

CODATA Recommended Values of the Fundamental Physical Constants: 1998*†

Peter J. Mohr^{a)} and Barry N. Taylor^{b)}

National Institute of Standards and Technology, Gaithersburg, Maryland 20899-8401

Received September 24, 1999

This paper gives the 1998 self-consistent set of values of the basic constants and conversion factors of physics and chemistry recommended by the Committee on Data for Science and Technology (CODATA) for international use. Further, it describes in detail the adjustment of the values of the subset of constants on which the complete 1998 set of recommended values is based. The 1998 set replaces its immediate predecessor recommended by CODATA in 1986. The new adjustment, which takes into account all of the data available through 31 December 1998, is a significant advance over its 1986 counterpart. The standard uncertainties (i.e., estimated standard deviations) of the new recommended values are in most cases about 1/5 to 1/12 and in some cases 1/160 times the standard uncertainties of the corresponding 1986 values. Moreover, in almost all cases the absolute values of the differences between the 1998 values and the corresponding 1986 values are less than twice the standard uncertainties of the 1986 values. The new set of recommended values is available on the World Wide Web at physics.nist.gov/constants. © 1999 American Institute of Physics and American Chemical Society. [S0047-2689(00)00301-9]

Key words: CODATA, conversion factors, data analysis, electrical units, fundamental constants, Josephson effect, least-squares adjustment, quantum electrodynamics, quantum Hall effect.

Contents

1. Introduction.	1718	2. Special Quantities and Units.	1722
1.1. Background.	1718	2.1. Speed of Light in Vacuum c and Realization of the Meter.	1722
1.2. Units, Quantity Symbols, Numerical Values, Numerical Calculations.	1719	2.2. Magnetic Constant μ_0 and Electric Constant ϵ_0	1723
1.3. Uncertainties.	1719	2.3. Electronvolt eV, Unified Atomic Mass Unit u, and Related Quantities.	1723
1.4. Data Categorization and Selection.	1720	2.4. Josephson Effect and Josephson Constant K_J , and Quantum Hall Effect and von Klitzing Constant R_K	1724
1.5. Data Evaluation Procedures.	1721	2.4.1. Josephson Effect.	1724
1.6. Outline of Paper.	1721	2.4.2. Quantum Hall Effect.	1724
		2.5. Conventional Josephson Constant K_{J-90} , Conventional von Klitzing Constant R_{K-90} , and Conventional Electric Units.	1725
		2.6. Acceleration of Free Fall g	1727
		3. Review of Data.	1727
		3.1. Relative Atomic Masses.	1727
		3.1.1. Atomic Mass Evaluation: 1995 Update.	1727
		3.1.2. Binding Energies.	1727
		3.1.3. Relative Atomic Masses of e, n, p, d, h, and α Particle.	1728
		3.1.3.a. Electron.	1729
		3.1.3.b. Proton, deuteron, helion, and α particle.	1730
		3.1.3.c. Neutron.	1730
		3.2. Hydrogenic Transition Frequencies and the Rydberg Constant R_∞	1732
		3.2.1. MPQ.	1733
		3.2.2. LKB/LPTF.	1735
		3.2.3. Yale University.	1736
		3.2.4. Harvard University.	1736
		3.2.5. University of Sussex.	1737

*This review is being published simultaneously by the *Reviews of Modern Physics*.

†This report was prepared by the authors under the auspices of the CODATA Task Group on Fundamental Constants. The members of the task group are:

F. Cabiati, Istituto Elettrotecnico Nazionale "Galileo Ferraris," Italy
E. R. Cohen, Science Center, Rockwell International (retired), United States of America
T. Endo, Electrotechnical Laboratory, Japan
R. Liu, National Institute of Metrology, China (People's Republic of)
B. A. Mamyrin, A. F. Ioffe Physical-Technical Institute, Russian Federation
P. J. Mohr, National Institute of Standards and Technology, United States of America
F. Nez, Laboratoire Kastler-Brossel, France
B. W. Petley, National Physical Laboratory, United Kingdom
T. J. Quinn, Bureau International des Poids et Mesures
B. N. Taylor, National Institute of Standards and Technology, United States of America
V. S. Tuninsky, D. I. Mendeleyev All-Russian Research Institute for Metrology, Russian Federation
W. Wöger, Physikalisch-Technische Bundesanstalt, Germany
B. M. Wood, National Research Council, Canada

^{a)}Electronic mail: peter.mohr@nist.gov

^{b)}Electronic mail: barry.taylor@nist.gov

©1999 by the U.S. Secretary of Commerce on behalf of the United States. All rights reserved. This copyright is assigned to the American Institute of Physics and the American Chemical Society.

Reprints available from ACS; see Reprints List at back of issue.

3.2.6.	Other Data.	1737	3.5.3.	Other Values.	1762
3.2.7.	Nuclear Radii.	1737	3.6.	von Klitzing Constant R_K	1763
3.3.	Magnetic Moments and g -Factors.	1738	3.6.1.	NIST: Calculable Capacitor.	1763
3.3.1.	Electron Magnetic Moment		3.6.2.	NML: Calculable Capacitor.	1764
	Anomaly a_e	1738	3.6.3.	NPL: Calculable Capacitor.	1765
3.3.2.	Bound-State Corrections for		3.6.4.	NIM: Calculable Capacitor.	1766
	Magnetic Moments.	1740	3.6.5.	Other Values.	1766
3.3.2.a.	Electron in hydrogen.	1740	3.7.	Product $K_J^2 R_K$	1766
3.3.2.b.	Proton in hydrogen.	1742	3.7.1.	NPL: Watt Balance.	1767
3.3.2.c.	Electron in deuterium.	1742	3.7.2.	NIST: Watt Balance.	1768
3.3.2.d.	Deuteron in deuterium.	1742	3.8.	Faraday Constant F	1769
3.3.2.e.	Electron in muonium.	1742	3.8.1.	NIST: Ag Coulometer.	1770
3.3.2.f.	Muon in muonium.	1742	3.8.2.	Other Values.	1771
3.3.2.g.	Comparison of theory and		3.9.	{220} Lattice Spacing of Silicon d_{220}	1771
	experiment.	1742	3.9.1.	PTB: X-ray/Optical	
3.3.3.	Electron to Proton Magnetic			Interferometer.	1773
	Moment Ratio μ_e/μ_p	1743	3.9.2.	IMGC: X-ray/Optical	
3.3.4.	Deuteron to Electron Magnetic			Interferometer.	1774
	Moment Ratio μ_d/μ_e	1743	3.9.3.	NRLM: X-ray/Optical	
3.3.5.	Deuteron to Proton Magnetic			Interferometer.	1775
	Moment Ratio μ_d/μ_p	1744	3.10.	Molar Volume of Silicon $V_m(\text{Si})$	1776
3.3.6.	Electron to Shielded Proton		3.11.	Quotient of Planck Constant and Particle	
	Magnetic Moment Ratio μ_e/μ'_p	1744		Mass $h/m(\text{X})$	1777
3.3.6.a.	Temperature dependence		3.11.1.	Quotient h/m_n	1777
	of shielded proton		3.11.2.	Quotient $h/m(^{133}\text{Cs})$	1779
	magnetic moment.	1745	3.12.	Hyperfine Structure.	1780
3.3.6.b.	Value of μ_e/μ'_p	1745	3.13.	Fine Structure.	1780
3.3.7.	Shielded Helion to Shielded Proton		3.14.	Molar Gas Constant R	1781
	Magnetic Moment Ratio μ'_h/μ'_p	1745	3.14.1.	NIST: Speed of Sound in Argon. . .	1781
3.3.8.	Neutron to Shielded Proton		3.14.2.	NPL: Speed of Sound in Argon. . .	1783
	Magnetic Moment Ratio μ_n/μ'_p	1746	3.15.	Boltzmann Constant k	1784
3.3.9.	Muon to Proton Magnetic Moment		3.16.	Stefan-Boltzmann Constant σ	1785
	Ratio μ_μ/μ_p and Muon to		3.17.	Newtonian Constant of Gravitation G	1786
	Electron Mass Ratio m_μ/m_e	1747	3.18.	X-ray Units.	1791
3.3.9.a.	SIN: μ_μ/μ_p	1747	3.19.	Other Quantities.	1793
3.3.9.b.	LAMPF 1982: μ_μ/μ_p	1748	4.	Analysis of Data.	1793
3.3.9.c.	LAMPF 1999: μ_μ/μ_p	1749	4.1.	Comparison of Data of the Same Type.	1794
3.3.9.d.	LAMPF: $\Delta\nu_{\text{Mu}}$	1750	4.1.1.	Rydberg Constant Data.	1794
3.3.9.e.	Other values.	1750	4.1.2.	Other Data.	1794
3.3.10.	Muon Magnetic Moment Anomaly		4.2.	Comparison of Data of Different Types.	1798
	a_μ	1751	4.2.1.	Rydberg Constant Data.	1798
3.3.10.a.	CERN.	1751	4.2.2.	Other Data.	1798
3.3.10.b.	Brookhaven.	1752	4.3.	Multivariate Analysis of Data.	1800
3.3.10.c.	Theory.	1752	4.3.1.	Rydberg Constant Data.	1801
3.4.	Shielded Gyromagnetic Ratios γ'	1753	4.3.2.	Other Data.	1802
3.4.1.	Proton p	1754	4.3.3.	All Data.	1807
3.4.1.a.	NIST: Low field.	1754	4.4.	Final Selection of Data and Least-Squares	
3.4.1.b.	NIM: Low field and high			Adjustment.	1807
	field.	1756	5.	The 1998 CODATA Recommended Values.	1807
3.4.1.c.	NPL: High field.	1757	5.1.	Tables of Values.	1808
3.4.2.	Helion h	1758	5.2.	Computational Details.	1808
3.4.2.a.	KRISS/VNIIM: Low field. .	1758	6.	Summary and Conclusion.	1819
3.4.2.b.	VNIIM: Low field.	1759	6.1.	Comparison of 1998 and 1986 CODATA	
3.4.3.	Other Values.	1760		Recommended Values.	1819
3.5.	Josephson Constant K_J	1760	6.2.	Some Implications for Physics and Metrology	
3.5.1.	NML: Hg Electrometer.	1760		of the 1998 CODATA Recommended	
3.5.2.	PTB: Capacitor Voltage Balance. .	1762		Values and Adjustment.	1821

6.3. Outlook and Suggestions for Future Work...	1822
7. Acknowledgments.....	1825
8. Appendices.....	1825
Appendix A. Theory Relevant to the Rydberg Constant.....	1825
1. Dirac Eigenvalue.....	1826
2. Relativistic Recoil.....	1826
3. Nuclear Polarization.....	1827
4. Self Energy.....	1827
5. Vacuum Polarization.....	1828
6. Two-Photon Corrections.....	1829
7. Three-Photon Corrections.....	1830
8. Finite Nuclear Size.....	1831
9. Nuclear-Size Correction to Self Energy and Vacuum Polarization.....	1832
10. Radiative-Recoil Corrections.....	1832
11. Nucleus Self Energy.....	1832
12. Total Energy and Uncertainty.....	1832
13. Transition Frequencies Between Levels with $n=2$	1833
Appendix B. Theory of Electron Magnetic Moment Anomaly.....	1833
Appendix C. Theory of Muon Magnetic Moment Anomaly.....	1836
Appendix D. Theory of Muonium Ground-State Hyperfine Splitting.....	1839
Appendix E. Method of Least Squares.....	1840
Appendix F. Use of the Covariance Matrix.....	1843
9. References.....	1844

List of Tables

1. Some exact quantities.....	1722
2. Values of the relative atomic masses of various neutral atoms.....	1728
3. Ground-state ionization energies.....	1728
4. Input values of mass ratios, and inferred values of relative atomic masses.....	1728
5. Variances, covariances, and correlation coefficients of relative atomic masses.....	1728
6. Summary of reported values of R_∞ with $10^{-10} < u_r < 10^{-9}$	1733
7. Summary of reported values of R_∞ with $u_r < 10^{-10}$	1733
8. Summary of measured transition frequencies for the determination of R_∞	1734
9. Summary of data related to magnetic moments, and inferred values of various quantities.....	1739
10. Summary of data related to shielded gyromagnetic ratios, and inferred values of α and h	1754
11. Summary of data related to K_J , R_K , and F , and inferred values of α and h	1761
12. Summary of data related to d_{220} of Si, and inferred values of α	1772
13. Summary of principal values of G	1788
14.A.1. Summary of principal input data relevant to	

the determination of the value of R_∞	1795
14.A.2. Non-negligible correlation coefficients of the data in Table 14.A.1.....	1796
14.B.1. Summary of principal input data relevant to the determination of the values of most constants.....	1797
14.B.2. Non-negligible correlation coefficients of the data in Table 14.B.1.....	1798
15. Comparison of data in Tables 14.B.1. and 14.B.2. through inferred values of α	1798
16. Comparison of data in Tables 14.B.1 and 14.B.2 through inferred values of h	1800
17.A.1. The 28 adjusted constants used in the analysis of the data relevant to R_∞	1800
17.A.2. Observational equations for the data relevant to R_∞	1801
18. Summary of results of adjustments used to analyze the data relevant to R_∞	1802
19.B.1. The 29 adjusted constants used in the analysis of the data relevant to most constants.....	1803
19.B.2. Observational equations for the data relevant to most constants.....	1804
20. Summary of the input data, relevant to most constants, omitted from various adjustments..	1805
21. Summary of the results of adjustments used to analyze the data relevant to most constants.....	1806
22. Summary of the results of adjustments used to analyze all of the data.....	1807
23. An abbreviated list of the 1998 CODATA recommended values.....	1808
24. The 1998 CODATA recommended values....	1809
25. The variances, covariances, and correlation coefficients of selected constants.....	1813
26. Internationally adopted values of various quantities.....	1814
27. Values of x-ray-related quantities.....	1814
28. Values in SI units of non-SI units.....	1815
29. Values of energy equivalents.....	1816
30. Values of energy equivalents.....	1816
31. Comparison of 1998 and 1986 CODATA recommended values.....	1819
32. Bethe logarithms relevant to the determination of R_∞	1828
33. Values of the function $G_{SE}(\alpha)$	1828
34. Values of the function $G_{VP}^{(1)}(\alpha)$	1828

List of Figures

1. Graphical comparison of values of G	1788
2. Graphical comparison of input data through inferred values of α	1799
3. Graphical comparison of five values of α^{-1}	1799
4. Graphical comparison of input data through inferred values of h	1800
5. Graphical comparison of 1998 and 1986 CODATA recommended values.....	1820

List of Symbols

AMDC	Atomic Mass Data Center, Centre de Spectrométrie Nucléaire et de Spectrométrie de Masse (CSNSM), Orsay, France	IMGC	Istituto di Metrologia “G. Colonnetti,” Torino, Italy
$A_r(X)$	Relative atomic mass of X: $A_r(X) = m(X)/m_u$	IRMM	Institute for Reference Materials and Measurements, Geel, Belgium
A_{90}	Conventional unit of electric current: $A_{90} = V_{90}/\Omega_{90}$	KRISS	Korea Research Institute of Standards and Science, Taedok Science Town, Republic of Korea
\AA^*	Ångström star: $\lambda(W K\alpha_1) = 0.209\,010\,0\text{ \AA}^*$	KR/VN	KRISS-VNIIM collaboration
a_e	Electron magnetic moment anomaly: $a_e = (g_e - 2)/2$	K_J	Josephson constant: $K_J = 2e/h$
a_μ	Muon magnetic moment anomaly: $a_\mu = (g_\mu - 2)/2$	K_{J-90}	Conventional value of the Josephson constant K_J : $K_{J-90} = 483\,597.9\text{ GHz V}^{-1}$
BIPM	Bureau International des Poids et Mesures (International Bureau of Weights and Measures), Sèvres, France	k	Boltzmann constant: $k = R/N_A$
BNL	Brookhaven National Laboratory, Upton, New York, USA	LAMPF	Clinton P. Anderson Meson Physics Facility at Los Alamos National Laboratory, Los Alamos, New Mexico, USA
CCEM	Comité Consultatif d'Électricité et Magnétisme	LKB	Laboratoire Kastler-Brossel, Paris, France
CERN	European Laboratory for Particle Physics, Geneva, Switzerland	LK/LP	LKB-LPTF collaboration
CIPM	Comité International des Poids et Mesures	LPTF	Laboratoire Primaire du Temps et des Fréquences, Paris, France
CODATA	Committee on Data for Science and Technology of the International Council for Science (ICSU, formerly the International Council of Scientific Unions)	MIT	Massachusetts Institute of Technology, Cambridge, Massachusetts, USA
CPT	Combined charge conjugation, parity inversion, and time reversal	MPQ	Max-Planck-Institute für Quantenoptik, Garching, Germany
c	Speed of light in vacuum	$M(X)$	Molar mass of X: $M(X) = A_r(X)M_u$
d	Deuteron (nucleus of deuterium D, or ^2H)	Mu	Muonium (μ^+e^- atom)
d_{220}	{220} lattice spacing of an ideal crystal of silicon	M_u	Molar mass constant: $M_u = 10^{-3}\text{ kg mol}^{-1}$
$d_{220}(X)$	{220} lattice spacing of silicon crystal X	m_u	Unified atomic mass constant: $m_u = m(^{12}\text{C})/12$
E_b	Binding energy	$m_X, m(X)$	Mass of X (for the electron e, proton p, and other elementary particles, the first symbol is used, i.e., m_e, m_p , etc.)
e	Symbol for either member of the electron-positron pair; when necessary, e^- or e^+ is used to signify the electron or positron	N_A	Avogadro constant
e	elementary charge: absolute value of the charge of the electron	NIM	National Institute of Metrology, Beijing, China (People's Republic of)
F	Faraday constant: $F = N_A e$	NIST	National Institute of Standards and Technology, Gaithersburg, Maryland and Boulder, Colorado, USA
FSU	Friedrich-Schiller University, Jena, Germany	NML	National Measurement Laboratory, Commonwealth Scientific and Industrial Research Organization (CSIRO), Lindfield, Australia
\mathcal{F}_{90}	$\mathcal{F}_{90} = (F/A_{90})\text{ A}$	NPL	National Physical Laboratory, Teddington, UK
G	Newtonian constant of gravitation	NRLM	National Research Laboratory of Metrology, Tsukuba, Japan
g	Local acceleration of free fall	n	Neutron
g_d	deuteron g -factor: $g_d = \mu_d/\mu_N$	PTB	Physikalisch-Technische Bundesanstalt, Braunschweig and Berlin, Germany
g_e	Electron g -factor: $g_e = 2\mu_e/\mu_B$	p	Proton
g_p	proton g -factor: $g_p = 2\mu_p/\mu_N$	QED	Quantum electrodynamics
g'_p	Shielded proton g -factor: $g'_p = 2\mu'_p/\mu_N$	$Q(\chi^2 \nu)$	Probability that an observed value of chi-square for ν degrees of freedom would exceed χ^2
$g_X(Y)$	g -factor of particle X in the ground (1S) state of hydrogenic atom Y	R	Molar gas constant
g_μ	Muon g -factor: $g_\mu = 2\mu_\mu/(e\hbar/2m_\mu)$	\bar{R}	Ratio of muon anomaly difference frequency to free proton NMR frequency
Harv	Harvard University, Cambridge, Massachusetts, USA		
h	Helion (nucleus of ^3He)		
\hbar	Planck constant; $\hbar = h/2\pi$		
ILL	Institut Max von Laue-Paul Langevin, Grenoble, France		

R_B	Birge ratio: $R_B = (\chi^2/\nu)^{1/2}$	$\Gamma'_{X-90}(lo)$	$\Gamma'_{X-90}(lo) = (\gamma'_X A_{90}) A^{-1}$, X=p or h
R_d	Bound-state nuclear rms charge radius of the deuteron	$\Gamma'_{p-90}(hi)$	$\Gamma'_{p-90}(hi) = (\gamma'_p/A_{90}) A$
R_K	von Klitzing constant: $R_K = h/e^2$	γ_p	Proton gyromagnetic ratio: $\gamma_p = 2\mu_p/\hbar$
R_{K-90}	Conventional value of the von Klitzing constant R_K : $R_{K-90} = 25\,812.807\,\Omega$	γ'_p	Shielded proton gyromagnetic ratio: $\gamma'_p = 2\mu'_p/\hbar$
R_p	Bound-state nuclear rms charge radius of the proton	γ'_h	Shielded helion gyromagnetic ratio: $\gamma'_h = 2 \mu'_h /\hbar$
R_∞	Rydberg constant: $R_\infty = m_e c \alpha^2/2h$	$\Delta\nu_{Mu}$	Muonium ground-state hyperfine splitting
$r(x_i, x_j)$	Correlation coefficient of estimated values x_i and x_j : $r(x_i, x_j) = u(x_i, x_j)/[u(x_i)u(x_j)]$	δ_e	Additive correction to the theoretical expression for the electron magnetic moment anomaly a_e
S_c	Self-sensitivity coefficient	δ_{Mu}	Additive correction to the X theoretical expression for the ground-state hyperfine splitting of muonium $\Delta\nu_{Mu}$
SI	Système International d'Unités (International System of Units)	$\delta_X(nL_j)$	Additive correction to the theoretical expression for an energy level of X (either hydrogen H or deuterium D) with quantum numbers n , L , and j
SIN	Schweizerisches Institut für Nuklearforschung, Villigen, Switzerland (now the Paul Scherrer Institute, PSI)	δ_μ	Additive correction to the theoretical expression for the muon magnetic moment anomaly a_μ
T	Thermodynamic temperature	ϵ_0	Electric constant: $\epsilon_0 = 1/\mu_0 c^2$
Type A	Uncertainty evaluation by the statistical analysis of series of observations	\doteq	Symbol used to relate an input datum to its theoretical expression in an observational equation
Type B	Uncertainty evaluation by means other than the statistical analysis of series of observations	$\kappa(t)$	Volume magnetic susceptibility of water at theoretical expression in an Celsius temperature t
t_{68}	Celsius temperature on the International Practical Temperature Scale of 1968 (IPTS-68)	$\lambda(X K\alpha_1)$	Wavelength of $K\alpha_1$ x-ray line of element X
t_{90}	Celsius temperature on the International Temperature Scale of 1990 (ITS-90)	λ_{meas}	Measured wavelength of the 2.2 MeV capture γ ray emitted in the reaction $n+p \rightarrow d+\gamma$
USus	University of Sussex, Sussex, UK	μ	Symbol for either member of the muon-antimuon pair; when necessary, μ^- or μ^+ is used to signify the negative muon or positive muon
UWash	University of Washington, Seattle, Washington, USA	μ_B	Bohr magneton: $\mu_B = e\hbar/2m_e$
u	Unified atomic mass unit: $1\ u = m_u = m(^{12}\text{C})/12$	μ_N	Nuclear magneton: $\mu_N = e\hbar/2m_p$
$u(x_i)$	Standard uncertainty (i.e., estimated standard deviation) of an estimated value x_i of a quantity X_i (also simply u)	$\mu_X(Y)$	Magnetic moment of particle X in atom Y
$u_r(x_i)$	Relative standard uncertainty of an estimated value x_i of a quantity X_i : $u_r(x_i) = u(x_i)/ x_i $, $x_i \neq 0$ (also simply u_r)	μ_0	Magnetic constant: $\mu_0 = 4\pi \times 10^{-7}\text{ N/A}^2$
$u(x_i, x_j)$	Covariance of estimated values x_i and x_j	μ_X, μ'_X	Magnetic moment, or shielded magnetic moment, of particle X
$u_r(x_i, x_j)$	Relative covariance of estimated values x_i and x_j : $u_r(x_i, x_j) = u(x_i, x_j)/(x_i x_j)$, $x_i x_j \neq 0$	ν	Degrees of freedom of a particular adjustment
VNIIM	D. I. Mendeleyev All-Russian Research Institute for Metrology, St. Petersburg, Russian Federation	$\nu(f_p)$	Difference between muonium hyperfine splitting Zeeman transition frequencies ν_{34} and ν_{12} at a magnetic flux density B corresponding to the free proton NMR frequency f_p
V_{90}	Conventional unit of voltage based on the Josephson effect and K_{J-90} : $V_{90} = (K_{J-90}/K_J) V$	σ	Stefan-Boltzmann constant: $\sigma = \pi^2 k^4/60\hbar^3 c^2$
W_{90}	Conventional unit of power: $W_{90} = V_{90}^2/\Omega_{90}$	τ	Symbol for either member of the tau-antitau pair; when necessary, τ^- or τ^+ is used to signify the negative tau or positive tau
XRCD	x-ray crystal density (method of determining the Avogadro constant N_A)	χ^2	The statistic "chi square"
XROI	Combined x ray and optical interferometer	Ω_{90}	Conventional unit of resistance based on the quantum Hall effect and $R_{K-90}:\Omega_{90}$
xu(Cu $K\alpha_1$)	Cu x unit: $\lambda(\text{Cu } K\alpha_1) = 1\,537.400\text{ xu}(\text{Cu } K\alpha_1)$		$= (R_K/R_{K-90})\Omega$
xu(Mo $K\alpha_1$)	Mo x unit: $\lambda(\text{Mo } K\alpha_1) = 707.831\text{ xu}(\text{Mo } K\alpha_1)$		
$x(X)$	Amount-of-substance fraction of X		
Yale	Yale University, New Haven, Connecticut, USA		
α	Fine-structure constant: $\alpha = e^2/4\pi\epsilon_0\hbar c$		
α	Alpha particle (nucleus of ^4He)		

1. Introduction

1.1. Background

CODATA, the Committee on Data for Science and Technology, was established in 1966 as an interdisciplinary committee of the International Council for Science (ICSU), formerly the International Council of Scientific Unions. It seeks to improve the quality, reliability, processing, management, and accessibility of data of importance to science and technology.

The CODATA Task Group on Fundamental Constants was established in 1969. Its purpose is to periodically provide the scientific and technological communities with a self-consistent set of internationally recommended values of the basic constants and conversion factors of physics and chemistry based on all of the relevant data available at a given point in time. The first such set was published in 1973 (CODATA, 1973; Cohen and Taylor, 1973) and the second in 1986 (Cohen and Taylor, 1986; Cohen and Taylor, 1987). This paper gives the third such set together with a detailed description of the 1998 adjustment of the values of the subset of constants on which it is based. Like its 1986 predecessor, the 1998 set of recommended values is available on the World Wide Web at physics.nist.gov/constants.

The 1973 CODATA adjustment, and to some extent that of 1986, built on the 1969 adjustment of Taylor, Parker, and Langenberg (1969), which in turn built on the 1965 adjustment of Cohen and DuMond (1965). Adjustments carried out in the 1950s include those of Bearden and Thomsen (1957) and of Cohen *et al.* (1955). The origin of such endeavors is the pioneering analysis of the values of the constants carried out in the late 1920s by Birge (1929). [Birge (1957) later made insightful observations concerning the evaluation of the constants based on 30 years of experience.] Viewed from this perspective, the 1998 adjustment is simply the latest in a continuing series that began 70 years ago.

The 1986 CODATA adjustment took into consideration all relevant data available by 1 January 1986. Since that closing date, a vast amount of new experimental and theoretical work has been completed. The relative standard uncertainties (that is, relative estimated standard deviations—see Sec. 1.3) of the results of this new work range from about 2×10^{-3} for measurements of the Newtonian constant of gravitation, to 3.4×10^{-13} for a measurement of the frequency of the 1S–2S transition in hydrogen, to essentially zero uncertainty for the analytic calculation of the sixth-order term in the theoretical expression for the magnetic moment anomaly of the electron.

The impact of the new results reported between the closing date of the 1986 adjustment and mid-1990 on the 1986 recommended values was examined in a status report by Taylor and Cohen (1990). They found that, in general, the new results would have led to new values of most of the constants with standard uncertainties one-fifth to one-seventh of the standard uncertainties assigned the 1986 values, and that the absolute values of the differences between the 1986 values and the new values would have been less than twice the assigned uncertainties of the earlier values. The reduction

in the 1986 uncertainties was mainly due to three new results: a value of the fine-structure constant α obtained from the electron magnetic moment anomaly, a value of the Planck constant h obtained from a moving-coil watt balance experiment, and a value of the molar gas constant R obtained from a measurement of the speed of sound in argon.

Because of the major role that these three additional data would play in determining the values and uncertainties of the constants in any future adjustment, Taylor and Cohen suggested that before a new adjustment was carried out, more data should be in hand that provide a value of α , of h , and of R with an uncertainty comparable to that of the corresponding new value and that corroborates it. Although only a value of h that meets this criterion has become available since their report, the CODATA Task Group has decided that, because the 1986 set is some 13 years old and because the data already in hand can yield values of the constants with significantly reduced uncertainties, it is time to provide a new set of recommended values.

Because data that influence our knowledge of the values of the constants become available nearly continuously, and because of the modern and highly beneficial trend of having new information immediately and widely available on the Web, the Task Group has also decided that 13 years between adjustments is no longer acceptable. In the future, by taking advantage of the high degree of automation incorporated by the authors in the 1998 adjustment, CODATA will issue a new set of recommended values at least every 4 years, and more frequently if a new result is reported that has a significant impact on the values of the constants. This paper has been written with this new approach in mind; we have attempted both to structure it and to include sufficient detail to allow future adjustments to be understood with only a discussion of new work.

It should be recognized that carrying out an adjustment provides two important results. The obvious one is a self-consistent set of recommended values of the basic constants and conversion factors of physics and chemistry; the less obvious one is an analysis of the broad spectrum of experimental and theoretical information relevant to the constants. In general, such an analysis may uncover errors in theoretical calculations or experiments, will reevaluate uncertainties so that all are expressed as standard uncertainties, may identify inconsistencies among results and weaknesses in certain areas, possibly stimulating new experimental and theoretical work, and will summarize a large amount of rather diverse information in one place.

It has long been recognized that a significant measure of the correctness and over-all consistency of the basic theories and experimental methods of physics is the comparison of the values of the constants as obtained from widely differing experiments. Nevertheless, throughout this adjustment, as a working principle, we assume the validity of the physical theory that underlies it including special relativity, quantum mechanics, quantum electrodynamics (QED), the standard model of particle physics, combined charge conjugation, par-

ity inversion, and time-reversal (CPT) invariance, and—as discussed in Sec. 2.4—the theory of the Josephson and quantum Hall effects, especially the exactness of the relationships between the Josephson and von Klitzing constants and the elementary charge e and Planck constant h .

1.2. Units, Quantity Symbols, Numerical Values, Numerical Calculations

We generally use in this paper units of the International System of Units, universally abbreviated SI from the French name *Système International d'Unités*. Detailed descriptions of the SI, which is founded on seven base units—the meter (m), kilogram (kg), second (s), ampere (A), kelvin (K), mole (mol), and candela (cd)—are given in a number of publications (BIPM, 1998; Taylor, 1995).

We also generally employ symbols for quantities recommended by the International Organization for Standardization (ISO), the International Electrotechnical Commission (IEC), the International Union of Pure and Applied Chemistry (IUPAC), and the International Union of Pure and Applied Physics (IUPAP) (ISO, 1993b; IEC, 1992; Mills *et al.*, 1993; Cohen and Giacomo, 1987). Following the recommendations of these bodies, unit symbols are printed in roman (upright) type and quantity symbols in italic (sloping) type. A subscript or superscript on a quantity symbol is in roman type if descriptive, such as the name of a person or a particle, and the subscript or superscript is in italic type if it represents a quantity, a variable, or an index that represents an integer.

The value of a quantity is expressed as a number times a unit. Formally, the value of quantity A can be written as $A = \{A\} \cdot [A]$, where $\{A\}$ is the *numerical value* of the quantity A when A is expressed in the unit $[A]$ (ISO, 1993b). The numerical value $\{A\}$ can therefore be written as $\{A\} = A/[A]$, where $A/[A]$ is interpreted to mean the ratio of quantity A to a quantity of the same kind with the value 1 $[A]$. An example of this notation is $1 \text{ eV} = (e/C) \text{ J} \approx 1.60 \times 10^{-19} \text{ J}$, where e/C is the numerical value of the elementary charge e when e is expressed in the SI derived unit the coulomb, symbol C.

Occasionally the reader may find that the stated result of a calculation involving several quantities differs slightly from the result one would obtain using the values of the quantities as given in the text. This is because values of quantities are presented with a number of significant figures appropriate to their associated standard uncertainties (see the following section), whereas the calculations are in general performed with values having more significant figures in order to minimize rounding error.

1.3. Uncertainties

Because the uncertainty assigned to a datum determines its level of agreement with other values of the same quantity as well as its weight in a least-squares adjustment, uncertainty evaluation is of critical importance.

In evaluating and expressing the uncertainty to be associated with a result obtained either by measurement or calculation, we follow to a great extent the philosophy, terminology, and notation of the *Guide to the Expression of Uncertainty in Measurement* published by ISO in the name of seven international organizations, including IUPAC and IUPAP (ISO, 1993a). [A concise summary is also available (Taylor and Kuyatt, 1994).]

The basic approach described in the *Guide* is straightforward and has been used in the field of precision measurement and fundamental constants for many years. The *standard uncertainty* $u(y)$ (or simply u) of a result y is taken to represent the estimated standard deviation (the square root of the estimated variance) of y . If the result y is obtained as a function of estimated values x_i of other quantities, $y = f(x_1, x_2, \dots)$, then the standard uncertainty $u(y)$ is obtained by combining the individual standard uncertainty components $u(x_i)$, and covariances $u(x_i, x_j)$ where appropriate, using the law of propagation of uncertainty as given in Eq. (F11) of Appendix F. [The law of propagation of uncertainty is also called the “root-sum-of squares” (square root of the sum of the squares) or rss method.] The *relative standard uncertainty* of a result y , $u_r(y)$ (or simply u_r), is defined by $u_r(y) = u(y)/|y|$, if $y \neq 0$, with an analogous definition for individual components of uncertainty.

Further, the evaluation of a standard uncertainty by the statistical analysis of series of observations is termed a *Type A evaluation*, while an evaluation by means other than the statistical analysis of series of observations is termed a *Type B evaluation*. A Type A evaluation of standard uncertainty is one based on any valid statistical method for treating data, while a Type B evaluation is usually based on scientific judgment using all the relevant information available and an assumed probability distribution for the possible values of the quantity in question.

As part of our review of the data for the 1998 adjustment, we carefully consider the uncertainty assigned to each result in order to ensure that it has been properly evaluated and that it represents a standard uncertainty. We clearly indicate in the text those cases where we have had to alter an uncertainty originally assigned by an author, either because of our reevaluation or our application of additional corrections. We also pay careful attention to correlations among the data, calculating covariances and the corresponding correlation coefficients whenever deemed necessary based on Eqs. (F7) and (F12) of Appendix F. However, if the absolute value of the correlation coefficient is less than about 0.01, the correlation between those particular items is usually ignored because of its insignificant consequences.

In many cases involving theoretical expressions for quantities it is necessary to evaluate the uncertainty due to terms that are likely to exist but are not yet calculated. In such cases we assign an uncertainty, based on experience with similar theoretical expressions where terms are known, such that the absolute value of the expected contribution of the uncalculated terms has a probability of 68 % of being smaller than the assigned uncertainty, and we assume that such the-

oretical uncertainties may be treated on an equal footing with statistically estimated standard deviations. The underlying probability distribution is taken to be normal to the extent that there is a 95 % probability that the absolute value of the contribution of the uncalculated terms is smaller than twice the assigned uncertainty. Further in regard to theoretical expressions for quantities, in cases where only some terms of a given magnitude have been calculated while other terms that are expected to be of similar magnitude or even larger have not, we occasionally follow the practice of not including the known terms and accounting for all omitted terms by means of an appropriate standard uncertainty.

In presenting numerical data in the text, we follow (in part) the general form that has become common in the precision measurement/fundamental constants field. That is, we usually write a result as, for example,

$$y = 1\,234.567\,89(12) \times 10^{-10} \text{ U } [9.7 \times 10^{-8}],$$

where U represents a unit symbol and the number in parentheses is the numerical value of the standard uncertainty of y referred to the last figures of the quoted value. The number in square brackets is the relative standard uncertainty of y . (Note that we do not use ppm, ppb, and the like to express relative standard uncertainties, because such symbols are not part of the SI.) Although not always justified, uncertainties are usually quoted with two-figure accuracy to limit rounding errors to an acceptable level. In general, numbers with more than four figures on either side of the decimal point are written with the figures in groups of three counting from the decimal point toward the left and right, with the exception that when there is a single separated figure followed by a two-figure standard uncertainty in parentheses, the single figure is grouped with the previous three figures. Thus we write, for example, 1.234 5678(12). It should also be understood that 12 345.6(1.2) means that the standard uncertainty of the figures 5.6 is 1.2.

1.4. Data Categorization and Selection

In the past, the data entering a least-squares adjustment of the constants were divided into two distinct categories: stochastic input data and auxiliary constants. In general, stochastic input data were those quantities whose values were simultaneously adjusted, while auxiliary constants were those quantities whose uncertainties were judged to be sufficiently small, based on the magnitude of the uncertainties and the way the quantities entered the adjustment, that they could be taken as exact. In other words, if the auxiliary constants were treated as stochastic data, their values would not be significantly changed by the adjustment. The motivation for this classification scheme was in part computational convenience (it reduces the number of “unknowns” in the adjustment and hence the size of the matrices that must be inverted).

However, for the following reasons we abandon such categorization in the 1998 adjustment and treat essentially all quantities on an equal footing. First, with modern computers

computational convenience is not a consideration. Second, dividing the data into these categories is somewhat arbitrary, and not doing so ensures that all components of uncertainty and correlations are taken into account. Finally, as discussed in Sec. 1.1, it is the intention of the CODATA Task Group on Fundamental Constants to issue sets of recommended values of the constants more frequently, and one of the purposes of this paper is to establish the framework for doing so. Treating all data in essentially the same way will provide continuity between adjustments by avoiding changes in the classification of quantities from one adjustment to the next.

On the other hand, in a few cases in the current adjustment a constant that enters the analysis of input data is taken as a fixed quantity rather than an adjusted quantity. An example of the most extreme case is the Fermi coupling constant, which is taken to have the fixed value given by the Particle Data Group (Caso *et al.*, 1998), because the data that enter the current adjustment have a negligible effect on its value. An intermediate case is where a quantity is in some contexts taken as a variable and in others as fixed. For example, the electron-muon mass ratio m_e/m_μ is taken as an adjusted quantity in the theoretical expression for the muonium hyperfine splitting, but it is taken as a fixed quantity in the calculation of the theoretical expression for the magnetic moment anomaly of the electron $a_e(\text{th})$. The reason is that $a_e(\text{th})$ depends so weakly on m_e/m_μ that the particular value used is unimportant. Consistent with these examples, we only omit the dependence when it is of no consequence. However, in the intermediate cases, rather than use arbitrary values for the fixed constants, we effectively use the 1998 recommended values by iterating the least-squares adjustment several times and replacing the fixed values by the adjusted values after each iteration.

As in the 1986 adjustment, the initial selection of the data for the 1998 adjustment is based on two main criteria: the date on which the result became available and its uncertainty.

Any datum considered for the 1998 adjustment had to be available by 31 December 1998. As noted in Sec. 1.1, data that influence our knowledge of the values of the constants become available nearly continuously, and it is never a straightforward task to decide when to carry out a new adjustment. Rather than delay the completion of the current adjustment until a particular experiment or calculation is completed, the above closing date was established with the knowledge that, based on the new schedule for adjustments (see Sec. 1.1), changes in the recommended values of the constants that might result from the completion of work currently underway could be taken into account within 2 years. A datum was considered to have met the 31 December 1998 closing date, even though not yet reported in an archival journal, as long as a detailed written description of the work was available and allowed a valid standard uncertainty to be assigned to the datum.

As in the 1986 adjustment, each datum considered for the 1998 adjustment had to have a standard uncertainty u sufficiently small that its weight $w = 1/u^2$ was nontrivial in com-

parison with the weight of other directly measured values of the same quantity. This requirement means that in most cases a result was not considered if its standard uncertainty was more than about five times the standard uncertainty of other similar results, corresponding to a weight smaller by a factor of less than 1/25. However, a datum that meets this criterion may still not be included as a final input datum if it affects the adjustment only weakly.

This “factor-of-five rule” accounts for the fact that an experiment that determines the value of a particular quantity with a valid uncertainty one-fifth to one-tenth of the uncertainty achieved in another experiment is necessarily qualitatively different from the other experiment. In particular, it must be assumed that the more accurate experiment achieved its significantly reduced uncertainty because it was designed and carried out in such a way that systematic effects at a level of only marginal concern in the less accurate experiment were carefully investigated.

In a number of cases, a particular laboratory has reported two or more values of the same quantity obtained from similar measurements carried out several years apart, with the most recent value having a smaller uncertainty due to improvements in apparatus and technique. Because of the many factors common to the results, such as personnel, method, equipment, and experimental environment, they cannot be viewed as fully independent. Hence, unless there are special circumstances (duly noted in the text), we adopt the general policy that the latest result, which is usually the most accurate, supersedes the earlier results of the same laboratory.

1.5. Data Evaluation Procedures

In the 1986 adjustment, the data were analyzed using two extended least-squares algorithms that were designed to incorporate information on the reliability of the initial standard uncertainty u assigned to each input datum. This information was quantitatively represented by ν , the effective degrees of freedom associated with u ; it was calculated from the Welch–Satterthwaite formula and the effective degrees of freedom of each component of uncertainty that contributed to u . In these calculations, the effective degrees of freedom of each Type B component of uncertainty was somewhat arbitrarily taken to be 1. This generally led to a comparatively small effective degrees of freedom for each datum.

We have taken the opportunity of the 1998 adjustment to review the idea of trying to quantify the “uncertainty of an uncertainty” and of using the result of such quantification in a modified least-squares algorithm. After due consideration, we have been forced to conclude that while such an attempt may seem attractive initially, it is virtually impossible to implement in a meaningful way. This conclusion was reached as a consequence of our detailed review of literally hundreds of experimental and theoretical results relevant to the fundamental constants, a review which has extended over nearly a 4 year period and has involved well in excess of 1000 email exchanges with both experimentalists and theorists in an effort to understand and evaluate the uncertainties

of results. Simply stated, because of the complexity of measurements and calculations in the field of fundamental constants, it is difficult enough to evaluate the uncertainty of a result in this field in a meaningful way, let alone the “uncertainty” of that uncertainty. We have therefore not calculated a value of ν for any input datum and use the standard least-squares algorithm in our data analyses.

In further support of our approach, we make the following three observations:

First, although carrying out Type B evaluations of uncertainty is rarely easy, it is our experience that such evaluations are usually done reliably for known effects. The difficulty with an experiment or theoretical calculation most often arises from an unrecognized effect, that is, an effect for which no component of uncertainty has been evaluated because its existence was not realized. Trying to assign an “uncertainty to an uncertainty” based only on known components of uncertainty is not necessarily reliable.

Second, as emphasized by one of the CODATA Task-Group-members, if there are doubts about the reliability of an initially assigned uncertainty, then one should use the information on which the doubts are based to reevaluate it (which in most cases means increasing the uncertainty) so that the doubts are removed. In short, all available information should be used in the evaluation of components of uncertainty.

The third and final observation concerns the possibility of including a margin of safety in the recommended values of the constants as is sometimes suggested. In particular, should the uncertainty of the values include an extra component so that they are “certain” to be correct? We do not include such an extra component of uncertainty, but rather give the best values based on all the available information, which in some cases means relying on the validity of the result of a single experiment or calculation. This approach, which is consistent with a view expressed earlier by one of the authors (Taylor, 1971), provides a faithful representation of our current state of knowledge with the unavoidable element of risk that that knowledge may include an error or oversight.

1.6. Outline of Paper

The remainder of the paper is organized as follows: Section 2 deals with special quantities and units such as the speed of light in vacuum c , the unified atomic mass unit u , the conventional values of the Josephson and von Klitzing constants K_{J-90} and R_{K-90} , and the conventional electric units that they imply.

Section 3 and Appendices A–D are the most critical portions of the paper because they are devoted to the review of all the available data that might be relevant to the 1998 adjustment. This includes theoretical expressions for bound-state corrections to magnetic moments (Sec. 3.3.2), energy levels of the hydrogen atom (Appendix A), the magnetic moment anomalies of the electron and muon a_e and a_μ (Appendices B and C), and the ground-state hyperfine splitting in muonium $\Delta\nu_{\text{Mu}}$ (Appendix D).

TABLE 1. Some exact quantities relevant to the 1998 adjustment.

Quantity	Symbol	Value
speed of light in vacuum	c, c_0	$299\,792\,458\,\text{m s}^{-1}$
magnetic constant	μ_0	$4\pi \times 10^{-7}\,\text{N A}^{-2} = 12.566\,370\,614 \dots \times 10^{-7}\,\text{N A}^{-2}$
electric constant	ϵ_0	$(\mu_0 c^2)^{-1} = 8.854\,187\,817 \dots \times 10^{-12}\,\text{F m}^{-1}$
molar mass of ^{12}C	$M(^{12}\text{C})$	$12 \times 10^{-3}\,\text{kg mol}^{-1}$
conventional value of Josephson constant	$K_{\text{J}-90}$	$483\,597.9\,\text{GHz V}^{-1}$
conventional value of von Klitzing constant	$R_{\text{K}-90}$	$25\,812.807\,\Omega$

The experimental data include relative atomic masses of various atoms, transition frequencies in hydrogen, magnetic moment ratios involving various atomic particles such as the electron and muon, values of $\Delta\nu_{\text{Mu}}$, shielded gyromagnetic ratios involving the proton and the helion (nucleus of the ^3He atom), values of the Josephson and von Klitzing constants K_{J} and R_{K} , the product $K_{\text{J}}^2 R_{\text{K}}$, the {220} lattice spacing of silicon d_{220} , the quotient $h/m_{\text{n}} d_{220}$ (m_{n} is the neutron mass), the Faraday and molar gas constants, and the Newtonian constant of gravitation.

In order to keep this paper to an acceptable length, theoretical calculations and experiments are described only in sufficient detail to allow the reader to understand our treatment of them and the critical issues involved, if any. It is left to the reader to consult the original papers for additional details and to understand fully the difficulty of experimentally determining the value of a quantity with a relative standard uncertainty of 1×10^{-8} (one part in 100 million), or of calculating a fractional contribution of 1×10^{-8} to the theoretical expression for a quantity such as $\Delta\nu_{\text{Mu}}$.

There is nothing special about the order in which the major categories of data are reviewed. It was selected on the basis of what seemed reasonable to us, but a different ordering could very well have been chosen. Similarly, there is nothing special about the order in which we review measurements of the same quantity from different laboratories. Factors that influenced our ordering choice in any particular case include the uncertainty quoted by the experimenters, the date the result was published, and the alphabetical order of the laboratories.

To avoid confusion, we identify a result by its year of publication rather than the year the result became available. For example, if a result was given at a meeting in 1988 but the publication date of the paper formally reporting the result is 1990, the date used in the result's identification is 1990 rather than 1988.

Section 4 gives our analysis of the data. Their consistency is examined by first comparing directly measured values of the same quantity, and then by comparing directly measured values of different quantities through the values of a third quantity such as the fine-structure constant α or Planck constant h that may be inferred from the values of the directly measured quantities. The data are then examined using the standard method of least squares, which is described in Appendix E, and based on this study the final input data (including their uncertainties) for the 1998 adjustment are determined.

Section 5 gives, in several tables, the 1998 CODATA recommended values of the basic constants and conversion factors of physics and chemistry. Included among the tables is the covariance matrix of a selected group of constants, the utilization of which, together with the law of propagation of uncertainty, is reviewed in Appendix F. The tables are followed by a summary of how the 1998 recommended values are obtained from the values of the subset of constants resulting from the least-squares fit of the final input data.

Section 6 concludes the main text with a comparison of the 1998 set of recommended values with the 1986 set, a discussion of the implications of some of the 1998 recommended values, the outlook for the future based on work currently underway, and suggestions for future work.

2. Special Quantities and Units

Some special quantities and units that are relevant to the 1998 adjustment are reviewed in the following sections. Those special quantities with exactly defined numerical values are given in Table 1.

2.1. Speed of Light in Vacuum c and Realization of the Meter

The current definition of the unit of length in the SI, the meter, was adopted by the 17th General Conference on Weights and Measures (CGPM, *Conférence Générale des Poids et Mesures*) in 1983. It reads (BIPM, 1998) "The meter is the length of the path traveled by light in vacuum during a time interval of $1/299\,792\,458$ of a second." This definition replaced the definition adopted by the 11th CGPM in 1960 based on the krypton 86 atom, which in turn replaced the original definition of the meter adopted by the 1st CGPM in 1889 based on the international Prototype of the meter. As a consequence of the 1983 definition, the speed of light in vacuum c is now an exact quantity:

$$c = 299\,792\,458\,\text{m/s.} \quad (1)$$

A number of the experiments relevant to the 1998 adjustment of the constants require an accurate practical realization of the meter. The three ways to realize the meter recommended by the International Committee for Weights and Measures (CIPM, *Comité International des Poids et Mesures*) are (BIPM, 1998) (a) by means of the length l traveled by electromagnetic waves in vacuum in a time t using the relation $l = c t$; (b) by means of the wavelength in

vacuum λ of a plane electromagnetic wave of frequency f using the relation $\lambda = c/f$; and (c) by means of one of the CIPM recommended radiations and its stated wavelength or stated frequency. The CIPM published its first list of recommended values of specified radiations in 1983 (called “*Mise en Pratique* of the Definition of the Meter”), and subsequently issued an improved and extended *Mise en Pratique* in 1992 and again in 1997 (Hudson, 1984; Quinn, 1993; BIPM, 1998).

For experiments requiring the accurate measurement of a length, except for those related to the determination of the Rydberg constant, the changes in the recommended values from one *Mise en Pratique* to the next are well below the uncertainties of the experiments and need not be taken into account. In the case of the Rydberg constant, the changes would need to be taken into account in analyzing data that span the changes in recommended values. However, as discussed in Sec. 3.2, the older data are no longer competitive, and in the newer experiments the frequencies of the relevant lasers used were determined in terms of the SI definition of the second based on the cesium atom. That definition is as follows (BIPM, 1998): “The second is the duration of 9 192 631 770 periods of the radiation corresponding to the transition between the two hyperfine levels of the ground state of the cesium 133 atom.”

2.2. Magnetic Constant μ_0 and Electric Constant ϵ_0

The definition of the ampere, the unit of electric current in the SI, reads (BIPM, 1998) “The ampere is that constant current which, if maintained in two straight parallel conductors of infinite length, of negligible circular cross section, and placed 1 meter apart in vacuum, would produce between these conductors a force equal to 2×10^{-7} N/m of length.”

The expression from electromagnetic theory for the force F per length l between two straight parallel conductors a distance d apart in vacuum, of infinite length and negligible cross section, and carrying currents I_1 and I_2 is

$$\frac{F}{l} = \frac{\mu_0 I_1 I_2}{2\pi d}. \quad (2)$$

This expression and the definition of the ampere in combination imply that the magnetic constant μ_0 , also called the permeability of vacuum, is an exact quantity given by

$$\begin{aligned} \mu_0 &= 4\pi \times 10^{-7} \text{ N A}^{-2} \\ &= 4\pi \times 10^{-7} \text{ H m}^{-1} \\ &= 12.566\,370\,614\ldots \times 10^{-7} \text{ N A}^{-2}. \end{aligned} \quad (3)$$

Because the electric constant ϵ_0 , also called the permittivity of vacuum, is related to μ_0 by the expression $\epsilon_0 = 1/\mu_0 c^2$, it too is an exact quantity:

$$\begin{aligned} \epsilon_0 &= \frac{1}{4\pi \times 10^{-7} \text{ N A}^{-2} \text{ c}^2} \\ &= 8.854\,187\,817\ldots \times 10^{-12} \text{ F m}^{-1}. \end{aligned} \quad (4)$$

2.3. Electronvolt eV, Unified Atomic Mass Unit u, and Related Quantities

The electron volt eV and the unified atomic mass unit u are not units of the SI but are accepted for use with the SI by the CIPM (BIPM, 1998). Energies and masses of atomic particles are more conveniently expressed in eV and u than in the corresponding SI units of energy and mass, the joule and the kilogram, and in the case of mass, with significantly smaller uncertainties.

One electronvolt is the kinetic energy acquired by an electron in passing through a potential difference of 1 V in vacuum. It is related to the joule by

$$1 \text{ eV} = (e/C) \text{ J} \approx 1.60 \times 10^{-19} \text{ J}, \quad (5)$$

where e is the elementary charge and e/C is the numerical value of the elementary charge when expressed in the unit Coulomb (see Sec. 1.2).

The unified atomic mass unit u is $\frac{1}{12}$ times the mass $m(^{12}\text{C})$ of a free (noninteracting) neutral atom of carbon 12 at rest and in its ground state:

$$1 \text{ u} = m_{\text{u}} = \frac{m(^{12}\text{C})}{12} \approx 1.66 \times 10^{-27} \text{ kg}, \quad (6)$$

where the quantity m_{u} is the atomic mass constant.

The relative atomic mass $A_{\text{r}}(\text{X})$ of an elementary particle, atom, or more generally an entity X, is defined by

$$A_{\text{r}}(\text{X}) = \frac{m(\text{X})}{m_{\text{u}}}, \quad (7)$$

where $m(\text{X})$ is the mass of X. Thus $A_{\text{r}}(\text{X})$ is the numerical value of $m(\text{X})$ when $m(\text{X})$ is expressed in u, and evidently $A_{\text{r}}(^{12}\text{C}) = 12$ exactly. [For particles such as the electron e and proton p, the symbol m_{X} rather than $m(\text{X})$ is used to denote the mass. Further, for molecules the term relative molecular mass and symbol $M_{\text{r}}(\text{X})$ are used.]

The quantity “amount of substance” of a specified elementary entity is one of the seven base quantities of the SI, and its unit the mole, with symbol mol, is one of the seven base units of the SI (BIPM, 1998). One mole is the amount of substance $n(\text{X})$ of a collection of as many specified entities X as there are atoms in 0.012 kg of carbon 12, where it is understood that the carbon atoms are free, neutral, at rest, and in their ground state.

The molar mass $M(\text{X})$ is the mass of a collection of entities X divided by the amount of substance $n(\text{X})$ of the collection. Clearly, the molar mass of free carbon 12 atoms at rest, $M(^{12}\text{C})$, is exactly

$$M(^{12}\text{C}) = 12 \times 10^{-3} \text{ kg mol}^{-1} = 12 M_{\text{u}}, \quad (8)$$

where for convenience we introduce the molar mass constant M_{u} defined by

$$M_{\text{u}} = 10^{-3} \text{ kg mol}^{-1}, \quad (9)$$

so that in general

$$M(\text{X}) = A_{\text{r}}(\text{X}) M_{\text{u}}. \quad (10)$$

[Mills *et al.* (1993) use M° to represent $10^{-3} \text{ kg mol}^{-1}$, but we believe that M_u is preferable, because it does not require a special font.]

The Avogadro constant $N_A \approx 6.02 \times 10^{23} \text{ mol}^{-1}$ is defined as the quotient of the molar mass and atomic mass constants:

$$N_A = \frac{M_u}{m_u}, \quad (11)$$

or equivalently

$$N_A = \frac{M(X)}{m(X)}. \quad (12)$$

For a collection of L different types of free entities X_1, X_2, \dots, X_L , the total amount of substance of the collective entity X is

$$n(X) = \sum_{i=1}^L n(X_i), \quad (13)$$

and

$$x(X_i) = \frac{n(X_i)}{n(X)} \quad (14)$$

is the amount-of-substance fraction (also called mole fraction) of entity X_i . The mean relative atomic mass of X is given by

$$A_r(X) = \sum_{i=1}^L x(X_i) A_r(X_i), \quad (15)$$

and the mean molar mass is

$$M(X) = A_r(X) M_u. \quad (16)$$

An example relevant to Sec. 3.8 is the mean molar mass $M(\text{Ag})$ of the silver atoms of a given sample containing the two naturally occurring isotopes ^{107}Ag and ^{109}Ag . In this case $M(\text{Ag}) = A_r(\text{Ag}) M_u$, where

$$A_r(\text{Ag}) = x(^{107}\text{Ag}) A_r(^{107}\text{Ag}) + x(^{109}\text{Ag}) A_r(^{109}\text{Ag}), \quad (17)$$

and $x(^A\text{Ag}) = n(^A\text{Ag})/n(\text{Ag})$ is the amount-of-substance fraction of the silver isotope of nucleon number (mass number) A .

2.4. Josephson Effect and Josephson Constant K_J , and Quantum Hall Effect and von Klitzing Constant R_K

This section briefly reviews two truly remarkable quantum phenomena of condensed-matter physics known as the Josephson effect (JE) and quantum Hall effect (QHE), as they relate to the fundamental physical constants.

2.4.1. Josephson Effect

It is now well known that the ac and dc Josephson effects are characteristic of weakly coupled superconductors, for example, a superconductor–insulator–superconductor (SIS) tunnel junction, or a superconductor–normal metal–superconductor (SNS) weak link [see, for example, the book

by Likharev (1986)]. When such a Josephson device is irradiated with electromagnetic radiation of frequency f , usually in the range 10 GHz to 100 GHz, its current vs. voltage curve exhibits current steps at precisely quantized Josephson voltages U_J . The voltage of the n th step, where n is an integer, is related to the frequency f by

$$U_J(n) = \frac{nf}{K_J}. \quad (18)$$

Here K_J is the Josephson constant, formerly called the Josephson frequency–voltage quotient, because it is equal to the step number n times the quotient of the frequency and voltage. [Note that, under certain circumstances, steps that accurately obey Eq. (18) with n replaced by $n \pm \frac{1}{2}$ may also be observed (Genevès *et al.*, 1993).]

An impressive body of experimental evidence has accumulated since the Josephson effect was predicted nearly 40 years ago (Josephson, 1962) that clearly demonstrates that K_J is a constant of nature. For example, with different but small uncertainties, K_J has been shown to be independent of experimental variables such as irradiation frequency and power, current, step number, type of superconductor, and type of junction [see Refs. 12–22 of Taylor and Witt (1989)]. In one experiment (Tsai, Jain, and Lukens, 1983) it was shown that K_J was the same for two SNS junctions composed of different superconductors (biased on their $n = 1$ steps) to within the 2×10^{-16} relative uncertainty of the comparison. More recently, it was shown that K_J for a weak link of the high T_c ceramic superconductor $\text{YBa}_2\text{Cu}_3\text{O}_{7-\delta}$ was equal to K_J for a weak link of Nb to within the 5×10^{-8} relative uncertainty of the experiment (Tarbeyev *et al.*, 1991).

The theory of the JE predicts, and the experimentally observed universality of K_J is consistent with the prediction, that

$$K_J = \frac{2e}{h} \approx 483\,598 \text{ GHz/V}, \quad (19)$$

where e is the elementary charge and h is the Planck constant (Clarke, 1970; Langenberg and Schrieffer, 1971; Hartle, Scalapino, and Sugar, 1971; Likharev, 1986). Some arguments given for the exactness of Eq. (19) are based on the quite general theoretical grounds of flux conservation (Bloch, 1968; Bloch, 1970; Fulton, 1973).

In keeping with the experimental and theoretical evidence, we assume for the purpose of the 1998 adjustment, as was assumed for the 1969, 1973, and 1986 adjustments (see Sec. 1.1), that any correction to Eq. (19) is negligible compared to the standard uncertainty of measurements involving K_J . At present this uncertainty is larger than $4 \times 10^{-8} K_J$, and it is likely to be larger than $1 \times 10^{-9} K_J$ for the foreseeable future.

2.4.2. Quantum Hall Effect

It is also now well known that the integral and fractional quantum Hall effects are characteristic of a two-dimensional

electron gas (or 2DEG) [see, for example, the book by Prange and Girvin (1990)]. In practice, a 2DEG may be realized in a high-mobility semiconductor device such as a GaAs–Al_xGa_{1–x}As heterostructure or a silicon-metal-oxide-semiconductor field-effect transistor (MOSFET), of usual Hall-bar geometry, when the applied magnetic flux density B is of order 10 T and the device is cooled to a temperature of order 1 K. Under these conditions, the 2DEG is fully quantized and for a fixed current I through the device, there are regions in the curve of U_H vs. B for a heterostructure, or of U_H vs. gate voltage U_g for a MOSFET, where the Hall voltage U_H remains constant as B or U_g is varied. These regions of constant U_H are called quantized Hall resistance (QHR) plateaus.

In the limit of zero dissipation in the direction of current flow, the QHR of the i th plateau $R_H(i)$, which is the quotient of the Hall voltage of the i th plateau $U_H(i)$ and the current I , is quantized:

$$R_H(i) = \frac{U_H(i)}{I} = \frac{R_K}{i}, \quad (20)$$

where i is an integer and R_K is the von Klitzing constant. (The integer i has been interpreted as the filling factor—the number of Landau levels fully occupied and equal to the number of electrons per flux quantum threading the sample. We confine our discussion to the integral QHE because, to date, no experimental work on the fractional QHE is relevant to the fundamental constants.) It follows from Eq. (20) that the von Klitzing constant R_K is equal to the QHR of the i th plateau times the plateau number, and hence is equal to the resistance of the first plateau.

As with the Josephson effect, a significant body of experimental evidence has accumulated since the discovery of the QHE nearly 20 years ago (von Klitzing, Dorda and Pepper, 1980) that clearly demonstrates that R_K as defined by Eq. (20) is a constant of nature. To measure this constant accurately, certain experimental criteria must be met. These criteria are given in technical guidelines developed by the CIPM's Consultative Committee for Electricity and Magnetism (CCEM, *Comité Consultatif d'Électricité et Magnétisme*, formerly *Comité Consultatif d'Electricité* or CCE) and published by Delahaye (1989). Although the universality of R_K has not yet been demonstrated to a level of uncertainty approaching that for the Josephson constant K_J , for dc currents in the range 10 μ A to 50 μ A and for ohmic contacts to the 2DEG with resistances $\leq 1 \Omega$, Jeckelmann, Jeanneret and Inglis (1997) have shown R_K to be independent of device type, device material, and plateau number within their experimental relative uncertainty of about 3.5×10^{-10} . In particular, these experimenters showed that the anomalous values of R_K observed for certain Si MOSFETs are very likely due to the resistances of the voltage contacts on the devices, and that the universal value of R_K is found if all the criteria of the CCEM technical guidelines are met. In addition, Jeanneret *et al.* (1995) have shown that for a specially prepared set of GaAs/AlGaAs heterostructures of widths that varied from 10 μ m to 1 mm, R_K was independent of device width to within

the 1×10^{-9} relative uncertainty of the measurements. [Tests of the universality of R_K have also been carried out by other researchers; see for example Refs. 28–34 of Taylor and Witt (1989) and also Delahaye, Satrapinsky and Witt (1989); Piquemal *et al.* (1991); Delahaye and Bournaud (1991); Hartland *et al.* (1991).]

The theory of the QHE predicts, and the experimentally observed universality of R_K is consistent with the prediction, that

$$R_K = \frac{h}{e^2} = \frac{\mu_0 c}{2\alpha} \approx 25\,813 \Omega, \quad (21)$$

where as usual α is the fine-structure constant. There is a vast literature on the QHE [see for example the bibliography compiled by Van Degrift, Cage, and Girvin (1991) of important papers of the 1980s]. In particular, there have been many publications on the theory behind Eq. (21) and why it is believed to be an exact relation, some of which invoke rather general principles [see, for example, the books by Prange and Girvin (1990), Stone (1992), and Janßen *et al.* (1994), the papers for nonspecialists by Yennie (1987) and Watson (1996), and the popular article by Halperin (1986)].

In analogy with the JE, in keeping with the experimental and theoretical evidence, we assume for the purpose of the 1998 adjustment, as was assumed for the 1986 adjustment, that any correction to Eq. (21) is negligible compared to the standard uncertainty of experiments involving R_K . Currently this uncertainty is larger than $2 \times 10^{-8} R_K$, and it is likely to be larger than $1 \times 10^{-9} R_K$ for the foreseeable future. Since μ_0 and c are exact constants in the SI, this assumption and Eq. (21) imply that a measurement of R_K in the unit Ω with a given relative standard uncertainty provides a value of α with the same relative standard uncertainty.

It is of interest to note that R_K , α , and the characteristic impedance of vacuum $Z_0 = \sqrt{\mu_0/\epsilon_0} = \mu_0 c \approx 377 \Omega$ are related by

$$Z_0 = 2\alpha R_K. \quad (22)$$

2.5. Conventional Josephson Constant K_{J-90} , Conventional von Klitzing Constant R_{K-90} , and Conventional Electric Units

It has long been recognized that the Josephson and quantum Hall effects can be used to realize accurate and reproducible representations of the (SI) volt and (SI) ohm (Taylor *et al.*, 1967; von Klitzing *et al.*, 1980). In order to achieve international uniformity in measurements of voltage and resistance, on 1 January 1990 the CIPM introduced new representations of the volt and the ohm for worldwide use based on these effects and conventional (i.e., adopted) values of the Josephson constant K_J and von Klitzing constant R_K (Quinn, 1989). These assigned exact values, denoted respectively by K_{J-90} and R_{K-90} , are

$$K_{J-90} = 483\,597.9 \text{ GHz/V} \quad (23a)$$

$$R_{K-90} = 25\,812.807 \Omega. \quad (23b)$$

They were derived by the CCEM of the CIPM from an analysis of all the relevant data available by 15 June 1988 (Taylor and Witt, 1989). These data included measurements of K_J and R_K as well as other fundamental constants. The goal was to select conventional values of the Josephson and von Klitzing constants (within certain constraints) that were as close to their SI values as possible so that the new volt and ohm representations would closely approximate the volt and the ohm.

For the purpose of the 1998 adjustment, we interpret the CIPM's adoption of K_{J-90} and R_{K-90} as establishing conventional, practical units of voltage and resistance V_{90} and Ω_{90} defined by

$$K_J = 483\,597.9 \text{ GHz}/V_{90} \quad (24a)$$

$$R_K = 25\,812.807 \Omega_{90}. \quad (24b)$$

(Note that V_{90} and Ω_{90} are printed in italic type in recognition of the fact that they are physical quantities.) The conventional units V_{90} and Ω_{90} are related to the SI units V and Ω by

$$V_{90} = \frac{K_{J-90}}{K_J} \text{ V} \quad (25a)$$

$$\Omega_{90} = \frac{R_K}{R_{K-90}} \Omega, \quad (25b)$$

which follow from Eqs. (23) and (24).

The conventional units V_{90} and Ω_{90} are readily realized in the laboratory: 1 V_{90} is the voltage across the terminals of an array of a large number of Josephson devices in series when the product of the total number of steps n of the array and the frequency f of the applied microwave radiation is exactly 483 597.9 GHz [see Eq. (18)]; and 1 Ω_{90} is exactly $i/25\,812.807$ times the resistance of the i th QHR plateau [see Eq. (20)].

In practice, V_{90} can be realized at the 1 V level with a relative standard uncertainty of less than 1×10^{-9} ; and Ω_{90} can be realized at the 1 Ω level with a relative standard uncertainty that approaches 1×10^{-9} . Such a small uncertainty for V_{90} is possible because of the development, beginning in the mid-1980s, of series arrays consisting of some 20 000 Josephson tunnel junctions on a single chip capable of generating well in excess of 10 V [see, for example, Hamilton, Burroughs, and Benz (1997); Pöpel (1992)]. The above uncertainties for V_{90} and Ω_{90} have been demonstrated, for example, through comparisons carried out by the International Bureau of Weights and Measures (BIPM, *Bureau International des Poids et Mesures*), of the Josephson effect voltage standards and the quantum Hall effect resistance standards of the national metrology institutes of various countries with BIPM transportable versions of such standards [for JE voltage standards see for example Reymann *et al.* (1998); Quinn (1996); Witt (1995); Quinn (1994); Reymann and Witt (1993); and for QHE resistance standards see Delahaye *et al.* (1997); Delahaye *et al.* (1996); Delahaye *et al.* (1995)].

Other conventional electric units follow directly from V_{90} and Ω_{90} . Examples are the conventional units of electric current and power, $A_{90} = V_{90}/\Omega_{90}$ and $W_{90} = V_{90}^2/\Omega_{90}$, which are related to the SI units A and W by

$$A_{90} = \frac{K_{J-90} R_{K-90}}{K_J R_K} \text{ A} \quad (26a)$$

$$W_{90} = \frac{K_{J-90}^2 R_{K-90}}{K_J^2 R_K} \text{ W}. \quad (26b)$$

Equation (26b) is noteworthy, because if one assumes $K_J = 2e/h$ and $R_K = h/e^2$, then

$$\frac{W_{90}}{W} = \frac{K_{J-90}^2 R_{K-90}}{4} h. \quad (27)$$

Since K_{J-90} and R_{K-90} have no uncertainty, an experimental determination of the unit ratio W_{90}/W with a given uncertainty determines the Planck constant h with the same relative uncertainty. This is the basis of the watt-balance measurements of h discussed in Sec. 3.7.

It is evident that for a voltage U ,

$$U = \frac{U}{V_{90}} V_{90} = \frac{U}{V_{90}} \frac{K_{J-90}}{K_J} \text{ V}. \quad (28)$$

That is, the numerical value of U when U is expressed in the SI unit V, is equal to the numerical value of U when U is expressed in the conventional unit V_{90} multiplied by the ratio K_{J-90}/K_J . Similar expressions apply to other electric quantities; those of interest here are resistance R , current I , and power P . To summarize,

$$U = \frac{U}{V_{90}} \frac{K_{J-90}}{K_J} \text{ V} \quad (29a)$$

$$R = \frac{R}{\Omega_{90}} \frac{R_K}{R_{K-90}} \Omega \quad (29b)$$

$$I = \frac{I}{A_{90}} \frac{K_{J-90} R_{K-90}}{K_J R_K} \text{ A} \quad (29c)$$

$$P = \frac{P}{W_{90}} \frac{K_{J-90}^2 R_{K-90}}{K_J^2 R_K} \text{ W}. \quad (29d)$$

Throughout the 1998 adjustment we attempt to express all electric-unit-dependent quantities in terms of conventional electric units. However, in some experiments carried out prior to 1990, an alternative value of K_J was adopted to define the laboratory unit of voltage V_{LAB} . We denote such values by $K_{J-\text{LAB}}$ and apply appropriate factors to convert to K_{J-90} . Further, prior to 1990, no laboratory unit of resistance was based on the conventional value of R_K , but in most cases of interest the laboratory unit of resistance was calibrated using the quantum Hall effect. That is, R_K is known in terms of Ω_{LAB} at the time of the experiment. On the other hand, if a laboratory's practical units of voltage and resistance were based on artifact voltage and resistance standards such as standard cells and standard resistors with no connection to the Josephson or quantum Hall effects, then

we have, for example, in analogy with Eq. (29a), $U = (U/V_{\text{LAB}})(V_{\text{LAB}}/V) V$, where in general the ratio V_{LAB}/V is not well known.

2.6. Acceleration of Free Fall g

The acceleration of free fall, or acceleration due to gravity g , is of course not really a fundamental physical constant: its fractional variation with height near the Earth's surface is $-3 \times 10^{-7}/\text{m}$, its fractional variation from equator to pole is about 0.5 %, and it can have significant fractional variations over a day at a fixed location, for example, of order 2×10^{-7} at 40° latitude, due mostly to the varying influences of the moon and sun. For reference purposes, a conventional value called "standard acceleration of gravity" given by

$$g_n = 9.806\,65 \text{ m/s}^2 \quad (30)$$

has been adopted internationally (BIPM, 1998).

A number of experiments relevant to the 1998 adjustment, for example the measurement of $K_J^2 R_K$ using a watt balance (see Sec. 3.7), require the determination of a force based on the weight of a standard of mass and hence the value of g at the site of the measurement. Fortunately, significant advances in the development of highly accurate, portable, and commercially available absolute gravimeters have been made in recent years [see, for example, Niebauer *et al.* (1995) and Sasagawa *et al.* (1995)]. Such instruments allow g to be determined at a given site with a sufficiently small uncertainty that lack of knowledge of g is not a significant contributor to the uncertainty of any experiment of interest in the adjustment. Indeed, the two most recent international comparisons of absolute gravimeters, carried out in 1994 (ICAG94) and in 1997 (ICAG97) at the BIPM and organized by Working Group 6 of the International Gravity Commission, show that g can be determined with modern absolute gravimeters with a relative standard uncertainty of the order of 4×10^{-9} (Marson *et al.*, 1995; Robertsson, 1999). Although this uncertainty is negligible compared to the approximate 9×10^{-8} relative standard uncertainty of the most accurate experiment that requires knowledge of g , namely, the most recent measurement of $K_J^2 R_K$ (see Sec. 3.7.2), the uncertainty of g may no longer be negligible if such experiments achieve their anticipated level of uncertainty.

3. Review of Data

This portion of the paper reviews the experimental data relevant to the 1998 adjustment of the values of the constants and in some cases the associated theory required for their interpretation. As summarized in Appendix E, in a least-squares analysis of the fundamental constants the numerical data, both experimental and theoretical, also called *observational data* or *input data*, are expressed as functions of a set of independent variables called *adjusted constants*. The functions that relate the input data to the adjusted constants are called *observational equations*, and the least-squares procedure provides best estimated values, in the least-squares

sense, of the adjusted constants. Thus the focus of this Review of Data section is the identification and discussion of the input data and observational equations of interest for the 1998 adjustment. Although not all observational equations that we use are explicitly given in the text, all are summarized in Tables 17.A.2 and 19.A.2 of Sec. 4.3.

3.1. Relative Atomic Masses

We consider here the relative atomic masses $A_r(X)$ (see Sec. 2.3.) of a number of particles and atoms that are of interest for the 1998 adjustment. In this work, the relative atomic masses of the electron $A_r(e)$, neutron $A_r(n)$, proton $A_r(p)$, deuteron $A_r(d)$, helion $A_r(h)$ (the helion h is the nucleus of the ^3He atom), and alpha particle $A_r(\alpha)$ are included in the set of adjusted constants. The relevant data are summarized in Tables 2 to 5, and are discussed in the following sections.

3.1.1. Atomic Mass Evaluation: 1995 Update

A self-consistent set of values of the relative atomic masses of the neutron and neutral atoms has been periodically generated for use by the scientific community for many years. The values listed in Table 2 are taken from the 1995 update of the 1993 atomic mass evaluation of Audi and Wapstra (1993). The update, also due to Audi and Wapstra, is available in printed form (Audi and Wapstra, 1995), and a more extensive electronic version is available at www-csns.m.in2p3.fr/amdc/amdc_en.html, the Web site of the Atomic Mass Data Center (AMDC), Centre de Spectrométrie Nucléaire et de Spectrométrie de Masse (CSNSM), Orsay, France.

The 1995 update and the 1993 full evaluation are the most recent compilations available. The latter replaced the 1983 full evaluation (Wapstra and Audi, 1985), the results of which were used in the 1986 adjustment, and the next full evaluation is scheduled for completion in 2000 (Audi and Wapstra, 1999). Many of the values given in the 1995 update that are of greatest interest to the 1998 adjustment are strongly influenced by the highly accurate mass ratio measurements made by both the MIT and the University of Washington groups using single ions stored in a Penning trap (DiFilippo *et al.*, 1995a; DiFilippo *et al.*, 1995b; DiFilippo *et al.*, 1994; Van Dyck, 1995; Van Dyck, Farnham, and Schwingberg, 1995; Van Dyck, Farnham, and Schwingberg, 1993a; Van Dyck, Farnham, and Schwingberg, 1993b).

The relative atomic mass of the neutron $A_r(n)$ and its treatment in the 1998 adjustment are discussed in Sec. 3.1.3.c.

3.1.2. Binding Energies

To calculate the relative atomic masses of various nuclei from the data of Table 2, and to calculate $A_r(e)$ from the measured ratio $6m_e/m(^{12}\text{C}^{6+})$ (see Sec. 3.1.3.a) and $A_r(p)$ from the measured ratio $m(^{12}\text{C}^{4+})/4m_p$ (see Sec. 3.1.3.b) requires the ionization energies E_I given in Table 3. In that table, the value quoted for each atom or ion is the energy

TABLE 2. Values of the relative atomic masses of various neutral atoms, as given in the 1995 update to the 1993 atomic mass evaluation.

Atom	Relative atomic mass $A_r(X)$	Relative standard uncertainty u_r
^1H	1.007 825 032 14(35)	3.5×10^{-10}
^2H	2.014 101 777 99(36)	1.8×10^{-10}
^3He	3.016 029 309 70(86)	2.8×10^{-10}
^4He	4.002 603 2497(10)	2.5×10^{-10}
^{28}Si	27.976 926 5327(20)	7.0×10^{-11}
^{29}Si	28.976 494 719(30)	1.0×10^{-9}
^{30}Si	29.973 770 218(45)	1.5×10^{-9}
^{36}Ar	35.967 546 28(27)	7.6×10^{-9}
^{38}Ar	37.962 732 16(53)	1.4×10^{-8}
^{40}Ar	39.962 383 1232(30)	7.6×10^{-11}
^{107}Ag	106.905 0930(60)	5.6×10^{-8}
^{109}Ag	108.904 7555(34)	3.1×10^{-8}

required to remove one electron from the ground state and leave the atom or ion in the ground state of the next higher charge state. The total ionization energies, or binding energies E_b (the sum of the individual ionization energies), of ^3He , ^4He , and ^{12}C are also given.

In Table 3, the wave numbers for the binding energies for ^1H and ^2H are obtained from the 1998 recommended values of the relevant constants and the analysis of Appendix A. For ^4He I we use the wave number given by Drake and Martin (1998), and for the ^3He I and ^4He I difference, we use the value recommended by Martin (1998). The other wave numbers are those given by Kelly (1987). However, since Kelly's values for hydrogenic helium and hydrogenic carbon are the same as the values calculated by Erickson (1977) who used the 1973 CODATA value of R_∞ (Cohen and Taylor, 1973), for completeness we rescale these values by the ratio of the 1998 to the 1973 recommended values of R_∞ . For information, we also give the binding energies in eV, obtained using

TABLE 3. Ground-state ionization energies for ^1H and ^2H , and for neutral and ionized ^3He , ^4He , and ^{12}C , where E represents E_1 or E_b as appropriate (see text).

Atom/ion	Ionization energy		
	(10^7 m^{-1})	(eV)	$10^9 E/m_e c^2$
^1H	1.096 787 717	13.5984	14.5985
^2H	1.097 086 146	13.6021	14.6025
^3He I	1.983 002	24.5861	26.3942
^3He II	4.388 892	54.4153	58.4173
^3He Total	6.371 894	79.0014	84.8115
^4He I	1.983 107	24.5874	26.3956
^4He II	4.389 089	54.4178	58.4199
^4He Total	6.372 195	79.0051	84.8155
^{12}C I	0.908 204	11.2603	12.0884
^{12}C II	1.966 647	24.3833	26.1766
^{12}C III	3.862 410	47.8878	51.4096
^{12}C IV	5.201 784	64.4939	69.2370
^{12}C V	31.623 950	392.087	420.923
^{12}C VI	39.520 614	489.993	526.029
^{12}C Total	83.083 610	1030.105	1105.864

TABLE 4. Input value of the mass ratio $6m_e/m(^{12}\text{C}^{6+})$ and the value of $A_r(e)$ it implies; values of $A_r(p)$, $A_r(d)$, $A_r(h)$, and $A_r(\alpha)$ that may be inferred from the relative atomic masses of the corresponding neutral atoms as given in Table 2; and input value of the mass ratio $m(^{12}\text{C}^{4+})/4m_p$ and the value of $A_r(p)$ it implies.

Quantity	Value	Relative standard uncertainty u_r
$6m_e/m(^{12}\text{C}^{6+})$	0.000 274 365 185 89(58)	2.1×10^{-9}
$A_r(e)$	0.000 548 579 9111(12)	2.1×10^{-9}
$A_r(p)$	1.007 276 466 83(35)	3.5×10^{-10}
$A_r(d)$	2.013 553 212 68(36)	1.8×10^{-10}
$A_r(h)$	3.014 932 234 69(86)	2.8×10^{-10}
$A_r(\alpha)$	4.001 506 1747(10)	2.5×10^{-10}
$m(^{12}\text{C}^{4+})/4m_p$	2.977 783 715 20(42)	1.4×10^{-10}
$A_r(p)$	1.007 276 466 89(14)	1.4×10^{-10}

the 1998 recommended value for the factor that relates wave numbers in m^{-1} to the equivalent energy in eV. The last column of the table gives the ratio of the binding energy to the energy equivalent of the atomic mass constant obtained using the 1998 recommended value for the factor that relates wave numbers in m^{-1} to the equivalent mass in u. The uncertainties of these two conversion factors are negligible in this application (see Table 30 for their values). No uncertainties are given for the binding energies in Table 3, because they are inconsequential compared to the uncertainties of the quantities with which the binding energies are used. Indeed, binding energies represent sufficiently small corrections that the number of significant digits shown in the last column of the table is more than needed.

3.1.3. Relative Atomic Masses of e, n, p, d, h, and α Particle

We give in Table 4 the measured value of the mass ratio $6m_e/m(^{12}\text{C}^{6+})$ and the value of the relative atomic mass of the electron $A_r(e)$ that it implies. These are followed by the values of the relative atomic masses $A_r(p)$, $A_r(d)$, $A_r(h)$, and $A_r(\alpha)$ inferred from the data in Tables 2 and 3. The last two entries are the measured value of the mass ratio $m(^{12}\text{C}^{4+})/4m_p$ and the value of $A_r(p)$ it implies. Each inferred value is indented for clarity and is given for comparison purposes only; in practice, it is the data from which they are obtained that are used as the input data in the 1998 adjustment (as noted above, the relative atomic masses of p, d,

TABLE 5. The variances, covariances, and correlation coefficients of the values of the relative atomic masses of hydrogen, deuterium, and the helium three atom [the covariances involving $A_r(^4\text{He})$ are negligible]. The numbers in boldface above the main diagonal are 10^{18} times the numerical values of the covariances; the numbers in boldface on the main diagonal are 10^{18} times the numerical values of the variances; and the numbers in italics below the main diagonal are the correlation coefficients.

	$A_r(^1\text{H})$	$A_r(^2\text{H})$	$A_r(^3\text{He})$
$A_r(^1\text{H})$	0.1234	0.0402	0.0027
$A_r(^2\text{H})$	<i>0.3141</i>	0.1328	0.0088
$A_r(^3\text{He})$	<i>0.0089</i>	<i>0.0281</i>	0.7330

h, and α are adjusted constants). These data are, in addition to $6m_e/m(^{12}\text{C}^{6+})$ and $m(^{12}\text{C}^{4+})/4m_p$, the values of $A_r(^1\text{H})$, $A_r(^2\text{H})$, $A_r(^3\text{He})$, $A_r(^4\text{He})$ given in Table 2, and their relevant covariances given in Table 5. The following sections discuss in some detail Tables 4 and 5 and our treatment of $A_r(n)$.

a. Electron. Using a Penning trap mass spectrometer, Farnham, Van Dyck, and Schwinberg (1995) at the University of Washington measured the ratio of the cyclotron frequency of a fully ionized carbon 12 atom $f_c(^{12}\text{C}^{6+}) = 6eB/2\pi m(^{12}\text{C}^{6+})$ to the cyclotron frequency of an electron $f_c(e) = eB/2\pi m_e$ in the same magnetic flux density B . The value of the ratio they report, which is based on the simple mean of six values obtained in separate runs, is

$$\frac{f_c(^{12}\text{C}^{6+})}{f_c(e)} = \frac{6m_e}{m(^{12}\text{C}^{6+})} = \frac{6A_r(e)}{A_r(^{12}\text{C}^{6+})} \\ = 0.000\,274\,365\,185\,89(58) \quad [2.1 \times 10^{-9}]. \quad (31)$$

Although adequate resolution was achieved for the determination of $f_c(^{12}\text{C}^{6+})$ using single ions, most of the electron cyclotron frequency data were taken using small clouds consisting of 5 to 13 electrons in order to achieve the necessary resolution. Because of the instability of the magnetic flux density B , it was necessary to acquire data over a time period sufficiently long to determine the fractional drift rate of B , which was about $2 \times 10^{-10} \text{ h}^{-1}$, and to average out short-term fluctuations that on occasion were observed to be as large as $\pm 3 \times 10^{-9} B$. For example, the value of the frequency ratio resulting from one of the six runs was obtained by comparing 3 d of $f_c(^{12}\text{C}^{6+})$ data with 2 d of $f_c(e)$ data.

In their experiment Farnham *et al.* (1995) investigated and took into account a number of systematic effects, including the influence of the number of electrons in the cloud and magnetic-field gradients. The net fractional correction for such effects that had to be applied to the simple mean of the six values was -1.6×10^{-9} . The statistical relative standard uncertainty of the mean was found to be 1.0×10^{-9} (Type A), while the relative standard uncertainty due to all systematic effects was 1.9×10^{-9} (Type B).

The relation of $A_r(e)$ to the ratio $6m_e/m(^{12}\text{C}^{6+})$ follows from the expression for the mass $m(X)$ of a neutral atom X in terms of its constituents:

$$m(X)c^2 = m(N)c^2 + Zm_e c^2 - E_b(X), \quad (32)$$

where $m(N)$ is the mass of the nucleus of the atom, Z is its atomic number, and E_b is the total binding energy of its Z electrons. This relation together with Eq. (31) and the definition $A_r(^{12}\text{C}) = 12$ yields

$$A_r(e) = \frac{1}{6} \left[12 + \frac{E_b(^{12}\text{C})}{m_u c^2} \right] \left[1 + \frac{m(^{12}\text{C}^{6+})}{6m_e} \right]^{-1}, \quad (33)$$

or the following observational equation for the value of the ratio given in Eq. (31):

$$\frac{6m_e}{m(^{12}\text{C}^{6+})} \doteq \frac{6A_r(e)}{12 - 6A_r(e) + E_b(^{12}\text{C})/m_u c^2}. \quad (34)$$

Here, the symbol \doteq is used, because in general an observational equation does not express an equality (see Sec. 4.3). Although the quantity

$$m_u c^2 = \frac{2R_\infty h c}{\alpha^2 A_r(e)} \quad (35)$$

in Eq. (34) is a function of adjusted constants (excepting c), we take the ratio $E_b(^{12}\text{C})/m_u c^2$ to be an exact fixed number, because in this context its uncertainty is negligible and Eq. (34) does not have a significant influence on its value. There are, however, cases in which the dependence of $m_u c^2$ on the adjusted constants must be taken into account.

Using the value of $6m_e/m(^{12}\text{C}^{6+})$ given in Eq. (31) and the value of $E_b(^{12}\text{C})/m_u c^2$ given in Table 3, we obtain from Eq. (33)

$$A_r(e) = 0.000\,548\,579\,9111(12) \quad [2.1 \times 10^{-9}]. \quad (36)$$

Unfortunately, there is no other direct measurement of $A_r(e)$ with which this result may be compared. However, using it and the 1998 recommended value of $A_r(p)$, which has a significantly smaller uncertainty, we can obtain a value of the mass ratio m_p/m_e and compare it to other measured values of this ratio. The result for m_p/m_e based on Eq. (36) is

$$\frac{m_p}{m_e} = 1\,836.152\,6670(39) \quad [2.1 \times 10^{-9}]. \quad (37)$$

This may be compared to $m_p/m_e = 1\,836.152\,701(37) [2.0 \times 10^{-8}]$, which was obtained from similar Penning trap cyclotron frequency measurements on single electrons and protons at the University of Washington by Van Dyck *et al.* (1986a), and which was used as an auxiliary constant in the 1986 adjustment. The two values are in agreement, differing by less than the standard uncertainty of their difference.

The two less accurate values $m_p/m_e = 1\,836.152\,680(88)$ and $m_p/m_e = 1\,836.152\,68(10)$ also agree with Eq. (37). The first was obtained by Gabrielse *et al.* (1990b) as a result of experiments at CERN (European Laboratory for Particle Physics, Geneva, Switzerland) to determine the antiproton–proton mass ratio from cyclotron frequency measurements in a Penning trap of a radically different geometry than that used in the University of Washington experiments. The second was obtained by de Beauvoir *et al.* (1997) from their analysis of earlier absolute frequency measurements of the 2S–8S/D transitions in hydrogen and deuterium carried out for the determination of the Rydberg constant (see Sec. 3.2).

Because the relative standard uncertainty of the Farnham *et al.* (1995) value of $A_r(e)$ is about one-tenth of the uncertainty of the value of $A_r(e)$ that could be derived from the Van Dyck *et al.* (1986a) result for m_p/m_e , and because both experiments were carried out in the same laboratory using similar techniques, we view the 1995 result as superseding the 1986 result. Therefore the earlier value is not included as an input datum in the 1998 adjustment.

b. Proton, deuteron, helion, and α particle. Values of the relative atomic masses $A_r(p)$, $A_r(d)$, $A_r(h)$, and $A_r(\alpha)$ may be calculated by dividing Eq. (32) by $m_u c^2$ and solving for the relative atomic mass of the nucleus $m(N)/m_u = A_r(N)$. The observational equation for the relative atomic mass of a neutral atom X in terms of $A_r(N)$ and $A_r(e)$ is thus

$$A_r(X) \doteq A_r(N) + Z A_r(e) - \frac{E_b(X)}{m_u c^2}. \quad (38)$$

Evaluation of this expression with the relative atomic masses of the atoms ^1H , ^2H , ^3He , and ^4He in Table 2, the 1998 recommended value of $A_r(e)$, and the ratios $E_b/m_u c^2$ in Table 3 yields the inferred values in Table 4. In this application, the uncertainty of $A_r(e)$ is negligible.

Because the values of $A_r(^1\text{H})$, $A_r(^2\text{H})$, $A_r(^3\text{He})$, and $A_r(^4\text{He})$ of Audi and Wapstra (1995) are the results of a least-squares calculation, they are correlated. Table 5 gives their non-negligible covariances and, for information, the corresponding correlation coefficients [see Appendix F, Eq. (F12)], all based on the covariances given by Audi and Wapstra in the electronic version of their 1995 update.

Recently, the University of Washington group has significantly improved its Penning trap mass spectrometer by replacing the existing magnet–cryostat system by a specially designed system that reduces fluctuations of the applied magnetic flux density B to about $2 \times 10^{-11} \text{ T h}^{-1}$ (Van Dyck *et al.*, 1999b). Such fluctuations were a major contributor to the uncertainties of the group's earlier mass ratio measurements [see Van Dyck (1995), Van Dyck *et al.* (1995), and the above discussion of the measurement of $6m_e/m(^{12}\text{C}^{6+})$ by Farnham *et al.* (1995)]. Using the new spectrometer, Van Dyck *et al.* (1999a) have determined the ratio of the cyclotron frequency of a proton $f_c(p)$ to that of a four-times ionized carbon 12 atom $f_c(^{12}\text{C}^{4+})$ in the same flux density and obtained (Van Dyck, 1999)

$$\begin{aligned} \frac{f_c(p)}{f_c(^{12}\text{C}^{4+})} &= \frac{m(^{12}\text{C}^{4+})}{4m_p} = \frac{A_r(^{12}\text{C}^{4+})}{4A_r(p)} \\ &= 2.977\,783\,715\,20(42) \quad [1.4 \times 10^{-10}]. \end{aligned} \quad (39)$$

In this first significant mass-ratio measurement with the new spectrometer, Van Dyck *et al.* (1999a) carefully investigated a number of systematic effects and assigned a component of relative standard uncertainty (Type B) to the frequency ratio in the range 1×10^{-11} to 8×10^{-11} for each effect. The two largest components are 8×10^{-11} for a residual temperature and/or pressure effect and 7×10^{-11} for the influence of the applied axial drive power. The statistical relative standard uncertainty (Type A) is given as 5×10^{-11} .

The observational equation for the measured ratio $m(^{12}\text{C}^{4+})/4m_p$ is, in analogy with Eq. (34),

$$\frac{m(^{12}\text{C}^{4+})}{4m_p} \doteq \frac{12 - 4A_r(e) + [E_b(^{12}\text{C}) - E_b(^{12}\text{C}^{4+})]/m_u c^2}{4A_r(p)}, \quad (40)$$

where $E_b(^{12}\text{C}^{4+})/m_u c^2$ is the relative atomic mass equivalent of the binding energy of a $^{12}\text{C}^{4+}$ atom and from Table 3 is equal to 946.952×10^{-9} . Using this result and the value of $E_b(^{12}\text{C})/m_u c^2$ also from Table 3, the 1998 recommended value of $A_r(e)$, the uncertainty of which is negligible in this context, and the value of $m(^{12}\text{C}^{4+})/4m_p$ given in Eq. (39), we find from Eq. (40)

$$A_r(p) = 1.007\,276\,466\,89(14) \quad [1.4 \times 10^{-10}]. \quad (41)$$

This inferred value, which is the last entry of Table 4, agrees with the inferred value of $A_r(p)$ also given in that table and which was obtained from $A_r(^1\text{H})$. However, the value of $A_r(p)$ implied by $m(^{12}\text{C}^{4+})/4m_p$ has an uncertainty 0.4 times that of the value implied by $A_r(^1\text{H})$. Although the 1995 value of $A_r(^1\text{H})$ of Audi and Wapstra is based in part on earlier University of Washington mass ratio measurements, we take both the 1995 value of $A_r(^1\text{H})$ and the value of $m(^{12}\text{C}^{4+})/4m_p$ as input data in the 1998 adjustment. This is justified by the fact that the new result was obtained from a significantly modified and improved apparatus.

c. Neutron. The relative atomic mass of the neutron $A_r(n)$ is one of the results of the least-squares adjustment carried out by Audi and Wapstra to obtain their 1995 recommended values of relative atomic masses. They give

$$A_r(n) = 1.008\,664\,9233(22) \quad [2.2 \times 10^{-9}]. \quad (42)$$

The input datum that most affects the adjusted value of $A_r(n)$, in the sense that its uncertainty makes the largest contribution to the uncertainty of $A_r(n)$, is the binding energy of the neutron in the deuteron $S_n(d)$. This binding energy is determined by measuring the 2.2 MeV capture γ ray emitted in the reaction $n + p \rightarrow d + \gamma$. The value of $S_n(d)$ employed by Audi and Wapstra in their adjustment is the result obtained by Wapstra (1990), who calculated the weighted mean of four different measured values (Greene *et al.*, 1986; Adam, Hnatowicz, and Kugler, 1983; Van Der Leun and Alderliesten, 1982; Vylov *et al.*, 1982). The analysis of Wapstra took into account the known error in all four results due to the approximate 1.8×10^{-6} fractional error in the measurement of the {220} lattice spacing of silicon (see Sec. 3.9.1). Of these four values, that of Greene *et al.* (1986) carried the dominant weight and thus played a major role in the determination of the 1995 value of $A_r(n)$ given in Eq. (42).

The relation between the neutron mass and the binding energy $S_n(d)$ is

$$m_n c^2 = m_d c^2 - m_p c^2 + S_n(d), \quad (43)$$

which is equivalent to

$$A_r(n) = A_r(d) - A_r(p) + \frac{S_n(d)}{m_u c^2}, \quad (44)$$

or

$$A_r(n) = A_r(^2\text{H}) - A_r(^1\text{H}) + \frac{S_n(d)}{m_u c^2} \quad (45)$$

if one neglects the inconsequential difference in binding energy of the electron in hydrogen and deuterium.

The Greene *et al.* (1986) result for the wavelength of the critical 2.2 MeV capture γ ray was obtained at the GAMS4 crystal diffraction facility at the high-flux reactor of the Institut Max von Laue-Paul Langevin (ILL), Grenoble, France, using a flat crystal spectrometer in a National Institute of Standards and Technology (NIST, formerly the National Bureau of Standards, NBS), Gaithersburg, Md, and ILL collaboration. In the following 10 years, a number of improvements were incorporated into the GAMS4 facility including a vibration-isolation platform for the crystal spectrometer, improved angle interferometers, a permanently installed angle calibration facility, advanced γ -ray detection instrumentation, and temperature stabilization of the spectrometer. Motivated by the fact that these improvements might have significantly reduced or eliminated errors that were possibly present in the Greene *et al.* (1986) determination, in a second NIST-ILL collaboration, Kessler *et al.* (1999a) remeasured the wavelength of the 2.2 MeV γ ray. Their result, obtained in two separate measurement campaigns (February–March 1995 and March 1998), has an uncertainty that is nearly one-sixth of the 1×10^{-6} relative standard uncertainty of the earlier result. However, the new result is smaller than the earlier result by the fractional amount 4.2×10^{-6} . Although the reason for the discrepancy between the two values is not fully understood, the NIST-ILL researchers put forward plausible reasons why the earlier result might be in error. In view of the many GAMS4 improvements and the agreement between the results obtained in two measurement campaigns 3 years apart and from three different crystal configurations, the researchers believe that the new result is significantly more reliable, and it is the only one we consider. [The uncertainties of the other values used by Wapstra (1990) in his analysis are so large compared to the uncertainty of the new result that those values are no longer competitive. Note that the work of Röttger, Paul, and Keyser (1997) is not relevant, because they did not employ an independent calibration of their Ge detector in the 2.2 MeV region.]

The new measurements were carried out with the ILL GAMS4 two-axis flat silicon crystal spectrometer in transmission at 26 °C and in air at a pressure $p \approx 100$ kPa. All angle measurements were corrected to a crystal temperature of 22.5 °C using the accepted linear thermal coefficient of expansion of silicon. Each silicon crystal in the spectrometer is a 2.5 mm thick plate cut in such a way that the (220) lattice planes are perpendicular to the crystal surface and oriented so that the normal to the crystal planes is normal to the axis of rotation (for a detailed discussion of the {220} lattice spacing of Si, see Sec. 3.9). The final value of the relevant first-order Bragg angle from all of the data, taking into account all known components of uncertainty (both Type A and Type B), is (in radians)

$$\theta_{\text{meas}} = 0.001\,452\,152\,24(25) \quad [1.7 \times 10^{-7}]. \quad (46)$$

This result is based on 52 Bragg-angle measurements made in February–March 1995 in two separate orders and 89 measurements made in March 1998 in three separate orders. The angle interferometer of the GAMS4 spectrometer was cali-

brated once at the time of the 1995 runs and three times at the time of the 1998 runs. The final result given in Eq. (46) is the weighted mean of the two values obtained in the two campaigns, and its relative standard uncertainty includes Type B components from systematic effects that total 1.1×10^{-7} .

Based on the Bragg relation, the measured wavelength of the emitted gamma ray λ_{meas} is given by

$$\lambda_{\text{meas}} = 2d_{220}(\text{ILL}) \left(1 - \frac{p}{c_{11} + 2c_{12}} \right) \sin \theta_{\text{meas}}. \quad (47)$$

In Eq. (47), $d_{220}(\text{ILL})$ is the {220} lattice spacing of the 2.5 mm thick silicon crystals of the ILL GAMS4 spectrometer at 22.5 °C in vacuum. Further, in Eq. (47), the volume-compressibility-related term in parentheses, with elastic constants $c_{11} = 165.7$ GPa and $c_{12} = 63.9$ GPa (McSkimin, 1953), accounts for the fact that the crystals were actually in air at $p \approx 100$ kPa and the lattice spacing variables we use in the adjustment apply to Si crystals at the reference temperature 22.5 °C in vacuum (see Sec. 3.9). Since the effect of pressure on the lattice spacing is small and the elastic constants are relatively well known, this factor introduces no uncertainty. The input datum determined in this measurement is therefore

$$\frac{\lambda_{\text{meas}}}{d_{220}(\text{ILL})} = 0.002\,904\,302\,46(50) \quad [1.7 \times 10^{-7}]. \quad (48)$$

In the NIST-ILL experiment, the protons are in hydrogen atoms of a plastic target and the incident neutrons have negligible kinetic energy, hence it may be assumed that the initial state is one of a proton and neutron at rest. The final state consists of a photon and a recoiling deuteron. The relativistic kinematics of this reaction gives

$$\frac{c\lambda_{\text{meas}}}{h} = 2 \frac{m_n + m_p}{(m_n + m_p)^2 - m_d^2}, \quad (49)$$

which, with the aid of Eq. (35), yields the following observational equation for the input datum given in Eq. (48):

$$\frac{\lambda_{\text{meas}}}{d_{220}(\text{ILL})} \div \frac{\alpha^2 A_r(e)}{R_\infty d_{220}(\text{ILL})} \frac{A_r(n) + A_r(p)}{[A_r(n) + A_r(p)]^2 - A_r(d)}, \quad (50)$$

where $d_{220}(\text{ILL})$ on the right-hand side is also an adjusted constant. Note that, although treating the recoil relativistically gives an observational equation that is simpler than its nonrelativistic analog, the nonrelativistic treatment is a good approximation. Further, because the value of $S_n(d)$ used by Audi and Wapstra, in their 1995 update has negligible impact on the determination of their 1995 values of $A_r(^1\text{H})$ and $A_r(^2\text{H})$ (Audi and Wapstra, 1998), it is legitimate to use the latter as input data by means of Eq. (38) together with Eqs. (48) and (50).

As part of their effort to redetermine $S_n(d)$, Kessler *et al.* (1999a) compared a presumably representative sample of the ILL Si crystals to samples of three other Si crystals in order to obtain the lattice spacing of the ILL crystal in meters. These three crystals, whose significance is discussed in Sec. 3.9, are labeled WASO 17, MO*4, and SH1. (Note that

throughout this paper, the designation WASO n is abbreviated as Wn in equations.) The results of the comparisons, which we also take as input data, are

$$\frac{d_{220}(\text{ILL}) - d_{220}(\text{W17})}{d_{220}(\text{ILL})} = -8(22) \times 10^{-9} \quad (51)$$

$$\frac{d_{220}(\text{ILL}) - d_{220}(\text{MO*4})}{d_{220}(\text{ILL})} = 86(27) \times 10^{-9} \quad (52)$$

$$\frac{d_{220}(\text{ILL}) - d_{220}(\text{SH1})}{d_{220}(\text{ILL})} = 34(22) \times 10^{-9}. \quad (53)$$

Related results from the Physikalisch-Technische Bundesanstalt (PTB), Braunschweig, Germany, are given in Sec. 3.9, together with additional discussion of lattice spacing comparisons. Here we note that the disagreement between NIST and PTB lattice comparison results reported by Kessler, Schweppe, and Deslattes (1997) has been reduced to a statistically acceptable level by subsequent work of the NIST group (Kessler *et al.*, 1999b). This was accomplished by employing an improved method of surface preparation of the silicon samples and eliminating temperature measurement errors. The above results were obtained after these advances were incorporated into the NIST lattice comparison protocol.

It is important to recognize that crystal designations such as ILL, WASO 17, MO*4, etc., refer to any one of several samples from a particular large single-crystal silicon boule, and in general precision measurements involving a silicon lattice spacing and lattice spacing comparisons are carried out with different samples. Measurements of lattice spacings as a function of position in a boule typically show fractional variations at the level of 1×10^{-8} or more over its volume, where the actual variations depend on the level of impurities in the boule (Kessler *et al.*, 1999b; Windisch and Becker, 1990). In general, to account for this variation, we assign a component of relative standard uncertainty of $\sqrt{2} \times 10^{-8}$ to the lattice spacing of each crystal sample, such that the measured lattice spacing difference between any two particular samples from the same boule includes a component of uncertainty of 2×10^{-8} . Thus the uncertainty of the value of $\lambda_{\text{meas}}/d_{220}(\text{ILL})$ given in Eq. (48) contains a component of relative standard uncertainty of $\sqrt{2} \times 10^{-8}$ in addition to the components assigned by Kessler *et al.* (1999b). For measurements involving MO*4 samples, the additional component of uncertainty assigned is $(3/\sqrt{2}) \times 10^{-8}$, because the MO*4 crystal contains an unusually large amount of carbon (Martin *et al.*, 1999). This uncertainty is consistent with the fractional difference results obtained at NIST and PTB using different samples of the MO*4 crystal.

The standard uncertainty of each of the above fractional differences includes appropriate uncertainty components for sample variation as just discussed, the 9.3×10^{-9} standard uncertainty (Type B) of the NIST instrument used to compare the lattice spacings of different crystals, and the statistically calculated standard uncertainty (Type A) of order 4×10^{-9} of each comparison (Kessler, 1999). This last uncertainty is the standard deviation of the mean of several mea-

surements made over the length of the sample being compared to the ILL crystal, but due to the limited size of the sample, this statistical component of uncertainty does not account for lattice spacing variations among different crystals from the same boule.

Because there is a total component of uncertainty of 1.6×10^{-8} common to the uncertainty of the NIST fractional differences given above, the covariance of any two of them is 258×10^{-18} [see Appendix F, Eq. (F7)] and leads to correlation coefficients of approximately 0.5.

The 1998 recommended value of $A_r(n)$, which relies heavily on the NIST-ILL measurement of the 2.2 MeV capture γ ray, is

$$A_r(n) = 1.008\,664\,915\,78(55) \quad [5.4 \times 10^{-10}]. \quad (54)$$

Comparison of this 1998 value to the 1995 value of Audi and Wapstra given in Eq. (42) shows that the uncertainty has been reduced by a factor of 4.0 and that the new value differs from the 1995 value by 3.4 times the uncertainty of the latter. This substantial change is apparently due to an error in the earlier γ -ray measurement of Greene *et al.* (1986).

3.2. Hydrogenic Transition Frequencies and the Rydberg Constant R_∞

The Rydberg constant is related to other constants by

$$R_\infty = \alpha^2 \frac{m_e c}{2h}. \quad (55)$$

It can be determined to high accuracy by combining the measured wavelengths or frequencies corresponding to transitions between levels in hydrogenic atoms having different principal quantum numbers n with the theoretical expressions for the wavelengths or frequencies.

Although the most accurate values of R_∞ are obtained from measurements on hydrogen and deuterium, for completeness we note that similar measurements have also been carried out in other hydrogenlike systems. Using Doppler-free two-photon laser spectroscopy, Maas *et al.* (1994) have measured the frequency of the 1S–2S transition in muonium (μ^+e^- atom) and find

$$\nu_{1,2}(\text{Mu}) = 2455\,529\,002(57) \text{ MHz} \quad [2.3 \times 10^{-8}]. \quad (56)$$

This measurement does not provide a competitive value of R_∞ at present, because its relative standard uncertainty is of the order of 10^5 times the uncertainties of measured transition frequencies in hydrogen. On the other hand, the value for the muon-electron mass ratio m_μ/m_e implied by this measurement is closer to being competitive with other values; see Sec. 3.3.9.e.

Also using Doppler-free two-photon spectroscopy, Fee *et al.* (1993) have measured the 1S–2S transition frequency in positronium (e^+e^- atom) and find

$$\nu_{1,2}(\text{Ps}) = 1233\,607\,216.4(3.2) \text{ MHz} \quad [2.6 \times 10^{-9}]. \quad (57)$$

TABLE 6. Summary of reported values of the Rydberg constant R_∞ with a relative standard uncertainty $10^{-10} < u_r < 10^{-9}$ and the 1986 CODATA value (H is hydrogen and D is deuterium).

Authors	Laboratory ^a	Atom and transition	Reported value R_∞ / m^{-1}	$10^{10} u_r$
CODATA 1986 (Cohen and Taylor, 1987)			10 973 731.534(13)	12
Biraben <i>et al.</i> (1986)	LKB	H,D: 2S–8D/10D	10 973 731.5692(60)	5.5
Zhao <i>et al.</i> (1986)	Yale	H,D: 2S–3P	10 973 731.5689(71)	6.5
Zhao <i>et al.</i> (1987); Zhao <i>et al.</i> (1989)	Yale	H,D: 2S–4P	10 973 731.5731(29)	2.6
Beausoleil <i>et al.</i> (1987); Beausoleil (1986)	Stanford	H: 1S–2S	10 973 731.5715(67)	6.1
Boshier <i>et al.</i> (1987); Boshier <i>et al.</i> (1989)	Oxford	H,D: 1S–2S	10 973 731.5731(31)	2.8
McIntyre <i>et al.</i> (1989)	Stanford	H: 1S–2S	10 973 731.5686(78)	7.1
Biraben <i>et al.</i> (1989); Garreau <i>et al.</i> (1990a); Garreau <i>et al.</i> (1990b); Garreau <i>et al.</i> (1990c)	LKB	H,D: 2S–8D/10D/12D	10 973 731.5709(18)	1.7

^aLKB: Laboratoire Kastler-Brossel, Paris (Laboratoire de Spectroscopie Hertzienne prior to 1994).

Because of its large uncertainty compared to the uncertainties of measured transition frequencies in hydrogen and because of the substantially larger uncertainty of the relevant theory (Sapirstein and Yennie, 1990), this result does not provide a competitive value of R_∞ .

The 1986 CODATA recommended value of R_∞ , which is given in Table 6, was based to a large extent on the 1981 value obtained by Amin, Caldwell, and Lichten (1981) at Yale University, suitably corrected for the 1983 redefinition of the meter. The experiment was subsequently repeated with a number of improvements, yielding the result also given in Table 6 (Zhao *et al.*, 1986). The difference between this result and the earlier result is not understood. However, a number of other measurements of R_∞ reported after the 1 January 1986 closing date for the 1986 adjustment with relative standard uncertainties $u_r < 10^{-9}$ agree with the 1986 value of Zhao *et al.* (1986). Such reported values with $10^{-10} < u_r < 10^{-9}$ are also listed in Table 6. [Two experiments with $u_r > 10^{-9}$ reported after the 1986 closing date are not included in the table (Hildum *et al.*, 1986; Barr *et al.*, 1986).]

Because experiments reported after 1990, which are based on optical frequency metrology, have uncertainties at least an order of magnitude smaller than those in Table 6, which are based on optical wavelength metrology, we do not consider the earlier results any further.

More recent measurements of R_∞ are given in Table 7. Note that the first six results for the Rydberg constant are based on two principal measurements of frequencies: that of

Andreae *et al.* (1992) and that of Nez *et al.* (1993); the various values for R_∞ from the same laboratory differ because of differences in the theoretical analysis and the auxiliary quantities used.

The measured transition frequencies that we consider as input data in our own analysis for the least-squares adjustment are given in Table 8. These have been appropriately adjusted to remove the hyperfine shift by the groups reporting the values. Covariances associated with values obtained in the same laboratory are, in general, not reported in the literature. However, for the purpose of the 1998 adjustment, we obtained from the experimental groups the information needed to evaluate the covariances, and we include them in the least-squares calculation. These covariances are given in the form of correlation coefficients in Table 14.A.2.

These data, as well as related data that we do not use, are reviewed in the following sections, but our discussion is necessarily brief because of the large number of data and complexity of the experiments; the references should be consulted for details. Following this review, we discuss the values of the bound-state root-mean-square (rms) charge radius of the proton and deuteron that we consider for use as input data. Such radii enter the theoretical expressions for hydrogenic energy levels, as discussed in Appendix A.

3.2.1. MPQ

The group at the Max Planck Institut für Quantenoptik (MPQ) in Garching, Germany and its predecessor at Stanford

TABLE 7. Summary of some reported values of the Rydberg constant R_∞ with a relative standard uncertainty $u_r < 10^{-10}$ (H is hydrogen and D is deuterium).

Authors	Laboratory ^a	Atom and transition	Reported value R_∞ / m^{-1}	$10^{12} u_r$
Andreae <i>et al.</i> (1992)	MPQ	H: 1S–2S	10 973 731.568 41(42)	38
Nez <i>et al.</i> (1992)	LKB	H: 2S–8S/8D	10 973 731.568 30(31)	29
Nez <i>et al.</i> (1993)	LKB	H: 2S–8S/8D	10 973 731.568 34(24)	22
Weitz <i>et al.</i> (1994); Schmidt-Kaler <i>et al.</i> (1995)	MPQ	H: 1S–2S	10 973 731.568 44(31)	28
Weitz <i>et al.</i> (1995)	MPQ	H: 1S–2S	10 973 731.568 49(30)	27
Bourzeix <i>et al.</i> (1996a)	LKB	H: 2S–8S/8D	10 973 731.568 36(18)	17
de Beauvoir <i>et al.</i> (1997)	LKB/LPTF	H,D: 2S–8S/8D	10 973 731.568 59(10)	9
Udem <i>et al.</i> (1997)	MPQ	H: 1S–2S	10 973 731.568 639(91)	8.3

^aMPQ: Max-Planck-Institut für Quantenoptik, Garching. LKB: Laboratoire Kastler-Brossel, Paris (Laboratoire de Spectroscopie Hertzienne prior to 1994). LPTF: Laboratoire Primaire du Temps et des Fréquences, Paris.

TABLE 8. Summary of measured transition frequencies ν considered in the present work for the determination of the Rydberg constant R_∞ (H is hydrogen and D is deuterium).

Authors	Laboratory ^a	Frequency interval(s)	Reported value ν/kHz	Rel. stand. uncert. u_r
Udem <i>et al.</i> (1997)	MPQ	$\nu_{\text{H}}(1\text{S}_{1/2}-2\text{S}_{1/2})$	2 466 061 413 187.34(84)	3.4×10^{-13}
Weitz <i>et al.</i> (1995)	MPQ	$\nu_{\text{H}}(2\text{S}_{1/2}-4\text{S}_{1/2}) - \frac{1}{4} \nu_{\text{H}}(1\text{S}_{1/2}-2\text{S}_{1/2})$	4 797 338(10)	2.1×10^{-6}
		$\nu_{\text{H}}(2\text{S}_{1/2}-4\text{D}_{5/2}) - \frac{1}{4} \nu_{\text{H}}(1\text{S}_{1/2}-2\text{S}_{1/2})$	6 490 144(24)	3.7×10^{-6}
		$\nu_{\text{D}}(2\text{S}_{1/2}-4\text{S}_{1/2}) - \frac{1}{4} \nu_{\text{D}}(1\text{S}_{1/2}-2\text{S}_{1/2})$	4 801 693(20)	4.2×10^{-6}
		$\nu_{\text{D}}(2\text{S}_{1/2}-4\text{D}_{5/2}) - \frac{1}{4} \nu_{\text{D}}(1\text{S}_{1/2}-2\text{S}_{1/2})$	6 494 841(41)	6.3×10^{-6}
Huber <i>et al.</i> (1998)	MPQ	$\nu_{\text{D}}(1\text{S}_{1/2}-2\text{S}_{1/2}) - \nu_{\text{H}}(1\text{S}_{1/2}-2\text{S}_{1/2})$	670 994 334.64(15)	2.2×10^{-10}
de Beauvoir <i>et al.</i> (1997)	LKB/LPTF	$\nu_{\text{H}}(2\text{S}_{1/2}-8\text{S}_{1/2})$	770 649 350 012.1(8.6)	1.1×10^{-11}
		$\nu_{\text{H}}(2\text{S}_{1/2}-8\text{D}_{3/2})$	770 649 504 450.0(8.3)	1.1×10^{-11}
		$\nu_{\text{H}}(2\text{S}_{1/2}-8\text{D}_{5/2})$	770 649 561 584.2(6.4)	8.3×10^{-12}
		$\nu_{\text{D}}(2\text{S}_{1/2}-8\text{S}_{1/2})$	770 859 041 245.7(6.9)	8.9×10^{-12}
		$\nu_{\text{D}}(2\text{S}_{1/2}-8\text{D}_{3/2})$	770 859 195 701.8(6.3)	8.2×10^{-12}
		$\nu_{\text{D}}(2\text{S}_{1/2}-8\text{D}_{5/2})$	770 859 252 849.5(5.9)	7.7×10^{-12}
Schwob <i>et al.</i> (1999)	LKB/LPTF	$\nu_{\text{H}}(2\text{S}_{1/2}-12\text{D}_{3/2})$	799 191 710 472.7(9.4)	1.2×10^{-11}
		$\nu_{\text{H}}(2\text{S}_{1/2}-12\text{D}_{5/2})$	799 191 727 403.7(7.0)	8.7×10^{-12}
		$\nu_{\text{D}}(2\text{S}_{1/2}-12\text{D}_{3/2})$	799 409 168 038.0(8.6)	1.1×10^{-11}
		$\nu_{\text{D}}(2\text{S}_{1/2}-12\text{D}_{5/2})$	799 409 184 966.8(6.8)	8.5×10^{-12}
Bourzeix <i>et al.</i> (1996b)	LKB	$\nu_{\text{H}}(2\text{S}_{1/2}-6\text{S}_{1/2}) - \frac{1}{4} \nu_{\text{H}}(1\text{S}_{1/2}-3\text{S}_{1/2})$	4 197 604(21)	4.9×10^{-6}
		$\nu_{\text{H}}(2\text{S}_{1/2}-6\text{D}_{5/2}) - \frac{1}{4} \nu_{\text{H}}(1\text{S}_{1/2}-3\text{S}_{1/2})$	4 699 099(10)	2.2×10^{-6}
Berkeland <i>et al.</i> (1995)	Yale	$\nu_{\text{H}}(2\text{S}_{1/2}-4\text{P}_{1/2}) - \frac{1}{4} \nu_{\text{H}}(1\text{S}_{1/2}-2\text{S}_{1/2})$	4 664 269(15)	3.2×10^{-6}
		$\nu_{\text{H}}(2\text{S}_{1/2}-4\text{P}_{3/2}) - \frac{1}{4} \nu_{\text{H}}(1\text{S}_{1/2}-2\text{S}_{1/2})$	6 035 373(10)	1.7×10^{-6}
Hagley and Pipkin (1994)	Harvard	$\nu_{\text{H}}(2\text{S}_{1/2}-2\text{P}_{3/2})$	9 911 200(12)	1.2×10^{-6}
Lundeen and Pipkin (1986)	Harvard	$\nu_{\text{H}}(2\text{P}_{1/2}-2\text{S}_{1/2})$	1 057 845.0(9.0)	8.5×10^{-6}
Newton <i>et al.</i> (1979)	U. Sussex	$\nu_{\text{H}}(2\text{P}_{1/2}-2\text{S}_{1/2})$	1 057 862(20)	1.9×10^{-5}

^aMPQ: Max-Planck-Institut für Quantenoptik, Garching. LKB: Laboratoire Kastler-Brossel, Paris. LPTF: Laboratoire Primaire du Temps et des Fréquences, Paris.

University have a long history of high-accuracy measurements of hydrogenic transition frequencies. The MPQ frequencies given in Table 8 are the most recent and accurate values reported by the group for the indicated transitions and transition differences. In keeping with the policy stated at the end of Sec. 1.4, we view the more recent results as superseding the earlier results. In particular, the 1997 measurement of the 1S–2S transition (first entry of Table 8) discussed in the following paragraph and on which the last value of R_∞ in Table 7 is based, supersedes the 1992 measurement of this transition on which the other MPQ values of R_∞ in Table 7 are based.

Prominent among the MPQ results is the $1\text{S}_{1/2}-2\text{S}_{1/2}$ transition frequency with a relative standard uncertainty of 3.4×10^{-13} (Udem *et al.*, 1997). This experiment used longitudinal Doppler-free two-photon spectroscopy of a cold atomic beam; the required light at 243 nm was obtained by doubling the frequency of an ultrastable 486 nm dye laser. Using as an intermediate reference a transportable CH_4 -stabilized He–Ne laser at 3.39 μm , Udem *et al.* (1997) compared the $1\text{S}(F=1) \rightarrow 2\text{S}(F=1)$ resonance frequency to the frequency of a cesium atomic clock using a phase-coherent laser frequency chain. The method takes advantage of the near coincidence of the 1S–2S resonance and the 28th harmonic of the He–Ne laser frequency. The 2.1 THz frequency mis-

match near the 7th harmonic was measured using a phase-locked chain of five frequency dividers. The 3.4×10^{-13} relative standard uncertainty is principally statistical (Type A) and arises mainly from the instability of the He–Ne reference; the resonant line shape is sufficiently understood that the line center could be determined with a relative uncertainty of 1.5×10^{-14} if a sufficiently stable optical frequency standard were available.

The approximately 5 GHz differences between the frequencies of the transitions $2\text{S}_{1/2}-4\text{S}_{1/2}/4\text{D}_{5/2}$ and one-fourth the frequency of the transition $1\text{S}_{1/2}-2\text{S}_{1/2}$ in hydrogen and deuterium were determined by direct optical frequency comparisons (Weitz *et al.*, 1995). The 1S–2S and 2S–4S/4D resonances were observed simultaneously in separate 1S and 2S atomic beams using two-photon excitation of each transition. The 243 nm radiation used to drive the 1S–2S two-photon transition was obtained by doubling the frequency of a 486 nm stabilized dye laser as in the 1S–2S experiment described above, and the 972 nm radiation used to drive the 2S–4S/4D two-photon transitions was obtained from a stabilized Ti–sapphire laser. The approximately 5 GHz frequency difference was determined by measuring the beat frequency between the doubled frequency of the 972 nm radiation and the 486 nm radiation using a fast photodiode. In order to achieve the quoted uncertainty, a number of effects had to be

investigated and appropriate corrections applied. The latter included corrections for (i) the rather large ac Stark effect in the 2S–4S/4D transitions; (ii) second-order Doppler shift based on measurements of the velocity distributions of the hydrogen and deuterium atoms in the beams; and (iii) second-order Zeeman shift. (The ac Stark effect was taken into account by incorporating it in the theoretical line shape and correcting for the residual dependence on laser power by extrapolating the beat frequency to zero power.) Nevertheless, the uncertainties of the frequency differences are dominated by the statistical uncertainties (Type A) of the beat frequency measurements. Based on a detailed uncertainty budget provided by these experimenters (Weitz, 1998), we have calculated the six independent pairwise covariances of the four difference frequencies and, as indicated above, include them in the calculations for the 1998 adjustment (the corresponding correlation coefficients range from 0.01 to 0.21).

The 671 GHz difference between the $1S_{1/2}$ – $2S_{1/2}$ transition frequency in deuterium and in hydrogen, commonly referred to as the 1S–2S isotope shift, was measured by comparing each frequency to a CH_4 -stabilized He–Ne laser at $3.39\text{ }\mu\text{m}$ via a phase-coherent frequency chain (Huber *et al.*, 1998). The experiment is somewhat similar to the measurement of the 1S–2S transition in hydrogen described above, but in this case the cold atomic beam contained both hydrogen and deuterium atoms. Using longitudinal Doppler-free two-photon excitation, Huber *et al.* (1998) sequentially observed the $1S(F=1)\rightarrow 2S(F=1)$ transition frequency in hydrogen and the $1S(F=3/2)\rightarrow 2S(F=3/2)$ transition frequency in deuterium. All but about 2% of the frequency difference between the two resonant frequencies was bridged with the aid of an optical frequency comb generator driven at a modulation frequency of 6.34 GHz, spanning a frequency range of 3.5 THz, and inserted in the frequency chain at a stage where each frequency of $2.5\times 10^{15}\text{ Hz}$ and the 671 GHz frequency difference is reduced to its eighth subharmonic. At this stage it was possible to compare this eighth subharmonic of each frequency to the fourth harmonic of the He–Ne reference laser by counting a frequency of 244 MHz in the case of hydrogen and 1702 MHz in the case of deuterium. The frequency of the He–Ne laser does not need to be known, because it drops out when calculating the difference frequency; it is only required to be stable. However, its stability is the dominant factor in determining the 0.15 kHz uncertainty of the final result. The uncertainty contributions from other effects such as ac Stark shifts, dc Stark shifts, and pressure shifts are insignificant by comparison.

3.2.2. LKB/LPTF

The group at the Laboratoire Kastler-Brossel (LKB), Ecole Normale Supérieure et Université Pierre et Marie Curie, Paris, France has a history of high-accuracy spectroscopy of simple atomic systems. Recently the LKB researchers have collaborated with colleagues at the Laboratoire Primaire du Temps et des Fréquences (LPTF), Bureau National de Métrologie-Observatoire de Paris, to make absolute fre-

quency measurements in hydrogen and deuterium with relative standard uncertainties of less than 1×10^{-11} . As in the case of the MPQ measurements, we view the more recent results of the LKB/LPTF group as superseding the earlier results of the LKB group. In particular, the 1997 measurements of the $2S_{1/2}$ – $8S_{1/2}$ /8D $_{3/2}$ /8D $_{5/2}$ transition frequencies in H and D (Table 8) discussed below supersede the values obtained earlier.

It should be noted that the LKB/LPTF values given in Table 8 are revised values provided by Biraben and Nez (1998) that reflect the remeasurement in terms of the SI definition of the second of the LPTF CO_2/OsO_4 secondary frequency standard (Rovera and Acef, 1999) as well as a number of improvements in the analysis of the original data, including corrections for the effects of stray electric fields and blackbody radiation. Further, these researchers provided a detailed uncertainty budget for each of the LKB/LPTF and LKB frequencies which allows us to calculate the covariances of any two values (the corresponding correlation coefficients range from 0.02 to 0.67).

The 2S–8S/8D transition frequencies were determined by inducing two-photon transitions in a metastable atomic beam of either H or D collinear with counterpropagating laser beams from a Ti–sapphire laser at 778 nm (de Beauvoir *et al.*, 1997). The theoretical line shape used to fit the observed resonances took into account the light shift, saturation of the transition, hyperfine structure of the 8D levels, second-order Doppler shift (based on the inferred velocity distribution of the atoms), and photoionization of the excited levels. To determine the absolute frequency of the transitions, the Ti–sapphire laser was compared to a 778 nm (385 THz) laser diode (LD) stabilized via a two-photon transition in Rb. The comparison was carried out using a Schottky diode to mix the two optical frequencies together with a 13 GHz microwave signal for H (48.4 GHz for D). The beat frequency between the third harmonic of the microwave frequency and the approximate 40 GHz optical frequency difference for H (144 GHz for D) was counted continuously. The frequency of this LD/Rb laser at LKB was compared to the frequency of a similar laser at LPTF by means of a 3 km long optical fiber. The frequency of the LPTF LD/Rb laser, in turn, was compared to a Cs clock using a phase-locked frequency chain and a CO_2/OsO_4 secondary frequency standard. In these measurements, as well as for the other LKB/LPTF and LKB measurements listed in Table 8, the statistical uncertainty (Type A) played a major role in determining the total uncertainty.

The determination of the 2S–12D transition frequencies was similar to that for the 2S–8S/8D frequencies; the main difference was in the measurement of the frequency of the 400 THz Ti–sapphire laser used to drive the two-photon transitions (Schwob *et al.*, 1999). In this case, the frequency of the Ti–sapphire laser was measured by comparing it to the frequency of a similar auxiliary Ti–sapphire laser and comparing the sum of this auxiliary laser's frequency and the frequency of a 371 THz (809 nm) diode laser to the doubled frequency of the 385 THz (778 nm) LD/Rb laser standard.

This measurement at the LKB only determined the sum of the frequencies of the two lasers. Their difference, and hence the absolute frequency of the 400 THz Ti-sapphire laser, was determined by comparison to lasers at the LPTF via two optical fibers connecting the two laboratories. One fiber was used to compare a 400 THz laser diode at the LPTF to the 400 THz auxiliary Ti-sapphire laser and the other to compare a 371 THz laser diode at the LPTF to the similar laser diode at the LKB. The 29 THz frequency difference between these two LPTF lasers was measured in terms of the frequency of the LPTF CO₂/OsO₄ secondary standard, using as an intermediary the P(8) line of a CO₂ laser (10 μ m band) in the case of H or the R(4) line in the case of D. The 2S–12D measurements complement the 2S–8S/8D measurements, because the observed 2S–12D transition frequencies are very sensitive to stray electric fields (the shift of an energy level due to the quadratic Stark effect varies with principal quantum number n as n^7). Hence the 2S–12D results provide a critical test of the Stark corrections.

Bourzeix *et al.* (1996b) determined the approximately 4 GHz differences between the frequencies of the transitions 2S_{1/2}–6S_{1/2}/6D_{5/2} and one-fourth the frequency of the transition 1S_{1/2}–3S_{1/2} in H by exciting the 2S–6S/6D two-photon resonance with a Ti-sapphire laser at 820 nm and the 1S–3S two-photon resonance with radiation from the same laser after two successive frequency-doubling stages. The approximately 2.4 GHz change in the frequency of the laser was measured using a Fabry–Pérot reference cavity. The second doubling of the 820 nm radiation required to induce the 1S–3S two-photon transition was challenging; the 205 nm UV radiation consisted of 3 μ s pulses at a frequency of 30 kHz and was obtained by modulating the length of the cavity containing the frequency-doubling crystal. The experiment was carried out in such a way that the frequency shift of the UV radiation due to the modulation of the cavity canceled between successive pulses, and the residual frequency shift was estimated to be less than 3 kHz. The researchers took a number of effects into account in analyzing the data and assigning uncertainties, including possible drift of the laser frequency, second-order Doppler effect, Zeeman shifts, dc Stark shifts, and light shifts.

3.2.3. Yale University

The measurement in hydrogen of the difference between the 2S_{1/2}–4P_{1/2}/4P_{3/2} transition frequencies and one-fourth the 1S_{1/2}–2S_{1/2} transition frequency carried out at Yale University used two tunable lasers at 486 nm, one the primary laser, the other the reference laser locked to an appropriate saturated absorption line in ¹³⁰Te₂ (Berkeland, Hinds, and Boshier, 1995). The primary laser was used to observe the 2S–4P single-photon resonance in one beam of H atoms and, after its frequency was doubled, the Doppler-free two-photon 1S–2S resonance in another beam of H atoms. The first-order Doppler shift of the 2S–4P resonance was reduced to a negligible level by ensuring that the laser beam was nearly perpendicular to the atomic beam. The change in frequency

of the primary laser required to alternately excite the two transitions was measured by heterodyning the primary and reference lasers. Each observed resonance was fitted with a theoretical line shape that took into account, as appropriate, background light, saturation, decreasing metastable beam intensity, measured laser intensity fluctuations, and pressure shift. Corrections were made for effects such as atomic recoil from the single-photon absorption, the second-order Doppler shift, and distribution of atoms among hyperfine sublevels of the 2S states. The effect of stray electric and magnetic fields was estimated to be negligible. The uncertainty of each transition frequency is dominated by its statistical uncertainty (Type A). Because the uncertainties of the second-order Doppler shift correction for the two transitions are common, the two frequencies are correlated with a correlation coefficient of 0.08 (Boshier, 1998).

3.2.4. Harvard University

The measurements in hydrogen of the 2S_{1/2}–2P_{3/2} interval (Hagley and Pipkin, 1994) and classic 2P_{1/2}–2S_{1/2} Lamb shift (Lundeen and Pipkin, 1986) carried out at Harvard University were done in a similar manner using a fast metastable atomic beam and the well-known Ramsey separated-oscillatory-field technique. This method, which employs two separated interaction regions, allows the observation of the transitions with a linewidth significantly less than the 100 MHz natural linewidth due to the 1.6 ns finite lifetime of the 2P state. The 50 keV to 100 keV metastable 2S beam of hydrogen atoms used in these measurements was produced by passing a beam of fast protons through nitrogen gas to capture an electron and then a state selection region to reduce the 2S($F=1$) population. (Both measurements employed $F=0 \rightarrow F=1$ transitions.) The technique requires a fast atomic beam so that the decay length of H atoms in the 2P state is a convenient laboratory distance (of order 5 cm). Microwave signals that have either 0 or π phase difference are applied in the two interaction regions and the depletion of the metastable population of the beam as a function of microwave frequency is observed. The narrow decay profile is obtained by taking the difference between the distributions for the 0 and π phase difference.

In these experiments, a critical factor was control of the relative phase of the oscillatory fields in the two interaction regions. The main effect of error in the relative phase was eliminated in both experiments by combining data with the relative time order of the two interaction regions interchanged. Similarly, residual first-order Doppler shifts were eliminated by reversing the direction of propagation of the oscillatory fields. Many other possible corrections and sources of uncertainty were also considered, including time dilation due to the fast beam motion, Bloch–Siegert and ac Stark shifts, incomplete cancellation of the phase-independent part of the 0 and π phase signals due to power variation, overlap of the oscillatory fields in the two interaction regions, and the effect of stray electric and magnetic fields. The statistical uncertainty (Type A) dominates the un-

certainty of the $2S_{1/2}-2P_{3/2}$ result of Hagley and Pipkin (1994), while Type B components of uncertainty dominate the uncertainty of the $2P_{1/2}-2S_{1/2}$ result of Lundeen and Pipkin (1986).

3.2.5. University of Sussex

The measurement of the classic $2P_{1/2}-2S_{1/2}$ Lamb shift at the University of Sussex (Newton, Andrews, and Unsworth, 1979) was done using a single microwave region in the form of a $50\ \Omega$ transmission line, which has the advantage of a higher signal strength, less complex apparatus, and a simpler line-shape analysis compared to the separated-oscillatory-field approach. In this experiment, a 21 keV beam of hydrogen atoms in the metastable $2S$ state was produced by charge-exchange collisions of protons with molecular hydrogen gas in a cell followed by hyperfine state selection to increase the fraction of atoms in the $2S(F=1)$ state. The beam entered the microwave region in which the microwaves propagated perpendicular to the beam direction in order to eliminate first-order Doppler shifts. Residual first-order Doppler effects were canceled by reversing the direction of propagation of the microwave fields. The applied microwave power was carefully controlled in order to keep it constant as the frequency was swept through the resonance in order to avoid a shift of the apparent line center. Since the goal of the experiment was to measure the center of the resonance with an uncertainty of less than $\frac{1}{2000}$ of the line-width, a reliable expression for the theoretical line shape was necessary and required precise knowledge of the electric field in the transmission line. Possible corrections and sources of uncertainty considered in this experiment include the Bloch–Siebert shift, motional electric fields due to the earth's magnetic field, time dilation, power and frequency measurement, stray electromagnetic fields, and $n=4$ resonances. The uncertainty of this result is in fact dominated by Type B components of uncertainty.

3.2.6. Other Data

A number of other potentially relevant results have been reported, but are not included in the 1998 adjustment for a variety of reasons.

The result 1 057 852(15) kHz for the classic hydrogen Lamb shift obtained by van Wijngaarden, Holuj, and Drake (1998), based on the anisotropy of emitted photons in an applied electric field, is not included, because its agreement with the Harvard University and University of Sussex values is viewed by van Wijngaarden *et al.* (1998) as a verification of the anisotropy method rather than an independent determination. This verification was deemed necessary because of the disagreement between the theoretical value of the Lamb shift in He^+ and the experimental result obtained using this method.

The result 1 057 851.4(1.9) kHz for the Lamb shift in hydrogen reported by Pal'chikov, Sokolov, and Yakovlev (1985) is also omitted. For this experiment, it was necessary to know the velocity of the metastable beam; it was deter-

mined by measuring the decay length of atoms in the $2P$ state and deducing the velocity from the theoretically calculated decay rate. This required measurement of the decay length and calculation of the decay rate with an unprecedented relative uncertainty of less than 2×10^{-6} . These and other issues have been discussed in the literature, and in our view the reliability of the measurement and calculation at this level of uncertainty has not been established (Hinds, 1988; Karshenboim, 1994; Pal'chikov, Sokolov, and Yakovlev, 1997; Karshenboim, 1995).

Earlier results (mainly for the classic Lamb shift, the $2S_{1/2}-2P_{3/2}$ interval, and the fine-structure interval $2P_{1/2}-2P_{3/2}$, all in hydrogen) are omitted either because of their large uncertainties or significant disagreement with the more modern measurements. Summaries and discussion of earlier work are given by Pipkin (1990), Cohen and Taylor (1973), and Taylor *et al.* (1969). [Note that the result of Safinya *et al.* (1980) listed in Pipkin (1990) is corrected by Hagley and Pipkin (1994).]

3.2.7. Nuclear Radii

The theoretical expressions for the finite nuclear size contributions to hydrogenic energy levels in Appendix A are given in terms of the bound-state nuclear rms charge radius R_N with $N \rightarrow p$, or $N \rightarrow d$ for H or D. The values of R_p and R_d that we consider as input data are determined from elastic electron–nucleon scattering experiments.

A comprehensive analysis of the relevant existing low- and high-energy $e-p$ data and low-energy neutron–atom data based on dispersion relations, together with various theoretical constraints, has yielded the result for the proton scattering radius $r_p = 0.847(8)$ fm (Mergell, Meißner, and Dreschel, 1996). This value differs somewhat from the earlier value $r_p = 0.862(12)$ fm (Simon *et al.*, 1980). Although this earlier result is based solely on low-energy data, such data are the most critical in determining the value of r_p . [We do not consider still earlier values, for example, $r_p = 0.805(11)$ fm (Hand, Miller, and Wilson, 1963), because the more recent results had available a larger set of data and improved methods of analysis.] Mergell *et al.* (1996) have stressed the importance of simultaneously fitting both the proton and the neutron data and note that if the value of 0.862 fm is used, one cannot simultaneously fit both sets of data in their dispersion-theoretical analysis. Clearly, to obtain a more accurate value of r_p , improved low-energy data are necessary. In the absence of additional information, for the purpose of the 1998 adjustment we take $r_p = 0.8545(120)$ fm, which is simply the unweighted mean of the values of Mergell *et al.* (1996) and Simon *et al.* (1980) with the larger of the two uncertainties.

For hydrogen, in the context of the expressions in Appendix A, R_p is the same as r_p , and hence

$$R_p = 0.8545(120) \text{ fm.} \quad (58)$$

[Note that for the proton, as well as for the deuteron discussed below, the interpretation of the quoted value obtained

from the scattering data depends on whether muonic and/or hadronic vacuum polarization has been included as a correction to the data (Friar, Martorell, and Sprung, 1999). However, at the level of uncertainty of current interest, such vacuum polarization effects may be neglected.]

The world data on elastic electron–deuteron scattering, consisting of some 340 data points below 10 GeV/c momentum transfer, has been used by Sick and Trautmann (1998) in a thorough analysis that includes Coulomb distortion to determine the deuteron rms charge radius; the result, including their dispersion correction of -0.0024 fm, is $r_d = 2.128(10)$ fm. These authors emphasize the importance of treating all of the available data simultaneously in order to maximally constrain the momentum-transfer dependence of the form factor and thereby obtain a reliable value for the rms radius. Because of the completeness of their treatment, this is the only result we consider for the 1998 adjustment. We note that it is consistent with the result of a model calculation by Friar, Martorell, and Sprung (1997) based on nucleon–nucleon scattering data.

As discussed in Sec. A.8 of Appendix A, R_d is related to r_d by

$$R_d = \sqrt{r_d^2 + \frac{3}{4} \left(\frac{m_e}{m_d} \right)^2 \chi_C^2}, \quad (59)$$

which yields, based on the 1998 recommended values of m_e/m_d and χ_C ,

$$R_d = 2.130(10) \text{ fm}. \quad (60)$$

3.3. Magnetic Moments and g -Factors

The magnetic moment of any of the three charged leptons (e , μ , τ) is written as

$$\boldsymbol{\mu} = g \frac{e}{2m} \mathbf{s}, \quad (61)$$

where g is the g -factor of the particle, m is its mass, and \mathbf{s} is its spin. In Eq. (61), e is the elementary charge and is positive. For the negatively charged leptons (e^- , μ^- , and τ^-), g is negative, and for the corresponding antiparticles (e^+ , μ^+ , and τ^+) g is positive. CPT invariance implies that the masses and absolute values of the g -factors are the same for each particle–antiparticle pair.

These leptons have eigenvalues of spin projection $s_z = \pm \hbar/2$, and in the case of the electron and positron it is conventional to write, based on Eq. (61),

$$\mu_e = \frac{g_e}{2} \mu_B, \quad (62)$$

where $\mu_B = e\hbar/2m_e$ is the Bohr magneton.

For nucleons or nuclei with spin \mathbf{I} , the magnetic moment can be written as

$$\boldsymbol{\mu} = g \frac{e}{2m_p} \mathbf{I}, \quad (63)$$

or

$$\mu = g \mu_N i. \quad (64)$$

In Eq. (64), $\mu_N = e\hbar/2m_p$ is the nuclear magneton, defined in analogy with the Bohr magneton, and i is the spin quantum number of the nucleus defined by $\mathbf{I}^2 = i(i+1)\hbar^2$ and $I_z = -i\hbar, \dots, (i-1)\hbar, i\hbar$, where I_z is the spin projection. However, in some publications moments of nucleons are expressed in terms of the Bohr magneton with a corresponding change in the definition of the g -factor.

Magnetic moments, magnetic moment ratios, and g -factors of various particles which impact the determination of other constants of interest are discussed in the following sections, and the relevant data are summarized in Table 9. (The shielded gyromagnetic ratios of some of the same particles are discussed in Sec. 3.4) Also given in Table 9 are values of quantities of interest that may be inferred from the data, as discussed in connection with each experiment. As in Table 4, each such inferred value is indented for clarity and is given only for comparison purposes. In practice, the source data are used as input data for the 1998 adjustment.

3.3.1. Electron Magnetic Moment Anomaly a_e

The electron magnetic moment anomaly a_e is defined as

$$a_e = \frac{|g_e| - 2}{2} = \frac{|\mu_e|}{\mu_B} - 1, \quad (65)$$

where $g_e = 2\mu_e/\mu_B$ is the g -factor of the electron and μ_e is its magnetic moment. The electron and positron anomalies have been measured in a classic series of experiments at the University of Washington in which individual electrons or positrons are stored in a Penning trap immersed in a liquid helium bath at 4.2 K in an applied magnetic flux density of order 5 T (Van Dyck, Schwinberg, and Dehmelt, 1986b; Van Dyck, 1990; Van Dyck, Schwinberg, and Dehmelt, 1991). The anomaly is obtained from the relation $a_e = f_a/f_c$ by measuring, in the same magnetic flux density B , the anomaly difference frequency $f_a = f_s - f_c$ and cyclotron frequency $f_c = eB/2\pi m_e$, where $f_s = g_e \mu_B B/h$ is the electron spin-flip (often called precession) frequency. In practice, the measured frequencies f'_a and f'_c are shifted from their free-space values f_a and f_c by the electrostatic field required to confine the electron in the trap, and corrections for these shifts must be made from a measurement of the frequency of the electron's axial motion f_z .

The values reported for the electron and positron anomalies by Van Dyck, Schwinberg, and Dehmelt (1987b) are

$$a_{e^-} = 1.159\,652\,1884(43) \times 10^{-3} \quad [3.7 \times 10^{-9}] \quad (66a)$$

$$a_{e^+} = 1.159\,652\,1879(43) \times 10^{-3} \quad [3.7 \times 10^{-9}]. \quad (66b)$$

The 4.3×10^{-12} standard uncertainty given by these authors for the electron is a combination of the 0.62×10^{-12} statistical standard uncertainty (Type A) of the weighted mean of four individual measurements, a standard uncertainty (Type B) of 1.3×10^{-12} to allow for a possible residual microwave power shift, and a standard uncertainty (Type B) of 4×10^{-12} associated with possible cavity resonance ef-

TABLE 9. Summary of data related to magnetic moments of various particles, and inferred values of various quantities.

Quantity	Value	Relative standard uncertainty u_r	Identification	Sec. and Eq.
a_e	$1.159\,652\,1883(42) \times 10^{-3}$	3.7×10^{-9}	UWash-87	3.3.1 (68)
$\alpha^{-1}(a_e)$	137.035 999 58(52)	3.8×10^{-9}		3.3.1 (72)
$\mu_{e^-}(\text{H})/\mu_{\text{p}}(\text{H})$	− 658.210 7058(66)	1.0×10^{-8}	MIT-72	3.3.3 (95)
μ_{e^-}/μ_{p}	− 658.210 6876(66)	1.0×10^{-8}		3.3.3 (99)
$\mu_{\text{d}}(\text{D})/\mu_{e^-}(\text{D})$	− 4.664 345 392(50) $\times 10^{-4}$	1.1×10^{-8}	MIT-84	3.3.4 (100)
μ_{d}/μ_{e^-}	− 4.664 345 537(50) $\times 10^{-4}$	1.1×10^{-8}		3.3.4 (104)
$\mu_{e^-}(\text{H})/\mu'_{\text{p}}$	− 658.215 9430(72)	1.1×10^{-8}	MIT-77	3.3.6 (115)
$\mu_{e^-}/\mu'_{\text{p}}$	− 658.227 5970(72)	1.1×10^{-8}		3.3.6 (116)
$\mu'_{\text{h}}/\mu'_{\text{p}}$	− 0.761 786 1313(33)	4.3×10^{-9}	NPL-93	3.3.7 (117)
$\mu_{\text{n}}/\mu'_{\text{p}}$	− 0.684 996 94(16)	2.4×10^{-7}	ILL-79	3.3.8 (122)
$\mu_{\mu^+}/\mu_{\text{p}}$	3.183 3442(17)	5.3×10^{-7}	SIN-82	3.3.9.a (133)
m_{μ}/m_e	206.768 34(11)	5.3×10^{-7}		3.3.9.a (135)
$\nu(f_{\text{p}})$	627 994.77(14) kHz	2.2×10^{-7}	LAMPF-82	3.3.9.b (145)
$\mu_{\mu^+}/\mu_{\text{p}}$	3.183 3461(11)	3.6×10^{-7}		3.3.9.b (147)
m_{μ}/m_e	206.768 219(74)	3.6×10^{-7}		3.3.9.b (148)
$\Delta\nu_{\text{Mu}}$	4 463 302.88(16) kHz	3.6×10^{-8}	LAMPF-82	3.3.9.b (144)
α^{-1}	137.036 000(20)	1.5×10^{-7}		3.3.9.d (158)
$\nu(f_{\text{p}})$	668 223 166(57) Hz	8.6×10^{-8}	LAMPF-99	3.3.9.c (153)
$\mu_{\mu^+}/\mu_{\text{p}}$	3.183 345 13(39)	1.2×10^{-7}		3.3.9.c (155)
m_{μ}/m_e	206.768 283(25)	1.2×10^{-7}		3.3.9.c (156)
$\Delta\nu_{\text{Mu}}$	4 463 302 765(53) Hz	1.2×10^{-8}	LAMPF-99	3.3.9.c (152)
α^{-1}	137.035 9932(83)	6.0×10^{-8}		3.3.9.d (159)
\bar{R}	0.003 707 213(27)	7.2×10^{-6}	CERN-79	3.3.10.a (164)
a_{μ}	$1.165\,9231(84) \times 10^{-3}$	7.2×10^{-6}		3.3.10.a (165)
α^{-1}	137.035 18(98)	7.2×10^{-6}		3.3.10.c (169)
\bar{R}^+	0.003 707 220(48)	1.3×10^{-5}	BNL-99	3.3.10.b (166)
a_{μ}	$1.16\,925(15) \times 10^{-3}$	1.3×10^{-5}		3.3.10.b (167)
α^{-1}	137.0349(18)	1.3×10^{-5}		3.3.10.c (170)

fects. For the positron, the statistical standard uncertainty of the weighted mean of five individual measurements is 0.93×10^{-12} and the other uncertainties are the same as for the electron. The two values agree to well within their combined statistical uncertainty.

Cavity resonance effects have long been recognized as a possible source of systematic error in the measurement of a_e (Dehmelt, 1981); a review has been given by Gabrielse, Tan, and Brown (1990a). For more recent work see Mittlemann, Dehmelt, and Kim (1995), Dehmelt (1994a), Dehmelt (1994b), Gabrielse and Tan (1994), Tan and Gabrielse (1993), Dehmelt, Van Dyck, and Palmer (1992), and Tan and Gabrielse (1991). The uncertainty of 4×10^{-12} assigned by Van Dyck, Schwinberg, and Dehmelt (1987b) to take into account possible cavity resonance effects is based on information derived from their additional experimental investigations (Van Dyck *et al.*, 1987a) together with an application of the theory of Brown *et al.* (1985a) and Brown *et al.* (1985b); see also Dehmelt *et al.* (1992).

To further study uncertainties due to cavity effects, Van Dyck *et al.* (1991) constructed a trap with a lower Q in order to produce an environment in which interactions with cavity

modes would be less significant. That the interactions with such cavity modes were reduced was revealed by the fact that in this trap the lifetime against spontaneous decay of cyclotron orbits was close to the free-space value, as compared to the trap used to obtain the results in Eq. (66), in which the lifetime of the cyclotron orbits was ten times longer than the free-space value.

Van Dyck *et al.* (1991) used this trap to measure a_e , but, due to the trap's sensitivity to variations of the ambient magnetic field, the results from the 14 runs were spread out in a distribution that does not appear to be due to purely random variations. Because of the nature of the distribution, these authors give the simple mean of the 14 values as their result for a_e and the experimental standard deviation of the 14 values (relative to the simple mean) as its uncertainty:

$$a_{e^-} = 1.159\,652\,1855(40) \times 10^{-3} \quad [3.4 \times 10^{-9}]. \quad (67)$$

No additional component of uncertainty for cavity shifts was included because the lifetime evidence mentioned above indicates that the interactions with cavity modes were negligible at the quoted level of uncertainty. Equation (67) is consistent with Eq. (66). However, in view of the nature of

the distribution of the results of the 14 runs, these authors do not consider this result as replacing the earlier work, but rather as a confirmation of their 4×10^{-12} uncertainty assigned to account for possible cavity effects (Dehmelt and Van Dyck, 1996).

In light of the above discussion, we use the data that lead to the results given in Eq. (66) to determine a single experimental value of a_e for use in the 1998 adjustment. Since we assume that CPT invariance holds for the electron–positron system, that value is obtained by taking the weighted mean of the data for both the electron and positron. The result is

$$a_e = 1.159\,652\,1883(42) \times 10^{-3} \quad [3.7 \times 10^{-9}], \quad (68)$$

where the standard uncertainty consists of the following components based on the values given by Van Dyck, Schwinberg and Dehmelt (1987b): 0.52×10^{-12} statistical standard uncertainty of the weighted mean of the nine individual measurements (Type A); 1.3×10^{-12} for a possible microwave power shift (Type B); and 4×10^{-12} for possible cavity resonance effects (Type B). The Birge ratio associated with this weighted mean for $\nu = 8$ degrees of freedom (see Appendix E) is $R_B = \sqrt{\chi^2/\nu} = 0.73$, indicating that the data are consistent. We also note that the unweighted mean of the nine measurements and the experimental standard deviation of this mean, which are $1.159\,652\,187\,9 \times 10^{-3}$ and 0.52×10^{-12} , respectively, agree well with the corresponding weighted values.

It is important to note that the result in Eq. (68) is in agreement with earlier results of the University of Washington group, but supersedes those results because of improvements in methodology and understanding. For example, the value $a_e = 1.159\,652\,193(4) \times 10^{-3}$ was reported in 1984 (Van Dyck, Schwinberg, and Dehmelt, 1984), which was in fact the value used in the 1986 adjustment but with the standard uncertainty increased from the 4×10^{-12} assigned by the authors to 10×10^{-12} to account for possible cavity effects. [The 1984 value was subsequently corrected to $a_e = 1.159\,652\,189(4) \times 10^{-3}$ by Van Dyck *et al.* (1991) as a result of taking into account the effect of the microwave power.] The values reported in 1981 were $a_e = 1.159\,652\,200(40) \times 10^{-3}$ and $a_{e^+} = 1.159\,652\,222(50) \times 10^{-3}$ (Schwinberg, Van Dyck, and Dehmelt, 1981; Schwinberg, Van Dyck, and Dehmelt, 1984; Van Dyck *et al.*, 1984).

A value of the fine-structure constant α can be obtained from the University of Washington weighted mean experimental value of a_e , given in Eq. (68), by determining the value $\alpha(a_e)$ for which $a_e(\text{exp}) = a_e(\text{th})$, where $a_e(\text{th})$ is the theoretical expression for a_e as a function of α . The theory of a_e is briefly summarized in Appendix B; a more detailed review will be the subject of a future publication. Following Appendix B, we have

$$a_e(\text{th}) = a_e(\text{QED}) + a_e(\text{weak}) + a_e(\text{had}), \quad (69)$$

with

$$a_e(\text{QED}) = C_e^{(2)} \left(\frac{\alpha}{\pi} \right) + C_e^{(4)} \left(\frac{\alpha}{\pi} \right)^2 + C_e^{(6)} \left(\frac{\alpha}{\pi} \right)^3 + C_e^{(8)} \left(\frac{\alpha}{\pi} \right)^4 + C_e^{(10)} \left(\frac{\alpha}{\pi} \right)^5 + \cdots, \quad (70)$$

where the coefficients $C_e^{(2n)}$, as well as $a_e(\text{weak})$ and $a_e(\text{had})$, are given in Appendix B. As indicated in that Appendix, the standard uncertainty of $a_e(\text{th})$ is

$$u[a_e(\text{th})] = 1.1 \times 10^{-12} = 0.98 \times 10^{-9} a_e \quad (71)$$

and is due almost entirely to the uncertainty of the coefficient $C_e^{(8)}$.

Equating the theoretical expression with $a_e(\text{exp})$ given in Eq. (68) yields

$$\alpha^{-1}(a_e) = 137.035\,999\,58(52) \quad [3.8 \times 10^{-9}], \quad (72)$$

which is the value included in Table 9. The uncertainty of $a_e(\text{th})$ is about one-fourth of the uncertainty of $a_e(\text{exp})$, and thus the uncertainty of this inferred value of α is determined mainly by the uncertainty of $a_e(\text{exp})$. This result has the smallest uncertainty of any value of α currently available.

3.3.2. Bound-State Corrections for Magnetic Moments

The experiments relevant to the magnetic moments of the particles of interest in this paper are done on hydrogenic atoms that contain these particles, namely, hydrogen, deuterium, and muonium, each in the ground (1S) state. In order to obtain the free-space magnetic moments of these particles, it is necessary to apply theoretical corrections to account for the fact that they are bound. These bound-state corrections are expressed in terms of the ratio of the bound g -factor to the free g -factor. Such bound state g -factors are defined by considering the contribution to the Hamiltonian from the interaction of the atom with an applied magnetic flux density \mathbf{B} written in terms of the magnetic moments of the constituent particles in the framework of the Pauli approximation. For example, for hydrogen we have

$$\begin{aligned} \mathcal{H} &= \beta(\text{H}) \boldsymbol{\mu}_e \cdot \boldsymbol{\mu}_p - \boldsymbol{\mu}_e \cdot (\text{H}) \cdot \mathbf{B} - \boldsymbol{\mu}_p(\text{H}) \cdot \mathbf{B} \\ &= \frac{2\pi}{\hbar} \Delta\nu_{\text{H}} s \cdot \mathbf{I} - g_e(\text{H}) \frac{\mu_{\text{B}}}{\hbar} s \cdot \mathbf{B} - g_p(\text{H}) \frac{\mu_{\text{N}}}{\hbar} \mathbf{I} \cdot \mathbf{B}, \end{aligned} \quad (73)$$

where $\beta(\text{H})$ characterizes the strength of the hyperfine interaction, $\Delta\nu_{\text{H}}$ is the ground-state hyperfine frequency, s is the spin of the electron, and \mathbf{I} is the spin of the nucleus, i.e., the proton. The individual cases of interest are discussed in the following paragraphs.

a. Electron in hydrogen. The main theoretical contributions to the g -factor of the electron $g_e(\text{H})$ in the 1S state of hydrogen may be categorized as follows: Dirac (relativistic) value g_{D} ; radiative corrections Δg_{rad} ; recoil corrections Δg_{rec} . Thus we write

$$g_e(\text{H}) = g_{\text{D}} + \Delta g_{\text{rad}} + \Delta g_{\text{rec}} + \cdots, \quad (74)$$

where terms accounting for finite nuclear size, nuclear polarization, weak interactions, etc., are assumed to be negligible at the current level of uncertainty of the relevant experiments (relative standard uncertainty $u_r \approx 1 \times 10^{-8}$).

Breit (1928) obtained the exact value

$$g_D = -\frac{2}{3}[1 + 2\sqrt{1 - (Z\alpha)^2}] \\ = -2[1 - \frac{1}{3}(Z\alpha)^2 - \frac{1}{12}(Z\alpha)^4 + \dots] \quad (75)$$

from the Dirac equation for an electron in the field of a fixed point charge of magnitude Ze . [Although we are concerned only with cases in which $Z=1$, in Eq. (75) and the following discussion we display the Z dependence explicitly to distinguish between binding corrections and corrections for a free particle, i.e., for the case $Z=0$.]

The radiative corrections may be written as

$$\Delta g_{\text{rad}} = -2 \left[C_e^{(2)}(Z\alpha) \left(\frac{\alpha}{\pi} \right) + C_e^{(4)}(Z\alpha) \left(\frac{\alpha}{\pi} \right)^2 + \dots \right], \quad (76)$$

where the coefficients $C_e^{(2n)}(Z\alpha)$ are slowly varying functions of $Z\alpha$ corresponding to n virtual photons. These coefficients are defined in direct analogy with the corresponding coefficients for the free electron given in Sec. 3.3.1 so that

$$\lim_{Z\alpha \rightarrow 0} C_e^{(2n)}(Z\alpha) = C_e^{(2n)}. \quad (77)$$

The coefficient $C_e^{(2)}(Z\alpha)$ has been calculated to second order in $Z\alpha$ by Grotch (1970a), who finds

$$C_e^{(2)}(Z\alpha) = C_e^{(2)} + \frac{1}{12}(Z\alpha)^2 + \dots \\ = \frac{1}{2} + \frac{1}{12}(Z\alpha)^2 + \dots \\ = 0.500\,004\,437 \dots + \dots \quad (78)$$

This result has been confirmed by Faustov (1970) and Close and Osborn (1971) [see also Lieb (1955); Hegstrom (1969); Grotch and Hegstrom (1971); Hegstrom (1971); and Grotch (1971)]. Recently, this coefficient has been calculated numerically to all orders in $Z\alpha$ with high accuracy by Persson *et al.* (1997). By assuming that $C_e^{(2)}(0) = \frac{1}{2}$ exactly and fitting their calculated values at higher Z to a polynomial in $Z\alpha$, they find for $Z=1$

$$C_e^{(2)}(\alpha) = 0.500\,004\,469(9). \quad (79)$$

[A similar calculation has been carried out by Blundell, Cheng, and Sapirstein (1997b), but their results for low Z have significantly larger uncertainties.] The difference between Eq. (79) and Eq. (78) is negligible in the present context, and thus only the lowest-order binding correction to $C_e^{(2)}(Z\alpha)$ needs to be considered. The binding corrections to the higher-order coefficients $C_e^{(4)}(Z\alpha)$, etc., have not been calculated but are expected to be small, so these coefficients are approximated by the free electron values. Thus, for the fourth-order coefficient, we have

$$C_e^{(4)}(Z\alpha) \approx C_e^{(4)} = -0.328\,478\,444\,00 \dots, \quad (80)$$

and we make the analogous approximation for the higher-order coefficients. With these approximations, the result for Δg_{rad} is

$$\Delta g_{\text{rad}} = -2 \left[\left(C_e^{(2)} + \frac{1}{12}(Z\alpha)^2 \right) \left(\frac{\alpha}{\pi} \right) + C_e^{(4)} \left(\frac{\alpha}{\pi} \right)^2 + C_e^{(6)} \left(\frac{\alpha}{\pi} \right)^3 + \dots \right]. \quad (81)$$

The preceding terms Δg_D and Δg_{rad} are based on the approximation that the nucleus of the hydrogenic atom has an infinite mass. The contribution to the bound-state g -factor associated with the finite mass of the nucleus, represented here by Δg_{rec} , has been calculated by Grotch (1970b) with the result

$$\Delta g_{\text{rec}} = -(Z\alpha)^2 \frac{m_e}{m_N} + \dots, \quad (82)$$

where m_N is the mass of the nucleus. This term and higher-order terms have been obtained by Grotch (1971); Hegstrom (1971); Faustov (1970); Close and Osborn (1971); and Grotch and Hegstrom (1971) [see also Hegstrom (1969) and Grotch (1970a)]. We have not included these higher-order terms in Eq. (82), because they are negligible compared to the uncertainty of the relevant experiments (less than 1 % of the experimental uncertainty in this case), and because additional terms that could well be larger, such as the binding corrections to the fourth-order coefficient $C_e^{(4)}$, have not yet been explicitly calculated.

The quantity of interest is the ratio of the bound-electron g -factor in hydrogen to the free-electron g -factor:

$$\frac{g_{e^-}(\text{H})}{g_{e^-}} = \frac{g_D + \Delta g_{\text{rad}} + \Delta g_{\text{rec}} + \dots}{g_{e^-}}. \quad (83)$$

Substitution of Eqs. (75), (81), and (82) in the numerator, with $m_N = m_p$, and substitution of the theoretical expression for $g_{e^-} = -2(1 + a_e)$ that follows from Sec. 3.3.1 in the denominator, yields

$$\frac{g_{e^-}(\text{H})}{g_{e^-}} = 1 - \frac{1}{3}(Z\alpha)^2 - \frac{1}{12}(Z\alpha)^4 \\ + \frac{1}{4}(Z\alpha)^2 \left(\frac{\alpha}{\pi} \right) + \frac{1}{2}(Z\alpha)^2 \frac{m_e}{m_p} + \dots \\ = 1 - 17.7053 \times 10^{-6}. \quad (84)$$

The numerical result is based on the 1998 recommended values of α and m_e/m_p , but the result is clearly not sensitive to the exact values used. This is also true for the binding correction to the g -factor of the proton in hydrogen and for the corrections to g -factors in deuterium and muonium, discussed below. The calculated or expected magnitude of any contribution not included in Eq. (84) is less than 1×10^{-9} , which is not significant compared to the uncertainty of the relevant experiments. This statement also applies to the corresponding expression for the proton g -factor in hydrogen

and to those for the electron and deuteron g -factors in deuterium. Therefore no uncertainty is quoted for the binding corrections to these g -factors.

b. Proton in hydrogen. For the proton $i = \frac{1}{2}$, and hence according to Eq. (64) its magnetic moment may be written as

$$\mu_p = \frac{g_p}{2} \mu_N, \quad (85)$$

where g_p is the g -factor of the free proton referred to the nuclear magneton $\mu_N = e\hbar/2m_p$. In analogy with the electron, the proton magnetic moment anomaly a_p is defined as

$$a_p = \frac{g_p - 2}{2} = \frac{\mu_p}{\mu_N} - 1 \approx 1.793. \quad (86)$$

However, unlike the electron anomaly a_e , the proton anomaly a_p cannot be calculated accurately. Therefore the bound-state corrections, particularly those involving a_p , are necessarily treated phenomenologically. The expression for the ratio of the bound proton g -factor $g_p(\text{H})$ to g_p analogous to Eq. (84) for the electron is

$$\begin{aligned} \frac{g_p(\text{H})}{g_p} &= 1 - \frac{1}{3} Z\alpha^2 + \frac{1}{6} Z\alpha^2 \frac{m_e}{m_p} \frac{3+4a_p}{1+a_p} + \dots \\ &= 1 - 17.7328 \times 10^{-6}. \end{aligned} \quad (87)$$

The leading correction $-Z\alpha^2/3$ can be viewed as a diamagnetic shielding correction that follows from the work of Lamb (1941). The mass-dependent term, as well as negligible higher-order mass-dependent terms not included here, have been obtained by Grotch (1971); Hegstrom (1971); Faustov (1970); Close and Osborn (1971); and Grotch and Hegstrom (1971); [see also Hegstrom (1969)].

c. Electron in deuterium. To calculate the binding correction for the g -factor of the electron in deuterium $g_{e^-}(\text{D})$, one may simply replace the proton mass m_p in Eq. (84) by the mass of the deuteron m_d . This yields

$$\begin{aligned} \frac{g_{e^-}(\text{D})}{g_{e^-}} &= 1 - \frac{1}{3} (Z\alpha)^2 - \frac{1}{12} (Z\alpha)^4 \\ &\quad + \frac{1}{4} (Z\alpha)^2 \left(\frac{\alpha}{\pi} \right) + \frac{1}{2} (Z\alpha)^2 \frac{m_e}{m_d} + \dots \\ &= 1 - 17.7125 \times 10^{-6}. \end{aligned} \quad (88)$$

d. Deuteron in deuterium. The deuteron g -factor is defined by $\mu_d = g_d \mu_N$ based on Eq. (64) and the fact that the spin quantum number i of the deuteron is 1. Although Eq. (87) was derived for the case $i = \frac{1}{2}$, Grotch (1997) and Eides and Grotch (1997a), have confirmed that this expression is also valid for the deuteron, where the deuteron magnetic moment anomaly a_d is defined by

$$a_d = \frac{\mu_d}{(e\hbar/m_d)} - 1 \approx -0.143. \quad (89)$$

Hence the binding correction for the g -factor of the deuteron in deuterium $g_d(\text{D})$ is obtained by making the replacements $m_p \rightarrow m_d$ and $a_p \rightarrow a_d$ in Eq. (87). The result is

$$\begin{aligned} \frac{g_d(\text{D})}{g_d} &= 1 - \frac{1}{3} Z\alpha^2 + \frac{1}{6} Z\alpha^2 \frac{m_e}{m_d} \frac{3+4a_d}{1+a_d} + \dots \\ &= 1 - 17.7436 \times 10^{-6}. \end{aligned} \quad (90)$$

e. Electron in muonium. Muonium, with chemical symbol Mu, is the bound state of a positive muon μ^+ and an electron e^- . The binding correction for the g -factor of the electron in muonium $g_{e^-}(\text{Mu})$ may be obtained by simply replacing the proton mass m_p in Eq. (84) by the mass of the muon m_μ . The result is

$$\begin{aligned} \frac{g_{e^-}(\text{Mu})}{g_{e^-}} &= 1 - \frac{1}{3} (Z\alpha)^2 \\ &\quad + \frac{1}{4} (Z\alpha)^2 \left(\frac{\alpha}{\pi} \right) + \frac{1}{2} (Z\alpha)^2 \frac{m_e}{m_\mu} + \dots \\ &= 1 - 17.591 \times 10^{-6}, \end{aligned} \quad (91)$$

where the term $-(Z\alpha)^4/12$ has been dropped from Eq. (84) because it is smaller than neglected higher-order mass-dependent terms. Although the mass ratio m_e/m_μ is nine times the mass ratio m_e/m_p , higher-order terms in the mass ratio, which are slightly greater than 1×10^{-9} , may be neglected compared to the uncertainty of the relevant experiment. The same statement applies to the expression for the g -factor of the muon in muonium discussed in the next paragraph. Therefore no uncertainty is quoted for either $g_{e^-}(\text{Mu})/g_{e^-}$ or $g_{\mu^+}(\text{Mu})/g_{\mu^+}$.

f. Muon in muonium. The g -factor of the muon g_μ is defined according to Eq. (61) by

$$\mu_\mu = \frac{g_\mu}{2} \frac{e\hbar}{2m_\mu} = \frac{g_\mu}{2} \frac{m_e}{m_\mu} \mu_B. \quad (92)$$

The binding correction for the g -factor of the muon in muonium $g_{\mu^+}(\text{Mu})$ follows from Eq. (87) by replacing m_p by m_μ and setting a_p to zero. We thereby obtain

$$\begin{aligned} \frac{g_{\mu^+}(\text{Mu})}{g_{\mu^+}} &= 1 - \frac{1}{3} Z\alpha^2 + \frac{1}{2} Z\alpha^2 \frac{m_e}{m_\mu} + \dots \\ &= 1 - 17.622 \times 10^{-6}. \end{aligned} \quad (93)$$

g. Comparison of theory and experiment. The theory of bound-state corrections to g -factors has been tested by a number of experiments. Based on their measurement of the ratio $g_{e^-}({}^{87}\text{Rb})/g_{e^-}$ and the earlier measurement of $g_{e^-}(\text{H})/g_{e^-}({}^{87}\text{Rb})$ by Hughes and Robinson (1969), Tiedeman and Robinson (1977) report the value $g_{e^-}(\text{H})/g_{e^-} = 1 - 17.709(13) \times 10^{-6}$. This agrees with the numerical result in Eq. (84), thereby checking the Breit correction $-(Z\alpha)^2/3$ and the term $(Z\alpha)^2(\alpha/\pi)/4$ to relative uncertainties of about 0.07 % and 40 %, respectively. An independent check of the Breit correction for $Z=2$ with a relative uncertainty of about 0.4 % is provided by the measurement of $g_{e^-}({}^4\text{He}^+)/g_{e^-}$ by Johnson and Robinson (1980).

Mass-dependent corrections to the bound-state g -factor have been tested by the work of Walther, Phillips, and Klepner (1972). Using a pulsed double-mode hydrogen maser, they obtained the ratio $g_{e^-}(\text{H})/g_{e^-}(\text{D}) = 1 + 7.22(3) \times 10^{-9}$.

The quotient of Eq. (84) and Eq. (88) gives the leading correction term in the theoretical expression for this ratio:

$$\begin{aligned}\frac{g_{e^-}(\text{H})}{g_{e^-}(\text{D})} &= 1 + \frac{1}{2}(Z\alpha)^2 \left(\frac{m_e}{m_p} - \frac{m_e}{m_d} \right) + \dots \\ &= 1 + 7.247 \times 10^{-9} + \dots\end{aligned}\quad (94)$$

The result of Walther *et al.* (1972) checks this leading correction term to a relative uncertainty of about 0.4 %. The next-order term [see the discussion following Eq. (82)], which contributes approximately -0.03×10^{-9} , improves the agreement between experiment and theory, but is checked only at a level equal to its value.

Earlier measurements of $g_{e^-}(\text{H})/g_{e^-}(\text{D})$, but with larger uncertainties, have been reported. Larson, Valberg, and Ramsey (1969) obtained $1 + 9.4(1.4) \times 10^{-9}$ for this ratio, and Hughes and Robinson (1969); Robinson and Hughes (1971), obtained $1 + 7.2(1.2) \times 10^{-9}$.

The leading correction term in Eq. (94) has been checked for a different mass to a relative uncertainty of about 15 % by Larson and Ramsey (1974) who carried out experiments with hydrogen and tritium. They obtained $g_{e^-}(\text{H})/g_{e^-}(\text{T}) = 1 + 10.7(1.5) \times 10^{-9}$, which is consistent with theory.

3.3.3. Electron to Proton Magnetic Moment Ratio μ_e/μ_p

The ratio μ_e/μ_p may be obtained from measurements of the ratio of the magnetic moment of the electron to the magnetic moment of the proton in the 1S state of hydrogen $\mu_{e^-}(\text{H})/\mu_p(\text{H})$. This bound-state ratio is determined from the energy eigenvalues of the Hamiltonian of Eq. (73), which are given by the Breit–Rabi equation (Breit and Rabi, 1931; Millman, Rabi, and Zacharias, 1938). Using a hydrogen maser operating in an applied magnetic flux density of 0.35 T to observe simultaneously both electron and proton spin-flip transitions between Zeeman energy levels, Winkler *et al.* (1972) at the Massachusetts Institute of Technology (MIT) found

$$\frac{\mu_{e^-}(\text{H})}{\mu_p(\text{H})} = -658.210\,7058(66) \quad [1.0 \times 10^{-8}], \quad (95)$$

where a minor typographical error in the original publication has been corrected (Kleppner, 1997). This value is the result of their preferred quadratic extrapolation method and is consistent with the value obtained by their linear extrapolation method. The standard uncertainty is that assigned by Winkler *et al.* (1972) and is meant to take into account possible systematic effects, mainly due to the extrapolation procedure used to analyze the data; the statistical relative uncertainty (Type A) was less than 4×10^{-9} . This result, which is in agreement with earlier measurements that have uncertainties at least a factor of 30 larger, is the only one we need to consider. [See Taylor *et al.* (1969) for a discussion of previous work.]

To obtain the free-particle ratio μ_e/μ_p from the bound-particle ratio given in Eq. (95), we apply binding corrections as follows. From Eq. (73) we have

$$\mu_{e^-}(\text{H}) = \frac{g_{e^-}(\text{H})}{2} \mu_B \quad (96)$$

and

$$\mu_p(\text{H}) = \frac{g_p(\text{H})}{2} \mu_N. \quad (97)$$

These relations together with Eqs. (62) and (85) yield

$$\frac{\mu_{e^-}}{\mu_p} = \frac{g_p(\text{H})}{g_p} \left(\frac{g_{e^-}(\text{H})}{g_{e^-}} \right)^{-1} \frac{\mu_{e^-}(\text{H})}{\mu_p(\text{H})}. \quad (98)$$

Substituting into this equation the numerical values from Eqs. (84), (87), and (95), we obtain

$$\begin{aligned}\frac{\mu_{e^-}}{\mu_p} &= (1 - 27.6 \times 10^{-9}) \frac{\mu_{e^-}(\text{H})}{\mu_p(\text{H})} \\ &= -658.210\,6876(66) \quad [1.0 \times 10^{-8}].\end{aligned}\quad (99)$$

The stated standard uncertainty is due entirely to the uncertainty of the experimental value of $\mu_{e^-}(\text{H})/\mu_p(\text{H})$ because the bound-state corrections are taken as exact, as discussed in the text following Eq. (84).

3.3.4. Deuteron to Electron Magnetic Moment Ratio μ_d/μ_e

In a manner similar to that for μ_e/μ_p , μ_d/μ_e may be obtained from measurements of the ratio $\mu_d(\text{D})/\mu_{e^-}(\text{D})$ in the 1S state of deuterium. Using essentially the same method as that employed by Winkler *et al.* (1972) to determine $\mu_{e^-}(\text{H})/\mu_p(\text{H})$ as discussed in the previous section, Phillips, Kleppner, and Walther (1984), also at MIT, measured $\mu_d(\text{D})/\mu_{e^-}(\text{D})$ and found

$$\frac{\mu_d(\text{D})}{\mu_{e^-}(\text{D})} = -4.664\,345\,392(50) \times 10^{-4} \quad [1.1 \times 10^{-8}]. \quad (100)$$

Although this result has not been published, we include it as an input datum, because the method is described in detail by Winkler *et al.* (1972) in connection with their measurement of $\mu_{e^-}(\text{H})/\mu_p(\text{H})$.

To obtain the free-particle ratio μ_d/μ_e , in analogy with the preceding section, we have

$$\mu_{e^-}(\text{D}) = \frac{g_{e^-}(\text{D})}{2} \mu_B, \quad (101)$$

$$\mu_d(\text{D}) = g_d(\text{D}) \mu_N, \quad (102)$$

and

$$\frac{\mu_d}{\mu_{e^-}} = \frac{g_{e^-}(\text{D})}{g_{e^-}} \left(\frac{g_d(\text{D})}{g_d} \right)^{-1} \frac{\mu_d(\text{D})}{\mu_{e^-}(\text{D})}. \quad (103)$$

With numerical values from Eqs. (88), (90), and (100), we find

$$\begin{aligned}\frac{\mu_d}{\mu_e} &= (1 + 31.1 \times 10^{-9}) \frac{\mu_d(\text{D})}{\mu_e(\text{D})} \\ &= -4.664\,345\,537(50) \times 10^{-4} \quad [1.1 \times 10^{-8}].\end{aligned}\quad (104)$$

3.3.5. Deuteron to Proton Magnetic Moment Ratio μ_d/μ_p

The ratio μ_d/μ_p may be determined by nuclear magnetic resonance (NMR) measurements on the molecule HD. The relevant expression is

$$\frac{\mu_d(\text{HD})}{\mu_p(\text{HD})} = \frac{[1 - \sigma_d(\text{HD})]\mu_d}{[1 - \sigma_p(\text{HD})]\mu_p}, \quad (105)$$

where $\mu_d(\text{HD})$ and $\mu_p(\text{HD})$ are the deuteron and proton magnetic moments in HD, respectively, and $\sigma_d(\text{HD})$ and $\sigma_p(\text{HD})$ are the corresponding nuclear magnetic shielding corrections similar to the atomic bound-state corrections discussed in Sec. 3.3.2. The ratio $\mu_d(\text{HD})/\mu_p(\text{HD})$ in turn is given by

$$\frac{\mu_d(\text{HD})}{\mu_p(\text{HD})} = 2 \frac{f_d(\text{HD})}{f_p(\text{HD})}, \quad (106)$$

where $f_d(\text{HD})$ and $f_p(\text{HD})$ are the NMR frequencies of the deuteron and proton in HD in the same magnetic flux density B . The factor 2 arises because the spin quantum number i of the deuteron is 1, while for the proton it is $\frac{1}{2}$. That is, in general we have for the NMR frequency f of a nucleus of magnetic moment μ in an applied flux density B

$$f = \frac{|\mu|}{i\hbar} B = \frac{|g|\mu_N}{h} B = \frac{\gamma}{2\pi} B, \quad (107)$$

reflecting the fact that in NMR measurements the selection rule on spin projection in the field direction is $\Delta i_z = \pm 1$, where $I_z = i_z \hbar$. In Eq. (107), the term $|g|\mu_N/h$ follows from Eq. (64), and the last term defines the gyromagnetic ratio of the nucleus γ . Equations (105) and (106) lead to

$$\begin{aligned}\frac{\mu_d}{\mu_p} &= 2 \frac{1 - \sigma_p(\text{HD}) f_d(\text{HD})}{1 - \sigma_d(\text{HD}) f_p(\text{HD})} \\ &= 2[1 + \sigma_d(\text{HD}) - \sigma_p(\text{HD})] \frac{f_d(\text{HD})}{f_p(\text{HD})} + \dots,\end{aligned}\quad (108)$$

where the second line follows from the fact that the nuclear magnetic shielding corrections are small.

Using the NMR method, Wimett (1953) obtained

$$\frac{\mu_d}{\mu_p} = 0.307\,012\,192(15) \quad [4.9 \times 10^{-8}] \quad (109)$$

based on the assumption that in HD the shielding correction is the same for the deuteron as it is for the proton, as suggested by Ramsey (1952), which implies $\sigma_d(\text{HD}) - \sigma_p(\text{HD}) = 0$ in Eq. (108). The uncertainty is that quoted by the author, who simply states that it is "five times the standard deviation of results obtained in four independent mea-

surements." Because the description of this experiment provided by Wimett is minimal, we are unable to give further consideration to the result in Eq. (109).

A more recent result for μ_d/μ_p , based on the theoretical estimate $\sigma_d(\text{HD}) - \sigma_p(\text{HD}) = 15.0 \times 10^{-9}$ of Neronov and Barzakh (1977), has been reported by Gorshkov *et al.* (1989):

$$\frac{\mu_d}{\mu_p} = 0.307\,012\,208\,1(4) \quad [1.3 \times 10^{-9}]. \quad (110)$$

The uncertainty, which is apparently only statistical (Type A), is that given by Gorshkov *et al.* (1989). Their measurements were designed to eliminate a particular systematic error of an earlier similar measurement by Neronov, Barzakh, and Mukhamadiev (1975). The estimate of Neronov and Barzakh (1977) for $\sigma_d(\text{HD}) - \sigma_p(\text{HD})$ supplants the earlier theoretical estimate also given by Neronov *et al.* (1975).

Because Gorshkov *et al.* (1989) do not provide sufficient information to allow an independent assessment of uncertainties due to other possible systematic effects, and also because there is no confirmation of the theoretical value for $\sigma_d(\text{HD}) - \sigma_p(\text{HD})$, we do not consider this result any further.

3.3.6. Electron to Shielded Proton Magnetic Moment Ratio μ_e/μ'_p

In many experiments requiring a magnetic field, the applied magnetic flux density B is calibrated in terms of the NMR frequency of protons in H_2O . Since the observed NMR frequency depends on the properties of the water sample, such as its purity, shape, and temperature, we write, based on Eq. (107) with $i = \frac{1}{2}$,

$$f_p = 2\mu_p^{\text{eff}} B/h, \quad (111)$$

which defines the effective magnetic moment of the proton μ_p^{eff} for that sample. In the field of fundamental constants, the sample is taken to be a sphere of pure H_2O at 25°C surrounded by vacuum, and the corresponding effective proton magnetic moment is denoted by μ'_p . Further, B is the flux density in vacuum before the sample is introduced, and the sources of B are assumed to be infinitely far away from the sample.

The relation between the shielded magnetic moment μ'_p and the free proton moment μ_p can be written as

$$\mu'_p = [1 - \sigma'_p] \mu_p, \quad (112)$$

which defines the shielding correction σ'_p . Results from experiments in which B is measured using such water samples can be related to fundamental quantities through knowledge of the shielded proton moment in Bohr magnetons μ'_p/μ_B . This quantity can be obtained from the measurement of μ_e/μ'_p discussed below. [We assume for the cases of interest in this review that any nonlinear dependence of the NMR frequency on B is negligible, and consequently that shielding corrections such as σ'_p are independent of B ; see Ramsey (1970).]

a. *Temperature dependence of shielded proton magnetic moment.* Petley and Donaldson (1984) have determined experimentally that the temperature-dependent shielded magnetic moment of the proton $\mu_p^*(t)$ in a spherical sample of pure H₂O over the range $5^\circ\text{C} \leq t \leq 45^\circ\text{C}$ can be written as

$$\frac{\mu_p^*(t)}{\mu_p'} = 1 - 10.36(30) \times 10^{-9} \text{ }^\circ\text{C}^{-1}(t - 25^\circ\text{C}), \quad (113)$$

where the uncertainty is that assigned by these researchers and is dominated by the component that allows for possible systematic effects. As pointed out by Petley and Donaldson (1984), earlier results have larger uncertainties and are consistent with their result. Although we use Eq. (113) to correct several experimental results to 25°C , the uncertainties of the corrections are sufficiently small that the correlations introduced among these results by using the same equation to calculate the corrections are negligible.

b. *Value of μ_e/μ_p' .* Phillips, Cooke, and Kleppner (1977) at MIT, in an experiment similar to that of Winkler *et al.* (1972) discussed in connection with μ_e/μ_p (see Sec. 3.3.3), measured the ratio of the electron magnetic moment in hydrogen to the proton magnetic moment in water. By comparing the electron spin-flip frequency obtained using a hydrogen maser operating at 0.35 T to the proton NMR frequency of a spherical sample of pure H₂O at a temperature $t = 34.7^\circ\text{C}$ in the same magnetic flux density, Phillips *et al.* (1977) found

$$\frac{\mu_e^-(\text{H})}{\mu_p^*(34.7^\circ\text{C})} = -658.216\,0091(69) \quad [1.0 \times 10^{-8}]. \quad (114)$$

The uncertainty is that assigned by these researchers and includes the statistical uncertainty (Type A) and a number of small uncertainty components arising from various systematic effects. This value disagrees with the reported value of the previous most accurate measurement, obtained by Lambe (1968) at Princeton University nearly 20 years earlier, which has a relative standard uncertainty of 6.6×10^{-8} . As discussed in detail by Phillips *et al.* (1977), there are a number of plausible explanations for this disagreement that favor the later value. Thus we consider only the MIT result.

To obtain μ_e/μ_p' , we first write

$$\begin{aligned} \frac{\mu_e^-(\text{H})}{\mu_p'} &= \frac{\mu_p^*(34.7^\circ\text{C})}{\mu_p'} \frac{\mu_e^-(\text{H})}{\mu_p^*(34.7^\circ\text{C})} \\ &= (1 - 1.005(29) \times 10^{-7}) \frac{\mu_e^-(\text{H})}{\mu_p^*(34.7^\circ\text{C})} \\ &= -658.215\,9430(72) \quad [1.1 \times 10^{-8}], \end{aligned} \quad (115)$$

based on Eqs. (113) and (114). Using $g_{e^-}(\text{H})/g_{e^-} = \mu_e^-(\text{H})/\mu_{e^-}$, which follows from Eqs. (96) and (62), and Eq. (84), we then have

$$\begin{aligned} \frac{\mu_{e^-}}{\mu_p'} &= \left(\frac{g_{e^-}(\text{H})}{g_{e^-}} \right)^{-1} \frac{\mu_{e^-}(\text{H})}{\mu_p'} \\ &= -658.227\,5970(72) \quad [1.1 \times 10^{-8}]. \end{aligned} \quad (116)$$

3.3.7. Shielded Helion to Shielded Proton Magnetic Moment Ratio μ_h'/μ_p'

Because of the inherent difficulties of using water as an NMR medium to calibrate magnetic flux densities to the level of accuracy required in present-day experiments in the field of fundamental constants, researchers at the National Physical Laboratory (NPL), Teddington, UK, have been developing optically pumped ^3He NMR (Flowers, Petley, and Richards, 1990; Flowers, Petley, and Richards, 1993; Flowers, Franks, and Petley, 1995a; Flowers, Franks, and Petley, 1995b; Flowers *et al.*, 1997; Flowers *et al.*, 1999). Employing their new techniques, Flowers *et al.* (1993) measured the ratio of the magnetic moment of the helion h , the nucleus of the ^3He atom, to the magnetic moment of the proton in H₂O and obtained the result

$$\frac{\mu_h'}{\mu_p'} = -0.761\,786\,1313(33) \quad [4.3 \times 10^{-9}]. \quad (117)$$

The assigned uncertainty is that of Flowers *et al.* (1993) and is mainly due to a number of nonstatistical (Type B) standard uncertainty components. The next most accurate experiment has an uncertainty that is about 24 times larger (Belyi, Il'ina, and Shifrin, 1986) and is not considered. (The prime on the symbol for the moment indicates that the helion is not free, but is bound in a helium atom. Further, although the magnetic shielding of the helion due to the susceptibility of the ^3He gas at the pressures typically used in such experiments is inconsequential, thereby making exact sample shape and temperature unimportant, we nevertheless assume that the sample is spherical, at 25°C , and surrounded by vacuum.)

Neronov and Barzakh (1978) have reported the value $\mu_h'/\mu_p(\text{H}_2) = -0.761\,786\,635(4) \quad [5.2 \times 10^{-9}]$ for the related ratio of the helion magnetic moment in ^3He to the magnetic moment of the proton in H₂. However, these authors do not give a detailed breakdown of the uncertainty components due to systematic effects that might contribute to their experiment, and, as noted by Flowers *et al.* (1993), there may be an additional component of uncertainty due to the effect subsequently discovered by Gorshkov *et al.* (1989). [Note that the next most accurate measurement of this quantity has an uncertainty that is nearly 20 times larger (Williams and Hughes, 1969).]

A value of either the ratio μ_h'/μ_p' or the ratio μ_h'/μ_p could be obtained from the above result of Neronov and Barzakh (1978) with the aid of a value for either the shielding correction difference $\sigma_p(\text{H}_2) - \sigma_p'$ or the shielding correction $\sigma_p(\text{H}_2)$ itself. Neronov and Barzakh give the measured value $\sigma_p(\text{H}_2) - \sigma_p(\text{H}_2\text{O}, 21^\circ\text{C}) = 0.596(13) \times 10^{-6}$, which implies $\sigma_p(\text{H}_2) - \sigma_p' = 0.555(13)$, based on the temperature dependence in Eq. (113). Taking the values and uncertainties as given, we find $\mu_h'/\mu_p' = -0.761\,786\,213(11) \quad [14 \times 10^{-9}]$,

which is in significant disagreement with the result in Eq. (117). In a similar manner, as noted by Fei (1996), if the quoted value $\sigma_p(\text{H}_2) = 26.363(4) \times 10^{-6}$ obtained by Raynes and Panteli (1983) from a combination of theory and experimental data is used together with the result for $\mu'_h/\mu'_p(\text{H}_2)$ of Neronov and Barzakh (1978) and the result for μ'_h/μ'_p of Flowers *et al.* (1993), one obtains $\sigma'_p = 25.702(8) \times 10^{-6}$ based on Eq. (112). At face value, this result is in agreement with and has a smaller uncertainty than the corresponding result $\sigma'_p = 25.689(15) \times 10^{-6}$ based on the experiments discussed above in Secs. 3.3.3 and 3.3.6. This agreement could be interpreted as providing confirmation of the result of Neronov and Barzakh for the ratio μ'_h/μ'_p , and could indicate that their value for the difference $\sigma_p(\text{H}_2) - \sigma_p(\text{H}_2\text{O}, 21^\circ\text{C})$ is the source of the discrepancy with Flowers *et al.* (1993). On the other hand, the reliability the value of the screening correction $\sigma_p(\text{H}_2)$ of Raynes and Panteli (1983) is open to question because of various assumptions on which it is based and a lack of experimental verification. Further, as discussed in the preceding paragraph, there are questions concerning the magnitude of the uncertainty that should be assigned to the result of Neronov and Barzakh (1978), and there is insufficient information available to resolve these questions. Therefore we do not include their result as an input datum.

3.3.8. Neutron to Shielded Proton Magnetic Moment Ratio

$$\mu_n/\mu'_p$$

The ratio of the magnetic moment of the neutron μ_n to that of the shielded proton μ'_p may be determined from the work of Greene *et al.* (1979), Greene *et al.* (1977) carried out at the Institut Laue-Langevin (ILL). Using the Ramsey separated-oscillatory-field magnetic resonance technique with protons in flowing water and slow neutrons in the same applied magnetic flux density, Greene *et al.* (1979) obtained

$$\frac{\mu_n}{\mu_p(\text{cyl}, 22^\circ\text{C})} = -0.684\,995\,88(16) \quad [2.4 \times 10^{-7}], \quad (118)$$

where “cyl” indicates that the water sample was cylindrical. The uncertainty in Eq. (118) is that assigned by Greene *et al.* (1979) and is due mainly to a statistical relative standard uncertainty (Type A) of 1.7×10^{-7} and an uncertainty in the velocity distribution of both the neutrons and protons which contributes a relative standard uncertainty (Type B) of 1.4×10^{-7} .

To determine μ_n/μ'_p from the ratio given in Eq. (118), we first note that that result is based on measurements made in air, while the symbol μ'_p denotes measurement in vacuum (see Sec. 3.3.6). However, from Eq. (120) below, it can be seen that, to first order in the magnetic susceptibility of air, the ratio of the neutron and proton resonant frequencies is the same whether measured in vacuum or air. (This statement also applies to those ratio measurements discussed in previous sections that were carried out in air.) The ratio in Eq. (118) can therefore be taken as the ratio in vacuum. This

vacuum ratio is then transformed to a result corresponding to a spherical H_2O sample in vacuum at the same temperature using the relation

$$\begin{aligned} \frac{\mu_p(\text{cyl}, 22^\circ\text{C})}{\mu_p^*(22^\circ\text{C})} &= \frac{1 + \frac{1}{3}\kappa(22^\circ\text{C})}{1 + \frac{1}{2}\kappa(22^\circ\text{C})} \\ &= 1 + 1.5093(10) \times 10^{-6}, \quad (119) \end{aligned}$$

where $\kappa(22^\circ\text{C}) = -9.0559(61) \times 10^{-6}$ [0.067 %] is the volume magnetic susceptibility of water at 22°C . This value of $\kappa(t)$ is the mass susceptibility result of Auer (1933) corrected to 22°C using the H_2O mass susceptibility versus temperature data of Philo and Fairbank (1980) and converted to a volume susceptibility using the H_2O mass density vs. temperature data of Patterson and Morris (1994). We have also corrected the result of Auer for the accepted difference between the international ampere, which he used in his experiment as a unit to express the values of currents, and the SI ampere (Hamer, 1965). We do not consider the work of Piccard and Devaud (1920) because of the disagreement between the values of the H_2O mass susceptibility obtained from their inductive measurements and their Cotton-balance measurements of the flux density in their experiment. [According to Davis (1997), the reason given by Cotton and Dupouy (1932) for possibly excluding the inductive flux-density result of Piccard and Devaud was later shown to be invalid by Dupouy and Jouaust (1935).] We have taken the 0.067 % relative uncertainty quoted by Auer (1933) as a relative standard uncertainty, although it was rather conservatively assigned, in order to account for the fact that the two results of Piccard and Devaud (1920) disagree not only with each other, but also with that of Auer. (If Auer had followed current practice, his assigned uncertainty would have been about 0.03 %.)

Fortunately, because the correction for the shape of the sample used by Greene *et al.* (1979) is small relative to the uncertainty of their result, the lack of modern data for κ is not of critical importance. Of course, there is no shape or temperature correction for μ_n because of the low density of the neutrons. (Although we use the volume magnetic susceptibility of H_2O to derive corrections to several experimental results in the 1998 adjustment, the uncertainty of the susceptibility of H_2O is sufficiently small that the correlations introduced among these results by using very nearly the same value of the susceptibility are negligible.)

Equation (119) follows from the relation for the magnetic flux density B_i inside an ellipsoid with a volume magnetic susceptibility κ_i placed in an originally uniform flux density B_o in a medium with volume magnetic susceptibility κ_o :

$$B_i = \frac{1 + \kappa_i}{1 + \kappa_o + \epsilon(\kappa_i - \kappa_o)} B_o, \quad (120)$$

where ϵ is the demagnetizing factor of the ellipsoid, and κ is related to the permeability μ by $\mu = (1 + \kappa)\mu_0$; in vacuum $\kappa = 0$. Further, ϵ has the value $\frac{1}{3}$ for a sphere and $\frac{1}{2}$ for an infinitely long cylinder with axis perpendicular to the lines of

flux [see Sec. 4.18 of Stratton (1941); Lowes (1974); and Bennett, Page, and Swartzendruber (1978)]. The fact that the water sample used by Greene *et al.* (1979) was a cylinder of finite length might have the effect of reducing the correction in Eq. (119) by an amount of the same order as its uncertainty. However such a decrease, like the uncertainty itself, would be insignificant in comparison to the uncertainty of the experiment of Greene *et al.* (1979).

The temperature dependence of the effective magnetic moment in water is taken into account by means of Eq. (113):

$$\frac{\mu_p^*(22^\circ\text{C})}{\mu_p'} = 1 + 3.108(90) \times 10^{-8}. \quad (121)$$

Equations (118), (119), and (121) together yield

$$\frac{\mu_n}{\mu_p'} = -0.684\,996\,94(16) \quad [2.4 \times 10^{-7}]. \quad (122)$$

Because the result of Greene *et al.* (1979) has an uncertainty that is 1 % of the uncertainty of the next most accurate measurement involving μ_n , it is the only one we need to consider.

3.3.9. Muon to Proton Magnetic Moment Ratio μ_μ/μ_p and Muon to Electron Mass Ratio m_μ/m_e

a. SIN: μ_μ/μ_p . A value of the ratio μ_μ/μ_p may be obtained from the measurements of Klempt *et al.* (1982) carried out at the Swiss Institute for Nuclear Research, Villigen, Switzerland (SIN, now the Paul Scherrer Institute or PSI). These workers measured, using a stroboscopic technique, the NMR frequency of positive muons stopped in spherical targets relative to the NMR frequency of protons in cylindrical water samples doped with NiSO_4 in the same magnetic flux density $B = 0.75$ T. The spherical targets contained either pure liquid bromine (Br_2), liquid bromine with a small admixture of H_2O , or pure H_2O . All measurements were made at a temperature of 25°C . In pure liquid bromine, the muonium and bromine atoms form the molecule MuBr , while in bromine with H_2O and in pure H_2O the molecule formed is MuOH . Thus, in terms of effective moments [see Eq. (111)], their results may be written as

$$\frac{\mu_{\mu^+}(\text{sph}, \text{MuBr})_{\text{Br}_2}}{\mu_p^{\text{eff}}(\text{cyl})} = 3.183\,3212(20) \quad [6.3 \times 10^{-7}] \quad (123)$$

$$\frac{\mu_{\mu^+}(\text{sph}, \text{MuOH})_{\text{Br}_2}}{\mu_p^{\text{eff}}(\text{cyl})} = 3.183\,3341(19) \quad [6.0 \times 10^{-7}] \quad (124)$$

$$\frac{\mu_{\mu^+}(\text{sph}, \text{MuOH})_{\text{H}_2\text{O}}}{\mu_p^{\text{eff}}(\text{cyl})} = 3.183\,3519(66) \quad [2.1 \times 10^{-6}], \quad (125)$$

where $\mu_p^{\text{eff}}(\text{cyl})$ is the effective magnetic moment of the protons in the field-measuring probe, and the uncertainties are statistical (Type A) only.

The corrections to the NMR frequency of the field-measuring probe found by Klempt *et al.* (1982), including a correction of $-0.20(25) \times 10^{-6}$ due to the stroboscopic background, can be expressed as

$$\frac{\mu_p^{\text{eff}}(\text{cyl})}{\mu_p(\text{cyl})} = 1 - 0.95(29) \times 10^{-6}, \quad (126)$$

where the uncertainty is mainly nonstatistical (Type B). Also in separate measurements, using a high-resolution NMR spectrometer operated at 25°C and with long cylindrical samples, Klempt *et al.* (1982) determined the NMR frequency of protons in HBr and in H_2O , both in liquid bromine, relative to the NMR frequency of protons in pure water. The results may be written as

$$\frac{\mu_p(\text{cyl}, \text{HBr})_{\text{Br}_2}}{\mu_p(\text{cyl})} = 1 - 6.55(5) \times 10^{-6} \quad (127)$$

$$\frac{\mu_p(\text{cyl}, \text{H}_2\text{O})_{\text{Br}_2}}{\mu_p(\text{cyl})} = 1 - 2.40(5) \times 10^{-6}. \quad (128)$$

[Note that the corresponding ratio for water is 1, because $\mu_p(\text{cyl}, \text{H}_2\text{O})_{\text{H}_2\text{O}} \equiv \mu_p(\text{cyl})$.]

The ratio of magnetic moments μ_{μ^+}/μ_p may be obtained using the experimental results given in Eqs. (123)–(128). The following is the relevant equation for the case in which muons are captured in a pure bromine target (similar equations may be written for the other two cases):

$$\begin{aligned} \frac{\mu_{\mu^+}}{\mu_p} = & \left(\frac{\mu_{\mu^+}(\text{sph}, \text{MuBr})_{\text{Br}_2}}{\mu_p^{\text{eff}}(\text{cyl})} \right) \left(\frac{\mu_p^{\text{eff}}(\text{cyl})}{\mu_p(\text{cyl})} \right) \\ & \times \left(\frac{\mu_p(\text{cyl}, \text{HBr})_{\text{Br}_2}}{\mu_p(\text{cyl})} \right)^{-1} \left(\frac{\mu_p(\text{cyl}, \text{HBr})_{\text{Br}_2}}{\mu_p(\text{sph}, \text{HBr})_{\text{Br}_2}} \right) \\ & \times \left(\frac{\mu_{\mu^+}}{\mu_p} \frac{\mu_p(\text{sph}, \text{HBr})_{\text{Br}_2}}{\mu_{\mu^+}(\text{sph}, \text{MuBr})_{\text{Br}_2}} \right). \end{aligned} \quad (129)$$

The first term on the right-hand side of this equation is approximately equal to the ratio of the magnetic moments of the free muon and proton. The other terms take into account the differences in the effective magnetic fields seen by the particles. In particular, the second term corrects for the characteristics of the field-measuring probe; the third term accounts for the difference between the bromine and water environments for the proton in a cylindrical sample; the fourth term takes into account the effect of the shape of the bromine samples; and the fifth term, called the isotope shift correction, corrects for the difference between the local environment seen by the muon in the MuBr molecule and the proton in the HBr molecule. The first three terms are determined experimentally, and are given by Eqs. (123), (126), and (127). The fourth and fifth terms are calculated.

The value of the fourth term is given, as in Eq. (119), by $1 - \frac{1}{6} \kappa(\text{Br}_2) = 1 + 2.19(5) \times 10^{-6}$, where $\kappa(\text{Br}_2) = -13.12(32) \times 10^{-6}$ at 25°C . This value for $\kappa(\text{Br}_2)$ is based on the volume susceptibility result obtained by Bro-

ersma (1949) at 20 °C, scaled to 25 °C using accepted values of the density of Br₂ (Kirk-Othmer, 1978). The result of Broersma appears to be the most reliable available. Based on the results for water [see Sec. 3.3.8], the temperature dependence of the mass susceptibility of Br₂ is assumed to be negligible compared to the temperature dependence of its density. The assigned uncertainty is our own estimate and is based on the variability of measurements of this type [see, for example, Savithri (1943); and Rao and Govindarajan (1942)].

The value of the fifth term in Eq. (129) is theoretically estimated by Klempt *et al.* (1982) to be $1 - 0.78(12) \times 10^{-6}$, based on work by Breskman and Kanofsky (1970); Williams (1971); and Castro, Keller, and Schenck (1979). Evaluation of Eq. (129) yields

MuBr in Br₂:

$$\frac{\mu_{\mu^+}}{\mu_p} = 3.183\,3435(20) \quad [6.4 \times 10^{-7}]. \quad (130)$$

In the case of MuOH in Br₂, the shape correction is the same as in the MuBr case. For the isotope shift correction, Klempt *et al.* (1982) give $1 - 0.28(12) \times 10^{-6}$, estimated in the same way as in the MuBr case. [Although the uncertainties of these isotope shift corrections were evaluated using a more conservative approach (absolute sum of the uncertainty components) than normally employed for other results discussed in this review, we take them to be standard uncertainties, as do Klempt *et al.* (1982), because an independent evaluation of the uncertainties cannot be done.]

Klempt *et al.* (1982) take $1 - 2.0(2.0) \times 10^{-6}$ as the corresponding correction for MuOH in H₂O from Crowe *et al.* (1972). Also in the latter case, the shape correction is $1 - \frac{1}{6} \kappa(25^\circ\text{C}) = 1 + 1.509(1) \times 10^{-6}$, where $\kappa(25^\circ\text{C}) = -9.0531(61) \times 10^{-6}$ and is obtained as described in Sec. 3.3.8. The results are

MuOH in Br₂:

$$\frac{\mu_{\mu^+}}{\mu_p} = 3.183\,3448(19) \quad [6.1 \times 10^{-7}] \quad (131)$$

MuOH in H₂O:

$$\frac{\mu_{\mu^+}}{\mu_p} = 3.183\,3473(92) \quad [29 \times 10^{-7}]. \quad (132)$$

The uncertainties quoted for the ratios in Eqs. (130)–(132) do not include the 2.9×10^{-7} uncertainty common to all three measurements arising from the relationship between μ_p^{eff} and $\mu_p(\text{cyl})$, as given in Eq. (126). Also not included in the uncertainties of the first two ratios is their common 0.54×10^{-7} uncertainty due to the Br₂ shape correction.

The three ratios are in good agreement. However, following Klempt *et al.* (1982), the final result is obtained by taking a weighted mean of only the first two, because the third has a significantly larger uncertainty arising from the theoretical estimate of the isotope shift correction. The weighted mean is

$$\frac{\mu_{\mu^+}}{\mu_p} = 3.183\,3442(17) \quad [5.3 \times 10^{-7}], \quad (133)$$

where the final quoted uncertainty consists of the 4.4×10^{-7} relative standard uncertainty of the mean, and the two common components of uncertainty. As stated by Klempt *et al.* (1982), the result given in Eq. (133) supersedes the initial result reported by Camani *et al.* (1978).

Earlier NMR measurements of μ_{μ}/μ_p have uncertainties that are sufficiently large that they need not be considered. This includes the most accurate previous result, $\mu_{\mu^+}/\mu_p = 3.183\,346\,7(82) \quad [2.6 \times 10^{-6}]$, which was obtained by Crowe *et al.* (1972) and is consistent with Eq. (133).

The muon to electron mass ratio m_{μ}/m_e and the muon to proton magnetic moment ratio μ_{μ}/μ_p are related by

$$\frac{m_{\mu}}{m_e} = \left(\frac{\mu_e}{\mu_p} \right) \left(\frac{\mu_{\mu}}{\mu_p} \right)^{-1} \left(\frac{g_{\mu}}{g_e} \right), \quad (134)$$

where g_{μ} is the g -factor of the muon. Because the relative standard uncertainties of μ_e/μ_p , g_{μ} , and g_e are 1×10^{-8} or less, m_{μ}/m_e may be obtained from μ_{μ}/μ_p (and vice versa) with an insignificant increase in uncertainty. Further, any dependence of g_{μ} and g_e on m_{μ}/m_e is extremely weak and may be ignored (see Appendices B and C). Using the 1998 recommended values of these quantities, we find that the Klempt *et al.* (1982) value of μ_{μ}/μ_p given in Eq. (133) implies

$$\frac{m_{\mu}}{m_e} = 206.768\,34(11) \quad [5.3 \times 10^{-7}]. \quad (135)$$

b. LAMPF 1982: μ_{μ}/μ_p . A value of μ_{μ}/μ_p may be obtained from measurements of the frequencies of transitions between Zeeman energy levels in muonium. Until very recently, the most accurate experiment in a long series of this type [see Hughes and zu Putlitz (1990) for a review] was carried out nearly 20 years ago at the Clinton P. Anderson Meson Physics Facility at Los Alamos (LAMPF), USA, by an international collaboration using a microwave resonance method. The experiment, the results of which were reported in 1982 (Mariam *et al.*, 1982; Mariam, 1981), used the high-intensity, low-momentum “surface” muon beam at LAMPF. Muons were stopped in a microwave cavity filled with krypton gas at a pressure of 0.5 or 1 atmosphere and in a magnetic flux density of approximately 1.4 T. A total of 184 pairs of resonance curves were analyzed for the frequencies of transitions between the energy levels labeled by the high-field quantum numbers (m_s, m_l). The frequencies are ν_{12} , corresponding to the transition $(\frac{1}{2}, \frac{1}{2}) \leftrightarrow (\frac{1}{2}, -\frac{1}{2})$; and ν_{34} , corresponding to the transition $(-\frac{1}{2}, -\frac{1}{2}) \leftrightarrow (-\frac{1}{2}, \frac{1}{2})$. Of these 184 resonance curves, 28 were from a similar experiment reported in 1977 (Casperson *et al.*, 1977) in which the pressure of the krypton in the microwave cavity was 1.7 or 5.2 atmospheres. The 184 pairs of frequencies, after correction to a free proton NMR reference frequency f_p of very nearly 57.972 993 MHz, corresponding to a magnetic flux density of about 1.3616 T, and after correction for a small

quadratic krypton gas density shift, were extrapolated linearly to zero gas density. The results obtained may be written as

$$\nu_{12} = 1\,917\,654.053(92) \text{ kHz} \quad [4.8 \times 10^{-8}] \quad (136)$$

$$\nu_{34} = 2\,545\,648.82(12) \text{ kHz} \quad [4.6 \times 10^{-8}] \quad (137)$$

$$r(\nu_{12}, \nu_{34}) = 0.18, \quad (138)$$

where $r(\nu_{12}, \nu_{34})$ is the correlation coefficient of ν_{12} and ν_{34} . The quoted uncertainties and correlation coefficient follow from the 19 components of uncertainty given by Mariam (1982). The statistical (Type A) uncertainty is 0.046 kHz for ν_{12} and 0.057 kHz for ν_{34} .

We have considered possible corrections to these frequencies due to the temperature dependence of the proton magnetic moment in water and due to modification of the values used by Mariam *et al.* (1982) for the diamagnetic susceptibility of water and the proton magnetic shielding correction σ'_p . We conclude that any change in the value of μ_{μ^+}/μ_p deduced from the frequencies given in Eqs. (136) and (137) should be well within its uncertainty. The value of the muonium ground-state hyperfine splitting $\Delta\nu_{\text{Mu}}$, which also follows from these frequencies, is essentially independent of such corrections.

The Hamiltonian for muonium is similar to that for hydrogen given in Eq. (73):

$$\begin{aligned} \mathcal{H} &= \beta(\text{Mu}) \mu_{e^-} \cdot \mu_{\mu^+} - \mu_{e^-}(\text{Mu}) \cdot \mathbf{B} - \mu_{\mu^+}(\text{Mu}) \cdot \mathbf{B} \\ &= \frac{2\pi}{\hbar} \Delta\nu_{\text{Mu}} \mathbf{S} \cdot \mathbf{I} - g_{e^-}(\text{Mu}) \frac{\mu_B}{\hbar} \mathbf{S} \cdot \mathbf{B} \\ &\quad - g_{\mu^+}(\text{Mu}) \frac{m_e}{m_\mu} \frac{\mu_B}{\hbar} \mathbf{I} \cdot \mathbf{B}. \end{aligned} \quad (139)$$

The energy eigenvalues of this Hamiltonian are again given by the Breit–Rabi equation (Breit and Rabi, 1931; Millman *et al.*, 1938). This yields

$$\Delta\nu_{\text{Mu}} = \nu_{34} + \nu_{12} \quad (140)$$

$$\nu(f_p) = \nu_{34} - \nu_{12} \quad (141)$$

$$\frac{\mu_{\mu^+}}{\mu_p} = \frac{\Delta\nu_{\text{Mu}}^2 - \nu^2(f_p) + 2s_e f_p \nu(f_p)}{4s_e f_p^2 - 2f_p \nu(f_p)} \left(\frac{g_{\mu^+}(\text{Mu})}{g_{\mu^+}} \right)^{-1}, \quad (142)$$

where f_p is the free proton NMR frequency given above. The quantity $g_{\mu^+}(\text{Mu})/g_{\mu^+}$ is the bound-state correction for the muon in muonium given in Eq. (93); and

$$s_e = \frac{\mu_{e^-}}{\mu_p} \frac{g_{e^-}(\text{Mu})}{g_{e^-}}, \quad (143)$$

where $g_{e^-}(\text{Mu})/g_{e^-}$ is the bound-state correction for the electron in muonium given in Eq. (91). Based on Eqs. (136)–(138), Eqs. (140) and (141) yield

$$\Delta\nu_{\text{Mu}} = 4\,463\,302.88(16) \text{ kHz} \quad [3.6 \times 10^{-8}] \quad (144)$$

$$\nu(f_p) = 627\,994.77(14) \text{ kHz} \quad [2.2 \times 10^{-7}] \quad (145)$$

$$r[\Delta\nu_{\text{Mu}}, \nu(f_p)] = 0.23. \quad (146)$$

Taking the 1998 recommended value of μ_{e^-}/μ_p , we find from Eqs. (142)–(146)

$$\frac{\mu_{\mu^+}}{\mu_p} = 3.183\,3461(11) \quad [3.6 \times 10^{-7}]. \quad (147)$$

(Note that all significant correlations are taken into account in this and subsequent calculations.)

The LAMPF-82 result given in Eq. (147) agrees with that obtained at SIN given in Eq. (133); the two differ by $0.94 u_{\text{diff}}$, where u_{diff} is the standard uncertainty of their difference.

A value of m_μ/m_e may be obtained from the LAMPF-82 value of μ_{μ^+}/μ_p and Eq. (134) as was done for the SIN value. The result is

$$\frac{m_\mu}{m_e} = 206.768\,219(74) \quad [3.6 \times 10^{-7}]. \quad (148)$$

c. LAMPF 1999: μ_μ/μ_p . Data from a new experiment initiated in the mid-1980s at LAMPF and designed to measure transition frequencies between Zeeman energy levels in muonium with higher accuracy than the earlier experiment of Mariam *et al.* (1982) have recently been reported by an international collaboration that includes some of the researchers in the earlier collaboration (Liu *et al.*, 1999). The measurements were carried out using basically the same method as in the previous experiment but with a number of significant improvements, leading to a reduction in the uncertainty of both μ_μ/μ_p and $\Delta\nu_{\text{Mu}}$ by a factor of 3. [For an early overview of the experiment, see Hughes (1997).] These advances were in three major areas: (i) magnetic field: a higher magnetic flux density with greater homogeneity and stability measured with a more accurate method (Fei, Hughes and Prigl, 1997; Prigl *et al.*, 1996). (ii) Muon beam: higher intensity, greater purity, and a narrower beam profile. (iii) Resonance line: higher signal-to-background ratio and narrower linewidth, especially when the resonance line-narrowing technique termed “old muonium” rather than the conventional technique was used (Boshier *et al.*, 1995).

In the new experiment, the resonance curves were obtained either by sweeping the magnetic flux density about a central value of approximately 1.7 T with fixed microwave frequency, or by sweeping the frequency with the flux density fixed at this central value. The centers of the resonance curves were obtained by fitting them with a theoretical line shape that takes into account a number of factors such as the measured magnetic flux density distribution over the microwave cavity, the ideal microwave power distributions, and the muon stopping distribution.

In total, 1270 resonance lines were analyzed: 154 conventional and 726 “old muonium” resonances obtained by the swept-field method; and 43 conventional and 347 “old muonium” resonances obtained by the swept-frequency method (Kawall, 1998). Each of the transition frequencies, ν_{12} and ν_{34} , resulting from the fitted line shape was then converted to the frequency that would have been obtained if the flux

density seen by the muonium atoms had been that corresponding to a free proton NMR frequency f_p of exactly 72.320 000 MHz, corrected for a small quadratic pressure shift due to the fact that the data were taken with the pressure of the krypton gas in the microwave cavity at either 0.8 or 1.5 atmospheres, and extrapolated linearly to zero gas pressure. The final results from all of the data are given as (Liu *et al.*, 1999; Liu and Kawall, 1998)

$$\nu_{12} = 1\,897\,539\,800(35) \text{ Hz} \quad [1.9 \times 10^{-8}] \quad (149)$$

$$\nu_{34} = 2\,565\,762\,965(43) \text{ Hz} \quad [1.7 \times 10^{-8}] \quad (150)$$

$$r(\nu_{12}, \nu_{34}) = -0.07, \quad (151)$$

where the quoted standard uncertainties are dominated by statistical components of uncertainty (Type A) but also contain a number of Type B components arising from different run-independent and run-dependent effects.

In the same manner discussed in the previous paragraph in connection with the 1982 LAMPF experiment, the 1999 LAMPF results lead to

$$\Delta\nu_{\text{Mu}} = 4\,463\,302\,765(53) \text{ Hz} \quad [1.2 \times 10^{-8}] \quad (152)$$

$$\nu(f_p) = 668\,223\,166(57) \text{ Hz} \quad [8.6 \times 10^{-8}] \quad (153)$$

$$r[\Delta\nu_{\text{Mu}}, \nu(f_p)] = 0.19, \quad (154)$$

$$\frac{\mu_{\mu^+}}{\mu_p} = 3.183\,345\,13(39) \quad [1.2 \times 10^{-7}], \quad (155)$$

and

$$\frac{m_{\mu}}{m_e} = 206.768\,283(25) \quad [1.2 \times 10^{-7}]. \quad (156)$$

A comparison of Eqs. (144) and (147) with Eqs. (152) and (155) shows that the 1999 and 1982 LAMPF determinations are in agreement. Because the two experiments are separated in time by some 15 years, the new experiment was carried out with a completely different apparatus, and the uncertainties of the earlier values of μ_{μ^+}/μ_p and $\Delta\nu_{\text{Mu}}$ are only three times larger than those of the newer values, we include the results of both experiments as input data in the 1998 adjustment.

d. LAMPF: $\Delta\nu_{\text{Mu}}$. The experimental value of the muonium ground-state hyperfine splitting $\Delta\nu_{\text{Mu}}$ obtained at LAMPF by Mariam *et al.* (1982) is given in Eq. (144) and the value obtained at LAMPF by Liu *et al.* (1999) is given in Eq. (152). The theoretical expression for the splitting is briefly discussed in Appendix D; a more detailed review is planned for a future publication. That expression may be written as

$$\begin{aligned} \Delta\nu_{\text{Mu}}(\text{th}) &= \frac{16}{3} c R_{\infty} \alpha^2 \frac{m_e}{m_{\mu}} \left(1 + \frac{m_e}{m_{\mu}}\right)^{-3} \mathcal{F}(\alpha, m_e/m_{\mu}) \\ &= \Delta\nu_{\text{F}}(\alpha, m_e/m_{\mu}), \end{aligned} \quad (157)$$

where, because it provides a significantly more accurate value, the theoretical expression for the muon magnetic moment anomaly a_{μ} , as discussed in Sec. 3.3.10 and Appendix C, is used in the function \mathcal{F} . Further, \mathcal{F} depends on α and m_e/m_{μ} only weakly compared to the dependence of $\Delta\nu_{\text{F}}$ on these quantities.

It follows from Eq. (157) that, given experimental values of $\Delta\nu_{\text{Mu}}$ and m_{μ}/m_e , one can calculate a value of α by equating $\Delta\nu_{\text{Mu}}(\text{exp})$ with $\Delta\nu_{\text{Mu}}(\text{th})$; or similarly, given values of $\Delta\nu_{\text{Mu}}(\text{exp})$ and α , one can calculate a value of m_{μ}/m_e . How the available information on μ_{μ}/μ_p , m_{μ}/m_e , and $\Delta\nu_{\text{Mu}}$ is treated in the 1998 adjustment is discussed in Sec. 4. Here we point out that using the 1998 recommended value of R_{∞} (the uncertainty of which is negligible in this application) and the combined LAMPF-82 and SIN values of m_{μ}/m_e , and equating the LAMPF-82 value of $\Delta\nu_{\text{Mu}}(\text{exp})$ with $\Delta\nu_{\text{Mu}}(\text{th})$, we find

$$\alpha^{-1} = 137.036\,000(20) \quad [1.5 \times 10^{-7}]. \quad (158)$$

The uncertainty of this result is due almost entirely to the uncertainty of the combined LAMPF-82 and SIN values of m_{μ}/m_e . (A value of α with a somewhat smaller uncertainty could be inferred from Eq. (157) by introducing an explicit factor of α^4 through the replacement of R_{∞} by the equivalent expression $c \alpha^2 A_r(e)/[A_r(n) d_{220}(\text{W04})(h/m_n d_{220}(\text{W04}))]$ from Eq. (283) and using the available experimental data to determine the values of the various quantities other than α that enter the resulting expression. However, we choose not to do so in order to obtain a value of α that is independent of x-ray data. Repeating this calculation with the LAMPF 1982 data replaced by the LAMPF 1999 data yields

$$\alpha^{-1} = 137.035\,9932(83) \quad [6.0 \times 10^{-8}], \quad (159)$$

where the uncertainty is again dominated by the uncertainty of the combined LAMPF-99 and SIN values of m_{μ}/m_e . Finally, by combining the SIN, LAMPF 1982, and LAMPF 1999 data we obtain what may be called a muonium value of the fine-structure constant:

$$\alpha^{-1}(\Delta\nu_{\text{Mu}}) = 137.035\,9952(79) \quad [5.7 \times 10^{-8}]. \quad (160)$$

On the other hand, using the value of $\alpha(a_e)$ from Eq. (72), which has a relative standard uncertainty of only 3.8×10^{-9} , and equating the combined 1982 and 1999 LAMPF values of $\Delta\nu_{\text{Mu}}(\text{exp})$ with $\Delta\nu_{\text{Mu}}(\text{th})$, we find

$$\frac{m_{\mu}}{m_e} = 206.768\,2656(64) \quad [3.1 \times 10^{-8}], \quad (161)$$

where the uncertainty arises primarily from the 2.7×10^{-8} relative standard uncertainty of the theory of $\Delta\nu_{\text{Mu}}$ and the 1.1×10^{-8} relative standard uncertainty of the 1982–1999 combined experimental value of the hyperfine splitting. Because the uncertainty of this value of m_{μ}/m_e is significantly smaller than that of any of the three values discussed above, the muonium hyperfine splitting plays a dominant role in the determination of this mass ratio in the 1998 adjustment.

e. Other values. There are other values of μ_{μ}/μ_p and m_{μ}/m_e , and they generally agree with those discussed

above. However, they are not competitive because of their relatively large uncertainties. One such value is the NMR-based result for μ_{μ^+}/μ_p of Crowe *et al.* (1972), with a relative standard uncertainty of 2.6×10^{-6} already given in connection with the SIN experiment. Another is $m_{\mu}/m_e = 206.768\,67(64) [3.1 \times 10^{-6}]$ based on measurements of x-ray transitions in muonic ^{24}Mg and ^{28}Si (Beltrami *et al.*, 1986). [Note that we have corrected the original result reported by Beltrami *et al.* (1986) for the approximate 1.8×10^{-6} fractional decrease in the value of the ^{170}Tm γ -ray wavelength λ_{γ} that they used as a reference due to a fractional error of about 1.8×10^{-6} in the value of the silicon lattice spacing employed in the determination of λ_{γ} ; see Sec. 3.9.1.] Still another is $m_{\mu}/m_e = 206.76907(102) [4.9 \times 10^{-6}]$ derived from measurements of the 1S–2S transition in muonium, hydrogen, and deuterium using Doppler-free two-photon laser spectroscopy, although a value of m_{μ}/m_e with a relative standard uncertainty of less than 8×10^{-7} derived from new measurements of the muonium 1S–2S transition is expected to be published in 2000 (Schwarz *et al.*, 1995; Jungmann, 1999). And finally we have $\mu_{\mu^-}/\mu_p = -3.183\,28(15) [47 \times 10^{-6}]$ obtained from measurements of the frequencies of transitions between Zeeman energy levels of the muonic helium atom $\alpha\mu^-e^-$ (Gardner *et al.*, 1982).

3.3.10. Muon Magnetic Moment Anomaly a_{μ}

In a manner similar to that for the electron [see Eq. (65)], the muon magnetic moment anomaly a_{μ} is defined as

$$a_{\mu} = \frac{|g_{\mu}| - 2}{2} = \frac{|\mu_{\mu}|}{e\hbar/2m_{\mu}} - 1, \quad (162)$$

where, as usual, $g_{\mu} = 2\mu_{\mu}/(e\hbar/2m_{\mu})$ is the g -factor of the muon and μ_{μ} is its magnetic moment. The muon anomaly has been determined experimentally with a relative standard uncertainty $u_r = 7.2 \times 10^{-6}$, and more recently a value with $u_r = 13 \times 10^{-6}$ has been obtained from the first run of an entirely new experiment. By contrast, a value with $u_r = 0.55 \times 10^{-6}$ may be obtained from the theoretical expression for a_{μ} . These three values are discussed in the following sections.

a. CERN. The most accurate experimental value of a_{μ} comes from the third $g-2$ experiment at CERN (European Laboratory for Particle Physics, Geneva, Switzerland), which was the culmination of nearly 20 years of effort (Bailey *et al.*, 1979). [For reviews of the early work, see Farley and Picasso (1990); Combley, Farley, and Picasso (1981); Farley and Picasso (1979); and Combley (1979).] The CERN result is based on nine separate runs or measurements with both positive and negative muons over the period 1974–1976 using the CERN 3.098 GeV/c, 1.47 T muon storage ring (Drumm *et al.*, 1979). The basic principle of the experiment is similar to that used for determining the electron anomaly a_e and involves measuring the anomaly difference frequency $f_a = f_s - f_c$, where $f_s = |g_{\mu}|(e\hbar/2m_{\mu})B/h$ is the muon spin-flip (often called precession) frequency in the magnetic flux

density B and where $f_c = eB/2\pi m_{\mu}$ is the corresponding muon cyclotron frequency. However, instead of eliminating B by measuring f_c as is done for the electron (see Sec. 3.3.1), B is determined from proton NMR measurements. As a consequence, the value of μ_{μ}/μ_p is required to deduce the value of a_{μ} from the data. The relevant equation is

$$a_{\mu} = \frac{\bar{R}}{|\mu_{\mu}/\mu_p| - \bar{R}}, \quad (163)$$

where $\bar{R} = f_a/\bar{f}_p$, and \bar{f}_p is the free proton NMR frequency corresponding to the average flux density seen by the muons in their orbits in the storage ring.

The value of \bar{R} reported by Bailey *et al.* (1979) from the third CERN $g-2$ experiment is

$$\bar{R} = 0.003\,707\,213(27) [7.2 \times 10^{-6}], \quad (164)$$

where the uncertainty consists of a 7.0×10^{-6} statistical (Type A) relative standard uncertainty component, arising from the determination of f_a , and a 1.5×10^{-6} relative standard uncertainty component (Type B), arising from a number of systematic effects associated with the determination of f_p . The NMR probes used in mapping, monitoring, and stabilizing the flux density of the storage ring were calibrated in terms of a long, cylindrical H_2O reference probe containing NiSO_4 (Borer and Lange, 1977). The observed NMR frequency of this reference probe was converted to the corresponding free proton NMR frequency by applying corrections to account for the paramagnetic Ni^{++} ions, the cylindrical shape of the probe, and the proton's magnetic shielding in H_2O . The first correction was determined experimentally; the second was based on the assumption that the cylinder was infinitely long and was calculated with the accepted value of the volume magnetic susceptibility of H_2O , κ ; and the third was based on the accepted value of the proton magnetic shielding correction σ'_p . [It should be noted that the difference between the value of κ used by Bailey *et al.* (1979) and the value of κ that follows from the discussion of Sec. 3.3.8 would lead to a change in the corresponding correction that is negligible compared to the uncertainty of \bar{f}_p . A similar statement applies to the value of σ'_p used by Bailey *et al.* (1979) and the 1998 recommended value.]

Equation (164) is the weighted mean of all nine independent measurements, five using positive muons and four using negative muons. The Birge ratio (see Appendix E) associated with this weighted mean ($\nu = 8$) is $R_B = \sqrt{\chi^2/\nu} = 0.96$, indicating that the data form a consistent set. The μ^+ and μ^- data alone give $\bar{R}^+ = 0.003\,707\,173(36)$ and $\bar{R}^- = 0.003\,707\,256(37)$, where each quoted uncertainty is the statistical (Type A) uncertainty only. The 84×10^{-9} difference between \bar{R}^- and \bar{R}^+ is equal to $1.6 u_{\text{diff}}$, where u_{diff} is the standard uncertainty of the difference (Type A only) and is not deemed statistically significant. Since the μ^+ and μ^- values are consistent and we assume that CPT invariance holds for the muon–antimuon system as we do for the

electron–positron system (see Sec. 3.3.1), taking the weighted mean of all nine values is the appropriate way to treat the data.

Because of the relatively large uncertainty of the CERN result for \bar{R} , the value of μ_μ/μ_p used to obtain a_μ from \bar{R} and Eq. (163) is not critical. Taking the 1998 recommended value for μ_μ/μ_p , we find

$$a_\mu = 1.165\,9231(84) \times 10^{-3} \quad [7.2 \times 10^{-6}]. \quad (165)$$

This result is consistent with the significantly less accurate result from the second CERN $g-2$ experiment, $a_\mu = 1.166\,16(31) \times 10^{-3} \quad [27 \times 10^{-5}]$ [Bailey *et al.* (1972)].

b. Brookhaven. A new muon $g-2$ experiment based on the same general method employed in the most recent CERN experiment was initiated in the mid-1980s by an international group of researchers at the Brookhaven National Laboratory (BNL), Upton, New York, USA using the BNL Alternating Gradient Synchrotron (AGS). The ultimate aim of the BNL $g-2$ collaboration is to reduce the uncertainty of the measured value of a_μ achieved at CERN by about a factor of 20, corresponding to a relative standard uncertainty $u_r = 3.5 \times 10^{-7}$. [For a detailed overview of the BNL $g-2$ effort, see Hughes (1998); Hughes (1994).]

The main characteristics of the new experiment that should make this significantly reduced uncertainty possible include (i) a smaller statistical uncertainty because of the larger number of stored muons due to the higher proton beam intensity of the BNL AGS and the eventual direct injection of muons into the BNL muon storage ring (the dominant uncertainty component by far in the CERN determination was the statistical uncertainty); (ii) a superferric 14 m diameter, 1.45 T ‘‘C’’ magnet of very high homogeneity and stability, together with a system of fixed and movable NMR probes with the potential of measuring the magnetic flux density distribution seen by the circulating muon beam in terms of the corresponding free proton NMR frequency with $u_r = 1 \times 10^{-7}$ (Fei *et al.*, 1997; Fei, 1995); and (iii) an advanced detector system with Pb-scintillating fiber electron calorimeters and the capability of measuring time intervals with an uncertainty of 20 ps over a time period of 200 μ s.

The principal equipment of the new experiment was checked out and initial data acquired in a 1997 engineering run using pion injection into the storage ring. All critical components performed successfully, including the positive pion beam line of the AGS, the superconducting inflector for bringing the pion (and eventually muon) beam into the storage ring, the storage ring itself, the NMR magnetic field measuring system, and the detectors. In early 1999, the BNL $g-2$ collaboration reported a value of f_a/\bar{f}_p for μ^+ with $u_r = 13 \times 10^{-6}$ as obtained from these initial data (Carey *et al.*, 1999):

$$\bar{R}^+ = 0.003\,707\,220(48) \quad [1.3 \times 10^{-5}], \quad (166)$$

where the 48×10^{-9} standard uncertainty arises from a 47×10^{-9} statistical uncertainty component (Type A) and a 11×10^{-9} uncertainty component (Type B) from eight differ-

ent systematic effects, the associated relative standard uncertainties of which range from 0.2×10^{-6} to 2.0×10^{-6} .

This first result from BNL agrees well with that from CERN given in Eq. (164) and has an uncertainty less than twice as large. Although a significantly more accurate BNL value is expected from the data acquired in 1998 and 1999 runs using muon injection rather than pion injection into the storage ring, the experiment is sufficiently well in hand and the uncertainty of the initial value of \bar{R}^+ is sufficiently small to allow it to be considered as an input datum in the 1998 adjustment together with the CERN value of \bar{R} given in Eq. (164).

Based on Eq. (163), the BNL value of \bar{R}^+ implies

$$a_\mu = 1.165\,925(15) \times 10^{-3} \quad [1.3 \times 10^{-5}]. \quad (167)$$

c. Theory. Appendix C gives a brief summary of the theory of a_μ ; a more detailed review is planned for a future publication. In accordance with Appendix C, we have

$$a_\mu(\text{th}) = a_\mu(\text{QED}) + a_\mu(\text{weak}) + a_\mu(\text{had}),$$

with

$$a_\mu(\text{QED}) = C_\mu^{(2)} \left(\frac{\alpha}{\pi} \right) + C_\mu^{(4)} \left(\frac{\alpha}{\pi} \right)^2 + C_\mu^{(6)} \left(\frac{\alpha}{\pi} \right)^3 + C_\mu^{(8)} \left(\frac{\alpha}{\pi} \right)^4 + C_\mu^{(10)} \left(\frac{\alpha}{\pi} \right)^5 + \dots,$$

where the coefficients $C_\mu^{(2n)}$, as well as $a_\mu(\text{weak})$ and $a_\mu(\text{had})$, are given in Appendix C. The standard uncertainty of $a_\mu(\text{th})$ due to the uncertainties of the coefficients and the weak and hadronic contributions is $u[a_\mu(\text{th})] = 6.4 \times 10^{-10} = 5.5 \times 10^{-7} a_\mu$ and is almost entirely due to the uncertainty of $a_\mu(\text{had})$.

Because of the relatively large uncertainty of the theoretical expression for a_μ , the value of α used to evaluate it is not particularly critical. The 1998 recommended value of α yields

$$a_\mu = 1.165\,916\,02(64) \times 10^{-3} \quad [5.5 \times 10^{-7}], \quad (168)$$

which agrees with the CERN and BNL experimental results given in Eqs. (165) and (167); the differences between the two experimental values and the theoretical value are $0.8 u_{\text{diff}}$ and $0.6 u_{\text{diff}}$, respectively, where u_{diff} is the standard uncertainty of the difference. The uncertainties of the CERN and BNL values of a_μ are 13 and 24 times that of the theoretical value, so the 1998 recommended value of a_μ is determined primarily by the theoretical expression.

The agreement between theory and experiment may also be seen by considering the value of α obtained by equating the theoretical expression for a_μ with the CERN and BNL experimental values. The results are

$$\alpha^{-1} = 137.035\,18(98) \quad [7.2 \times 10^{-6}] \quad (169)$$

and

$$\alpha^{-1} = 137.0349(18) \quad [1.3 \times 10^{-5}], \quad (170)$$

which agree with more accurate values such as $\alpha^{-1}(a_e)$ given in Eq. (72).

3.4. Shielded Gyromagnetic Ratios γ'

It follows from Eq. (107) that the gyromagnetic ratio γ of a particle of spin quantum number i and magnetic moment μ is given by

$$\gamma = \frac{2\pi f}{B} = \frac{\omega}{B} = \frac{|\mu|}{i\hbar}, \quad (171)$$

where f is the precession (i.e., spin-flip) frequency and ω is the angular precession frequency of the particle in the magnetic flux density B . The SI unit of γ is $\text{s}^{-1}\text{T}^{-1} = \text{C kg}^{-1} = \text{A s kg}^{-1}$. In this section we review measurements of the gyromagnetic ratio of the shielded proton

$$\gamma'_p = \frac{2\mu'_p}{\hbar} \quad (172)$$

and of the shielded helion

$$\gamma'_h = \frac{2|\mu'_h|}{\hbar}, \quad (173)$$

where, as in previous sections that dealt with magnetic moment ratios involving these particles, the protons are those in a spherical sample of pure H_2O at 25°C surrounded by vacuum; and the helions are those in a spherical sample of low-pressure, pure ^3He gas at 25°C surrounded by vacuum. Also, as was assumed in these previous sections, B is the flux density in vacuum before the sample is introduced and the sources of B are infinitely far from the sample.

In practice, two methods are used to determine the shielded gyromagnetic ratio γ' of a particle. In the low-field method B is of the order of 1 mT and is usually generated by a single-layer precision solenoid carrying an electric current I . The flux density B is calculated from the dimensions of the solenoid and the current: $B = \mu_0 k_s I$, where k_s is the measured solenoid constant and has the dimension of reciprocal length. In the high-field method B is of the order of 0.5 T, is generated by an electromagnet or a permanent magnet, and is measured in terms of the force F_e it produces on a straight conducting wire of length l carrying an electric current I : $B = F_e / l I$.

In either case the current I is measured in terms of a practical laboratory unit of current $A_{\text{LAB}} = V_{\text{LAB}} / \Omega_{\text{LAB}}$, where V_{LAB} and Ω_{LAB} are practical laboratory units of voltage and resistance. As indicated in Sec. 2.5, the unit V_{LAB} may be based on the Josephson effect, or possibly on the mean emf of a group of standard cells, and the unit Ω_{LAB} may be based on the quantum Hall effect or possibly on the mean resistance of a group of standard resistors.

Since in the low-field method γ' is inversely proportional to the current I , and in the high-field method γ' is directly proportional to I , it follows from the discussion of Sec. 2.5 that for a low-field experiment

$$\gamma' = \frac{\omega}{\mu_0 k_s I} = \Gamma'_{\text{LAB}}(\text{lo}) \left(\frac{A_{\text{LAB}}}{A} \right)^{-1}, \quad (174)$$

where $\Gamma'_{\text{LAB}}(\text{lo})$ is the value of $\omega / \mu_0 k_s I$ when I is replaced by $(I/A_{\text{LAB}})A$, that is, when I is taken to be the numerical value of the current measured in the unit A_{LAB} times the unit A . For a high-field experiment

$$\gamma' = \frac{\omega l I}{F_e} = \Gamma'_{\text{LAB}}(\text{hi}) \left(\frac{A_{\text{LAB}}}{A} \right), \quad (175)$$

where $\Gamma'_{\text{LAB}}(\text{hi})$ is the value of $\omega l I / F_e$ when I is replaced as above. The square root of the product of Eqs. (174) and (175) is

$$\gamma' = [\Gamma'_{\text{LAB}}(\text{lo}) \Gamma'_{\text{LAB}}(\text{hi})]^{1/2}, \quad (176)$$

which shows that if low- and high-field measurements of γ' are based on the same unit of current A_{LAB} , irrespective of how that unit is realized, then the two measurements together yield γ' in its SI unit $\text{s}^{-1}\text{T}^{-1}$.

If $V_{\text{LAB}} = V_{90}$ and $\Omega_{\text{LAB}} = \Omega_{90}$, where V_{90} and Ω_{90} are based on the Josephson and quantum Hall effects and the exact, conventional values K_{J-90} and R_{K-90} for the Josephson and von Klitzing constants (see Sec. 2.5), then from Eqs. (174) and (175) we have

$$\gamma' = \Gamma'_{90}(\text{lo}) \frac{K_J R_K}{K_{J-90} R_{K-90}} \quad (177a)$$

$$\gamma' = \Gamma'_{90}(\text{hi}) \frac{K_{J-90} R_{K-90}}{K_J R_K}, \quad (177b)$$

where the subscript “90” on Γ' indicates that A_{LAB} is taken to be the conventional unit $A_{90} = V_{90} / \Omega_{90}$.

Low- and high-field measurements of γ' contribute to the determination of a set of recommended values of the constants because of the relationship of γ' to constants of fundamental interest, particularly the fine-structure constant α and Planck constant h , which are central to the 1998 adjustment. For example, starting from Eq. (172) and taking advantage of the fact that the ratio μ_{e^-} / μ'_p has been accurately measured (see Sec. 3.3.6), we can relate μ'_p to μ_{e^-} , where the latter is well known in terms of the Bohr magneton $\mu_B = e\hbar/2m_e$ (see Sec. 3.3.1):

$$\gamma'_p = \frac{2}{\hbar} \frac{\mu'_p}{\mu_{e^-}} \frac{\mu_{e^-}}{\mu_B} \mu_B = \frac{\mu'_p}{\mu_{e^-}} \frac{g_{e^-}}{2} \frac{e}{m_e}. \quad (178)$$

Since $e^2 = 2\alpha h / \mu_0 c$ and $m_e = 2R_\infty h / \alpha^2 c$, Eq. (178) may be written as

$$\gamma'_p = \frac{\mu'_p}{\mu_{e^-}} \frac{g_{e^-}}{R_\infty} \left(\frac{c}{8\mu_0} \frac{\alpha^5}{h} \right)^{1/2}. \quad (179)$$

The results of the gyromagnetic ratio experiments that we review in the following sections are summarized in Table 10. Also included in the table is the value of α inferred from each low-field result and the value of h inferred from each high-field result, as discussed in connection with each experiment. Each inferred value is indented for clarity and is given for comparison purposes only; in actuality the values

TABLE 10. Summary of data related to shielded gyromagnetic ratios, and inferred values of α and h .

Quantity	Value	Relative standard uncertainty u_r	Identification	Sec. and Eq.
$\Gamma'_{p-90}(\text{lo})$	$2.675\,154\,05(30) \times 10^8 \text{ s}^{-1} \text{ T}^{-1}$	1.1×10^{-7}	NIST-89	3.4.1.a (183)
α^{-1}	137.035 9880(51)	3.7×10^{-8}		3.4.1.a (193)
$\Gamma'_{p-90}(\text{lo})$	$2.675\,1530(18) \times 10^8 \text{ s}^{-1} \text{ T}^{-1}$	6.6×10^{-7}	NIM-95	3.4.1.b (197)
α^{-1}	137.036 006(30)	2.2×10^{-7}		3.4.1.b (200)
$\Gamma'_{p-90}(\text{hi})$	$2.675\,1525(43) \times 10^8 \text{ s}^{-1} \text{ T}^{-1}$	1.6×10^{-6}	NIM-95	3.4.1.b (198)
h	$6.626\,071(11) \times 10^{-34} \text{ J s}$	1.6×10^{-6}		3.4.1.b (202)
$\Gamma'_{p-90}(\text{hi})$	$2.675\,1518(27) \times 10^8 \text{ s}^{-1} \text{ T}^{-1}$	1.0×10^{-6}	NPL-79	3.4.1.c (205)
h	$6.626\,0729(67) \times 10^{-34} \text{ J s}$	1.0×10^{-6}		3.4.1.c (206)
$\Gamma'_{h-90}(\text{lo})$	$2.037\,895\,37(37) \times 10^8 \text{ s}^{-1} \text{ T}^{-1}$	1.8×10^{-7}	KR/VN-98	3.4.2.a (210)
α^{-1}	137.035 9853(82)	6.0×10^{-8}		3.4.2.a (212)
$\Gamma'_{h-90}(\text{lo})$	$2.037\,897\,29(72) \times 10^8 \text{ s}^{-1} \text{ T}^{-1}$	3.5×10^{-7}	VNIIM-89	3.4.2.b (214)
α^{-1}	137.035 942(16)	1.2×10^{-7}		3.4.2.b (215)

of Γ' are taken as input data for the 1998 adjustment. (The consistency of the data of Table 10 is discussed in Sec. 4.)

3.4.1. Proton p

A number of national metrology institutes have long histories of measuring the gyromagnetic ratio of the shielded proton. The motivation for such measurements was, in part, the need to develop a method of measuring magnetic fields using NMR and to monitor the stability of the laboratory's practical unit of current based on groups of standard cells and standard resistors.

a. NIST: Low field. The National Institute of Standards and Technology reported its first low-field measurement of γ'_p , which had a relative standard uncertainty of about 4×10^{-6} , in 1958 (Bender and Driscoll, 1958). Its most recent low-field result was reported in 1989 by Williams *et al.* (1989) and has a relative standard uncertainty of 1.1×10^{-7} .

In this experiment, the single-layer precision solenoid had a length of 2.1 m, a diameter of 0.3 m, and was wound with 2100 turns of gold-plated copper wire 0.8 mm in diameter; the winding pitch was about 1 mm per turn. The current through the solenoid was about 1 A, but additional current was added to segments of the wire in such a way that the magnetic flux density was insensitive to the diameter of the solenoid to the same extent that it would be for a 1.5 km long solenoid, and the flux density was uniform with a fractional variation of less than 2×10^{-7} over a spherical volume 8 cm in diameter at the solenoid's center. In all, five current sources were used to energize the solenoid. A movable probe consisting of a set of five coils was guided along the axis of the solenoid by a fused silica straightedge in order to determine variations in the diameter and pitch of the windings. This was done by injecting an ac current having a special wave form in sequentially selected groups of ten turns. The probe itself was in vacuum and its position was measured by laser interferometry (Williams *et al.*, 1985; Williams, Olsen, and Phillips, 1984; Williams and Olsen 1979; Olsen and

Williams, 1974; Williams and Olsen, 1972). The proton NMR measurements were carried out at 25 °C using a 3.5 cm diameter spherical sample of pure H₂O. The NMR frequency in the 1.2 mT magnetic flux density of the solenoid was about 52 kHz and was measured by the method of nuclear induction.

The result obtained by Williams *et al.* (1989) may be written as

$$\gamma_p^* = \Gamma_{p-\text{NIST}}^*(\text{lo}) \frac{K_J}{K_{J-\text{NIST}}} \frac{\Omega_{\text{NIST}}}{\Omega}, \quad (180a)$$

with

$$\Gamma_{p-\text{NIST}}^*(\text{lo}) = 2.675\,133\,76(29) \times 10^8 \text{ s}^{-1} \text{ T}^{-1} [1.1 \times 10^{-7}], \quad (180b)$$

where the standard uncertainty is that assigned by the experimenters. Here the asterisk indicates that the experiment was carried out in air rather than vacuum, $K_{J-\text{NIST}} = 483\,593.420 \text{ GHz/V}$ was the adopted value of the Josephson constant K_J used by NIST to define its laboratory unit of voltage V_{NIST} , and Ω_{NIST} was the NIST laboratory unit of resistance based on standard resistors at the time of the experiment, the mean date of which was 3 April 1988. From measurements of the von Klitzing constant in terms of Ω_{NIST} made in the period August 1983 to May 1988 (Cage *et al.*, 1989a), together with two additional measurements, one made in December 1988 and the other in August 1989 (Cage, 1989a), we find that on this mean date $R_K = 25\,812.848\,21(29) \Omega_{\text{NIST}} [1.1 \times 10^{-8}]$.

A number of systematic effects were investigated and accounted for in the experiment of Williams *et al.* (1989), including the magnetic susceptibility of the Earth, of the fused silica solenoid form, and of the tuned pickup coil used to detect the 52 kHz NMR signal. The principal sources of uncertainty in the experiment were the NMR measurements, the susceptibility of the pickup coil, the measurements of the winding pitch, and the power coefficient of the resistor used to measure the solenoid current.

A number of corrections must be applied to the result given in Eq. (180) to convert it to a value based on the unit

A_{90} and to account for other effects not initially considered by Williams *et al.* (1989). The fractional values of these corrections, and their standard uncertainties where applicable, are as follows: 9.264×10^{-6} to convert from K_{J-NIST} to K_{J-90} ; $-1.596(11) \times 10^{-6}$ to convert from Ω_{NIST}/Ω to R_K/R_{K-90} based on the above value of R_K ; $-4.0(1.3) \times 10^{-9}$ to account for the under-estimation of the current dependence (loading) of the 6453.2 Ω transfer resistors used in the 1980s measurements of R_K in terms of Ω_{NIST} (Elmquist and Dziuba, 1997; Elmquist, 1997; Cage, 1997); $3.6(1.0) \times 10^{-8}$ due to the effect of the field of the solenoid on the magnetometer that was used to null the magnetic field of the Earth (Williams, 1997); and finally, a relatively large correction of $-1.160(18) \times 10^{-7}$ due to the fact that the experiment was done in air, but was assumed to be done in vacuum.

A correction for this latter effect, which in this case is slightly larger than the quoted standard uncertainty, is also applied to the results of the other shielded gyromagnetic ratio experiments considered here. Although this correction is of only marginal significance for some of the experiments, we apply it to all in order not to introduce artificial relative shifts in results for the 1998 adjustment. Based on Eq. (120), one can show that for low-field experiments, to first order in the volume magnetic susceptibilities of H_2O and air,

$$\gamma'_p = (1 - \epsilon_s \kappa_a) \gamma'^q_{(lo)}, \quad (181)$$

where $\epsilon_s = \frac{1}{3}$ is the demagnetizing factor for a sphere, κ_a is the volume magnetic susceptibility of the air, and $\gamma'^q_{(lo)}$ is the quoted value of γ'_p as obtained from NMR measurements carried out in air, but with the corresponding flux density B calculated as if the solenoid generating B were in vacuum. For high-field experiments, the corresponding equation is

$$\gamma'_p = [1 + (1 - \epsilon_s) \kappa_a] \gamma'^q_{(hi)}. \quad (182)$$

The difference between Eqs. (181) and (182) is due to the difference in the methods of obtaining B .

To calculate the fractional correction $\epsilon_s \kappa_a$, we use the equation for κ_a as a function of temperature, pressure, relative humidity, and amount-of-substance fraction of CO_2 derived by Davis (1998), based on a thorough review of the available experimental and theoretical data. The relative standard uncertainty given by Davis for the resulting value of κ_a is 1 % assuming that all four of these variables are exactly known, but generally increases to above 1.5 % if the uncertainties of these variables in a particular experiment are taken into account. It should be noted that the 1 % uncertainty is sufficiently small that the correlations among the various values of Γ' in Table 10 introduced by using essentially the same value of κ_a to calculate the air correction are negligible.

Application of all the above corrections to the value given in Eq. (180) yields

$$\Gamma'_{p-90}(lo) = 2.675\,154\,05(30) \times 10^8 \text{ s}^{-1} \text{ T}^{-1} [1.1 \times 10^{-7}], \quad (183)$$

where Γ'_{p-90} is related to γ'_p by Eq. (177a).

This result may be compared to that obtained from the previous NIST low-field γ'_p experiment using similar techniques, but with a solenoid of length 1 m (Williams and Olsen, 1979). The measurements were carried out with two different current distributions, one that produced a nearly uniform magnetic flux density over the sample volume and one that not only provided an adequately uniform flux density, but also significantly reduced the sensitivity of the flux density to the average diameter of the solenoid. The result reported by Williams and Olsen (1979) is, in analogy with Eq. (180),

$$\Gamma^*_{p-NIST}(lo) = 2.675\,132\,29(57) \times 10^8 \text{ s}^{-1} \text{ T}^{-1} [2.1 \times 10^{-7}], \quad (184)$$

but in this case Ω_{NIST} was the NIST unit of resistance on 22 March 1978, the mean date of the experiment.

A number of corrections must be applied to this result, most of which are similar to those applied to the result reported in 1989. The fractional values of these corrections, and their uncertainties where applicable, are as follows: 9.264×10^{-6} to convert from K_{J-NIST} to K_{J-90} ; $-1.089(26) \times 10^{-6}$ to convert from Ω_{NIST}/Ω to R_K/R_{K-90} ; $1.39(39) \times 10^{-8}$ to correct for the effect of the solenoid's field on the magnetometer (Williams, 1997); $-1.160(18) \times 10^{-7}$ for the effect of the air; and $-4.7(1.2) \times 10^{-8}$ for the effect of the Earth's magnetic susceptibility as obtained by scaling the corresponding correction of -1.1×10^{-7} given by Williams *et al.* (1989) by the ratio of the magnetic dipole moments of the solenoids used in the two experiments (Williams, 1997).

The correction for Ω_{NIST} is based on the following three results: (i) the value

$$R_K = 25\,812.808\,31(62) \, \Omega [2.4 \times 10^{-8}] \quad (185)$$

obtained from NIST R_K -calculable capacitor measurements carried out in 1994–1995 (Jeffery *et al.*, 1998; Jeffery *et al.*, 1997) and discussed in detail in Sec. 3.6.1; (ii) the value

$$R_K = 25\,812.848\,35(30) \, \Omega_{NIST} [1.1 \times 10^{-8}] \quad (186)$$

corresponding to 12 April 1988 based on the measurements of R_K in terms of Ω_{NIST} from 1983 to 1989 discussed above, but including the loading correction (this date gives the smallest uncertainty for R_K); and (iii) the value

$$\Omega_{NIST} = [1 - 0.819(27) \times 10^{-6}] \, \Omega \quad (187)$$

obtained from NIST calculable capacitor measurements with a mean date of 2 December 1973 (Cutkosky, 1974). [Note that because of the 21 year time difference between the NIST 1973 and 1994–1995 calculable capacitor measurements, and changes in equipment, personnel, and technique over this period, the values in Eqs. (185) and (187) are treated as independent data.] Equations (185) and (186) imply that on 12 April 1988

$$\Omega_{NIST} = [1 - 1.551(27) \times 10^{-6}] \, \Omega, \quad (188)$$

which together with Eq. (187) implies that the drift rate of Ω_{NIST} is

$$\frac{d\Omega_{\text{NIST}}}{dt} = -5.10(26) \times 10^{-8} \text{ a}^{-1}, \quad (189)$$

where a is the unit symbol for year. This drift rate agrees with the value $d\Omega_{\text{NIST}}/dt = -5.32(29) \times 10^{-8} \text{ a}^{-1}$ based on the 1983 to 1989 R_K measurements. We do not use the result

$$\Omega_{\text{NIST}} = [1 - 1.594(22) \times 10^{-6}] \Omega \quad (190)$$

based on the NIST calculable capacitor measurements with a mean date of 17 May 1988 (Shields, Dziuba, and Layer, 1989), because the more recent NIST work Jeffery *et al.*, 1998; Jeffery *et al.*, 1997) indicates that the earlier measurements are likely to be in error. We have used the value of $d\Omega_{\text{NIST}}/dt$ from the NIST 1973 and 1994–1995 calculable capacitor ohm realizations rather than the value from the NIST R_K measurements, because the time span of the ohm realizations includes the mean date of the γ'_p experiment.

Application of all of the above corrections to the value given in Eq. (184) leads to

$$\Gamma'_{p-90}(\text{lo}) = 2.675\,153\,76(57) \times 10^8 \text{ s}^{-1} \text{ T}^{-1} [2.1 \times 10^{-7}], \quad (191)$$

which agrees with the value given in Eq. (183); the two differ by about one-half of the standard uncertainty of the 1979 value. Although the uncertainty of the 1979 NIST result is less than twice that of the 1989 NIST result, in keeping with the policy discussed in Sec. 1.4., only the 1989 value of $\Gamma'_{p-90}(\text{lo})$ is included in the 1998 adjustment.

The value of α that may be inferred from Eq. (183) follows from the relation

$$\Gamma'_{p-90}(\text{lo}) = \frac{K_{J-90} R_{K-90} g_e^-}{4 \mu_0 R_\infty} \frac{\mu'_p}{\mu_e^-} \alpha^3, \quad (192)$$

which is obtained by combining Eqs. (177a) and (179) and assuming the validity of the relations $K_J = 2e/h = \sqrt{8\alpha/\mu_0 c h}$ and $R_K = h/e^2 = \mu_0 c/2\alpha$. Using the 1998 recommended values for the other relevant quantities, the uncertainties of which are significantly smaller than the uncertainty of the NIST experimental result, we find

$$\alpha^{-1} = 137.035\,9880(51) [3.7 \times 10^{-8}], \quad (193)$$

where the uncertainty is about one-third the uncertainty of the NIST value of $\Gamma'_{p-90}(\text{lo})$ because of the cube-root dependence of α on $\Gamma'_{p-90}(\text{lo})$.

b. NIM: Low field and high field. Researchers at the National Institute of Metrology (NIM), Beijing, PRC, have measured γ'_p in both low and high fields starting in the 1970s. The basic apparatus for each experiment has remained essentially unchanged since the first NIM low- and high-field results were reported by Chiao, Liu, and Shen (1980), but a number of significant improvements in technique and ancillary equipment have been incorporated over the years (Liu *et al.*, 1988; Liu *et al.*, 1995). In the low-field experiment the magnetic flux density B was produced by either Helmholtz coil No. 2 or Helmholtz coil No. 3. Coil No. 2 had a diameter of 296 mm and consisted of two windings of 38 turns each of gold-plated copper wire 0.8 mm in

diameter with a winding pitch of 1 mm per turn; coil No. 3 was similar—it was 320 mm in diameter and its two windings contained 40 turns each. For either coil, B was about 0.23 mT for a current of 1 A. The dimensions of the coils, including the diameter of the wire itself, were determined using laser interferometry. The comparatively small magnetic dipole moment of each coil and the small magnetic susceptibility of the ground at the remote site of the experiment eliminated the need for a correction due to the coil's image moment. However, a correction for the effect of the magnetic field of a coil on the system used to compensate the Earth's magnetic field was necessary (Liu, 1997). The experiment was carried out in air with a spherical pure H_2O NMR sample at a mean temperature of 21 °C, and the NMR frequencies were measured by the free-precession method. The dominant components of uncertainty, mainly Type B, arose from determining the following quantities: the susceptibilities of the NMR polarization and detection coils; the power coefficient of the standard resistor used to measure the coil current; the NMR frequencies; the location of the current lead to a coil; and the diameters of the windings, their pitch, and the diameter of the wire itself.

In the high-field experiment the magnetic flux density B , produced by a permanent magnet, was about 0.47 T. The resonance absorption frequency of the cylindrical, CuSO_4 -doped H_2O proton NMR sample was held constant at 20 MHz by using a signal derived from a crystal oscillator and by incorporating the sample in a magnet stabilization system. The conductor used to measure B was a rectangular coil of four turns of oxygen-free copper wire 0.8 mm in diameter cemented to the edges of a rectangular fused silica plate 600 mm high, 100 mm wide, and 10 mm thick. The coil was hung from a balance beam with its lower edge in the center of the gap of the magnet. Since the width of the coil was not perfectly uniform, the effective length l of the current segment is calculated from measurements of the coil width along its height together with the difference between the magnetic flux density at the points of measurement and the flux density at the lower edge of the coil. The largest components of uncertainty were due to the following: random variations among the six groups of measurements carried out, thought to arise mainly from the change in zero position of the balance and its automatic balance system; calibration of the mass standard; and determination of both the width of the coil and the diameter of the wire.

The most recent NIM measurements yielded (Liu *et al.*, 1995)

$$\gamma_p^* = \Gamma_{p-\text{NIM}}^*(\text{lo}) \frac{K_J}{K_{J-90}} \frac{\Omega_{\text{NIM}}}{\Omega}, \quad (194a)$$

with

$$\Gamma_{p-\text{NIM}}^*(\text{lo}) = 2.675\,1534(17) \times 10^8 \text{ s}^{-1} \text{ T}^{-1} [6.5 \times 10^{-7}], \quad (194b)$$

and

$$\gamma_p^* = \Gamma_{p-NIM}^*(hi) \frac{K_{J-90}}{K_J} \frac{\Omega}{\Omega_{NIM}}, \quad (195a)$$

with

$$\Gamma_{p-NIM}^*(hi) = 2.675\,1536(43) \times 10^8 \text{ s}^{-1} \text{ T}^{-1} \\ [1.6 \times 10^{-6}]. \quad (195b)$$

Here the asterisk indicates that the experiments were carried out in air rather than vacuum, the average temperature of the NMR samples was 21 °C (Liu, 1997), and for the high-field experiment that the NMR sample was a cylinder containing H₂O with dissolved CuSO₄. Further, Ω_{NIM} was the NIM laboratory unit of resistance at the time of the experiments and was based on standard resistors. The fractional corrections that must be applied to these results are as follows: $0.002(121) \times 10^{-6}$ and $-0.002(121) \times 10^{-6}$ to convert from Ω_{NIM} to R_{K-90} for the low- and high-field results, respectively, based on NIM measurements of both R_K and Ω_{NIM} in terms of the ohm as realized by the NIM calculable capacitor (Liu *et al.*, 1996; Liu, 1997); $-4.14(12) \times 10^{-8}$ to correct from 21 °C to 25 °C, based on Eq. (113); $-1.180(21) \times 10^{-7}$ to convert from air to vacuum for the low-field result; and $-0.38(20) \times 10^{-6}$ to account for the fact that the high-field experiment was carried out in air with a finite-length cylindrical NMR sample of H₂O containing CuSO₄, in place of $0.43(13) \times 10^{-6}$, which was the correction included in the result reported by Liu *et al.* (1995) (Liu, 1997). Our high-field correction is the sum of two terms: $0.40(8) \times 10^{-6}$ to take into account the fact that the water contained CuSO₄; and $-0.78(19) \times 10^{-6}$ to convert the result for a cylindrical probe with demagnetizing factor ϵ_c containing pure water surrounded by air to a result corresponding to a spherical probe in vacuum. This term is based on the equation

$$\gamma_p' = [1 + (\epsilon_c - \epsilon_s)\kappa(21^\circ\text{C}) + (1 - \epsilon_c)\kappa_a] \gamma_p'^q(hi), \quad (196)$$

which is a generalization of Eq. (182), and where $\kappa(21^\circ\text{C})$ is the volume magnetic susceptibility of water at 21 °C. Our correction for the CuSO₄ is based on the data of Dickinson (1951) and an estimated value of $\epsilon_c = 0.44(4)$.

Application of these corrections yields

$$\Gamma_{p-90}'(lo) = 2.675\,1530(18) \times 10^8 \text{ s}^{-1} \text{ T}^{-1} \\ [6.6 \times 10^{-7}] \quad (197)$$

and

$$\Gamma_{p-90}'(hi) = 2.675\,1525(43) \times 10^8 \text{ s}^{-1} \text{ T}^{-1} \\ [1.6 \times 10^{-6}], \quad (198)$$

with a correlation coefficient of

$$r(lo, hi) = -0.014 \quad (199)$$

due to the uncertainty of the common $0.002(121) \times 10^{-6}$ Ω_{NIM} to R_{K-90} correction. (The uncertainty arises mainly

from the comparison of a 10 k Ω resistance standard calibrated in terms of the quantum Hall effect and the 1 Ω resistance standards used to maintain Ω_{NIM} .)

Based on Eq. (192), we find that the value of α that may be inferred from the NIM low-field result in Eq. (197) is

$$\alpha^{-1} = 137.036\,006(30) \quad [2.2 \times 10^{-7}]. \quad (200)$$

Similarly, based on the relation

$$\Gamma_{p-90}'(hi) = \frac{c \alpha^2 g_e}{2K_{J-90} R_{K-90} R_\infty} \frac{\mu_p'}{\mu_e} \frac{1}{h}, \quad (201)$$

which follows from Eqs. (177b) and (179), we find that the value of h that may be inferred from the NIM high-field result in Eq. (198) is

$$h = 6.626\,071(11) \times 10^{-34} \text{ J s} \quad [1.6 \times 10^{-6}]. \quad (202)$$

In both cases we have used the 1998 recommended values for the other relevant quantities; their uncertainties are negligible compared to the NIM values of $\Gamma_{p-90}'(lo)$ and $\Gamma_{p-90}'(hi)$.

Because the earlier NIM low- and high-field results are well known only in terms of the NIM laboratory units V_{NIM} and Ω_{NIM} based on standard cells and standard resistors, the 1995 results may best be compared to the earlier results by considering the value of γ_p' obtained from Eq. (176). Using that equation, and the results given in Eqs. (197) and (198), we find

$$\gamma_p' = 2.675\,1527(23) \times 10^8 \text{ s}^{-1} \text{ T}^{-1} \quad [8.6 \times 10^{-7}]. \quad (203)$$

This result agrees with the value $\gamma_p' = 2.675\,1541(23) \times 10^8 \text{ s}^{-1} \text{ T}^{-1}$ $[8.7 \times 10^{-7}]$ based on low- and high-field measurements reported in 1988 (Liu *et al.*, 1988) and the value $\gamma_p' = 2.675\,1482(49) \times 10^8 \text{ s}^{-1} \text{ T}^{-1}$ $[1.8 \times 10^{-6}]$ based on measurements reported in 1980 (Chiao *et al.*, 1980), where we have again applied corrections for temperature, air, and probe shape/CuSO₄ as appropriate. In keeping with our policy (see Sec. 1.4), only the 1995 results are included in the 1998 adjustment.

c. NPL: High field. The most accurate high-field γ_p' experiment was carried out at NPL by Kibble and Hunt (1979). In this experiment, the current-carrying conductor used to measure the 0.47 T magnetic flux density B of the electromagnet was a rectangular coil of three turns of 2.5 mm wide by 0.7 mm thick rectangular silver strip conductor cemented to a rectangular pyrex form 800 mm in height, 187 mm wide, and 3 mm thick and which hung from one arm of a balance. The current in the coil was 0.5 A to 5 A, the number of ampere turns used was 1.5 to 15, and the maximum force on the coil, upon reversal of the current through it, was equal to the weight of a 250 g standard of mass. The proton NMR sample containing pure H₂O was in the shape of a cylinder with rounded ends and with a length-to-diameter ratio of about five. The NMR signal was observed using a tuned circuit formed by an inductive coil wound on the sample and driven

at about 20 MHz. The largest sources of uncertainty in the experiment were the determination of the width of the coil and its position in the gap of the magnet.

The result reported by Kibble and Hunt (1979) (Kibble, 1981) may be written as

$$\gamma_p^* = \Gamma_{p-NPL}^*(\text{hi}) \frac{K_{J-NPL}}{K_J} \frac{\Omega}{\Omega_{NPL}}, \quad (204a)$$

with

$$\Gamma_{p-NPL}^*(\text{hi}) = 2.675\,1701(27) \times 10^8 \text{ s}^{-1} \text{ T}^{-1} [1.0 \times 10^{-6}]. \quad (204b)$$

Here the asterisk indicates that the experiment was carried out in air rather than vacuum and the average temperature of the NMR sample was 20.2 °C (Kibble, 1997). Further, $K_{J-NPL} = 483\,594 \text{ GHz/V}$ was the adopted value of K_J used by NPL to define its laboratory unit of voltage, and Ω_{NPL} was the NPL laboratory unit of resistance based on standard resistors at the time of the experiment, the mean date of which may be taken as 15 March 1974. The fractional corrections that must be applied to this result are as follows: -8.065×10^{-6} to convert from K_{J-NPL} to K_{J-90} ; $0.90(15) \times 10^{-6}$ to convert from Ω/Ω_{NPL} to R_{K-90}/R_K ; $-4.97(14) \times 10^{-8}$ to correct from 20.2 °C to 25 °C based on Eq. (113); and $-1.139(94) \times 10^{-6}$ to account for the fact that the experiment was carried out in air with a cylindrical H_2O NMR sample of finite length, in place of $-1.50(10) \times 10^{-6}$, which assumes that the experiment was carried out in vacuum with a cylinder of infinite length and was included as a correction in the result reported by Kibble and Hunt (1979) (Kibble, 1997).

The ohm correction is based on the relation $\Omega_{NPL} = [1 - 0.017(150) \times 10^{-6}] \Omega_{\text{NIST}}$ for 15 March 1974 obtained from the periodic resistance intercomparisons involving the BIPM and the national metrology institutes (Taylor and Witt, 1986) and on the same procedure to convert $\Omega_{\text{NIST}}/\Omega$ to R_K/R_{K-90} discussed above in connection with the NIST 1979 low-field γ'_p experiment (see Sec. 3.4.1.a). An additional relative standard uncertainty of 0.1×10^{-6} has been included in the resistance transfers between NPL and BIPM and between NIST and BIPM to allow for a variety of possible systematic effects, and these together account for most of the assigned uncertainty of the correction. The air and sample shape correction is based on Eq. (196) where in this case $\kappa(21^\circ\text{C})$ is replaced by $\kappa(20.2^\circ\text{C})$ and our estimated value of ϵ_c is 0.48(1).

The result after application of the above corrections is

$$\Gamma'_{p-90}(\text{hi}) = 2.675\,1518(27) \times 10^8 \text{ s}^{-1} \text{ T}^{-1} [1.0 \times 10^{-6}], \quad (205)$$

from which we infer

$$h = 6.626\,0729(67) \times 10^{-34} \text{ J s} [1.0 \times 10^{-6}]. \quad (206)$$

[It should be noted that various input data in the 1998 adjustment such as that in Eq. (205) depend on the same NIST QHE and/or calculable capacitor measurements; nevertheless, their covariances are negligible.]

3.4.2. Helion h

There are two independent low-field determinations of the gyromagnetic ratio of the shielded helion γ'_h to be considered: one carried out at the Korea Research Institute of Standards and Science (KRISS), Taedok Science Town, Republic of Korea, in a collaborative effort with researchers from the Mendeleyev All-Russian Research Institute for Metrology (VNIIM), St. Petersburg, Russian Federation (Shifrin *et al.*, 1999; Shifrin *et al.*, 1998a; Shifrin *et al.*, 1998b; Kim *et al.*, 1995); and one carried out at VNIIM itself (Tarbeev *et al.*, 1989). [Note that although we have defined γ'_h to correspond to 25 °C, the temperature dependence of the shielded helion gyromagnetic ratio is expected to be significantly less than that of the shielded proton gyromagnetic ratio as given in Eq. (113). Thus small differences in temperature from 25 °C are ignored.]

a. *KRISS/VNIIM: Low field.* The sample used in the precision solenoid of the KRISS/VNIIM experiment was a low-pressure gaseous ^4He and ^{133}Cs cylindrical sample 40 mm in length and diameter. The quantity measured was the shielded gyromagnetic ratio of the $^4\text{He}(2^3\text{S}_1)$ atom using atomic magnetic resonance (AMR). (In the ^4He AMR technique, the ^4He atoms are polarized by means of metastable exchange with alkaline metal atoms polarized by optical pumping.) In a separate experiment the same ^4He sample was compared in air at an average temperature of 25 °C with a spherical low-pressure gaseous ^3He sample, thereby allowing γ'_h to be obtained (Shifrin *et al.*, 1997).

The single-layer precision solenoid had a winding length of 1020 mm, a diameter of 229 mm, and a winding pitch of 1 mm; it was wound with silver-plated copper wire 0.8 mm in diameter. The NIST technique of injecting current into the solenoid from five different current sources was used to generate a uniform magnetic flux density with significantly reduced dependence on the mean diameter of the solenoid. The dimensional measurement system was also very similar to that used in the NIST experiment, but it incorporated a number of refinements, including modification of the method of injecting ac current into selected groups of ten turns. Because the magnetic susceptibility of the ground under the solenoid was comparatively small, as was the magnetic dipole moment of the solenoid, a correction for the effect of the Earth was not required. Similarly, because of the comparatively small size of the solenoid's magnetic dipole moment and the distance between the solenoid and the sensor used in the system to compensate the Earth's magnetic field, a correction for the effect of the solenoid on the sensor was also not required. The working voltage and resistance standards employed in the experiment were calibrated in terms of the Josephson and quantum Hall effects using K_{J-90} and

R_{K-90} . The uncertainty of the experiment was dominated by Type B components associated with the measurement of the dimensions of the solenoid.

The result of the ^4He gyromagnetic ratio experiment, which was carried out at an average temperature of 25 °C, is (Shifrin *et al.*, 1998a; Shifrin, 1997)

$$\gamma^*(^4\text{He}) = \Gamma_{90}^*(^4\text{He}, \text{lo}) \frac{K_J R_K}{K_{J-90} R_{K-90}}, \quad (207a)$$

with

$$\Gamma_{90}^*(^4\text{He}, \text{lo}) = 1.760\,788\,19(31) \times 10^{11} \text{ s}^{-1} \text{ T}^{-1} \\ [1.8 \times 10^{-7}]; \quad (207b)$$

and the result of the ^4He – ^3He comparison experiment is (Shifrin *et al.*, 1997; Shifrin, 1997)

$$\frac{\gamma^*(^4\text{He})}{\gamma_h^*} = 864.022\,761(25) \quad [2.9 \times 10^{-8}], \quad (208)$$

where for both experiments the asterisk indicates that the measurements were carried out in air. Together these equations yield

$$\gamma_h^* = \Gamma_{h-90}^*(\text{lo}) \frac{K_J R_K}{K_{J-90} R_{K-90}}, \quad (209a)$$

with

$$\Gamma_{h-90}^*(\text{lo}) = 2.037\,895\,61(37) \times 10^8 \text{ s}^{-1} \text{ T}^{-1} \\ [1.8 \times 10^{-7}]. \quad (209b)$$

The only correction that needs to be applied to this result to convert it to the required form is $-1.156(20) \times 10^{-7} \Gamma_{h-90}^*(\text{lo})$ to account for the fact that the experiments were done in air. This leads to

$$\Gamma'_{h-90}(\text{lo}) = 2.037\,895\,37(37) \times 10^8 \text{ s}^{-1} \text{ T}^{-1} \\ [1.8 \times 10^{-7}]. \quad (210)$$

The value of α that may be inferred from Eq. (210) follows from the expression

$$\Gamma'_{h-90}(\text{lo}) = - \frac{K_{J-90} R_{K-90} g_e \mu'_h}{4 \mu_0 R_\infty} \frac{\mu'_h}{\mu_e} \alpha^3, \quad (211)$$

which is analogous to Eq. (192). We find

$$\alpha^{-1} = 137.035\,9853(82) \quad [6.0 \times 10^{-8}]. \quad (212)$$

b. VNIIM: Low field. The VNIIM low-field helion experiment was carried out in air at 23 °C with spherical low-pressure ^3He samples. The NMR frequency was measured by free precession with the ^3He atoms first polarized by optical pumping as was done in the VNIIM experiment that determined the shielded helion to shielded proton magnetic moment ratio (Belyi *et al.*, 1986). The magnetic field was produced by a four-section, single-layer precision solenoid 294 mm in diameter and 500 mm long with a total of 256 turns that generated a magnetic flux density of 0.57 mT with a

current of 1 A. The same solenoid was used in the magnetic moment ratio experiment of Belyi *et al.* (1986) and in the earlier VNIIM low-field proton gyromagnetic ratio experiment of Studentsov, Khorev, and Shifrin (1981). Many improvements were incorporated in the helion gyromagnetic ratio experiment based on the experience gained in the earlier proton gyromagnetic ratio experiment. For example, special attention was paid to the stability and calibration of the emfs of the standard cells used as the working voltage reference inasmuch as the site at which the experiment was carried out was 40 km away from the main VNIIM laboratories. Also, because the largest uncertainty component in the earlier proton gyromagnetic ratio experiment was due to the measurement of the diameter of the windings, the apparatus used to carry out those measurements was improved and the data were more complete—the diameter of each turn was determined at 12 points. Because the magnetic dipole moment of the solenoid used in the VNIIM experiment was comparatively small, as was the magnetic susceptibility of the ground underneath the solenoid, any correction for the effect of the ground was expected to be insignificant (Shifrin, 1997). The effect of the magnetic field of the solenoid on the system used to compensate the Earth's magnetic field was taken into account and an appropriate component of uncertainty was included in the experiment's uncertainty budget (Shifrin, 1997).

The result reported by Tarbeev *et al.* (1989) (Shifrin, 1997) may be written as

$$\gamma_h^* = \Gamma_{h-VNIIM}^*(\text{lo}) \frac{K_J}{K_{J-VNIIM}} \frac{\Omega_{VNIIM}}{\Omega} \quad (213a)$$

with

$$\Gamma_{h-VNIIM}^*(\text{lo}) = 2.037\,890\,11(71) \times 10^8 \text{ s}^{-1} \text{ T}^{-1} \\ [3.5 \times 10^{-7}], \quad (213b)$$

where the asterisk indicates that the experiment was performed in air. Additionally, $K_{J-VNIIM} = 483\,596.176 \text{ GHz/V}$ was the adopted value of K_J used by VNIIM to define its laboratory unit of voltage, and Ω_{VNIIM} is the VNIIM laboratory unit of resistance based on standard resistors at the time of the experiment, the mean date of which was 20 November 1987 (Shifrin, 1997). The principal components of uncertainty contributing to the quoted uncertainty arise from the measurements of the diameter and position of each turn, the diameter of the wire, the distribution of the current over the cross section of the wire, the overall shape of the winding, and the instability of the emfs of the standard cells.

The fractional corrections to be applied to this result are 3.565×10^{-6} to convert from $K_{J-VNIIM}$ to K_{J-90} ; $0.072(50) \times 10^{-6}$ to convert Ω_{VNIIM}/Ω to R_K/R_{K-90} ; and $-1.149(20) \times 10^{-7}$ for the effect of the air. The correction for Ω_{VNIIM} is based on a recent VNIIM analysis of a large body of data from VNIIM as well as other laboratories (Shifrin, 1997). Application of these corrections to Eq. (213) yields

$$\Gamma'_{h-90}(\text{lo}) = 2.037\,897\,29(72) \times 10^8 \text{ s}^{-1} \text{ T}^{-1}, \\ [3.5 \times 10^{-7}] \quad (214)$$

from which one may infer

$$\alpha^{-1} = 137.035\,942(16) \quad [1.2 \times 10^{-7}] \quad (215)$$

based on Eq. (211).

It is of interest to compare the VNIIM 1989 helion low-field result with the VNIIM 1981 proton low-field result. The value obtained by Studentsov *et al.* (1981) may be written as

$$\gamma_p^* = \Gamma_{p-VNIIM}^*(1\sigma) \frac{V}{\tilde{V}_{VNIIM}} \frac{\Omega_{VNIIM}}{\Omega} \quad (216a)$$

with

$$\Gamma_{p-VNIIM}^*(1\sigma) = 2.675\,1257(16) \times 10^8 \text{ s}^{-1} \text{ T}^{-1} \quad [6.0 \times 10^{-7}], \quad (216b)$$

where the asterisk indicates that the NMR sample was spherical, contained pure H_2O , and was at 24°C , and that the experiment was carried out in air. The quantities \tilde{V}_{VNIIM} and Ω_{VNIIM} are, respectively, the working unit of voltage based on standard cells used in the experiment and the VNIIM laboratory unit of resistance based on standard resistors on the mean date of the experiment, which was 1 September 1980 (Tarbeev, 1981). The value of α that we infer from the result in Eq. (216) is

$$\alpha^{-1} = 137.036\,208(28) \quad [2.0 \times 10^{-7}] \quad (217)$$

based on Eq. (192), the result $K_J = 483\,594.983(12) \times 10^9 \text{ GHz}/\tilde{V}_{VNIIM}$ (Tarbeev, 1981), the result $\Omega_{VNIIM} = [1 - 0.118(71) \times 10^{-6}] \Omega_{90}$ from the recent VNIIM analysis mentioned above (Shifrin, 1997), and corrections for temperature and air. We see that the difference between the 1989 and 1981 results is $8.3 u_{\text{diff}}$, where u_{diff} is the standard uncertainty of the difference, and thus that they strongly disagree. The origin of this disagreement is unknown, but the many improvements incorporated into the 1989 experiment give it preference over the 1981 experiment. Further, the value of α that one may infer from the 1981 result strongly disagrees with all other values. Thus, in keeping with our policy (see Sec. 1.4), we view the 1989 result as superseding the 1981 result.

3.4.3. Other Values

There are a number of other results from low- and high-field γ_p' experiments, some of which are nearly 50 years old. We do not consider these for a variety of reasons, such as a noncompetitive uncertainty, the tentative or preliminary nature of the result, the unavailability of critical information regarding the experiment, difficulties in relating laboratory electrical units to V_{90} and Ω_{90} , or such gross disagreement of the result with other data that it is obvious it contains a large systematic error. The more recent of these other values are from the following: a low-field experiment at the Electrotechnical Laboratory (ETL), Tsukuba, Japan (Nakamura, Kasai, and Sasaki, 1987); low- and high-field experiments at the Amt für Standardisierung, Messwesen und Warenprüfung (ASMW), Berlin, the former GDR (Forkert and Schle-

sok, 1986); a low-field experiment at the PTB (Weyand, 1985); and a low-field experiment at the NPL (Vigoureux and Dupuy, 1980). For reviews of these values as well as others, see Taylor and Cohen (1990); Cohen and Taylor (1987); Cohen and Taylor (1973); and Taylor *et al.* (1969).

3.5. Josephson Constant K_J

In this section we consider measurements of the Josephson constant K_J in its SI unit Hz/V . In the following three sections we consider measurements of the von Klitzing constant R_K in its SI unit Ω , the quantity $K_J^2 R_K$ in its SI unit $\text{J}^{-1} \text{s}^{-1}$, and the Faraday constant F in the unit $A_{90} \text{ s mol}^{-1}$, where A_{90} is the conventional unit of current based on the Josephson and quantum Hall effects and the conventional values K_{J-90} and R_{K-90} (see Sec. 2.5). Since all of these measurements involve K_J and/or R_K , the results are grouped in Table 11, together with the values of α and h that may be inferred from the data, assuming the validity of the relations $K_J = 2e/h$ and $R_K = h/e^2$.

The quantity K_J is determined by measuring a voltage U in terms of both a Josephson voltage $U_J(n) = nf/K_J$ (see Sec. 2.4.1) and the SI unit $\text{V} = \text{m}^2 \text{ kg s}^{-3} \text{ A}^{-1}$. The comparison can be direct, which leads to

$$K_J = nf \frac{U/U_J(n)}{U/V} \text{ V}^{-1}, \quad (218)$$

where U/V is the numerical value of U when U is expressed in the unit V (see Sec. 1.2). Alternatively, the voltage U can be compared to a laboratory unit of voltage V_{LAB} known in terms of a particular value of the Josephson constant $K_{J-\text{LAB}}$. In this case, the appropriate expression, in analogy with Eq. (29a), is

$$K_J = K_{J-\text{LAB}} \frac{U/V_{\text{LAB}}}{U/V}, \quad (219)$$

where U/V_{LAB} is the numerical value of U when U is expressed in the unit V_{LAB} . In either case (direct or in terms of V_{LAB}), U/V is determined by counterbalancing an electrostatic force arising from the voltage U with a known gravitational force.

3.5.1. NML: Hg Electrometer

The determination of K_J at the National Measurement Laboratory (NML) of the Commonwealth Scientific and Industrial Research Organization (CSIRO), Lindfield, Australia, was carried out by Clothier *et al.* (1989) using a liquid-mercury electrometer which was first proposed by Clothier (1965b) and had its origin in the attracted-disk electrometer described 130 years earlier by Harris (1834).

The NML Hg electrometer used a vertical electric field applied to the surface of a pool of Hg to elevate the pool to a height s of somewhat less than 1 mm relative to two adjacent Hg pools coupled to it but to which no field was applied. The electric field was produced by a voltage U of the order of several kilovolts or more applied to a metal film electrode

TABLE 11. Summary of data related to the Josephson constant K_J , the von Klitzing constant R_K , and the Faraday constant F , and inferred values of α and h .

Quantity	Value	Relative standard uncertainty u_r	Identification	Sec. and Eq.
K_J	483 597.91(13) GHz V ⁻¹	2.7×10^{-7}	NML-89	3.5.1 (221)
h	$6.626\,0684(36) \times 10^{-34}$ J s	5.4×10^{-7}		3.5.1 (223)
K_J	483 597.96(15) GHz V ⁻¹	3.1×10^{-7}	PTB-91	3.5.2 (226)
h	$6.626\,0670(42) \times 10^{-34}$ J s	6.3×10^{-7}		3.5.2 (227)
R_K	25 812.808 31(62) Ω	2.4×10^{-8}	NIST-97	3.6.1 (232)
α	137.036 0037(33)	2.4×10^{-8}		3.6.1 (233)
R_K	25 812.8071(11) Ω	4.4×10^{-8}	NML-97	3.6.2 (235)
α	137.035 9973(61)	4.4×10^{-8}		3.6.2 (236)
R_K	25 812.8092(14) Ω	5.4×10^{-8}	NPL-88	3.6.3 (237)
α	137.036 0083(73)	5.4×10^{-8}		3.6.3 (238)
R_K	25 812.8084(34) Ω	1.3×10^{-7}	NIM-95	3.6.4 (239)
α	137.036 004(18)	1.3×10^{-7}		3.6.4 (240)
$K_J^2 R_K$	$6.036\,7625(12) \times 10^{33}$ J ⁻¹ s ⁻¹	2.0×10^{-7}	NPL-90	3.7.1 (245)
h	$6.626\,0682(13) \times 10^{-34}$ J s	2.0×10^{-7}		3.7.1 (246)
$K_J^2 R_K$	$6.036\,761\,85(53) \times 10^{33}$ J ⁻¹ s ⁻¹	8.7×10^{-8}	NIST-98	3.7.2 (248)
h	$6.626\,068\,91(58) \times 10^{-34}$ J s	8.7×10^{-8}		3.7.2 (249)
\mathcal{F}_{90}	96 485.39(13) C mol ⁻¹	1.3×10^{-6}	NIST-80	3.8.1 (264)
h	$6.626\,0657(88) \times 10^{-34}$ J s	1.3×10^{-6}		3.8.1 (265)

on a fused silica optical flat a distance d of several millimeters above the pool. The relationship of s , U , and d is $|U| = kds^{1/2}$ with $k = (2\rho g/\epsilon_0\epsilon_r)^{1/2}$, where ρ is the density of the Hg, g is the local acceleration of free fall, $\epsilon_0 = 1/\mu_0 c^2$ is the electric constant, and ϵ_r is the relative permittivity of the gas between the electrode and the surface of the Hg pool. To eliminate surface effects on both U and d , the measurements were carried out at two different voltages U_1 and U_2 , with $|U_2| > |U_1|$, and spacings d_1 and d_2 chosen such that the electric field strengths U_1/d_1 and U_2/d_2 (and hence pool elevations s_1 and s_2) were approximately the same. In all cases d and s were measured interferometrically (Clothier, Sloggett, and Bairnsfather, 1980). The voltage difference $\Delta U = |U_2| - |U_1|$ is given by

$$\Delta U = k(d_2 s_2^{1/2} - d_1 s_1^{1/2}). \quad (220)$$

Since the values of k , d , and s were determined in SI units, the value of ΔU obtained from Eq. (220) was in the unit V. Further, since ΔU was also determined in terms of V_{NML} and the latter was based on the value $K_{J-\text{NML}} = 483\,594$ GHz/V, K_J could be obtained from Eq. (219).

Clothier *et al.* (1989) carried out their difficult experiment with great care; many subtle systematic effects were thoroughly investigated, including those associated with the interferometric measurements of d and s and with the forces acting on the Hg other than the assumed electrostatic and gravitational forces. The density of the Hg used in the experiment was determined by Patterson and Prowse (1985) [see also Patterson and Prowse (1988)] through comparisons with samples of known density as determined by Cook (1961) [see also Cook and Stone (1957)]. A total of 27 measurements of K_J were carried out in 1983 at three different

pairs of electrode spacings and two voltage polarities. The final result given by Clothier *et al.* (1989) based on 16 of those measurements is

$$K_J = 483\,594[1 + 8.087(269) \times 10^{-6}] \text{ GHz/V} \\ = 483\,597.91(13) \text{ GHz/V} \quad [2.7 \times 10^{-7}], \quad (221)$$

where the two principal relative standard uncertainty components contributing to the quoted uncertainty are 19×10^{-8} arising from the determination of k and 13×10^{-8} arising from the optical interferometry.

The value of g used by Clothier *et al.* (1989) was based on measurements carried out at NML in 1979 by a Russian team (Sloggett, 1994) using the absolute gravimeter ‘‘GABL’’ (Arnautov *et al.*, 1979). Similar measurements carried out at the same site in 1993 by a Japanese team (Sloggett, 1994; Hanada *et al.*, 1994) gave a result for g that was smaller than that obtained in 1979 by a fractional amount of about 0.14×10^{-6} , which may be compared to the 0.03×10^{-6} relative standard uncertainty of their difference. The 1993 value of g implies an increase in the value of K_J given in Eq. (221) by the fractional amount 0.07×10^{-6} . However, there is no basis for replacing the the Russian result by the Japanese result since the former has as an assigned uncertainty half that of the latter, the Russian result includes an assessment of possible systematic effects while the Japanese result does not, and difficulties with the Japanese apparatus during the course of the measurements severely curtailed the amount of data obtained (Sloggett, 1994). Further, in the international comparison of absolute gravimeters carried out at the BIPM in 1981 (Boulangier, Arnautov, and Scheglov, 1983), the Rus-

sian value of g obtained using GABL was consistent with the mean value of g obtained using a number of instruments at the fractional level of 1×10^{-8} .

As pointed out in Sec. 3.4, the fine-structure constant α and Planck constant h are central to the 1998 adjustment. Since the relative standard uncertainty of α is considerably less than that of the NML value of K_J , the value of h that may be inferred from it, if one assumes the validity of the relation $K_J = 2e/h$, is of particular interest. Based on the expression $\alpha = e^2/4\pi\epsilon_0\hbar = \mu_0ce^2/2h$, we have

$$h = \frac{8\alpha}{\mu_0cK_J^2}. \quad (222)$$

Using the value of K_J in Eq. (221) and the 1998 recommended value of α , we find

$$h = 6.626\,0684(36) \times 10^{-34} \text{ J s} \quad [5.4 \times 10^{-7}]. \quad (223)$$

3.5.2. PTB: Capacitor Voltage Balance

The determination of K_J at PTB was carried out by Funck and Sienknecht (1991) using a voltage balance consisting of two coaxial cylindrical electrodes 126 mm and 142 mm in diameter (Sienknecht and Funck, 1986; Sienknecht and Funck, 1985). The smaller, fixed inner electrode was suspended from a beam of a balance and the larger, movable outer electrode could be displaced in the vertical z direction relative to the suspended electrode. The nominal value of the change in capacitance C between the electrodes with displacement Δz was $\Delta C/\Delta z = 0.38 \text{ pF/mm}$. The displacement was measured interferometrically and was about 27 mm, corresponding to a change in capacitance of 10 pF. A 10 kV voltage U applied between the electrodes and measured in terms of the Josephson effect using the conventional value of the Josephson constant K_{J-90} , produced an electrostatic force F_e between them equal to the gravitational force on a 2 g standard of mass m_s . More specifically, $F_e = m_s g [1 - \rho(N_2)/\rho_s]$, where g is the local acceleration of free fall at the site of the balance, $\rho(N_2)$ is the mass density of the nitrogen gas with which the apparatus was filled, and ρ_s is the mass density of the standard of mass used to counterbalance the electrostatic force F_e .

The basic equation for the voltage balance is

$$U = \left[\frac{2(1+D)F_e}{\Delta C/\Delta z} \right]^{1/2}, \quad (224)$$

where the correction D is determined experimentally and accounts for the slight variation of F_e with displacement. This expression shows that in order to determine the voltage U in the unit V so that Eq. (219) can be used to obtain K_J , ΔC must be measured in its SI unit the farad F. This was done by means of a substitution bridge that compared ΔC to a 10 pF reference capacitor whose capacitance was determined in farads with a relative standard uncertainty of about 3.5×10^{-8} using the PTB calculable cross capacitor (Bachmair *et al.*, 1995); the total relative standard uncertainty assigned to the measurement of ΔC was about 1×10^{-7} .

The result reported by Funck and Sienknecht (1991) based on the mean of 48 pairs of values of K_J obtained in 1989, with the outer electrode both positive and negative with respect to the grounded inner electrode, is

$$K_J = K_{J-90} [1 - 0.027(274) \times 10^{-6}] \\ = 483\,597.89(13) \text{ GHz/V} \quad [2.7 \times 10^{-7}]. \quad (225)$$

The quoted uncertainty is dominated by Type B relative standard uncertainty components of approximately 2×10^{-7} , 1×10^{-7} , and 1×10^{-7} associated with the determination of m_s , U in terms of the Josephson effect and K_{J-90} , and Δz , respectively.

A comparison of capacitance standards in the late 1990s involving several European national metrology institutes indicated the existence of a possible error in the PTB calculable cross capacitor (Bachmair, 1997). The error, confirmed by the early results of a similar but international comparison being carried out under the auspices of the CCEM of the CIPM, was traced to a systematic error in the fringe-counting system used to determine the approximate 0.5 m displacement of the movable electrode of the PTB calculable capacitor and was exactly one fringe (Bachmair, 1999) [see Sec. 3.6 for a brief description of such capacitors]. This means that any capacitor calibrated in terms of the PTB calculable capacitor when the fringe-counting system was malfunctioning was assigned a value that was too small by the fractional amount 6.18×10^{-7} . Unfortunately, PTB researchers are unable to establish whether or not this error existed at the time in late 1989 when the 10 pF reference capacitor used in the PTB volt-balance experiment was calibrated; they believe that it is equally likely that the error was present as not present (Bachmair, 1999). Since K_J depends on the square root of the value assigned to the 10 pF reference capacitor, this could have introduced a fractional error of -3.09×10^{-7} in the value of K_J . To account for this possibility, we apply a fractional correction of $1.55(1.55) \times 10^{-7}$ to the originally reported value given in Eq. (225). This leads to

$$K_J = 483\,597.96(15) \text{ GHz/V} \quad [3.1 \times 10^{-7}], \quad (226)$$

from which we infer using Eq. (222),

$$h = 6.626\,0670(42) \times 10^{-34} \text{ J s} \quad [6.3 \times 10^{-7}]. \quad (227)$$

3.5.3. Other Values

A result from the Laboratoire Central des Industries Électrique (LCIE), Fontenay-aux-Roses, France with a relative standard uncertainty of 2.4×10^{-6} , obtained using a Kelvin electrometer, was initially considered as an input datum in the 1986 adjustment, but was later deleted because of its noncompetitive uncertainty (Cohen and Taylor, 1987); it was not considered by the CCEM in its analysis of values of K_J that led to K_{J-90} (Taylor and Witt, 1989).

The result of Bego and colleagues with a relative standard uncertainty of 3.5×10^{-7} obtained in 1987–1988 at the University of Zagreb, Republic of Croatia, using a capacitor voltage balance with flat-plate electrodes, was initially con-

sidered by the CCEM in its analysis but was ultimately rejected because of its significant disagreement with other values (Taylor and Witt, 1989). Subsequently, Bego and colleagues identified several unsuspected systematic errors in their experiment due mainly to the difference in the ac and dc capacitance of the balance electrodes arising from surface effects, the measurement of the displacement of the movable electrode, and the voltage dependence of the capacitance of the electrodes, but they were unable to retroactively correct their 1987–1988 result (Bego *et al.*, 1993).

In principle, ampere balance experiments could provide information on the value of K_J , and the results of six such experiments with relative standard uncertainties in the range 4.1×10^{-6} to 9.7×10^{-6} were initially considered in the 1986 adjustment (Cohen and Taylor, 1987). However, all were eventually discarded because of their disagreement with the other data and/or their negligible weight. No new ampere balance results have become available or are expected in the future; such experiments have been replaced by those involving voltage balances or moving-coil watt balances (see Sec. 3.7).

3.6. von Klitzing Constant R_K

The quantity R_K is determined by measuring a resistance R in terms of both the resistance $R_H(i) = R_K/i$ of the i th quantized Hall resistance (QHR) plateau (see Sec. 2.4.2) and the SI unit $\Omega = \text{m}^2 \text{kg s}^{-3} \text{A}^{-2}$. The comparison can be direct, in which case we have

$$R_K = i \frac{R/\Omega}{R/R_H(i)} \Omega, \quad (228)$$

where R/Ω is the numerical value of R when R is expressed in the unit Ω (see Sec. 1.2); or instead, the resistance R can be compared to a laboratory unit of resistance Ω_{LAB} known in terms of a particular value of the von Klitzing constant $R_{K-\text{LAB}}$. In this case the relevant relation, in analogy with Eq. (29b), is

$$R_K = R_{K-\text{LAB}} \frac{R/\Omega}{R/\Omega_{\text{LAB}}}, \quad (229)$$

where R/Ω_{LAB} is the numerical value of R when R is expressed in the unit Ω_{LAB} . In either case (direct or in terms of Ω_{LAB}), R/Ω is determined using a calculable cross capacitor.

The calculable cross capacitor is based on a theorem in electrostatics discovered by Thompson and Lampard (1956) (Lampard, 1957). The theorem allows one to construct a cylindrical capacitor (Thompson, 1959) whose capacitance, to high accuracy, depends only on its length. (The electric constant $\epsilon_0 = 1/\mu_0 c^2$ is also required but is exactly known, since in the SI μ_0 and c are exactly known.) In its most accurate practical form (Clothier, 1965a), the calculable cross capacitor consists of four long, parallel, identical cylindrical bars in vacuum with small gaps between their surfaces and oriented vertically with their axes forming a square array. In addition, there are grounded cylindrical guard electrodes centered between the bars at either end of the array, one of which is

movable and the other fixed, and both of which are inserted part way into the array along its axis. For such a configuration, the cross capacitance between diagonally opposite bars is independent of their diameter and is determined by the distance between the two guard electrodes. In practice, the known change in capacitance due to an interferometrically measured displacement of the movable electrode relative to the fixed electrode is compared to the resistance of a reference resistor through a chain of impedance comparisons which we discuss in connection with particular experiments. A displacement of the movable electrode of about 25 cm leads to a change in cross capacitance of about 0.5 pF.

The uncertainty of R_K is determined mainly by the quality and implementation of the design of the calculable capacitor and the apparatus used to compare its capacitance to the resistance of the reference resistor, and the extent to which systematic effects are understood. These effects include geometrical imperfections in the calculable capacitor, voltage dependences of capacitance standards, calibrations of transformer ratios, and the difference in ac and dc resistance of the reference resistor, since the impedance measurements are carried out at ac (for example, $\omega = 10^4$ rad/s or approximately 1592 Hz) and the QHR measurements are carried out at dc. The uncertainty of the comparison of R with $R_H(i)$ or Ω_{LAB} is usually rather smaller than the combined uncertainties of the calculable capacitor and impedance chain.

As noted in Sec. 2.4.2, if one assumes the validity of the relation $R_K = h/e^2$, R_K and the fine-structure constant α are related by

$$\alpha = \frac{\mu_0 c}{2R_K}. \quad (230)$$

Since μ_0 and c are exactly known, the relative uncertainty of the value of α that may be inferred from a particular experimental value of R_K is the same as the relative uncertainty of that value.

3.6.1. NIST: Calculable Capacitor

The first NIST calculable cross-capacitor measurements were reported nearly 40 years ago by Cutkosky (1961). He used a capacitor consisting of horizontal bars to determine the NIST (then the National Bureau of Standards, NBS) laboratory unit of resistance based on 1 Ω standard resistors in terms of the ohm, $\Omega_{\text{NIST}}/\Omega$, with a relative standard uncertainty of about 3×10^{-6} . A new vertical capacitor of the now classic geometry described above and pioneered by Clothier (1965a) at NML (then the National Standards Laboratory, NSL) was constructed starting in the late 1960s and culminated in a measurement of $\Omega_{\text{NIST}}/\Omega$, reported in 1974, with a relative standard uncertainty of 2.7×10^{-8} (Cutkosky, 1974). Using the same system, but with a number of improvements, a value for $\Omega_{\text{NIST}}/\Omega$ was reported in 1989 by Shields *et al.* (1989) with a relative standard uncertainty of 2.2×10^{-8} ; and based on this result and measurements at the same time by Cage *et al.* (1989a) of $R_H(4)$ of a GaAs/AlGaAs heterostructure in terms of Ω_{NIST} , Cage *et al.* (1989b) reported

$$R_K = 25\,812.8[1 + 0.280(24) \times 10^{-6}] \, \Omega$$

$$= 25\,812.807\,23(61) \, \Omega \quad [2.4 \times 10^{-8}]. \quad (231)$$

The NIST work to determine R_K continued, focusing on the acquisition of more data and the investigation and elimination of possible sources of systematic error. Based on this new effort, in 1997 Jeffery *et al.* (1997) and Jeffery *et al.* (1998) reported

$$R_K = 25\,812.8[1 + 0.322(24) \times 10^{-6}] \, \Omega$$

$$= 25\,812.808\,31(62) \, \Omega \quad [2.4 \times 10^{-8}], \quad (232)$$

which exceeds the 1989 result by the fractional amount 4.2×10^{-8} .

The calculable capacitor and impedance chain used to obtain the 1997 result were essentially the same as those used to obtain the 1974 and 1989 results. In brief, the known 0.5 pF change of capacitance of the NIST calculable cross capacitor is compared, using a two-terminal-pair transformer bridge, to the capacitance of a fixed 10 pF portable standard, which in turn is used to calibrate a bank of five similar 10 pF standards maintained in an oil bath using a two-terminal-pair 10:1 transformer bridge. These standards and a 10:1 four-terminal-pair direct reading ratio set are then used to calibrate a 100 pF capacitor, and that capacitor and the ratio set are used to calibrate two 1000 pF capacitors. These in turn are employed as two arms of a frequency-dependent quadrature bridge to determine the ac resistance of two 100 k Ω resistors. Each of these is then compared, using a 100:1 equal-power resistance bridge, to a 1000 Ω transportable resistor called R311. The difference in ac and dc resistance of R311 is determined by comparing it to a special coaxial straight-wire resistor of calculable ac/dc difference. All ac measurements are done at 1592 Hz.

Starting in the early 1990s, a cryogenic current comparator (CCC) was used to compare $R_H(4)$ and $R_H(2)$ to a 100 Ω reference resistor and to compare that resistor to R311. Prior to this time, $R_H(4)$ was compared to 6453.2 Ω reference resistors using a potentiometric technique and these were then compared, using classical dc scaling methods based on a Hamon resistor, to the 1 Ω resistors that defined Ω_{NIST} . The resistor R311 was also compared to the 1 Ω resistors using such classical methods.

The likelihood that the 1989 NIST value of R_K was in error became fully apparent to the NIST researchers in the early 1990s. Every effort was then made to understand the cause of the error. All critical aspects of the experiment, on both the ac side and the dc side, were exhaustively checked but to little avail. It was concluded that about 0.4×10^{-8} of the 4.2×10^{-8} shift between the 1989 and 1997 values was probably due to a loading effect on the 6453.2 Ω resistors used in the pre-1990 measurements of $R_H(4)$, as mentioned in Sec. 3.4.1.a, and that the ratio of the current transformer in the 100:1 resistance bridge used to measure R311 in terms of the 100 k Ω ac resistors (see above), which had a history of being

extremely stable and thus was not checked in the earlier experiment, might have shifted unexpectedly at the time of those measurements.

Because the 1997 NIST value of R_K given in Eq. (232) is based on a much more extensive body of data than is the 1989 value, including the results of an extremely thorough investigation of possible systematic errors, we use only the 1997 value in the 1998 adjustment. This is consistent with the view of Jeffery *et al.* (1998) that the newer result supersedes the earlier result. The 2.4×10^{-8} relative standard uncertainty of this value, which is smaller by about a factor of 2 than the next most accurate measured value of R_K , consists of the following major components (mainly Type B): 1.9×10^{-8} associated with measurement of the bank of 10 pF capacitors in terms of the NIST calculable cross capacitor, which includes 1.5×10^{-8} from possible geometrical imperfections of the calculable capacitor; 1.3×10^{-8} associated with measurement of R311 in terms of the 10 pF bank; and 0.7×10^{-8} associated with measurement of R311 in terms of $R_H(2)$ and $R_H(4)$. The value of α that may be inferred from the NIST 1997 value of R_K is, from Eq. (230),

$$\alpha^{-1} = 137.036\,0037(33) \quad [2.4 \times 10^{-8}]. \quad (233)$$

3.6.2. NML: Calculable Capacitor

Clothier (1965a) completed the construction of his pioneering calculable cross capacitor at NML in the early 1960s. At the same time he and NML colleagues developed the ac and dc apparatus required to relate its known capacitance to the 1 Ω resistance standards on which Ω_{NML} was based. The complete system was functional in 1963, at which time measurements of $\Omega_{\text{NML}}/\Omega$ commenced. Results obtained in 1964 and 1967, together with a detailed description of the system and its uncertainty, were given by Thompson (1968). The system was used on a regular basis to maintain Ω_{NML} until the introduction by the CIPM, starting 1 January 1990, of the ohm representation based on the QHE and the conventional value R_{K-90} (see Sec. 2.5). Small (1987) briefly summarized the results obtained through 1986, described the improvements made to the system since it was first used, discussed a correction that had to be applied retroactively to the results obtained starting in 1974, and reassessed the uncertainty of the system. He concluded that a resistance of one ohm could be determined in ohms with a relative standard uncertainty of 6.2×10^{-8} .

Based on such calculable capacitor measurements and measurements of $R_H(4)$ of one GaAs/AlGaAs heterostructure and $R_H(2)$ of another in terms of 1 Ω resistance standards, Ricketts and Cage (1987) reported $R_K = 25\,812.8099(20) \, \Omega \quad [7.8 \times 10^{-8}]$. This work was carried out from November 1985 to May 1986. Subsequently the NML calculable capacitor was dismantled, carefully checked, and reassembled, the QHR measurement system was improved, and additional measurements were carried out over the period December 1987 to April 1988. From the new data, and the earlier data after minor adjustment based on

information gained during the course of the new measurements, Small, Ricketts, and Coogan (1989) obtained

$$R_K = 25\,812.8[1 + 0.363(66) \times 10^{-6}] \, \Omega \\ = 25\,812.8094(17) \, \Omega \quad [6.6 \times 10^{-8}]. \quad (234)$$

In the NML system, a $\frac{1}{6}$ pF change in capacitance of the calculable capacitor is compared to that of a $\frac{1}{6}$ pF reference capacitor, which in turn is compared to the capacitance of two other similar capacitors. The 0.5 pF capacitance of the three in parallel is then compared to the capacitance of two 5 nF capacitors in four 10:1 steps. These two capacitors are subsequently used in a frequency-dependent quadrature bridge to determine the ac resistance of two 20 k Ω resistors, and the ac/dc difference in resistance of the two in parallel is determined using a 10 k Ω transfer resistor of known ac/dc difference. Finally, the dc resistance of the two parallel 20 k Ω resistors is compared to the 1 Ω reference resistors used to maintain Ω_{NML} using a Hamon resistor of ratio $10^4:1$. All ac measurements are carried out at 1592 Hz. In the NML QHR measurement system, $R_H(4)$ is compared potentiometrically to a 6453.2 Ω reference resistor, $R_H(2)$ to two such resistors in series, and the 6453.2 Ω resistors are compared to the 1 Ω reference resistors used to maintain Ω_{NML} via a Hamon resistor of ratio $6453\frac{4}{9}:1$.

As part of the December 1987 to April 1988 redetermination of R_K , a possible error in the NML calculable capacitor due to the spreading of the four main bars as the upper movable guard electrode is lowered was investigated and a fractional correction for this effect of 6.4×10^{-8} was incorporated into the reported result. To check the reliability of this correction and to eliminate the need for it in future measurements, a compensating spike was added to the end of the fixed guard electrode after the redetermination was completed. Subsequent measurements uncovered an unsuspected error in the calculable capacitor arising from the need to tilt the lower guard electrode in order to align the interferometer used to determine the displacement of the movable guard electrode (Small *et al.*, 1997). This error was eliminated and a new determination of R_K undertaken after the calculable capacitor was dismantled, cleaned, and reassembled, and after a number of improvements were incorporated in both the ac and dc measurement systems. The reliability of the QHR portion of the system was subsequently confirmed through comparisons with BIPM (Small *et al.*, 1997) and NIST (Jeffery *et al.*, 1997) using 1 Ω traveling resistors.

Based on measurements carried out from December 1994 to April 1995 and a complete reassessment of uncertainties, in 1997 Small *et al.* (1997) reported

$$R_K = R_{K-90}[1 + 0.4(4.4) \times 10^{-8}] \\ = 25\,812.8071(11) \, \Omega \quad [4.4 \times 10^{-8}], \quad (235)$$

where the quoted relative standard uncertainty consists of the following principal components: 3.2×10^{-8} associated with the calculable capacitor, which includes 3.0×10^{-8} due to geometrical imperfections; 2.4×10^{-8} associated with linking of the calculable capacitor to the 1 Ω standard resistors

used to maintain Ω_{NML} ; and 1.9×10^{-8} associated with measurement of $R_H(i)$ in terms of these resistors. Because of the problems associated with the 1989 value of R_K , we use the result reported in 1997 as the NML value of R_K in the 1998 adjustment. The value of α it implies is

$$\alpha^{-1} = 137.035\,9973(61) \quad [4.4 \times 10^{-8}]. \quad (236)$$

3.6.3. NPL: Calculable Capacitor

The NPL calculable cross capacitor (Rayner, 1972) is similar in design to those of NIST and NML and the impedance chain that links it to a 1 k Ω resistor (Jones and Kibble, 1985) is similar to that of NIST with all ac measurements being carried out at 1592 Hz. The 0.4 pF capacitance change of the NPL calculable capacitor is stepped up to 10 pF, then to 1000 pF in three 10:1 steps, transferred to a 100 k Ω ac resistance using a frequency-dependent quadrature bridge, and stepped down to a 1 k Ω ac resistance in a single 100:1 step. In the initial work (Jones and Kibble, 1985; Hartland, Davies and Wood, 1985) the dc resistance of this resistor was determined by comparing it at ac and dc to two quadrifilar resistors whose ac resistance at 1592 Hz and dc resistance is the same. In subsequent work (Hartland *et al.*, 1987; Hartland, Jones, and Legg, 1988), instead of determining the ac/dc difference of the 1 k Ω resistor, such a quadrifilar resistor was measured at ac and then compared at dc with a group of four 1 k Ω resistors, two of which were then used to determine the resistance of the 100 Ω resistors used in the QHR measurements. The relative standard uncertainty for linking a 10 pF capacitor to the calculable capacitor is 2.8×10^{-8} , which includes the uncertainty associated with the calculable capacitor itself, and that for linking a so-calibrated 10 pF capacitor to one of the 100 Ω QHR resistors is 4.4×10^{-8} .

The result for R_K reported in 1988 by NPL is (Hartland *et al.*, 1988)

$$R_K = R_{K-90}[1 + 0.356(54) \times 10^{-6}] \\ = 25\,812.8092(14) \, \Omega \quad [5.4 \times 10^{-8}] \quad (237)$$

and was obtained by comparing the $i=2$ plateau of a GaAs/AlGaAs heterostructure to a 200 Ω resistor using a cryogenic current comparator. The latter resistor consisted of two 100 Ω resistors calibrated in terms of the 1 k Ω resistors known in terms of the calculable capacitor as described above. The relative standard uncertainty of the $R_H(2)$ to 200 Ω resistance comparison is 1.0×10^{-8} . The 1988 NPL value of R_K is consistent with values given earlier when the calculable capacitor and the impedance chain were in a less refined state and when the QHR measurement system was being developed; in 1987 Hartland *et al.* (1987) reported $R_K = 25\,812.8106(17) \, \Omega$ [6.7×10^{-8}], while in 1985 Hartland *et al.* (1985) reported $R_K = 25\,812.8083(46) \, \Omega$ [1.8×10^{-7}]. The value of α that one may infer from the NPL 1988 value of R_K is

$$\alpha^{-1} = 137.036\,0083(73) \quad [5.4 \times 10^{-8}]. \quad (238)$$

3.6.4. NIM: Calculable Capacitor

The NIM calculable cross capacitor (Zhang, 1985) differs markedly from the now classic version of Clothier used at NIST, NML, and NPL. The four bars are horizontal and the length that determines its known 0.5 pF capacitance is the fixed distance between two narrow insulating gaps about 8 μm wide in two of the four bars. This distance, about 256 mm, is determined by the NIM length metrology laboratory using modern dimensional measurement techniques. The two bars with gaps, called detector electrodes, are actually well-ground fused silica tubes covered with a vacuum-evaporated Cr–Al–Cr composite film 0.1 μm thick with the gaps formed using a photoetching technique.

In the NIM experiment to determine R_K , the dc resistance of a transportable 1 k Ω resistor used in connection with the QHR measurements was determined in terms of the known 0.5 pF capacitance of the NIM calculable capacitor through an impedance chain in which the 0.5 pF capacitance is stepped up to 1 nF in one 2:1 and three 10:1 steps using a two-terminal transformer bridge, and then to 10 nF using a four-terminal arrangement of the bridge. This capacitance is compared to the ac resistance of a 10 k Ω resistor using a quadrature bridge, which is then compared to the resistance of the 1 k Ω transportable resistor using a four-terminal transformer bridge (Ruan *et al.*, 1988; Zhang *et al.*, 1995). The difference between the ac and dc resistance of this resistor was determined by comparing it to a special 1 k Ω resistor whose ac/dc difference could be calculated from its dimensions. Again, all ac measurements were carried out at 1592 Hz.

The NIM QHR measurements were carried out using several different GaAs/AlGaAs heterostructures biased on the $i=2$ plateau (Zhang *et al.*, 1995; Zhang *et al.*, 1993; Zhang *et al.*, 1992; Zhang *et al.*, 1991). The NIM system for relating $R_H(2)$ to a resistance of 1 k Ω is based on 1:1 potentiometric resistance comparisons and two specialized resistance networks. A number of improvements were incorporated in the system since it was first described by Zhang *et al.* (1991) and the quoted relative standard uncertainty of relating $R_H(2)$ to the resistance of the 1 k Ω transportable resistor is now 1.4×10^{-8} (Zhang *et al.*, 1995). The relative standard uncertainty of the 0.5 pF capacitance of the calculable capacitor is given as 10×10^{-8} and that for relating the impedance of the capacitor to the resistance of the 1 k Ω transportable resistor is 8.4×10^{-8} . The final result for R_K , as reported in 1995 by Zhang *et al.* (1995), is

$$R_K = 25\,812.8084(34) \, \Omega \quad [1.3 \times 10^{-7}], \quad (239)$$

where it should be noted that the significantly smaller uncertainty of the NIM calculable capacitor and impedance chain given by Zhang *et al.* (1995) compared to that given by Ruan *et al.* (1988) and by Zhang (1985) is due to significant improvements in the apparatus and the evaluation of all uncertainty components as estimated standard deviations (Liu, 1998).

The value of R_K given in Eq. (239) agrees with the value $25\,812.8055(156) \, \Omega$ [6.1×10^{-7}] reported in 1988 by Zhang *et al.* (1988). It was obtained using the NIM calculable capacitor in a less developed state, a more conservative approach to uncertainty evaluation in use at NIM at the time, and a different and less accurate QHR measurement system. The value of α that may be inferred from the 1995 NIM result is

$$\alpha^{-1} = 137.036\,004(18) \quad [1.3 \times 10^{-7}]. \quad (240)$$

3.6.5. Other Values

In addition to those discussed above, three values of R_K directly based on calculable capacitor measurements, with quoted relative standard uncertainties of 22×10^{-8} , 26×10^{-8} , and 32×10^{-8} , have been reported. These values were obtained by researchers at LCIE (Delahaye *et al.*, 1987), ETL (Shida *et al.*, 1989), and at VNIIM together with colleagues at the Institute of Metrological Service (IMS), Moscow (Kuznetsov *et al.*, 1988). Because their uncertainties are 9 to 13 times larger than the 2.4×10^{-8} uncertainty of the NIST value of R_K , which has the smallest uncertainty, and because all seven values of R_K are consistent, we follow the principles given in Sec. 1.4 and do not include these three additional values as input data.

3.7. Product $K_J^2 R_K$

A value of the product $K_J^2 R_K$ is of importance to the determination of the Planck constant h , because if one assumes the relations $K_J = 2e/h$ and $R_K = h/e^2$ are valid, then

$$h = \frac{4}{K_J^2 R_K}. \quad (241)$$

In analogy with the determination of K_J and R_K (see Secs. 3.5 and 3.6), the product $K_J^2 R_K$ can be determined by measuring a power P in terms of both a power $P_e(n, i) = U_J^2(n)/R_H(i)$ and the SI unit $\text{W} = \text{m}^2 \text{kg s}^{-3}$, with $U_J(n) = n f/K_J$ and $R_H(i) = R_K/i$. If the comparison is direct, the applicable expression is

$$K_J^2 R_K = n^2 f^2 i \frac{P/P_e(n, i)}{P/W} \text{W}^{-1}, \quad (242)$$

where P/W is the numerical value of P when P is expressed in the unit W . If instead the power P is compared to a laboratory unit of power $W_{\text{LAB}} = V_{\text{LAB}}^2/\Omega_{\text{LAB}}$, where the laboratory units of voltage and resistance V_{LAB} and Ω_{LAB} are known in terms of particular values of the Josephson constant $K_{J-\text{LAB}}$ and von Klitzing constant $R_{K-\text{LAB}}$, respectively, then the applicable expression, in analogy with Eq. (29d), is

$$K_J^2 R_K = K_{J-\text{LAB}}^2 R_{K-\text{LAB}} \frac{P/W_{\text{LAB}}}{P/W}. \quad (243)$$

A practical approach that allows $K_J^2 R_K$ to be determined with high accuracy based on the above formulation was first proposed by Kibble at NPL nearly 25 years ago (Kibble,

1975). Kibble's idea is elegantly simple and was a direct outgrowth of his measurement with Hunt of the shielded proton gyromagnetic ratio γ'_p by the high-field method (see Sec. 3.4.1.c).

The basic principle is illustrated by the following simplified example. Consider a straight, conducting wire of length l carrying a current I in a uniform applied magnetic flux density B perpendicular to l . The force on the conductor is $F_e = BIl$, and if this force is balanced by the gravitational force on a mass standard with mass m_s , then $BIl = m_s g$, where g is the local acceleration of free fall. If the same conductor without an applied current is moved with velocity v in a direction perpendicular to B and l , a voltage $U_v = Blv$ is induced across its ends. The elimination of the product Bl leads to

$$U_v I = F_e v = m_s g v. \quad (244)$$

If U_v is measured by means of the Josephson effect, I is measured by means of both the Josephson and quantum Hall effects, and m_s , g , and v are measured in their respective SI units, then the same power $P = U_v I$ will be known both in terms of these effects and in terms of the SI watt, thereby determining $K_J^2 R_K$. The beauty of Kibble's approach is that it does not require measuring the dimensions of an object or a magnetic flux density; the only length measurement required is that needed to determine a velocity. In practice, the movable conductor is a coil with many turns, hence such an apparatus has come to be called a moving-coil watt balance. To date two laboratories, NPL and NIST, have determined $K_J^2 R_K$ using this method.

3.7.1. NPL: Watt Balance

Shortly after Kibble's original proposal of 1975, Kibble and Robinson (1977) carried out a theoretical study of its feasibility based on the NPL apparatus used to determine γ'_p by the high-field method (Kibble and Hunt, 1979). This apparatus was then appropriately modified, and the promising progress made with it was reported in 1983 by Kibble, Smith, and Robinson (1983). The final result of the experiment was given in 1990 by Kibble, Robinson, and Belliss (1990). That result may be written as

$$\begin{aligned} K_J^2 R_K &= K_{J-NPL}^2 R_{K-NPL} [1 + 16.14(20) \times 10^{-6}] \\ &= 6.036\,7625(12) \times 10^{33} \text{ J}^{-1} \text{ s}^{-1} \\ &\quad [2.0 \times 10^{-7}], \end{aligned} \quad (245)$$

where $K_{J-NPL} = 483\,594 \text{ GHz/V}$ and $R_{K-NPL} = 25\,812.809\,2 \text{ } \Omega$.

The magnetic flux density used in the NPL experiment was 0.7 T and was generated by a permanent magnet. The moving coil consisted of two flat rectangular coils above one another in a vertical plane and connected in series opposition. Its total number of turns was 3362, its mean width 0.25 m, and its mass about 30 kg. When carrying a current I of 10 mA in the 0.7 T flux density, the change in force ΔF on the coil upon reversal of the current, which corresponds to

twice the force F_e of Eq. (244), was equal to the gravitational force on a 1 kg standard of mass. The current I was determined by placing a reference resistor of resistance $R = 100 \text{ } \Omega$ known in terms of R_{K-NPL} in series with the coil and measuring the 1 V potential difference U_r across its terminals in terms of V_{NPL} , which was defined in terms of the Josephson effect and K_{J-NPL} . The coil was suspended between the pole faces of the magnet from one end of a massive balance beam and the change in force ΔF was determined by substitution weighing in such a way that the balance beam was always in a horizontal position.

The measurement of ΔF and I as just described gives the quotient F_e/I of the quantities F_e and I in Eq. (244). The quotient U_v/v of the quantities U_v and v in Eq. (244) was obtained by rotating the balance around its central knife edge in such a way that the coil, now in its open circuit mode, moved $\pm 15 \text{ mm}$ about its central position (i.e., balance beam horizontal) at a velocity of 2 mm/s. The velocity was determined interferometrically and the 1 V induced voltage U_v across the coil was measured in terms of V_{NPL} and hence in terms of K_{J-NPL} . The quotient v/U_v was determined at five different points along the coil's trajectory when it was ascending or descending, a parabolic curve fitted to these points, and the quotient at the coil's central position calculated. This procedure was necessary, because the flux density was not perfectly uniform over the coil's trajectory.

The final NPL result given in Eq. (245) is the unweighted mean of 50 values obtained from July 1987 to May 1988. A result based on the unweighted mean of 27 values obtained from January 1985 to June 1985 agrees with it, but the uncertainty of the earlier result is four times larger. Because of this large difference in uncertainty and the many minor improvements in equipment and measurement technique incorporated in the 1987/1988 measurements, Kibble *et al.* (1990) took no account of the earlier data in arriving at their final result. Of the 50 1987/1988 values, 12 were obtained with a coil current of 5 mA and a 0.5 kg mass standard. The statistical (Type A) relative standard deviation of the 50 values is 3.3×10^{-7} and the relative standard deviation of their mean is 0.47×10^{-7} . The principal components of relative standard uncertainty due to possible systematic effects, all of which were obtained from Type B evaluations, are 1.1×10^{-7} associated with the measurement of voltage and 0.5×10^{-7} associated with the refractive index and density of air (the entire experiment was carried out in air, including the interferometric measurements of v and the weighings).

During the course of their work, Kibble *et al.* (1990) searched for and eliminated many systematic errors. The effects studied included coil misalignment, simple and torsional pendulum-like motions of the coil, the effect of the current in the coil on the permanent magnet, and the dependence of the measured value of $K_J^2 R_K$ on coil velocity. However, Kibble *et al.* (1990) could not completely account for the observed variations among the 50 values. In particular, the four values obtained from 15 February 1988 to 24 February 1988 deviated from the mean of all 50 values by an unexpectedly large amount. Nevertheless, since in general as

many changes as possible were made between measurement runs and there was no reason to believe that any of these changes introduced a systematic error, Kibble *et al.* (1990) did not include any additional component of uncertainty to account for the possibility that the variations between values were not entirely due to random effects.

For the purpose of the 1998 adjustment, Kibble and Robinson (1998) reconsidered their uncertainty assignment and suggested that, to allow for this possibility, the data should be viewed as a collection of five uncorrelated groups of data with different means, and therefore the statistical standard deviation of the mean is obtained by dividing the 3.3×10^{-7} statistical relative standard deviation of the 50 values by $\sqrt{5}$ rather than $\sqrt{50}$. The uncertainty quoted in Eq. (245) reflects this suggestion. The value of h that may be inferred from the 1990 NPL value of $K_J^2 R_K$ according to Eq. (241) is

$$h = 6.626\,0682(13) \times 10^{-34} \text{ J s} \quad [2.0 \times 10^{-7}]. \quad (246)$$

Based on the experience gained in the experiment just described, a new apparatus has been designed and constructed at NPL by Robinson and Kibble (1997) that is expected to yield a relative standard uncertainty of the order of 1×10^{-8} . The apparatus, which has the cylindrical symmetry of the NIST apparatus to be described in the next section, uses the same balance beam but little else from the earlier experiment. Two horizontal circular coils, one above the other on the same cylindrical form, are suspended from one end of the balance beam. Each coil is in the radial magnetic flux density in the gap between two concentric annular permanent magnets.

The coils have 340 turns each and are about 330 mm in diameter. Much of the apparatus—magnet, coils, interferometer for measuring the position of the coils, and balance—are in a vacuum chamber to eliminate the uncertainty associated with the refractive index and density of air. The magnitude of the induced voltage U_v and force F_e are the same as in the earlier apparatus. However, to significantly reduce the uncertainty of the voltage measurements in both the U_v/v and F_e/I portions of the experiment, and to simplify how the experiment is carried out, the apparatus is directly connected to the NPL Josephson array voltage standard. Although the array standard is some 60 m away in another building, the watt-balance experimenters are able to select, with a relative standard uncertainty of about 1×10^{-9} , any Josephson voltage less than 1.5 V and directly measure both the induced voltage U_v and the voltage U_r across the series reference resistor. As a consequence, within broad ranges, coil traversals may be carried out at any velocity and weighings with any standard of mass. Further, although the NPL quantum Hall effect resistance standard is also located 60 m away, it too has been connected to the apparatus; an automated calibration of the reference resistor in terms of R_{K-90} is now done every few months with a relative standard uncertainty approaching 1×10^{-9} . Many other improvements and refinements have been incorporated in the new apparatus as well, including an on-site absolute gravimeter for determining g as

needed with a relative standard uncertainty significantly less than 1×10^{-8} . However, no result for $K_J^2 R_K$ has been reported at the time of writing (October 1999).

3.7.2. NIST: Watt Balance

Work on a moving-coil watt balance at NIST began shortly after Kibble proposed his new approach. Preliminary studies were carried out with a Pellat-type “electrodynamometer” consisting of a rotatable coil with its axis vertical resting on a balance and immersed in the uniform horizontal magnetic flux density at the center of a long solenoid (Olsen, Phillips, and Williams, 1984; Olsen *et al.*, 1980a).

At the same time, a special vertical magnet (1.5 m high, 240 mm nominal radius) consisting of upper and lower superconducting solenoids and smaller compensation windings, connected in series opposition, was designed and constructed (Olsen, Phillips, and Williams, 1980b; Chen *et al.*, 1982). The solenoids generate, for a current of about 5 A in the solenoids and 66 mA in the compensation windings, an axially symmetric radial flux density of about 0.1 T in the region traversed by a moving coil that encircles the solenoids in the watt-balance experiment. The magnetic flux density over the vertical extent of this region has a fractional variation of less than 0.05 % and the product Br , where r is the radial distance from the axis of the solenoids, has a fractional variation of a few times 10^{-6} . These characteristics of the flux density keep the variations of U_v/v and F_e/I over the moving coil’s trajectory within reasonable bounds and ensure that, if the diameter of the moving coil changes due to small changes in temperature, or if the coil’s axis does not exactly coincide with the axis of the solenoids, significant errors do not occur. The superconducting solenoid is, of course, in a liquid helium Dewar, with the moving coil in the air outside.

In order to avoid the additional complexities that the superconducting solenoid would introduce while they developed the other portions of the apparatus, the NIST researchers constructed a similar room-temperature solenoid cooled by immersion in an oil bath and which provided a maximum flux density of about 2 mT (Olsen *et al.*, 1985). For this value of B , the voltage induced in a 2355-turn moving coil of mean radius 350 mm and traveling at 2 mm/s was 20 mV. Reversing a current of 50 mA in the coil resulted in a change in force on the coil equal to the gravitational force on a standard of mass of about 100 g. Using this apparatus and methods comparable to those discussed below, in 1989 Olsen *et al.* (1989) and Cage *et al.* (1989b) reported

$$\begin{aligned} K_J^2 R_K &= K_{J-\text{NIST}}^2 R_{K-\text{NIST}} [1 + 16.69(1.33) \times 10^{-6}] \\ &= 6.036\,7605(80) \times 10^{33} \text{ J}^{-1} \text{ s}^{-1} \\ &\quad [1.3 \times 10^{-6}], \end{aligned} \quad (247)$$

where $K_{J-\text{NIST}} = 483\,593.420 \text{ GHz/V}$; and $R_{K-\text{NIST}} = 25\,812.848\,47(30) \, \Omega_{\text{NIST}}$ on the mean date of the experiment, which was 15 May 1988, based on our analysis discussed in connection with the NIST low-field γ_p' determination [see Eq. (184) and the subsequent text].

Upon completion of the 1988 measurements, the NIST researchers installed the superconducting solenoid and undertook the additional work necessary to obtain a value of $K_J^2 R_K$ with a significantly reduced uncertainty (Steiner *et al.*, 1997; Gillespie *et al.*, 1997; Fujii *et al.*, 1997; Stenbakken *et al.*, 1996; Olsen *et al.*, 1991). The final result from this phase of the NIST effort was reported in 1998 by Williams *et al.* (1998) and is

$$\begin{aligned} K_J^2 R_K &= K_{J-90}^2 R_{K-90} [1 - 0.008(87) \times 10^{-6}] \\ &= 6.036\,761\,85(53) \times 10^{33} \text{ J}^{-1} \text{ s}^{-1} \\ &\quad [8.7 \times 10^{-8}]. \end{aligned} \quad (248)$$

The earlier NIST value is consistent with this value, but has an uncertainty about 15 times larger.

The moving coil in the new measurements was the same as in the 1988 measurements. However, when traversing its 85 mm trajectory in the 0.1 T flux density of the superconducting solenoids at a velocity of 2 mm/s, it generated an induced voltage of 1 V; and the change in force on the coil when the 10 mA current through it was reversed was equal to the gravitational force of a 1 kg mass standard. Thus the use of the new magnet led to increases in the force and voltage by factors of 10 and 50, respectively, thereby allowing these quantities to be determined with considerably smaller uncertainties.

The balance was also essentially the same as that used in the earlier measurements, but with an improved main knife edge. It consisted of a wheel about 610 mm in diameter and 25 mm thick with the knife edge serving as its axle. The moving coil was suspended from a three-arm spider, which in turn was suspended from the wheel by a band of fine wires that went around the wheel and hung from both sides. An absolute gravimeter, a refractometer for help in determining the index of refraction of air, and a three-axis interferometer were incorporated in the new experiment as well as many new instruments and procedures, especially for aligning the apparatus. In this and the earlier experiment, to reduce voltage noise from ambient ac electromagnetic fields and from vibrational motion of the moving coil relative to the superconducting solenoids, the voltage and velocity differences between the moving coil and a similar but fixed suspended reference coil were the quantities actually measured.

In the 1998 NIST measurements, U_v/v was sampled approximately 650 times during a single up or down traversal of the moving coil. In a typical run, the data from ten pairs of such transversals, interspersed with weighings at a particular point to determine F_e/I , were used to determine the profile of the flux density. This profile in turn was used to correct the data from each traversal. These corrected data were then used to determine the value of U_v/v at the point where F_e/I was determined, thereby yielding a single measurement of $K_J^2 R_K$. The result given in Eq. (248) is the mean of 989 values obtained over the period January 1998 to April 1998. The statistical relative standard deviation of these values (Type A) is 14×10^{-8} . Although the 989 values were very nearly normally distributed, because of occasional small

changes in the measured value of $K_J^2 R_K$ that could not be completely explained, Williams *et al.* (1998), took as their statistical relative standard uncertainty 3.0×10^{-8} , based on treating the 989 individual values as a collection of 22 uncorrelated groups of data. Thus the 14×10^{-8} statistical relative standard deviation of the 989 values was divided by $\sqrt{22}$ rather than $\sqrt{989}$ to obtain the statistical relative standard uncertainty of the mean. The three largest components of relative standard uncertainty due to possible systematic effects, as obtained from Type B evaluations, are 4.3×10^{-8} for the index of refraction of the air, 4.0×10^{-8} for apparatus alignment, and 3.0×10^{-8} for relating the measured voltages to K_{J-90} .

During the course of their work, the NIST researchers investigated many possible sources of error. For example, special attention was paid to possible errors due to misalignment of the apparatus (Gillespie *et al.*, 1997; Stenbakken *et al.*, 1996). Determining the index of refraction of air was particularly troublesome, due in part to the size of the apparatus, outgassing of the components, and gaseous helium leaking into the air. Improvements now being introduced into the apparatus should alleviate this as well as other difficulties and lead to a reduced uncertainty (Steiner, Newell, and Williams, 1999). The improvements include converting to vacuum operation, incorporating a programmable Josephson array voltage standard directly into the experiment, and possibly replacing the wheel balance with a dual flexure-strip balance.

As in other similar cases, we consider the 1989 NIST result as being superseded by the 1998 result given in Eq. (248) and include only the latter in the 1998 adjustment. The value of h that it implies is

$$h = 6.626\,068\,91(58) \times 10^{-34} \text{ J s} \quad [8.7 \times 10^{-8}]. \quad (249)$$

3.8. Faraday Constant F

The Faraday constant F is equal to the Avogadro constant N_A times the elementary charge e , $F = N_A e$; its SI unit is coulomb per mole, $\text{C mol}^{-1} = \text{A s mol}^{-1}$. It determines the amount of substance $n(\text{X})$ of an entity X that is deposited or dissolved during electrolysis by the passage of a quantity of electricity or charge $Q = It$ due to the flow of a current I in a time t . The Faraday constant is related to the molar mass $M(\text{X})$ (see Sec. 2.3), electrochemical equivalent $E(\text{X})$, and valence z of entity X by

$$F = \frac{M(\text{X})}{zE(\text{X})}, \quad (250)$$

where $E(\text{X})$ is the mass $m_d(\text{X})$ of entity X deposited or dissolved divided by the amount of charge $Q = It$ transferred during the electrolysis:

$$E(\text{X}) = \frac{m_d(\text{X})}{It}. \quad (251)$$

Obtaining F experimentally thus involves determining $E(X)$ with SI unit kg A s^{-1} and $M(X)$ with SI unit kg mol^{-1} .

In practice, as in other experiments that require the measurement of an electric current, the quantity I in Eq. (251) is measured in terms of a laboratory unit of current $A_{\text{LAB}} = V_{\text{LAB}}/\Omega_{\text{LAB}}$ (see Sec. 2.5). Since $E(X)$ varies inversely with I , and hence F varies directly with I , the situation is identical to that for low- and high-field measurements of shielded gyromagnetic ratios. Based on the discussion of Sec. 3.4 and Eqs. (177a) and (177b), we may immediately write

$$E(X) = \mathcal{E}_{90}(X) \frac{K_J R_K}{K_{J-90} R_{K-90}}, \quad (252)$$

where $\mathcal{E}_{90}(X)$ is the value of $m_d(X)/It$ when I is replaced by $(I/A_{90}) \text{ A}$; that is, when I is taken to be the numerical value of the current measured in the unit A_{90} times the unit A ; and

$$F = \mathcal{F}_{90} \frac{K_{J-90} R_{K-90}}{K_J R_K}, \quad (253)$$

where

$$\mathcal{F}_{90} = \frac{M(X)}{z \mathcal{E}_{90}(X)}. \quad (254)$$

As in the case of shielded gyromagnetic ratios, if V_{LAB} and Ω_{LAB} are not based on the Josephson and quantum Hall effects and the conventional values K_{J-90} and R_{K-90} , then Eq. (252) has a modified but similar form. In particular, in the one experiment considered here, the appropriate expression is obtained by replacing $\mathcal{E}_{90}(X)$, K_{J-90} , and R_K/R_{K-90} by $\mathcal{E}_{\text{LAB}}(X)$, $K_{J-\text{LAB}}$, and $\Omega_{\text{LAB}}/\Omega$, respectively, and it is necessary to apply corrections to $\mathcal{E}_{\text{LAB}}(X)$ to convert it to $\mathcal{E}_{90}(X)$.

It follows from the relations $F = N_A e$, $e^2 = 2\alpha h/\mu_0 c$, $m_e = 2R_\infty h/c\alpha^2$, and $N_A = A_r(e)M_u/m_e$, where $M_u = 10^{-3} \text{ kg mol}^{-1}$ (see Sec. 2.3), that

$$F = \frac{A_r(e)M_u}{R_\infty} \left(\frac{c}{2\mu_0} \frac{\alpha^5}{h} \right)^{1/2}, \quad (255)$$

and thus, from Eq. (253), that

$$\mathcal{F}_{90} = \frac{K_J R_K}{K_{J-90} R_{K-90}} \frac{A_r(e)M_u}{R_\infty} \left(\frac{c}{2\mu_0} \frac{\alpha^5}{h} \right)^{1/2}. \quad (256)$$

If one assumes the validity of the expressions $K_J = 2e/h$ and $R_K = h/e^2$, the latter equation can be written as

$$\mathcal{F}_{90} = \frac{cM_u}{K_{J-90} R_{K-90}} \frac{A_r(e)\alpha^2}{R_\infty h}, \quad (257)$$

which would be the observational equation for \mathcal{F}_{90} .

Also of interest is the relation

$$N_A = \frac{K_{J-90} R_{K-90}}{2} \mathcal{F}_{90}. \quad (258)$$

Because K_{J-90} and R_{K-90} have no uncertainty, a determination of the Faraday constant when the relevant current is measured in the unit A_{90} is a determination of N_A .

3.8.1. NIST: Ag Coulometer

There is one high-accuracy experimental value of \mathcal{F}_{90} available, that from NIST. The NIST determination of $E(\text{Ag})$ by Bower and Davis (1980) used the silver dissolution coulometer pioneered by Craig *et al.* (1960) in their earlier determination of F at NIST. It is based on the anodic dissolution by electrolysis of silver, which is monovalent, into a solution of perchloric acid containing a small amount of silver perchlorate. The basic chemical reaction is $\text{Ag} \rightarrow \text{Ag}^+ + e^-$ and occurs at the anode, which in the NIST work was a highly purified silver bar. By operating the coulometer at the proper potential, one can ensure that any chemical reactions of the constituents of the solutions other than the desired reaction are negligible.

The amount of silver dissolved for the passage of a given amount of charge $Q = It$ is found by weighing the bar before and after electrolysis. However, some of the anode is lost by mechanical separation rather than by electrolytic dissolution. Craig *et al.* (1960) addressed this problem of silver residue by recovering the mechanically separated silver and weighing it, a most difficult task. To reduce the uncertainty arising from such weighings, Davis and Bower (1979) developed a novel electrolytic method of determining the residue. In their approach, the silver particles were converted into silver ions dissolved in an electrolyte and the ionic silver plated onto a platinum cathode. The correction applied to Eq. (251) was then the amount of charge that passed during the electrolysis rather than the mass of the silver particles lost.

Bower and Davis (1980) carried out eight definitive measurements of $E(\text{Ag})$, the mean date of which was 15 March 1975. In these eight runs, the mass of the silver dissolved and the current used was either 3 g and 100 mA or 5 g and 200 mA; the duration of the runs was between 13 ks and 44 ks (3.6 h and 12.2 h). The final result based on the mean of the eight values may be expressed as

$$E(\text{Ag}) = \mathcal{E}_{\text{NIST}}(\text{Ag}) \frac{K_J}{K_{J-\text{NIST}}} \frac{\Omega_{\text{NIST}}}{\Omega}, \quad (259)$$

with

$$\mathcal{E}_{\text{NIST}}(\text{Ag}) = 1.117\,9646(15) \times 10^{-6} \text{ kg C}^{-1}$$

$$[1.3 \times 10^{-6}], \quad (260)$$

and includes a fractional correction of $1.68(49) \times 10^{-6}$ to account for impurities in the silver samples. This correction is based on additional analyses of the impurity content of the silver that were motivated by the 1986 adjustment (Taylor, 1985). The relative statistical standard deviation of the mean of the eight values is 0.85×10^{-6} (Type A), and the relative standard uncertainty due to weighing, and measuring voltage, resistance, time, and the residue is 0.85×10^{-6} (Type B).

The fractional values of the corrections that must be applied to $\mathcal{E}_{\text{NIST}}(\text{Ag})$ in Eq. (260) to convert it to a value based on A_{90} are obtained in the same manner as in the case of $\Gamma_{\text{p-NIST}}^*(\text{Io})$ in Eq. (184) and are as follows: 9.264×10^{-6} to convert from $K_{\text{J-NIST}} = 483\,593.420 \text{ GHz/V}$ to $K_{\text{J-90}}$; and $-0.935(33) \times 10^{-6}$ to convert from $\Omega_{\text{NIST}}/\Omega$ to $R_{\text{K}}/R_{\text{K-90}}$ based on the value $R_{\text{K}} = 25\,812.831\,14(85) \Omega_{\text{NIST}}$ on the 15 March 1975 mean date of the eight runs. Application of these corrections yields

$$\mathcal{E}_{90} = 1.117\,9739(15) \times 10^{-6} \text{ kg C}^{-1} \quad [1.3 \times 10^{-6}], \quad (261)$$

Naturally occurring silver contains the two isotopes ^{107}Ag and ^{109}Ag in nearly equal abundance. In a separate experiment, Powell, Murphy, and Gramlich (1982) determined the ratio $r_{79} = n(^{107}\text{Ag})/n(^{109}\text{Ag})$, the ratio of the amount of substance of ^{107}Ag to the amount of substance of ^{109}Ag , for the silver used in the $E(\text{Ag})$ measurements. The result is

$$r_{79} = 1.076\,376(60) \quad [5.6 \times 10^{-5}], \quad (262)$$

where the uncertainty has been recalculated by Eberhardt, (1981) of NIST following the method used throughout the 1998 adjustment (see Sec. 1.3). This result was obtained by the arduous but well-developed technique known as absolute isotopic-ratio mass spectrometry, which combines high-accuracy chemical assay with high-accuracy mass spectrometry. In this technique, the mass spectrometers used to determine amount-of-substance ratios are calibrated using synthetic mixtures of known isotopic composition prepared from nearly pure separated isotopes.

Based on Eq. (17) with $x(^{107}\text{Ag}) = r_{79}/(1 + r_{79})$, $x(^{109}\text{Ag}) = 1/(1 + r_{79})$, r_{79} given in Eq. (262), and $A_{\text{r}}(^{107}\text{Ag})$ and $A_{\text{r}}(^{109}\text{Ag})$ given in Table 2, the mean relative atomic mass of the silver used in the NIST measurements of $E(\text{Ag})$ is

$$A_{\text{r}}(\text{Ag}) = 107.868\,147(28) \quad [2.6 \times 10^{-7}], \quad (263)$$

where we have taken into account the fact that $A_{\text{r}}(^{107}\text{Ag})$ and $A_{\text{r}}(^{109}\text{Ag})$ are correlated with a correlation coefficient of 0.087 (Audi and Wapstra, 1998). However, the uncertainty of $A_{\text{r}}(\text{Ag})$ is dominated by the uncertainty of r_{79} , hence the covariances of $A_{\text{r}}(\text{Ag})$ and other values of $A_{\text{r}}(\text{X})$ used as input data in the 1998 adjustment are negligible.

The relation $M(\text{Ag}) = A_{\text{r}}(\text{Ag})M_{\text{u}}$, and Eqs. (254), (261), and (263) lead to

$$\mathcal{F}_{90} = 96\,485.39(13) \text{ C mol}^{-1} \quad [1.3 \times 10^{-6}]. \quad (264)$$

Following our usual policy, we view the 1980 NIST result in Eq. (264) as superseding the earlier and similar 1960 NIST result reported by Craig *et al.* (1960), which has an uncertainty five times larger (Cohen and Taylor, 1973). The value of h that may be inferred from Eq. (257) using the 1980 result for \mathcal{F}_{90} and the values from the 1998 adjustment for the other quantities in that equation is

$$h = 6.626\,0657(88) \times 10^{-34} \text{ J s} \quad [1.3 \times 10^{-6}], \quad (265)$$

where the uncertainties of the other quantities are negligible compared to the uncertainty of \mathcal{F}_{90} .

3.8.2. Other Values

The two other values of the Faraday constant available have relative standard uncertainties of about 1×10^{-5} and are not considered competitive for use in the 1998 adjustment. One was obtained at NIST by Marinenko and Taylor (1968) [see also Cohen and Taylor (1973)] from measurements of the electrochemical equivalent of benzoic acid and of oxalic acid dihydrate. The other was obtained at NIST by Koch (1980) from measurements of the electrochemical equivalent of 4-aminopyridine.

3.9. {220} Lattice Spacing of Silicon d_{220}

The crystal plane spacings of silicon and related topics have been reviewed over the last several years by a number of authors (Martin *et al.*, 1998; Becker *et al.*, 1996; Mana and Zosi, 1995; Becker and Mana, 1994). In brief, silicon is a cubic crystal with the same crystal structure as diamond; it has eight atoms per face-centered cubic unit cell of edge length $a \approx 357 \text{ pm}$, which is commonly called the silicon lattice parameter. The lattice spacing d_{hkl} of any plane characterized by Miller indices h, k, l in the full set of planes $\{h, k, l\}$ that are equivalent by symmetry is related to a by $d_{hkl} = a/\sqrt{h^2 + k^2 + l^2}$.

The three naturally occurring isotopes of silicon are ^{28}Si , ^{29}Si , and ^{30}Si . The amount of substance fractions $x(^{28}\text{Si})$, $x(^{29}\text{Si})$, and $x(^{30}\text{Si})$ of natural silicon are approximately 0.92, 0.05, and 0.03, respectively. The linear temperature coefficient of expansion of silicon at room temperature, and hence of a and d_{hkl} , is about $2.56 \times 10^{-6} \text{ K}^{-1}$. Its elastic constants are such that $(\Delta a/a)/\Delta p \approx -3.4 \times 10^{-12} \text{ Pa}^{-1}$, and thus the fractional change in a for a pressure change Δp of 100 kPa or about 1 standard atmosphere is -3.4×10^{-7} .

The {220} lattice spacing of silicon is obviously not a fundamental constant in the usual sense. Nevertheless, for practical purposes one can consider the lattice parameter a , and hence d_{220} , of an impurity-free crystallographically perfect or “ideal” silicon crystal under specified conditions (principally temperature, pressure, and isotopic composition) to be an invariant quantity of nature. Currently the reference temperature and pressure adopted are $t_{90} = 22.5^\circ \text{C}$ and $p = 0$ (i.e., vacuum), where t_{90} is Celsius temperature as defined on the International Temperature Scale of 1990, ITS-90 (Preston-Thomas, 1990). However, to date no reference values for isotopic composition have been adopted, because the variation of a due to the variations of the composition of the crystals used is taken to be negligible at the current level of experimental uncertainty.

The degree to which a particular high-quality silicon crystal grown by the floating-zone technique represents an ideal silicon crystal depends primarily on the amount of carbon (C) and oxygen (O) impurities it contains. Based on experimental and theoretical investigations of the effect of C and O on silicon lattice spacings (Windisch and Becker, 1990), it is

TABLE 12. Summary of data related to the {220} lattice spacing of particular silicon crystals and the quotient $h/m_n d_{220}(\text{W04})$ together with inferred values of α .

Quantity	Value	Relative standard uncertainty u_r	Identification	Sec. and Eq.
$h/m_n d_{220}(\text{W04})$	2 060.267 004(84) m s ⁻¹	4.1×10^{-8}	PTB-99	3.11.1 (282)
$d_{220}(\text{W4.2a})$	192 015.563(12) fm	6.2×10^{-8}	PTB-81	3.9.1 (272)
α^{-1}	137.036 0119(51)	3.7×10^{-8}		3.11.1 (284)
$d_{220}(\text{MO*4})$	192 015.551(6) fm	3.4×10^{-8}	IMGC-94	3.9.2 (273)
α^{-1}	137.036 0100(37)	2.7×10^{-8}		3.11.1 (285)
$d_{220}(\text{SH1})$	192 015.587(11) fm	5.6×10^{-8}	NRLM-97	3.9.3 (274)
α^{-1}	137.036 0017(47)	3.4×10^{-8}		3.11.1 (286)

believed possible to relate the lattice parameter of such a crystal using its measured C and O content (if sufficiently small) to the lattice parameter of an ideal crystal with a relative standard uncertainty of about 1×10^{-8} (Martin *et al.*, 1998).

To relate the lattice spacings of crystals used in different experiments, it is necessary in the 1998 adjustment to include information on lattice spacing differences. The fractional difference $[d_{220}(\text{X}) - d_{220}(\text{ref})]/d_{220}(\text{ref})$ of the {220} lattice spacing of a sample of crystal X and that of a sample of a reference crystal ref can be determined with a relative standard uncertainty in the range 5×10^{-9} to about 2×10^{-8} , depending on the instrument used and the lattice spacing uniformity of the samples. Both PTB (Windisch and Becker, 1988) and NIST (Kessler *et al.*, 1994) have constructed lattice comparators based on x-ray double crystal nondispersive diffractometry, and these instruments are used regularly to compare the lattice spacings of different samples. In particular, as a result of improvements recently made to the PTB apparatus (Martin *et al.*, 1999), PTB comparisons have achieved a high degree of internal consistency; measured lattice spacing fractional differences and calculated differences based on measured C and O content agree to within about 2×10^{-8} (Martin *et al.*, 1998).

Lattice spacing fractional differences obtained at NIST by Kessler *et al.* (1999a) that we take as input data are given in Sec. 3.1.3.c, Eqs. (51) to (53), in connection with the discussion of the relative atomic mass of the neutron $A_r(n)$. The following are the fractional differences obtained at PTB by Martin *et al.* (1998) that we also take as input data:

$$\frac{d_{220}(\text{W4.2a}) - d_{220}(\text{W04})}{d_{220}(\text{W04})} = -1(21) \times 10^{-9} \quad (266)$$

$$\frac{d_{220}(\text{W17}) - d_{220}(\text{W04})}{d_{220}(\text{W04})} = 22(22) \times 10^{-9} \quad (267)$$

$$\frac{d_{220}(\text{MO*4}) - d_{220}(\text{W04})}{d_{220}(\text{W04})} = -103(28) \times 10^{-9} \quad (268)$$

$$\frac{d_{220}(\text{SH1}) - d_{220}(\text{W04})}{d_{220}(\text{W04})} = -23(21) \times 10^{-9}. \quad (269)$$

In analogy with our treatment of the uncertainties of the NIST lattice spacing fractional differences (see Sec. 3.1.3.c),

the uncertainties we assign to these PTB differences consist of the following components: 5×10^{-9} associated with the PTB lattice comparator itself; a statistical component arising from the observed variation of the lattice spacing along the length of the sample being compared to the WASO 04 reference sample; and $\sqrt{2} \times 10^{-8} d_{220}(\text{X})$ for each sample X entering a comparison (including the WASO 04 sample), except that for the MO*4 sample $\sqrt{2} \times 10^{-8}$ is replaced by $(3/\sqrt{2}) \times 10^{-8}$. As discussed in connection with the NIST results, this last uncertainty component accounts for the fact that in general, the {220} lattice spacing of different samples from the same boule deviate from the mean value of the boule. The total component of uncertainty common to the uncertainty of each of these PTB lattice spacing differences is 1.5×10^{-8} (Becker, 1998), and hence the covariance of any two of these fractional differences is 219×10^{-18} (the correlation coefficients are about 0.4). Note that since the same reference sample of WASO 04 was used in the PTB lattice spacing comparisons and we take these covariances into account, the extra component of uncertainty assigned to d_{220} of the WASO 04 reference sample does not increase the uncertainty of the difference between the lattice spacings of two other crystal samples derived from the comparison of each to the WASO 04 sample.

The {220} lattice spacing of silicon is relevant to the 1998 adjustment not only because of its relationship to $A_r(n)$, but also because of the availability of an accurate value of $h/m_n d_{220}(\text{W04})$, where h/m_n is the quotient of the Planck constant and the neutron mass. Further, current measurements of the Avogadro constant N_A by the x-ray crystal density method involve $d_{220}(\text{X})$. We discuss below three determinations of $d_{220}(\text{X})$ in meters using a combined x-ray and optical interferometer carried out at three different laboratories: PTB, crystal WASO 4.2a; the Istituto di Metrologia ‘‘G. Colonnetti’’ (IMGC), Torino, Italy, crystal MO*4; and the National Research Laboratory of Metrology (NRLM), Tsukuba, Japan, crystal SH1. In Sec. 3.10 we discuss the status of measurements of the molar volume of silicon $V_m(\text{Si})$ in the context of determining N_A ; and in Sec. 3.11 we discuss the measurement of $h/m_n d_{220}(\text{W04})$ as well as the quotient $h/m(^{133}\text{Cs})$. Table 12 summarizes the data and gives values of the fine-structure constant α that may be inferred from the data; the calculation of these values is dis-

cussed in the relevant portion of the text. As in previous similar tables, the inferred values are indented for clarity and are given for comparison purposes only. [No values of $V_m(\text{Si})$ and $h/m(^{133}\text{Cs})$ are given for the reasons discussed in Secs. 3.10 and 3.11.2.]

As discussed at the beginning of this section, the lattice spacing of an ideal silicon crystal of naturally occurring isotopic composition d_{220} can be deduced from the lattice spacing of a real crystal sample. Based on both experiment and theory, Martin *et al.* (1998) have proposed a number of criteria that a silicon crystal should meet in order to allow d_{220} to be obtained from its lattice spacing. Further, these workers established that WASO 04 meets these criteria reasonably well and that d_{220} can be calculated from $d_{220}(\text{W04})$ simply by taking into account the effect of C and O on the latter. The relevant expression is (Martin *et al.*, 1999)

$$\frac{d_{220} - d_{220}(\text{W04})}{d_{220}(\text{W04})} = 15(11) \times 10^{-9}, \quad (270)$$

where the standard uncertainty arises from the 4×10^{-9} standard uncertainty of the correction for C and O and a 10×10^{-9} standard uncertainty assigned to account for the fact that WASO 04 may not fully meet all of the criteria. Equation (270) is also taken as an input datum in order to obtain a recommended value of d_{220} as well as its covariances with the other 1998 recommended values. As pointed out by Martin *et al.* (1998), because MO*4 contains a large amount of carbon and SH1 may possibly contain voids, it is less clear how well these crystals meet the criteria needed to deduce d_{220} from their lattice spacings.

3.9.1. PTB: X-ray/Optical Interferometer

X-ray interferometry began nearly 35 years ago with the publication of the now classic letter of Bonse and Hart (1965). The field developed rapidly, and the many significant accomplishments of its first decade were reviewed by Hart (1975), Deslattes (1980), and Bonse and Graeff (1977). The first high-accuracy x-ray interferometric value of the {220} lattice spacing of silicon was obtained at NIST in the 1970s in pioneering work by Deslattes and colleagues, initiated in the 1960s, using a combined x-ray and optical interferometer or “XROI” (Deslattes and Henins, 1973; Deslattes *et al.*, 1974; Deslattes *et al.*, 1976; Deslattes, 1980). Its assigned relative standard uncertainty was $u_r = 1.5 \times 10^{-7}$. Subsequently the NIST value was found to be too large by a fractional amount of approximately 1.8×10^{-6} , but a final value from an improved NIST x-ray/optical interferometer (designated XROI-II) designed to eliminate the apparent cause of the error has not been reported (Becker, Seyfried, and Siegert, 1982; Deslattes *et al.*, 1987; Deslattes, 1988; Deslattes and Kessler, 1991).

In brief, an XROI used to measure the {220} lattice spacing of a particular silicon crystal in meters consists of three thin, flat, and parallel crystals cut from the same silicon single crystal in such a way that the (220) lattice planes are perpendicular to the surfaces of the three crystals. The initial

structure is monolithic (the three crystals or lamellae are like “fins”), but the monolith is then cut so that one of the end crystals, called the analyzer, can be moved relative to the other two. A monoenergetic x-ray beam (for example, 17 keV Mo $K\alpha_1$ radiation) impinges upon the first fixed crystal, called the splitter, and is coherently split into two beams by Laue diffraction. The two beams impinge upon the second (middle) fixed crystal, called the mirror, and are again Laue diffracted. Two of the four diffracted beams overlap and produce an interference pattern at the position of the analyzer. The analyzer is moved in a direction parallel to the mirror so that its planes are aligned, then “antialigned” with the interference pattern maxima, and intensity variations of the x rays passing through the analyzer are measured. The spatial period of these intensity variations, or x-ray fringes, is equal to the (220) lattice plane spacing of the analyzer. By measuring the displacement of the analyzer relative to the fixed splitter and mirror via optical interferometry as the analyzer is moved parallel to the mirror, one can determine d_{220} of the analyzer by comparing the period of the x-ray fringes to the period of the optical fringes. The relevant relation is $d_{220} = (m/n)\lambda/2$, where n is the number of x-ray fringes corresponding to m optical fringes of period $\lambda/2$, and $\lambda \approx 633$ nm is the wavelength of the laser used to illuminate the optical interferometer. For this value of λ , $n/m \approx 1648$. Typically (but see the following section), the x-ray fringes are scanned by displacing the analyzer less than $80 \mu\text{m}$ ($m < 250$). Successful operation of an XROI is a challenge, and the geometric, thermal, and vibrational requirements are severe. Of particular importance is controlling (or, so that appropriate corrections can be applied, measuring) the unwanted motions of the analyzer—the goal is to move it along a perfectly straight line. Indeed, the error in the NIST lattice spacing determination is attributed to a problem with the trajectory of the analyzer (Deslattes *et al.*, 1987; Deslattes, 1988; Deslattes and Kessler, 1991).

The XROI determination of the {220} lattice spacing of silicon at the PTB was initiated in the 1970s, and measurements of d_{220} of silicon crystal WASO 4.2a were carried out in the early 1980s (Becker *et al.*, 1981; Seyfried, 1984; Becker and Siegert, 1984; Siegert and Becker, 1984; Becker *et al.*, 1982). The special features of the PTB XROI included: (i) a double parallel spring translation stage to move the analyzer with very small guiding errors, thereby maintaining the visibility of the x-ray fringes for displacements as large as $40 \mu\text{m}$, or about 120 optical fringes; (ii) polished ends of the splitter/mirror monolith and of the analyzer portion of the XROI used for the optical interferometry, forming mirrors that were part of the three crystals themselves; (iii) displacement of the analyzer determined by the two-beam interferometry technique using an optical polarization interferometer; and (iv) optimization of the point of impact of the optical interferometer’s laser beam on the analyzer in order to reduce the correction (but not the uncertainty) for Abbe offset error to a negligible level, and choice of the waist of the laser beam so that only a very small correction due to

wave-front nonplanarity (Fresnel phase shift or diffraction) was necessary.

In the initial PTB determination, 170 values of the ratio n/m were obtained from 170 bidirectional scans carried out in vacuum over about 18 d at temperatures $t_{68}=22.42\text{ }^{\circ}\text{C}$ to $t_{68}=22.50\text{ }^{\circ}\text{C}$, where t_{68} is Celsius temperature as defined on the International Practical Temperature Scale of 1968 or IPTS-68 (Preston-Thomas, 1969). Each value was corrected as necessary to the reference temperature $t_{68}=22.5\text{ }^{\circ}\text{C}$ using the accepted linear thermal coefficient of expansion of silicon. In addition, the mean of the 170 values (obtained by fitting a Gaussian probability distribution to them) was corrected by the fractional amount -3.9×10^{-8} to account for Fresnel diffraction and cosine error. The mean value of n/m was then combined with the measured value of λ to obtain $d_{220}(\text{W4.2a})$. The result reported by Becker *et al.* (1981) is

$$d_{220}^*(\text{W4.2a}) = 192\,015.560(12)\text{ fm} \quad [6.2\times 10^{-8}], \quad (271)$$

where the asterisk indicates that the reference temperature is $t_{68}=22.5\text{ }^{\circ}\text{C}$. [Note that the $\sqrt{2}\times 10^{-8}d_{220}(\text{W4.2a})$ component of uncertainty to account for sample variation discussed in Sec. 3.9 has been included in the uncertainty of this value.] However, in the 1998 adjustment we take as the reference temperature for measurements involving the crystal plane spacings of silicon $t_{90}=22.5\text{ }^{\circ}\text{C}$ (see Sec. 3.9). Since $t_{90}-t_{68}=-5.5\text{ mK}$ at the temperature of interest (Preston-Thomas, 1990) and the linear temperature coefficient of expansion of silicon at these temperatures is $2.56\times 10^{-6}\text{ K}^{-1}$ (Becker *et al.*, 1981), the value of $d_{220}(\text{W4.2a})$ given in Eq. (271) must be increased by the fractional amount 1.4×10^{-8} . The final result is

$$d_{220}(\text{W4.2a}) = 192\,015.563(12)\text{ fm} \quad [6.2\times 10^{-8}]. \quad (272)$$

In the PTB experiment, the two principal relative standard uncertainty components (both Type B) are 5.1×10^{-8} for the measurement of temperature and lack of exact knowledge of the thermal expansion coefficient of WASO 4.2a and 3.0×10^{-8} for possible Abbe error. The statistical relative standard uncertainty (Type A) of the mean value of n/m as obtained from the Gaussian fit of the 170 values is only 0.4×10^{-8} .

Because the PTB result of Becker *et al.* (1981) disagreed with the earlier NIST result of Deslattes *et al.* (1976), the PTB researchers repeated their determination of $d_{220}(\text{W4.2a})$ under varied experimental conditions in order to investigate possible errors due to unsuspected systematic effects (Becker *et al.*, 1982). Prior to the remeasurement, they disassembled and then reassembled the apparatus, realigned the x-ray and optical interferometers, made other adjustments, and improved their measurement of temperature. They then derived 13 values of $d_{220}(\text{W4.2a})$ from 13 runs, with from 13 to 78 bidirectional scans per run for a total of 414 values. Run 1 was carried out with the analyzer and interferometer laser beam optimally aligned, while runs 2 to 12 were carried out with the analyzer tilted from its optimal orientation by different amounts and the laser beam displaced from its optimal position by different amounts. After correction for the errors

thereby introduced, the values of $d_{220}(\text{W4.2a})$ obtained from runs 2 to 12 as well as run 1 were found to agree with each other and with the original result reported by Becker *et al.* (1981). Although the remeasurement consisted of 414 scans compared to the 170 scans of the initial determination, the remeasurement is viewed as supporting the result of that determination, not replacing it. (As part of their effort to understand the disagreement between the NIST and PTB lattice spacing values, the PTB researchers also showed, via direct lattice spacing comparisons, that d_{220} of the crystals used by NIST and PTB was the same within $2\times 10^{-7}d_{220}$, and hence that the 1.8×10^{-6} fractional difference between the NIST and PTB values could not be explained by a difference in the lattice spacing of the crystals.)

3.9.2. IMGC: X-ray/Optical Interferometer

Researchers at IMGC began their XROI determination of the $\{220\}$ lattice spacing of silicon in the 1970s and first observed x-ray fringes late in the decade (Basile *et al.*, 1978). The work continued and a preliminary value of d_{220} for a particular sample of silicon with an assigned relative standard uncertainty $u_r=2.8\times 10^{-7}$ was presented in 1988, together with a detailed description of the IMGC XROI (Basile *et al.*, 1989). Subsequently the apparatus as well as the procedures used to analyze the data were significantly improved, and the value

$$d_{220}(\text{MO*4}) = 192\,015.551(6)\text{ fm} \quad [3.4\times 10^{-8}] \quad (273)$$

for the crystal MO*4 at the reference conditions $p=0$ and $t_{90}=22.5\text{ }^{\circ}\text{C}$ was reported by Basile *et al.* (1994), Basile *et al.* (1995a). [Note that the $(3/\sqrt{2})\times 10^{-8}d_{220}(\text{MO*4})$ component of uncertainty to account for sample variation discussed in Sec. 3.9 has been included in the uncertainty of this value.] Their result is based on the mean of 196 values of n/m obtained over a period of many months by moving the analyzer between optical orders $m=0$ and $m=270$ (85 μm displacement), where each value is typically the average of 20 data collected in a 30 min measurement cycle. The largest correction by far that had to be applied to the mean value is -2.5×10^{-8} due to Fresnel diffraction, and the largest contribution to the relative standard uncertainty of $d_{220}(\text{MO*4})$ is 1.8×10^{-8} (Type B) due to lack of exact knowledge of the analyzer's trajectory. Other Type B relative standard uncertainty components include 0.8×10^{-8} for each of the following effects: Fresnel diffraction, XROI temperature, Abbe error, and variations of the thickness of the analyzer.

The many refinements incorporated into the IMGC experiment that enabled $d_{220}(\text{MO*4})$ to be determined with such a small uncertainty are described in a series of papers cited by Basile *et al.* (1994) [see also Bergamin *et al.* (1999)]. The key advances were a larger displacement of the analyzer, an XROI with a two-beam polarization-encoded optical interferometer that allowed the displacement of the analyzer and its unwanted rotations to be simultaneously measured, and a detailed analysis and understanding of the x-ray and optical

interference patterns. In particular, the unwanted rotations of the analyzer as it is displaced were measured by monitoring the differential displacements (phase shifts) between four portions of the optical interference pattern and automatically adjusting the tilt of the analyzer translation stage to compensate for the rotation.

Upon completion of the measurements on which the result given in Eq. (273) is based, the IMGC researchers began work that should eventually allow d_{220} of a particular crystal to be determined with a relative standard uncertainty approaching 1×10^{-9} . The issues addressed so far include the theory of the scanning x-ray interferometer (Mana and Vittone, 1997a; Mana and Vittone, 1997b), beam astigmatism in laser interferometry (Bergamin *et al.*, 1997b), and how to displace the analyzer by up to 2 mm, corresponding to some 6000 optical fringes or 10^7 x-ray fringes (Bergamin *et al.*, 1997c). Recently, Bergamin *et al.* (1999) reported the results of a series of additional measurements of $d_{220}(\text{MO*4})$ carried out from October 1996 to January 1997. The same x-ray interferometer was used in this remeasurement as was used to obtain the result given in Eq. (273), but first the entire XROI was disassembled and reassembled, the laser of the optical interferometer replaced, and a new translation stage or guide for the analyzer crystal as described by Bergamin *et al.* (1997c) was installed. The new guide allowed the analyzer to smoothly scan the x-ray fringes at a speed of 1 pm/s to 0.1 mm/s for displacements of up to 2 mm; unwanted rotations of the analyzer were no larger than 1 nrad. By averaging the results obtained from a typical sequence of 45 scans with analyzer displacements of about 1.6 mm or 5000 optical fringes, the statistical relative standard deviation of the mean value of n/m was reduced to less than 1×10^{-9} . This implies that in a time period of 1 h, one can investigate a possible systematic error as small as about $1 \times 10^{-9} d_{220}$.

Using this improved XROI, Bergamin *et al.* (1999) studied the effect of crystal temperature [the coefficient of thermal expansion of MO*4 was determined from measurements of $d_{220}(\text{MO*4})$ over the range $t_{90} = 21^\circ\text{C}$ to $t_{90} = 23.5^\circ\text{C}$ (Bergamin *et al.*, 1997a)], lattice strain, unwanted rotations and transverse displacements of the analyzer, laser diffraction in the optical interferometer, and residual gas pressure in the vacuum chamber housing the XROI. The five values of $d_{220}(\text{MO*4})$ obtained in these studies varied from 192 015.547 fm to 192 015.552 fm with standard uncertainties of 0.004 fm assigned to each, corresponding to $u_r = 2.1 \times 10^{-8}$. Because these additional values are viewed by Bergamin *et al.* (1999) as providing confirmation of the 1994 result rather than replacing it, we take Eq. (273) as the input datum for $d_{220}(\text{MO*4})$ in the 1998 adjustment.

3.9.3. NRLM: X-ray/Optical Interferometer

The effort at NRLM to determine the $\{220\}$ lattice spacing of silicon began in the 1970s; a review of the initial work was presented in 1988 by Tanaka, Nakayama, and Kuroda (1989). A first result for d_{220} of crystal SH1 with a relative standard uncertainty $u_r = 1.6 \times 10^{-7}$ was reported several

years later by Fujimoto *et al.* (1995a), following the further development of the NRLM XROI [see, for example, Nakayama, Tanaka and Kuroda, (1991a); Nakayama *et al.* (1991b); Nakayama *et al.* (1993); Fujimoto, Tanaka, and Nakayama, (1995b)]. Improvements made to the early apparatus include a new polarization-type optical interferometer with picometer resolution to measure the displacement of the analyzer, a new translation stage for the analyzer that significantly reduced its unwanted motions, a feedback system based on an angular interferometer with 3 nrad resolution to correct for unwanted rotations of the analyzer during displacements of up to 100 μm , and the addition of a trajectory interferometer to measure unwanted rectilinear movements of the analyzer.

The dominant contribution by far to the 1.6×10^{-7} relative standard uncertainty of the 1995 result was the 1.6×10^{-7} statistical relative standard deviation (Type A) of the approximately 900 individual values of $d_{220}(\text{SH1})$ obtained from bidirectional scans of up to 250 optical fringes, corresponding to analyzer displacements of about 80 μm . The scatter of the data, which was periodic in time and correlated with the temperature of the XROI, and which over the 18 d of measurements was as large as $6 \times 10^{-7} d_{220}(\text{SH1})$ peak-to-peak, was identified by Fujimoto *et al.* (1995a) to be due to the reflection of light from the surface of a quarter wave plate inserted in the optical path of the interferometer used to measure analyzer displacements. This problem was addressed in a new series of measurements by inclining the plate so that the reflected light did not interfere with the interferometer's main optical beam. As a consequence, the scatter decreased by a factor of 3. Based on 829 temperature-corrected values of n/m obtained from 829 bidirectional scans of up to $m = 214$ (displacements up to about 70 μm), each lasting about 23 min and carried out over 15 d at temperatures within 200 mK of $t_{90} = 22.5^\circ\text{C}$, Nakayama and Fujimoto (1997) found for the reference conditions $p = 0$ and $t_{90} = 22.5^\circ\text{C}$

$$d_{220}(\text{SH1}) = 192\,015.587(11) \text{ fm} \quad [5.6 \times 10^{-8}]. \quad (274)$$

[Note that the $\sqrt{2} \times 10^{-8} d_{220}(\text{SH1})$ component of uncertainty to account for sample variation discussed in Sec. 3.9 has been included in the uncertainty of this value.]

The 829 values of n/m varied slowly but periodically over the 15 d of data taking, with an amplitude of about $5 \times 10^{-8} (n/m)$ relative to the mean. This effect was investigated by carrying out a considerable number of the 829 scans with the x-ray interferometer rotated from its optimum alignment with respect to the optical interferometer by up to ± 8000 nrad. Based on the values of n/m obtained from these scans and their lack of correlation with the temperature of the XROI, Nakayama and Fujimoto (1997) concluded that the value of n/m lies within the $5 \times 10^{-8} (n/m)$ amplitude of the periodic variation.

The principal fractional correction that Nakayama and Fujimoto (1997) had to apply to the observed mean value of n/m was -16.0×10^{-8} to account for the 251 μm width of the beam of the optical interferometer (Fresnel diffraction);

the two other required fractional corrections, that for cosine error and scan direction, were less than 1×10^{-8} each. The 5.6×10^{-8} relative standard uncertainty of the result is mainly due to the 5.0×10^{-8} statistical relative standard deviation of the 829 values (Type A). This can be compared to the relative standard uncertainties (Type B) assigned for possible Abbe error and for the Fresnel diffraction correction, the two largest additional components (other than our $\sqrt{2} \times 10^{-8}$ for sample variation), which are only 1.0×10^{-8} and 0.8×10^{-8} , respectively.

We use the value given in Eq. (274) as the input datum for $d_{220}(\text{SHI})$ in the 1998 adjustment.

3.10. Molar Volume of Silicon $V_m(\text{Si})$

It follows from Eq. (12) as applied to silicon that the Avogadro constant N_A is given by

$$N_A = \frac{M(^A\text{Si})}{m(^A\text{Si})}, \quad (275)$$

where $M(^A\text{Si})$ and $m(^A\text{Si})$ are the molar mass and mass of silicon atoms of a particular nucleon number A , respectively. However, in keeping with the discussion of Sec. 3.9, we suppose that we are dealing with an ideal silicon crystal at $t_{90} = 22.5^\circ\text{C}$ in vacuum with a particular isotopic composition. Hence $M(^A\text{Si})$ and $m(^A\text{Si})$ in Eq. (275) are replaced by $M(\text{Si})$ and $m(\text{Si})$, the mean molar mass and mean mass of the silicon atoms (see Sec. 2.3). Further, since the binding energy of each silicon atom in a silicon crystal is only about 5 eV, $M(\text{Si})$ and $m(\text{Si})$ may be viewed as the molar mass and mass of free silicon atoms instead of silicon atoms in a crystal.

The mean mass $m(\text{Si})$ is related to the mean volume of a silicon atom a^3/n and the mass density of the silicon crystal $\rho(\text{Si})$ by

$$m(\text{Si}) = \rho(\text{Si}) \frac{a^3}{n}, \quad (276)$$

where a is the edge length of the cubic unit cell as defined in Sec. 3.9 and n is the number of silicon atoms per unit cell, and where it is understood that the same reference conditions apply to $\rho(\text{Si})$ as to a (that is, $t_{90} = 22.5^\circ\text{C}$ and vacuum). In terms of the mean molar volume of silicon,

$$V_m(\text{Si}) = \frac{M(\text{Si})}{\rho(\text{Si})} = \frac{A_r(\text{Si})M_u}{\rho(\text{Si})}, \quad (277)$$

Eq. (275) can be written as

$$N_A = \frac{V_m(\text{Si})}{a^3/n} = \frac{A_r(\text{Si})M_u}{\sqrt{8}d_{220}^3\rho(\text{Si})}, \quad (278)$$

since $n = 8$ for an ideal silicon crystal and $a = \sqrt{8}d_{220}$ (see Sec. 3.9). From this point of view, the Avogadro constant is equal to the quotient of the mean molar volume of silicon to the mean volume of a silicon atom.

It is clear from the above discussion that a value of N_A can be obtained from measurements of $V_m(\text{Si})$ and d_{220} . This

method of determining N_A is called the x-ray crystal density or XRCD method, and in its modern form as applied to silicon was pioneered at NIST by Deslattes and colleagues in the early 1970s (Deslattes *et al.*, 1974). It follows from Eq. (278) that an XRCD determination of N_A involves three separate experiments: determination of d_{220} using a combined x-ray and optical interferometer or XROI as discussed in Sec. 3.9.1; determination of the amount of substance ratios $n(^{29}\text{Si})/n(^{28}\text{Si})$ and $n(^{30}\text{Si})/n(^{28}\text{Si})$ —and hence amount-of-substance fractions $x(^A\text{Si})$ —using the absolute isotopic ratio mass spectrometry technique in order to determine the mean relative atomic mass $A_r(\text{Si})$; and determination of $\rho(\text{Si})$. However, real silicon crystals contain chemical impurities (see Sec. 3.9), which implies that the measured values of d_{220} and $V_m(\text{Si}) = A_r(\text{Si})M_u/\rho(\text{Si})$ may not correspond to those of an ideal crystal, n may not be exactly equal to eight, and the unit cell may be distorted (Siebert, Becker, and Seyfried, 1984). Further, because in practice lattice spacing and density measurements are carried out on different samples of a particular boule, information about sample homogeneity is required. This means that the silicon crystals must be carefully characterized both structurally and chemically so that appropriate corrections can be applied to the measured values of d_{220} and $V_m(\text{Si})$, thereby allowing Eq. (278) to be used to determine N_A .

Since the pioneering work at NIST, significant progress has been made in all three experimental areas, but also in characterizing and understanding the imperfections of real silicon crystals. The most accurate measurement of d_{220} of a particular crystal sample is that carried out at IMGC and has a quoted relative standard uncertainty $u_r = 2.6 \times 10^{-8}$ (Basile *et al.*, 1994); amount-of-substance ratio measurements at the Institute of Reference Materials and Measurements (IRMM), Geel, Belgium, have now reached the point where the quoted relative standard uncertainty of $A_r(\text{Si})$ for a particular sample is $u_r = 1.3 \times 10^{-7}$ (Gonfiantini *et al.*, 1997); the most accurate measurement of $\rho(\text{Si})$ is that carried out at NRLM and has a quoted relative standard uncertainty $u_r = 1.1 \times 10^{-7}$ (Fujii *et al.*, 1995); and it is believed that d_{220} of a high-quality real crystal can represent d_{220} of an ideal crystal with a relative standard uncertainty of 1×10^{-8} (see Sec. 3.9).

The considerable effort being expended internationally on the improved determination of N_A is motivated in part by the desire to replace the current artifact-based definition of the unit of mass in the SI—the international prototype of the kilogram—by a definition based on an invariant property of nature such as the mass of a specified number of particular atoms (Quinn, 1991; Taylor, 1991) or a specified sum for the frequencies of a collection of photons (Taylor and Mohr, 1999). To coordinate this international effort, the Consultative Committee for Mass and Related Quantities (CCM, *Comité Consultatif pour la Masse et les grandeurs apparentées*) of the CIPM has formed a subcommittee, the CCM Working Group on the Avogadro Constant, with representatives from all major research groups working in areas relevant to the determination of N_A by the XRCD method. Its present chairman is P. Becker of the PTB.

Nevertheless, in spite of the impressive advances made in the last decade or so, not the least of which is the improved understanding of the imperfections of real silicon crystals, the current well-known (De Bièvre *et al.*, 1997), but not yet well-understood, inconsistencies in a number of experimental values of $V_m(\text{Si})$ are deemed sufficiently troublesome to preclude the use of any value of $V_m(\text{Si})$ in the 1998 adjustment. The decision to exclude such values was reached in collaboration with, and has the full support of, the CCM Working Group on the Avogadro Constant (Becker, 1997). The possible cause of these inconsistencies is currently under intensive investigation, and it is expected that once it is identified values of $V_m(\text{Si})$ can be included in future adjustments. For completeness we very briefly summarize the current situation.

As indicated in Sec. 3.9, the fractional variation of d_{220} with the observed variation of the isotopic composition of the silicon crystals used in high-accuracy experiments is considered negligible. Hence Eq. (278) implies that, after correction for impurities, values of $V_m(\text{Si})$ should be nearly invariant. However, the values of $V_m(\text{Si})$ obtained at IMGC for two crystals (Basile *et al.*, 1995b), as well as the value obtained at NRLM for its crystal, differ from other IMGC values and values obtained at PTB by unexpectedly large amounts (De Bièvre *et al.*, 1997). Indeed, the NRLM value exceeds that of PTB by $3.4 \times 10^{-6} V_m(\text{Si})$. Because for each of these values $M(\text{Si})$ is based on similar measurements carried out at IRMM, and the comparison of silicon density standards among laboratories shows that the fractional difference between measurements of density at NRLM and at PTB is less than 2×10^{-7} (Bettin *et al.*, 1997), the observed anomalously low density of the NRLM silicon is very likely to be real. Such a low density could be explained by the presence of unexpected voids (Deslattes and Kessler, 1999), which would have to account for about 1.5 mm^3 of missing silicon in a 1 kg sample.

It is worthwhile to note that from Eq. (278) and the relations $m_e = 2R_\infty h/c\alpha^2$ and $N_A = A_r(e)M_u/m_e$ one obtains the observational equation

$$V_m(\text{Si}) \doteq \frac{\sqrt{2} c M_u A_r(e) \alpha^2 d_{220}^3}{R_\infty h} \quad (279)$$

for measured values of $V_m(\text{Si})$.

3.11. Quotient of Planck Constant and Particle Mass $h/m(X)$

It follows from the relation $R_\infty = \alpha^2 m_e c/2h$ that

$$\alpha = \left[\frac{2R_\infty A_r(X)}{c} \frac{h}{A_r(e)} \frac{1}{m(X)} \right]^{1/2}, \quad (280)$$

where $A_r(X)$ is the relative atomic mass of particle X with mass $m(X)$ and $A_r(e)$ is the relative atomic mass of the electron (see Sec. 3.1). Since c is an exactly known constant, the relative standard uncertainty of R_∞ is less than 1×10^{-11} , that of $A_r(e)$ is about 2×10^{-9} , and the relative atomic masses of many particles and atoms have relative

standard uncertainties comparable to or smaller than that of the electron, Eq. (280) yields a value of α with a competitive uncertainty if $h/m(X)$ is determined with a sufficiently small uncertainty. In this section we review two determinations of $h/m(X)$, one for the neutron and the other for the ^{133}Cs atom. As already noted in Sec. 3.9, the neutron result is included in Table 12 of that section.

3.11.1. Quotient h/m_n

Although the PTB determination of h/m_n had its origins in a proposal by Stedman (1968), Weirauch (1975) had serious difficulties in implementing the particular method suggested and developed an alternative approach (Weirauch, 1978). The basic idea is to use the de Broglie relation $p = m_n v = h/\lambda$ to determine $h/m_n = \lambda v$ for the neutron by measuring both the de Broglie wavelength λ and the corresponding velocity v of slow neutrons. The PTB experiment (Krüger, Nistler, and Weirauch, 1998; Krüger, Nistler, and Weirauch, 1995) was carried out at the high-flux reactor of ILL after initial investigations at PTB using the PTB reactor (Krüger, Nistler, and Weirauch, 1984b; Weirauch, Krüger, and Nistler, 1980). In the experiment, the de Broglie wavelength $\lambda \approx 0.25 \text{ nm}$ of slow neutrons in a monochromatic horizontal beam was determined by back reflection (Bragg angle of 90°) from the (311) lattice planes perpendicular to v of a single crystal of silicon; and the velocity $v \approx 1600 \text{ m/s}$ of the neutrons was determined by a special time-of-flight method. In brief, the neutrons in the beam were first spin polarized and then the direction of the polarization modulated at a known frequency $\nu \approx 750 \text{ kHz}$ by having the beam pass through a ‘meander’ coil. The modulated beam then traveled to the silicon crystal, was back-reflected along its original path, and again passed through the meander coil, which again modulated the direction of the spin of the neutrons in the beam. The resulting total modulation, which is the superposition of the two modulations and depends on the round-trip time-of-flight of the neutrons, was analyzed and measured as a function of the distance l between the center of the meander coil and the silicon crystal. The mean neutron current $\bar{I}(l)$ at the detector is of the form

$$\bar{I}(l) = \frac{I_0}{2} \left\{ 1 - J_0 \left[2\hat{\Phi} \cos \left(\frac{2\pi\nu l}{v} \right) \right] \right\}, \quad (281)$$

where $\hat{\Phi} \approx 1.6\pi$ is the modulation amplitude and J_0 is the zero-order Bessel function. The velocity v is related to the distance $\Delta l \approx 1 \text{ mm}$ between the main minima of $\bar{I}(l)$ by $v = 2\nu\Delta l = 2\Delta l/\tau$, where τ is the modulation period. Thus the neutrons traverse a distance $2\Delta l$ in the time τ . To achieve high accuracy, the distance between the crystal and the meander coil was changed by 10 m, corresponding to over 9400 main minima, $\bar{I}(l)$ was measured for one main minimum at either end of the path, and a curve fitted to $\bar{I}(l)$ over the entire path based on Eq. (281) with $\hat{\Phi}$ and Δl as free parameters. The experiment was carried out in a vacuum chamber at a pressure of between 1 Pa and 10 Pa. The distance l was

measured interferometrically and a small correction applied to account for the index of refraction of the residual air.

The work at ILL was documented in a number of progress reports published in the 1980s (Krüger, Nistler, and Weirauch, 1984a; Krüger, Nistler, and Weirauch, 1986; Krüger, Nistler, and Weirauch, 1989b; Krüger, Nistler, and Weirauch, 1989a). The result from a series of 13 measurements carried out from April 1989 to March 1991, when the ILL reactor closed for about 4 years for repairs and improvements, was reported in 1995 by Krüger *et al.* (1995). The final result of the PTB effort reported by Krüger *et al.* (1998) was based on a second series of ten measurements carried out from August 1995 to November 1996 together with the first series of 13 measurements. This result may be written as (Krüger, Nistler, and Weirauch, 1999)

$$\frac{h}{m_n d_{220}(\text{W04})} = 2\,060.267\,004(84) \text{ m s}^{-1} \quad [4.1 \times 10^{-8}], \quad (282)$$

where, as discussed in Sec. 3.9, $d_{220}(\text{W04})$ is the {220} lattice spacing of the crystal WASO 04 at $t_{90} = 22.5^\circ\text{C}$ in vacuum. The assigned uncertainty is that of the PTB researchers combined with $1 \times 10^{-8} h/m_n d_{220}(\text{W04})$, which accounts for possible lattice spacing variations of the samples of the crystals used in the $h/m_n d_{220}(\text{X})$ measurements, and $\sqrt{2} \times 10^{-8} h/m_n d_{220}(\text{W04})$, which accounts for the possible lattice spacing variation of the crystal WASO 04. [See the discussion in Sec. 3.9 following Eqs. (266)–(269); as explained below, the silicon crystals used in the PTB h/m_n experiment were compared to WASO 04.] Because the relative standard uncertainty of the value of $h/m_n d_{220}(\text{W04})$ given in Eq. (282) includes the 1.5×10^{-8} total component of uncertainty common to the PTB fractional lattice spacing differences given in Eqs. (266)–(269), the covariance of this value and any of the fractional differences is $451 \times 10^{-15} \text{ m s}^{-1}$ (the correlation coefficients are about 0.2).

The result of the second series of measurements is in excellent agreement with that of the first, even though nearly 4 years separated the two series and a number of potentially significant changes were made in the experiment for the second series. These modifications included the removal of some major components of the apparatus and their subsequent reinstallation and readjustment; replacement of the lasers used in the interferometric determination of l and the synthesizer used to generate the $\nu \approx 750 \text{ kHz}$ modulation frequency; recalibration of the resistors used to measure the temperature of the silicon crystal; the use of two new silicon crystals; and significantly increased measuring time, which led to a reduction in the statistical uncertainty in determining the period of the fitted $\bar{I}(l)$ curve. The uncertainty of $h/m_n d_{220}(\text{W04})$ is in fact largely due to this statistical uncertainty (Type A), which arises to a significant extent from the thermal expansion of components associated with the interferometry. The largest nonstatistical (Type B) component of relative standard uncertainty, about 1.1×10^{-8} , is associated with measuring the temperature of the silicon crystal.

Knowledge of the temperature of the crystal is of critical importance, because the linear temperature coefficient of expansion of silicon α_{Si} , and hence of its lattice spacings, is large: $\alpha_{\text{Si}} = 2.56 \times 10^{-6} \text{ K}^{-1}$.

Two silicon crystals, Si 1 and Si 2, were employed in the first series and three crystals, Si 2, Si 4, and Si 5, in the second. After the first series, the lattice spacing of a sample of Si 1 was compared to that of reference crystal WASO REF, and the result of the comparison was used for both Si 1 and Si 2, because these were cut one after the other from the same boule. After the second series, the lattice spacings of samples of Si 1, Si 2, Si 4, and Si 5 were compared to that of the new reference crystal WASO 04, thereby determining the lattice spacing of each crystal in terms of the lattice spacing of WASO 04. As for the samples used in the first series, these comparisons were carried out in the PTB X-Ray Metrology Section, but the improved instrument mentioned in Sec. 3.9 was used in the latter set. The fact that the differences among the 23 individual values of $h/m_n d_{220}(\text{W04})$ are consistent with the uncertainties assigned to each value indicates that the lattice spacing differences of the h/m_n crystals, arising from C and O impurities and other imperfections, are adequately accounted for by the difference measurements relative to WASO 04.

The observational equation, which follows from Eq. (280), for the measured value of $h/m_n d_{220}(\text{W04})$ given in Eq. (282) is

$$\frac{h}{m_n d_{220}(\text{W04})} \doteq \frac{c \alpha^2 A_r(e)}{2 R_\infty A_r(n) d_{220}(\text{W04})}. \quad (283)$$

From this expression and the value of $h/m_n d_{220}(\text{W04})$, one can infer a value of α using any one of the three available absolute silicon lattice spacing measurements (PTB, IMGC, or NRLM—see Sec. 3.9) together with its relation to $d_{220}(\text{W04})$ as determined from the NIST and PTB lattice spacing fractional differences given in Secs. 3.1.3.c and 3.9. Using the 1998 recommended value of R_∞ , values of $A_r(e)$ and $A_r(n)$ consistent with Eqs. (31), (34), (48), (50), and (283), we obtain from the PTB measurement

$$\alpha^{-1} = 137.036\,0119(51) \quad [3.7 \times 10^{-8}], \quad (284)$$

from the IMGC measurement

$$\alpha^{-1} = 137.036\,0100(37) \quad [2.7 \times 10^{-8}], \quad (285)$$

and from the NRLM measurement

$$\alpha^{-1} = 137.036\,0017(47) \quad [3.4 \times 10^{-8}]. \quad (286)$$

(These are the inferred values included in Table 12 of Sec. 3.9.) The three absolute lattice spacing measurements together yield what may be called an h/m_n value of alpha:

$$\alpha^{-1}(h/m_n) = 137.036\,0084(33) \quad [2.4 \times 10^{-8}]. \quad (287)$$

It is important to note that the observational equations for $\lambda_{\text{meas}}/d_{220}(\text{ILL})$ and $h/m_n d_{220}(\text{W04})$ [Eqs. (50) and (283)] may be combined to give

$$A_r(n) = \frac{1}{1-2\epsilon} \{ [(1-2\epsilon)A_r^2(d) + \epsilon^2 A_r^2(p)]^{1/2} - (1-\epsilon)A_r(p) \}, \quad (288)$$

where

$$\epsilon = \frac{1}{c} \left[\frac{h}{m_n d_{220}(\text{W04})} \right] \left[\frac{\lambda_{\text{meas}}}{d_{220}(\text{ILL})} \right]^{-1} \frac{d_{220}(\text{W04})}{d_{220}(\text{ILL})} \approx 0.0024. \quad (289)$$

Of particular interest here is the fact that $A_r(n)$ depends only on the relative lattice spacing of the two crystals, and not on the absolute values of their lattice spacings in meters. Indeed, if the same silicon crystal were used to measure the two quotients in square brackets, then not even a lattice spacing comparison would be necessary. This route to $A_r(n)$ is important in the determination of the 1998 recommended value of the mass of the neutron m_n in the unified atomic mass unit $m_n/u = A_r(n)$.

3.11.2. Quotient $h/m(^{133}\text{Cs})$

The atomic recoil frequency shift of photons absorbed and emitted by cesium atoms is being measured at Stanford University in order to determine the quotient $h/m(^{133}\text{Cs})$ and thus the fine-structure constant (Young, Kasevich, and Chu, 1997; Peters *et al.*, 1997).

In its simplest form, the atomic recoil frequency shift follows from energy and momentum conservation. If a photon of frequency ν_1 propagating in the x direction is absorbed by an atom of mass m initially at rest, and a second photon of frequency ν_2 is emitted by the atom in the $-x$ direction, then the difference between the two frequencies is given by

$$\Delta\nu = \nu_1 - \nu_2 = \frac{2h\nu^2}{mc^2} \left(1 - \frac{\Delta\nu}{2\nu} + \dots \right), \quad (290)$$

where $\nu_1 \approx \nu_2 \approx \nu$, and ν is the relevant resonant transition frequency in the atom. For the cesium atom with ν equal to the frequency of the D_1 line, the correction term $\Delta\nu/2\nu$ is about 1×10^{-11} . Under the assumption that such terms are negligible, h/m is given by

$$\frac{h}{m} = \frac{c^2 \Delta\nu}{2\nu^2}. \quad (291)$$

This recoil frequency shift leads to spectral doubling in saturation absorption spectroscopy as predicted by Kol'chenko, Rautian, and Sokolovskii (1968) and optically resolved by Hall, Bordé, and Uehara (1976). Hall *et al.* (1976) also pointed out that the splitting provides a measure of h/m .

The determination of h/m with high accuracy by measuring the atomic recoil frequency shift of photons is rather more difficult than the above discussion might imply. In the experiment to measure $\Delta\nu_{\text{Cs}}$ at Stanford, full use is made of the laser cooling of neutral atoms, velocity-selective stimulated Raman transitions to observe matter-wave interference, and the concept of Ramsey separated-oscillatory-field spectroscopy. By employing these light-pulse atom-

interferometry techniques, Weiss, Young, and Chu (1994) and Weiss, Young and Chu (1993) were able to obtain a value of $\Delta\nu_{\text{Cs}}$ in 2 h of data taking with a statistical relative standard uncertainty (Type A) of 1×10^{-7} , but found that the resulting value of $h/m(^{133}\text{Cs})$ was smaller than the expected value by the fractional amount 8.5×10^{-7} . Although Weiss *et al.* (1994) could not identify a particular systematic effect in the measurement of $\Delta\nu_{\text{Cs}}$ that might have caused such a difference, they believed that it was mainly due to imperfections of the Raman laser beams. In order to reduce this and a number of other possible systematic effects, as well as to significantly reduce the scatter of the data, the Stanford researchers made major modifications to their apparatus (Young, 1997). The focus of these changes was the following: improved vibration isolation, reduced magnetic-field shifts, longer interferometer interaction times, more efficient atomic state transfers, smaller errors from wave-front distortions, and reduced ac Stark shifts. As a consequence of their efforts, a statistical relative standard uncertainty of 1×10^{-7} for $\Delta\nu_{\text{Cs}}$ could be obtained with the improved apparatus in 1 min of data taking rather than in 2 h of data taking as with the unmodified apparatus. Moreover, from the observed variation of values of $\Delta\nu_{\text{Cs}}$ with changes in experimental parameters, it was concluded that systematic effects were also reduced (Young, 1997).

The value of $\Delta\nu_{\text{Cs}}$ based on data obtained with the improved apparatus, as given by Young (1997) in his Ph.D. thesis, is assigned a relative standard uncertainty $u_r = 5.6 \times 10^{-8}$, which consists of a statistical component of 2.2×10^{-8} (Type A) and components totaling 5.2×10^{-8} (Type B) to account for various systematic effects. Of these components, the largest by far is 5.0×10^{-8} to account for the observed variations of $\Delta\nu_{\text{Cs}}$ with the number N of mirror (π) laser pulses occurring between the two pairs of beam splitter ($\pi/2$) laser pulses of the atom interferometer and with the time T between the two pulses of a given pair.

Since the cause of this systematic effect was not understood, it was decided not to formally publish Young's result for $\Delta\nu_{\text{Cs}}$ but to continue to try to understand and improve the apparatus (Chu, Hensley, and Young, 1998). As a result of this additional work, variation of the experimental values of $\Delta\nu_{\text{Cs}}$ was discovered to be due in part to unwanted phase shifts in the atom interferometer when the frequency of a synthesizer used to compensate for the Doppler shift from gravity was changed (Chu *et al.*, 1998). Replacement of the synthesizer solved this problem. The experiment is continuing and efforts to eliminate the observed dependence of the $\Delta\nu_{\text{Cs}}$ data on the shape (intensity vs. time) of the beam splitter pulses are underway (Hensley, 1999).

It is noteworthy that a significantly improved value ($u_r \approx 1 \times 10^{-10}$) of the relevant ^{133}Cs resonance frequency ν_{eff} characteristic of the Stanford experiment is now available from the frequency measurements of the ^{133}Cs D_1 line reported by Udem *et al.* (1999); and that a similarly improved value ($u_r < 2 \times 10^{-10}$) of $A_r(^{133}\text{Cs})$ has been obtained by Bradley *et al.* (1999). Since the relative standard uncertainty of $A_r(e)$ is about 2×10^{-9} and that of R_∞ is less than 1

$\times 10^{-11}$, the uncertainty of the value of α that can be inferred from Eq. (280) as applied to ^{133}Cs ,

$$\alpha = \left[\frac{2R_\infty}{c} \frac{A_r(^{133}\text{Cs})}{A_r(e)} \frac{h}{m(^{133}\text{Cs})} \right]^{1/2} \quad (292)$$

with

$$\frac{h}{m(^{133}\text{Cs})} = \frac{c^2 \Delta\nu_{\text{Cs}}}{2\nu_{\text{eff}}^2}, \quad (293)$$

is to a large extent dictated by the uncertainty of the experimental value of $\Delta\nu_{\text{Cs}}$. If $\Delta\nu_{\text{Cs}}$ were to be measured with a relative standard uncertainty $u_r = 5 \times 10^{-9}$, which seems feasible (Chu *et al.*, 1998), one would have a value of α with $u_r = 2.7 \times 10^{-9}$. This is to be compared to the uncertainty of the value of α inferred from the electron magnetic moment anomaly a_e : $u_r = 3.8 \times 10^{-9}$ [see Eq. (72)].

In view of the fact that possible systematic errors are still being investigated, no value of $\Delta\nu_{\text{Cs}}$ is included in the 1998 adjustment.

3.12. Hyperfine Structure

The ground-state hyperfine splittings of hydrogen, muonium, and positronium, $\Delta\nu_{\text{H}}$, $\Delta\nu_{\text{Mu}}$, and $\Delta\nu_{\text{Ps}}$, respectively, are nearly proportional to $\alpha^2 R_\infty$, hence a value of α can be obtained by equating an experimental value for a splitting to its corresponding theoretical expression. Because of the simplicity of these atoms, one expects that both the experimental value and theoretical expression can be known with high accuracy. Indeed, a value of α with a relative standard uncertainty $u_r = 5.7 \times 10^{-8}$ is deduced in this way in Sec. 3.3.9.d from data on muonium.

For hydrogen, the uncertainties of experimental values of $\Delta\nu_{\text{H}}$ as obtained by measuring the frequency of a well characterized hydrogen maser are extraordinarily small. For example, 20 years ago Petit, Desaintfussien, and Audoin (1980) reported

$$\Delta\nu_{\text{H}} = 1\,420\,405\,751.773(1) \text{ Hz} \quad [7 \times 10^{-13}]. \quad (294)$$

Nevertheless, a useful value of α cannot be derived from this impressive result, because the uncertainty of the theoretical expression for $\Delta\nu_{\text{H}}$ is $u_r \approx 5 \times 10^{-6}$, nearly seven orders of magnitude larger than that of the experimental value. The problem is that the contributions to $\Delta\nu_{\text{H}}$ due to the finite size and internal structure of the proton are large and difficult to calculate accurately (Karshenboim, 1997b; Bodwin and Yennie, 1988). Especially troublesome is the contribution arising from the polarizability of the proton. For example, based on an analysis of spin-dependent inelastic electron-proton scattering data, the fractional contribution δ_{pol} of the proton polarizability to $\Delta\nu_{\text{H}}$ can only be bounded by $|\delta_{\text{pol}}| < 4 \times 10^{-6}$ (Hughes and Kuti, 1983). [Because the muon is a structureless point-like particle, the problems of finite size and internal structure do not exist for $\Delta\nu_{\text{Mu}}$.]

It is also not yet possible to obtain a useful value of α from $\Delta\nu_{\text{Ps}}$. The experimental value with the smallest uncertainty is that reported by Ritter *et al.* (1984):

$$\Delta\nu_{\text{Ps}} = 203.389\,10(74) \text{ GHz} \quad [3.6 \times 10^{-6}]. \quad (295)$$

Further, although progress has been made in recent years in the calculation of $\Delta\nu_{\text{Ps}}$, Czarnecki, Melnikov, and Yelkhovsky (1999) estimate that its uncertainty due to uncalculated terms is $u_r = 2.3 \times 10^{-6}$.

In summary, only the muonium hyperfine splitting $\Delta\nu_{\text{Mu}}$, which is discussed in detail in Secs. 3.3.9.b to 3.3.9.d and in Appendix D, is of interest in the 1998 adjustment.

3.13. Fine Structure

As in the case of hyperfine splittings (see the previous section), fine-structure transition frequencies are nearly proportional to $\alpha^2 R_\infty$, and hence may also be used to deduce a value of α . Data related to the fine structure of hydrogen and deuterium are discussed in Sec. 3.2 in connection with the Rydberg constant. The three experimental results deemed useful for the 1998 adjustment are a value for the frequency of the interval $2S_{1/2} - 2P_{3/2}$ obtained at Harvard University by Hagley and Pipkin (1994), and two values for the frequency of the interval $2P_{1/2} - 2S_{1/2}$ (the classic Lamb shift), one obtained at Harvard University by Lundeen and Pipkin (1986), and the other at the University of Sussex by Newton *et al.* (1979). Combining the values for these intervals and comparing experiment and theory for the inferred interval $2P_{1/2} - 2P_{3/2}$ would provide a value of α with relative standard uncertainty $u_r \approx 7 \times 10^{-7}$, where the uncertainty would be largely from experiment. Although such a value is not competitive, we include these data in the adjustment because they influence the value of R_∞ .

The accuracy of the experimental determination of fine-structure frequencies involving hydrogen or deuterium $2P$ states is limited by the large natural widths of the levels. On the other hand, the 2^3P_J states of ^4He cannot decay to the ground 1^1S_0 state by allowed electric dipole transitions, so their levels are relatively narrow. Because the transition frequencies corresponding to the differences in energy of the three 2^3P levels can be both measured and calculated with reasonable accuracy, the fine structure of ^4He has long been viewed as a potential source of a reliable value of α .

The three frequencies of interest are $\nu_{01} \approx 29.6 \text{ GHz}$, $\nu_{12} \approx 2.29 \text{ GHz}$, and $\nu_{02} \approx 31.9 \text{ GHz}$, which correspond to the intervals $2^3P_1 - 2^3P_0$, $2^3P_2 - 2^3P_1$, and $2^3P_2 - 2^3P_0$, respectively. Improvements in experiment have been especially significant during the last decade [for a review of the early work, see Pichanick and Hughes (1990)]. For example, the group at the European Laboratory for Non-Linear Spectroscopy (LENS), Firenze, Italy has reported the value (Minardi *et al.*, 1999)

$$\nu_{01} = 29\,616\,949.7(2.0) \text{ kHz} \quad [6.8 \times 10^{-8}], \quad (296)$$

and three other groups are carrying out similar measurements: one at Harvard University (Roach, Levy, and Gabrielse, 1998), one at York University, Canada (Storrs and Hesses, 1998), and one at the University of North Texas (Koehler *et al.*, 1999; Shiner, Dixon, and Zhao, 1994). If the

theoretical expression for ν_{01} were exactly known, the result of Minardi *et al.* (1999) given in Eq. (296) would yield a value of α with $u_r = 3.4 \times 10^{-8}$.

Although the last decade has seen progress in the calculation of the 2^3P_J transition frequencies, the uncertainty of the theoretical expression for ν_{01} due to uncalculated terms is estimated to be of the order of ten times that of the LENS result (Zhang and Drake, 1996) and would lead to an uncertainty $u_r = 3 \times 10^{-7}$ in the value of α . Because a value of α with this uncertainty is not competitive, the ^4He fine-structure data are not included in the 1998 adjustment. On the other hand, as with the experimental measurements, theoretical calculations are in progress, and the ^4He fine structure could eventually provide a useful value of α .

3.14. Molar Gas Constant R

The equation of state of a real gas of atoms or molecules in thermal equilibrium at the thermodynamic temperature T , of amount of substance n , and occupying a volume V , can be written as a virial expansion (Colclough, 1973):

$$p = RT \frac{n}{V} \left[1 + \frac{n}{V} B(T) + \frac{n^2}{V^2} C(T) + \dots \right]. \quad (297)$$

Here p is the pressure of the gas, $R \approx 8.31 \text{ J mol}^{-1}$ is the molar gas constant, and $B(T)$ is the first virial coefficient, $C(T)$ is the second, etc. For an ideal gas the atoms or molecules do not interact, all of the virial coefficients are zero, and the equation of state reduces to the familiar $pV = nRT$.

In a similar manner, the square of the speed of sound $c_a^2(p, T)$ in a real gas at the pressure p and thermodynamic temperature T can be written as (Colclough, 1973)

$$c_a^2(p, T) = A_0(T) + A_1(T)p + A_2(T)p^2 + A_3(T)p^3 + \dots, \quad (298)$$

where $A_1(T)$ is the first acoustic virial coefficient, $A_2(T)$ is the second, etc. In the limit $p \rightarrow 0$, we have

$$c_a^2(0, T) = A_0(T) = \frac{\gamma_0 RT}{A_r(X)M_u}, \quad (299)$$

where the expression on the right-hand side is the square of the speed of sound for an unbounded ideal gas, and where $\gamma_0 = c_p/c_v$ is the ratio of the specific heat capacity of the gas at constant pressure to that at constant volume, $A_r(X)$ is the relative atomic mass of the atoms or molecules of the gas, and $M_u = 10^{-3} \text{ kg mol}^{-1}$. For a monatomic ideal gas, $\gamma_0 = 5/3$.

The most important of the historical measurements of R , which are based on Eq. (297) and were carried out by the so-called method of limited density, have been carefully reviewed by Colclough (1984b) [see also Quinn, Colclough, and Chandler (1976)]. In this approach one measures p and the mass $m(p)$ of different amounts of a gas (usually O_2 or N_2) occupying a constant volume V at the temperature $T_0 = 273.15 \text{ K}$ (the ice point). The quantity $L(p) = (p_0/p)m(p)/V$, where $p_0 = 101.325 \text{ kPa}$ (one standard atmosphere), is then extrapolated to $p = 0$ and R is calculated

from the relation $R = p_0 A_r(X) M_u / L(0) T_0$. Although it was thought that the values of R obtained by this method had relative standard uncertainties of the order of $u_r = 3 \times 10^{-5}$, Quinn *et al.* (1976) and Colclough (1984b) conclude that errors from a number of systematic effects had been overlooked and that u_r is significantly larger than 3×10^{-5} . Thus these values of R were not considered for use in the 1986 adjustment (Cohen and Taylor, 1987), and we exclude them here as well.

The 1986 recommended value of R was based on measurements of the speed of sound in argon carried out at NPL in the 1970s using an acoustic interferometer (Quinn *et al.*, 1976; Colclough, Quinn, and Chandler, 1979). Values of $c_a^2(p, T_{\text{tw}})$, where $T_{\text{tw}} = 273.16 \text{ K}$ is the triple point of water, were obtained in the pressure range $p = 30 \text{ kPa}$ to 1.3 MPa and extrapolated to $p = 0$ in order to determine $A_0(T_{\text{tw}}) = c_a^2(0, T_{\text{tw}})$, and hence R from the relation

$$R = \frac{c_a^2(0, T_{\text{tw}}) A_r(\text{Ar}) M_u}{\gamma_0 T_{\text{tw}}}, \quad (300)$$

which follows from Eq. (299). [Recall that in the SI the triple point of water, $T_{\text{tw}} = 273.16 \text{ K}$, defines the kelvin: “The kelvin, unit of thermodynamic temperature, is the fraction $1/273.16$ of the thermodynamic temperature of the triple point of water.” (BIPM, 1998)] The uncertainty assigned to the 1986 recommended value is $u_r = 8.4 \times 10^{-6}$.

In the latter half of the 1980s, after completion of the 1986 adjustment, researchers at NIST also determined the molar gas constant from measurements of the speed of sound in argon at $T = T_{\text{tw}}$ (Moldover *et al.*, 1988a; Moldover *et al.*, 1988b). However, they used a spherical acoustic resonator in the pressure range $p = 25 \text{ kPa}$ to $p = 0.5 \text{ MPa}$ to determine $A_0(T_{\text{tw}})$ rather than an acoustic interferometer. Consequently, they were able to obtain a value of R with $u_r = 1.8 \times 10^{-6}$, an uncertainty that is about one-fifth that of the NPL result. Both values, which are in agreement and are discussed in the following two sections, are included as input data in the 1998 adjustment.

Since R cannot be expressed as a function of any other of our adjusted constants, we take R itself as an adjusted constant and the relation

$$R \doteq R \quad (301)$$

as the observational equation for the NIST and NPL measured values of R .

3.14.1. NIST: Speed of Sound in Argon

In contrast to the variable path length, 5.6 kHz fixed-frequency cylindrical acoustic interferometer used by Colclough *et al.* (1979) at NPL to measure $c_a^2(p, T_{\text{tw}})$ [see the following section], Moldover *et al.* (1988a) at NIST employed a spherical acoustic resonator of fixed dimensions (180 mm inside diameter) operated near five different radially symmetric modes at frequencies in the range 2.4 kHz to 9.5 kHz . The applicable relation is

$$c_a^2(p, T_{\text{tw}}) = \left[\frac{f_{0n}(p, T_{\text{tw}})}{\nu_{0n}} \right]^2 V^{2/3}, \quad (302)$$

where p is the pressure of the argon gas in the resonator at $T = T_{\text{tw}}$, $f_{0n}(p, T_{\text{tw}})$ is the measured resonance frequency of the n th mode of the resonator, ν_{0n} is an eigenfrequency which is exactly known from the theory of such resonators, and V is the volume of the resonator. In practice, corrections must be applied to the measured frequencies in order to use this equation. The largest such corrections are due to the absorption effect of the thermal boundary layer between the argon gas and the inside surface of the resonator and to the motion of the resonator wall. (Because of the boundary layer, the measured value of c_a is less than that in the unbounded fluid.) These corrections were obtained from theory, the known thermodynamic transport properties of Ar, and the known mechanical properties of the stainless steel from which the resonator was fabricated. Further, they were confirmed by various experimental studies, including acoustic measurements of the half-widths of the resonances.

As emphasized by Moldover *et al.* (1988a), there are two important advantages of the NIST spherical resonator over the NPL cylindrical interferometer. First, corrections to the radial-mode frequencies $f_{0n}(p, T_{\text{tw}})$ from the boundary layer are a factor of 10 smaller for the 180 mm diameter spherical resonator than for the longitudinal-mode frequencies of the 30 mm diameter cylindrical interferometer. Second, because resonances in the sphere are an order of magnitude narrower than in the cylinder, significantly smaller electroacoustic transducers can be used to excite them. As a consequence, the radially symmetric resonances are perturbed only in a minor, easily corrected manner.

In the NIST experiment, the volume V of the resonator at $T = T_{\text{tw}}$ was measured by determining the mass of the amount of mercury of known density that was required to fill it when the resonator was at this temperature. The mercury used was traceable to the mercury whose density was measured by Cook (1961) [see also Cook and Stone (1957)] with a relative standard uncertainty $u_r = 4.2 \times 10^{-7}$. The mercury employed in the NML Hg electrometer determination of K_J (see Sec. 3.5.1) was also traceable to the same mercury. Converting the resonator's volume determined in the weighing configuration to the resonator's volume in the acoustic resonances configuration required a net fractional correction of $4.82(17) \times 10^{-6}$ to account for a variety of effects, the largest of which was due to replacing the "drive" and "receive" transducers by plugs when the resonator was filled with mercury.

The volume of the resonator was measured three times, twice in September 1985 and once in April 1986, and speed-of-sound measurements were carried out during three separate fillings of the resonator with argon, two in late March 1986 and one in early April 1986. The total data set used to obtain $A_0(T) = c_a^2(0, T)$ by extrapolation to $p = 0$ consisted of 70 $c_a^2(p, T_{\text{tw}})$ vs. p data points obtained from measurements of the frequencies of the five modes f_{02} to f_{06} at each of 14 different values of p in the range 25 kPa to 0.5 MPa. In

extrapolating to $p = 0$, Moldover *et al.* (1988a) used a value of the third acoustic virial coefficient $A_3(T)$ from the literature and also included an additional term in Eq. (298) of the form $A_{-1}p^{-1}$ to account for imperfect thermal accommodation. The result of the extrapolation is

$$\begin{aligned} A_0(T_{\text{tw}}) &= c_a^2(0, T_{\text{tw}}) \\ &= 94\,756.178(144) \text{ m}^2 \text{ s}^{-2} \quad [1.5 \times 10^{-6}], \end{aligned} \quad (303)$$

where the quoted uncertainty consists of 11 relative standard uncertainty components, the two largest of which are statistical (Type A): 8.0×10^{-7} from the calibration of the platinum resistance thermometer used to measure the temperature of the resonator and 6.8×10^{-7} from the extrapolation to $p = 0$. Other significant components (Type B) are 6.7×10^{-7} due to the thermal expansion of the mercury; 5.9×10^{-7} from the effect on the determination of the resonator's volume of a possible error in the location of the resonator's transducers; and 3.7×10^{-7} due to a vertical temperature gradient from the bottom to the top of the resonator.

The speed-of-sound measurements were made on a working argon gas sample designated Ar-M. The value of $A_r(\text{Ar-M})/\gamma_0$ was determined by comparing the speed of sound in Ar-M to the speed of sound in an isotopically enriched, highly purified ^{40}Ar sample, designated Ar-40, whose relative atomic mass could be calculated from the relative atomic masses of its constituent gases and the measured amount-of-substance fractions of those gases. Using the fractions given by Moldover *et al.* (1988a), the 1995 values of $A_r(^{40}\text{Ar})$, $A_r(^{38}\text{Ar})$, and $A_r(^{36}\text{Ar})$ given in Table 2, and the 1995 recommended values of the relative atomic masses of naturally occurring Ne, Kr, and Xe (Coplen, 1996), the only significant impurities in the Ar-40 sample, one finds

$$A_r(\text{Ar-40}) = 39.962\,519(34) \quad [8.4 \times 10^{-7}], \quad (304)$$

where the uncertainty is dominated by the uncertainty of the chromatographically determined amount-of-substance fraction of Xe in the Ar-40 sample. Moldover *et al.* (1988a) argue that since Ar, Ne, Kr, and Xe are monatomic gases and the electronic contributions to γ_0 are negligible at the values of p and T used in the measurements of $c_a^2(p, T)$, it can be assumed that $\gamma_0 = 5/3$ for this sample. Thus Eq. (304) leads to

$$\frac{A_r(\text{Ar-40})}{\gamma_0} = 23.977\,511(20) \quad [8.5 \times 10^{-7}]. \quad (305)$$

Moldover *et al.* (1988a) were only able to set an upper limit of 4.5×10^{-6} on the amount-of-substance fraction of N_2 in the Ar-40 sample. Based on their analysis, the fractional decrease in the above value of $A_r(\text{Ar-40})/\gamma_0$ that the N_2 might cause due to its different relative atomic mass and different values of c_p and c_v is less than 1.5×10^{-7} , which may be compared to the 8.4×10^{-7} relative standard uncertainty of $A_r(\text{Ar-40})$. However, since only an upper limit was set for the amount-of-substance fraction of nitrogen and the

actual amount could have been considerably smaller, we have not included a correction for this effect, but instead have included an additional relative standard uncertainty component of half of this possible fractional error in the uncertainty of the above value of $A_r(\text{Ar-40})/\gamma_0$.

The result of the Ar–M to Ar-40 speed-of-sound comparisons, done at $p \approx 115$ kPa and $T \approx 273.2$ K, is

$$\frac{c_a(\text{Ar-40})}{c_a(\text{Ar-M})} = 1 - 0.000\,184\,09(20) \quad [2.0 \times 10^{-7}]. \quad (306)$$

Following the well-founded assumption of Moldover *et al.* (1988a) that with sufficient accuracy for the present experiment one can take

$$\frac{c_a^2(\text{Ar-40})}{c_a^2(\text{Ar-M})} = \frac{A_r(\text{Ar-M})/\gamma_0}{A_r(\text{Ar-40})/\gamma_0} \quad (307)$$

[see Eq. (300)], one finds from Eqs. (305) and (306)

$$\frac{A_r(\text{Ar-M})}{\gamma_0} = 23.968\,684(22) \quad [9.4 \times 10^{-7}]. \quad (308)$$

This result, the result for $c_a^2(0, T_{\text{tw}})$ given in Eq. (303), and Eq. (300) yield

$$R = 8.314\,471(15) \text{ J mol}^{-1} \text{ K}^{-1} \quad [1.8 \times 10^{-6}]. \quad (309)$$

It should be emphasized that Moldover *et al.* (1988a) carefully investigated both experimentally and theoretically many possible sources of error in the experiment in order to substantiate their assigned uncertainty.

Recently, Moldover *et al.* (1999) reported the results of measurements at NIST of thermodynamic temperature in the range 217 K to 303 K using the same spherical resonator as was used to determine R . From data mainly acquired in 1992, they deduced a value for the triple point of gallium T_{tg} that was 4.3(8) mK larger than the value obtained by Moldover and Trusler (1988) in May 1986 with the gas-constant resonator, shortly after the acquisition of the data on which the NIST value of R is based. From data acquired when the resonator was filled with xenon in the course of the new measurements, Moldover *et al.* (1999) conjecture that the 1986 value of T_{tg} was in error because the argon used in the measurements became progressively contaminated over time. However, because all of the gas-constant resonator data used to determine R were obtained over an 8 d period and were mutually consistent, Moldover *et al.* (1999) and Moldover (1990) conclude that there is no evidence that contamination was a problem when the gas-constant data were acquired.

Because both the NIST result for R and the NML result for K_J are based on the same measured value of the density of mercury, and the uncertainty of that value is not negligible in either experiment, the two values are correlated with the non-negligible correlation coefficient $r = 0.068$.

3.14.2. NPL: Speed of Sound in Argon

In 1976, Quinn *et al.* (1976) reported the final result of the first NPL determination of R using a variable-path-length,

cylindrical acoustic interferometer. In the NPL experiment, a transducer of frequency $f = 5.6$ kHz was located at the bottom end of a 30 mm diameter cylindrical vertical cavity immersed in an ice bath and filled with Ar at a pressure p . The transducer, with an accelerometer attached to its diaphragm to measure its total impedance, excited and monitored the cavity's resonant frequencies as the acoustic reflector forming the top of the cavity was moved and its displacement measured by means of optical interferometry. Resonances were separated by $\Delta l = \lambda/2$, where Δl is the change in length of the cavity and λ is the wavelength of the standing wave in the cavity. The speed of sound was calculated from the known excitation frequency f and the value of λ , which was determined from the measured separations of five resonances.

The most significant correction that Quinn *et al.* (1976) had to make to their measured values of $c_a^2(p, T_{\text{tw}})$ was due to the thermal boundary layer. In the NPL experiment the fractional correction applied to c_a was rather large because of the comparatively small diameter of the cylindrical cavity: about 3×10^{-3} at $p = 30$ kPa and 1×10^{-3} at $p = 200$ kPa. The absorption coefficient required to evaluate this correction was determined from measurements, by means of the accelerometer, of the complex impedance of the transducer (arising from its own mechanical impedance and that due to the gas loading) when the acoustic reflector was moved through the five resonances. The total data set employed for this purpose consisted of the 98 $c_a^2(p, T_{\text{tw}})$ vs. p data points used to obtain $c_a^2(0, T_{\text{tw}})$ by extrapolation to $p = 0$, with p in the range 30 kPa to 200 kPa, plus seven additional data points acquired at pressures of about 10 kPa and 20 kPa.

Because the 98 data points showed significant curvature, Quinn *et al.* (1976) fit them with the function $c_a^2(p, T_{\text{tw}}) = A_0(T) + A_1(T)p + A_2(T)p^2$ to obtain $c_a^2(0, T_{\text{tw}})$. This gave a very small value for $A_1(T)$ and a surprisingly large value for $A_2(T)$. Subsequently, based on work on Ar–Ar intermolecular potentials and measurements of $A_2(T)$, Rowlinson and Tildesley (1977) argued that the Quinn *et al.* (1976) value of $A_1(T)$ was too small and that the $c_a^2(p, T_{\text{tw}})$ vs. p isotherm in the pressure range 30 kPa to 200 kPa should be essentially linear. This led to the discovery that a systematic error due to the nonlinearity of the transducer had been overlooked by Quinn *et al.* (1976) (Colclough, 1979a; Colclough, 1979b). When the correction for this error was applied to the 98 original data points, together with additional corrections for some relatively minor effects, Colclough *et al.* (1979) found that the resulting isotherm was nearly linear with a slope close to that predicted by Rowlinson and Tildesley (1977). Further, they found that the implied value of R was smaller by the fractional amount 1.6×10^{-4} than the value reported by Quinn *et al.* (1976).

Colclough *et al.* (1979) also obtained 48 new data points in the pressure range 200 kPa to 1.3 MPa in order to further clarify the earlier measurements. The new data were acquired by essentially the same method, but with an apparatus modified to withstand higher pressures. A new transducer was installed as well, and in the new work all of the critical

electronic and mechanical components were carefully adjusted before the measurements began so that subsequent corrections for small misadjustments would not be required as in the work of Quinn *et al.* (1976). Colclough *et al.* (1979) readily observed a reduced low-pressure nonlinear behavior in the new transducer; however, the effect was negligible at $p > 20$ kPa and hence was not a problem in the new measurements.

Inasmuch as the corrected data of Quinn *et al.* (1976) and the new high-pressure data of Colclough *et al.* (1979) were highly consistent, the latter workers combined all of the data (146 data points) and fit them with a function containing $A_2(T)$. The final result is (Colclough *et al.*, 1979; Colclough, 1984a)

$$c_a^2(0, T_{\text{tw}}) = 94\,756.75(78) \text{ m}^2 \text{ s}^{-2} \quad [8.2 \times 10^{-6}], \quad (310)$$

where the principal relative standard uncertainty components are a 6.1×10^{-6} Type A component from the fit to the data, and the following Type B components: 4×10^{-6} from the calibration of the instrumentation used to measure the absorption coefficient, 2.7×10^{-6} each for the transducer non-linearity correction and the correction for molecular slip, and 1.7×10^{-6} from the measurement of temperature.

To calculate the relative atomic mass of the argon sample used in the NPL experiment, we follow the general approach employed in the 1986 adjustment (Cohen and Taylor, 1987). We use the amount of substance ratio $n(^{36}\text{Ar})_{\text{atm}}/n(^{40}\text{Ar})_{\text{atm}} = 0.003\,378(17)$ for atmospheric argon as determined by Nier (1950), and the ratios $n(^{38}\text{Ar})_{\text{NPL}}/n(^{36}\text{Ar})_{\text{NPL}} = 0.189(1)$ and $[n(^{36}\text{Ar})_{\text{NPL}}/n(^{40}\text{Ar})_{\text{NPL}}]/[n(^{36}\text{Ar})_{\text{atm}}/n(^{40}\text{Ar})_{\text{atm}}] = 0.994\,44(21)$ as determined at IRMM, Geel, Belgium and given by Quinn *et al.* (1976). Here the subscript “atm” indicates “Ar naturally occurring in the atmosphere” and the subscript “NPL” indicates the argon used in the NPL speed-of-sound measurements. We assume that the atmospheric argon prepared at IRMM by purifying air has the same isotopic composition as the atmospheric argon prepared in a similar manner by Nier (1950). The assigned uncertainties are our own estimates. For the ratios obtained by Nier (1950), we take into account his assigned probable error (50 % confidence level) and the range of values expected for the ratios in naturally occurring argon as deduced by the IUPAC Commission on Atomic Weights and Isotopic Abundances (Rosman and Taylor, 1998). For the ratios determined by IRMM, we assume that the uncertainties quoted by Quinn *et al.* (1976) are standard uncertainties. Using these data and the 1995 values of $A_r(^{40}\text{Ar})$, $A_r(^{38}\text{Ar})$, and $A_r(^{36}\text{Ar})$ given in Table 2, we obtain for the relative atomic mass of the NPL argon

$$A_r(\text{Ar})_{\text{NPL}} = 39.947\,752(75) \quad [1.9 \times 10^{-6}]. \quad (311)$$

Quinn *et al.* (1976) found that their argon sample typically contained N_2 and water vapor with amount-of-substance fractions x of 14×10^{-6} and 2×10^{-6} , respectively, and that in 1 day's data taking the amount of substance fraction of N_2 never increased to more than 20×10^{-6} . Taking into account

the differences between the relative atomic masses and values of c_p and c_v of N_2 and Ar, we find, based on the treatment of Moldover *et al.* (1988a), that $x(\text{N}_2) = 14 \times 10^{-6}$ leads to a fractional decrease in R of 0.45×10^{-6} . Similarly, we find that $x(\text{H}_2\text{O}) = 2 \times 10^{-6}$ decreases R by the fractional amount 0.23×10^{-6} . Although these corrections are marginal at best, we apply them for completeness, assuming that in each case the uncertainty is equal to one-half of the correction. Combining the value of $A_r(\text{Ar})_{\text{NPL}}$ in Eq. (311) with the value of $c_a^2(0, T_{\text{tw}})$ given in Eq. (310), we thus obtain from Eq. (300)

$$R = 8.314\,504(70) \text{ J mol}^{-1} \text{ K}^{-1} \quad [8.4 \times 10^{-6}]. \quad (312)$$

Although both the NIST and NPL values of R are based on the same values of $A_r(^{40}\text{Ar})$, $A_r(^{38}\text{Ar})$, and $A_r(^{36}\text{Ar})$, the uncertainties of these relative atomic masses are sufficiently small that the covariance of the two values of R is negligible.

3.15. Boltzmann Constant k

As is well known (Feynman, Leighton, and Sands, 1963), the Boltzmann constant $k \approx 1.38 \times 10^{-23} \text{ J K}^{-1}$, the basic constant of statistical mechanics and thermodynamics, is the constant of proportionality between thermodynamic temperature T and the mean kinetic energy of an atom or molecule of an ideal gas in thermal equilibrium at the temperature T :

$$\frac{1}{2} m \langle v^2 \rangle = \frac{3}{2} k T. \quad (313)$$

Here m is the mass of the atom or molecule and $\langle v^2 \rangle$ is its mean-square velocity. The Boltzmann constant is related to the molar gas constant R and Avogadro constant N_A by

$$k = \frac{R}{N_A}. \quad (314)$$

Since $m_e = 2R_\infty h / c \alpha^2$ and $N_A = A_r(\text{e}) M_u / m_e$, where $M_u = 10^{-3} \text{ kg mol}^{-1}$, one may write

$$N_A = \frac{c A_r(\text{e}) M_u \alpha^2}{2 R_\infty h}, \quad (315)$$

which leads to

$$k = \frac{2 R_\infty h}{c A_r(\text{e}) M_u \alpha^2} R. \quad (316)$$

The most accurate directly measured value of R has a relative standard uncertainty $u_r = 1.8 \times 10^{-6}$ (see Sec. 3.14.1), while for the group of constants multiplying R in Eq. (316) we have $u_r < 1 \times 10^{-7}$. This implies that a value of k with $u_r = 1.8 \times 10^{-6}$ can be inferred from that equation, and hence to be at all useful in the 1998 adjustment a directly measured value of k should have $u_r < 1 \times 10^{-5}$.

Unfortunately, no such value is currently available, although an experiment that could conceivably reach this level of uncertainty was undertaken in the 1980s by Storm (1986). It was based on measuring the mean-square-voltage $\langle U^2 \rangle$, or Johnson noise voltage, in a bandwidth Δf across the terminals of a resistor of resistance R_s in thermal equilibrium at the temperature T . According to the Nyquist theorem, these

quantities are related by $\langle U^2 \rangle = 4kTR_s \Delta f$, an expression with a fractional error of less than 1×10^{-6} for frequencies less than 1 MHz and $T < 25$ K. [For a status report on Johnson noise thermometry, see White *et al.* (1996).] Since in such experiments the voltage and resistance can best be measured in terms of the conventional electric units V_{90} and Ω_{90} (see Sec. 2.5), in analogy with the measurement of gyromagnetic ratios and of the Faraday constant (see Secs. 3.4 and 3.8), one has

$$k = \mathcal{K}_{90} \frac{K_{J-90}^2 R_{K-90}}{4} h, \quad (317)$$

where \mathcal{K}_{90} is the numerical value of $\langle U^2 \rangle / 4TR_s \Delta f$ obtained in the experiment multiplied by the unit W s K^{-1} . Since K_{J-90} and R_{K-90} are defined quantities with no uncertainty, Eq. (317) shows that the experiment actually determines k/h in SI units, not k .

If a measured value of the quantity \mathcal{K}_{90} with a sufficiently small uncertainty becomes available, it can be included in a least-squares adjustment based on the 1998 set of adjusted constants by means of the observational equation

$$\mathcal{K}_{90} \doteq \frac{8R_\infty R}{c K_{J-90}^2 R_{K-90} A_r(e) M_u \alpha^2}, \quad (318)$$

which follows from Eqs. (316) and (317).

Another approach to the possible determination of k , emphasized recently by Pendrill (1996), is based on the virial expansion of the Clausius–Mossotti equation for a real gas of atoms of amount of substance n occupying a volume V :

$$\frac{\epsilon - \epsilon_0}{\epsilon + 2\epsilon_0} = \frac{n}{V} A_\epsilon \left(1 + \frac{n}{V} B_\epsilon + \frac{n^2}{V^2} C_\epsilon + \dots \right). \quad (319)$$

Here ϵ is the permittivity of the gas, ϵ_0 is the exactly known electric constant (see Sec. 2.2), A_ϵ is the molar polarizability of the atoms, and B_ϵ , C_ϵ , etc., are the dielectric virial coefficients. The molar polarizability A_ϵ is related to the molar gas constant R , the Boltzmann constant k , and the static electric dipole polarizability of the atoms α_0 by

$$A_\epsilon = \frac{R\alpha_0}{3\epsilon_0 k}. \quad (320)$$

Hence a measurement of A_ϵ/R together with a theoretical value for α_0 yields a value of k .

By expressing the quotient n/V in Eq. (319) in terms of pressure p , temperature T , and R by means of Eq. (297), one can in fact determine the quantity A_ϵ/R experimentally using dielectric constant gas thermometry or DCGT (Luther, Grohmann, and Fellmuth, 1996). In this technique, the fractional change in capacitance $\Delta C(p) = C(p)/C(0) - 1$ of a suitable gas-filled capacitor at a constant temperature T is determined as a function of the pressure p of the gas: The capacitance C of the capacitor is measured with the space between its electrodes filled with the gas at various pressures p and with the space evacuated so that $p=0$. A polynomial fit to the resulting p vs. $\Delta C(p)$ data points, together with knowledge of the dependence of the dimensions of the capacitor on p , yields

A_ϵ/R . The value with the smallest uncertainty determined to date is that obtained by Luther *et al.* (1996) for ^4He over the temperature range 4.2 K to 27 K (Fellmuth, 1999):

$$\frac{A_\epsilon}{R} = 6.221\,12(19) \times 10^{-8} \text{ K Pa}^{-1} \quad [3.0 \times 10^{-5}]. \quad (321)$$

Equation (321) is the final result of work that had yielded the preliminary value reported by Grohmann and Luther (1992), but in contrast to their value the assigned uncertainty in Eq. (321) includes all known components. [Note that Eq. (321) is not actually given by Luther *et al.* (1996), but can be inferred from the agreement of the DCGT temperature scale and the NPL-75 constant volume gas thermometry scale (Fellmuth, 1999).]

Ab initio calculations of the static electric dipole polarizability of the 1^1S ground state of the ^4He atom in the ^4He reduced atomic unit of electric polarizability, $\alpha_0^*(^4\text{He}) = \alpha_0(^4\text{He})/4\pi\epsilon_0 a_0^3 (1 + m_e/m_\alpha)^3$, have been carried out over the years by a number of workers (a_0 is the Bohr radius and m_e/m_α is the electron to α particle mass ratio). In terms of this calculated value and the experimentally determined value of A_ϵ/R for ^4He , Eq. (320) yields

$$k = \frac{4\pi a_0^3 (1 + m_e/m_\alpha)^3}{3} \frac{\alpha_0^*(^4\text{He})}{(A_\epsilon/R)^4_{\text{He}}}. \quad (322)$$

A value of $\alpha_0^*(^4\text{He})$ can be obtained by combining the nonrelativistic result $\alpha_0^*(^4\text{He})_{\text{NR}} = 1.383\,241\dots$ of Bhatia and Drachman (1994) with the relativistic correction $\Delta\alpha_0^*(^4\text{He})_{\text{R}} = -7.65 \times 10^{-5}$ of Johnson and Cheng (1996):

$$\alpha_0^*(^4\text{He}) = 1.383\,165. \quad (323)$$

Using this value with the experimental value of A_ϵ/R given in Eq. (321), we obtain from Eq. (322) and the 1998 recommended values of a_0 and m_e/m_α , whose uncertainties are negligible in this context,

$$k = 1.380\,625 \times 10^{-23} \text{ J K}^{-1}. \quad (324)$$

We have deliberately avoided assigning an uncertainty to the above value of $\alpha_0^*(^4\text{He})$, and hence to this deduced value of k , because of the large variations in the values of $\alpha_0^*(^4\text{He})$ obtained by different authors and the omission of potentially important terms. Pendrill (1996) assigns $u_r = 1 \times 10^{-5}$ to the above value of $\alpha_0^*(^4\text{He})$, but Luther *et al.* (1996), after a careful review of the literature, assign $u_r = 1.9 \times 10^{-5}$. Our own review supports a larger value as well. We therefore conclude that, although improvements in both experiment and theory may make it useful for a future adjustment, this route to k is not useful for the 1998 adjustment. As a consequence, the 1998 recommended value of k is calculated from Eq. (316) using the recommended values of the adjusted constants R_∞ , h , R , $A_r(e)$, and α .

3.16. Stefan–Boltzmann Constant σ

The radiant exitance M of an ideal thermal radiator or blackbody (also called a Planckian radiator) at the thermodynamic temperature T is given by

$$M = \sigma T^4, \quad (325)$$

where $\sigma \approx 5.67 \times 10^{-8} \text{ W m}^{-2} \text{ K}^{-4}$ is the Stefan–Boltzmann constant (Quinn and Martin, 1985). It is related to c , h , and the Boltzmann constant k by

$$\sigma = \frac{2\pi^5 k^4}{15h^3 c^2}, \quad (326)$$

which becomes, with the aid of Eq. (316) of the previous section,

$$\sigma = \frac{32\pi^5 h}{15c^6} \left(\frac{R_\infty R}{A_r(e) M_u \alpha^2} \right)^4. \quad (327)$$

In analogy with our discussion of k , the value of σ that can be inferred from Eq. (327) using the most accurate directly measured value of the molar gas constant R has a relative standard uncertainty $u_r = 7.1 \times 10^{-6}$ (essentially four times that of R). Thus to be at all useful in the 1998 adjustment, a directly measured value of σ should have $u_r < 4 \times 10^{-5}$.

Unfortunately, the most accurate direct value of σ has an uncertainty of $u_r = 1.3 \times 10^{-4}$. It was obtained by Quinn and Martin (1985) at NPL using a cryogenic absolute radiometer in which the radiant power emitted by a blackbody is compared to electric power. [The principle of operation of such radiometers is sometimes called “electrical substitution radiometry” (Martin, Fox, and Key, 1985).] The result of Quinn and Martin (1985), as revised for comparison purposes in the 1986 adjustment (Cohen and Taylor, 1987), is $\sigma = 5.669\,59(76) \times 10^{-8} \text{ W m}^{-2} \text{ K}^{-4}$ [1.3×10^{-4}], which may be compared to the 1998 recommended value $\sigma = 5.670\,400(40) \times 10^{-8} \text{ W m}^{-2} \text{ K}^{-4}$ [7.0×10^{-6}]. (Any change in the revised value resulting from our improved knowledge of the value of the NPL representation of the watt at the time of the experiment in terms of the watt is not expected to be significant.) A new experiment using a much improved radiometer is now underway at NPL with the goal of obtaining a direct value of σ with $u_r = 1 \times 10^{-5}$ (Martin and Haycocks, 1998). Clearly, such a result would be quite competitive.

In the new NPL experiment the electric power is measured in terms of the conventional electric unit W_{90} , not the watt W (see Sec. 2.5). This means that, in analogy with the discussion of the previous section regarding the Johnson noise determination of k , one has

$$\sigma = S_{90} \frac{K_{J-90}^2 R_{K-90}}{4} h, \quad (328)$$

where S_{90} is the numerical value of M/T^4 obtained in the experiment multiplied by the unit $\text{W m}^{-2} \text{ K}^{-4}$. Also in analogy with the Johnson noise determination of k , since K_{J-90} and R_{K-90} are defined quantities with no uncertainty, Eq. (328) shows that the experiment actually determines σ/h in SI units, not σ . When the anticipated measured value of the quantity S_{90} becomes available, it can be included in a least-squares adjustment based on the 1998 set of adjusted constants by means of the observational equation

$$S_{90} \doteq \frac{128\pi^5}{15c^6 K_{J-90}^2 R_{K-90}} \left(\frac{R_\infty R}{A_r(e) M_u \alpha^2} \right)^4, \quad (329)$$

which follows from Eqs. (327) and (328).

Because there are no direct data related to the Stefan–Boltzmann constant for use in the 1998 adjustment, the recommended value of σ is calculated from Eq. (327) in the same way the recommended value of k is calculated from Eq. (316).

3.17. Newtonian Constant of Gravitation G

There is no recognized quantitative theoretical relationship between the Newtonian constant of gravitation G and other fundamental physical constants. Moreover, because the experimental values of G currently available are independent of the other data relevant to the 1998 adjustment, they contribute only to the determination of the 1998 recommended value of G itself and can be considered independently of the other data.

The 1986 CODATA recommended value of G is (Cohen and Taylor, 1987)

$$G = 6.672\,59(85) \times 10^{-11} \text{ m}^3 \text{ kg}^{-1} \text{ s}^{-2} \quad [1.3 \times 10^{-4}]. \quad (330)$$

This value, but with one-half the uncertainty, was obtained at NIST in a NIST–University of Virginia (NIST–UVA) collaboration by Luther and Towler (1982) [see also Luther and Towler (1984)]. The experiment employed a rather classic torsion balance operated in the dynamic mode and the time-of-swing method. In this approach the angular oscillation frequency of the balance is determined by measuring the angular position of the balance as a function of time. The NIST–UVA balance consisted of a quartz torsion fiber about $12 \mu\text{m}$ in diameter and 40 cm long with a 7 g , dumbbell-like small-mass system, or test mass, suspended from its center at the end of the fiber with its axis horizontal. The test mass consisted of two tungsten disks about 2.5 mm thick and 7.2 mm in diameter, the centers of which were connected by a tungsten rod about 1 mm in diameter and 29 mm long. A small mirror attached to the fiber was used with an autocollimator to determine the balance’s angular position. The large-mass system, or source mass, which provided the gravitational torque on the balance, consisted of two tungsten spheres, each about 10.2 cm in diameter and with a mass of about 10.5 kg . With the source masses in their “far” position (in this case, removed), the period of oscillation of the balance was about 6 min , and the change in period with the source masses in their “near” position was a few percent. In this position, the source masses were located at opposite ends of the dumbbell in its rest position with their centers in line with the axis of the dumbbell and separated by about 14 cm . The value of G was obtained from the change in angular frequency of the torsion balance and the calculation of the gravitational potential energy of the small-mass system in the gravitational field of the large-mass system, based on measurements of the dimensions, angles, masses, and densi-

ties of the components of the apparatus, as appropriate. (Calculations of this type are required in all experiments to determine G .) Although Luther and Towler (1982) had originally assigned a relative standard uncertainty $u_r = 6.4 \times 10^{-5}$ to their result, this was doubled by the CODATA Task Group on Fundamental Constants to reflect the fact that measurements of G have historically been rather difficult to carry out and, since the experiment was expected to continue, the result of Luther and Towler (1982) was not final.

Four other values of G were initially considered for use in the 1986 adjustment but were subsequently rejected for one or more of the following reasons: the uncertainty was not competitive, the data were internally inconsistent, or there was insufficient information to make a reliable uncertainty assessment. These four values were the 1973 CODATA recommended value (Cohen and Taylor, 1973)

$$G = 6.6720(41) \times 10^{-11} \text{ m}^3 \text{ kg}^{-1} \text{ s}^{-2} \quad [6.1 \times 10^{-4}], \quad (331)$$

which is the weighted mean of the result obtained in the 1920s by Heyl (1930) and the result obtained in 1940 by Heyl and Chrzanowski (1942); the result of Pontikis (1972)

$$G = 6.6714(6) \times 10^{-11} \text{ m}^3 \text{ kg}^{-1} \text{ s}^{-2} \quad [9.0 \times 10^{-5}], \quad (332)$$

the value reported by Sagitov *et al.* (1979)

$$G = 6.6745(8) \times 10^{-11} \text{ m}^3 \text{ kg}^{-1} \text{ s}^{-2} \quad [1.2 \times 10^{-4}], \quad (333)$$

and the result of Karagyoz, Silin, and Iszmaylov (1981)

$$G = 6.6364(15) \times 10^{-11} \text{ m}^3 \text{ kg}^{-1} \text{ s}^{-2} \quad [2.3 \times 10^{-4}]. \quad (334)$$

Each of these values was obtained using a fiber-based torsion balance operated in the dynamic mode. Heyl (1930) and Heyl and Chrzanowski (1942) used the time-of-swing method to determine the angular oscillation frequency of the balance, as did Sagitov *et al.* (1979) and Karagyoz *et al.* (1981), while Pontikis (1972) used a resonance method.

Since the completion of the 1986 adjustment, a number of values of G with uncertainties sufficiently small to be of interest have been reported. Those available prior to 1997 are reviewed by Gillies (1997). More recent results were reviewed at the November 1998 conference in London organized by the Institute of Physics to mark the bicentenary of the publication of Cavendish's classic determination of G . The conference was entitled "The Gravitational Constant: Theory and Experiment 200 Years after Cavendish," and the papers presented at it appear in the June 1999 issue of *Measurement Science and Technology*.

Prominent among the post-1986 values is the result obtained at PTB by Michaelis, Haars, and Augustin (1996),

$$G = 6.715\,40(56) \times 10^{-11} \text{ m}^3 \text{ kg}^{-1} \text{ s}^{-2} \quad [8.3 \times 10^{-5}], \quad (335)$$

using a horizontal balance beam supported by a body floating in liquid mercury. A gravitational torque applied to the beam was balanced, and thereby measured, against a compensating

torque produced electrostatically by a quadrant electrometer. By employing a mercury bearing rather than a torsion fiber, Michaelis *et al.* (1996) were able to use a 240 g test-mass system, significantly increasing the gravitational force in the experiment. The system consisted of two glass-ceramic 120 g cylindrical test masses suspended from opposite ends of the beam with their axes horizontal and perpendicular to the axis of the beam. The source-mass system that provided the torsional couple on the test masses consisted of four cylindrical masses, one at each end of each test mass with its axis in line with the axis of the test mass. The pair of source masses on opposite sides and ends of the balance beam were alternately brought to their near and far positions, thereby applying an alternating torsional couple to the balance of equal magnitude and opposite sign.

A voltage applied to the quadrant electrometer produced the compensating torque required to prevent an angular displacement of the balance. The value of G was calculated from this voltage and the dependence of the capacitance of the electrometer on angular displacement of the balance beam $dC/d\theta$, which was measured with a capacitance bridge in a separate experiment.

The PTB value for G exceeds the 1986 CODATA recommended value by $42\,u_{\text{diff}}$, where u_{diff} is the standard uncertainty of their difference, and hence the two values are in severe disagreement. Michaelis *et al.* (1996) looked intensively for a possible error in their work which could explain the discrepancy, but to no avail.

Since the 1986 adjustment, a factor affecting torsion-balance experiments has come to light. The determination of G using a fiber-based torsion balance operated in the dynamic mode and the time-of-swing method requires the measurement of a small change in the long oscillation period of the balance. For this application the torsional spring constant of the fiber should ideally be independent of frequency at extremely low frequencies, for example, at 3 mHz. From theoretical considerations based on accepted theories of the anelasticity of solids, Kuroda (1995) proposed that the anelasticity of such fibers is large enough to cause a value of G determined in this way to be biased by the multiplicative factor $(1 + 1/\pi Q)$, where Q is the quality factor of the main torsional mode of the fiber and it is assumed that the damping of the torsional balance is solely due to losses in the fiber. For $Q = 10^3$, the fractional error is about 3×10^{-4} . The existence of such a frequency-dependent torsional spring constant has in fact been demonstrated experimentally by Bagley and Luther (1997) as part of their experiment to determine G (discussed briefly below) and by Matsumura *et al.* (1998) [see also Kuroda (1999)].

Table 13 summarizes the most important of the values of G with $u_r < 2 \times 10^{-3}$ that have been reported since 1986, and Fig. 1 compares them graphically. The stated value of G , including its uncertainty, is that quoted by the laboratory and is the most recent value available (one or more earlier results have been published by a number of the laboratories).

For purposes of comparison, Table 13 and Fig. 1 also

TABLE 13. Summary of the principal experimental values of the Newtonian constant of gravitation G with relative standard uncertainties $u_r < 2 \times 10^{-3}$ reported since the completion of the 1986 CODATA adjustment of the values of the constants, together with the 1986 and 1998 CODATA recommended values. (See the text for brief discussions of the experiments.)

Item No.	Source	Identification	Method	$10^{11} G$ $\text{m}^3 \text{kg}^{-1} \text{s}^{-2}$	Rel. stand. uncert. u_r
1.	1986 CODATA, from Luther and Towler (1982)	CODATA-86	Fiber torsion balance, dynamic mode	6.672 59(85)	1.3×10^{-4}
2.	Michaelis <i>et al.</i> (1996)	PTB-95	Floating balance beam, compensation mode	6.715 40(56)	8.3×10^{-5}
3.	Bagley and Luther (1997)	LANL-97	Fiber torsion balance, dynamic mode	6.6740(7)	1.0×10^{-4}
4.	Karagioz <i>et al.</i> (1998)	TR&D-98	Fiber torsion balance, dynamic mode	6.6729(5)	7.8×10^{-5}
5.	Schwarz <i>et al.</i> (1999); and Schwarz <i>et al.</i> (1998)	JILA-98	Freely-falling body, acceleration change	6.6873(94)	1.4×10^{-3}
6.	Luo <i>et al.</i> (1999)	HUST-99	Fiber torsion balance, dynamic mode	6.6699(7)	1.0×10^{-4}
7.	Fitzgerald and Armstrong (1999)	MSL-99	Fiber torsion balance, compensation mode	6.6742(7)	1.0×10^{-4}
8.	Richman <i>et al.</i> (1999)	BIPM-99	Strip torsion balance, static deflection	6.683(11)	1.7×10^{-3}
9.	Nolting <i>et al.</i> (1999)	UZur-99	Stationary body, weight change	6.6754(15)	2.2×10^{-4}
10.	Kleinevoss <i>et al.</i> (1999)	UWup-99	Suspended body, displacement	6.6735(29)	4.3×10^{-4}
11.	1998 CODATA	CODATA-98	1986 CODATA value, increased uncertainty	6.673(10)	1.5×10^{-3}

include the 1986 and 1998 recommended values of G . The 1998 value,

$$G = 6.673(10) \times 10^{-11} \text{ m}^3 \text{ kg}^{-1} \text{ s}^{-2} \quad [1.5 \times 10^{-3}], \tag{336}$$

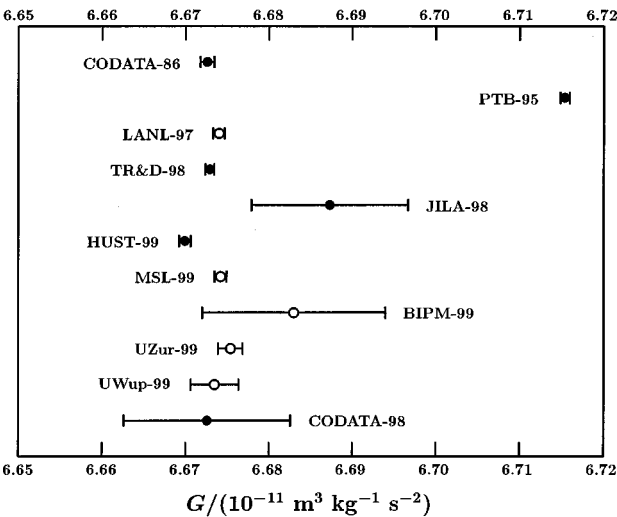


FIG. 1. Graphical comparison of the values of the Newtonian constant of gravitation G summarized in Table 13. An open circle indicates that the value is preliminary. (For the meanings of the identifying abbreviations in the figure, see the text.)

is the same as the 1986 value but its uncertainty is about a factor of 12 larger. The 1998 recommended value is the result of a careful review of the status of measurements of G by the CODATA Task Group on Fundamental Constants and is based on the following considerations:

- (i) Although the PTB experiment was carefully carried out, the resulting value of G is in severe disagreement with most other values, and a plausible explanation has not yet been found.
- (ii) The effect of torsion fiber anelasticity, which can be quite large, is still under investigation.
- (iii) Most of the experiments that have yielded the post-1986 values of G in Table 13 are still underway, and in each such case a result with a smaller uncertainty is anticipated. In fact, the Los Alamos National Laboratory (LANL-97), Measurement Standards Laboratory (MSL-99), BIPM (BIPM-99), University of Zurich (UZur-99), and University of Wuppertal (UWup-99) results are preliminary. Also, as discussed at the Cavendish conference, there are at least two other experiments well underway that could yield values of G with $u_r \approx 1 \times 10^{-5}$ in the next several years (Gundlach, 1999; Newman and Bantel, 1999).
- (iv) The 1986 CODATA recommended value of G has become a convenient reference against which all other

values are compared, and there are insufficient data on which to base a new value that is significantly different.

- (v) The uncertainty assigned to the 1998 recommended value G_{98} must reflect the existence of the PTB result G_{PTB} , the anelasticity problem, and the historic difficulty of determining G .
- (vi) The convenient standard uncertainty $u(G_{98}) = 0.010 \times 10^{-11} \text{ m}^3 \text{ kg}^{-1} \text{ s}^{-2}$ meets these requirements. Chosen so that $G_{\text{PTB}} - G_{98} \approx 4 u_{\text{diff}}$, it has the effect of reducing the discrepancy between the PTB value and the recommended value by a factor of 10 and producing a recommended value that encompasses all other values, except that from PTB, to within about 1.5 times the recommended value's standard uncertainty.

Because we do not obtain the 1998 recommended value of G from an in-depth numerical analysis of the available data, we do not give a detailed review of the values of G and their uncertainties, which are summarized in Table 13. Rather, we simply make a few cogent remarks about a value and/or provide a brief overview of the experiment as we have done above for the NIST-UVA and PTB efforts. In each case the cited paper should be consulted for references to earlier work.

(1) CODATA-86. A rough estimate of the Q of the quartz fiber employed in the NIST-UVA experiment of Luther and Towler (1982) is 2000 (Kuroda, 1999), which implies that the resulting value of G could be fractionally too large due to torsion fiber anelasticity by as much as 1.6×10^{-4} or about $1.2 u_r$.

(2) PTB-95. Michaelis *et al.* (1996) obtained two different values of G in their experiment, one with tungsten source masses of mass 900 g and one with source masses of identical size but made of the same glass-ceramic material as the test masses. The tungsten result is given in the table; the glass-ceramic result is $G = 6.7174(20) \times 10^{-11} \text{ m}^3 \text{ kg}^{-1} \text{ s}^{-2}$ [3.0×10^{-4}]. The two agree, but the uncertainty of the latter value is 3.6 times larger because of a much reduced signal due to the significantly smaller density (a factor of 1/7.5) of the glass-ceramic source masses.

(3) LANL-97. The experiment of Bagley and Luther (1997) at the Los Alamos National Laboratory (LANL) is in many ways similar to the NIST-UVA experiment of Luther and Towler (1982); it used the same dumbbell test mass and tungsten source masses. However, in the measurement of Bagley and Luther (1997), the far position of the source masses was a 90° rotation from their near position rather than removal. To test the anelasticity hypothesis of Kuroda (1995), Bagley and Luther (1997) used two different tungsten fibers, one with a Q of 950, the other with a Q of about 490. They found that the $Q=490$ result for G exceeded the $Q=950$ result by the fractional amount 345×10^{-6} compared to 315×10^{-6} predicted by the theory of Kuroda (1995). This level of agreement was interpreted by Bagley and Luther (1997) as confirming the theory. They therefore applied the appropriate fractional correction to each result

(650×10^{-6} and 335×10^{-6} , respectively) and combined the two to obtain the value given in Table 13. This work is being continued, and the reported results are considered preliminary.

(4) TR&D-98. The long-term researchers involved in the torsion-balance determination of G published by Karagioz, Izmaylov and Gillies (1998) are now at the Tribotech Research and Development Company (TR&D), Moscow, Russian Federation. The reported result, obtained using a torsion balance operated in the dynamic mode and the time-of-swing method, is the weighted mean of 12 values obtained from 12 series of measurements carried out from 1985 to 1989 as part of an effort to determine G that was initiated in Moscow over 25 years ago. The experiment was continuously improved over this period, with the measurements in 1985 and 1986 being done with version 1 of the apparatus, in 1987 with version 2, and in 1988 and 1989 with version 3. In version 3, a 25 μm diameter, 23 cm long fiber supported a 5.3 g test mass at its center. The test mass consisted of a cylindrical beam 23 cm long and 1.8 mm in diameter with its axis horizontal and with a 1.6 g spherical mass of diameter 7.2 mm at each end. The source-mass system consisted of two spherical masses at opposite ends of the suspended test mass with their centers aligned with the axis of the suspended beam. These masses could be moved individually or together along this axis. The different source masses used throughout the 5 years of measurements were one of brass (12.2 cm in diameter, mass of 8.0 kg), one of bronze (10.2 cm in diameter, mass of 4.9 kg), and several made of bearing steel (10.1 cm in diameter, mass of 4.3 kg).

In the early series of measurements only a single source mass was used and it was placed sequentially in four positions at distances 19.2 cm, 21.2 cm, 25.2 cm, and 47.2 cm from the torsion fiber. In the later series of measurements two source masses were used and placed symmetrically about the rotation axis at the same four distances as above. During the course of the measurements, a temporal shift of up to $0.001G$ and of unknown cause was observed in the values obtained. Karagioz *et al.* (1998) expect to publish an article on this aspect of their observations.

(5) JILA-98. The "free fall" experiment of Schwarz *et al.* (1999); and Schwarz *et al.* (1998) carried out at JILA (NIST-University of Colorado Joint Institute) in Boulder, Colorado is perhaps conceptually the simplest of all measurements of G . In this approach, one measures the change in the acceleration of free fall g of a freely falling test mass whose trajectory is perturbed by a source mass placed alternately above and below the region in which the test mass falls. Conducting the experiment in this differential mode eliminates errors present in conventional absolute gravimetry that would be five times larger than acceptable to reach the goal of determining G with $u_r = 2 \times 10^{-3}$.

The basis of the JILA experiment was a commercial absolute gravimeter in which the position as a function of time of a falling corner-cube reflector that defines one arm of a Michelson-type interferometer is measured by laser interferometry. The acceleration of the reflector (the test mass) as a

function of vertical position is determined from a fourth-order polynomial fit to the 700 position vs. time points obtained over the 20 cm drop. The polynomial employed is that appropriate for an object falling in a linear gravitational field. The fractional change in acceleration was about 8×10^{-8} when the toroidal (doughnut shaped) 500 kg primarily tungsten source mass surrounding the gravimeter was moved the 35 cm from its upper to its lower position. The value of G was extracted from the measured values of the change in acceleration by calculating the perturbing gravitational field of the source mass as a function of the position of the test mass and G , integrating the equation of motion to produce a series of theoretical position vs. time points and fitting them to the same fourth-order polynomial as was used to determine the acceleration of the test mass.

Two series of measurements were carried out, one in May 1997 and one in May 1998. A number of modifications were made to the apparatus between the series in order to reduce the scatter of the data, but quite surprisingly the scatter of the 1998 data was worse than that of the 1997 data. The weighted mean of the two values of G obtained in the two series, which agree well, has a relative standard uncertainty $u_r = 4.1 \times 10^{-4}$. Schwarz *et al.* (1999) combined this uncertainty with a component of 1.35×10^{-3} to account for the low-frequency scatter, thereby obtaining $u_r = 1.4 \times 10^{-3}$. The value given in Table 13 is the weighted mean together with this uncertainty.

(6) HUST-99. The determination of G by Luo *et al.* (1999) at the Huazhong University of Science and Technology (HUST), Wuhan, People's Republic of China used a torsion balance operated in the dynamic mode and the time-of-swing method. The balance consisted of a horizontal aluminum beam with a mass and length of about 55 g and 400 mm, respectively, suspended from its center by a 25 μm diameter tungsten torsion fiber about 0.5 m in length and with a Q of approximately 3.6×10^4 . A copper test mass of mass approximately 32 g was suspended from each end of the balance beam by 50 μm diam tungsten fibers, about 435 mm and 20 mm in length, respectively, so that the vertical separation of the two test masses was about 415 mm. Because of the high Q of the fiber, Luo *et al.* (1999) believe that fiber anelasticity is not a problem in their experiment.

The source-mass system consisted of two 6.25 kg stainless steel cylinders, 100 mm in length and diameter, placed with their axes horizontal and perpendicular to the axes of the balance beam and on either side of the lower test mass in such a way that the axes of the test mass and the two source masses were in line. In their near position, the faces of the source masses opposite one another and between which the test mass hung were separated by 60 mm; in the far position the source masses were removed. With the source masses in place, the period of the torsion balance was about 74 min; with the source masses removed, the period was about 58 min, corresponding to a fractional change of about 27 %. The angular position of the beam was determined as a function of time by means of a small mirror attached to the beam and an optical lever employing a He-Ne laser.

Luo *et al.* (1999) recognized the serious and well-known nonlinear effects characteristic of their torsion balance configuration: a very long torsion balance beam and test masses at significantly different heights exacerbate the nonlinear effects in the angular motion of the torsion balance due to inhomogeneities in the background gravitational field. Thus the angular oscillation frequencies with the source masses in their near and far positions were extracted from the angle-time data by a nonlinear least-squares fitting procedure. Luo *et al.* (1999) are planning to design a new torsion balance in order to reduce the nonlinear effects in their apparatus and obtain a value of G with a reduced uncertainty.

(7) MSL-99. The measurements of G using a torsion balance operating in the compensation mode at the Measurement Standards Laboratory (MSL), Industrial Research, Lower Hutt, New Zealand was initiated in the early 1990s by Fitzgerald and Armstrong (1999). In the MSL approach, the gravitational torque produced on the test mass by the source masses is compensated by an electrostatically induced torque. Because the torsion fiber does not twist (the suspended test mass remains stationary), fiber anelasticity is not a problem.

In the current version of the MSL apparatus, the fiber is made of tungsten, is 1 m in length, and has a rectangular cross section of 0.340 μm by 17 μm . The test mass suspended from the fiber, which also serves as the vane of the electrometer that provides the electrostatic torque to compensate the gravitational torque, is a horizontal 532 g copper cylinder 19 mm in diameter and 220 mm long. The two source masses are 28 kg stainless steel cylinders 438 mm long and 101 mm in diameter with their axes vertical; they rest on a turntable centered on the axis of the fiber and are positioned on opposite sides of the fiber. The turntable is rotated around the test mass and in each revolution is stopped in the four positions that produce maximum torque on the test mass. The value of G is calculated from the voltage that must be applied to the electrometer to balance the gravitational torque on the test mass when the turntable is stopped and from $dC/d\theta$, the change in capacitance of the electrometer with angular displacement of the test mass. This quantity is determined in a separate experiment by measuring the angular acceleration of the test mass when a voltage U_A is applied to the electrometer. The angular acceleration is measured by giving the entire torsion balance the same acceleration as the suspended test mass, thereby keeping the fiber from twisting.

The value of G given in Table 13 is from measurements done in 1998 with the version of the balance just described. This balance, as well as the experiment as a whole, contains a number of improvements compared to the balance and techniques used in a series of measurements carried out in 1995. In fact, the new work uncovered a fractional error in the earlier result of about 1.3×10^{-3} caused by the omission of a second-order term in the calculation of the torque between the source masses and the suspended test mass. Fitzgerald and Armstrong (1999) give as the corrected result of the earlier experiment $G = 6.6746(10)$

$\times 10^{-11} \text{ m}^3 \text{ kg}^{-1} \text{ s}^{-2}$, which agrees with the new result.

(8) BIPM-99. The torsion balance experiment of Richman *et al.* (1999) at the BIPM was begun in the mid-1990s and is in its early stages. The key ingredient of the balance is a thin, heavily loaded, copper–beryllium alloy torsion strip 160 mm long, 2.5 mm wide, and 30 μm thick that serves as its suspension element. Because 90 % of the stiffness of the strip is due to its load and only 10 % to its elasticity, anelasticity effects are greatly reduced. Four symmetrically arranged (i.e., 90° apart) test masses rest on a circular plate suspended from its center by the torsion strip and together with the plate form the oscillating “pendulum” of the balance; they are 1.2 kg cylinders of about 56 mm diameter and height with their axes vertical and made of a copper–tellurium alloy. The four source masses are 15.5 kg cylinders of about 130 mm diameter and height made from the same alloy; they rest on a carousel, again with their axes vertical. The axis of the carousel also coincides with that of the torsion strip and the source masses resting on it are arranged so that they are farther from the torsion strip than are the test masses. When aligned with the four test masses, the radial distance between the surfaces of each source mass and its corresponding test mass is 7 mm. Torque on the torsion strip is generated when the carousel is rotated from the aligned position ($\pm 2 \times 10^{-8} \text{ N m}$ maximum for $\pm 19^\circ$ angular displacement).

The value of G in Table 13 is the first result of the experiment and was obtained by measuring the difference in the angular displacement of the balance with the source masses in the two maximum torque positions and determining the stiffness of the torsional strip from the measured oscillation frequency of the balance. Future work with the balance under servo control with the gravitational torque balanced by an electrostatic torque is underway, and a value of G with $u_r \leq 1 \times 10^{-4}$ is anticipated by operating the balance in this compensation mode.

(9) UZur-99. The University of Zurich determination of G by Nolting *et al.* (1999) was initiated in the early 1990s and is being carried out at the Paul Scherrer Institute, Villigen, Switzerland; it grew out of the Geigerwald storage-lake measurement of G by Hubler, Cornaz, and Kündig (1995). In the new experiment, a commercial single-pan, flexure-strip balance, modified to achieve a resolution of 100 ng and a reproducibility of 300 ng, is used to measure the change in the difference in weight of two cylindrical test masses when the position of two source masses is changed. The test masses are 1 kg copper weights in fixed positions; the movable source masses, which surround the test masses, are toroidal stainless steel tanks 0.7 m high, of outer and inner diameters 1.05 m and 0.1 m, and of volume 500 L. The axes of the test masses and source masses are vertical and coincident, and the test masses are about 1.4 m apart. In position I the source masses are almost touching and the upper test mass is at the upper end of the upper source mass and the lower test mass is at the lower end of the lower source mass. In position II, the two source masses are separated by about 1.4 m so that the upper test mass is at the lower end of the upper source mass and the lower test mass is at the upper end of the lower

source mass. In each position, the difference in weight of the test masses is determined by weighing them alternately many times with the single-pan balance.

In the first University of Zurich determination of G with this apparatus, the tanks were filled with water and produced a change in the difference in weight of the two test masses equivalent to 110 μg when the tanks were in positions I and II. The value of G given in Table 13 is the result of 20 d of such measurements from which the change in the weight difference was determined with a statistical uncertainty (Type A) equivalent to 9 ng.

In the winter of 1997/1998, the tanks were filled with mercury, thereby increasing the change in weight difference to the equivalent of 800 μg . Two series of measurements with Hg were carried out that yielded values of G that differed by the fractional amount 1.6×10^{-4} , which was somewhat larger than the random variations within each run. Nevertheless, for the moment Nolting *et al.* (1999) take the simple mean of the two values, $G = 6.6749(14) \times 10^{-11} \text{ m}^3 \text{ kg}^{-1} \text{ s}^{-2}$ [2.2×10^{-4}], as the result of the two series for Hg, but have included in their assigned relative standard uncertainty a component of 8.0×10^{-5} to account for the discrepancy. Although no satisfactory explanation of the disagreement has yet been found, Nolting *et al.* (1999) suppose that balance nonlinearity may play a role. Work to resolve this problem is continuing, and Nolting *et al.* (1999) believe that their goal of determining G with $u_r = 1.0 \times 10^{-5}$ is still achievable.

(10) UWup-99. The experiment of Kleinevoss *et al.* (1999) at the University of Wuppertal, Wuppertal, Germany was begun in 1988. The apparatus consists of two microwave reflectors a distance $b = 24 \text{ cm}$ apart, each with a polished concave spherical surface and suspended by tungsten wires 2.6 m long. The reflectors, with their concave surfaces facing each other, form a Fabry–Pérot microwave resonator. A 576 kg brass cylindrical source mass is placed on the outer side of each reflector with its axis coincident with the axis of the resonator and the other source mass. The two source masses are moved symmetrically and simultaneously at intervals of 12 min from a reference position away from the reflectors to a measuring position near the reflectors. This causes the distance between the reflectors to change due to the change in gravitational forces acting on them. The measured quantity is the change in resonant frequency of the resonator Δf arising from the change in its length $\Delta b \approx 12 \text{ nm}$. The value of G in the table is the mean of three values obtained in mid-1998 from three different measuring positions. The work is continuing and Kleinevoss *et al.* (1999) hope to obtain a value of G with $u_r < 1 \times 10^{-4}$ from the current apparatus.

3.18. X-ray Units

The three most important units that historically have been used to express the wavelengths of x-ray lines are the copper $\text{K}\alpha_1$ x unit, symbol $\text{xu}(\text{Cu K}\alpha_1)$, the molybdenum $\text{K}\alpha_1$ x unit, symbol $\text{xu}(\text{Mo K}\alpha_1)$, and the ångström star, symbol

Å*. These units are defined by assigning an exact conventional value to the wavelength of the Cu K α_1 , Mo K α_1 , and W K α_1 x-ray lines when each is expressed in its corresponding unit:

$$\lambda(\text{Cu K}\alpha_1) = 1\,537.400 \text{ xu}(\text{Cu K}\alpha_1) \quad (337)$$

$$\lambda(\text{Mo K}\alpha_1) = 707.831 \text{ xu}(\text{Mo K}\alpha_1) \quad (338)$$

$$\lambda(\text{W K}\alpha_1) = 0.209\,010\,0 \text{ Å}^*. \quad (339)$$

Following the practice initiated in the 1986 adjustment, we also give in this adjustment a recommended value in meters for each of these units. The relevant data from which these values are derived and how we include that data in the 1998 adjustment are briefly discussed below. Other measurements involving the lattice spacings of silicon crystals and the comparison of the lattice spacings of different crystals are discussed in Sec. 3.1.3.c and in Sec. 3.9. Based on that discussion, when necessary we take 0.01×10^{-6} , $6.40(8) \times 10^{-6}$, and -0.34×10^{-6} as the fractional corrections to convert $d_{220}(\text{Si})$ at $t_{68} = 22.5^\circ\text{C}$ to $t_{90} = 22.5^\circ\text{C}$, $d_{220}(\text{Si})$ at $t_{90} = 22.5^\circ\text{C}$ to $t_{90} = 25^\circ\text{C}$, and $d_{220}(\text{Si})$ at $p = 0$ to $p = 100 \text{ kPa}$, respectively.

In a collaboration between Friedrich–Schiller University (FSU), Jena, Germany and the PTB, Härtwig *et al.* (1991) determined the wavelength of the Cu K α_1 line in terms of the lattice parameter a of a sample of the PTB crystal WASO 9 using the Bond method, an x-ray diffractometer technique that is a special version of the classic Bragg spectrometer technique. Based on the measured difference between a of crystal WASO 9 and a of PTB crystal WASO 4.2a as reported by Windisch and Becker (1990), the result of Härtwig *et al.* (1991) can be written as

$$\frac{\lambda(\text{Cu K}\alpha_1)}{d_{220}(\text{W4.2a})} = \frac{\lambda(\text{Cu K}\alpha_1)}{d_{220}^*(\text{W9})} \frac{d_{220}^*(\text{W9})}{d_{220}(\text{W4.2a})} = 0.802\,327\,11(24) \quad [3.0 \times 10^{-7}]. \quad (340)$$

Here the asterisk indicates that the reference conditions for d_{220} of crystal WASO 9 are $p = 101.325 \text{ kPa}$ and $t_{68} = 20^\circ\text{C}$ rather than our standard reference conditions $p = 0$, $t_{90} = 22.5^\circ\text{C}$. The assigned uncertainty is dominated by the 2.8×10^{-7} total relative standard uncertainty component arising from different aspects of the determination of the ratio $\lambda(\text{Cu K}\alpha_1)/d_{220}^*(\text{W9})$, the largest of which is 2.3×10^{-7} due to the uncertainties of various corrections; the relative standard deviation of the mean of the 146 individual measurements of the ratio is only 5×10^{-8} . The relative standard uncertainty of the ratio $d_{220}^*(\text{W9})/d_{220}(\text{W4.2a})$ is $u_r = 11 \times 10^{-8}$ and contains a component of 7×10^{-8} (Type B) to account for the observed large variations of the lattice parameter of the WASO 9 crystal due to the inhomogeneity of its impurity content (Windisch and Becker, 1990). [Note that the covariances of the result given in Eq. (340) with all the other PTB x-ray results are negligible.]

Using a double flat silicon crystal spectrometer, Kessler, Deslattes, and Henins (1979) at NIST compared the wave-

length of the W K α_1 line to the lattice parameter of the diffraction crystal of the spectrometer. Their result can be expressed as

$$\frac{\lambda(\text{W K}\alpha_1)}{d_{220}(\text{N})} = \frac{\lambda(\text{W K}\alpha_1)}{d_{220}^*(\text{W})} \frac{d_{220}^*(\text{W})}{d_{220}(\text{N})} = 0.108\,852\,175(98) \quad [9.0 \times 10^{-7}], \quad (341)$$

where $d_{220}(\text{N})$ denotes the {220} lattice spacing of the NIST XROI crystal (see Sec. 3.9.1.) at our standard reference conditions $p = 0$ and $t_{90} = 22.5^\circ\text{C}$, and $d_{220}^*(\text{W})$ is the {220} lattice spacing of the spectrometer's diffraction crystal at $p = 100 \text{ kPa}$ and $t_{68} = 22.5^\circ\text{C}$. The uncertainty is dominated by the 8.8×10^{-7} statistical relative standard uncertainty (Type A) associated with the measurements of the ratio $\lambda(\text{W K}\alpha_1)/d_{220}^*(\text{W})$; the ratio of the lattice parameters of the W and N crystals was determined by Kessler *et al.* (1979) in a separate experiment with the significantly smaller uncertainty $u_r = 7 \times 10^{-8}$.

Also at NIST and using a spectrometer similar to that of Kessler *et al.* (1979) but with the two crystals cut from the same boule from which the NIST XROI crystal was cut and only 10 mm from it, Deslattes and Henins (1973) compared the Mo K α_1 and Cu K α_1 x-ray lines to the lattice parameter of the diffraction crystal. The reference conditions for these measurements are $p = 100 \text{ kPa}$ and $t_{68} = 25^\circ\text{C}$. Data were taken in both transmission and reflection for each x-ray line and averaged; the final results can be written as

$$\frac{\lambda(\text{Mo K}\alpha_1)}{d_{220}(\text{N})} = 0.369\,406\,04(19) \quad [5.3 \times 10^{-7}] \quad (342)$$

$$\frac{\lambda(\text{Cu K}\alpha_1)}{d_{220}(\text{N})} = 0.802\,328\,04(77) \quad [9.6 \times 10^{-7}]. \quad (343)$$

The uncertainties are essentially those assigned by the experimenters and include components due to the index of refraction of silicon (required to evaluate the Bragg equation for the reflection data), measurement of temperature and angle, alignment of the apparatus, and scatter of the data. Although the two ratios have some common components of uncertainty, their covariance can be assumed to be negligible.

More recently, NIST researchers have measured the difference between $d_{220}(\text{N})$ and d_{220} of PTB crystal WASO 17, where the {220} lattice spacing of WASO 17 is relevant to the determination of the relative atomic mass of the neutron (see Secs. 3.1.3.c and 3.9). The result is (Kessler *et al.*, 1997; Kessler, 1999)

$$\frac{d_{220}(\text{W17}) - d_{220}(\text{N})}{d_{220}(\text{W17})} = 7(17) \times 10^{-9} \quad (344)$$

and reflects the new NIST lattice comparison protocol (see Sec. 3.1.3.c). The correlation coefficients of this fractional difference and the other NIST fractional differences given in Eqs. (51) to (53) are in the range -0.37 to 0.15 .

In order to obtain best values in the least-squares sense for $xu(\text{Cu K}\alpha_1)$, $xu(\text{Mo K}\alpha_1)$, and \AA^* , we take these units to be adjusted constants. Thus the observational equations for the data of Eqs. (340) to (343) are

$$\frac{\lambda(\text{Cu K}\alpha_1)}{d_{220}(\text{N})} \doteq \frac{1\,537.400\, xu(\text{Cu K}\alpha_1)}{d_{220}(\text{N})} \quad (345)$$

$$\frac{\lambda(\text{Mo K}\alpha_1)}{d_{220}(\text{N})} \doteq \frac{707.831\, xu(\text{Mo K}\alpha_1)}{d_{220}(\text{N})} \quad (346)$$

$$\frac{\lambda(\text{W K}\alpha_1)}{d_{220}(\text{N})} \doteq \frac{0.209\,010\,0\, \text{\AA}^*}{d_{220}(\text{N})} \quad (347)$$

$$\frac{\lambda(\text{Cu K}\alpha_1)}{d_{220}(\text{W4.2a})} \doteq \frac{1\,537.400\, xu(\text{Cu K}\alpha_1)}{d_{220}(\text{W4.2a})}, \quad (348)$$

where $d_{220}(\text{N})$ is taken to be an adjusted constant and $d_{220}(\text{W17})$ and $d_{220}(\text{W4.2a})$ are adjusted constants as well. In this context, the NIST XROI crystal simply plays the role of an intermediate reference crystal; a directly measured value of its $\{220\}$ lattice spacing $d_{220}(\text{N})$ in meters is not required.

3.19. Other Quantities

As pointed out in Sec. 1.4, there are a few cases in the 1998 adjustment where an inexact constant that enters the analysis of input data is taken to be a fixed quantity rather than an adjusted quantity, because the input data have a negligible effect on its value. Three such constants, used in the calculation of the theoretical expressions for the electron and muon magnetic moment anomalies a_e and a_μ (see Appendices B and C), are the mass of the tau lepton m_τ , the Fermi coupling constant G_F , and sine squared of the weak mixing angle $\sin^2 \theta_W$. The values we adopt for these constants are based on the most recent report of the Particle Data Group (Caso *et al.*, 1998):

$$m_\tau c^2 = 1\,777.05(29)\, \text{MeV} \quad [1.6 \times 10^{-4}] \quad (349)$$

$$\frac{G_F}{(\hbar c)^3} = 1.166\,39(1) \times 10^{-5}\, \text{GeV}^{-2} \quad [8.6 \times 10^{-6}] \quad (350)$$

$$\sin^2 \theta_W = 0.2224(19) \quad [8.7 \times 10^{-3}]. \quad (351)$$

Note, however, that the uncertainty assigned to $m_\tau c^2$ by the Particle Data Group is unsymmetrical and equal to $+0.29\, \text{MeV}$, $-0.26\, \text{MeV}$. For simplicity and because it is not at all critical, we have symmetrized the uncertainty by taking it to be $0.29\, \text{MeV}$. Also, the definition of $\sin^2 \theta_W$ depends on the renormalization prescription used. We take as its definition $\sin^2 \theta_W = s_W^2 \equiv 1 - (m_W/m_Z)^2$ based on the on-shell scheme, where m_W and m_Z are the masses of the W^\pm and Z^0 bosons, respectively, because this definition is conceptually simple and is that employed in the calculation of the electroweak contributions to a_e and a_μ (Czarnecki, Krause, and Marciano, 1996). The recommended value for the mass ratio of these bosons is $m_W/m_Z = 0.8818(11)$, which leads to our adopted value of $\sin^2 \theta_W$ given above. On the other hand, the value recommended by the Particle Data

Group (Caso *et al.*, 1998) is based on a particular variant of the modified minimal subtraction ($\overline{\text{MS}}$) scheme, which gives the much more accurate value $\sin^2 \theta_W(M_Z) = 0.231\,24(24)$.

4. Analysis of Data

In this portion of the paper, we analyze the previously discussed input data with the exception of the values of the Newtonian constant of gravitation G , since the latter have already been dealt with in Sec. 3.17. Based on this analysis, the focus of which is the compatibility of the data and the extent to which a particular datum would contribute to the determination of the 1998 recommended values of the constants, we select the final input data for the 1998 adjustment, decide how the data are to be treated, and carry out the final least-squares calculation from which the 1998 recommended values are obtained. Our analysis proceeds in three stages.

First we compare directly measured values of the same quantity, that is, data of the same type. An example is the four measured values of the von Klitzing constant R_K .

Next we compare directly measured values of different quantities, that is, data of different types, through the values of a third quantity that may be inferred from the values of the directly measured quantities. Prominent among these inferred values are the fine-structure constant α and the Planck constant h . For example, the four directly measured values of R_K are compared to the one directly measured value of the magnetic moment anomaly a_e through the five values of α that can be inferred from the five directly measured values. We have, of course, anticipated such comparisons by calculating values of α and h whenever appropriate as part of our review of the data. Such calculations are meaningful because many of the data of interest can be viewed as belonging to either one of two categories: data that determine α or data that determine h . Contributing to this dichotomy is the fact that the uncertainties of the measured values of those quantities that can be expressed as a combination of α and h , such as the Josephson constant $K_J = (8\alpha/\mu_0\hbar c)^{1/2}$, are significantly larger than the uncertainty of α . Thus these measured values only provide competitive information regarding h , not α .

Finally, we carry out a multivariate analysis of the data using the well-known method of least squares, which we briefly summarize in Appendix E as it is normally applied to the determination of recommended values of the fundamental constants. (Because computing a weighted mean is equivalent to applying the method of least squares in one dimension, that is, to the case of one variable, we in fact also employ the method of least squares in the first and second stages of our data analysis.)

Although the multivariate analysis of the data provides the most detailed, quantitative information regarding its overall consistency and the relative importance of individual items of data, because of the large number of such items and their diversity, and because a multivariate analysis is somewhat complex, this approach is not especially transparent. On the other hand, although less complete than the multivariate

analysis, comparisons of data of the same type, and comparisons of data of different types through the inferred value of a third quantity, are convenient methods for obtaining a general overview of the compatibility of the data and for identifying those data that are of greatest importance.

The principal input data relevant to the determination of the Rydberg constant R_∞ are not strongly coupled to the principal input data relevant to the determination of the other constants. We therefore carry out the first two stages of our data analysis on the two categories of data—Rydberg constant and other—independently. The third stage, multivariate analysis, is at first also carried out independently, but then on all of the data together. In fact, because of the complex nature of the Rydberg constant data, its second-stage analysis is actually done as a multivariate analysis. The two categories of data, with individual items appropriately numbered, are given in Tables 14.A.1 and 14.B.1. The covariances of the data in each table are given in the form of correlation coefficients in companion Tables 14.A.2 and 14.B.2. (Note that throughout this Analysis of Data portion of the paper, the letters “A” and “B” are associated with data in the first and second categories, respectively. Also, there are no correlations between the data in Table 14.A.1 and the data in Table 14.B.1.) The portions of the text where the data and their correlations are discussed are indicated in the last column of Tables 14.A.1 and 14.B.1. [In Table 14.B.1, the quantity \bar{R}^+ given in Eq. (166), Sec. 3.3.10.b, is denoted by \bar{R} , since by CPT invariance the sign of the charge is immaterial.]

The δ 's given in Tables 14.A.1 and 14.B.1 are additive corrections to various theoretical expressions that represent our lack of knowledge of those expressions. That is, each of the expressions includes an appropriate δ as an additive correction, where the initial estimate of each δ is zero but with an appropriate standard uncertainty. In Table 14.A.1 the δ 's are associated with the theoretical expressions for the energy levels of hydrogen (H) or deuterium (D) as indicated, while in Table 14.B.1 the δ 's are associated with the theoretical expressions for the electron and muon magnetic moment anomalies a_e and a_μ , and the ground-state hyperfine splitting of muonium $\Delta\nu_{\text{Mu}}$. These expressions are required to relate measured values of the frequencies of transitions between energy levels in H and D, a_e , a_μ , and $\Delta\nu_{\text{Mu}}$ to adjusted constants such as α and R_∞ . The expressions and our initial values for the uncertainties of the δ 's are discussed in Appendices A to D. Although the uncertainties depend on values of various constants, the uncertainties of the constants themselves are negligible in the calculation of the uncertainties of the δ 's.

4.1. Comparison of Data of the Same Type

This mode of comparison is obviously applicable only when there are two or more measurements of the same quantity. If there are only two measurements x_1 and x_2 , we simply compare them through their difference $\Delta = |x_1 - x_2|$ and the standard deviation of their difference $u_{\text{diff}} = \sqrt{u^2(x_1) + u^2(x_2)}$, since in this case the Birge ratio is

given by $R_B = \sqrt{\chi^2/\nu} = \Delta/u_{\text{diff}}$ with degrees of freedom $\nu = 1$ (see Appendix E). If there are N measurements with $N > 2$, we compare them by computing their weighted mean and resulting χ^2 and/or Birge ratio $R_B = \sqrt{\chi^2/\nu}$ with $\nu = N - 1$.

4.1.1. Rydberg Constant Data

The classic hydrogen Lamb shift is the only quantity in Table 14.A.1 with more than one measured value. The Harvard University and the University of Sussex results for this interval, items A14.1 and A14.2, agree: $\Delta = 0.8 u_{\text{diff}}$. The uncertainty of the Sussex value is 2.2 times that of the Harvard value, hence the weights of the two values in the calculation of their weighted mean are 0.83 and 0.17, respectively. Although these are the weights for their weighted mean, the effective weights of these data in the full least-squares calculation involving all of the data of Table 14.A.1 is less, because the remaining experimental and theoretical data provide information about this interval as well. In the case of the Lamb shift, they produce an *indirect* value of the interval with a significantly smaller uncertainty than either directly measured value. This is a common feature of a least-squares analysis and, in fact, in some cases the uncertainty of the indirect value is so small that one or more of the directly measured values are inconsequential.

4.1.2. Other Data

Other data refers to the input data related to the constants (R_∞ and G excepted) given in Tables 14.B.1 and 14.B.2. There are nine different quantities in Table 14.B.1 that have more than one measured value. We discuss each in turn.

$\Delta\nu_{\text{Mu}}$. The LAMPF 1982 and the LAMPF 1999 values of the muonium ground-state hyperfine splitting, items B17.1 and B17.2, are in agreement: $\Delta = 0.7 u_{\text{diff}}$. The uncertainty of the 1982 result exceeds that of the 1999 result by the factor 3.0, leading to a weight of 0.90 for the 1999 value and a weight of 0.10 for the 1982 value in the calculation of their weighted mean.

\bar{R} . The CERN value of \bar{R} , item B19.1, and the Brookhaven value of \bar{R} , item B19.2, agree: $\Delta = 0.1 u_{\text{diff}}$. Because the uncertainty of the Brookhaven value is 1.8 times that of the CERN value, the weights of the CERN and Brookhaven values in the calculation of their weighted mean are 0.77 and 0.23, respectively.

$\Gamma'_{p-90}(\text{lo})$. For the NIST and NIM values of $\Gamma'_{p-90}(\text{lo})$, items B21.1 and B21.2, $\Delta = 0.6 u_{\text{diff}}$, and hence they agree. However, the uncertainty of the NIM value exceeds that of the NIST value by a factor of 6.0, implying that in the calculation of the weighted mean of the two values, the weight of the NIST value is 0.97 and that of the NIM value is 0.03. We therefore conclude that the NIM value provides a limited amount of additional information.

$\Gamma'_{p-90}(\text{hi})$. The NIM and NPL values of $\Gamma'_{p-90}(\text{hi})$, items B22.1 and B22.2, agree; $\Delta = 0.1 u_{\text{diff}}$. Further, the uncertainty of the NIM value is 1.6 times that of the NPL value,

TABLE 14.A.1. Summary of principal input data for the determination of the 1998 recommended value of the Rydberg constant R_∞ . [The notation for the additive corrections $\delta_X(nL_j)$ in this table has the same meaning as the notation $\delta_{nL_j}^X$ in Appendix A, Sec. 12.]

Item number	Input datum	Value	Relative standard uncertainty ^a u_r	Identification	Sec.
A1	$\nu_H(1S_{1/2}-2S_{1/2})$	2 466 061 413 187.34(84) kHz	3.4×10^{-13}	MPQ-97	3.2.1
A2	$\nu_H(2S_{1/2}-8S_{1/2})$	770 649 350 012.1(8.6) kHz	1.1×10^{-11}	LK/LP-97	3.2.2
A3	$\nu_H(2S_{1/2}-8D_{3/2})$	770 649 504 450.0(8.3) kHz	1.1×10^{-11}	LK/LP-97	3.2.2
A4	$\nu_H(2S_{1/2}-8D_{5/2})$	770 649 561 584.2(6.4) kHz	8.3×10^{-12}	LK/LP-97	3.2.2
A5	$\nu_H(2S_{1/2}-12D_{3/2})$	799 191 710 472.7(9.4) kHz	1.2×10^{-11}	LK/LP-99	3.2.2
A6	$\nu_H(2S_{1/2}-12D_{5/2})$	799 191 727 403.7(7.0) kHz	8.7×10^{-12}	LK/LP-99	3.2.2
A7	$\nu_H(2S_{1/2}-4S_{1/2}) - \frac{1}{4} \nu_H(1S_{1/2}-2S_{1/2})$	4 797 338(10) kHz	2.1×10^{-6}	MPQ-95	3.2.1
A8	$\nu_H(2S_{1/2}-4D_{5/2}) - \frac{1}{4} \nu_H(1S_{1/2}-2S_{1/2})$	6 490 144(24) kHz	3.7×10^{-6}	MPQ-95	3.2.1
A9	$\nu_H(2S_{1/2}-6S_{1/2}) - \frac{1}{4} \nu_H(1S_{1/2}-3S_{1/2})$	4 197 604(21) kHz	4.9×10^{-6}	LKB-96	3.2.2
A10	$\nu_H(2S_{1/2}-6D_{5/2}) - \frac{1}{4} \nu_H(1S_{1/2}-3S_{1/2})$	4 699 099(10) kHz	2.2×10^{-6}	LKB-96	3.2.2
A11	$\nu_H(2S_{1/2}-4P_{1/2}) - \frac{1}{4} \nu_H(1S_{1/2}-2S_{1/2})$	4 664 269(15) kHz	3.2×10^{-6}	Yale-95	3.2.3
A12	$\nu_H(2S_{1/2}-4P_{3/2}) - \frac{1}{4} \nu_H(1S_{1/2}-2S_{1/2})$	6 035 373(10) kHz	1.7×10^{-6}	Yale-95	3.2.3
A13	$\nu_H(2S_{1/2}-2P_{3/2})$	9 911 200(12) kHz	1.2×10^{-6}	Harv-94	3.2.4
A14.1	$\nu_H(2P_{1/2}-2S_{1/2})$	1 057 845.0(9.0) kHz	8.5×10^{-6}	Harv-86	3.2.4
A14.2	$\nu_H(2P_{1/2}-2S_{1/2})$	1 057 862(20) kHz	1.9×10^{-5}	USus-79	3.2.5
A15	R_p	0.8545(120) fm	1.4×10^{-2}	Rp-98	3.2.7
A16	$\nu_D(2S_{1/2}-8S_{1/2})$	770 859 041 245.7(6.9) kHz	8.9×10^{-12}	LK/LP-97	3.2.2
A17	$\nu_D(2S_{1/2}-8D_{3/2})$	770 859 195 701.8(6.3) kHz	8.2×10^{-12}	LK/LP-97	3.2.2
A18	$\nu_D(2S_{1/2}-8D_{5/2})$	770 859 252 849.5(5.9) kHz	7.7×10^{-12}	LK/LP-97	3.2.2
A19	$\nu_D(2S_{1/2}-12D_{3/2})$	799 409 168 038.0(8.6) kHz	1.1×10^{-11}	LK/LP-99	3.2.2
A20	$\nu_D(2S_{1/2}-12D_{5/2})$	799 409 184 966.8(6.8) kHz	8.5×10^{-12}	LK/LP-99	3.2.2
A21	$\nu_D(2S_{1/2}-4S_{1/2}) - \frac{1}{4} \nu_D(1S_{1/2}-2S_{1/2})$	4 801 693(20) kHz	4.2×10^{-6}	MPQ-95	3.2.1
A22	$\nu_D(2S_{1/2}-4D_{5/2}) - \frac{1}{4} \nu_D(1S_{1/2}-2S_{1/2})$	6 494 841(41) kHz	6.3×10^{-6}	MPQ-95	3.2.1
A23	R_d	2.130(10) fm	4.7×10^{-3}	Rd-98	3.2.7
A24	$\nu_D(1S_{1/2}-2S_{1/2}) - \nu_H(1S_{1/2}-2S_{1/2})$	670 994 334.64(15) kHz	2.2×10^{-10}	MPQ-98	3.2.1
A25	$\delta_H(1S_{1/2})/h$	0(90) kHz	$[2.7 \times 10^{-11}]$	theory	App. A
A26	$\delta_H(2S_{1/2})/h$	0(11) kHz	$[1.4 \times 10^{-11}]$	theory	App. A
A27	$\delta_H(3S_{1/2})/h$	0.0(3.3) kHz	$[9.1 \times 10^{-12}]$	theory	App. A
A28	$\delta_H(4S_{1/2})/h$	0.0(1.4) kHz	$[6.8 \times 10^{-12}]$	theory	App. A
A29	$\delta_H(6S_{1/2})/h$	0.00(42) kHz	$[4.5 \times 10^{-12}]$	theory	App. A
A30	$\delta_H(8S_{1/2})/h$	0.00(18) kHz	$[3.4 \times 10^{-12}]$	theory	App. A
A31	$\delta_H(2P_{1/2})/h$	0.0(1.1) kHz	$[1.3 \times 10^{-12}]$	theory	App. A
A32	$\delta_H(4P_{1/2})/h$	0.00(14) kHz	$[6.6 \times 10^{-13}]$	theory	App. A
A33	$\delta_H(2P_{3/2})/h$	0.0(1.1) kHz	$[1.3 \times 10^{-12}]$	theory	App. A
A34	$\delta_H(4P_{3/2})/h$	0.00(14) kHz	$[6.6 \times 10^{-13}]$	theory	App. A
A35	$\delta_H(8D_{3/2})/h$	0.000(17) kHz	$[3.3 \times 10^{-13}]$	theory	App. A
A36	$\delta_H(12D_{3/2})/h$	0.0000(50) kHz	$[2.2 \times 10^{-13}]$	theory	App. A
A37	$\delta_H(4D_{5/2})/h$	0.00(14) kHz	$[6.6 \times 10^{-13}]$	theory	App. A
A38	$\delta_H(6D_{5/2})/h$	0.000(40) kHz	$[4.4 \times 10^{-13}]$	theory	App. A
A39	$\delta_H(8D_{5/2})/h$	0.000(17) kHz	$[3.3 \times 10^{-13}]$	theory	App. A
A40	$\delta_H(12D_{5/2})/h$	0.0000(50) kHz	$[2.2 \times 10^{-13}]$	theory	App. A
A41	$\delta_D(1S_{1/2})/h$	0(89) kHz	$[2.7 \times 10^{-11}]$	theory	App. A
A42	$\delta_D(2S_{1/2})/h$	0(11) kHz	$[1.4 \times 10^{-11}]$	theory	App. A
A43	$\delta_D(4S_{1/2})/h$	0.0(1.4) kHz	$[6.8 \times 10^{-12}]$	theory	App. A
A44	$\delta_D(8S_{1/2})/h$	0.00(17) kHz	$[3.4 \times 10^{-12}]$	theory	App. A
A45	$\delta_D(8D_{3/2})/h$	0.000(11) kHz	$[2.2 \times 10^{-13}]$	theory	App. A
A46	$\delta_D(12D_{3/2})/h$	0.0000(34) kHz	$[1.5 \times 10^{-13}]$	theory	App. A
A47	$\delta_D(4D_{5/2})/h$	0.000(92) kHz	$[4.5 \times 10^{-13}]$	theory	App. A
A48	$\delta_D(8D_{5/2})/h$	0.000(11) kHz	$[2.2 \times 10^{-13}]$	theory	App. A
A49	$\delta_D(12D_{5/2})/h$	0.0000(34) kHz	$[1.5 \times 10^{-13}]$	theory	App. A

^aThe values in brackets are relative to the frequency equivalent of the binding energy of the indicated level.

TABLE 14.A.2. Non-negligible correlation coefficients $r(x_i, x_j)$ of the input data related to R_∞ given in Table 14.A.1. For simplicity, the two items of data to which a particular correlation coefficient corresponds are identified by their item numbers in Table 14.A.1.

$r(A2, A3)=0.348$	$r(A5, A20)=0.114$	$r(A25, A27)=0.999$	$r(A30, A44)=0.998$
$r(A2, A4)=0.453$	$r(A6, A9)=0.028$	$r(A25, A28)=0.999$	$r(A31, A32)=0.990$
$r(A2, A5)=0.090$	$r(A6, A10)=0.055$	$r(A25, A29)=0.999$	$r(A33, A34)=0.990$
$r(A2, A6)=0.121$	$r(A6, A16)=0.151$	$r(A25, A30)=0.999$	$r(A35, A36)=0.990$
$r(A2, A9)=0.023$	$r(A6, A17)=0.165$	$r(A25, A41)=0.998$	$r(A35, A45)=0.944$
$r(A2, A10)=0.045$	$r(A6, A18)=0.175$	$r(A25, A42)=0.998$	$r(A35, A46)=0.935$
$r(A2, A16)=0.123$	$r(A6, A19)=0.121$	$r(A25, A43)=0.998$	$r(A36, A45)=0.935$
$r(A2, A17)=0.133$	$r(A6, A20)=0.152$	$r(A25, A44)=0.997$	$r(A36, A46)=0.944$
$r(A2, A18)=0.142$	$r(A7, A8)=0.105$	$r(A26, A27)=0.999$	$r(A37, A38)=0.990$
$r(A2, A19)=0.098$	$r(A7, A21)=0.210$	$r(A26, A28)=0.999$	$r(A37, A39)=0.990$
$r(A2, A20)=0.124$	$r(A7, A22)=0.040$	$r(A26, A29)=0.999$	$r(A37, A40)=0.990$
$r(A3, A4)=0.470$	$r(A8, A21)=0.027$	$r(A26, A30)=0.998$	$r(A37, A47)=0.944$
$r(A3, A5)=0.093$	$r(A8, A22)=0.047$	$r(A26, A41)=0.998$	$r(A37, A48)=0.935$
$r(A3, A6)=0.125$	$r(A9, A10)=0.141$	$r(A26, A42)=0.998$	$r(A37, A49)=0.935$
$r(A3, A9)=0.023$	$r(A9, A16)=0.028$	$r(A26, A43)=0.997$	$r(A38, A39)=0.990$
$r(A3, A10)=0.047$	$r(A9, A17)=0.031$	$r(A26, A44)=0.997$	$r(A38, A40)=0.990$
$r(A3, A16)=0.127$	$r(A9, A18)=0.033$	$r(A27, A28)=0.999$	$r(A38, A47)=0.935$
$r(A3, A17)=0.139$	$r(A9, A19)=0.023$	$r(A27, A29)=0.998$	$r(A38, A48)=0.935$
$r(A3, A18)=0.147$	$r(A9, A20)=0.028$	$r(A27, A30)=0.998$	$r(A38, A49)=0.935$
$r(A3, A19)=0.102$	$r(A10, A16)=0.056$	$r(A27, A41)=0.997$	$r(A39, A40)=0.990$
$r(A3, A20)=0.128$	$r(A10, A17)=0.061$	$r(A27, A42)=0.997$	$r(A39, A47)=0.935$
$r(A4, A5)=0.121$	$r(A10, A18)=0.065$	$r(A27, A43)=0.997$	$r(A39, A48)=0.944$
$r(A4, A6)=0.162$	$r(A10, A19)=0.045$	$r(A27, A44)=0.997$	$r(A39, A49)=0.935$
$r(A4, A9)=0.030$	$r(A10, A20)=0.057$	$r(A28, A29)=0.998$	$r(A40, A47)=0.935$
$r(A4, A10)=0.060$	$r(A11, A12)=0.083$	$r(A28, A30)=0.998$	$r(A40, A48)=0.935$
$r(A4, A16)=0.165$	$r(A16, A17)=0.570$	$r(A28, A41)=0.998$	$r(A40, A49)=0.944$
$r(A4, A17)=0.180$	$r(A16, A18)=0.612$	$r(A28, A42)=0.997$	$r(A41, A42)=0.999$
$r(A4, A18)=0.191$	$r(A16, A19)=0.123$	$r(A28, A43)=0.998$	$r(A41, A43)=0.999$
$r(A4, A19)=0.132$	$r(A16, A20)=0.155$	$r(A28, A44)=0.997$	$r(A41, A44)=0.999$
$r(A4, A20)=0.166$	$r(A17, A18)=0.667$	$r(A29, A30)=0.998$	$r(A42, A43)=0.999$
$r(A5, A6)=0.475$	$r(A17, A19)=0.134$	$r(A29, A41)=0.997$	$r(A42, A44)=0.998$
$r(A5, A9)=0.021$	$r(A17, A20)=0.169$	$r(A29, A42)=0.997$	$r(A43, A44)=0.998$
$r(A5, A10)=0.041$	$r(A18, A19)=0.142$	$r(A29, A43)=0.997$	$r(A45, A46)=0.990$
$r(A5, A16)=0.113$	$r(A18, A20)=0.179$	$r(A29, A44)=0.996$	$r(A47, A48)=0.990$
$r(A5, A17)=0.123$	$r(A19, A20)=0.522$	$r(A30, A41)=0.997$	$r(A47, A49)=0.990$
$r(A5, A18)=0.130$	$r(A21, A22)=0.011$	$r(A30, A42)=0.997$	$r(A48, A49)=0.990$
$r(A5, A19)=0.090$	$r(A25, A26)=0.999$	$r(A30, A43)=0.997$	

implying that the weights of the NPL and NIM values in the calculation of their weighted mean are 0.72 and 0.28, respectively.

$\Gamma'_{h-90}(lo)$. The KRISS/VNIIM and VNIIM values of $\Gamma'_{h-90}(lo)$, items B23.1 and B23.2, do not agree; $\Delta = 2.4 u_{\text{diff}}$. The ratio of the uncertainty of the VNIIM value to that of the KRISS/VNIIM value is 2.0, so that in the calculation of their weighted mean, the weight of the KRISS/VNIIM value is 0.79 and that of the VNIIM value is 0.21.

K_J . For the NML and PTB values of K_J , items B24.1 and B24.2, $\Delta = 0.3 u_{\text{diff}}$, indicating agreement. The uncertainty of the NML value is 1.2 times that of the PTB value, implying that the weights of the NML and PTB values in the calculation of their weighted mean are 0.58 and 0.42, respectively.

R_K . The values of R_K from NIST, NML, NPL, and NIM, items B25.1, B25.2, B25.3, and B25.4, are in agreement. Calculation of their weighted mean \hat{R}_K yields $\chi^2 = 1.46$ for $\nu = 3$, $R_B = 0.70$, and $Q(1.46|3) = 0.69$, where $Q(\chi^2|\nu)$ is the probability that an observed value of χ^2 for ν degrees of freedom would exceed χ^2 (see Appendix E). The normalized residuals, $r_i = [R_{K,i} - \hat{R}_K]/u(R_{K,i})$, for the four values are

0.18, -0.95 , 0.72, and 0.06, respectively, and their weights in the calculation of their weighted mean are 0.65, 0.19, 0.13, and 0.02. Clearly, the amount of additional information provided by the NIM result is limited.

$K_J^2 R_K$. Items B26.1 and B26.2, the NPL and NIST values of $K_J^2 R_K$, are consistent; $\Delta = 0.5 u_{\text{diff}}$. The ratio of the uncertainty of the NPL value to that of the NIST value is 2.3, leading to weights for the NIST and NPL values in the calculation of their weighted mean of 0.84 and 0.16, respectively.

R . The NIST and NPL values of R , items B42.1 and B42.2, are consistent; $\Delta = 0.5 u_{\text{diff}}$. However, because the uncertainty of the NPL value is 4.7 times that of the NIST value, the respective weights of the NIST and NPL values in the calculation of their weighted mean are 0.96 and 0.04. Thus the additional information contributed by the NPL result is limited.

In summary, we have identified a significant inconsistency between the two measurements of $\Gamma'_{h-90}(lo)$, items B23.1 and B23.2; and three data that provide limited information: the NIM value of $\Gamma'_{p-90}(lo)$, item B21.2; the NIM value of

TABLE 14.B.1. Summary of principal input data for the determination of the 1998 recommended values of the fundamental constants (R_∞ and G excepted).

Item number	Input datum	Value	Relative standard uncertainty ^a u_r	Identification	Sec. and Eq.
B1	$A_r(^1\text{H})$	1.007 825 032 14(35)	3.5×10^{-10}	AMDC-95	3.1.1
B2	$A_r(^2\text{H})$	2.014 101 777 99(36)	1.8×10^{-10}	AMDC-95	3.1.1
B3	$A_r(^3\text{He})$	3.016 029 309 70(86)	2.8×10^{-10}	AMDC-95	3.1.1
B4	$A_r(^4\text{He})$	4.002 603 2497(10)	2.5×10^{-10}	AMDC-95	3.1.1
B5	$6m_e/m(^{12}\text{C}^{6+})$	0.000 274 365 185 89(58)	2.1×10^{-9}	UWash-95	3.1.3.a (31)
B6	$m(^{12}\text{C}^{4+})/4m_p$	2.977 783 715 20(42)	1.4×10^{-10}	UWash-99	3.1.3.b (39)
B7	a_e	$1.159\,652\,1883(42) \times 10^{-3}$	3.7×10^{-9}	UWash-87	3.3.1. (68)
B8	δ_e	$0.0(1.1) \times 10^{-12}$	$[0.98 \times 10^{-9}]$	theory	App. B (B24)
B9	$\mu_{e-}(\text{H})/\mu_p(\text{H})$	$-658.210\,7058(66)$	1.0×10^{-8}	MIT-72	3.3.3 (95)
B10	$\mu_d(\text{D})/\mu_{e-}(\text{D})$	$-4.664\,345\,392(50) \times 10^{-4}$	1.1×10^{-8}	MIT-84	3.3.4 (100)
B11	$\mu_{e-}(\text{H})/\mu'_p$	$-658.215\,9430(72)$	1.1×10^{-8}	MIT-77	3.3.6.b (115)
B12	μ'_h/μ'_p	$-0.761\,786\,1313(33)$	4.3×10^{-9}	NPL-93	3.3.7 (117)
B13	μ_n/μ'_p	$-0.684\,996\,94(16)$	2.4×10^{-7}	ILL-79	3.3.8. (122)
B14	μ_{μ^+}/μ_p	$3.183\,3442(17)$	5.3×10^{-7}	SIN-82	3.3.9.a (133)
B15	$\nu(58\text{ MHz})$	$627\,994.77(14)\text{ kHz}$	2.2×10^{-7}	LAMPF-82	3.3.9.b (145)
B16	$\nu(72\text{ MHz})$	$668\,223\,166(57)\text{ Hz}$	8.6×10^{-8}	LAMPF-99	3.3.9.c (153)
B17.1	$\Delta\nu_{\text{Mu}}$	$4\,463\,302.88(16)\text{ kHz}$	3.6×10^{-8}	LAMPF-82	3.3.9.b (144)
B17.2	$\Delta\nu_{\text{Mu}}$	$4\,463\,302\,765(53)\text{ Hz}$	1.2×10^{-8}	LAMPF-99	3.3.9.c (152)
B18	δ_{Mu}	$0.0(1.2) \times 10^{-1}\text{ kHz}$	$[2.7 \times 10^{-8}]$	theory	App. D (D13)
B19.1	\bar{R}	$0.003\,707\,213(27)$	7.2×10^{-6}	CERN-79	3.3.10.a (164)
B19.2	\bar{R}	$0.003\,707\,220(48)$	1.3×10^{-5}	BNL-99	3.3.10.b (166)
B20	δ_μ	$0.0(6.4) \times 10^{-10}$	$[5.5 \times 10^{-7}]$	theory	App. C (C35)
B21.1	$\Gamma'_{p-90}(\text{lo})$	$2.675\,154\,05(30) \times 10^8\text{ s}^{-1}\text{ T}^{-1}$	1.1×10^{-7}	NIST-89	3.4.1.a (183)
B21.2	$\Gamma'_{p-90}(\text{lo})$	$2.675\,1530(18) \times 10^8\text{ s}^{-1}\text{ T}^{-1}$	6.6×10^{-7}	NIM-95	3.4.1.b (197)
B22.1	$\Gamma'_{p-90}(\text{hi})$	$2.675\,1525(43) \times 10^8\text{ s}^{-1}\text{ T}^{-1}$	1.6×10^{-6}	NIM-95	3.4.1.b (198)
B22.2	$\Gamma'_{p-90}(\text{hi})$	$2.675\,1518(27) \times 10^8\text{ s}^{-1}\text{ T}^{-1}$	1.0×10^{-6}	NPL-79	3.4.1.c (205)
B23.1	$\Gamma'_{h-90}(\text{lo})$	$2.037\,895\,37(37) \times 10^8\text{ s}^{-1}\text{ T}^{-1}$	1.8×10^{-7}	KR/VN-98	3.4.2.a (210)
B23.2	$\Gamma'_{h-90}(\text{lo})$	$2.037\,897\,29(72) \times 10^8\text{ s}^{-1}\text{ T}^{-1}$	3.5×10^{-7}	VNIIM-89	3.4.2.b (214)
B24.1	K_J	$483\,597.91(13)\text{ GHz V}^{-1}$	2.7×10^{-7}	NML-89	3.5.1 (221)
B24.2	K_J	$483\,597.96(15)\text{ GHz V}^{-1}$	3.1×10^{-7}	PTB-91	3.5.2 (226)
B25.1	R_K	$25\,812.808\,31(62)\,\Omega$	2.4×10^{-8}	NIST-97	3.6.1 (232)
B25.2	R_K	$25\,812.8071(11)\,\Omega$	4.4×10^{-8}	NML-97	3.6.2 (235)
B25.3	R_K	$25\,812.8092(14)\,\Omega$	5.4×10^{-8}	NPL-88	3.6.3 (237)
B25.4	R_K	$25\,812.8084(34)\,\Omega$	1.3×10^{-7}	NIM-95	3.6.4. (239)
B26.1	$K_J^2 R_K$	$6.036\,7625(12) \times 10^{33}\text{ J}^{-1}\text{ s}^{-1}$	2.0×10^{-7}	NPL-90	3.7.1 (245)
B26.2	$K_J^2 R_K$	$6.036\,761\,85(53) \times 10^{33}\text{ J}^{-1}\text{ s}^{-1}$	8.7×10^{-8}	NIST-98	3.7.2 (248)
B27	\mathcal{F}_{90}	$96\,485.39(13)\text{ C mol}^{-1}$	1.3×10^{-6}	NIST-80	3.8.1 (264)
B28	$\lambda_{\text{meas}}/d_{220}(\text{ILL})$	$0.002\,904\,302\,46(50)$	1.7×10^{-7}	NIST-99	3.1.3.c (48)
B29	$h/m_n d_{220}(\text{W04})$	$2\,060.267\,004(84)\text{ m s}^{-1}$	4.1×10^{-8}	PTB-99	3.11.1 (282)
B30	$1 - d_{220}(\text{W17})/d_{220}(\text{ILL})$	$-8(22) \times 10^{-9}$	$[2.2 \times 10^{-8}]$	NIST-99	3.1.3.c (51)
B31	$1 - d_{220}(\text{MO*4})/d_{220}(\text{ILL})$	$86(27) \times 10^{-9}$	$[2.7 \times 10^{-8}]$	NIST-99	3.1.3.c (52)
B32	$1 - d_{220}(\text{SH1})/d_{220}(\text{ILL})$	$34(22) \times 10^{-9}$	$[2.2 \times 10^{-8}]$	NIST-99	3.1.3.c (53)
B33	$1 - d_{220}(\text{N})/d_{220}(\text{W17})$	$7(17) \times 10^{-9}$	$[1.7 \times 10^{-8}]$	NIST-99	3.18 (344)
B34	$d_{220}(\text{W4.2A})/d_{220}(\text{W04}) - 1$	$-1(21) \times 10^{-9}$	$[2.1 \times 10^{-8}]$	PTB-98	3.9 (266)
B35	$d_{220}(\text{W17})/d_{220}(\text{W04}) - 1$	$22(22) \times 10^{-9}$	$[2.2 \times 10^{-8}]$	PTB-98	3.9 (267)
B36	$d_{220}(\text{MO*4})/d_{220}(\text{W04}) - 1$	$-103(28) \times 10^{-9}$	$[2.8 \times 10^{-8}]$	PTB-98	3.9 (268)
B37	$d_{220}(\text{SH1})/d_{220}(\text{W04}) - 1$	$-23(21) \times 10^{-9}$	$[2.1 \times 10^{-8}]$	PTB-98	3.9 (269)
B38	$d_{220}/d_{220}(\text{W04}) - 1$	$15(11) \times 10^{-9}$	$[1.1 \times 10^{-8}]$	PTB-99	3.9 (270)
B39	$d_{220}(\text{W4.2a})$	$192\,015.563(12)\text{ fm}$	6.2×10^{-8}	PTB-81	3.9.1 (272)
B40	$d_{220}(\text{MO*4})$	$192\,015.551(6)\text{ fm}$	3.4×10^{-8}	IMGC-94	3.9.2 (273)
B41	$d_{220}(\text{SH1})$	$192\,015.587(11)\text{ fm}$	5.6×10^{-8}	NRLM-97	3.9.3 (274)
B42.1	R	$8.314\,471(15)\text{ J mol}^{-1}\text{ K}^{-1}$	1.8×10^{-6}	NIST-88	3.14.1 (309)
B42.2	R	$8.314\,504(70)\text{ J mol}^{-1}\text{ K}^{-1}$	8.4×10^{-6}	NPL-79	3.14.2 (312)
B43	$\lambda(\text{Cu K}\alpha_1)/d_{220}(\text{W4.2a})$	$0.802\,327\,11(24)$	3.0×10^{-7}	FSU/PTB-91	3.18 (340)
B44	$\lambda(\text{W K}\alpha_1)/d_{220}(\text{N})$	$0.108\,852\,175(98)$	9.0×10^{-7}	NIST-79	3.18 (341)
B45	$\lambda(\text{Mo K}\alpha_1)/d_{220}(\text{N})$	$0.369\,406\,04(19)$	5.3×10^{-7}	NIST-73	3.18 (342)
B46	$\lambda(\text{Cu K}\alpha_1)/d_{220}(\text{N})$	$0.802\,328\,04(77)$	9.6×10^{-7}	NIST-73	3.18 (343)

^aThe values in brackets are relative to $a_e, a_\mu, \Delta\nu_{\text{Mu}}$, or 1, as appropriate.

TABLE 14.B.2. Non-negligible correlation coefficients $r(x_i, x_j)$ of the input data related to the constants (R_∞ and G excepted) given in Table 14.B.1. For simplicity, the two items of data to which a particular correlation coefficient corresponds are identified by their item numbers in Table 14.B.1.

$r(B1, B2)=0.314$	$r(B29, B34)=0.258$	$r(B30, B33)=-0.375$	$r(B34, B37)=0.502$
$r(B1, B3)=0.009$	$r(B29, B35)=0.241$	$r(B31, B32)=0.421$	$r(B35, B36)=0.347$
$r(B2, B3)=0.028$	$r(B29, B36)=0.192$	$r(B31, B33)=0.125$	$r(B35, B37)=0.469$
$r(B15, B17.1)=0.227$	$r(B29, B37)=0.258$	$r(B32, B33)=0.153$	$r(B36, B37)=0.372$
$r(B16, B17.2)=0.195$	$r(B30, B31)=0.421$	$r(B34, B35)=0.469$	
$r(B21.2, B22.1)=-0.014$	$r(B30, B32)=0.516$	$r(B34, B36)=0.372$	

R_K , item B25.4; and the NPL value of R , item B42.2.

4.2. Comparison of Data of Different Types

For the data related to the Rydberg constant, the comparisons are mainly through inferred values of R_∞ . However, some comparisons are possible through inferred values of the bound-state rms charge radius of the proton R_p or of the deuteron R_d . For the data not closely related to the Rydberg constant, the comparisons are mainly through inferred values of α and h .

4.2.1. Rydberg Constant Data

As mentioned in the first part of Sec. 4, because of the complex nature of the Rydberg constant data, their second-stage analysis is best done using a multivariate analysis. Hence we postpone comparing the data through the values of R_∞ , R_p , and R_d they imply until Sec. 4.3.

4.2.2. Other Data

Although the data of Tables 14.B.1 and 14.B.2 are compared in this section by means of inferred values of α and h , we first recall that the SIN value of μ_{μ^+}/μ_p , item B14, the LAMPF value of $\nu(58\text{ MHz})$, item B15, and the LAMPF value of $\nu(72\text{ MHz})$, item B16, can be compared through

inferred values of the muon-electron mass ratio m_μ/m_e . These values of m_μ/m_e , which are summarized in Table 9, Sec. 3.3, are in agreement and have relative standard uncertainties of 5.3×10^{-7} , 3.6×10^{-7} , and 1.2×10^{-7} , respectively. However, because the value of m_μ/m_e that can be inferred from the 1982 and 1999 LAMPF values of $\Delta\nu_{\text{Mu}}$, items B17.1 and B17.2, together with the theoretical expression for this splitting has a relative standard uncertainty of only $u_r \approx 3 \times 10^{-8}$ [see Eq. (161), Sec. 3.3.9.d], the 1998 recommended value of m_μ/m_e is principally determined by the indirect value generated from items B17.1, B17.2, α , and the theoretical expression.

Table 15 and Fig. 2 numerically and graphically compare a significant portion of the data of Tables 14.B.1 and 14.B.2 through inferred values of α . (For simplicity, the figure compares only data whose inferred values of α have a relative standard uncertainty $u_r < 1 \times 10^{-7}$.)

Inspection of the table and figure shows that some of the values of α are not in good agreement, implying that some of the data of Table 14.B.1 disagree. Most notable in this regard is the VNIIM value of $\Gamma'_{p-90}(\text{lo})$, item B23.2; its inferred value of α is significantly larger than any other value and exceeds the value of α with the smallest uncertainty, that implied by the University of Washington measured value of a_e , item B7, by over $3.5 u_{\text{diff}}$. Moreover, its uncertainty is

TABLE 15. Comparison of the input data given in Tables 14.B.1 and 14.B.2 via inferred values of the fine-structure constant α in order of increasing standard uncertainty.

Primary source	Item number	Identification	Sec. and Eq.	α^{-1}	Relative standard uncertainty u_r
a_e	B7	UWash-87	3.3.1 (72)	137.035 999 58(52)	3.8×10^{-9}
R_K	B25.1	NIST-97	3.6.1 (233)	137.036 0037(33)	2.4×10^{-8}
$h/m_n d_{220}(\text{W04})$	B29	PTB-99	3.11.1 (282)		
$d_{220}(\text{MO*4})$	B40	IMGC-94	3.11.1 (285)	137.036 0100(37)	2.7×10^{-8}
$d_{220}(\text{SH1})$	B41	NRLM-97	3.11.1 (286)	137.036 0017(47)	3.4×10^{-8}
$d_{220}(\text{W4.2a})$	B39	PTB-81	3.11.1 (284)	137.036 0119(51)	3.7×10^{-8}
$\Gamma'_{p-90}(\text{lo})$	B21.1	NIST-89	3.4.1.a (193)	137.035 9880(51)	3.7×10^{-8}
R_K	B25.2	NML-97	3.6.2 (236)	137.035 9973(61)	4.4×10^{-8}
R_K	B25.3	NPL-88	3.6.3 (238)	137.036 0083(73)	5.4×10^{-8}
$\Gamma'_{h-90}(\text{lo})$	B23.1	KR/VN-98	3.4.2.a (212)	137.035 9853(82)	6.0×10^{-8}
$\Delta\nu_{\text{Mu}}$	B17.2	LAMPF-99	3.3.9.d (159)	137.035 9932(83)	6.0×10^{-8}
$\Gamma'_{h-90}(\text{lo})$	B23.2	VNIIM-89	3.4.2.b (215)	137.035 942(16)	1.2×10^{-7}
R_K	B25.4	NIM-95	3.6.4. (240)	137.036 004(18)	1.3×10^{-7}
$\Delta\nu_{\text{Mu}}$	B17.1	LAMPF-82	3.3.9.d (158)	137.036 000(20)	1.5×10^{-7}
$\Gamma'_{p-90}(\text{lo})$	B21.2	NIM-95	3.4.1.b (200)	137.036 006(30)	2.2×10^{-7}
\bar{R}	B19.1	CERN-79	3.3.10.c (169)	137.035 18(98)	7.2×10^{-6}
\bar{R}	B19.2	BNL-99	3.3.10.c (170)	137.0349(18)	1.3×10^{-5}

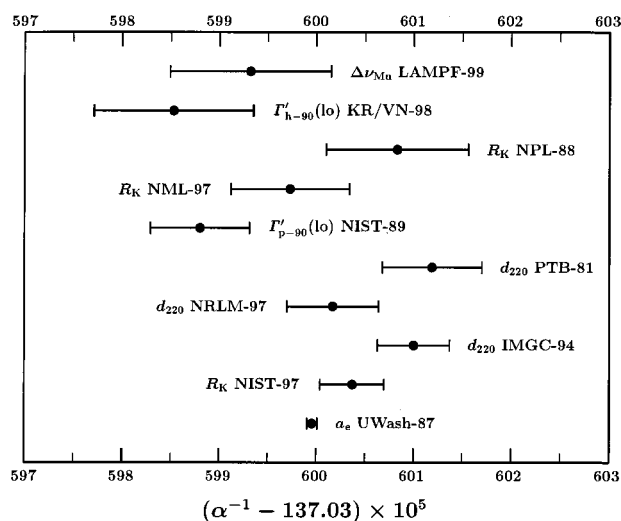


FIG. 2. Graphical comparison of the input data related to the constants (R_K and G excepted) given in Tables 14.B.1 and 14.B.2 via inferred values of the fine-structure constant α as summarized in Table 15, in order of increasing standard uncertainty.

nearly 30 times larger, implying that its contribution to any least-squares adjustment that includes this value of a_e and the theoretical expression for a_e will be negligible. This statement applies as well to the NIM value of R_K , item B25.4, the NIM value of $\Gamma'_{p-90}(\text{lo})$, item B21.2, and the CERN and BNL values of \bar{R} , items B19.1 and B19.2, because of their comparatively large uncertainties and the fact that they mainly determine α . However, the statement does not apply to the LAMPF values of $\Delta\nu_{\text{Mu}}$, items B17.1 and B17.2, because, as noted at the beginning of this section, these items, α , and the theoretical expression for $\Delta\nu_{\text{Mu}}$ generate an indirect value of m_μ/m_e with an uncertainty significantly smaller than any other value.

The compatibility of the inferred values of α of Table 15, and hence of the input data from which they were principally obtained, may be brought into sharper focus in the following way: We put aside the first of the last six values in the table because of its severe disagreement with the other values, and also the last five values because their uncertainties are so large that they contribute little additional information, even though they agree among themselves and with the other data. We then combine the remaining values to obtain (in order of increasing value for α^{-1})

$$\alpha^{-1}(\Gamma'_{90}) = 137.035\,9871(43) \quad [3.2 \times 10^{-8}] \quad (352)$$

$$\alpha^{-1}(\Delta\nu_{\text{Mu}}) = 137.035\,9952(79) \quad [5.7 \times 10^{-8}] \quad (353)$$

$$\alpha^{-1}(a_e) = 137.035\,999\,58(52) \quad [3.8 \times 10^{-9}] \quad (354)$$

$$\alpha^{-1}(R_K) = 137.036\,0030(27) \quad [2.0 \times 10^{-8}] \quad (355)$$

$$\alpha^{-1}(h/m_n) = 137.036\,0084(33) \quad [2.4 \times 10^{-8}], \quad (356)$$

where $\alpha^{-1}(\Gamma'_{90})$ is the combined result from the NIST measurement of $\Gamma'_{p-90}(\text{lo})$ and the KRISS/VNIIM measurement of $\Gamma'_{h-90}(\text{lo})$, items B.21.1 and B.23.1 (the experiments are similar and the two inferred values of α agree); $\alpha^{-1}(\Delta\nu_{\text{Mu}})$

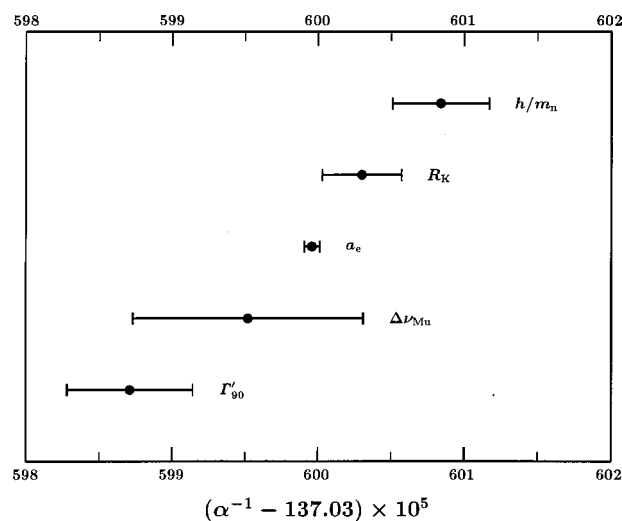


FIG. 3. Graphical comparison of the five values of the inverse fine-structure constant α^{-1} given in Eqs. (352) to (356), in order of increasing value of α^{-1} .

is the muonium value of the fine-structure constant given in Eq. (160), Sec. 3.3.9.d; $\alpha^{-1}(a_e)$ is the electron magnetic moment anomaly value (the first entry of Table 15); $\alpha^{-1}(R_K)$ is the weighted mean of the three values from the NIST, NML, and NPL measurements of R_K (they are in agreement—see Sec. 4.1.2); and $\alpha^{-1}(h/m_n)$ is the h/m_n value of α given in Eq. (287), Sec. 3.11.1 [for the calculation of this value, $Q(4.6|4)=0.33$, and $d_{220}(\text{SH1})$ has the largest normalized residual: $r=1.67$]. These five values of α are compared graphically in Fig. 3.

Ignoring the small correlations between some of the values, we find for their weighted mean $137.035\,999\,72(50) [3.6 \times 10^{-9}]$, with $R_B=2.1$ and $Q(17.5|4)=0.0016$. The normalized residuals of the five values are -2.9 , -0.6 , -0.3 , 1.2 , and 2.7 , with $\alpha^{-1}(\Gamma'_{90})$ responsible for 48 % of χ^2 and $\alpha^{-1}(h/m_n)$ for 41 %. Clearly, the data do not agree well. However, note that because the uncertainty of $\alpha^{-1}(a_e)$ is significantly smaller than that of any of the other values, and because $\alpha^{-1}(\Gamma'_{90})$ and $\alpha^{-1}(h/m_n)$ tend to counterbalance one another, the weighted mean exceeds $\alpha^{-1}(a_e)$ by less than 0.3 times the standard uncertainty of $\alpha^{-1}(a_e)$, a shift that is not particularly significant. We thus expect that even if all of the input data of Table 14.B.1 are retained, the 1998 recommended value of α will be determined mainly by $\alpha(a_e)$.

Table 16 and Fig. 4 numerically and graphically compare by means of inferred values of h many of the data of Tables 14.B.1 and 14.B.2 that have not been compared in Table 15 and Fig. 2 through inferred values of α . Examination of Table 16 and Fig. 4 shows that the values of h are in agreement, implying that the seven input data from which they primarily are derived are consistent: the absolute value of the difference Δ between any two values of h is less than the standard uncertainty of their difference u_{diff} , and in most cases Δ is significantly less than u_{diff} . (To obtain h from K_J requires a value of α and to obtain h from $\Gamma'_{p-90}(\text{hi})$ or \mathcal{F}_{90}

TABLE 16. Comparison of the input data given in Tables 14.B.1 and 14.B.2 via inferred values of the Planck constant h in order of increasing standard uncertainty.

Primary source	Item number	Identification	Sec. and Eq.	$h/(\text{J s})$	Relative standard uncertainty u_r
$K_J^2 R_K$	B26.2	NIST-98	3.7.2 (249)	$6.626\,068\,91(58) \times 10^{-34}$	8.7×10^{-8}
$K_J^2 R_K$	B26.1	NPL-90	3.7.1 (246)	$6.626\,0682(13) \times 10^{-34}$	2.0×10^{-7}
K_J	B24.1	NML-89	3.5.1 (223)	$6.626\,0684(36) \times 10^{-34}$	5.4×10^{-7}
K_J	B24.2	PTB-91	3.5.2 (227)	$6.626\,0670(42) \times 10^{-34}$	6.3×10^{-7}
$\Gamma'_{p-90}(\text{hi})$	B22.2	NPL-79	3.4.1.c (206)	$6.626\,0729(67) \times 10^{-34}$	1.0×10^{-6}
\mathcal{F}_{90}	B27	NIST-80	3.8.1 (265)	$6.626\,0657(88) \times 10^{-34}$	1.3×10^{-6}
$\Gamma'_{p-90}(\text{hi})$	B22.1	NIM-95	3.4.1.b (202)	$6.626\,071(11) \times 10^{-34}$	1.6×10^{-6}

requires a value of α^2 . Although the above discussion indicates that a number of values of α are available, the possible variation of α is sufficiently small that its impact on the agreement among the values of h is inconsequential.)

Because the uncertainties of the values of h from the NIST and NPL values of $K_J^2 R_K$, items B26.2 and B26.1, are rather smaller than the uncertainties of the other values of h , we expect that the 1998 recommended value of h will be determined to a large extent by these two input data.

4.3. Multivariate Analysis of Data

Our third stage of data analysis proceeds in three steps. First we analyze the Rydberg-constant data of Tables 14.A.1 and 14.A.2, then the other data of Tables 14.B.1 and 14.B.2 and then all of the data together. In this analysis, the input data are related to the adjusted constants by means of appropriate observational equations. In those equations, the symbol \doteq is used to indicate that an observed value of an input datum of the particular type shown on the left-hand side is ideally given by the function of the adjusted constants on the right-hand side. In general, an observational equation in a least-squares adjustment does not express an equality, be-

cause it is one of an overdetermined set of equations relating the data to the adjusted constants. In particular, in an observational equation of the form $Z \doteq Z$, the measured value (left-hand side) of a quantity does not in general equal the adjusted value (right-hand side) of that quantity. The best estimate of a quantity is given by its observational equation evaluated with the least-squares estimated values of the adjusted constants on which it depends (see Appendix E).

TABLE 17.A.1. The 28 adjusted constants (variables) used in the least-squares multivariate analysis of the Rydberg constant data given in Tables 14.A.1 and 14.A.2. These adjusted constants appear as arguments of the functions on the right-hand side of the observational equations of Table 17.A.2. [The notation for hydrogenic energy levels $E_X(nL_j)$ and for additive corrections $\delta_X(nL_j)$ in this table have the same meaning as the notations $E_{nL_j}^X$ and $\delta_{nL_j}^X$ in Appendix A, Sec. 12.]

Adjusted constant	Symbol
Rydberg constant	R_∞
bound-state proton rms charge radius	R_p
additive correction to $E_H(1S_{1/2})$	$\delta_H(1S_{1/2})$
additive correction to $E_H(2S_{1/2})$	$\delta_H(2S_{1/2})$
additive correction to $E_H(3S_{1/2})$	$\delta_H(3S_{1/2})$
additive correction to $E_H(4S_{1/2})$	$\delta_H(4S_{1/2})$
additive correction to $E_H(6S_{1/2})$	$\delta_H(6S_{1/2})$
additive correction to $E_H(8S_{1/2})$	$\delta_H(8S_{1/2})$
additive correction to $E_H(2P_{1/2})$	$\delta_H(2P_{1/2})$
additive correction to $E_H(4P_{1/2})$	$\delta_H(4P_{1/2})$
additive correction to $E_H(2P_{3/2})$	$\delta_H(2P_{3/2})$
additive correction to $E_H(4P_{3/2})$	$\delta_H(4P_{3/2})$
additive correction to $E_H(8D_{3/2})$	$\delta_H(8D_{3/2})$
additive correction to $E_H(12D_{3/2})$	$\delta_H(12D_{3/2})$
additive correction to $E_H(4D_{5/2})$	$\delta_H(4D_{5/2})$
additive correction to $E_H(6D_{5/2})$	$\delta_H(6D_{5/2})$
additive correction to $E_H(8D_{5/2})$	$\delta_H(8D_{5/2})$
additive correction to $E_H(12D_{5/2})$	$\delta_H(12D_{5/2})$
bound-state deuteron rms charge radius	R_d
additive correction to $E_D(1S_{1/2})$	$\delta_D(1S_{1/2})$
additive correction to $E_D(2S_{1/2})$	$\delta_D(2S_{1/2})$
additive correction to $E_D(4S_{1/2})$	$\delta_D(4S_{1/2})$
additive correction to $E_D(8S_{1/2})$	$\delta_D(8S_{1/2})$
additive correction to $E_D(8D_{3/2})$	$\delta_D(8D_{3/2})$
additive correction to $E_D(12D_{3/2})$	$\delta_D(12D_{3/2})$
additive correction to $E_D(4D_{5/2})$	$\delta_D(4D_{5/2})$
additive correction to $E_D(8D_{5/2})$	$\delta_D(8D_{5/2})$
additive correction to $E_D(12D_{5/2})$	$\delta_D(12D_{5/2})$

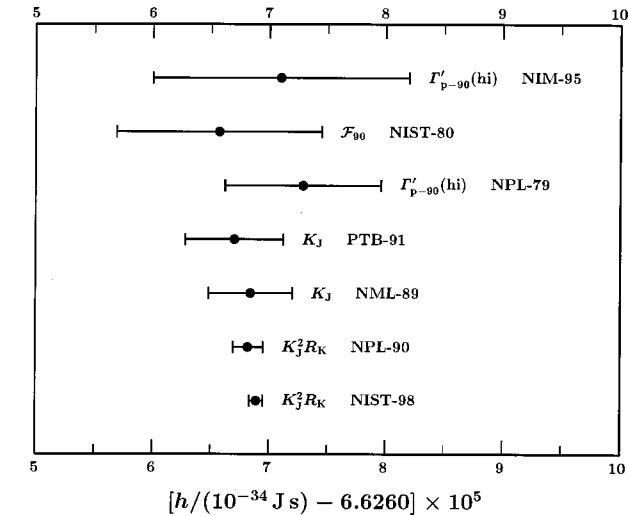


FIG. 4. Graphical comparison of the input data related to the constants (R_∞ and G excepted) given in Tables 14.B.1 and 14.B.2 via inferred values of the Planck constant h as summarized in Table 16, in order of increasing standard uncertainty.

TABLE 17.A.2. Observational equations that express the input data related to R_∞ in Tables 14.A.1 and 14.A.2 as functions of the adjusted constants in Table 17.A.1. The numbers in the first column correspond to the numbers in the first column of Table 14.A.1. The expressions for the energy levels of hydrogenic atoms are discussed in Appendix A. As pointed out in Sec. 12 of that Appendix, $E_X(nL_j)/h$ is in fact proportional to cR_∞ and independent of h , hence h is not an adjusted constant in these equations. [The notation for hydrogenic energy levels $E_X(nL_j)$ and for additive corrections $\delta_X(nL_j)$ in this table have the same meaning as the notations $E_{nL_j}^X$ and $\delta_{nL_j}^X$ in Appendix A, Sec. 12.] See Sec. 4.3 for an explanation of the symbol \doteq .

Type of input datum	Observational equation
A1–A6, A13, A14	$\nu_H(n_1L_{1j_1} - n_2L_{2j_2}) \doteq [E_H(n_2L_{2j_2}; R_\infty, \alpha, A_r(e), A_r(p), R_p, \delta_H(n_2L_{2j_2})) - E_H(n_1L_{1j_1}; R_\infty, \alpha, A_r(e), A_r(p), R_p, \delta_H(n_1L_{1j_1}))]/h$
A7–A12	$\nu_H(n_1L_{1j_1} - n_2L_{2j_2}) - \frac{1}{4} \nu_H(n_3L_{3j_3} - n_4L_{4j_4}) \doteq \{E_H(n_2L_{2j_2}; R_\infty, \alpha, A_r(e), A_r(p), R_p, \delta_H(n_2L_{2j_2})) - E_H(n_1L_{1j_1}; R_\infty, \alpha, A_r(e), A_r(p), R_p, \delta_H(n_1L_{1j_1})) - \frac{1}{4} [E_H(n_4L_{4j_4}; R_\infty, \alpha, A_r(e), A_r(p), R_p, \delta_H(n_4L_{4j_4})) - E_H(n_3L_{3j_3}; R_\infty, \alpha, A_r(e), A_r(p), R_p, \delta_H(n_3L_{3j_3}))]\}/h$
A15	$R_p \doteq R_p$
A16–A20	$\nu_D(n_1L_{1j_1} - n_2L_{2j_2}) \doteq [E_D(n_2L_{2j_2}; R_\infty, \alpha, A_r(e), A_r(d), R_d, \delta_D(n_2L_{2j_2})) - E_D(n_1L_{1j_1}; R_\infty, \alpha, A_r(e), A_r(d), R_d, \delta_D(n_1L_{1j_1}))]/h$
A21–A22	$\nu_D(n_1L_{1j_1} - n_2L_{2j_2}) - \frac{1}{4} \nu_D(n_3L_{3j_3} - n_4L_{4j_4}) \doteq \{E_D(n_2L_{2j_2}; R_\infty, \alpha, A_r(e), A_r(d), R_d, \delta_D(n_2L_{2j_2})) - E_D(n_1L_{1j_1}; R_\infty, \alpha, A_r(e), A_r(d), R_d, \delta_D(n_1L_{1j_1})) - \frac{1}{4} [E_D(n_4L_{4j_4}; R_\infty, \alpha, A_r(e), A_r(d), R_d, \delta_D(n_4L_{4j_4})) - E_D(n_3L_{3j_3}; R_\infty, \alpha, A_r(e), A_r(d), R_d, \delta_D(n_3L_{3j_3}))]\}/h$
A23	$R_d \doteq R_d$
A24	$\nu_D(1S_{1/2} - 2S_{1/2}) - \nu_H(1S_{1/2} - 2S_{1/2}) \doteq \{E_D(2S_{1/2}; R_\infty, \alpha, A_r(e), A_r(d), R_d, \delta_D(2S_{1/2})) - E_D(1S_{1/2}; R_\infty, \alpha, A_r(e), A_r(d), R_d, \delta_D(1S_{1/2})) - [E_H(2S_{1/2}; R_\infty, \alpha, A_r(e), A_r(p), R_p, \delta_H(2S_{1/2})) - E_H(1S_{1/2}; R_\infty, \alpha, A_r(e), A_r(p), R_p, \delta_H(1S_{1/2}))]\}/h$
A25–A40	$\delta_H(nL_j) \doteq \delta_H(nL_j)$
A41–A49	$\delta_D(nL_j) \doteq \delta_D(nL_j)$

4.3.1. Rydberg Constant Data

The input data of Table 14.A.1, together with their correlation coefficients in Table 14.A.2, are examined by carrying out various fits or adjustments based on the method of least squares as summarized in Appendix E. These 50 input data are of 49 different types and can be expressed in terms of 28 adjusted constants. It is these variables that are the “unknowns” of the adjustment and for which best estimated values in the least-squares sense are obtained. The 28 adjusted constants are given in Table 17.A.1, and the observational equations that relate the 49 different types of input data to the adjusted constants are given in Table 17.A.2.

The following comments apply to the observational equations given in Table 17.A.2 and our use of them in this section.

(i) The first argument in the expression for the energy of a level does not denote an adjusted constant, but indicates the state under consideration.

(ii) Because in this section we are interested only in the internal consistency of the data that pertain to R_∞ , and because the results of our least-squares analysis of those data depend only weakly on the values of α , $A_r(e)$, $A_r(p)$, and

$A_r(d)$ employed, we temporarily take for these quantities their 1998 recommended values with no uncertainties.

Our multivariate analysis of the Rydberg-constant data of Tables 14.A.1 and 14.A.2 has involved many individual least-squares adjustments; the results of the most informative of these are summarized in Table 18. Since the key adjusted physical constants in the observational equations used to analyze the data are R_∞ and the bound-state rms charge radii R_p and R_d , we include in that table the values of these quantities resulting from each adjustment. We discuss in turn each of the six adjustments listed in the table.

Adjustment 1. This adjustment involves all 50 input data of Table 14.A.1, together with the correlation coefficients of Table 14.A.2, expressed in terms of the 28 adjusted constants of Table 17.A.1 by means of the 49 different observational equations of Table 17.A.2; the degrees of freedom for this adjustment is $\nu=22$.

Since this adjustment includes all of the data related to R_∞ and the Birge ratio is $R_B=0.76$ with $Q(12.7|22)=0.94$, the data are shown to be consistent. Further, no normalized residual r_i exceeds 1.5. However, the normalized residual of each $\delta_X(nS_{1/2})$, $n=1,2,3,4,6,8$, is in the narrow range

TABLE 18. Summary of the results of some of the least-squares adjustments used to analyze the input data related to R_∞ given in Tables 14.A.1 and 14.A.2. The values of R_∞ , R_p , and R_d are those obtained in the indicated adjustment, N is the number of input data, M is the number of adjusted constants, $\nu = N - M$ is the degrees of freedom, $R_B = \sqrt{\chi^2/\nu}$ is the Birge ratio, and $Q(\chi^2|\nu)$ is the probability that the observed value of χ^2 for ν degrees of freedom would have exceeded that observed value.

Adj.	N	M	ν	χ^2	R_B	$Q(\chi^2 \nu)$	R_∞/m^{-1}	$u_r(R_\infty)$	R_p/fm	R_d/fm
1	50	28	22	12.7	0.76	0.94	10 973 731.568 521(81)	7.3×10^{-12}	0.859(10)	2.1331(42)
2	48	28	20	10.4	0.72	0.96	10 973 731.568 549(83)	7.5×10^{-12}	0.907(32)	2.153(14)
3	31	18	13	7.4	0.75	0.88	10 973 731.568 556(96)	8.7×10^{-12}	0.908(33)	
4	16	11	5	2.1	0.65	0.84	10 973 731.568 32(30)	2.7×10^{-11}		2.133(28)
5	36	28	8	4.8	0.78	0.78	10 973 731.568 59(16)	1.5×10^{-11}	0.910(35)	2.154(15)
6	39	25	14	8.5	0.78	0.86	10 973 731.568 53(10)	9.2×10^{-12}	0.903(35)	2.151(16)

$-1.410 < r_i < -1.406$, which shows a systematic deviation between theory and experiment corresponding to $126/n^3$ kHz for $nS_{1/2}$ states. The most likely sources for this difference are a deviation of the value of the proton charge radius and/or the deuteron charge radius predicted by the spectroscopic data from the values deduced from scattering experiments, an uncalculated contribution to the energy levels from the two-photon QED correction that exceeds the estimated uncertainty for this term, or a combination of these. Although the normalized residuals of the input data for R_p and R_d in this adjustment are -0.34 and -0.35 , respectively, these small values are a result of the small uncertainties of the input data compared to the uncertainties associated with the spectroscopic predictions.

Adjustment 2. This adjustment is the same as adjustment 1, except that the input data for the charge radii R_p , item A15, and R_d , item A23, are omitted. Thus the transition frequencies alone determine the adjusted values of these constants.

If the proton and deuteron charge radii are allowed to vary freely, they take on values that eliminate the systematic deviation seen in adjustment 1 regardless of its source. In fact, the absolute value of the normalized residuals of all of the δ 's in this adjustment are less than 0.04, and for $nS_{1/2}$ states, 0.0001 or less. The difference between the deduced values of the Rydberg constant from this adjustment and adjustment 1 is about $\frac{1}{3}u_r(R_\infty)$, while the uncertainty itself is increased by less than 3%. This value of R_∞ is preferable to the value from adjustment 1, because the adjustment from which it is obtained provides significantly better consistency between theory and experiment, while its uncertainty is not significantly larger.

Adjustments 3 and 4. Here the hydrogen data (adjustment 3) and deuterium data (adjustment 4) are considered separately in order to investigate the consistency of the H and D data. For the reasons given in the discussion of adjustment 2, the input datum for R_p is not included in adjustment 3 and the input datum for R_d is not included in adjustment 4. In either case the measurement of the H–D isotope shift, item A24, is also omitted.

We see from Table 18 that the values of R_∞ resulting from these two adjustments agree, although the uncertainty of R_∞ from adjustment 4 (deuterium) is about three times larger than the uncertainty from adjustment 3 (hydrogen).

Adjustments 5 and 6. The aim of these adjustments is to check the consistency of the MPQ and the LKB-LKB/LPTF data. Hence the MPQ data (adjustment 5) and the LKB and LKB/LPTF data (adjustment 6) are considered separately, again with R_p and R_d omitted. In both adjustments, the Yale, Harvard, and Sussex data, items A11, A12, A13, A14.1, and A14.2, are included.

We see that the adjusted values of R_∞ agree, as do the adjusted values of R_p and R_d .

Based on the above analysis, we conclude that the preferred way of treating the Rydberg-constant data is adjustment 2. The reason is that by omitting as input data the values of R_p and R_d obtained from electron-scattering data and allowing their values to be determined entirely by the spectroscopic data, we eliminate the systematic difference between theory and experiment observed in adjustment 1, whatever its source. Although doing so increases the uncertainty in the deduced value of the Rydberg constant, the increase is very small and the resulting value of the Rydberg constant has the advantage of being based on a consistent set of data. For all of the adjustments with the input data for R_p and R_d omitted, the values for these quantities predicted by the spectroscopic data are in agreement with each other and differ (particularly for the proton) from the input values deduced from electron-scattering experiments. However, since the difference between the spectroscopic and the scattering values for the two radii corresponds to a change of only 1.4 times the uncertainty of $\delta_X(nS_{1/2})$, one cannot make a conclusive statement about the implications of the difference.

4.3.2. Other Data

As we did in the previous section for the Rydberg-constant data, we examine here the input data related to the constants (R_∞ and G excepted) of Table 14.B.1, together with the correlation coefficients in Table 14.B.2, by means of a multivariate analysis based on the method of least squares as summarized in Appendix E. These 57 input data are of 46 different types and can be expressed in terms of the 29 adjusted constants given in Table 19.B.1. The observational equations that relate the 46 different types of input data to

the adjusted constants are given in Table 19.B.2. The following comments apply to these equations and our use of them in this section.

(i) The last column of the table gives the section in which the basis of the observational equation in question is discussed. (Equations of the form $Z \doteq Z$ are self explanatory and no section is indicated.)

(ii) The various ratios of binding energies $E_b(X)$ to the energy equivalent of the atomic mass constant $m_u c^2$ in the observational equations for input data of type *B1* to *B6* are taken as exact (see Sec. 3.1.2).

(iii) The bound-state corrections $g_{e^-}(H)/g_{e^-}$, $g_p(H)/g_p$, $g_{e^-}(D)/g_{e^-}$, and $g_d(D)/g_d$ in the observational equations for input data of type *B9* to *B11* are taken as exact; and similarly, the bound state corrections $g_{e^-}(Mu)/g_{e^-}$ and $g_{\mu^+}(Mu)/g_{\mu^+}$ in the observational equations for input data of type *B15* and *B16*, but which are not explicitly shown, are taken as exact (see Sec. 3.3.2.). Note also that in the observational equation for these two input data, the exact proton NMR reference frequency f_p is not an adjusted constant but is included in the equation to indicate that it is a function of f_p .

(iv) The theoretical expression for the electron magnetic moment anomaly a_e in terms of α and δ_e is given in Appendix B, Eq. (B23); and that for the muon magnetic moment anomaly a_μ in terms of α and δ_μ is given in Appendix C, Eq. (C34).

(v) The theoretical expressions for a_e and/or a_μ are part of the observational equations for input data of type *B14* to *B17*, *B19*, and *B21* to *B23*, but are not explicitly shown in the equations for *B15* to *B17*, since for simplicity the observational equations for input data of type *B15* to *B17* are not written as explicit functions of the adjusted constants.

(vi) The observational equation for items *B15* and *B16* is based on Eqs. (134), (142), and (143) of Sec. 3.3.9, and includes the functions $a_e(\alpha, \delta_e)$ and $a_\mu(\alpha, \delta_\mu)$, as well as the theoretical expression for input data of type *B17*, $\Delta\nu_{Mu}$. The latter expression is discussed in Appendix D and is a function of R_∞ , α , m_e/m_μ , $a_\mu(\alpha, \delta_\mu)$, and δ_{Mu} .

(vii) In analogy with the analysis of the Rydberg-constant data, in this section we are interested only in the internal consistency of the other data. Because the results of our least-squares analysis of these data depend only weakly on the value of R_∞ employed, we temporarily take the 1998 recommended value for it with no uncertainty.

As for our multivariate analysis of the Rydberg-constant data, our multivariate analysis of the data of Tables 14.B.1 and 14.B.2 has involved many individual least-squares adjustments. The data used in some of the more informative of these adjustments are summarized in Table 20 by indicating the items of data omitted, and the results of the adjustments themselves are summarized in Table 21. Since the key quantities in determining a large number of the 1998 recommended values of the constants are α and h , the values of these quantities resulting from each adjustment are the focus of the analysis and are given in the table. We discuss each of the nine adjustments in turn.

TABLE 19.B.1. The 29 adjusted constants (variables) used in the least-squares multivariate analysis of the input data given in Tables 14.B.1 and 14.B.2. These adjusted constants appear as arguments of the functions on the right-hand side of the observational equations of Table 19.B.2.

Adjusted constant	Symbol
electron relative atomic mass	$A_r(e)$
proton relative atomic mass	$A_r(p)$
neutron relative atomic mass	$A_r(n)$
deuteron relative atomic mass	$A_r(d)$
helion relative atomic mass	$A_r(h)$
alpha particle relative atomic mass	$A_r(\alpha)$
fine-structure constant	α
correction to a_e (th)	δ_e
electron-proton magnetic moment ratio	μ_{e^-}/μ_p
deuteron-electron magnetic moment ratio	μ_d/μ_{e^-}
electron to shielded proton	
magnetic moment ratio	μ_{e^-}/μ'_p
shielded helion to shielded proton	
magnetic moment ratio	μ'_h/μ'_p
neutron to shielded proton	
magnetic moment ratio	μ_n/μ'_p
electron-muon mass ratio	m_e/m_μ
correction to $\Delta\nu_{Mu}$ (th)	δ_{Mu}
correction to a_μ (th)	δ_μ
Planck constant	h
molar gas constant	R
copper $K\alpha_1$ x unit	xu(Cu $K\alpha_1$)
molybdenum $K\alpha_1$ x unit	xu(Mo $K\alpha_1$)
ångstrom star	\AA^*
d_{220} of Si crystal ILL	$d_{220}(\text{ILL})$
d_{220} of Si crystal N	$d_{220}(\text{N})$
d_{220} of Si crystal WASO 17	$d_{220}(\text{W17})$
d_{220} of Si crystal WASO 04	$d_{220}(\text{W04})$
d_{220} of Si crystal WASO 4.2a	$d_{220}(\text{W4.2a})$
d_{220} of Si crystal MO*4	$d_{220}(\text{MO*4})$
d_{220} of Si crystal SH1	$d_{220}(\text{SH1})$
d_{220} of an ideal Si crystal	d_{220}

Adjustment 1. This adjustment involves all $N=57$ input data of Tables 14.B.1 and 14.B.2, expressed in terms of the $M=29$ adjusted constants of Table 19.B.1 through the 46 different observational equations of Table 19.B.2; the degrees of freedom for this adjustment is $\nu=N-M=28$.

As anticipated from the analyses of Secs. 4.1.2 and 4.2.2, the value of χ^2 for this adjustment is significantly larger than ν . Also as anticipated, the principal contributor to the unacceptably large value of χ^2 is item *B23.2*, the VNIIM value of $\Gamma'_{h-90}(\text{lo})$. Its normalized residual is $r=3.6$ and it is responsible for 31 % of χ^2 . However, its self-sensitivity coefficient S_c is only 0.20 %. (S_c is a measure of how the least-squares estimated value of a given type of input datum depends on a particular measured value of that type of datum; see Appendix E.) This value of S_c confirms the limited potential of this datum for contributing to the 1998 adjustment that was identified in Sec. 4.2.2.

Adjustment 2. When the VNIIM value of $\Gamma'_{h-90}(\text{lo})$ is eliminated, one obtains a quite acceptable value of χ^2 . The three input data with the largest normalized residuals are then the NIST value of $\Gamma'_{p-90}(\text{lo})$, item *B21.1*, with $r=2.3$; the PTB value of $h/m_n d_{220}(\text{W04})$, item *B29*, with

TABLE 19.B.2. Observational equations that express the input data in Tables 14.B.1 and 14.B.2 as functions of the adjusted constants in Table 19.B.1. The numbers in the first column correspond to the numbers in the first column of Table 14.B.1. For simplicity, the lengthier functions are not explicitly given. See Sec. 4.3 for an explanation of the symbol \doteq .

Type of input datum	Observational equation	Sec.
B1	$A_r(^1\text{H}) \doteq A_r(\text{p}) + A_r(\text{e}) - E_b(^1\text{H})/m_u c^2$	3.1.3.b
B2	$A_r(^2\text{H}) \doteq A_r(\text{d}) + A_r(\text{e}) - E_b(^2\text{H})/m_u c^2$	3.1.3.b
B3	$A_r(^3\text{He}) \doteq A_r(\text{h}) + 2A_r(\text{e}) - E_b(^3\text{He})/m_u c^2$	3.1.3.b
B4	$A_r(^4\text{He}) \doteq A_r(\alpha) + 2A_r(\text{e}) - E_b(^4\text{He})/m_u c^2$	3.1.3.b
B5	$\frac{6m_e}{m(^{12}\text{C}^{6+})} \doteq \frac{6A_r(\text{e})}{12 - 6A_r(\text{e}) + E_b(^{12}\text{C})/m_u c^2}$	3.1.3.a
B6	$\frac{m(^{12}\text{C}^{4+})}{4m_p} \doteq \frac{12 - 4A_r(\text{e}) + [E_b(^{12}\text{C}) - E_b(^{12}\text{C}^{4+})]/m_u c^2}{4A_r(\text{p})}$	3.1.3.b
B7	$a_e \doteq a_e(\alpha, \delta_e)$	App. B
B8	$\delta_e \doteq \delta_e$	
B9	$\frac{\mu_{e^-}(\text{H})}{\mu_p(\text{H})} \doteq \frac{g_{e^-}(\text{H})}{g_{e^-}} \left(\frac{g_p(\text{H})}{g_p} \right)^{-1} \frac{\mu_{e^-}}{\mu_p}$	3.3.3
B10	$\frac{\mu_d(\text{D})}{\mu_{e^-}(\text{D})} \doteq \frac{g_d(\text{D})}{g_d} \left(\frac{g_{e^-}(\text{D})}{g_{e^-}} \right)^{-1} \frac{\mu_d}{\mu_{e^-}}$	3.3.4
B11	$\frac{\mu_{e^-}(\text{H})}{\mu'_p} \doteq \frac{g_{e^-}(\text{H})}{g_{e^-}} \frac{\mu_{e^-}}{\mu'_p}$	3.3.6.b
B12	$\frac{\mu'_h}{\mu'_p} \doteq \frac{\mu'_h}{\mu'_p}$	
B13	$\frac{\mu_n}{\mu'_p} \doteq \frac{\mu_n}{\mu'_p}$	
B14	$\frac{\mu_{\mu^+}}{\mu_p} \doteq - \frac{1 + a_\mu(\alpha, \delta_\mu)}{1 + a_e(\alpha, \delta_e)} \frac{m_e}{m_\mu} \frac{\mu_{e^-}}{\mu_p}$	3.3.9.a
B15, B16	$\nu(f_p) \doteq \nu \left(f_p, R_\infty, \alpha, \frac{m_e}{m_\mu}, \frac{\mu_{e^-}}{\mu_p}, \delta_e, \delta_\mu, \delta_{\text{Mu}} \right)$	3.3.9.b
B17	$\Delta\nu_{\text{Mu}} \doteq \Delta\nu_{\text{Mu}} \left(R_\infty, \alpha, \frac{m_e}{m_\mu}, \delta_\mu, \delta_{\text{Mu}} \right)$	App. D
B18	$\delta_{\text{Mu}} \doteq \delta_{\text{Mu}}$	
B19	$\bar{R} \doteq - \frac{a_\mu(\alpha, \delta_\mu)}{1 + a_e(\alpha, \delta_e)} \frac{m_e}{m_\mu} \frac{\mu_{e^-}}{\mu_p}$	3.3.10.a
B20	$\delta_\mu \doteq \delta_\mu$	
B21	$\Gamma'_{p-90}(\text{lo}) \doteq - \frac{K_{J-90} R_{K-90} [1 + a_e(\alpha, \delta_e)] \alpha^3}{2\mu_0 R_\infty} \left(\frac{\mu_{e^-}}{\mu'_p} \right)^{-1}$	3.4.1.a
B22	$\Gamma'_{p-90}(\text{hi}) \doteq - \frac{c[1 + a_e(\alpha, \delta_e)] \alpha^2}{K_{J-90} R_{K-90} R_\infty h} \left(\frac{\mu_{e^-}}{\mu'_p} \right)^{-1}$	3.4.1.b
B23	$\Gamma'_{h-90}(\text{lo}) \doteq \frac{K_{J-90} R_{K-90} [1 + a_e(\alpha, \delta_e)] \alpha^3}{2\mu_0 R_\infty} \left(\frac{\mu_{e^-}}{\mu'_p} \right)^{-1} \frac{\mu'_h}{\mu'_p}$	3.4.2.a
B24	$K_J \doteq \left(\frac{8\alpha}{\mu_0 c h} \right)^{1/2}$	3.5.1
B25	$R_K \doteq \frac{\mu_0 c}{2\alpha}$	3.6
B26	$K_J^2 R_K \doteq \frac{4}{h}$	3.7
B27	$\mathcal{F}_{90} \doteq \frac{c M_u A_r(\text{e}) \alpha^2}{K_{J-90} R_{K-90} R_\infty h}$	3.8
B28	$\frac{\lambda_{\text{meas}}}{d_{220}(\text{ILL})} \doteq \frac{\alpha^2 A_r(\text{e})}{R_\infty d_{220}(\text{ILL})} \frac{A_r(\text{n}) + A_r(\text{p})}{[A_r(\text{n}) + A_r(\text{p})]^2 - A_r^2(\text{d})}$	3.1.3.c
B29	$\frac{h}{m_n d_{220}(\text{W04})} \doteq \frac{c A_r(\text{e}) \alpha^2}{2 R_\infty A_r(\text{n}) d_{220}(\text{W04})}$	3.11.1

TABLE 19.B.2. Observational equations that express the input data in Tables 14.B.1 and 14.B.2 as functions of the adjusted constants in Table 19.B.1. The numbers in the first column correspond to the numbers in the first column of Table 14.B.1. For simplicity, the lengthier functions are not explicitly given. See Sec. 4.3 for an explanation of the symbol \doteq —Continued.

Type of input datum	Observational equation	Sec.
<i>B30–B33</i>	$1 - \frac{d_{220}(\text{Y})}{d_{220}(\text{X})} \doteq 1 - \frac{d_{220}(\text{Y})}{d_{220}(\text{X})}$	
<i>B34–B37</i>	$\frac{d_{220}(\text{X})}{d_{220}(\text{Y})} - 1 \doteq \frac{d_{220}(\text{X})}{d_{220}(\text{Y})} - 1$	
<i>B38</i>	$\frac{d_{220}}{d_{220}(\text{W04})} - 1 \doteq \frac{d_{220}}{d_{220}(\text{W04})} - 1$	
<i>B39–B41</i>	$d_{220}(\text{X}) \doteq d_{220}(\text{X})$	
<i>B42</i>	$R \doteq R$	
<i>B43, B46</i>	$\frac{\lambda(\text{Cu K}\alpha_1)}{d_{220}(\text{X})} \doteq \frac{1\,537.400\text{ xu}(\text{Cu K}\alpha_1)}{d_{220}(\text{X})}$	3.18
<i>B44</i>	$\frac{\lambda(\text{W K}\alpha_1)}{d_{220}(\text{N})} \doteq \frac{0.209\,010\,0\text{ \AA}^*}{d_{220}(\text{N})}$	3.18
<i>B45</i>	$\frac{\lambda(\text{Mo K}\alpha_1)}{d_{220}(\text{N})} \doteq \frac{707.831\text{ xu}(\text{Mo K}\alpha_1)}{d_{220}(\text{N})}$	3.18

$r = -2.0$; and the KRISS/VNIIM value of $\Gamma'_{\text{h-90}}(\text{lo})$, item *B23.1*, with $r = 1.8$. The self-sensitivity coefficients S_c of the three input data are 1.9 %, 38 %, and 0.78 %. The comparatively large normalized residuals are no surprise in view of the discussion of Sec. 4.2.2. The fact that S_c for item *B29* is only 38 % can be understood by recognizing that the adjusted value of α and the mean of the three values of $d_{220}(\text{X})$ to-

gether produce an indirect value of $h/m_{\text{e}}d_{220}(\text{W04})$ with a comparatively small uncertainty.

Adjustment 3. This adjustment demonstrates formally that the VNIIM value of $\Gamma'_{\text{h-90}}(\text{lo})$ is not incompatible just with a_{e} . As shown in Sec. 4.2.2, a_{e} provides a value of α with an uncertainty that is significantly smaller than that of any other value. To eliminate $\alpha(a_{\text{e}})$, we increase the standard uncer-

TABLE 20. Summary of the input data given in Tables 14.B.1 and 14.B.2 that are omitted from one or more of the adjustments 1 to 9 summarized in Table 21 and discussed in the text. (Omission is indicated by \circ , inclusion by \bullet .)

Item number	Symbol	Identification	Adjustment number								
			1	2	3	4	5	6	7	8	9
<i>B8</i>	δ_{e}	theory	\bullet	\bullet	\circ	\circ	\bullet	\bullet	\bullet	\bullet	\bullet
<i>B14</i>	$\mu_{\text{e}^+}/\mu_{\text{p}}$	SIN-82	\bullet	\bullet	\bullet	\bullet	\bullet	\bullet	\bullet	\circ	\circ
<i>B19.1</i>	\bar{R}	CERN-79	\bullet	\bullet	\bullet	\bullet	\bullet	\bullet	\bullet	\circ	\circ
<i>B19.2</i>	\bar{R}	BNL-99	\bullet	\bullet	\bullet	\bullet	\bullet	\bullet	\bullet	\circ	\circ
<i>B21.1</i>	$\Gamma'_{\text{p-90}}(\text{lo})$	NIST-89	\bullet	\bullet	\bullet	\bullet	\circ	\bullet	\circ	\bullet	\circ
<i>B21.2</i>	$\Gamma'_{\text{p-90}}(\text{lo})$	NIM-95	\bullet	\bullet	\bullet	\bullet	\circ	\bullet	\circ	\circ	\circ
<i>B22.1</i>	$\Gamma'_{\text{p-90}}(\text{hi})$	NIM-95	\bullet	\bullet	\bullet	\bullet	\bullet	\bullet	\bullet	\circ	\circ
<i>B22.2</i>	$\Gamma'_{\text{p-90}}(\text{hi})$	NPL-79	\bullet	\bullet	\bullet	\bullet	\bullet	\bullet	\bullet	\circ	\circ
<i>B23.1</i>	$\Gamma'_{\text{h-90}}(\text{lo})$	KR/VN-98	\bullet	\bullet	\bullet	\bullet	\circ	\bullet	\circ	\circ	\circ
<i>B23.2</i>	$\Gamma'_{\text{h-90}}(\text{lo})$	VNIIM-89	\bullet	\circ	\bullet	\circ	\circ	\circ	\circ	\circ	\circ
<i>B24.2</i>	K_{J}	PTB-91	\bullet	\bullet	\bullet	\bullet	\bullet	\bullet	\bullet	\bullet	\circ
<i>B25.2</i>	R_{K}	NML-97	\bullet	\bullet	\bullet	\bullet	\bullet	\bullet	\bullet	\circ	\circ
<i>B25.3</i>	R_{K}	NPL-88	\bullet	\bullet	\bullet	\bullet	\bullet	\bullet	\bullet	\circ	\circ
<i>B25.4</i>	R_{K}	NIM-95	\bullet	\bullet	\bullet	\bullet	\bullet	\bullet	\bullet	\circ	\circ
<i>B26.1</i>	$K_{\text{J}}^2 R_{\text{K}}$	NPL-90	\bullet	\bullet	\bullet	\circ	\bullet	\bullet	\bullet	\bullet	\bullet
<i>B26.2</i>	$K_{\text{J}}^2 R_{\text{K}}$	NIST-98	\bullet	\bullet	\bullet	\circ	\bullet	\bullet	\bullet	\bullet	\bullet
<i>B27</i>	\mathcal{F}_{90}	NIST-80	\bullet	\bullet	\bullet	\bullet	\bullet	\bullet	\bullet	\circ	\circ
<i>B39</i>	$d_{220}(\text{W4.2a})$	PTB-81	\bullet	\bullet	\bullet	\bullet	\bullet	\circ	\circ	\bullet	\bullet
<i>B40</i>	$d_{220}(\text{MO}^*4)$	IMGC-94	\bullet	\bullet	\bullet	\bullet	\bullet	\circ	\circ	\bullet	\bullet
<i>B41</i>	$d_{220}(\text{SH1})$	NRLM-97	\bullet	\bullet	\bullet	\bullet	\bullet	\circ	\circ	\bullet	\bullet

TABLE 21. Summary of the results of some of the least-squares adjustments used to analyze the input data given in Tables 14.B.1 and 14.B.2. The values of α and h are those obtained in the indicated adjustment, N is the number of input data, M is the number of adjusted constants, $\nu = N - M$ is the degrees of freedom, $R_B = \sqrt{\chi^2/\nu}$ is the Birge ratio, and $Q(\chi^2|\nu)$ is the probability that the observed value of χ^2 for ν degrees of freedom would have exceeded that observed value.

Adj.	N	M	ν	χ^2	R_B	$Q(\chi^2 \nu)$	α^{-1}	$u_r(\alpha^{-1})$	$h/(J\ s)$	$u_r(h)$
1	57	29	28	41.4	1.2	0.05	137.035 999 68(50)	3.6×10^{-9}	$6.626\ 068\ 78(52) \times 10^{-34}$	7.8×10^{-8}
2	56	29	27	28.7	1.0	0.38	137.035 999 73(50)	3.6×10^{-9}	$6.626\ 068\ 78(52) \times 10^{-34}$	7.8×10^{-8}
3	57	29	28	40.9	1.2	0.05	137.036 0008(18)	1.3×10^{-8}	$6.626\ 068\ 78(52) \times 10^{-34}$	7.8×10^{-8}
4	54	29	25	27.4	1.0	0.34	137.036 0015(18)	1.3×10^{-8}	$6.626\ 0684(24) \times 10^{-34}$	3.6×10^{-7}
5	53	29	24	20.0	0.9	0.70	137.035 999 90(50)	3.7×10^{-9}	$6.626\ 068\ 78(52) \times 10^{-34}$	7.8×10^{-8}
6	53	29	24	17.5	0.9	0.83	137.035 999 52(50)	3.7×10^{-9}	$6.626\ 068\ 78(52) \times 10^{-34}$	7.8×10^{-8}
7	50	29	21	9.1	0.7	0.99	137.035 999 69(51)	3.7×10^{-9}	$6.626\ 068\ 78(52) \times 10^{-34}$	7.8×10^{-8}
8	45	29	16	21.8	1.2	0.15	137.035 999 76(50)	3.7×10^{-9}	$6.626\ 068\ 76(52) \times 10^{-34}$	7.8×10^{-8}
9	43	29	14	16.1	1.1	0.30	137.035 999 88(51)	3.7×10^{-9}	$6.626\ 068\ 79(52) \times 10^{-34}$	7.9×10^{-8}

tainty $u(\delta_e)$ of δ_e by the multiplicative factor 10^6 . (This is what an open circle means in the row corresponding to δ_e in Table 20.) In this case the normalized residual of the VNIIM value is 3.6; it is responsible for 32 % of χ^2 , and its self-sensitivity coefficient is 1.3 %. Because of the obvious severe disagreement of this input datum with the other data and negligible contribution to any reasonable adjustment, we omit it from all other adjustments without comment.

Adjustment 4. To examine the robustness of the values of α and h , we eliminate those input data that contribute most significantly to their determination. Based on the discussions of Secs. 4.1.2 and 4.2.2, these are $\alpha(a_e)$ for α and the NIST and NPL values of $K_K^2 R_K$, items *B26.1* and *B26.2*, for h . We see that the value of α of adjustment 2 differs from the value of α of adjustment 4 by 1.0 times the uncertainty of α of adjustment 4, and the latter uncertainty is 3.6 times the uncertainty of α of adjustment 2. For h , the corresponding numbers are 0.18 and 4.6.

We conclude that the values of α and h are in fact fairly robust.

Adjustments 5, 6, and 7. The first of these adjustments shows the effect of deleting all three remaining low-field gyromagnetic ratio results, especially the NIST value of $\Gamma'_{p-90}(lo)$, item *B21.1*, and the KRISS/VNIIM value of $\Gamma'_{h-90}(lo)$, item *B23.1*; the second shows the effect of deleting the PTB, IMCG, and NRLM values of $d_{220}(X)$, items *B39*, *B40*, and *B41*; and the third shows the effect of deleting all six of these input data. The adjustments reflect the results that would have been obtained in Sec. 4.2.2 if the weighted mean of the five values of α had been computed with $\alpha(\Gamma'_{90})$ deleted, then with $\alpha(h/m_n)$ deleted, and finally with both deleted.

Adjustment 8. A considerable number of input data contribute only marginally to the determination of the values of the adjusted constants as measured by their values of S_c in adjustment 1. In adjustment 8, we omit those input data that have values of $S_c < 1\%$ unless they are a subset of the data of an experiment that provides input data with $S_c > 1\%$. The only input datum considered in this section that falls in the latter category is the 1982 LAMPF value of $\nu(58\text{ MHz})$, item *B15*. (There are four input data related to the Rydberg

constant that also fall into the latter category based on adjustment 1 of Sec. 4.3.1: items *A8*, *A9*, *A21*, and *A22*.)

As expected, the changes in the values of α and h and in their uncertainties are inconsequential; the absolute value of the change in α between adjustments 2 and 8 is about 1/18 times the standard uncertainty of α , and the absolute value of the change in h is about 1/26 times the standard uncertainty of h .

Adjustment 9. Here we extend the concept of adjustment 8 by eliminating all input data that in adjustment 1 have values of $S_c < 2\%$. Because this cutoff for S_c now eliminates the NIST value of $\Gamma'_{p-90}(lo)$, item *B21.1*, which in adjustment 8 provides a higher value of α that counterbalances the lower values of α from R_K and $h/m_n d_{220}(W04)$, the absolute value of the change in α is larger than that between adjustments 2 and 8. Nevertheless, the absolute value of the change in α between adjustments 2 and 9 is still only about 1/3.4 times the standard uncertainty of α . On the other hand, the absolute value of the change in h is smaller; it is only about 1/75 times the standard uncertainty of h .

In summary, we have identified and eliminated one significantly discrepant input datum, item *B23.2*, the VNIIM value of $\Gamma'_{h-90}(lo)$, and have demonstrated the robustness of the adjusted values of α and h .

Based on the analysis and discussion of the other data as given here and in Secs. 4.1.2 and 4.2.2, we conclude that adjustment 8 as summarized in Tables 20 and 21 is the preferred way of treating these data. To reiterate, 45 of the 57 input data of Tables 14.B.1 and 14.B.2 are used in the adjustment, its 29 adjusted constants are as given in Table 19.B.1, $R_B = 1.17$, and $Q(21.8|16) = 0.15$. Each input datum comes from an experiment that provides data with a self-sensitivity coefficient of $S_c > 1\%$. We choose this adjustment, rather than adjustment 2 or 9 of Table 21, because the data of truly marginal significance have been eliminated from it, but those data of slightly greater significance and which have some impact on the adjusted value of α are retained. We choose not to expand the uncertainties initially assigned the input data that determine the value of α in order to reflect the lack of agreement of some of these data, because the data principally involved in the disagreements have

TABLE 22. Summary of the results of some of the least-squares adjustments used to analyze all of the input data given in Tables 14.A.1, 14.A.2, 14.B.1, and 14.B.2. The values of R_∞ , α , and h are those obtained in the indicated adjustment, N is the number of input data, M is the number of adjusted constants, $\nu = N - M$ is the degrees of freedom, $R_B = \sqrt{\chi^2/\nu}$ is the Birge ratio, and $Q(\chi^2|\nu)$ is the probability that the observed value of χ^2 for ν degrees of freedom would have exceeded that observed value.

Adj.	N	M	ν	χ^2	R_B	$Q(\chi^2 \nu)$	R_∞/m^{-1}	α^{-1}	$h/(\text{J s})$
1	93	57	36	32.2	0.95	0.65	10 973 731.568 549(83)	137.035 999 76(50)	$6.626\,068\,76(52) \times 10^{-34}$
2	107	57	50	54.1	1.04	0.32	10 973 731.568 521(81)	137.035 999 67(50)	$6.626\,068\,78(52) \times 10^{-34}$
3	106	57	49	41.4	0.92	0.77	10 973 731.568 521(81)	137.035 999 73(50)	$6.626\,068\,78(52) \times 10^{-34}$

such magnitudes and uncertainties that their effect on the value of α is small. More to the point, we see little justification for expanding the uncertainties initially assigned the data that determine the adjusted value of α , which includes $\alpha_e(\text{exp})$ and δ_e and which would lead to an increased uncertainty of the adjusted value, because of disagreements involving data that contribute only in a marginal way to that value.

It should also be recognized that deleting input data with values of $S_c < 1\%$ is consistent with the criterion used in the initial data selection process, namely, that each input datum considered for the 1998 adjustment had to have a weight that was nontrivial in comparison with the weight of other directly measured values of the same quantity; see Sec. 1.4.

4.3.3. All Data

Here we summarize the multivariate analysis of all of the input data given in Tables 14.A.1, 14.A.2, 14.B.1, and 14.B.2 together. In fact, there is little to discuss that has not already been covered in the previous two sections, in which we have summarized the independent multivariate analysis of the two categories of data. Because the data in these two categories—Rydberg constant and other—are only weakly coupled, the preferred adjustment for the data in each category, adjustment 2 of Table 18 and adjustment 8 of Table 21, can be combined to yield the preferred adjustment for all of the data together.

In summary, the preferred adjustment uses as input data all of the data related to R_∞ given in Tables 14.A.1 and 14.A.2 except the values of R_p and R_d , items A15 and A23; and all of the data related to the constants (R_∞ and G excepted) given in Tables 14.B.1 and 14.B.2 except the 1982 SIN value of μ_{μ^+}/μ_p , item B14; the 1979 CERN and 1999 Brookhaven values of \bar{R} , items B19.1 and B19.2; the 1995 NIM values of $\Gamma'_{p-90}(\text{lo})$ and $\Gamma'_{p-90}(\text{hi})$, items B21.2 and B22.1; the 1979 NPL value of $\Gamma'_{p-90}(\text{hi})$, item B22.2; the 1998 KRISS-VNIIM and 1989 VNIIM values of $\Gamma'_{h-90}(\text{lo})$, items B23.1 and B23.2; the 1997 NML, 1988 NPL, and 1995 NIM values of R_K , items B25.2, B25.3, and B25.4; and the NIST value of \mathcal{F}_{90} , item B27. The input data with the largest residuals, and hence those that make the dominant contributions to χ^2 , are the 1989 NIST value of $\Gamma'_{p-90}(\text{lo})$, item B21.1 with $r = 2.33$; the 1999 PTB value of $h/m_n d_{220}(\text{W04})$, item B29 with $r = -1.97$; the 1994 IMGC value of

$d_{220}(\text{MO}^*4)$, item B40 with $r = -1.48$; and the 1981 PTB value of $d_{220}(\text{W4.2a})$, item B39 with $r = -1.48$. All other input data have $|r| < 1.2$.

Some of the results of this adjustment, denoted as adjustment 1, are summarized in Table 22. A comparison of the values of R_∞ , α , and h that follow from it to the corresponding values of the preferred independent adjustments of the data shows the weak dependence of the data in each category on the data in the other category. For comparison purposes, we also summarize in Table 22 the results from two other adjustments based on the combined data. Adjustment 2 uses all of the data, including item B23.2, the inconsistent 1989 VNIIM value of $\Gamma'_{h-90}(\text{lo})$; and adjustment 3 uses all of the data except this item. Clearly, there are no surprises in the results.

4.4. Final Selection of Data and Least-Squares Adjustment

Based on the data analysis and discussion of the previous sections, we choose adjustment 1 as summarized in Table 22 of the previous section to obtain the 1998 recommended values of the constants. In this adjustment, 93 of the 107 items of data given in Tables 14.A.1 and 14.B.1, together with their correlation coefficients given in Tables 14.A.2 and 14.B.2, are used as input data. The adjustment has degrees of freedom $\nu = 36$, $\chi^2 = 32.2$, $R_B = 0.95$, and $Q(32.4|36) = 0.65$, and the 57 adjusted constants employed are those given in Tables 17.A.1 and 19.B.1. Each input datum comes from an experiment that provides data with a self-sensitivity coefficient $S_c > 1\%$. The values of the constants deduced from adjustment 1 are given in the following section.

5. The 1998 CODATA Recommended Values

As indicated in Sec. 4.4, the 1998 recommended values of the constants are based on least-squares adjustment 1 of Table 22. The direct result of this adjustment is best estimated values in the least-squares sense of the 57 adjusted constants given in Tables 17.A.1 and 19.B.1 together with their variances and covariances. All of the 1998 recommended values and their uncertainties are obtained from these 57 constants and, as appropriate: (i) those constants that have defined values such as c and μ_0 ; (ii) the value of G adopted in Sec 3.17; and (iii) values of m_τ , G_F , and

TABLE 23. An abbreviated list of the CODATA recommended values of the fundamental constants of physics and chemistry based on the 1998 adjustment.

Quantity	Symbol	Numerical value	Unit	Relative std. uncert. u_f
speed of light in vacuum	c, c_0	299 792 458	m s^{-1}	(exact)
magnetic constant	μ_0	$4\pi \times 10^{-7}$	N A^{-2}	(exact)
		$= 12.566 370 614 \dots \times 10^{-7}$	N A^{-2}	(exact)
electric constant $1/\mu_0 c^2$	ϵ_0	$8.854 187 817 \dots \times 10^{-12}$	F m^{-1}	(exact)
Newtonian constant of gravitation	G	$6.673(10) \times 10^{-11}$	$\text{m}^3 \text{kg}^{-1} \text{s}^{-2}$	1.5×10^{-3}
Planck constant	h	$6.626 068 76(52) \times 10^{-34}$	J s	7.8×10^{-8}
$h/2\pi$	\hbar	$1.054 571 596(82) \times 10^{-34}$	J s	7.8×10^{-8}
elementary charge	e	$1.602 176 462(63) \times 10^{-19}$	C	3.9×10^{-8}
magnetic flux quantum $h/2e$	Φ_0	$2.067 833 636(81) \times 10^{-15}$	Wb	3.9×10^{-8}
conductance quantum $2e^2/h$	G_0	$7.748 091 696(28) \times 10^{-5}$	S	3.7×10^{-9}
electron mass	m_e	$9.109 381 88(72) \times 10^{-31}$	kg	7.9×10^{-8}
proton mass	m_p	$1.672 621 58(13) \times 10^{-27}$	kg	7.9×10^{-8}
proton-electron mass ratio	m_p/m_e	1 836.152 6675(39)		2.1×10^{-9}
fine-structure constant $e^2/4\pi\epsilon_0\hbar c$	α	$7.297 352 533(27) \times 10^{-3}$		3.7×10^{-9}
inverse fine-structure constant	α^{-1}	137.035 999 76(50)		3.7×10^{-9}
Rydberg constant $\alpha^2 m_e c/2h$	R_∞	10 973 731.568 549(83)	m^{-1}	7.6×10^{-12}
Avogadro constant	N_A, L	$6.022 141 99(47) \times 10^{23}$	mol^{-1}	7.9×10^{-8}
Faraday constant $N_A e$	F	96 485.3415(39)	C mol^{-1}	4.0×10^{-8}
molar gas constant	R	8.314 472(15)	$\text{J mol}^{-1} \text{K}^{-1}$	1.7×10^{-6}
Boltzmann constant R/N_A	k	$1.380 6503(24) \times 10^{-23}$	J K^{-1}	1.7×10^{-6}
Stefan-Boltzmann constant $(\pi^2/60)k^4/\hbar^3 c^2$	σ	$5.670 400(40) \times 10^{-8}$	$\text{W m}^{-2} \text{K}^{-4}$	7.0×10^{-6}
Non-SI units accepted for use with the SI				
electron volt: $(e/\text{C}) \text{ J}$	eV	$1.602 176 462(63) \times 10^{-19}$	J	3.9×10^{-8}
(unified) atomic mass unit				
$1 \text{ u} = m_u = \frac{1}{12} m(^{12}\text{C})$	u	$1.660 538 73(13) \times 10^{-27}$	kg	7.9×10^{-8}
$= 10^{-3} \text{ kg mol}^{-1}/N_A$				

$\sin^2 \theta_W$ given in Sec. 3.19. How this is done is described in Sec. 5.2, which immediately follows the tables of recommended values given in Sec. 5.1.

5.1. Tables of Values

The 1998 CODATA recommended values of the basic constants and conversion factors of physics and chemistry, including the values of related quantities, are given in Tables 23–30. Table 23 is a highly abbreviated list containing the values of the constants and conversion factors most commonly used. Table 24 is a much more extensive list of values categorized as follows: UNIVERSAL; ELECTROMAGNETIC; ATOMIC AND NUCLEAR; and PHYSICOCHEMICAL. The ATOMIC AND NUCLEAR category is subdivided into ten subcategories: General; Electroweak; Electron, e^- ; Muon, μ^- ; Tau, τ^- ; Proton, p ; Neutron, n ; Deuteron, d ; Helion, h ; and Alpha particle, α . Table 25 gives the variances, covariances, and correlation coefficients of a selected group of constants. (Application of the covariance matrix is discussed in Appendix F.) Table 26 gives the internationally adopted values of various quantities; Table 27 lists the values of a number of x-ray-related quantities; Table 28 lists the values of various non-SI units; and Tables 29 and 30 give the values of various energy equivalents.

All of the values given in Tables 23 to 30 are available on

the Web pages of the Fundamental Constants Data Center of the NIST Physics Laboratory at physics.nist.gov/constants. This electronic version of the 1998 CODATA recommended values of the constants also includes a much more extensive correlation coefficient matrix. Indeed, the correlation coefficient of any two constants listed in the tables is accessible on the Web site, as well as the automatic conversion of the value of an energy-related quantity expressed in one unit to the corresponding value expressed in another unit (in essence, an automated version of Tables 29 and 30).

5.2 Computational Details

Here we provide some particulars of how the 1998 recommended values and their uncertainties as given in the tables of the previous section are obtained from the values of the 57 adjusted constants listed in Tables 17.A.1 and 19.B.1 of Secs. 4.3.1. and 4.3.2. and from the values of other quantities such as c and G as appropriate (see the beginning of Sec. 5).

We first note that the values of many of the adjusted constants are themselves included in the tables. Their standard uncertainties are the positive square roots of the diagonal elements of the covariance matrix of the adjusted constants (see Appendix E). Their covariances, some of which are given in Table 25 in relative form as well as in the form of correlation coefficients, are the off-diagonal elements. As in-

TABLE 24. The CODATA recommended values of the fundamental constants of physics and chemistry based on the 1998 adjustment.

Quantity	Symbol	Numerical value	Unit	Relative std. uncert. u_r
UNIVERSAL				
speed of light in vacuum	c, c_0	299 792 458	m s^{-1}	(exact)
magnetic constant	μ_0	$4\pi \times 10^{-7}$ $= 12.566\,370\,614 \dots \times 10^{-7}$	N A^{-2} N A^{-2}	(exact)
electric constant $1/\mu_0 c^2$	ϵ_0	$8.854\,187\,817 \dots \times 10^{-12}$	F m^{-1}	(exact)
characteristic impedance of vacuum $\sqrt{\mu_0/\epsilon_0} = \mu_0 c$	Z_0	376.730 313 461 ...	Ω	(exact)
Newtonian constant of gravitation	G $G/\hbar c$	$6.673(10) \times 10^{-11}$ $6.707(10) \times 10^{-39}$	$\text{m}^3 \text{ kg}^{-1} \text{ s}^{-2}$ $(\text{GeV}/c^2)^{-2}$	1.5×10^{-3} 1.5×10^{-3}
Planck constant	h	$6.626\,068\,76(52) \times 10^{-34}$	J s	7.8×10^{-8}
in eV s		$4.135\,667\,27(16) \times 10^{-15}$	eV s	3.9×10^{-8}
$h/2\pi$	\hbar	$1.054\,571\,596(82) \times 10^{-34}$	J s	7.8×10^{-8}
in eV s		$6.582\,118\,89(26) \times 10^{-16}$	eV s	3.9×10^{-8}
Planck mass $(\hbar c/G)^{1/2}$	m_{P}	$2.1767(16) \times 10^{-8}$	kg	7.5×10^{-4}
Planck length $\hbar/m_{\text{P}}c = (\hbar G/c^3)^{1/2}$	l_{P}	$1.6160(12) \times 10^{-35}$	m	7.5×10^{-4}
Planck time $l_{\text{P}}/c = (\hbar G/c^5)^{1/2}$	t_{P}	$5.3906(40) \times 10^{-44}$	s	7.5×10^{-4}
ELECTROMAGNETIC				
elementary charge	e	$1.602\,176\,462(63) \times 10^{-19}$	C	3.9×10^{-8}
	e/h	$2.417\,989\,491(95) \times 10^{14}$	A J^{-1}	3.9×10^{-8}
magnetic flux quantum $h/2e$	Φ_0	$2.067\,833\,636(81) \times 10^{-15}$	Wb	3.9×10^{-8}
conductance quantum $2e^2/h$	G_0	$7.748\,091\,696(28) \times 10^{-5}$	S	3.7×10^{-9}
inverse of conductance quantum	G_0^{-1}	$12\,906.403\,786(47)$	Ω	3.7×10^{-9}
Josephson constant ^a $2e/h$	K_{J}	$483\,597.898(19) \times 10^9$	Hz V^{-1}	3.9×10^{-8}
von Klitzing constant ^b $h/e^2 = \mu_0 c/2\alpha$	R_{K}	$25\,812.807\,572(95)$	Ω	3.7×10^{-9}
Bohr magneton $e\hbar/2m_{\text{e}}$	μ_{B}	$927.400\,899(37) \times 10^{-26}$	J T^{-1}	4.0×10^{-8}
in eV T ⁻¹		$5.788\,381\,749(43) \times 10^{-5}$	eV T^{-1}	7.3×10^{-9}
	μ_{B}/h	$13.996\,246\,24(56) \times 10^9$	Hz T^{-1}	4.0×10^{-8}
	μ_{B}/hc	$46.686\,4521(19)$	$\text{m}^{-1} \text{ T}^{-1}$	4.0×10^{-8}
	μ_{B}/k	$0.671\,7131(12)$	K T^{-1}	1.7×10^{-6}
nuclear magneton $e\hbar/2m_{\text{p}}$	μ_{N}	$5.050\,783\,17(20) \times 10^{-27}$	J T^{-1}	4.0×10^{-8}
in eV T ⁻¹		$3.152\,451\,238(24) \times 10^{-8}$	eV T^{-1}	7.6×10^{-9}
	μ_{N}/h	$7.622\,593\,96(31)$	MHz T^{-1}	4.0×10^{-8}
	μ_{N}/hc	$2.542\,623\,66(10) \times 10^{-2}$	$\text{m}^{-1} \text{ T}^{-1}$	4.0×10^{-8}
	μ_{N}/k	$3.658\,2638(64) \times 10^{-4}$	K T^{-1}	1.7×10^{-6}
ATOMIC AND NUCLEAR				
General				
fine-structure constant $e^2/4\pi\epsilon_0\hbar c$	α	$7.297\,352\,533(27) \times 10^{-3}$		3.7×10^{-9}
inverse fine-structure constant	α^{-1}	$137.035\,999\,76(50)$		3.7×10^{-9}
Rydberg constant $\alpha^2 m_{\text{e}} c/2\hbar$	R_{∞}	$10\,973\,731.568\,549(83)$	m^{-1}	7.6×10^{-12}
	$R_{\infty} c$	$3.289\,841\,960\,368(25) \times 10^{15}$	Hz	7.6×10^{-12}
	$R_{\infty} \hbar c$	$2.179\,871\,90(17) \times 10^{-18}$	J	7.8×10^{-8}
$R_{\infty} \hbar c$ in eV		$13.605\,691\,72(53)$	eV	3.9×10^{-8}
Bohr radius $\alpha/4\pi R_{\infty} = 4\pi\epsilon_0\hbar^2/m_{\text{e}}e^2$	a_0	$0.529\,177\,2083(19) \times 10^{-10}$	m	3.7×10^{-9}
Hartree energy $e^2/4\pi\epsilon_0 a_0 = 2R_{\infty} \hbar c$ $= \alpha^2 m_{\text{e}} c^2$	E_{h}	$4.359\,743\,81(34) \times 10^{-18}$	J	7.8×10^{-8}
in eV		$27.211\,3834(11)$	eV	3.9×10^{-8}
quantum of circulation	$h/2m_{\text{e}}$ h/m_{e}	$3.636\,947\,516(27) \times 10^{-4}$ $7.273\,895\,032(53) \times 10^{-4}$	$\text{m}^2 \text{ s}^{-1}$ $\text{m}^2 \text{ s}^{-1}$	7.3×10^{-9} 7.3×10^{-9}
Electroweak				
Fermi coupling constant ^c	$G_{\text{F}}/(\hbar c)^3$	$1.166\,39(1) \times 10^{-5}$	GeV^{-2}	8.6×10^{-6}
weak mixing angle ^d θ_{W} (on-shell scheme) $\sin^2 \theta_{\text{W}} = s_{\text{W}}^2 \equiv 1 - (m_{\text{W}}/m_{\text{Z}})^2$	$\sin^2 \theta_{\text{W}}$	$0.2224(19)$		8.7×10^{-3}
Electron, e ⁻				
electron mass	m_{e}	$9.109\,381\,88(72) \times 10^{-31}$	kg	7.9×10^{-8}
in u, $m_{\text{e}} = A_{\text{r}}(\text{e})$ u (electron relative atomic mass times u)		$5.485\,799\,110(12) \times 10^{-4}$	u	2.1×10^{-9}
energy equivalent	$m_{\text{e}} c^2$	$8.187\,104\,14(64) \times 10^{-14}$	J	7.9×10^{-8}
in MeV		$0.510\,998\,902(21)$	MeV	4.0×10^{-8}
electron–muon mass ratio	m_{e}/m_{μ}	$4.836\,332\,10(15) \times 10^{-3}$		3.0×10^{-8}
electron–tau mass ratio	m_{e}/m_{τ}	$2.875\,55(47) \times 10^{-4}$		1.6×10^{-4}
electron–proton mass ratio	$m_{\text{e}}/m_{\text{p}}$	$5.446\,170\,232(12) \times 10^{-4}$		2.1×10^{-9}
electron–neutron mass ratio	$m_{\text{e}}/m_{\text{n}}$	$5.438\,673\,462(12) \times 10^{-4}$		2.2×10^{-9}

TABLE 24. The CODATA recommended values of the fundamental constants of physics and chemistry based on the 1998 adjustment—Continued.

Quantity	Symbol	Numerical value	Unit	Relative std. uncert. u_r
electron–deuteron mass ratio	m_e/m_d	$2.724\,437\,1170(58) \times 10^{-4}$		2.1×10^{-9}
electron to alpha particle mass ratio	m_e/m_α	$1.370\,933\,5611(29) \times 10^{-4}$		2.1×10^{-9}
electron charge to mass quotient	$-e/m_e$	$-1.758\,820\,174(71) \times 10^{11}$	C kg^{-1}	4.0×10^{-8}
electron molar mass $N_A m_e$	$M(e), M_e$	$5.485\,799\,110(12) \times 10^{-7}$	kg mol^{-1}	2.1×10^{-9}
Compton wavelength $h/m_e c$	λ_C	$2.426\,310\,215(18) \times 10^{-12}$	m	7.3×10^{-9}
$\lambda_C/2\pi = \alpha a_0 = \alpha^2/4\pi R_\infty$	λ_C	$386.159\,2642(28) \times 10^{-15}$	m	7.3×10^{-9}
classical electron radius $\alpha^2 a_0$	r_e	$2.817\,940\,285(31) \times 10^{-15}$	m	1.1×10^{-8}
Thomson cross section $(8\pi/3)r_e^2$	σ_e	$0.665\,245\,854(15) \times 10^{-28}$	m^2	2.2×10^{-8}
electron magnetic moment	μ_e	$-928.476\,362(37) \times 10^{-26}$	J T^{-1}	4.0×10^{-8}
to Bohr magneton ratio	μ_e/μ_B	$-1.001\,159\,652\,1869(41)$		4.1×10^{-12}
to nuclear magneton ratio	μ_e/μ_N	$-1\,838.281\,9660(39)$		2.1×10^{-9}
electron magnetic moment anomaly $ \mu_e /\mu_B - 1$	a_e	$1.159\,652\,1869(41) \times 10^{-3}$		3.5×10^{-9}
electron g -factor $-2(1+a_e)$	g_e	$-2.002\,319\,304\,3737(82)$		4.1×10^{-12}
electron–muon magnetic moment ratio	μ_e/μ_μ	$206.766\,9720(63)$		3.0×10^{-8}
electron–proton magnetic moment ratio	μ_e/μ_p	$-658.210\,6875(66)$		1.0×10^{-8}
electron to shielded proton magnetic moment ratio (H ₂ O, sphere, 25 °C)	μ_e/μ'_p	$-658.227\,5954(71)$		1.1×10^{-8}
electron–neutron magnetic moment ratio	μ_e/μ_n	$960.920\,50(23)$		2.4×10^{-7}
electron–deuteron magnetic moment ratio	μ_e/μ_d	$-2\,143.923\,498(23)$		1.1×10^{-8}
electron to shielded helion ^c magnetic moment ratio (gas, sphere, 25 °C)	μ_e/μ'_h	$864.058\,255(10)$		1.2×10^{-8}
electron gyromagnetic ratio $2 \mu_e /\hbar$	γ_e	$1.760\,859\,794(71) \times 10^{11}$	$\text{s}^{-1} \text{T}^{-1}$	4.0×10^{-8}
	$\gamma_e/2\pi$	$28\,024.9540(11)$	MHz T^{-1}	4.0×10^{-8}
		Muon, μ^-		
muon mass	m_μ	$1.883\,531\,09(16) \times 10^{-28}$	kg	8.4×10^{-8}
in u, $m_\mu = A_r(\mu)$ u (muon relative atomic mass times u)		$0.113\,428\,9168(34)$	u	3.0×10^{-8}
energy equivalent	$m_\mu c^2$	$1.692\,833\,32(14) \times 10^{-11}$	J	8.4×10^{-8}
in MeV		$105.658\,3568(52)$	MeV	4.9×10^{-8}
muon–electron mass ratio	m_μ/m_e	$206.768\,2657(63)$		3.0×10^{-8}
muon–tau mass ratio	m_μ/m_τ	$5.945\,72(97) \times 10^{-2}$		1.6×10^{-4}
muon–proton mass ratio	m_μ/m_p	$0.112\,609\,5173(34)$		3.0×10^{-8}
muon–neutron mass ratio	m_μ/m_n	$0.112\,454\,5079(34)$		3.0×10^{-8}
muon molar mass $N_A m_\mu$	$M(\mu), M_u$	$0.113\,428\,9168(34) \times 10^{-3}$	kg mol^{-1}	3.0×10^{-8}
muon Compton wavelength $h/m_\mu c$	$\lambda_{C,\mu}$	$11.734\,441\,97(35) \times 10^{-15}$	m	2.9×10^{-8}
$\lambda_{C,\mu}/2\pi$	$\lambda_{C,\mu}$	$1.867\,594\,444(55) \times 10^{-15}$	m	2.9×10^{-8}
muon magnetic moment	μ_μ	$-4.490\,448\,13(22) \times 10^{-26}$	J T^{-1}	4.9×10^{-8}
to Bohr magneton ratio	μ_μ/μ_B	$-4.841\,970\,85(15) \times 10^{-3}$		3.0×10^{-8}
to nuclear magneton ratio	μ_μ/μ_N	$-8.890\,597\,70(27)$		3.0×10^{-8}
muon magnetic moment anomaly $ \mu_\mu /(e\hbar/2m_\mu) - 1$	a_μ	$1.165\,916\,02(64) \times 10^{-3}$		5.5×10^{-7}
muon g -factor $-2(1+a_\mu)$	g_μ	$-2.002\,331\,8320(13)$		6.4×10^{-10}
muon–proton magnetic moment ratio	μ_μ/μ_p	$-3.183\,345\,39(10)$		3.2×10^{-8}
		Tau, τ^-		
tau mass ^f	m_τ	$3.167\,88(52) \times 10^{-27}$	kg	1.6×10^{-4}
in u, $m_\tau = A_r(\tau)$ u (tau relative atomic mass times u)		$1.907\,74(31)$	u	1.6×10^{-4}
energy equivalent	$m_\tau c^2$	$2.847\,15(46) \times 10^{-10}$	J	1.6×10^{-4}
in MeV		$1\,777.05(29)$	MeV	1.6×10^{-4}
tau–electron mass ratio	m_τ/m_e	$3\,477.60(57)$		1.6×10^{-4}
tau–muon mass ratio	m_τ/m_μ	$16.8188(27)$		1.6×10^{-4}
tau–proton mass ratio	m_τ/m_p	$1.893\,96(31)$		1.6×10^{-4}
tau–neutron mass ratio	m_τ/m_n	$1.891\,35(31)$		1.6×10^{-4}
tau–molar mass $N_A m_\tau$	$M(\tau), M_\tau$	$1.907\,74(31) \times 10^{-3}$	kg mol^{-1}	1.6×10^{-4}
tau Compton wavelength $h/m_\tau c$	$\lambda_{C,\tau}$	$0.697\,70(11) \times 10^{-15}$	m	1.6×10^{-4}
$\lambda_{C,\tau}/2\pi$	$\lambda_{C,\tau}$	$0.111\,042(18) \times 10^{-15}$	m	1.6×10^{-4}

TABLE 24. The CODATA recommended values of the fundamental constants of physics and chemistry based on the 1998 adjustment—Continued.

Quantity	Symbol	Numerical value	Unit	Relative std. uncert. u_r
Proton, p				
proton mass	m_p	$1.672\,621\,58(13) \times 10^{-27}$	kg	7.9×10^{-8}
in u, $m_p = A_r(p)$ u (proton relative atomic mass times u)		1.007 276 466 88(13)	u	1.3×10^{-10}
energy equivalent	$m_p c^2$	$1.503\,277\,31(12) \times 10^{-10}$	J	7.9×10^{-8}
in MeV		938.271 998(38)	MeV	4.0×10^{-8}
proton–electron mass ratio	m_p/m_e	1 836.152 6675(39)		2.1×10^{-9}
proton–muon mass ratio	m_p/m_μ	8.880 244 08(27)		3.0×10^{-8}
proton–tau mass ratio	m_p/m_τ	0.527 994(86)		1.6×10^{-4}
proton–neutron mass ratio	m_p/m_n	0.998 623 478 55(58)		5.8×10^{-10}
proton charge to mass quotient	e/m_p	$9.578\,834\,08(38) \times 10^7$	C kg ⁻¹	4.0×10^{-8}
proton molar mass $N_A m_p$	$M(p), M_p$	$1.007\,276\,466\,88(13) \times 10^{-3}$	kg mol ⁻¹	1.3×10^{-10}
proton Compton wavelength $h/m_p c$	$\lambda_{C,p}$	$1.321\,409\,847(10) \times 10^{-15}$	m	7.6×10^{-9}
$\lambda_{C,p}/2\pi$	$\lambda_{C,p}/2\pi$	$0.210\,308\,9089(16) \times 10^{-15}$	m	7.6×10^{-9}
proton magnetic moment	μ_p	$1.410\,606\,633(58) \times 10^{-26}$	J T ⁻¹	4.1×10^{-8}
to Bohr magneton ratio	μ_p/μ_B	$1.521\,032\,203(15) \times 10^{-3}$		1.0×10^{-8}
to nuclear magneton ratio	μ_p/μ_N	2.792 847 337(29)		1.0×10^{-8}
proton g -factor $2\mu_p/\mu_N$	g_p	5.585 694 675(57)		1.0×10^{-8}
proton–neutron				
magnetic moment ratio	μ_p/μ_n	−1.459 898 05(34)		2.4×10^{-7}
shielded proton magnetic moment (H ₂ O, sphere, 25 °C)	μ'_p	$1.410\,570\,399(59) \times 10^{-26}$	J T ⁻¹	4.2×10^{-8}
to Bohr magneton ratio	μ'_p/μ_B	$1.520\,993\,132(16) \times 10^{-3}$		1.1×10^{-8}
to nuclear magneton ratio	μ'_p/μ_N	2.792 775 597(31)		1.1×10^{-8}
proton magnetic shielding correction $1 - \mu'_p/\mu_p$ (H ₂ O, sphere, 25 °C)	σ'_p	$25.687(15) \times 10^{-6}$		5.7×10^{-4}
proton gyromagnetic ratio $2\mu_p/\hbar$	γ_p	$2.675\,222\,12(11) \times 10^8$	s ⁻¹ T ⁻¹	4.1×10^{-8}
	$\gamma_p/2\pi$	42.577 4825(18)	MHz T ⁻¹	4.1×10^{-8}
shielded proton gyromagnetic ratio $2\mu'_p/\hbar$ (H ₂ O, sphere, 25 °C)	γ'_p	$2.675\,153\,41(11) \times 10^8$	s ⁻¹ T ⁻¹	4.2×10^{-8}
	$\gamma'_p/2\pi$	42.576 3888(18)	MHz T ⁻¹	4.2×10^{-8}
Neutron, n				
neutron mass	m_n	$1.674\,927\,16(13) \times 10^{-27}$	kg	7.9×10^{-8}
in u, $m_n = A_r(n)$ u (neutron relative atomic mass times u)		1.008 664 915 78(55)	u	5.4×10^{-10}
energy equivalent	$m_n c^2$	$1.505\,349\,46(12) \times 10^{-10}$	J	7.9×10^{-8}
in MeV		939.565 330(38)	MeV	4.0×10^{-8}
neutron–electron mass ratio	m_n/m_e	1 838.683 6550(40)		2.2×10^{-9}
neutron–muon mass ratio	m_n/m_μ	8.892 484 78(27)		3.0×10^{-8}
neutron–tau mass ratio	m_n/m_τ	0.528 722(86)		1.6×10^{-4}
neutron–proton mass ratio	m_n/m_p	1.001 378 418 87(58)		5.8×10^{-10}
neutron molar mass $N_A m_n$	$M(n), M_n$	$1.008\,664\,915\,78(55) \times 10^{-3}$	kg mol ⁻¹	5.4×10^{-10}
neutron Compton wavelength $h/m_n c$	$\lambda_{C,n}$	$1.319\,590\,898(10) \times 10^{-15}$	m	7.6×10^{-9}
$\lambda_{C,n}/2\pi$	$\lambda_{C,n}/2\pi$	$0.210\,019\,4142(16) \times 10^{-15}$	m	7.6×10^{-9}
neutron magnetic moment	μ_n	$-0.966\,236\,40(23) \times 10^{-26}$	J T ⁻¹	2.4×10^{-7}
to Bohr magneton ratio	μ_n/μ_B	$-1.041\,875\,63(25) \times 10^{-3}$		2.4×10^{-7}
to nuclear magneton ratio	μ_n/μ_N	−1.913 042 72(45)		2.4×10^{-7}
neutron g -factor $2\mu_n/\mu_N$	g_n	−3.826 085 45(90)		2.4×10^{-7}
neutron–electron				
magnetic moment ratio	μ_n/μ_e	$1.040\,668\,82(25) \times 10^{-3}$		2.4×10^{-7}
neutron–proton				
magnetic moment ratio	μ_n/μ_p	−0.684 979 34(16)		2.4×10^{-7}
neutron to shielded proton magnetic moment ratio (H ₂ O, sphere, 25 °C)	μ_n/μ'_p	−0.684 996 94(16)		2.4×10^{-7}
neutron gyromagnetic ratio $2 \mu_n /\hbar$	γ_n	$1.832\,471\,88(44) \times 10^8$	s ⁻¹ T ⁻¹	2.4×10^{-7}
	$\gamma_n/2\pi$	29.164 6958(70)	MHz T ⁻¹	2.4×10^{-7}
Deuteron, d				
deuteron mass	m_d	$3.343\,583\,09(26) \times 10^{-27}$	kg	7.9×10^{-8}
in u, $m_d = A_r(d)$ u (deuteron relative atomic mass times u)		2.013 553 212 71(35)	u	1.7×10^{-10}
energy equivalent	$m_d c^2$	$3.005\,062\,62(24) \times 10^{-10}$	J	7.9×10^{-8}
in MeV		1 875.612 762(75)	MeV	4.0×10^{-8}

TABLE 24. The CODATA recommended values of the fundamental constants of physics and chemistry based on the 1998 adjustment—Continued.

Quantity	Symbol	Numerical value	Unit	Relative std. uncert. u_r
deuteron–electron mass ratio				
deuteron–proton mass ratio	m_d/m_p	1.999 007 500 83(41)		2.0×10^{-10}
deuteron molar mass $N_A m_d$	$M(d), M_d$	$2.013\,553\,212\,71(35) \times 10^{-3}$	kg mol ⁻¹	1.7×10^{-10}
deuteron magnetic moment	μ_d	$0.433\,073\,457(18) \times 10^{-26}$	J T ⁻¹	4.2×10^{-8}
to Bohr magneton ratio	μ_d/μ_B	$0.466\,975\,4556(50) \times 10^{-3}$		1.1×10^{-8}
to nuclear magneton ratio	μ_d/μ_N	0.857 438 2284(94)		1.1×10^{-8}
deuteron–electron magnetic moment ratio	μ_d/μ_e	$-4.664\,345\,537(50) \times 10^{-4}$		1.1×10^{-8}
deuteron–proton magnetic moment ratio	μ_d/μ_p	0.307 012 2083(45)		1.5×10^{-8}
deuteron–neutron magnetic moment ratio	μ_d/μ_n	-0.448 206 52(11)		2.4×10^{-7}
helion mass ^e	m_h	Helion, h $5.006\,411\,74(39) \times 10^{-27}$	kg	7.9×10^{-8}
in u, $m_h = A_r(h)$ u (helion relative atomic mass times u)		3.014 932 234 69(86)	u	2.8×10^{-10}
energy equivalent	$m_h c^2$	$4.499\,538\,48(35) \times 10^{-10}$	J	7.9×10^{-8}
in MeV		2 808.391 32(11)	MeV	4.0×10^{-8}
helion–electron mass ratio	m_h/m_e	5 495.885 238(12)		2.1×10^{-9}
helion–proton mass ratio	m_h/m_p	2.993 152 658 50(93)		3.1×10^{-10}
helion molar mass $N_A m_h$	$M(h), M_h$	$3.014\,932\,234\,69(86) \times 10^{-3}$	kg mol ⁻¹	2.8×10^{-10}
shielded helion magnetic moment (gas, sphere, 25 °C)	μ'_h	$-1.074\,552\,967(45) \times 10^{-26}$	J T ⁻¹	4.2×10^{-8}
to Bohr magneton ratio	μ'_h/μ_B	$-1.158\,671\,474(14) \times 10^{-3}$		1.2×10^{-8}
to nuclear magneton ratio	μ'_h/μ_N	-2.127 497 718(25)		1.2×10^{-8}
shielded helion to proton magnetic moment ratio (gas, sphere, 25 °C)	μ'_h/μ_p	-0.761 766 563(12)		1.5×10^{-8}
shielded helion to shielded proton magnetic moment ratio (gas/H ₂ O, spheres, 25 °C)	μ'_h/μ'_p	-0.761 786 1313(33)		4.3×10^{-9}
shielded helion gyromagnetic ratio $2 \mu'_h /\hbar$ (gas, sphere, 25 °C)	γ'_h	$2.037\,894\,764(85) \times 10^8$	s ⁻¹ T ⁻¹	4.2×10^{-8}
	$\gamma'_h/2\pi$	32.434 1025(14)	MHz T ⁻¹	4.2×10^{-8}
alpha particle mass	m_α	Alpha particle, α $6.644\,655\,98(52) \times 10^{-27}$	kg	7.9×10^{-8}
in u, $m_\alpha = A_r(\alpha)$ u (alpha particle relative atomic mass times u)		4.001 506 1747(10)	u	2.5×10^{-10}
energy equivalent	$m_\alpha c^2$	$5.971\,918\,97(47) \times 10^{-10}$	J	7.9×10^{-8}
in MeV		3 727.379 04(15)	MeV	4.0×10^{-8}
alpha particle to electron mass ratio	m_α/m_e	7 294.299 508(16)		2.1×10^{-9}
alpha particle to proton mass ratio	m_α/m_p	3.972 599 6846(11)		2.8×10^{-10}
alpha particle molar mass $N_A m_\alpha$	$M(\alpha), M_\alpha$	$4.001\,506\,1747(10) \times 10^{-3}$	kg mol ⁻¹	2.5×10^{-10}
PHYSICOCHEMICAL				
Avogadro constant	N_A, L	$6.022\,141\,99(47) \times 10^{23}$	mol ⁻¹	7.9×10^{-8}
atomic mass constant				
$m_u = \frac{1}{12} m(^{12}\text{C}) = 1 \text{ u}$ $= 10^{-3} \text{ kg mol}^{-1}/N_A$	m_u	$1.660\,538\,73(13) \times 10^{-27}$	kg	7.9×10^{-8}
energy equivalent	$m_u c^2$	$1.492\,417\,78(12) \times 10^{-10}$	J	7.9×10^{-8}
in MeV		931.494 013(37)	MeV	4.0×10^{-8}
Faraday constant ^g $N_A e$	F	96 485.3415(39)	C mol ⁻¹	4.0×10^{-8}
molar Planck constant	$N_A h$	$3.990\,312\,689(30) \times 10^{-10}$	J s mol ⁻¹	7.6×10^{-9}
	$N_A h c$	0.119 626 564 92(91)	J m mol ⁻¹	7.6×10^{-9}
molar gas constant	R	8.314 472(15)	J mol ⁻¹ K ⁻¹	1.7×10^{-6}
Boltzmann constant R/N_A	k	$1.380\,6503(24) \times 10^{-23}$	J K ⁻¹	1.7×10^{-6}
in eV K ⁻¹		8.617 342(15) $\times 10^{-5}$	eV K ⁻¹	1.7×10^{-6}
	k/h	$2.083\,6644(36) \times 10^{10}$	Hz K ⁻¹	1.7×10^{-6}
	k/hc	69.503 56(12)	m ⁻¹ K ⁻¹	1.7×10^{-6}

TABLE 24. The CODATA recommended values of the fundamental constants of physics and chemistry based on the 1998 adjustment—Continued.

Quantity	Symbol	Numerical value	Unit	Relative std. uncert. u_r
molar volume of ideal gas RT/p $T = 273.15 \text{ K}$, $p = 101.325 \text{ kPa}$	V_m	$22.413\,996(39) \times 10^{-3}$	$\text{m}^3 \text{mol}^{-1}$	1.7×10^{-6}
Loschmidt constant N_A/V_m $T = 273.15 \text{ K}$, $p = 100 \text{ kPa}$	n_0	$2.686\,7775(47) \times 10^{25}$	m^{-3}	1.7×10^{-6}
Sackur-Tetrode constant (absolute entropy constant) ^h $\frac{5}{2} + \ln[(2\pi m_u k T_1 / h^2)^{3/2} k T_1 / p_0]$ $T_1 = 1 \text{ K}$, $p_0 = 100 \text{ kPa}$ $T_1 = 1 \text{ K}$, $p_0 = 101.325 \text{ kPa}$	S_0/R	$-1.151\,7048(44)$ $-1.164\,8678(44)$		3.8×10^{-6} 3.7×10^{-6}
Stefan-Boltzmann constant ($\pi^2/60$) $k^4/\hbar^3 c^2$	σ	$5.670\,400(40) \times 10^{-8}$	$\text{W m}^{-2} \text{K}^{-4}$	7.0×10^{-6}
first radiation constant $2\pi\hbar c^2$	c_1	$3.741\,771\,07(29) \times 10^{-16}$	W m^2	7.8×10^{-8}
first radiation constant for spectral radiance $2\hbar c^2$	c_{1L}	$1.191\,042\,722(93) \times 10^{-16}$	$\text{W m}^2 \text{sr}^{-1}$	7.8×10^{-8}
second radiation constant $\hbar c/k$	c_2	$1.438\,7752(25) \times 10^{-2}$	m K	1.7×10^{-6}
Wien displacement law constant $b = \lambda_{\text{max}} T = c_2/4.965\,114\,231 \dots$	b	$2.897\,7686(51) \times 10^{-3}$	m K	1.7×10^{-6}

^aSee Table 26 for the conventional value adopted internationally for realizing representations of the volt using the Josephson effect.

^bSee Table 26 for the conventional value adopted internationally for realizing representations of the ohm using the quantum Hall effect.

^cValue recommended by the Particle Data Group (Caso *et al.*, 1998).

^dBased on the ratio of the masses of the W and Z bosons m_W/m_Z recommended by the Particle Data Group (Caso *et al.*, 1998). The value for $\sin^2 \theta_W$ they recommend, which is based on a particular variant of the modified minimal subtraction ($\overline{\text{MS}}$) scheme, is $\sin^2 \theta_W(M_Z) = 0.231\,24(24)$.

^eThe helion, symbol h, is the nucleus of the ^3He atom.

^fThis and all other values involving m_t are based on the value of $m_t c^2$ in MeV recommended by the Particle Data Group (Caso *et al.*, 1998), but with a standard uncertainty of 0.29 MeV rather than the quoted uncertainty of -0.26 MeV , $+0.29 \text{ MeV}$.

^gThe numerical value of F to be used in coulometric chemical measurements is $96\,485.3432(76) [7.9 \times 10^{-8}]$ when the relevant current is measured in terms of representations of the volt and ohm based on the Josephson and quantum Hall effects and the internationally adopted conventional values of the Josephson and von Klitzing constants K_{J-90} and R_{K-90} given in Table 26.

^hThe entropy of an ideal monoatomic gas of relative atomic mass A_r is given by $S = S_0 + \frac{3}{2} R \ln A_r - R \ln(p/p_0) + \frac{5}{2} R \ln(T/K)$.

dedicated in Appendix E, the evaluation of the uncertainty of a quantity calculated from two or more adjusted constants requires their covariances. Appendix F reviews the law of propagation of uncertainty and gives an example of how such evaluations are done. This is the basis for expanding Table 25 to include the relative covariances and correlation coefficients of, for example, the constants e and m_e with each other and with the adjusted constants α and h . Indeed, on this basis, and as noted at the start of the previous section,

the Web version of Table 25 allows one to access the correlation coefficient of any two constants listed in the tables of the previous section.

We now consider the tables of that section, our goal being to indicate how all quantities of interest are related to the 57 adjusted constants. For each entry, unless otherwise indicated, the value of the quantity is derived from the expression given in the column labeled “Quantity” or the column labeled “Symbol,” or both. For example, consider the elec-

TABLE 25. The variances, covariances, and correlation coefficients of the values of a selected group of constants based on the 1998 CODATA adjustment. The numbers in boldface above the main diagonal are 10^{16} times the values of the relative covariances; the numbers in boldface on the main diagonal are 10^{16} times the values of the relative variances; and the numbers in italics below the main diagonal are the correlation coefficients.^a

	α	h	e	m_e	N_A	m_e/m_μ	F
α	0.135	0.005	0.070	−0.265	0.264	−0.259	0.334
h	<i>0.002</i>	61.129	30.567	61.119	−61.119	−0.009	−30.552
e	<i>0.049</i>	<i>0.999</i>	15.318	30.427	−30.428	−0.134	−15.109
m_e	<i>−0.092</i>	<i>0.996</i>	<i>0.990</i>	61.648	−61.647	0.509	−31.220
N_A	<i>0.092</i>	<i>−0.995</i>	<i>−0.990</i>	<i>−1.000</i>	61.691	−0.508	31.263
m_e/m_μ	<i>−0.233</i>	<i>0.000</i>	<i>−0.011</i>	<i>0.021</i>	<i>−0.021</i>	9.189	−0.642
F	<i>0.226</i>	<i>−0.972</i>	<i>−0.960</i>	<i>−0.989</i>	<i>0.990</i>	<i>−0.053</i>	16.154

^aThe relative covariance $u_r(x_i, x_j)$ is defined according to $u_r(x_i, x_j) = u(x_i, x_j)/(x_i x_j)$, where $u(x_i, x_j)$ is the covariance of x_i and x_j ; the relative variance $u_r^2(x_i)$ is defined according to $u_r^2(x_i) = u^2(x_i)/x_i^2 = u_r(x_i, x_i) = u(x_i, x_i)/x_i^2$, where $u^2(x_i)$ is the variance of x_i ; and the correlation coefficient is defined according to $r(x_i, x_j) = u(x_i, x_j)/[u(x_i)u(x_j)] = u_r(x_i, x_j)/[u_r(x_i)u_r(x_j)]$.

TABLE 26. Internationally adopted values of various quantities.

Quantity	Symbol	Numerical value	Unit	Relative std. uncert. u_r
molar mass of ^{12}C	$M(^{12}\text{C})$	12×10^{-3}	kg mol^{-1}	(exact)
molar mass constant ^a $M(^{12}\text{C})/12$	M_u	1×10^{-3}	kg mol^{-1}	(exact)
conventional value of Josephson constant ^b	$K_{\text{J-90}}$	483 597.9	GHz V^{-1}	(exact)
conventional value of von Klitzing constant ^c	$R_{\text{K-90}}$	25 812.807	Ω	(exact)
standard atmosphere		101 325	Pa	(exact)
standard acceleration of gravity	g_n	9.806 65	m s^{-2}	(exact)

^aThe relative atomic mass $A_r(X)$ of particle X with mass $m(X)$ is defined by $A_r(X) = m(X)/m_u$, where $m_u = m(^{12}\text{C})/12 = M_u/N_A = 1 \text{ u}$ is the atomic mass constant, N_A is the Avogadro constant, and u is the (unified) atomic mass unit. Thus the mass of particle X is $m(X) = A_r(X) \text{ u}$ and the molar mass of X is $M(X) = A_r(X)M_u$.

^bThis is the value adopted internationally for realizing representations of the volt using the Josephson effect.

^cThis is the value adopted internationally for realizing representations of the ohm using the quantum Hall effect.

tron mass m_e and the quantum of circulation $h/2m_e$. The electron mass is derived from the adjusted constants via

$$m_e = \frac{2R_\infty h}{c\alpha^2}, \quad (357)$$

and it is understood that the quantum of circulation is derived from the adjusted constants by replacing m_e in h/m_e with this expression. The result is

$$\frac{h}{2m_e} = \frac{c\alpha^2}{4R_\infty}. \quad (358)$$

We begin our discussion with Table 24, since all quantities in Table 23 are contained in subsequent tables.

UNIVERSAL: The value of G is that adopted in Sec. 3.17.

The numerical value of h when h is expressed in the unit eV is $[h/(\text{J s})]/[e/C]$, where the elementary charge e is derived from the expression

$$e = \left(\frac{2\alpha h}{\mu_0 c} \right)^{1/2}. \quad (359)$$

All energies expressed in joules are reexpressed in electron volts by dividing by e/C .

ELECTROMAGNETIC: The elementary charge e and electron mass m_e are obtained as already indicated.

The Boltzmann constant k is derived from the molar gas constant R , which is an adjusted constant, and the Avogadro constant N_A :

$$k = \frac{R}{N_A}, \quad N_A = \frac{A_r(e)M_u}{m_e}, \quad (360)$$

where $A_r(e)$ is an adjusted constant and $M_u = 10^{-3} \text{ kg/mol}$ is the molar mass constant.

The Bohr magneton μ_B is obtained from the expression given in the table, namely,

$$\mu_B = \frac{e\hbar}{2m_e} = \left(\frac{c\alpha^5 h}{32\pi^2 \mu_0 R_\infty^2} \right)^{1/2}, \quad (361)$$

and the nuclear magneton μ_N follows from

TABLE 27. Values of some x-ray-related quantities based on the 1998 CODATA adjustment of the values of the constants.

Quantity	Symbol	Numerical value	Unit	Relative std. uncert. u_r
Cu x unit: $\lambda(\text{Cu K}\alpha_1)/1537.400$	$xu(\text{Cu K}\alpha_1)$	$1.002\,077\,03(28) \times 10^{-13}$	m	2.8×10^{-7}
Mo x unit: $\lambda(\text{Mo K}\alpha_1)/707.831$	$xu(\text{Mo K}\alpha_1)$	$1.002\,099\,59(53) \times 10^{-13}$	m	5.3×10^{-7}
ångstrom star: $\lambda(\text{W K}\alpha_1)/0.209\,010\,0$	\AA^*	$1.000\,015\,01(90) \times 10^{-10}$	m	9.0×10^{-7}
lattice parameter ^a of Si (in vacuum, 22.5 °C)	a	$543.102\,088(16) \times 10^{-12}$	m	2.9×10^{-8}
{220} lattice spacing of Si $a/\sqrt{8}$ (in vacuum, 22.5 °C)	d_{220}	$192.015\,5845(56) \times 10^{-12}$	m	2.9×10^{-8}
molar volume of Si $M(\text{Si})/\rho(\text{Si}) = N_A a^3/8$ (in vacuum, 22.5 °C)	$V_m(\text{Si})$	$12.058\,8369(14) \times 10^{-6}$	$\text{m}^3 \text{ mol}^{-1}$	1.2×10^{-7}

^aThis is the lattice parameter (unit cell edge length) of an ideal single crystal of naturally occurring Si free of impurities and imperfections, and is deduced from measurements on extremely pure and nearly perfect single crystals of Si by correcting for the effects of impurities.

TABLE 28. The values in SI units of some non-SI units based on the 1998 CODATA adjustment of the values of the constants.

Quantity	Symbol	Numerical value	Unit	Relative std. uncert. u_r
Non-SI units accepted for use with the SI				
electron volt: (e/C) J	eV	$1.602\,176\,462(63) \times 10^{-19}$	J	3.9×10^{-8}
(unified) atomic mass unit: $1\,u = m_u = \frac{1}{12} m(^{12}\text{C})$ $= 10^{-3}\,\text{kg mol}^{-1}/N_A$	u	$1.660\,538\,73(13) \times 10^{-27}$	kg	7.9×10^{-8}
Natural units (n.u.)				
n.u. of velocity: speed of light in vacuum	c, c_0	299 792 458	m s^{-1}	(exact)
n.u. of action: reduced Planck constant $(\hbar/2\pi)$	\hbar	$1.054\,571\,596(82) \times 10^{-34}$	J s	7.8×10^{-8}
in eV s		$6.582\,118\,89(26) \times 10^{-16}$	eV s	3.9×10^{-8}
n.u. of mass: electron mass	m_e	$9.109\,381\,88(72) \times 10^{-31}$	kg	7.9×10^{-8}
n.u. of energy in MeV	$m_e c^2$	$8.187\,104\,14(64) \times 10^{-14}$	J	7.9×10^{-8}
		0.510 998 902(21)	MeV	4.0×10^{-8}
n.u. of momentum in MeV/c	$m_e c$	$2.730\,923\,98(21) \times 10^{-22}$	kg m s^{-1}	7.9×10^{-8}
		0.510 998 902(21)	MeV/c	4.0×10^{-8}
n.u. of length $(\hbar/m_e c)$	λ_C	$386.159\,2642(28) \times 10^{-15}$	m	7.3×10^{-9}
n.u. of time	$\hbar/m_e c^2$	$1.288\,088\,6555(95) \times 10^{-21}$	s	7.3×10^{-9}
Atomic units (a.u.)				
a.u. of charge: elementary charge	e	$1.602\,176\,462(63) \times 10^{-19}$	C	3.9×10^{-8}
a.u. of mass: electron mass	m_e	$9.109\,381\,88(72) \times 10^{-31}$	kg	7.9×10^{-8}
a.u. of action: reduced Planck constant $(\hbar/2\pi)$	\hbar	$1.054\,571\,596(82) \times 10^{-34}$	J s	7.8×10^{-8}
a.u. of length: Bohr radius (bohr) $(\alpha/4\pi R_\infty)$	a_0	$0.529\,177\,2083(19) \times 10^{-10}$	m	3.7×10^{-9}
a.u. of energy: Hartree energy (hartree) $(e^2/4\pi\epsilon_0 a_0 = 2R_\infty \hbar c = \alpha^2 m_e c^2)$	E_h	$4.359\,743\,81(34) \times 10^{-18}$	J	7.8×10^{-8}
a.u. of time	\hbar/E_h	$2.418\,884\,326\,500(18) \times 10^{-17}$	s	7.6×10^{-12}
a.u. of force	E_h/a_0	$8.238\,721\,81(64) \times 10^{-8}$	N	7.8×10^{-8}
a.u. of velocity (αc)	$a_0 E_h/\hbar$	$2.187\,691\,2529(80) \times 10^6$	m s^{-1}	3.7×10^{-9}
a.u. of momentum	\hbar/a_0	$1.992\,851\,51(16) \times 10^{-24}$	kg m s^{-1}	7.8×10^{-8}
a.u. of current	$e E_h/\hbar$	$6.623\,617\,53(26) \times 10^{-3}$	A	3.9×10^{-8}
a.u. of charge density	e/a_0^3	$1.081\,202\,285(43) \times 10^{12}$	C m^{-3}	4.0×10^{-8}
a.u. of electric potential	E_h/e	27.211 3834(11)	V	3.9×10^{-8}
a.u. of electric field	E_h/ea_0	$5.142\,206\,24(20) \times 10^{11}$	V m^{-1}	3.9×10^{-8}
a.u. of electric field gradient	E_h/ea_0^2	$9.717\,361\,53(39) \times 10^{21}$	V m^{-2}	4.0×10^{-8}
a.u. of electric dipole moment	ea_0	$8.478\,352\,67(33) \times 10^{-30}$	C m	3.9×10^{-8}
a.u. of electric quadrupole moment	ea_0^2	$4.486\,551\,00(18) \times 10^{-40}$	C m^2	4.0×10^{-8}
a.u. of electric polarizability	$e^2 a_0^2/E_h$	$1.648\,777\,251(18) \times 10^{-41}$	$\text{C}^2 \text{m}^2 \text{J}^{-1}$	1.1×10^{-8}
a.u. of 1 st hyperpolarizability	$e^3 a_0^3/E_h^2$	$3.206\,361\,57(14) \times 10^{-53}$	$\text{C}^3 \text{m}^3 \text{J}^{-2}$	4.2×10^{-8}
a.u. of 2 nd hyperpolarizability	$e^4 a_0^4/E_h^3$	$6.235\,381\,12(51) \times 10^{-65}$	$\text{C}^4 \text{m}^4 \text{J}^{-3}$	8.1×10^{-8}
a.u. of magnetic flux density	\hbar/ea_0^2	$2.350\,517\,349(94) \times 10^5$	T	4.0×10^{-8}
a.u. of magnetic dipole moment $(2\mu_B)$	$\hbar e/m_e$	$1.854\,801\,799(75) \times 10^{-23}$	J T^{-1}	4.0×10^{-8}
a.u. of magnetizability	$e^2 a_0^2/m_e$	$7.891\,036\,41(14) \times 10^{-29}$	J T^{-2}	1.8×10^{-8}
a.u. of permittivity $(10^7/c^2)$	$e^2/a_0 E_h$	$1.112\,650\,056 \dots \times 10^{-10}$	F m^{-1}	(exact)

TABLE 29. Values of some energy equivalents derived from the relations $E=mc^2=hc/\lambda=h\nu=kT$, and based on the 1998 CODATA adjustment of the values of the constants; $1\text{ eV}=(e/C)\text{ J}$, $1\text{ u}=m_{\text{u}}=\frac{1}{12}m(^{12}\text{C})=10^{-3}\text{ kg mol}^{-1}/N_{\text{A}}$, and $E_{\text{h}}=2R_{\infty}hc=\alpha^2m_{\text{e}}c^2$ is the Hartree energy (hartree).

Relevant unit				
	J	kg	m^{-1}	Hz
1 J	(1 J)= 1 J	(1 J)/ c^2 = $1.112\,650\,056\times10^{-17}\text{ kg}$	(1 J)/ hc = $5.034\,117\,62(39)\times10^{24}\text{ m}^{-1}$	(1 J)/ h = $1.509\,190\,50(12)\times10^{33}\text{ Hz}$
1 kg	(1 kg) c^2 = $8.987\,551\,787\times10^{16}\text{ J}$	(1 kg)= 1 kg	(1 kg) c/h = $4.524\,439\,29(35)\times10^{41}\text{ m}^{-1}$	(1 kg) c^2/h = $1.356\,392\,77(11)\times10^{50}\text{ Hz}$
1 m^{-1}	(1 m^{-1}) hc = $1.986\,445\,44(16)\times10^{-25}\text{ J}$	(1 m^{-1}) h/c = $2.210\,218\,63(17)\times10^{-42}\text{ kg}$	(1 m^{-1})= 1 m^{-1}	(1 m^{-1}) c = $299\,792\,458\text{ Hz}$
1 Hz	(1 Hz) h = $6.626\,068\,76(52)\times10^{-34}\text{ J}$	(1 Hz) h/c^2 = $7.372\,495\,78(58)\times10^{-51}\text{ kg}$	(1 Hz)/ c = $3.335\,640\,952\times10^{-9}\text{ m}^{-1}$	(1 Hz)= 1 Hz
1 K	(1 K) k = $1.380\,6503(24)\times10^{-23}\text{ J}$	(1 K) k/c^2 = $1.536\,1807(27)\times10^{-40}\text{ kg}$	(1 K) k/hc = $69.503\,56(12)\text{ m}^{-1}$	(1 K) k/h = $2.083\,6644(36)\times10^{10}\text{ Hz}$
1 eV	(1 eV)= $1.602\,176\,462(63)\times10^{-19}\text{ J}$	(1 eV)/ c^2 = $1.782\,661\,731(70)\times10^{-36}\text{ kg}$	(1 eV)/ hc = $8.065\,544\,77(32)\times10^5\text{ m}^{-1}$	(1 eV)/ h = $2.417\,989\,491(95)\times10^{14}\text{ Hz}$
1 u	(1 u) c^2 = $1.492\,417\,78(12)\times10^{-10}\text{ J}$	(1 u)= $1.660\,538\,73(13)\times10^{-27}\text{ kg}$	(1 u) c/h = $7.513\,006\,658(57)\times10^{14}\text{ m}^{-1}$	(1 u) c^2/h = $2.252\,342\,733(17)\times10^{23}\text{ Hz}$
1 E_{h}	(1 E_{h})= $4.359\,743\,81(34)\times10^{-18}\text{ J}$	(1 E_{h}) c^2 = $4.850\,869\,19(38)\times10^{-35}\text{ kg}$	(1 E_{h}) hc = $2.194\,746\,313\,710(17)\times10^7\text{ m}^{-1}$	(1 E_{h}) h = $6.579\,683\,920\,735(50)\times10^{15}\text{ Hz}$

$$\mu_{\text{N}}=\mu_{\text{B}}\frac{A_{\text{r}}(\text{e})}{A_{\text{r}}(\text{p})}, \tag{362}$$

where $A_{\text{r}}(\text{p})$ is an adjusted constant.

ATOMIC AND NUCLEAR: General. The quantities α , R_{∞} , and h are, of course, adjusted constants. The Bohr radius is derived from $a_0=\alpha/4\pi R_{\infty}$ and the Hartree energy from $E_{\text{h}}=2R_{\infty}hc$.

ATOMIC AND NUCLEAR: Electroweak. The Fermi coupling constant $G_{\text{F}}/(\hbar c)^3$ and $\sin^2\theta_{\text{W}}$, where θ_{W} is the weak mixing angle, are as stated in Sec. 3.19.

ATOMIC AND NUCLEAR: Electron, e^- . The electron mass is obtained as indicated above, and the numerical value of m_{e} in u is $A_{\text{r}}(\text{e})$.

The electron–muon mass ratio m_{e}/m_{μ} is an adjusted constant, and the electron–tau mass ratio m_{e}/m_{τ} is obtained

TABLE 30. Values of some energy equivalents derived from the relations $E=mc^2=hc/\lambda=h\nu=kT$, and based on the 1998 CODATA adjustment of the values of the constants; $1\text{ eV}=(e/C)\text{ J}$, $1\text{ u}=m_{\text{u}}=\frac{1}{12}m(^{12}\text{C})=10^{-3}\text{ kg mol}^{-1}/N_{\text{A}}$, and $E_{\text{h}}=2R_{\infty}hc=\alpha^2m_{\text{e}}c^2$ is the Hartree energy (hartree).

Relevant unit				
	K	eV	u	E_{h}
1 J	(1 J)/ k = $7.242\,964(13)\times10^{22}\text{ K}$	(1 J)= $6.241\,509\,74(24)\times10^{18}\text{ eV}$	(1 J)/ c^2 = $6.700\,536\,62(53)\times10^9\text{ u}$	(1 J)= $2.293\,712\,76(18)\times10^{17}\text{ E}_{\text{h}}$
1 kg	(1 kg) c^2/k = $6.509\,651(11)\times10^{39}\text{ K}$	(1 kg) c^2 = $5.609\,589\,21(22)\times10^{35}\text{ eV}$	(1 kg)= $6.022\,141\,99(47)\times10^{26}\text{ u}$	(1 kg) c^2 = $2.061\,486\,22(16)\times10^{34}\text{ E}_{\text{h}}$
1 m^{-1}	(1 m^{-1}) hc/k = $1.438\,7752(25)\times10^{-2}\text{ K}$	(1 m^{-1}) hc = $1.239\,841\,857(49)\times10^{-6}\text{ eV}$	(1 m^{-1}) h/c = $1.331\,025\,042(10)\times10^{-15}\text{ u}$	(1 m^{-1}) hc = $4.556\,335\,252\,750(35)\times10^{-8}\text{ E}_{\text{h}}$
1 Hz	(1 Hz) h/k = $4.799\,2374(84)\times10^{-11}\text{ K}$	(1 Hz) h = $4.135\,667\,27(16)\times10^{-15}\text{ eV}$	(1 Hz) h/c^2 = $4.439\,821\,637(34)\times10^{-24}\text{ u}$	(1 Hz) h = $1.519\,829\,846\,003(12)\times10^{-16}\text{ E}_{\text{h}}$
1 K	(1 K)= 1 K	(1 K) k = $8.617\,342(15)\times10^{-5}\text{ eV}$	(1 K) k/c^2 = $9.251\,098(16)\times10^{-14}\text{ u}$	(1 K) k = $3.166\,8153(55)\times10^{-6}\text{ E}_{\text{h}}$
1 eV	(1 eV)/ k = $1.160\,4506(20)\times10^4\text{ K}$	(1 eV)= 1 eV	(1 eV)/ c^2 = $1.073\,544\,206(43)\times10^{-9}\text{ u}$	(1 eV)= $3.674\,932\,60(14)\times10^{-2}\text{ E}_{\text{h}}$
1 u	(1 u) c^2/k = $1.080\,9528(19)\times10^{13}\text{ K}$	(1 u) c^2 = $931.494\,013(37)\times10^6\text{ eV}$	(1 u)= 1 u	(1 u) c^2 = $3.423\,177\,709(26)\times10^7\text{ E}_{\text{h}}$
1 E_{h}	(1 E_{h}) k = $3.157\,7465(55)\times10^5\text{ K}$	(1 E_{h})= $27.211\,3834(11)\text{ eV}$	(1 E_{h}) c^2 = $2.921\,262\,304(22)\times10^{-8}\text{ u}$	(1 E_{h})= 1 E_{h}

from the ratio of $m_e c^2$ expressed in MeV to $m_\tau c^2$ expressed in MeV, where the latter is as stated in Sec. 3.19.

The mass ratios m_e/m_p , m_e/m_n , m_e/m_d , and m_e/m_α are given by $A_r(e)/A_r(p)$, $A_r(e)/A_r(n)$, $A_r(e)/A_r(d)$, and $A_r(e)/A_r(\alpha)$, respectively, where all of these relative atomic masses are adjusted constants. The electron molar mass follows from $M(e) = A_r(e)M_u$.

The electron magnetic moment μ_{e^-} is derived from

$$\mu_{e^-} = \left(\frac{\mu_{e^-}}{\mu_B} \right) \mu_B, \quad (363)$$

where the electron magnetic moment to Bohr magneton ratio follows from

$$\frac{\mu_{e^-}}{\mu_B} = \frac{g_{e^-}}{2} = -(1 + a_e), \quad (364)$$

and g_{e^-} is the electron g -factor. The electron magnetic moment anomaly a_e , in turn, is derived from the theoretical expression for a_e evaluated with the adjusted constants α and δ_e . The latter is

$$\delta_e = 0.1(1.1) \times 10^{-12}. \quad (365)$$

The electron magnetic moment to nuclear magneton ratio follows from

$$\frac{\mu_{e^-}}{\mu_N} = \frac{\mu_{e^-}}{\mu_B} \frac{A_r(p)}{A_r(e)}. \quad (366)$$

The adjusted constants μ_{e^-}/μ_p , μ_{e^-}/μ'_p , μ_n/μ'_p , μ'_h/μ'_p , and m_e/m_μ are the basis of the various magnetic moment ratios under Electron, e^- . We first note that

$$\frac{\mu_{\mu^-}}{\mu_p} = \frac{m_e}{m_\mu} \frac{\mu_{e^-}}{\mu_p} \frac{g_{\mu^-}}{g_{e^-}}, \quad (367)$$

where $g_{\mu^-} = -2(1 + a_\mu)$ and the muon magnetic moment anomaly a_μ is derived from the theoretical expression for a_μ , evaluated with the adjusted constants α and δ_μ . The latter is

$$\delta_\mu = 0.0(6.4) \times 10^{-10}. \quad (368)$$

(By taking the theoretical value to be the recommended value, we implicitly assume that contributions to a_μ beyond the standard model are negligible.) We then have

$$\begin{aligned} \frac{\mu_{e^-}}{\mu_{\mu^-}} &= \frac{\mu_{e^-}}{\mu_p} \left(\frac{\mu_{\mu^-}}{\mu_p} \right)^{-1} \\ \frac{\mu_{e^-}}{\mu_n} &= \frac{\mu_{e^-}}{\mu'_p} \left(\frac{\mu_n}{\mu'_p} \right)^{-1} \\ \frac{\mu_{e^-}}{\mu'_h} &= \frac{\mu_{e^-}}{\mu'_p} \left(\frac{\mu'_h}{\mu'_p} \right)^{-1}. \end{aligned} \quad (369)$$

ATOMIC AND NUCLEAR: Muon, μ^- . The muon mass is obtained from

$$m_\mu = m_e \left(\frac{m_e}{m_\mu} \right)^{-1}. \quad (370)$$

Its numerical value in u is $A_r(e)/(m_e/m_\mu)$, and the muon molar mass is given by $M(\mu) = A_r(e)M_u/(m_e/m_\mu)$. The mass ratio m_μ/m_τ is derived in the same way as m_e/m_τ (see Electron, e^-). The muon–proton mass ratio follows from

$$\frac{m_\mu}{m_p} = \frac{A_r(e)}{A_r(p)} \left(\frac{m_e}{m_\mu} \right)^{-1}, \quad (371)$$

and the muon–neutron mass ratio follows from the same expression but with p replaced by n .

The quantities a_μ , g_{μ^-} , and μ_{μ^-}/μ_p are discussed above in Electron, e^- . The other quantities involving the muon magnetic moment are derived from

$$\begin{aligned} \mu_{\mu^-} &= \left(\frac{\mu_{\mu^-}}{\mu_p} \right) \mu_p, \\ \frac{\mu_{\mu^-}}{\mu_B} &= \frac{\mu_{\mu^-}}{\mu_p} \frac{\mu_p}{\mu_B}, \\ \frac{\mu_{\mu^-}}{\mu_N} &= \frac{\mu_{\mu^-}}{\mu_B} \frac{A_r(p)}{A_r(e)}, \end{aligned} \quad (372)$$

where the quantities μ_p and μ_p/μ_B are discussed in Proton, p .

ATOMIC AND NUCLEAR: Tau, τ^- . The mass of the positive tau in kg is obtained by multiplying its value in MeV by $10^6(e/C)/c^2$. Its numerical value in u is $A_r(e)(m_\tau/m_e)$, where the electron–tau mass ratio m_e/m_τ is discussed in Electron, e^- . The other mass ratios follow from $m_\tau/m_\mu = (m_\tau/m_e)(m_e/m_\mu)$, $m_\tau/m_p = (m_\tau/m_e)[A_r(e)/A_r(p)]$, and $m_\tau/m_n = (m_\tau/m_e)[A_r(e)/A_r(n)]$. The molar mass of the tau is given by $M(\tau) = A_r(e)M_u(m_\tau/m_e)$.

ATOMIC AND NUCLEAR: Proton, p . The proton mass is derived from

$$m_p = m_e \frac{A_r(p)}{A_r(e)}, \quad (373)$$

and the numerical value of m_p in u is $A_r(p)$, $m_p/m_e = A_r(p)/A_r(e)$, $m_p/m_\mu = (m_p/m_e)(m_e/m_\mu)$, $m_p/m_\tau = (m_e/m_\tau)[A_r(p)/A_r(e)]$, $m_p/m_n = A_r(p)/A_r(n)$, and $M(p) = A_r(p)M_u$.

The adjusted constants μ_{e^-}/μ_p , μ_{e^-}/μ'_p , and μ_n/μ'_p are the basis of the quantities involving μ_p or μ'_p . One has

$$\begin{aligned} \mu_p &= \frac{\mu_p}{\mu_B} \mu_B \\ \frac{\mu_p}{\mu_B} &= \frac{\mu_{e^-}}{\mu_B} \left(\frac{\mu_{e^-}}{\mu_p} \right)^{-1} \\ \frac{\mu_p}{\mu_N} &= \frac{\mu_p}{\mu_B} \frac{A_r(p)}{A_r(e)} \\ \frac{\mu_p}{\mu_n} &= \frac{\mu_{e^-}}{\mu'_p} \left(\frac{\mu_{e^-}}{\mu_p} \right)^{-1} \left(\frac{\mu_n}{\mu'_p} \right)^{-1}. \end{aligned} \quad (374)$$

The quantities μ'_p , μ'_p/μ_B , and μ'_p/μ_N also follow from the first three of these expressions but with μ_p replaced everywhere by μ'_p .

The proton magnetic shielding correction is derived from

$$\sigma'_p = 1 - \left(\frac{\mu_{e^-}}{\mu_p} \right) \left(\frac{\mu_{e^-}}{\mu'_p} \right)^{-1}. \quad (375)$$

ATOMIC AND NUCLEAR: Neutron, n. The neutron mass follows from

$$m_n = m_e \frac{A_r(n)}{A_r(e)}, \quad (376)$$

and the numerical value of m_n in u is $A_r(n)$, $m_n/m_e = A_r(n)/A_r(e)$, $m_n/m_\mu = (m_n/m_e)(m_e/m_\mu)$, $m_n/m_\tau = (m_e/m_\tau)[A_r(n)/A_r(e)]$, $m_n/m_p = A_r(n)/A_r(p)$, and $M(n) = A_r(n)M_u$.

The basis of all quantities involving μ_n is the adjusted constant μ_n/μ'_p . We have

$$\begin{aligned} \mu_n &= \left(\frac{\mu_n}{\mu'_p} \right) \mu'_p \\ \frac{\mu_n}{\mu_B} &= \frac{\mu_n}{\mu'_p} \frac{\mu'_p}{\mu_B} \\ \frac{\mu_n}{\mu_N} &= \frac{\mu_n}{\mu_B} \frac{A_r(p)}{A_r(e)} \\ \frac{\mu_n}{\mu_{e^-}} &= \frac{\mu_n}{\mu'_p} \left(\frac{\mu_{e^-}}{\mu'_p} \right)^{-1} \\ \frac{\mu_n}{\mu_p} &= \frac{\mu_n}{\mu_{e^-}} \frac{\mu_{e^-}}{\mu_p}. \end{aligned} \quad (377)$$

ATOMIC AND NUCLEAR: Deuteron, d. The deuteron mass is derived from

$$m_d = m_e \frac{A_r(d)}{A_r(e)}, \quad (378)$$

and the numerical value of m_d in u is $A_r(d)$, $m_d/m_e = A_r(d)/A_r(e)$, $m_d/m_p = A_r(d)/A_r(p)$, and $M(d) = A_r(d)M_u$.

The basis of all quantities involving μ_d is the adjusted constant μ_d/μ_{e^-} . One has

$$\begin{aligned} \mu_d &= \left(\frac{\mu_d}{\mu_{e^-}} \right) \mu_{e^-} \\ \frac{\mu_d}{\mu_B} &= \frac{\mu_d}{\mu_{e^-}} \frac{\mu_{e^-}}{\mu_B} \\ \frac{\mu_d}{\mu_N} &= \frac{\mu_d}{\mu_B} \frac{A_r(p)}{A_r(e)} \\ \frac{\mu_d}{\mu_p} &= \frac{\mu_d}{\mu_{e^-}} \frac{\mu_{e^-}}{\mu_p} \\ \frac{\mu_d}{\mu_n} &= \frac{\mu_d}{\mu_{e^-}} \frac{\mu_{e^-}}{\mu'_p} \left(\frac{\mu_n}{\mu'_p} \right)^{-1}. \end{aligned} \quad (379)$$

ATOMIC AND NUCLEAR: Helion, h. The helion mass follows from

$$m_h = m_e \frac{A_r(h)}{A_r(e)}, \quad (380)$$

and the numerical value of m_h in u is $A_r(h)$, $m_h/m_e = A_r(h)/A_r(e)$, $m_h/m_p = A_r(h)/A_r(p)$, and $M(h) = A_r(h)M_u$.

The basis of all quantities involving μ'_h is the adjusted constant μ'_h/μ'_p . We have

$$\begin{aligned} \mu'_h &= \left(\frac{\mu'_h}{\mu'_p} \right) \mu'_p \\ \frac{\mu'_h}{\mu_B} &= \frac{\mu'_h}{\mu'_p} \frac{\mu'_p}{\mu_B} \\ \frac{\mu'_h}{\mu_N} &= \frac{\mu'_h}{\mu'_p} \frac{\mu'_p}{\mu_N} \\ \frac{\mu'_h}{\mu_p} &= \frac{\mu'_h}{\mu'_p} \frac{\mu'_p}{\mu_p} \left(\frac{\mu_{e^-}}{\mu'_p} \right)^{-1}. \end{aligned} \quad (381)$$

ATOMIC AND NUCLEAR: Alpha particle, α . As in previous similar cases, the alpha particle mass is derived from

$$m_\alpha = m_e \frac{A_r(\alpha)}{A_r(e)}, \quad (382)$$

and the numerical value of m_α in u is $A_r(\alpha)$, $m_\alpha/m_e = A_r(\alpha)/A_r(e)$, $m_\alpha/m_p = A_r(\alpha)/A_r(p)$, and $M(\alpha) = A_r(\alpha)M_u$.

PHYSICOCHEMICAL: All of the values follow from the relations given in the Quantity and/or Symbol columns and the expressions for k , N_A , and e given above. The number 4.965 114 231 ... in the equation for the Wien displacement law constant b is the nonzero root of the equation $5(e^{-x} - 1) + x = 0$ (Stone, 1963).

Table 25. This table was discussed at the beginning of this section on calculational details.

Table 26. The first two entries are discussed in Sec. 2.3, the next two in Sec. 2.5, and the last two entries are from the BIPM SI Brochure (BIPM, 1998). [The quantity g_n is also discussed in Sec. 2.6.]

Table 27. The Cu x unit $xu(\text{Cu K}\alpha_1)$, the Mo x unit $xu(\text{Mo K}\alpha_1)$, and the \AA^* are adjusted constants. The quantity d_{220} , which is the $\{220\}$ lattice spacing of an ideal single crystal of naturally occurring silicon in vacuum at $t_{90} = 22.5^\circ\text{C}$, is also an adjusted constant, and the lattice parameter a of silicon (the edge length of the silicon cubic unit cell) is related to d_{220} by $a = \sqrt{8}d_{220}$. The expression for N_A is given under ELECTROMAGNETIC, Eq. (360).

Table 28. The values in this table follow directly from the relations given in the Quantity and/or Symbol columns and the expressions given above for the constants e , N_A , and m_e .

Table 29. The numerical values given in the first four rows are the numerical values of the constants indicated above the values when those constants are expressed in their respective SI units. For example, the number $1.356\,392\,77(11) \times 10^{50}$ (last entry of row 2) is $[c^2/(\text{m s}^{-1})^2]/[h/(\text{J s})]$, which can be conveniently denoted by $\{c^2/h\}_{\text{SI}}$. For the last three rows,

the full combination of constants whose numerical values give the numerical value indicated are, respectively by row, e , e/c^2 , e/hc , and e/h ; $m_e c^2$, m_e , $m_e c/h$, and $m_e c^2/h$; $2R_\infty hc$, $2R_\infty h/c$, $2R_\infty$, and $2R_\infty c$.

Table 30. The situation for this table is similar to that for Table 29 but somewhat more involved. The full combination of constants of the last three rows of the column labeled “K” are e/k , $m_e c^2/k$, and $2R_\infty hc/k$. For the columns labeled “eV,” “u,” and “ E_h ,” the full combination of constants for the seven nontrivial rows of each column are, respectively by column, $1/e$, c^2/e , hc/e , h/e , k/e , $m_e c^2/e$, and $2R_\infty hc/e$; $1/m_e c^2$, $1/m_e$, $h/m_e c$, $h/m_e c^2$, $k/m_e c^2$, $e/m_e c^2$, and $2R_\infty h/m_e c$; $1/2R_\infty hc$, $c/2R_\infty h$, $1/2R_\infty$, $1/2R_\infty c$, $k/2R_\infty hc$, $e/2R_\infty hc$, and $m_e c/2R_\infty h$.

6. Summary and Conclusion

We close by first comparing the 1998 and 1986 CODATA recommended values of the fundamental physical constants and identifying those advances made since 1986 that are most responsible for our current improved knowledge of the constants. This is followed by a brief discussion of some of the conclusions that can be drawn from the 1998 values and adjustment. Finally, we look to the future and make some suggestions regarding the experimental and theoretical work required to solidify and continue the progress of the last 13 years.

6.1. Comparison of 1998 and 1986 CODATA Recommended Values

The 1998 CODATA set of recommended values of the fundamental physical constants is a major step forward relative to its 1986 predecessor. The 1998 and 1986 adjustments considered all data available by 31 December 1998 and 1 January 1986, respectively. As one would hope, the 13 year period between these adjustments has seen extraordinary experimental and theoretical advances in the precision measurement/fundamental constants (PMFC) field. The fact that the standard uncertainties of many of the 1998 recommended values are about $\frac{1}{5}$ to $\frac{1}{12}$, and in the case of R_∞ and some associated constants, $\frac{1}{160}$, times the standard uncertainties of the corresponding 1986 values is an indication of the remarkable nature of these advances. Moreover, the absolute values of the differences between the 1986 values and the corresponding 1998 values are almost all less than twice the standard uncertainties of the 1986 values. The reduction of uncertainties and the relatively small shifts of values is apparent from Table 31, which compares the recommended values of a representative group of constants from the two adjustments. A subset of the constants of this group is compared graphically in Fig. 5.

Table 31 also exhibits regularities that can be attributed to the interdependence of the various constants. This behavior is not influenced by the fact that the adjusted constants (i.e., variables of the adjustment) employed in 1986 and 1998 are different, but it does depend on the fact that for both adjustments $u_r(R) \gg u_r(h) \gg u_r(\alpha) \gg u_r(R_\infty)$. In the context of the

TABLE 31. Comparison of the 1998 and 1986 CODATA adjustments of the values of the constants by the comparison of the corresponding recommended values of a representative group of constants. Here D_r is the 1998 value minus the 1986 value divided by the standard uncertainty u of the 1986 value (i.e., D_r is the change in the value of the constant from 1986 to 1998 relative to its 1986 standard uncertainty).

Quantity	1998 rel. std. uncert. u_r	1986 rel. std. uncert. u_r	Ratio 1986 u_r to 1998 u_r	D_r
α	3.7×10^{-9}	4.5×10^{-8}	12.2	-1.7
R_K	3.7×10^{-9}	4.5×10^{-8}	12.2	1.7
a_0	3.7×10^{-9}	4.5×10^{-8}	12.2	-1.7
λ_C	7.3×10^{-9}	8.9×10^{-8}	12.2	-1.7
r_e	1.1×10^{-8}	1.3×10^{-7}	12.2	-1.7
σ_e	2.2×10^{-8}	2.7×10^{-7}	12.2	-1.7
h	7.8×10^{-8}	6.0×10^{-7}	7.7	-1.7
m_e	7.9×10^{-8}	5.9×10^{-7}	7.5	-1.5
N_A	7.9×10^{-8}	5.9×10^{-7}	7.5	1.5
E_h	7.8×10^{-8}	6.0×10^{-7}	7.7	-1.7
c_1	7.8×10^{-8}	6.0×10^{-7}	7.7	-1.7
e	3.9×10^{-8}	3.0×10^{-7}	7.8	-1.8
K_J	3.9×10^{-8}	3.0×10^{-7}	7.6	1.6
F	4.0×10^{-8}	3.0×10^{-7}	7.5	1.1
γ'_p	4.2×10^{-8}	3.0×10^{-7}	7.3	1.1
μ_B	4.0×10^{-8}	3.4×10^{-7}	8.3	-2.1
μ_N	4.0×10^{-8}	3.4×10^{-7}	8.3	-2.0
μ_e	4.0×10^{-8}	3.4×10^{-7}	8.3	2.1
μ_p	4.1×10^{-8}	3.4×10^{-7}	8.1	-2.1
R	1.7×10^{-6}	8.4×10^{-6}	4.8	-0.5
k	1.7×10^{-6}	8.5×10^{-6}	4.8	-0.6
V_m	1.7×10^{-6}	8.4×10^{-6}	4.8	-0.5
c_2	1.7×10^{-6}	8.4×10^{-6}	4.8	0.5
σ	7.0×10^{-6}	3.4×10^{-5}	4.8	-0.6
G	1.5×10^{-3}	1.3×10^{-4}	0.1	0.0
R_∞	7.6×10^{-12}	1.2×10^{-9}	157.1	2.7
m_e/m_p	2.1×10^{-9}	2.0×10^{-8}	9.5	0.9
m_e/m_μ	3.0×10^{-8}	1.5×10^{-7}	4.9	-0.1
$A_r(e)$	2.1×10^{-9}	2.3×10^{-8}	11.1	0.7
$A_r(p)$	1.3×10^{-10}	1.2×10^{-8}	91.6	-0.2
$A_r(n)$	5.4×10^{-10}	1.4×10^{-8}	25.6	0.8
$A_r(d)$	1.7×10^{-10}	1.2×10^{-8}	68.9	0.0
d_{220}	2.9×10^{-8}	2.1×10^{-7}	7.1	1.1
g_e	4.1×10^{-12}	1.0×10^{-11}	2.4	0.6
g_μ	6.4×10^{-10}	8.4×10^{-9}	13.1	0.8
μ_p/μ_B	1.0×10^{-8}	1.0×10^{-8}	1.0	0.1
μ_p/μ_N	1.0×10^{-8}	2.2×10^{-8}	2.2	-0.8
μ_n/μ_N	2.4×10^{-7}	2.4×10^{-7}	1.0	0.1
μ_d/μ_N	1.1×10^{-8}	2.8×10^{-8}	2.6	-0.1
μ_e/μ_p	1.0×10^{-8}	1.0×10^{-8}	1.0	0.1
μ_n/μ_p	2.4×10^{-7}	2.4×10^{-7}	1.0	0.0
μ_d/μ_p	1.5×10^{-8}	1.7×10^{-8}	1.1	0.9

1998 adjustment, much of this behavior can be understood by examining the functional dependence of the derived constants on the adjusted constants R_∞ , α , h , and R . This dependence is such that the uncertainties of the derived constants are mainly determined by the uncertainty of either α , h , or R .

For example, α and the Bohr radius a_0 have the same relative standard uncertainty, and that of the Compton wavelength is twice as large: $u_r(\lambda_C) = 2u_r(a_0) = 2u_r(\alpha)$. This is because the value of a_0 is calculated from the relation $a_0 = \alpha/4\pi R_\infty$ and since $u_r(\alpha) \gg u_r(R_\infty)$, $u_r(a_0)$ is essentially

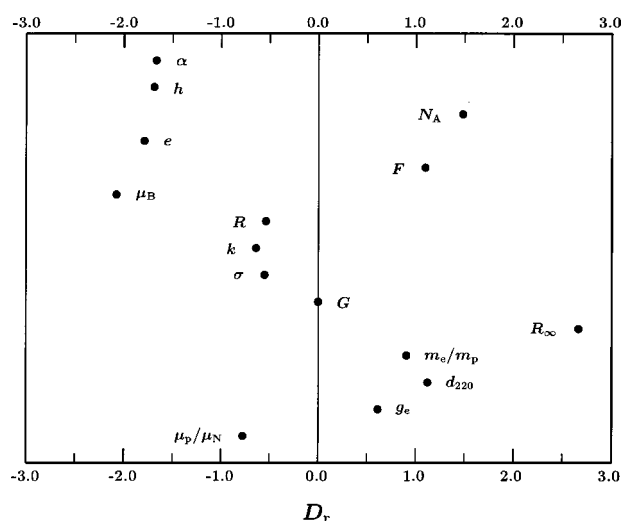


FIG. 5. Graphical comparison of the 1998 and 1986 CODATA recommended values of some of the constants listed in Table 31. As in that table, D_r is the 1998 value minus the 1986 value divided by the standard uncertainty u of the 1986 value (i.e., D_r is the change in the value of the constant from 1986 to 1998 relative to its 1986 standard uncertainty).

equal to $u_r(\alpha)$. Similarly, λ_C is obtained from the relation $\lambda_C = \alpha^2 / 2\pi R_\infty$, hence $u_r(\lambda_C) \approx u_r(\alpha^2) = 2u_r(\alpha)$. A further consequence of these relations is the near equality of the ratios of the 1986 uncertainties to the 1998 uncertainties, as well as the near equality of their values of D_r , where D_r is the change in the value of a constant from 1986 to 1998 relative to its 1986 standard uncertainty. The classical electron radius r_e with $u_r(r_e) = 3u_r(\alpha)$ and the Thomson cross section σ_e with $u_r(\sigma_e) = 6u_r(\alpha)$ follow a similar pattern, since r_e is calculated from $r_e = \alpha^2 a_0 = \alpha^3 / 4\pi R_\infty$ and σ_e from $\sigma_e = (8\pi/3)r_e^2 = \alpha^6 / 6\pi R_\infty^2$. (Since the von Klitzing constant is calculated from $R_K = \mu_0 c / 2\alpha$, D_r for α and R_K have opposite signs.)

In an analogous way, the 12 constants m_e through μ_p in column 1 of Table 31 are calculated from expressions that contain a factor h^p , where $p = 1, -1, \frac{1}{2}$, or $-\frac{1}{2}$, as well as other constants (such as α) that have relative standard uncertainties rather smaller than $u_r(h)$. Thus the uncertainties of these 12 constants are approximately $u_r(h)$ or $\frac{1}{2}u_r(h)$. Also, the values of the ratios of the 1986 to 1998 uncertainties for h and these constants are the same to within about 15%. On the other hand, their values of $|D_r|$ vary more widely, because of changes in the values of the other constants on which they depend. [It is mere coincidence that the value of $|D_r|$ for those constants whose uncertainties are mainly determined by $u_r(\alpha)$ is the same as it is for some of those constants whose uncertainties are mainly determined by $u_r(h)$.]

Table 31 exhibits analogous behavior for the constants R , k , V_m , c_2 , and σ ; the values of the last four are calculated from expressions that contain a factor R^p , where $p = 1, -1$, or 4 , as well as other constants that have relative standard uncertainties much smaller than $u_r(R)$.

Unique among all of the 1998 recommended values is the

Newtonian constant of gravitation G ; its uncertainty is larger than that of the 1986 value by nearly a factor of 12. As explained in detail in Sec. 3.17, for several reasons, including the existence of a value of G from a credible experiment that differs significantly from the 1986 value, the CODATA Task Group on Fundamental Constants decided to increase the relative standard uncertainty of the 1986 value from $u_r = 1.28 \times 10^{-4}$ to $u_r = 1.5 \times 10^{-3}$, but to retain the value itself.

The largest relative shift in the value of a constant between 1986 and 1998 is $D_r = 2.7$ for R_∞ . On the other hand, with a 1986 to 1998 uncertainty ratio of 157, the value of R_∞ has undergone the largest reduction in uncertainty. The shift in value is due to the fact that the 1986 recommended value of R_∞ was mainly based on a 1981 experimental result that was subsequently shown to be in error. The large uncertainty reduction is due mainly to the fact that starting at about the beginning of the 1990s, optical frequency metrology replaced optical wavelength metrology as the method of choice for determining transition frequencies of hydrogenic atoms. Major improvements in the theory of the energy levels of such atoms also contributed significantly to the reduction in uncertainty.

Although a more accurate value of R_∞ is partially responsible for our current improved knowledge of the values of the constants, three other post-1986 advances have also played important roles.

(i) A better experimental determination of the anomalous magnetic moment of the electron a_e and an improved theoretical expression for a_e are to a large extent responsible for the 1998 recommended value of α , which has the impressively small uncertainty $u_r = 3.7 \times 10^{-9}$. As pointed out above, α plays a key role in determining the recommended values of many constants.

(ii) The moving-coil watt balance, which was conceived some 25 years ago and was first brought to a useful operational state in the late 1980s, provided two results for $K_J^2 R_K = 4/h$ with comparatively small uncertainties. The 1998 recommended value of h with $u_r = 7.8 \times 10^{-8}$ is mainly due to these results, and, as also discussed above, h plays a major role in determining the recommended values of many constants.

(iii) The determination of R by measuring the speed of sound in argon using a spherical acoustic resonator yielded a value with $u_r = 1.8 \times 10^{-6}$, approximately $\frac{1}{5}$ times the uncertainty $u_r = 8.4 \times 10^{-6}$ of the value obtained earlier using a cylindrical acoustic interferometer and on which the 1986 recommended value is based. The new result is primarily responsible for the 1998 recommended value with $u_r = 1.7 \times 10^{-6}$ and consequently for the improved values of the various constants that depend on R .

Of course, better measurements and calculations of a number of other quantities also contributed to improving our overall knowledge of the values of the constants. Noteworthy are the Penning-trap mass ratio measurements that led to the improved values of the relative atomic masses $A_r(e)$, $A_r(p)$, $A_r(d)$, etc; the crystal diffraction determination of the bind-

ing energy of the neutron in the deuteron that led to the improved value of $A_r(n)$; the Zeeman transition-frequency determination of $\Delta\nu_{\text{Mu}}$ that, together with the QED-based, theoretically calculated expression for $\Delta\nu_{\text{Mu}}$, led to the improved value of m_e/m_μ ; and the new and more accurate measurements of the d_{220} lattice spacing of nearly perfect silicon crystals, together with the measurement of the quotient $h/m_n d_{220}(\text{W04})$ and better methods of comparing the lattice spacings of crystals and characterizing their quality, that led to the improved value of d_{220} of an ideal crystal. By comparison, there has been no improvement in our knowledge of magnetic-moment related constants such as μ_p/μ_B , μ_n/μ_N , μ_e/μ_p , and μ_n/μ_p , because there have been no new relevant measurements. (The reductions in uncertainties of μ_p/μ_N and μ_d/μ_N are mainly due to the reduction in uncertainty of m_e/m_p .)

6.2. Some Implications for Physics and Metrology of the 1998 CODATA Recommended Values and Adjustment

Reliable values of the fundamental physical constants and related energy conversion factors have long been necessary for a variety of practical applications. Prominent among these are calculations required for the analysis and compilation of data and the preparation of databases in various areas of science and technology including high energy, nuclear, atomic and molecular, condensed matter, chemical, and statistical physics. The 1998 recommended values with their significantly smaller uncertainties should, therefore, have a positive influence on a broad range of activities in many fields.

More recently, values of constants have become increasingly important to metrology. As discussed in Sec. 2.5, starting 1 January 1990 the CIPM introduced new, practical representations of the volt and the ohm for international use based on the Josephson and quantum Hall effects and exact conventional values of the Josephson and von Klitzing constants. As noted in that section, the adoption of these exact values, $K_{J-90}=483\,597.9\text{ GHz/V}$ and $R_{K-90}=25\,812.807\,\Omega$, can be interpreted as establishing conventional, practical units of voltage and resistance, V_{90} and Ω_{90} , that are related to the volt V and ohm Ω by

$$V_{90} = \frac{K_{J-90}}{K_J} V \quad (383)$$

$$\Omega_{90} = \frac{R_K}{R_{K-90}} \Omega. \quad (384)$$

These equations and the 1998 recommended values of K_J and R_K lead to

$$V_{90} = [1 + 0.4(3.9) \times 10^{-8}] V \quad (385)$$

$$\Omega_{90} = [1 + 2.21(37) \times 10^{-8}] \Omega, \quad (386)$$

which show that the practical unit of voltage V_{90} exceeds V by the fractional amount $0.4(3.9) \times 10^{-8}$, and the practical

unit of resistance Ω_{90} exceeds Ω by the fractional amount $2.21(37) \times 10^{-8}$. This means that measured voltages traceable to the Josephson effect and K_{J-90} and measured resistances traceable to the quantum Hall effect and R_{K-90} are too small relative to the SI by the same fractional amounts. Although these deviations from the SI, which follow from the 1998 adjustment, are inconsequential for the vast majority of measurements and are well within the original estimates of the CCEM (Taylor and Witt, 1989), corrections to account for them may need to be applied in those rare cases where consistency with the SI is critical.

A possible future use of fundamental constants in metrology is in the redefinition of the kilogram. As the authors have recently pointed out (Taylor and Mohr, 1999), if moving-coil watt-balance determinations of h can achieve a relative standard uncertainty of $u_r = 1 \times 10^{-8}$, then it becomes attractive to redefine the kilogram in such a way that the value of h is fixed, thereby allowing the watt balance to be used to directly calibrate standards of mass. [Such a definition would be analogous to the current definition of the meter, which has the effect of fixing the value of c . A redefinition of the kilogram that fixes the value of N_A has been proposed as well (Taylor, 1991).] It is also conceivable that if the Boltzmann constant k can be determined with a sufficiently small uncertainty, the kelvin could be redefined in such a way as to fix the value of k . Increasing the number of SI units and their practical representations that are based on invariants of nature—the fundamental constants—rather than on a material artifact or a property of a body that depends on the body's composition is highly appealing for both practical and esthetic reasons.

The focus of this paper has been the review of the currently available experimental and theoretical data relevant to the fundamental constants and how those data are used to obtain the 1998 CODATA set of recommended values, rather than what the data can tell us about the basic theories and experimental methods of physics. Although we plan to address this question in greater detail in a future publication, we briefly delineate in the following paragraphs a few of the conclusions that may be drawn from the 1998 adjustment regarding physics and metrology. These specific conclusions can be prefaced with the general conclusion that the 1998 adjustment provides no evidence of problems with either: (1) the basic theories of physics—special relativity, quantum mechanics, QED, the standard model, etc.; or (2) the broad range of metrological techniques used in experiments to determine values of the constants: Penning-trap mass spectrometry, optical frequency metrology, optical interferometry, voltage and resistance measurements based on the Josephson and quantum Hall effects, etc.

Josephson effect. The observed consistency of the values of h deduced from measurements of $K_J^2 R_K$, K_J , $\Gamma'_{p-90}(\text{hi})$, and \mathcal{F}_{90} (see Table 16) supports the important assumption that $K_J = 2e/h$. Further, since these measurements required the use of a wide variety of metrological techniques—from laser interferometry to analytical chemistry—the consistency of the values of h also suggests that the uncertainties associ-

ated with these techniques are understood and have been properly evaluated.

Quantum Hall effect and QED. The values of α inferred from measurements of the diverse group of constants a_e , R_K , $h/m_n d_{220}(\text{W04})$, $\Gamma'_{p-90}(\text{lo})$, $\Gamma'_{h-90}(\text{lo})$, $\Delta\nu_{\text{Mu}}$, and R_∞ , together with measurements of $d_{220}(\text{X})$, μ_{e^-}/μ'_{p^-} , μ'_{h^-}/μ'_{p^-} , and μ_{μ^+}/μ_p , are broadly consistent (see Table 15). This consistency supports the important assumption that $R_K = h/e^2 = \mu_0 c/2\alpha$. It also supports the validity of the QED calculations required to obtain theoretical expressions for a_e , a_μ , $\Delta\nu_{\text{Mu}}$, $g_{e^-}(\text{H})/g_{e^-}$, $g_p(\text{H})/g_p$, $g_{e^-}(\text{D})/g_{e^-}$, $g_d(\text{D})/g_d$, $g_{e^-}(\text{Mu})/g_{e^-}$, and $g_{\mu^+}(\text{Mu})/g_{\mu^+}$.

On the other hand, the various values of α are not as consistent as one would perhaps like; of special concern are those values of α obtained from gyromagnetic ratio measurements and from neutron/x-ray diffraction measurements. Although the causes of the differences between some of these values of α and the other values are not yet known, they may indicate that the measurement methods required to determine the dimensions of a precision solenoid and the lattice spacing of a crystal of silicon are not fully understood.

Hydrogenic energy levels, p and d bound-state rms charge radii, and QED. As pointed out in Sec. 4.3.1, there is a systematic deviation between theory and experiment for hydrogenic energy levels corresponding to $126/n^3$ kHz for $nS_{1/2}$ states. Its most likely causes are a difference between the proton and/or the deuteron rms charge radius predicted by the hydrogenic spectroscopic data from the values derived from scattering data, an uncalculated contribution to hydrogenic energy levels from the two-photon QED correction that exceeds its assigned uncertainty, or a combination of the two.

Nevertheless, the agreement of the value of R_∞ deduced from all of the Rydberg-constant data with the values deduced from subsets of that data (see Table 18) supports the overall validity of the QED-based calculations of hydrogenic energy levels.

Molar volume of silicon. As discussed in Sec. 3.10, values of the molar volume of silicon $V_m(\text{Si})$ are not included as input data in the 1998 adjustment because of discrepancies among them. These discrepancies indicate that our understanding of the FZ (floating zone) crystal-growing process as applied to silicon and the effects of impurities, vacancies, and self-interstitials on the properties of silicon may not yet be complete.

Molar gas constant, speed of sound, and thermometry. The two existing high-accuracy determinations of R , one from measurements of the speed-of-sound in argon using a spherical acoustic resonator and the other from similar measurements using a cylindrical acoustic interferometer, are consistent. This agreement indicates that the complex nature of the propagation of sound in such devices is satisfactorily understood and that the determination of thermodynamic temperatures from speed-of-sound measurements should be reliable.

Newtonian constant of gravitation. The current value of G

has the largest relative standard uncertainty by far of any of the basic constants of physics given in the 1998 CODATA set of recommended values, with the exception of $\sin^2 \theta_W$. It has long been recognized that the reason this measure of the strength of the most pervasive force in the universe is so poorly known is the weakness of the gravitational force compared to the weak, electromagnetic (electroweak), and strong forces. Nevertheless, because of gravity's central role in physics, the large uncertainty of G is disconcerting. One hopes that work currently underway (see the following section) will solve the problem.

6.3. Outlook and Suggestions for Future Work

It is difficult to imagine how the rate of progress of the past 13 years in improving our knowledge of the values of the constants can be sustained. The relative standard uncertainties of some constants are now in the range $4 \times 10^{-12} < u_r < 6 \times 10^{-10}$, and the uncertainties of most others are in the range $1 \times 10^{-9} < u_r < 1 \times 10^{-7}$. One wonders if experimentalists can continue to devise ever more ingenious methods of overcoming the limitations of electrical and mechanical noise and if theorists can continue to devise ever more sophisticated techniques of calculating contributions from an expanding number of complex Feynman diagrams so that our knowledge of the constants can continue to advance at the current pace. Although it is obvious that this question cannot be answered unequivocally, the impressive level of achievements of researchers in the PMFC field over the past century is a sound reason to be optimistic about the future. Indeed, there are a number of experiments already underway that, if successful, will lead to values of important constants with significantly reduced uncertainties. We touch upon some of these experiments in the paragraphs below, in which we make suggestions regarding future work based on what we believe are the main weaknesses of the 1998 adjustment.

It is an axiom in the PMFC field that the best way to establish confidence in the result of an experiment or calculation is to have it repeated in another laboratory, preferably by a dissimilar method. (The different results should have comparable uncertainties.) Although it does not guarantee that an unsuspected error in a result will be found, history shows that it is an excellent way of discovering an error if one exists.

Unfortunately, such redundancy is all too rare among the input data of the 1998 adjustment. As seen above, α , h , and R play a major role in the determination of many constants, yet the adjusted value of each is to a large extent determined by a pair of input data or a single input datum. These data are briefly summarized below, accompanied by our related suggestions for future work.

Fine-structure constant. In the case of α , the two critical data are the experimental value of a_e determined at the University of Washington and δ_e , the additive correction to the theoretical expression for a_e . The uncertainty of δ_e is dominated by the 0.0384 uncertainty of the eighth-order coefficient $A_1^{(8)}$ as calculated by Kinoshita; it leads to $u_r[a_e(\text{th})]$

$= 1.0 \times 10^{-9}$, which is about $\frac{1}{4}$ times the uncertainty $u_r = 3.7 \times 10^{-9}$ of the experimental value. The uncertainty of α that can be inferred from a_e is $u_r = 3.8 \times 10^{-9}$, about $\frac{1}{6}$ times that of the next most accurate value. We therefore believe that the most important tasks regarding alpha are

- (i) a second experimental determination of a_e with $u_r < 5 \times 10^{-9}$;
- (ii) a second calculation of $A_1^{(8)}$ with $u_r < 0.04$; and
- (iii) a determination of α with $u_r < 5 \times 10^{-9}$ by an entirely different method.

Point (i) is currently being addressed by the University of Washington group (Mittlemann, Ioannou, and Dehmelt, 1999) and by a group at Harvard University (Peil and Gabrielse, 1999). To the best of our knowledge, point (ii) is not being addressed, although Kinoshita continues to check and improve his calculation of $A_1^{(8)}$ and his assessment of its uncertainty. With regard to point (iii), it could actually be addressed in the very near future by the experiment at Stanford University to obtain α from a measurement of $h/m(^{133}\text{Cs})$ [see Sec. 3.11.2].

Planck constant. In the case of h , the most critical datum is the value of $K_J^2 R_K = 4/h$ obtained at NIST using a moving-coil watt balance; its relative standard uncertainty $u_r = 8.7 \times 10^{-8}$ is $\frac{1}{23}$ times that of the next most accurate value of h , which was determined at NPL also using a moving-coil watt balance. Thus it is our view that the highest-priority tasks with regard to h are

- (i) a second moving-coil watt balance determination of h with $u_r < 9 \times 10^{-8}$;
- (ii) determination of other constants such as N_A and F with sufficiently small uncertainties that a value of h with $u_r < 9 \times 10^{-8}$ can be inferred from them; and
- (iii) a moving-coil watt balance determination of h with $u_r \approx 2 \times 10^{-8}$ and determinations of other constants such as N_A and F from which such values of h can be inferred.

Point (i) and the first part of (iii) are being addressed by efforts at both NIST and NPL to significantly improve their watt-balance experiments; results with relative standard uncertainties of a few times 10^{-8} or less are expected in several years. Further, a new moving-coil watt balance experiment that should be competitive with those at NIST and NPL has been initiated at the Swiss Federal Office of Metrology (OFMET), Bern–Wabern, Switzerland (Beer *et al.*, 1999).

Point (ii) and the second part of (iii) are mainly being addressed by the international effort to determine the Avogadro constant by the XRCd method with the smallest possible uncertainty in order to replace the current definition of the kilogram. The Planck constant h may be obtained from N_A from the relation

$$h = \frac{cA_r(e)M_u\alpha^2}{2R_\infty N_A}. \quad (387)$$

Since $u_r < 8 \times 10^{-9}$ for the group of constants multiplying

$1/N_A$, a value of N_A with $u_r \approx 2 \times 10^{-8}$ will yield a value of h with nearly the same uncertainty. Although it is not yet clear that the XRCd method is capable of providing such a value of h , it is the best alternate route to h that we presently have. It should, therefore, continue to be vigorously pursued, even though to achieve this uncertainty will require major advances in characterizing near-ideal single crystals of silicon and in measuring their density and isotopic composition.

Although the route to N_A and hence h through the Faraday constant F using the relations

$$N_A = \frac{K_{J-90}R_{K-90}}{2} \mathcal{F}_{90} \quad (388)$$

$$h = \frac{cA_r(e)M_u\alpha^2}{K_{J-90}R_{K-90}R_\infty\mathcal{F}_{90}} \quad (389)$$

is being investigated at PTB in an experiment that is equivalent to determining \mathcal{F}_{90} in vacuum rather than in an electrolyte (Gläser, 1991), it is in its very early stages. Nevertheless, it should also be vigorously pursued so that its potential can be realistically assessed.

Other experiments that, like the moving-coil watt balance, compare electric power with mechanical power (or equivalently, electric energy to mechanical energy) are also in various stages of development. These include the levitated superconducting body experiment at NRLM (Fujii *et al.*, 1999) and an experiment using a moving-capacitor balance at the University of Zagreb (Bego, Butorac, and Ilić, 1999). Variations of the moving-coil watt balance itself are being investigated at the Istituto Elettrotecnico Nazionale (IEN) “Galileo Ferraris,” Torino, Italy (Cabiati, 1991). In view of the importance of h to the determination of the values of many constants, all of these efforts are highly warranted.

Molar gas constant. For R , the key datum is the NIST value with $u_r = 1.8 \times 10^{-6}$ obtained from measurements of the speed of sound in argon using a spherical acoustic resonator; its uncertainty is $\frac{1}{47}$ times that of the NPL value, the only other result of interest, which was also obtained from speed-of-sound measurements in argon but using a cylindrical acoustic interferometer. We therefore believe that the most important tasks with regard to R are

- (i) a second direct determination of R with u_r no larger than 2×10^{-6} ;
- (ii) determinations of other constants such as k and σ with sufficiently small uncertainties that a value of R with $u_r \approx 2 \times 10^{-6}$ or less can be inferred from them; and
- (iii) speed-of-sound determinations of R with $u_r \approx 5 \times 10^{-7}$ and determinations of other constants such as k and σ from which such values of R can be inferred.

Of the three critical constants α , h , and R , the molar gas constant is the most problematic; there are no other values of R with an uncertainty as small as that of the NIST value on the horizon from any source, let alone a value with a significantly smaller uncertainty. As far as we are aware, the only relevant experiment being actively pursued is the NPL deter-

mination of σ/h using electrical substitution radiometry (see Sec. 3.16). If it achieves its goal of $u_r(\sigma/h) = 1 \times 10^{-5}$, it could provide a value of R with $u_r(R) = 2.5 \times 10^{-6}$, compared to $u_r(R) = 1.8 \times 10^{-6}$ for the NIST value and $u_r(R) = 8.4 \times 10^{-6}$ for the NPL value. Although the new NPL experiment will not really address any of the above points, it is still highly important: it does not depend on speed-of-sound measurements in argon, and the uncertainty of the value of R that one expects to be able to infer from it is only about 1.4 times larger than that of the NIST value.

A possible approach to improving our knowledge of R is for metrologists at the national metrology institutes to join forces in an international collaborative effort much like the effort now underway to improve our knowledge of N_A . Perhaps the CCM Working Group on the Avogadro Constant (see Sec. 3.10) can serve as a model for a CCT Working Group on the Molar Gas Constant (CCT is the abbreviation of the *Comité Consultatif de Thermométrie* of the CIPM). In view of the key role played by R in the determination of important thermodynamic and radiometric constants such as k , σ , V_m , c_2 , and b , such an effort would be well justified.

Our discussion of α , h , and R can be summarized as follows: In the next few years, work already well underway has the possibility of confirming the 1998 recommended values of these constants, and hence the values of the many other constants deduced from them, as well as providing values of α and h with uncertainties about $\frac{1}{4}$ times those of the 1998 recommended values. Such new values of α and h will lead to new values of many other constants with comparably reduced uncertainties, thereby continuing the rapid progress of the past 13 years.

Although confirming and reducing the current uncertainties of α , h , and R through improved measurements and calculations would have the greatest impact on advancing our overall knowledge of the values of the constants, confirming and reducing the uncertainties of other constants would also have significant benefits. We address this issue with the following comments.

Josephson and quantum Hall effects. Although the current experimental and theoretical evidence for the exactness of the relations $K_J = 2e/h$ and $R_K = h/e^2 = \mu_0 c / 2\alpha$ is quite strong, efforts by both experimentalists and theorists to increase this evidence are encouraged. Soundly based quantitative estimates of the limitations of these relations are especially of interest.

Relative atomic masses. Of the basic particles e , n , p , d , h , and α , the relative atomic mass of the electron $A_r(e)$ is the least well known; its uncertainty is $u_r = 2.1 \times 10^{-9}$ compared to, for example, the uncertainty $u_r = 1.3 \times 10^{-10}$ of $A_r(p)$. Because $A_r(e)$ enters the expressions from which a number of constants are derived, for example, those for the energy levels of hydrogenic atoms, in order to fully use the anticipated advances in the measured and calculated values of various quantities, an improved value of $A_r(e)$ with an uncertainty of say $u_r = 2 \times 10^{-10}$ will be necessary. Moreover, there is only one high-accuracy input datum related to $A_r(e)$ currently available.

Experiment and theory relevant to the Rydberg constant. Because of limitations in the theory of the energy levels of hydrogen and deuterium, full advantage cannot yet be taken of the existing measurements of H and D transition frequencies to deduce a value of R_∞ . Since the uncertainty in the theory is dominated by the uncertainty of the two-photon corrections, reducing this uncertainty is crucial for continued progress. Of comparable importance is sorting out the relationships between the bound-state proton and deuteron rms charge radii and those obtained from scattering data. Improved experimental determinations of these radii would be of great help in this regard; such a result for the proton radius is expected from the determination of the Lamb shift in muonic hydrogen by an international group at PSI (Taqqu *et al.*, 1999). Of course, results from additional high-accuracy measurements of transition frequencies in H and D are always of value.

Experiment and theory relevant to the magnetic moment anomaly of the muon. The uncertainty of the theoretical expression for a_μ is dominated by the uncertainty of the hadronic contribution $a_\mu(\text{had})$, which in turn is dominated by the uncertainty of the cross section for the production of hadrons in e^+e^- collisions at low energies. Because at present the theoretical value of a_μ has a significantly smaller uncertainty than the experimental value, the 1998 recommended value of a_μ is the theoretical value. This means that, at least for the moment, to advance our knowledge of a_μ requires an improved measurement of the cross section. Such a measurement is also required to test the standard model through the comparison of the theoretical value of a_μ with the significantly improved experimental value anticipated from the ongoing muon $g-2$ experiment at Brookhaven National Laboratory, which could eventually produce a result for a_μ with an uncertainty comparable to that of the best anticipated theoretical result. How a more accurate value of the cross section can be obtained at the ϕ factory DAΦNE of the Laboratori Nazionali di Frascati, Italy is described by Spagnolo (1999).

Experiment and theory relevant to magnetic moment ratios. Measurements of various magnetic moment ratios such as $\mu_{e^-}(\text{H})/\mu_p(\text{H})$ and μ_n/μ_p' and theoretical calculations of bound-state corrections for those measurements carried out in atoms are to a large extent responsible for the recommended values of such important constants as μ_{e^-}/μ_p , μ_p/μ_N , μ_n/μ_p , μ_h'/μ_N , μ_d , etc. However, in each case there is only one input datum available—other values are simply not competitive. Additional measurements are clearly called for, we would hope with smaller uncertainties, so that our knowledge of these important constants can advance. Current work at NPL associated with its helium NMR program (see Sec. 3.3.7) should in fact lead to better values of $\mu_{e^-}(\text{H})/\mu_p(\text{H})$ and $\mu_{e^-}(\text{H})/\mu_p'$, but this is the only effort of its type of which we are aware. When such improved results become available, it may be necessary to improve the calculation of bound-state corrections so that full advantage can be taken of their small uncertainties.

Experiment and theory relevant to the muonium hyperfine splitting. The existing measurements of the frequencies of transitions between Zeeman energy levels in muonium presently have uncertainties such that the value of α that can be obtained by comparing the experimentally determined value of $\Delta\nu_{\text{Mu}}$ with its theoretical expression has a relative standard uncertainty of $u_r = 5.7 \times 10^{-8}$. This uncertainty is dominated by the uncertainty of the value of m_e/m_μ that can be deduced from the measurements. On the other hand, the experimental value of $\Delta\nu_{\text{Mu}}$, which has an uncertainty $u_r = 1.1 \times 10^{-8}$, together with its QED-based theoretical expression and the most accurate individual value of α yields a value for this mass ratio whose uncertainty is dominated by the uncertainty $u_r = 2.7 \times 10^{-8}$ of the theoretical expression. Thus reduction of this uncertainty by an order of magnitude through improvement in the theory would lead to a reduction in the uncertainty of this important ratio by nearly a factor of 3. We believe that this is motivation enough to improve the theory. However, such theoretical advances might also stimulate new efforts to improve the transition-frequency measurements, the end result of which could be a highly competitive value of α from muonium.

Theory of hydrogen hyperfine splitting. To take advantage of the phenomenally small uncertainty $u_r = 7 \times 10^{-13}$ of the experimentally determined value of $\Delta\nu_{\text{H}}$ to derive a competitive value of α will require major theoretical work. Most important at present is the contribution to $\Delta\nu_{\text{H}}$ of the polarizability of the proton $|\delta_{\text{pol}}| < 4 \times 10^{-6}$. In view of the great potential $\Delta\nu_{\text{H}}$ has in providing a highly accurate value of α , any improvement in its theoretical expression would be of value.

Experiment and theory relevant to the fine structure of ^4He . Measurements and theoretical calculations of the transition frequencies corresponding to the differences in energy of the three 2^3P levels of ^4He currently underway have the potential of eventually providing a value of α with $u_r \approx 5 \times 10^{-9}$. In view of the importance of such a value, both experimental and theoretical work in this area warrants sustained effort.

Experiment and theory relevant to the Boltzmann constant. The route to the molar gas constant R via the Boltzmann constant k was not specifically mentioned in our discussion of R in the earlier part of this section, because the possible routes to k are problematic. Of the two approaches described in Sec. 3.15, the ^4He molar polarizability/dielectric constant gas thermometry method would seem to be the most promising. Although major advances in both theory and experiment are required in order to use it to obtain a competitive value of k and hence R , they seem to be within the realm of possibility. [On the experimental side, see, for example, Moldover (1998).] Thus we encourage continued theoretical and experimental work in this field.

Newtonian constant of gravitation. As discussed in detail in Sec. 3.17, the present situation regarding G is quite unsatisfactory; new measurements with $u_r \approx 1 \times 10^{-5}$ are critically needed. Fortunately, as also discussed in that section, a num-

ber of experiments that should achieve this level of uncertainty are well underway.

In summary, two broad conclusions can be drawn from this review: The first is that the uncertainties of the values of the fundamental constants have been reduced to a remarkably low level by extraordinary research in the recent past. The second is that there are numerous and challenging opportunities for both experimentalists and theorists to make important contributions to the advancement of our knowledge of the values of the fundamental constants in the future. The reason that these opportunities must be seized is, of course, no mystery; as F. K. Richtmyer (1932) said nearly 70 years ago, "... the whole history of physics proves that a new discovery is quite likely to be found lurking in the next decimal place."

7. Acknowledgments

We sincerely thank our many colleagues in the field of precision measurement and fundamental constants for answering our myriad questions regarding their experiments and calculations, for providing us results prior to formal publication, and for educating us on a variety of topics with which we had only a limited familiarity. Their willingness to do so has made this paper possible. We particularly thank both Jonathan D. Baker for his technical advice, support, and critical reading of the manuscript and E. Richard Cohen for his incisive comments.

8. Appendices

Appendix A. Theory Relevant To The Rydberg Constant

This appendix gives a brief summary of the theory of the energy levels of the hydrogen atom relevant to the determination of the Rydberg constant R_∞ based on measurements of the frequencies of transitions between those levels. It is an updated version of an earlier review by one of the authors (Mohr, 1996). For brevity, references to most historical works are not included.

The energy levels of hydrogen-like atoms are determined mainly by the Dirac eigenvalue, QED effects such as self energy and vacuum polarization, and nuclear size and motion effects. We consider each of these contributions in turn.

Although the uncertainties of the theoretical contributions to a particular energy level are independent, in many cases the uncertainties of contributions of the same type to different energy levels are not independent and (mainly for S states) vary as $1/n^3$. (Note that for historical reasons, contributions that vary as $1/n^3$ are called "state independent.") As discussed at the end of this Appendix, in such cases we take the covariances of the theoretical expressions for different energy levels into account. To facilitate the calculation of covariances, we distinguish between two types of uncertainty components for each contribution to an energy level: u_0 and u_n . For a given isotope (H or D), an uncertainty u_0/n^3 is associated with an uncalculated term (or terms) of the form

$A(L,j)/n^3$, where $A(L,j)$ is a particular but unknown constant for a set of levels n, L, j for a given L and j and any n ($L=S, P, \dots$). An uncertainty u_n/n^3 is associated with terms of the form $B(n,L,j)/n^3$, where $B(n,L,j)$ is an unknown function of n . The former lead to nonzero covariances while the latter do not [the $B(n,L,j)$ are assumed to be independent], except possibly for the same energy levels of different isotopes. In addition, many of the contributions to the theoretical expression for a particular energy level of H or D are the same (except for the effect of the mass difference of the nuclei) and thus in general no distinction is made in the text between their uncertainties. In those few cases where the uncertainties are independent, we so indicate. The level of uncertainty in the theory of current S states corresponds to values of u_0/h in the range 1 kHz to 100 kHz and to values of u_n/h in the range 1 kHz to 10 kHz. In fact, as discussed below, u_0/h exceeds 10 kHz only for the two-photon correction. Uncertainty components of interest in the theory of the difference between the 1S–2S transition frequencies in hydrogen and deuterium are also at the level of 1 kHz to 10 kHz. In keeping with Sec. 1.3, all uncertainties discussed in this and the following three appendices, including those due to uncalculated terms, are meant to be standard uncertainties.

1. Dirac Eigenvalue

The binding energy of an electron in a static Coulomb field (the external electric field of a point nucleus of charge Ze with infinite mass) is determined predominantly by the Dirac eigenvalue

$$E_D = \left[1 + \frac{(Z\alpha)^2}{(n-\delta)^2} \right]^{-1/2} m_e c^2, \quad (\text{A1})$$

where n is the principal quantum number,

$$\delta = |\kappa| - [\kappa^2 - (Z\alpha)^2]^{1/2}, \quad (\text{A2})$$

and κ is the angular momentum-parity quantum number ($\kappa = -1, 1, -2, 2, -3$ for $S_{1/2}, P_{1/2}, P_{3/2}, D_{3/2},$ and $D_{5/2}$ states, respectively). States with the same principal quantum number n and angular momentum quantum number $j = |\kappa| - \frac{1}{2}$ have degenerate eigenvalues. The nonrelativistic orbital angular momentum is given by $l = |\kappa + \frac{1}{2}| - \frac{1}{2}$. (Although we are interested only in the case where the nuclear charge is e , we retain the atomic number Z in order to indicate the nature of various terms.)

Corrections to the Dirac eigenvalue that take into account the finite mass of the nucleus m_N are included in the more general expression for atomic energy levels, which replaces Eq. (A1) (Barker and Glover, 1955; Sapirstein and Yennie, 1990):

$$E_M = M c^2 + [f(n,j) - 1] m_r c^2 - [f(n,j) - 1]^2 \frac{m_r^2 c^2}{2M} + \frac{1 - \delta_{l0}}{\kappa(2l+1)} \frac{(Z\alpha)^4 m_r^3 c^2}{2n^3 m_N^2} + \dots, \quad (\text{A3})$$

where

$$f(n,j) = \left[1 + \frac{(Z\alpha)^2}{(n-\delta)^2} \right]^{-1/2}, \quad (\text{A4})$$

$M = m_e + m_N$, and $m_r = m_e m_N / (m_e + m_N)$ is the reduced mass.

2. Relativistic Recoil

Relativistic corrections to Eq. (A3) associated with motion of the nucleus are considered relativistic-recoil corrections. The leading term, to lowest order in $Z\alpha$ and all orders in m_e/m_N , is (Erickson, 1977; Sapirstein and Yennie, 1990)

$$E_S = \frac{m_r^3}{m_e^2 m_N} \frac{(Z\alpha)^5}{\pi n^3} m_e c^2 \times \left\{ \frac{1}{3} \delta_{l0} \ln(Z\alpha)^{-2} - \frac{8}{3} \ln k_0(n,l) - \frac{1}{9} \delta_{l0} - \frac{7}{3} a_n - \frac{2}{m_N^2 - m_e^2} \delta_{l0} \left[m_N^2 \ln\left(\frac{m_e}{m_r}\right) - m_e^2 \ln\left(\frac{m_N}{m_r}\right) \right] \right\}, \quad (\text{A5})$$

where

$$a_n = -2 \left[\ln\left(\frac{2}{n}\right) + \sum_{i=1}^n \frac{1}{i} + 1 - \frac{1}{2n} \right] \delta_{l0} + \frac{1 - \delta_{l0}}{l(l+1)(2l+1)}. \quad (\text{A6})$$

To lowest order in the mass ratio, higher-order corrections in $Z\alpha$ have been extensively investigated; the contribution of next order in $Z\alpha$ can be written as

$$E_R = \frac{m_e}{m_N} \frac{(Z\alpha)^6}{n^3} m_e c^2 D_{60}, \quad (\text{A7})$$

where

$$D_{60} = 4 \ln 2 - \frac{7}{2} \quad \text{for } nS_{1/2}, \quad (\text{A8})$$

$$D_{60} = \left[3 - \frac{l(l+1)}{n^2} \right] \frac{2}{(4l^2 - 1)(2l+3)} \quad \text{for } l \geq 1,$$

and the contribution to the 1S state is -7.4 kHz. The result for S states was first obtained by Pachucki and Grotch (1995) and subsequently confirmed by Eides and Grotch (1997c). It is supported by a complete numerical calculation to all orders in $Z\alpha$, which gives $-7.16(1)$ kHz for the terms of order $(Z\alpha)^6$ and higher for the 1S state at $Z=1$ (Shabaev *et al.*, 1998). Because of this consensus, we do not take into account two other results, 2.77 kHz and -16.4 kHz, for the same contribution (Elkhovskii, 1996; Yelkhovsky, 1998). The expression for D_{60} for P states was first obtained by Golosov *et al.* (1995), and the general expression for all $l \geq 1$ given in Eq. (A8) was obtained by Elkhovskii (1996). We include the result of Elkhovskii (1996) for states with $l > 1$ even though we do not consider the corresponding result for S states, because the ambiguity associated with the short-distance behavior of the relevant operators that leads to the disagreements for S states is not present in the contributions for $l \geq 1$.

The all-order results of Shabaev *et al.* (1998), expressed in their notation, are

$$E_R = \frac{m_e}{m_N} \frac{(Z\alpha)^6}{n^3} m_e c^2 \left[\frac{\Delta P(Z\alpha)}{\pi Z\alpha} \right], \quad (\text{A9})$$

where

$$\Delta P(\alpha) = \begin{cases} -0.016\,16(3) & 1S_{1/2}, \\ -0.016\,17(5) & 2S_{1/2}, \\ 0.007\,72(1) & 2P_{1/2}. \end{cases} \quad (\text{A10})$$

These are the values that we use for these states. (Note that for the $2P_{1/2}$ state we have added an explicit uncertainty to the originally quoted number 0.007 72 to reflect its implied uncertainty.)

On the other hand, no all-order calculation exists for states for $n \geq 3$. Since the theoretical expression for D_{60} for S states in Eq. (A8) is independent of n and the complete calculated values in Eq. (A10) for $n=1$ and $n=2$ are nearly equal, we take the value $\Delta P(\alpha) = -0.016\,17(5)$ for all higher S states. By similar reasoning, since the general expression in Eq. (A8) for $l=1$ is only weakly dependent on n , we take the value $\Delta P(\alpha) = 0.007\,72(1)$ for the $2P_{1/2}$ state and $\Delta P(\alpha) = 0.007\,72(10)$ for all other $P_{1/2}$ and $P_{3/2}$ states, where the uncertainty is expanded to reflect the approximate nature of the value. [We do not use the result $\Delta P(\alpha) = 0.0075(4)$ for the $P_{3/2}$ state obtained by Artemyev, Shabaev, and Yerokin (1995) because of its large uncertainty.] For D states, we use the contribution given by Eq. (A7) and the general expression in Eq. (A8) with a relative uncertainty of 1 % to account for higher-order terms in $Z\alpha$, guided by the P state all-orders calculation. Higher-order terms in m_e/m_N beyond Eq. (A5) are expected to be negligible at the level of uncertainty of current interest. [See, for example, Boikova, Tyukhtyaev, and Faustov (1998)]. In fact, all of the relativistic-recoil uncertainties discussed in this section are negligible at this level and are not included in our calculations.

3. Nuclear Polarization

Another effect involving specific properties of the nucleus, in addition to relativistic recoil, is nuclear polarization. It arises from interactions between the electron and nucleus in which the nucleus is excited from the ground state to virtual higher states.

This effect has been calculated for hydrogen for the 1S state by Khriplovich and Sen'kov (1998), who find $E_P/h = -0.071(13)$ kHz, and is currently of marginal significance. For n S states we employ that value multiplied by $1/n^3$, since it is mainly proportional to the square of the wave function at the origin. We take the effect to be zero in states of higher l .

For deuterium, the effect is much larger. A recent calculation by Friar and Payne (1997a), which includes corrections that go beyond their unretarded-dipole approximation calculation (Friar and Payne, 1997c), gives 18.58(7) kHz for the 1S–2S transition. Because of the near $1/n^3$ dependence

of this contribution, the value for the 1S state is $-21.23(8)$ kHz (Friar, 1998). In addition to this deuteron polarizability, the polarizability contributions of the constituent particles, $-0.071(13)$ kHz from the proton and $-0.061(12)$ kHz from the neutron for the 1S state, should be taken into account, although the contribution of the proton polarizability to the H–D isotope shift vanishes (Khriplovich, 1998; Friar, 1998; Pachucki, 1998). As for hydrogen, we assume that the effect is negligible in higher- l states.

In summary, the results for deuterium as well as hydrogen are

$$E_P(\text{H}) = -0.071(13)h \frac{\delta_{l0}}{n^3} \text{ kHz} \\ E_P(\text{D}) = -21.37(8)h \frac{\delta_{l0}}{n^3} \text{ kHz}. \quad (\text{A11})$$

Although we include these contributions to the energy levels, we do not include their uncertainties because they are negligible.

4. Self Energy

The second-order (in e , first-order in α) level shift due to the one-photon electron self energy, the lowest-order radiative correction, is given by

$$E_{\text{SE}}^{(2)} = \frac{\alpha}{\pi} \frac{(Z\alpha)^4}{n^3} F(Z\alpha) m_e c^2, \quad (\text{A12})$$

where

$$F(Z\alpha) = A_{41} \ln(Z\alpha)^{-2} + A_{40} + A_{50}(Z\alpha) \\ + A_{62}(Z\alpha)^2 \ln^2(Z\alpha)^{-2} + A_{61}(Z\alpha)^2 \ln(Z\alpha)^{-2} \\ + G_{\text{SE}}(Z\alpha)(Z\alpha)^2, \quad (\text{A13})$$

with (Erickson and Yennie, 1965)

$$A_{41} = \frac{4}{3} \delta_{l0} \\ A_{40} = -\frac{4}{3} \ln k_0(n, l) + \frac{10}{9} \delta_{l0} - \frac{1}{2\kappa(2l+1)} (1 - \delta_{l0}) \\ A_{50} = \left(\frac{139}{32} - 2 \ln 2 \right) \pi \delta_{l0} \\ A_{62} = -\delta_{l0} \\ A_{61} = \left[4 \left(1 + \frac{1}{2} + \cdots + \frac{1}{n} \right) + \frac{28}{3} \ln 2 - 4 \ln n \right. \\ \left. - \frac{601}{180} - \frac{77}{45n^2} \right] \delta_{l0} + \left(1 - \frac{1}{n^2} \right) \left(\frac{2}{15} + \frac{1}{3} \delta_{j\frac{1}{2}} \right) \delta_{l1} \\ + \frac{96n^2 - 32l(l+1)}{3n^2(2l-1)(2l)(2l+1)(2l+2)(2l+3)} \\ \times (1 - \delta_{l0}). \quad (\text{A14})$$

[As usual, the first subscript on the A 's in Eq. (A13) refers to the power of $Z\alpha$ and the second subscript to the power of

TABLE 32. Bethe logarithms $\ln k_0(n, l)$ relevant to the determination of R_∞ .

n	S	P	D
1	2.984 128 556		
2	2.811 769 893	−0.030 016 709	
3	2.767 663 612	−0.038 190 229	−0.005 232 148
4	2.749 811 840	−0.041 954 895	−0.006 740 939
6	2.735 664 207	−0.045 312 198	−0.008 147 204
8	2.730 267 261	−0.046 741 352	−0.008 785 043
12	2.726 179 341	−0.047 917 112	−0.009 342 954

$\ln(Z\alpha)^{-2}$.] Bethe logarithms $\ln k_0(n, l)$ that appear in Eq. (A14), needed for this and possibly future work, are given in Table 32 (Drake and Swainson, 1990).

The function $G_{\text{SE}}(Z\alpha)$ in Eq. (A13) gives the higher-order contribution (in $Z\alpha$) to the self energy. The low- Z limit of this function, $G_{\text{SE}}(0) = A_{60}$, has been calculated for various states by Pachucki and others (Pachucki, 1993b; Jentschura and Pachucki, 1996; Jentschura, Soff, and Mohr, 1997). Values for the function at $Z = 1$, $G_{\text{SE}}(\alpha)$, are given in Table 33. For the $1S_{1/2}$ state the value in the table is based on a direct numerical evaluation (Jentschura, Mohr, and Soff, 1999), and for the other states the values are based on extrapolation to $Z = 1$ of numerical values for $G_{\text{SE}}(Z\alpha)$ calculated at higher Z (Kotochigova, Mohr, and Taylor, 1999; Mohr and Kim, 1992; Mohr, 1992). The extrapolations for P states take into account the values of $G_{\text{SE}}(0)$ when known. Similar extrapolations of $G_{\text{SE}}(Z\alpha)$ to $Z = 1$ and 2 for states with $n = 1$ and 2 based on earlier numerical calculations have been done by van Wijngaarden, Kwela, and Drake (1991). Karshenboim, (1994) has done extrapolations to $Z = 1$ for the $1S_{1/2} - 2S_{1/2}$ difference and for the $P_{1/2}$ state, obtaining results slightly different from those given in Table 33. We use the values in the table because of their broader coverage and better agreement with the independent semianalytic calculations at $Z = 0$. These values are also in agreement with earlier results of Mohr (1996).

The dominant effect of the finite mass of the nucleus on the self energy correction is taken into account by multiplying each term of $F(Z\alpha)$ by the reduced-mass factor $(m_r/m_e)^3$, except that the magnetic moment term $-1/[2\kappa(2l+1)]$ in A_{40} is instead multiplied by the factor $(m_r/m_e)^2$. This prescription is consistent with the result for P states obtained by Golosov *et al.* (1995). In addition, the argument $(Z\alpha)^{-2}$ of the logarithms is replaced by $(m_e/m_r) \times (Z\alpha)^{-2}$ (Sapirstein and Yennie, 1990).

TABLE 33. Values of the function $G_{\text{SE}}(\alpha)$.

n	$S_{1/2}$	$P_{1/2}$	$P_{3/2}$	$D_{3/2}$	$D_{5/2}$
1	−30.290 24(2)				
2	−31.17(3)	−0.98(1)	−0.48(1)		
3	−31.01(6)	−1.13(1)	−0.57(1)	0.00(1)	0.00(1)
4	−30.87(5)	−1.17(1)	−0.61(1)	0.00(1)	0.00(1)
6	−30.82(8)	−1.23(3)	−0.63(3)	0.00(1)	0.00(1)
8	−30.80(9)	−1.25(4)	−0.64(4)	0.00(1)	0.00(1)
12	−30.77(13)	−1.28(6)	−0.66(6)	0.00(1)	0.00(1)

TABLE 34. Values of the function $G_{\text{VP}}^{(1)}(\alpha)$.

n	$S_{1/2}$	$P_{1/2}$	$P_{3/2}$	$D_{3/2}$	$D_{5/2}$
1	−0.618 724				
2	−0.808 872	−0.064 006	−0.014 132		
3	−0.814 530	−0.075 859	−0.016 750	−0.000 000	−0.000 000
4	−0.806 579	−0.080 007	−0.017 666	−0.000 000	−0.000 000
6	−0.791 450	−0.082 970	−0.018 320	−0.000 000	−0.000 000
8	−0.781 197	−0.084 007	−0.018 549	−0.000 000	−0.000 000
12	−0.769 151	−0.084 748	−0.018 713	−0.000 000	−0.000 000

The uncertainty of the self energy contribution to a given level arises entirely from the uncertainty of $G_{\text{SE}}(\alpha)$ listed in Table 33 and is taken to be entirely of type u_n .

5. Vacuum Polarization

The second-order vacuum polarization level shift, due to the creation of a virtual electron–positron pair in the exchange of photons between the electron and the nucleus, is

$$E_{\text{VP}}^{(2)} = -\frac{\alpha}{\pi} \frac{(Z\alpha)^4}{n^3} H(Z\alpha) m_e c^2, \quad (\text{A15})$$

where the function $H(Z\alpha)$ is divided into the part corresponding to the Uehling potential, denoted here by $H^{(1)}(Z\alpha)$, and the higher-order remainder $H^{(R)}(Z\alpha) = H^{(3)}(Z\alpha) + H^{(5)}(Z\alpha) + \dots$, where the superscript denotes the order in powers of the external field. The individual terms are expanded in a power series in $Z\alpha$ as

$$H^{(1)}(Z\alpha) = C_{40} + C_{50}(Z\alpha) + C_{61}(Z\alpha)^2 \ln(Z\alpha)^{-2} + G_{\text{VP}}^{(1)}(Z\alpha)(Z\alpha)^2 \quad (\text{A16})$$

$$H^{(R)}(Z\alpha) = G_{\text{VP}}^{(R)}(Z\alpha)(Z\alpha)^2, \quad (\text{A17})$$

with

$$\begin{aligned} C_{40} &= -\frac{4}{15} \delta_{l0} \\ C_{50} &= \frac{5}{48} \pi \delta_{l0} \\ C_{61} &= -\frac{2}{15} \delta_{l0}. \end{aligned} \quad (\text{A18})$$

The part $G_{\text{VP}}^{(1)}(Z\alpha)$ arises from the Uehling potential, and is readily calculated numerically (Mohr, 1982; Kotochigova *et al.*, 1999); values are given in Table 34. The higher-order remainder $G_{\text{VP}}^{(R)}(Z\alpha)$ has been considered by Wichmann and Kroll, and the leading terms in powers of $Z\alpha$ are (Wichmann and Kroll, 1956; Mohr, 1975; Mohr, 1983)

$$G_{\text{VP}}^{(R)}(Z\alpha) = \left(\frac{19}{45} - \frac{1}{27} \pi^2\right) \delta_{l0} + \left(\frac{1}{16} - \frac{31}{2880} \pi^2\right) \pi(Z\alpha) \delta_{l0} + \dots \quad (\text{A19})$$

Complete numerical calculations of $H(Z\alpha)$ have been done to all orders in $Z\alpha$ for high Z , and those results are consistent with the low- Z expression in Eq. (A19) (Johnson and Soff, 1985). The uncertainty in the vacuum polarization con-

tribution is due to higher-order omitted terms that are estimated to contribute $1 \times (Z\alpha)^2$ in Eq. (A19) and hence is negligible

In a manner similar to that for the self energy, the effect of the finite mass of the nucleus is taken into account by multiplying Eq. (A15) by the factor $(m_r/m_e)^3$ and including a multiplicative factor of (m_e/m_r) in the argument of the logarithm in Eq. (A16).

There is also a second-order vacuum polarization level shift due to the creation of virtual particle pairs other than the e^+e^- pair. The predominant contribution for nS states arises from $\mu^+\mu^-$, with the leading term being (Karshenboim, 1995)

$$E_{\mu\text{VP}}^{(2)} = \frac{\alpha}{\pi} \frac{(Z\alpha)^4}{n^3} \left(-\frac{4}{15} \right) \left(\frac{m_e}{m_\mu} \right)^2 \left(\frac{m_r}{m_e} \right)^3 m_e c^2. \quad (\text{A20})$$

The next-order term in the contribution of muon vacuum polarization to nS states is of relative order $Z\alpha m_e/m_\mu$ and is therefore negligible. The analogous contribution $E_{\tau\text{VP}}^{(2)}$ from $\tau^+\tau^-$ (-18 Hz for the $1S$ state) is also negligible at the level of uncertainty of current interest.

For the hadronic vacuum polarization contribution, we take the recent result given by Friar *et al.* (1999) that utilizes all available e^+e^- scattering data:

$$E_{\text{had VP}}^{(2)} = 0.671(15) E_{\mu\text{VP}}^{(2)}, \quad (\text{A21})$$

where the uncertainty is of type u_0 . This result is consistent with but has a smaller uncertainty than earlier results (Friar *et al.*, 1999).

The muonic and hadronic vacuum polarization contributions are negligible for P and D states.

6. Two-Photon Corrections

Corrections from two virtual photons, of order α^2 , have been calculated as a power series in $Z\alpha$:

$$E^{(4)} = \left(\frac{\alpha}{\pi} \right)^2 \frac{(Z\alpha)^4}{n^3} m_e c^2 F^{(4)}(Z\alpha), \quad (\text{A22})$$

where

$$\begin{aligned} F^{(4)}(Z\alpha) &= B_{40} + B_{50}(Z\alpha) + B_{63}(Z\alpha)^2 \ln^3(Z\alpha)^{-2} \\ &\quad + B_{62}(Z\alpha)^2 \ln^2(Z\alpha)^{-2} + \dots \\ &= B_{40} + (Z\alpha) G^{(4)}(Z\alpha). \end{aligned} \quad (\text{A23})$$

Because the possible terms $B_{61}(Z\alpha)^2 \ln(Z\alpha)^{-2}$, $B_{60}(Z\alpha)^2$, and higher-order terms are essentially unknown, they are not included in Eq. (A23), although fragmentary information about B_{61} exists (Eides and Grotch, 1995a, Karshenboim, 1996; Mallampalli and Sapirstein, 1996; Mallampalli and Sapirstein, 1998). Uncertainties to account for omitted terms are discussed at the end of this section.

The level shifts of order $(\alpha/\pi)^2 (Z\alpha)^4 m_e c^2$ that give rise to B_{40} are well known and are characterized as a self-energy correction

$$\begin{aligned} E_{\text{SE}}^{(4)} &= \left(\frac{\alpha}{\pi} \right)^2 \frac{(Z\alpha)^4}{n^3} m_e c^2 \\ &\quad \times \left[2\pi^2 \ln 2 - \frac{49}{108} \pi^2 - \frac{4819}{1296} - 3\zeta(3) \right] \delta_{l0}, \end{aligned} \quad (\text{A24})$$

a magnetic moment correction

$$\begin{aligned} E_{\text{MM}}^{(4)} &= \left(\frac{\alpha}{\pi} \right)^2 \frac{(Z\alpha)^4}{n^3} m_e c^2 \\ &\quad \times \left[\frac{1}{2} \pi^2 \ln 2 - \frac{1}{12} \pi^2 - \frac{197}{144} - \frac{3}{4} \zeta(3) \right] \frac{1}{\kappa(2l+1)}, \end{aligned} \quad (\text{A25})$$

and a vacuum polarization correction

$$E_{\text{VP}}^{(4)} = \left(\frac{\alpha}{\pi} \right)^2 \frac{(Z\alpha)^4}{n^3} m_e c^2 \left[-\frac{82}{81} \right] \delta_{l0}, \quad (\text{A26})$$

where ζ is the Riemann zeta function. The total for B_{40} is

$$\begin{aligned} B_{40} &= \left[2\pi^2 \ln 2 - \frac{49}{108} \pi^2 - \frac{6131}{1296} - 3\zeta(3) \right] \delta_{l0} \\ &\quad + \left[\frac{1}{2} \pi^2 \ln 2 - \frac{1}{12} \pi^2 - \frac{197}{144} - \frac{3}{4} \zeta(3) \right] \frac{1}{\kappa(2l+1)}. \end{aligned} \quad (\text{A27})$$

The terms of order $(\alpha/\pi)^2 (Z\alpha)^5 m_e c^2$ that give rise to B_{50} can be divided into two classes depending on whether the corresponding Feynman diagrams do or do not have closed electron loops. The former category gives (Pachucki, 1993a; Eides, Grotch, and Shelyuto, 1997)

$$E_{\text{EL}}^{(4)} = \left(\frac{\alpha}{\pi} \right)^2 \frac{(Z\alpha)^5}{n^3} m_e c^2 [2.710\,614(10)] \delta_{l0}, \quad (\text{A28})$$

while the latter category gives (Eides and Shelyuto, 1995; Pachucki, 1994)

$$E_{\text{NL}}^{(4)} = \left(\frac{\alpha}{\pi} \right)^2 \frac{(Z\alpha)^5}{n^3} m_e c^2 [-24.2668(31)] \delta_{l0}. \quad (\text{A29})$$

By combining these results, one obtains

$$B_{50} = -21.5561(31) \delta_{l0}. \quad (\text{A30})$$

The next coefficient, as obtained by Karshenboim, (1993a), is

$$B_{63} = -\frac{8}{27} \delta_{l0}. \quad (\text{A31})$$

It has been confirmed by Pachucki (1998), provided the assumptions made by Karshenboim (1993a) are employed. The term arises from a single diagram, which we label $\ell\ell$, consisting of two self-energy loops, and we define $G_{\ell\ell}^{(4)}(Z\alpha)$ to be the part of $G^{(4)}(Z\alpha)$ that corresponds to this diagram. It is given by

$$G_{\ell\ell}^{(4)}(Z\alpha) = 2.299\,53 \delta_{l0} - \frac{8}{27} \delta_{l0}(Z\alpha) \ln^3(Z\alpha)^{-2} + \dots, \quad (\text{A32})$$

where

$$B_{50}'' = 2.299\,53 \quad (\text{A33})$$

is the portion of B_{50} corresponding to this diagram (the diagram makes no contribution to B_{40} : $B_{40}'' = 0$). On the other hand, Mallampalli and Sapirstein (1998) have done a numerical calculation of $G_{\mathcal{P}}^{(4)}(Z\alpha)$ for the 1S state for various values of Z to all orders in $Z\alpha$. From their results, they obtain an estimate for B_{63} which differs from the value in Eq. (A31). Moreover, the calculated contribution of the diagram at $Z=1$ is negative, while the lowest-order term B_{50}'' is positive, which could be taken as a possible indication of the necessity of an all-orders calculation. Mallampalli and Sapirstein (1998) obtained $G_{\mathcal{P}}^{(4)}(\alpha) = -2.87(5)$, in contrast to the value $G_{\mathcal{P}}^{(4)}(\alpha) = 0.24 \dots$ in Eq. (A32). More recently, Goidenko *et al.* (1999) have calculated the contribution of the same diagram and obtain a result consistent with the coefficient in Eq. (A31), although they do not give values for $Z=1$ or 2, because the numerical uncertainty is too large. They find that for $3 \leq Z \leq 20$ their results can be fitted by the function

$$G_{\mathcal{P}}^{(4)}(Z\alpha) = 2.299\,53 - \frac{8}{27}(Z\alpha)\ln^3(Z\alpha)^{-2} - [1.0(1)](Z\alpha)\ln^2(Z\alpha)^{-2}, \quad (\text{A34})$$

which gives $G_{\mathcal{P}}^{(4)}(\alpha) = -0.47$ at $Z=1$. In view of the disagreement of these values of $G_{\mathcal{P}}^{(4)}(\alpha)$, for the purpose of our evaluation, we take the average of the two extreme results above (-2.87 and 0.24) with an uncertainty of half their difference:

$$G_{\mathcal{P}}^{(4)}(\alpha) = -1.3(1.6), \quad (\text{A35})$$

where we assume a $1/n^3$ scaling to obtain values for nS states other than 1S, as done by Mallampalli and Sapirstein (1998).

For S states the coefficient B_{62} has been calculated to be (Karshenboim, 1996b)

$$B_{62} = \frac{16}{9} \left(C + \psi(n) - \ln n - \frac{1}{n} + \frac{1}{4n^2} \right), \quad (\text{A36})$$

where ψ is the psi function (Abromowitz and Stegun, 1965) and C is an unknown constant independent of n [only the difference $B_{62}(1) - B_{62}(n)$ was calculated]. For P states the calculated value is (Karshenboim, 1996b)

$$B_{62} = \frac{4}{27} \frac{n^2 - 1}{n^2}. \quad (\text{A37})$$

There is no calculation of B_{62} for D states.

In summary, the two-photon contribution is calculated from Eq. (A22) with $F^{(4)}(Z\alpha)$ approximated by

$$B_{40} + (Z\alpha)(B_{50} - B_{50}'') + (Z\alpha)G_{\mathcal{P}}^{(4)}(Z\alpha) + B_{62}(Z\alpha)^2 \ln^2(Z\alpha)^{-2} \quad (\text{A38})$$

for nS states, by

$$B_{40} + B_{62}(Z\alpha)^2 \ln^2(Z\alpha)^{-2} \quad (\text{A39})$$

for nP states, and by

$$B_{40} \quad (\text{A40})$$

for states with $l > 1$. As in the case of the order- α self-energy and vacuum polarization contributions, the dominant effect of the finite mass of the nucleus is taken into account by multiplying each term of the two-photon contribution by the reduced-mass factor $(m_r/m_e)^3$, except that the magnetic moment term, Eq. (A25), is instead multiplied by the factor $(m_r/m_e)^2$. In addition, the argument $(Z\alpha)^{-2}$ of the logarithms is replaced by $(m_e/m_r)(Z\alpha)^{-2}$.

The uncertainties associated with the two-photon corrections in addition to those given in Eqs. (A30) and (A35) are as follows:

nS states: The leading uncalculated term is the constant C in B_{62} [see Eq. (A36)]. Based on the relative magnitudes of the coefficients of the power series of the one-photon self energy and the calculated coefficients of the two-photon corrections, we take $C=0$ with $u_0(C)=5$. We expect that this will also account for the uncertainties $u_0(B_{61})$ and $u_0(B_{60})$ due to the fact that the coefficients B_{61} and B_{60} are uncalculated. Thus we have $u_0(B_{62}) = \frac{80}{9}$ and $u_n(B_{62}) = 0$. (In general, we shall assume that a reasonable estimate for the uncertainty of the first uncalculated term is sufficiently large to account for the uncertainty of higher-order terms, which is consistent with the known results for the one-photon diagrams.) The first two-photon component of uncertainty of the type u_n evidently is $u_n(B_{61})$. As suggested by the value of the difference $B_{62}(n=1) - B_{62}(n=2) = \frac{16}{9} \ln 2 - \frac{7}{3} = -1.1 \dots$, and the pattern of values of the one-photon power-series coefficients, we take $u_n(B_{61}) = 2$ for this component of uncertainty. The uncertainty of the two-photon contribution is by far the dominant uncertainty for the 1S state: $u_0/h = 89$ kHz and $u_n/h = 2$ kHz.

nP states: Based on the calculated value for B_{62} in Eq. (A37) and the one-photon power-series pattern, we take $u_0(B_{61}) = 0.2$ and $u_n(B_{61}) = 0.02$.

nD states: Because there is no information regarding B_{62} for D states, we simply take the P-state values as uncertainties for the corresponding D-state uncertainties: $u_0(B_{62}) = 0.1$ and $u_n(B_{62}) = 0.01$.

7. Three-Photon Corrections

Corrections from three virtual photons, of order α^3 , have not been calculated, although an isolated term has been considered (Eides and Grotch, 1995a). Presumably they take the form

$$E^{(6)} = \left(\frac{\alpha}{\pi} \right)^3 \frac{(Z\alpha)^4}{n^3} m_e c^2 [T_{40} + \dots], \quad (\text{A41})$$

in analogy with the two-photon corrections. To account for such uncalculated terms, we take T_{40} to be zero but with standard uncertainties $u_0(T_{40}) = 1$ and $u_n(T_{40}) = 0.01$, based on the values of the one- and two-photon contributions. These values are taken for all states, because the two-photon contribution is comparable for all states.

8. Finite Nuclear Size

At low Z , the leading contribution due to the finite size of the nucleus is

$$E_{\text{NS}}^{(0)} = \mathcal{E}_{\text{NS}} \delta_{l0}, \quad (\text{A42})$$

where

$$\mathcal{E}_{\text{NS}} = \frac{2}{3} \left(\frac{m_r}{m_e} \right)^3 \frac{(Z\alpha)^2}{n^3} m_e c^2 \left(\frac{Z\alpha R_N}{\lambda_C} \right)^2; \quad (\text{A43})$$

R_N is the bound-state root-mean-square (rms) charge radius of the nucleus and λ_C is the Compton wavelength of the electron divided by 2π . The bound-state rms charge radius R_N is defined by the formulation in this Appendix and, except for the proton, differs from the scattering rms charge radius r_N . (The difference in the conventional definitions of r_N for the proton and deuteron and its significance is discussed later in this section.) The leading higher-order contributions have been examined by Friar (1979b) with the following results:

For S states the total contribution is

$$E_{\text{NS}} = \mathcal{E}_{\text{NS}}(1 + \eta + \theta), \quad (\text{A44})$$

where η is a correction of nonrelativistic origin and θ is a relativistic correction. Friar (1979b) gives general expressions for these corrections in terms of various moments of the nuclear charge distribution. The values of the corrections depend only weakly on the model assumed for the distribution. The expressions for η and θ are

$$\eta = -C_\eta \frac{m_r}{m_e} \frac{Z\alpha R_N}{\lambda_C} \quad (\text{A45})$$

and

$$\theta = \theta_0 + \theta_n, \quad (\text{A46})$$

where

$$\theta_0 = (Z\alpha)^2 \left[-\ln \left(\frac{m_r}{m_e} \frac{Z\alpha R_N}{\lambda_C} \right) + C_\theta \right] \quad (\text{A47})$$

and

$$\theta_n = (Z\alpha)^2 \left[\ln n - \psi(n) - \gamma + \frac{(5n+9)(n-1)}{4n^2} \right]. \quad (\text{A48})$$

In the latter expression, $\gamma = 0.577215\dots$ is Euler's constant. The quantities C_η and C_θ are numerical constants that contain all of the model dependence. The term θ_0 is independent of n and gives the largest correction due to the model-independent logarithm. The n -dependent term θ_n is model independent. This latter term has been confirmed by Karshenboim (1997a).

For hydrogen we assume a Gaussian charge distribution for the proton, which gives

$$C_\eta = \frac{16}{3\sqrt{3}\pi} \approx 1.7 \quad (\text{A49})$$

$$C_\theta = 0.465457\dots \quad (\text{A50})$$

The variations of C_η and C_θ are less than 0.16 and 0.06, respectively, between the Gaussian distribution and either the uniform or the exponential distribution. For deuterium we take the results given by Friar and Payne (1997b), which lead to (Friar, 1998)

$$C_\eta = 2.0 \quad (\text{A51})$$

$$C_\theta = 0.383(3), \quad (\text{A52})$$

where the uncertainty of C_θ simply indicates the spread in values resulting from various potential models for the deuteron.

For the $P_{1/2}$ states in hydrogen we have (Friar, 1979b)

$$E_{\text{NS}} = \mathcal{E}_{\text{NS}} \frac{(Z\alpha)^2(n^2 - 1)}{4n^2}. \quad (\text{A53})$$

For $P_{3/2}$ states and D states the nuclear-size contribution is negligible.

As alluded to above, the conventional definitions of the scattering rms charge radius r_p of the proton and r_d of the deuteron differ. For hydrogen, the nuclear-size effects are evaluated with

$$R_p = r_p. \quad (\text{A54})$$

However, in the case of the deuteron, the Darwin–Foldy (DF) contribution

$$E_{\text{DF}} = -\frac{(Z\alpha)^4 m_r^3 c^2}{2n^3 m_N^2} \delta_{l0}, \quad (\text{A55})$$

which appears as the term proportional to δ_{l0} in Eq. (A3), is included in the definition of r_d (Friar *et al.*, 1997). Consequently, for deuterium the nuclear-size effects can be evaluated with

$$R_d = \sqrt{r_d^2 + \frac{3}{4} \left(\frac{m_e}{m_d} \right)^2 \lambda_C^2} \quad (\text{A56})$$

to avoid double counting of the DF contribution. Alternatively, one could take R_d equal to r_d and omit the DF term in Eq. (A3). We take the former approach in the 1998 adjustment, because it is consistent with the existing atomic physics bound-state literature and with a nuclear-size contribution to energy levels that vanishes for a finite-mass point nucleus.

The uncertainty in the finite nuclear-size contribution, apart from that of the value of R_N , is assigned as follows:

nS states: The uncertainty associated with the model dependence of the nuclear charge distribution gives the largest contribution of type u_0 . For hydrogen, a reasonable estimate is $u_0(C_\eta) = 0.1$ and $u_0(C_\theta) = 0.04$ based on the difference between the Gaussian and uniform models. For deuterium, as noted by Friar and Payne (1997b), the uncertainty quoted for C_θ could be larger than the value in Eq. (A52) if various aspects of the charge distribution model of the deuteron were changed. To allow for this variation, we consider the uncertainties $u_0(C_\eta)$ and $u_0(C_\theta)$ to be the same for deuterium as

for hydrogen. However, the uncertainty arising from these values of u_0 as well as from omitted higher-order uncalculated terms, such as $\frac{1}{2}\theta_0^2$, is negligible. Because θ_n is model independent, the uncertainty u_n is due entirely to omitted higher-order uncalculated terms. Nevertheless, since such terms are negligible at the current level of interest, we take $u_n=0$ in both hydrogen and deuterium.

$nP_{1/2}$ states: The expression for the $nP_{1/2}$ -state contribution given in Eq. (A53) has no model dependence, and omitted higher-order uncalculated terms are negligible. We therefore take $u_0=u_n=0$.

In summary, the uncertainty of the nuclear-size contribution, apart from that due to the rms radius of the nucleus, is negligible.

9. Nuclear-Size Correction to Self Energy and Vacuum Polarization

In addition to the direct effect of finite nuclear size on energy levels, its effect on the previously discussed self energy and vacuum polarization contributions must also be considered.

For the self energy, the additional contribution due to the finite size of the nucleus is (Eides and Grotch, 1997b; Pachucki, 1993c)

$$E_{NSE} = a \frac{3}{2} \alpha(Z\alpha) \mathcal{E}_{NS} \delta_{l0}, \quad (A57)$$

where $a = -1.985(1)$, and for the vacuum polarization it is (Friar, 1979a)

$$E_{NVP} = \frac{3}{4} \alpha(Z\alpha) \mathcal{E}_{NS} \delta_{l0}. \quad (A58)$$

The contribution E_{NSE} is consistent with an extrapolation to $Z=0$ of the numerical results of Mohr and Soff (1993), and E_{NVP} has been obtained independently by Hylton (1985) and Eides and Grotch (1997b). These contributions are sufficiently small that their uncertainties may be ignored. The contributions are negligible for P and D states.

10. Radiative-Recoil Corrections

The dominant effect of nuclear motion on the self energy and vacuum polarization has been taken into account by including appropriate reduced-mass factors. The additional contributions over and above this prescription are termed radiative-recoil effects. The leading such term has been considered by Bhatt and Grotch (1987) and by Pachucki (1995), but the two results are not in complete agreement. In this article we employ the more recent result of Pachucki (1995),

$$E_{RR} = -1.36449(1) \alpha \frac{(Z\alpha)^5}{n^3} \frac{m_e}{m_N} m_e c^2 \delta_{l0}, \quad (A59)$$

which incorporated a number of crosschecks because of the disagreement. One of the small corrections included by Pachucki (1995) but not by Bhatt and Grotch (1987) has been confirmed by Eides and Grotch (1995b). (As indicated by the factor δ_{l0} , this contribution is zero for all states with $l \geq 1$.)

For the uncertainty, we take the next term, which is of relative order $Z\alpha$, with numerical coefficients 100 for u_0 and 10 for u_n . These coefficients are roughly what one would expect for the higher-order uncalculated terms, where the large coefficients arise from terms of order $\ln^2(Z\alpha)^{-2}$ and $\ln(Z\alpha)^{-2}$. We note that this uncertainty estimate is larger than the difference between the results of Bhatt and Grotch (1987) and Pachucki (1995).

11. Nucleus Self Energy

An additional contribution due to the self energy of the nucleus has been given by Pachucki (1995):

$$E_{SEN} = \frac{4Z^2 \alpha(Z\alpha)^4}{3\pi n^3} \frac{m_r^3}{m_N^2} c^2 \times \left[\ln \left(\frac{m_N}{m_r(Z\alpha)^2} \right) \delta_{l0} - \ln k_0(n, l) \right]. \quad (A60)$$

Although we include this term in our calculation, we essentially take the term itself as its uncertainty, $\sqrt{u_0^2 + u_n^2/n^3} = |E_{SEN}|$, where $u_n = |E_{SEN}(1S) - 8E_{SEN}(2S)|$ for $l=0$, $u_n = |8E_{SEN}(2P) - 27E_{SEN}(3P)|$ for $l=1$, and $u_n = |27E_{SEN}(3D) - 64E_{SEN}(4D)|$ for $l=2$. The reasons for assigning such a large uncertainty include the fact that this term is associated with the definition of the rms charge radius of the nucleus, and there is ambiguity in the definition of the radius at the level of the second term in Eq. (A60). Further, there are the questions of whether, in the case of the deuteron, m_N should be the mass of the deuteron or of the proton and whether this contribution can be treated without regard to nuclear polarization (Friar, 1998).

12. Total Energy and Uncertainty

The total energy E_{nLj}^X of a particular level (where $L=S, P, \dots$ and $X=H, D$) is just the sum of the various contributions listed above plus an additive correction δ_{nLj}^X that accounts for the uncertainty in the theoretical expression for E_{nLj}^X . Our theoretical estimate of the value of δ_{nLj}^X for a particular level is zero with a standard uncertainty of $u(\delta_{nLj}^X)$ equal to the square root of the sum of the squares of the individual uncertainties of the contributions, since, as they are defined above, the contributions to the energy of a given level are independent. (Components of uncertainty associated with the fundamental constants are not included here, because they are determined by the least-squares adjustment itself.) Thus we have

$$u^2(\delta_{nLj}^X) = \sum_i \frac{u_{0i}^2(XLj) + u_{ni}^2(XLj)}{n^6}, \quad (A61)$$

where the individual values $u_{0i}(XLj)$ and $u_{ni}(XLj)$ are enumerated in the sections above (denoted there simply as u_0 and u_n).

The covariance of any two δ 's follows from Eq. (F7) of Appendix F and for a given isotope X is

$$u(\delta_{n_1 L j}^X, \delta_{n_2 L j}^X) = \sum_i \frac{u_{0i}^2(XLj)}{(n_1 n_2)^3}. \quad (\text{A62})$$

For covariances between δ 's for hydrogen and deuterium, we have for states of the same n

$$\begin{aligned} u(\delta_{n L j}^H, \delta_{n L j}^D) \\ = \sum_{i=i_c} \frac{u_{0i}(\text{HL}j)u_{0i}(\text{DL}j) + u_{ni}(\text{HL}j)u_{ni}(\text{DL}j)}{n^6}, \end{aligned} \quad (\text{A63})$$

and for $n_1 \neq n_2$

$$u(\delta_{n_1 L j}^H, \delta_{n_2 L j}^D) = \sum_{i=i_c} \frac{u_{0i}(\text{HL}j)u_{0i}(\text{DL}j)}{(n_1 n_2)^3}, \quad (\text{A64})$$

where the summation is over the uncertainties common to hydrogen and deuterium. In most cases, the uncertainties can in fact be viewed as common except for a known multiplicative factor that contains all of the mass dependence. We assume that $u(\delta_{n_1 L j}^X, \delta_{n_2 L' j'}^{X'})$ is negligible if $L \neq L'$ or $j \neq j'$.

The values of $u(\delta_{n L j}^X)$ of interest for the 1998 adjustment are given in Table 14.A.1 of Sec. 4., and the nonnegligible covariances of the δ 's are given in the form of correlation coefficients in Table 14.A.2 of that section. These coefficients are as large as 0.999.

Since the transitions between levels are measured in frequency units (Hz), in order to apply the above equations for the energy level contributions we divide the theoretical expression for the energy difference ΔE of the transition by the Planck constant h to convert it to a frequency. Further, since we take the Rydberg constant $R_\infty = \alpha^2 m_e c^2 / 2h$ (expressed in m^{-1}) rather than the electron mass m_e to be an adjusted constant, we replace the group of constants $\alpha^2 m_e c^2 / 2h$ in $\Delta E/h$ by cR_∞ .

13. Transition Frequencies Between Levels with $n=2$

As an indication of the consistency of the theory summarized above and the experimental data, we list values of the transition frequencies between levels with $n=2$ in hydrogen. These results are based on values of the constants obtained in a variation of the 1998 least-squares adjustment in which the measurements of the directly related transitions (items A13, A14.1, and A14.2 in Table 14.A.1) are not included. The results are

$$\begin{aligned} \nu_H(2P_{1/2} - 2S_{1/2}) &= 1\,057\,844.9(3.2) \text{ kHz} \quad [3.0 \times 10^{-6}] \\ \nu_H(2S_{1/2} - 2P_{3/2}) &= 9\,911\,196.3(3.2) \text{ kHz} \quad [3.2 \times 10^{-7}] \\ \nu_H(2P_{1/2} - 2P_{3/2}) &= 10\,969\,041.2(1.5) \text{ kHz} \quad [1.4 \times 10^{-7}], \end{aligned} \quad (\text{A65})$$

which agree well with the relevant experimental results of that table. The uncertainty of the Lamb shift $\nu_H(2P_{1/2} - 2S_{1/2})$ obtained this way is about an order of magnitude smaller

than the theoretical uncertainty of the $2S_{1/2}$ level itself, because the experimental information reduces the uncertainty of $\delta_{2S_{1/2}}^H$.

Appendix B. Theory of Electron Magnetic Moment Anomaly

This Appendix gives a brief summary of the current theory of a_e , the magnetic moment anomaly of the electron. A summary of the theory of a_μ , the muon anomaly, is given in Appendix C. As indicated in Sec. 3.3.1, Eq. (65), a_e is defined according to

$$a_e = \frac{|g_e| - 2}{2} = \frac{|\mu_e|}{\mu_B} - 1. \quad (\text{B1})$$

The theoretical expression for a_e may be written as

$$a_e(\text{th}) = a_e(\text{QED}) + a_e(\text{weak}) + a_e(\text{had}), \quad (\text{B2})$$

where the terms denoted by QED, weak, and had account for the purely quantum electrodynamic, predominantly electroweak, and predominantly hadronic (i.e., strong interaction) contributions to a_e , respectively. The QED contribution may be written as (Kinoshita, Nižić, and Okamoto, 1990)

$$\begin{aligned} a_e(\text{QED}) &= A_1 + A_2(m_e/m_\mu) + A_2(m_e/m_\tau) \\ &\quad + A_3(m_e/m_\mu, m_e/m_\tau). \end{aligned} \quad (\text{B3})$$

The term A_1 is mass independent and the other terms are functions of the indicated mass ratios. For these terms the lepton in the numerator of the mass ratio is the particle under consideration, while the lepton in the denominator of the ratio is the virtual particle that is the source of the vacuum polarization that gives rise to the term.

Each of the four terms on the right-hand side of Eq. (B3) is expressed as a power series in the fine-structure constant α :

$$\begin{aligned} A_i &= A_i^{(2)} \left(\frac{\alpha}{\pi} \right) + A_i^{(4)} \left(\frac{\alpha}{\pi} \right)^2 + A_i^{(6)} \left(\frac{\alpha}{\pi} \right)^3 \\ &\quad + A_i^{(8)} \left(\frac{\alpha}{\pi} \right)^4 + \cdots. \end{aligned} \quad (\text{B4})$$

The fine-structure constant α is proportional to the square of the elementary charge e , so the order of a term containing $(\alpha/\pi)^n$ is $2n$ and its coefficient is called the $2n$ th-order coefficient.

The second-order coefficient $A_1^{(2)}$, which is the leading coefficient in $a_e(\text{QED})$, arises from one Feynman diagram and is the famous Schwinger term (Schwinger, 1948; Schwinger, 1949):

$$A_1^{(2)} = \frac{1}{2}. \quad (\text{B5})$$

The fourth-order coefficient $A_1^{(4)}$ arises from seven diagrams and has been known analytically for about 40 years (Sommerfield, 1957; Petermann, 1957; Sommerfield, 1958; Petermann, 1958):

$$A_1^{(4)} = \frac{3\zeta(3)}{4} - \frac{\pi^2 \ln 2}{2} + \frac{\pi^2}{12} + \frac{197}{144} \\ = -0.328\,478\,965\,579 \dots, \quad (\text{B6})$$

where $\zeta(n)$ is the Riemann zeta function of argument n .

The sixth-order coefficient $A_1^{(6)}$ arises from 72 diagrams and is now also known analytically after nearly 30 years of effort by many researchers [see Roskies, Remiddi, and Levine (1990) for a review of the early work]. It was not until 1996 that the last three remaining distinct diagrams were calculated analytically, thereby completing the theoretical expression for $A_1^{(6)}$. The final result is

$$A_1^{(6)} = \frac{100a_4}{3} - \frac{215\zeta(5)}{24} + \frac{83\pi^2\zeta(3)}{72} + \frac{139\zeta(3)}{18} \\ + \frac{25\ln^4 2}{18} - \frac{25\pi^2 \ln^2 2}{18} - \frac{298\pi^2 \ln 2}{9} - \frac{239\pi^4}{2160} \\ + \frac{17101\pi^2}{810} + \frac{28259}{5184} \\ = 1.181\,241\,456 \dots, \quad (\text{B7})$$

where $a_4 = \sum_{n=1}^{\infty} 1/(2^n n^4) = 0.517\,479\,061 \dots$. Recent work leading to this expression has been carried out by Laporta and Remiddi (1991); Laporta (1993c); Laporta (1995); Laporta and Remiddi (1995); and Laporta and Remiddi (1996).

A total of 891 Feynman diagrams give rise to the eighth-order coefficient $A_1^{(8)}$, and only a few of these are known analytically. However, in a major effort begun in the 1970s, Kinoshita and collaborators have calculated $A_1^{(8)}$ numerically [see Kinoshita (1990) for a review of the early work]. The current best estimate of this coefficient reported by Kinoshita is (Kinoshita, 1998; Hughes and Kinoshita, 1999)

$$A_1^{(8)} = -1.5098(384). \quad (\text{B8})$$

This value differs from $A_1^{(8)} = -1.4092(384)$ reported previously (Kinoshita, 1996; Kinoshita, 1997), but it is believed to be more accurate because of a significant increase in the number of integration points used in the calculation. Kinoshita has retained the uncertainty of the earlier result in the new result despite the higher accuracy of the calculations on which the new result is based, pending his completion of a more precise error analysis. Note that the numerical results agree with the analytic results for those few eighth-order diagrams that are known analytically. Further, the same numerical techniques used to evaluate the eighth-order diagrams have been used to evaluate all fourth- and sixth-order diagrams, and good agreement with the corresponding analytic results is found. For example, the numerical results obtained by Kinoshita (1995) for eight subgroups, consisting of 50 out of the 72 diagrams that give rise to $A_1^{(6)}$, are in good agreement with the corresponding analytic results.

To place in perspective the contributions to $a_e(\text{th})$ of $A_1^{(8)}$ and other relatively small terms discussed in the remainder of this Appendix, we recall that the most accurate experi-

mental value of a_e has a standard uncertainty of $4.2 \times 10^{-12} = 3.7 \times 10^{-9} a_e$ [see Eq. (68), Sec. 3.3.1] and note that $(\alpha/\pi)^4 = 29 \times 10^{-12} = 25 \times 10^{-9} a_e$. Thus the 0.0384 standard uncertainty of $A_1^{(8)}$ contributes a standard uncertainty to $a_e(\text{th})$ of $1.1 \times 10^{-12} = 0.96 \times 10^{-9} a_e$.

Little is known about the tenth-order coefficient $A_1^{(10)}$ and higher-order coefficients. However, since $(\alpha/\pi)^5 = 0.068 \times 10^{-12} = 0.058 \times 10^{-9} a_e$, $A_1^{(10)}$ and higher coefficients are not yet a major concern. To evaluate the contribution to the uncertainty of $a_e(\text{th})$ due to lack of knowledge of $A_1^{(10)}$, we assume that the probable error (50 % confidence level) is equal to the absolute value of $A_1^{(10)}$ as roughly estimated by $|(A_1^{(8)}/A_1^{(6)})A_1^{(8)}| = 1.9$. For a normal distribution this corresponds to a standard uncertainty of 2.9, and hence we take $A_1^{(10)} = 0.0(2.9)$ to calculate $a_e(\text{th})$. Because the 2.9 standard uncertainty of $A_1^{(10)}$ contributes a standard uncertainty component to $a_e(\text{th})$ of only $0.19 \times 10^{-12} = 0.17 \times 10^{-9} a_e$, the uncertainty contributions to $a_e(\text{th})$ from all other higher-order coefficients are assumed to be negligible.

The lowest-order nonvanishing mass-dependent coefficient is $A_2^{(4)}(x)$, where x denotes either m_e/m_μ or m_e/m_τ , as indicated in Eq. (B3). A complete series expansion for $A_2^{(4)}(x)$ in powers of x and $\ln x$ ($x < 1$) is known (Samuel and Li, 1991; Li, Mendel, and Samuel, 1993; Czarnecki and Skrzypek, 1999). Evaluation of the power series using the 1998 recommended values of the mass ratios yields

$$A_2^{(4)}(m_e/m_\mu) = 5.197\,387\,62(32) \times 10^{-7} \quad (\text{B9})$$

$$A_2^{(4)}(m_e/m_\tau) = 1.837\,50(60) \times 10^{-9}, \quad (\text{B10})$$

where the standard uncertainties are due to the uncertainties of the mass ratios. To place these coefficients in perspective, we note that their contributions to $a_e(\text{th})$ are

$$A_2^{(4)}(m_e/m_\mu) \left(\frac{\alpha}{\pi} \right)^2 = 2.804 \times 10^{-12} \\ = 2.418 \times 10^{-9} a_e \\ A_2^{(4)}(m_e/m_\tau) \left(\frac{\alpha}{\pi} \right)^2 = 0.010 \times 10^{-12} \\ = 0.009 \times 10^{-9} a_e. \quad (\text{B11})$$

These contributions are so small that the uncertainties of the mass ratios are not significant. This statement also applies to all other mass-dependent contributions to $a_e(\text{th})$.

The next coefficient in the series is $A_2^{(6)}(x)$. It is known in terms of a series expansion in x with a sufficient number of powers of x to ensure that the omitted terms are negligible (Laporta, 1993b; Laporta and Remiddi, 1993). Using the 1998 recommended values of the mass ratios, one obtains

$$A_2^{(6)}(m_e/m_\mu) = -7.373\,942\,53(33) \times 10^{-6} \\ A_2^{(6)}(m_e/m_\tau) = -6.5815(19) \times 10^{-8}. \quad (\text{B12})$$

To put these coefficients in perspective, we note that

$$\begin{aligned}
A_2^{(6)}(m_e/m_\mu) \left(\frac{\alpha}{\pi}\right)^3 &= -0.092 \times 10^{-12} \\
&= -0.080 \times 10^{-9} a_e \\
A_2^{(6)}(m_e/m_\tau) \left(\frac{\alpha}{\pi}\right)^3 &= -0.001 \times 10^{-12} \\
&= -0.001 \times 10^{-9} a_e. \quad (\text{B13})
\end{aligned}$$

In view of the smallness of these contributions, the next coefficient in the series, $A_2^{(8)}(x)$, as well as higher-order coefficients, may be ignored.

The lowest-order nonvanishing coefficient in the term $A_3(m_e/m_\mu, m_e/m_\tau)$ is $A_3^{(6)}(m_e/m_\mu, m_e/m_\tau)$. Evaluating the expression for this coefficient (Lautrup, 1977; Samuel and Li, 1991) by numerical integration using the 1998 recommended values of the mass ratios, we obtain

$$A_3^{(6)}(m_e/m_\mu, m_e/m_\tau) = 1.91 \times 10^{-13}. \quad (\text{B14})$$

The contribution of this coefficient to $a_e(\text{th})$ is $2.4 \times 10^{-21} = 2.1 \times 10^{-18} a_e$, which is so small that it may be ignored. Higher-order coefficients in this series may, of course, also be ignored.

The calculation of electroweak and hadronic contributions to lepton magnetic moment anomalies initially focused on the muon rather than the electron, because the contributions are significantly larger and thus of greater importance for heavier leptons. We therefore discuss them in greater detail in the following Appendix, which deals with the theory of a_μ . Here we simply give the results as they apply to the electron.

For the electroweak contribution we have

$$\begin{aligned}
a_e(\text{weak}) &= \frac{G_F m_e^2}{8\pi^2 \sqrt{2}} \frac{5}{3} \\
&\quad \times \left[1 + \frac{1}{5} (1 - 4 \sin^2 \theta_W)^2 + C \frac{\alpha}{\pi} + \dots \right] \\
&= 0.0297(7) \times 10^{-12} \\
&= 0.0256(6) \times 10^{-9} a_e, \quad (\text{B15})
\end{aligned}$$

where G_F is the Fermi coupling constant; θ_W is the weak mixing angle with $\sin^2 \theta_W = 1 - (m_W/m_Z)^2$, where m_W/m_Z is the ratio of the mass of the W^\pm to the mass of the Z^0 ; and $C = -150$ as calculated by Czarnecki *et al.* (1996) and accounts for two-loop contributions to $a_e(\text{weak})$. The quoted standard uncertainty is taken to be the 3×10^{-11} uncertainty of the electroweak contribution to $a_\mu(\text{th})$ multiplied by the factor $(m_e/m_\mu)^2$, since $a_\mu(\text{weak})$ varies approximately as m_μ^2 . In obtaining the numerical value of $a_e(\text{weak})$, we have used the 1998 recommended values of the relevant constants that appear in Eq. (B15). Clearly, $a_e(\text{weak})$ is not yet a significant contribution to $a_e(\text{th})$.

The hadronic contribution is

$$\begin{aligned}
a_e(\text{had}) &= 1.631(19) \times 10^{-12} \\
&= 1.407(17) \times 10^{-9} a_e \quad (\text{B16})
\end{aligned}$$

and is the sum of the following three contributions: $a_e^{(4)}(\text{had}) = 1.875(18) \times 10^{-12}$ obtained by Davier and Höcker (1998b); $a_e^{(6a)}(\text{had}) = -0.225(5) \times 10^{-12}$ given by Krause (1997); and $a_e^{(\gamma\gamma)}(\text{had}) = -0.0185(36) \times 10^{-12}$ obtained by multiplying the corresponding result for the muon of Hayakawa and Kinoshita (1998) by the factor $(m_e/m_\mu)^2$, since $a_\mu^{(\gamma\gamma)}(\text{had})$ is assumed to vary approximately as m_μ^2 . The contribution $a_e(\text{had})$, although larger than $a_e(\text{weak})$, is not yet of major significance.

For our least-squares adjustment, we require $a_e(\text{th})$ as a function of α . Since the dependence on α of any contribution other than $a_e(\text{QED})$ is negligible, we obtain a convenient form for the function by combining terms in $a_e(\text{QED})$ that have like powers of α/π . This leads to the following summary of the above results:

$$a_e(\text{th}) = a_e(\text{QED}) + a_e(\text{weak}) + a_e(\text{had}), \quad (\text{B17})$$

where

$$\begin{aligned}
a_e(\text{QED}) &= C_e^{(2)} \left(\frac{\alpha}{\pi}\right) + C_e^{(4)} \left(\frac{\alpha}{\pi}\right)^2 + C_e^{(6)} \left(\frac{\alpha}{\pi}\right)^3 \\
&\quad + C_e^{(8)} \left(\frac{\alpha}{\pi}\right)^4 + C_e^{(10)} \left(\frac{\alpha}{\pi}\right)^5 + \dots, \quad (\text{B18})
\end{aligned}$$

with

$$\begin{aligned}
C_e^{(2)} &= 0.5 \\
C_e^{(4)} &= -0.328\,478\,444\,00 \\
C_e^{(6)} &= 1.181\,234\,017 \\
C_e^{(8)} &= -1.5098(384) \\
C_e^{(10)} &= 0.0(2.9), \quad (\text{B19})
\end{aligned}$$

and where

$$a_e(\text{weak}) = 0.030(1) \times 10^{-12} \quad (\text{B20})$$

and

$$a_e(\text{had}) = 1.631(19) \times 10^{-12}. \quad (\text{B21})$$

The standard uncertainty of $a_e(\text{th})$ from the uncertainties of the terms listed above, other than that due to α , is

$$u[a_e(\text{th})] = 1.1 \times 10^{-12} = 1.0 \times 10^{-9} a_e. \quad (\text{B22})$$

It is dominated by the uncertainty of the coefficient $C_e^{(8)}$. In fact, if $C_e^{(8)}$ were exactly known, the standard uncertainty of $a_e(\text{th})$ would be only $0.19 \times 10^{-12} = 0.17 \times 10^{-9} a_e$. (Note that the uncertainties of $C_e^{(4)}$ and $C_e^{(6)}$ are beyond the digits shown and contribute negligible components of uncertainty to $u[a_e(\text{th})]$.)

For the purpose of the least-squares calculations carried out in Sec. 4, we define an additive correction δ_e to $a_e(\text{th})$ to account for the lack of exact knowledge of $a_e(\text{th})$, and hence the complete theoretical expression for the electron anomaly is

$$a_e(\alpha, \delta_e) = a_e(\text{th}) + \delta_e. \quad (\text{B23})$$

Our theoretical estimate of δ_e is zero and its standard uncertainty is $u[a_e(\text{th})]$:

$$\delta_e = 0.0(1.1) \times 10^{-12}. \quad (\text{B24})$$

Appendix C. Theory of Muon Magnetic Moment Anomaly

This Appendix gives a brief summary of the current theory of the magnetic moment anomaly of the muon a_μ . A similar summary of the theory of the electron anomaly a_e is given in Appendix B. [For a review of the early work on the theory of a_μ , see Kinoshita and Marciano (1990).] As indicated in Sec. 3.3.10, Eq. (162), a_μ is defined according to

$$a_\mu = \frac{|g_\mu| - 2}{2} = \frac{|\mu_\mu|}{e\hbar/2m_\mu} - 1. \quad (\text{C1})$$

As for the electron, the theoretical expression for a_μ may be written as

$$a_\mu(\text{th}) = a_\mu(\text{QED}) + a_\mu(\text{weak}) + a_\mu(\text{had}), \quad (\text{C2})$$

where the terms denoted by QED, weak, and had account for the purely quantum electrodynamic, predominantly electroweak, and predominantly hadronic (i.e., strong interaction) contributions to a_μ , respectively. Also in the same manner as for the electron, the QED contribution may be written as (Kinoshita *et al.*, 1990)

$$a_\mu(\text{QED}) = A_1 + A_2(m_\mu/m_e) + A_2(m_\mu/m_\tau) + A_3(m_\mu/m_e, m_\mu/m_\tau). \quad (\text{C3})$$

The mass-dependent terms are a function of the indicated mass ratios, and we again note that for these terms the lepton in the numerator of the mass ratio is the particle under consideration, while the lepton in the denominator of the ratio is the virtual particle that is the source of the vacuum polarization that gives rise to the term.

As for the electron, each of the four terms on the right-hand side of Eq. (C3) is expressed as a power series in the fine-structure constant α :

$$A_i = A_i^{(2)}\left(\frac{\alpha}{\pi}\right) + A_i^{(4)}\left(\frac{\alpha}{\pi}\right)^2 + A_i^{(6)}\left(\frac{\alpha}{\pi}\right)^3 + A_i^{(8)}\left(\frac{\alpha}{\pi}\right)^4 + \dots \quad (\text{C4})$$

The mass-independent term A_1 , which is given in Appendix B, is the same for all three charged leptons. The standard uncertainty of A_1 is $0.11 \times 10^{-11} = 0.097 \times 10^{-8} a_\mu$. To place this uncertainty in perspective, as well as the values and uncertainties of other contributions to $a_\mu(\text{th})$ discussed in this Appendix, we note that the standard uncertainty of $a_\mu(\text{th})$ is currently dominated by the $64 \times 10^{-11} = 55 \times 10^{-8} a_\mu$ uncertainty of $a_\mu(\text{had})$, and it will be a challenge to reduce the uncertainty of $a_\mu(\text{had})$ by as much as a factor of 10 (Czarnecki and Krause, 1996). Further, the standard uncertainty of the most accurate experimental value of a_μ is $840 \times 10^{-11} = 720 \times 10^{-8} a_\mu$ [see Eq. (165), Sec. 3.3.10.a], and the goal of the new experiment underway at Brookhaven

National Laboratory is to reduce this uncertainty by a factor of about 20 (see Sec. 3.3.10.b), which would imply an uncertainty of about $40 \times 10^{-11} \approx 35 \times 10^{-8} a_\mu$.

As for the electron, the lowest-order nonvanishing mass-dependent coefficient is $A_2^{(4)}(x)$. In the case of the muon [see Eq. (C3)], x is either m_μ/m_e , which is greater than 1, or m_μ/m_τ , which is less than 1. A complete series expansion in powers of $1/x$ and $\ln x$ for $x > 1$ is known and, as indicated in Appendix B, a series expansion in x and $\ln x$ for $x < 1$ is also known (Samuel and Li, 1991; Li, Mendel, and Samuel, 1993; Czarnecki and Skrzypek, 1999). Evaluation of these power series using the 1998 recommended values of the mass ratios yields

$$A_2^{(4)}(m_\mu/m_e) = 1.094\,258\,2828(98) \quad (\text{C5})$$

$$A_2^{(4)}(m_\mu/m_\tau) = 0.000\,078\,059(25), \quad (\text{C6})$$

where the standard uncertainties are due to the uncertainties of the mass ratios. The contributions of these coefficients to $a_\mu(\text{th})$ are

$$\begin{aligned} A_2^{(4)}(m_\mu/m_e) \left(\frac{\alpha}{\pi}\right)^2 &= 590\,405.9860(53) \times 10^{-11} \\ &= 506\,387.5988(45) \times 10^{-8} a_\mu \\ A_2^{(4)}(m_\mu/m_\tau) \left(\frac{\alpha}{\pi}\right)^2 &= 42.117(14) \times 10^{-11} \\ &= 36.123(12) \times 10^{-8} a_\mu. \end{aligned} \quad (\text{C7})$$

(For comparisons of this type we use the 1998 recommended values of α and a_μ , but ignore their uncertainties.) For these terms, as well as all other mass-dependent terms, the uncertainties of the mass ratios are of no practical significance.

The next coefficient, $A_2^{(6)}(x)$, is known in terms of a series expansion in x , for both $x < 1$ and $x > 1$, with a sufficient number of powers of x to ensure that the omitted terms are negligible (Laporta, 1993b; Laporta and Remiddi, 1993). Using the 1998 recommended values of the mass ratios, one obtains

$$A_2^{(6)}(m_\mu/m_e) = 22.868\,379\,36(23) \quad (\text{C8})$$

$$A_2^{(6)}(m_\mu/m_\tau) = 0.000\,360\,54(21). \quad (\text{C9})$$

The contributions of these coefficients to $a_\mu(\text{th})$ are

$$\begin{aligned} A_2^{(6)}(m_\mu/m_e) \left(\frac{\alpha}{\pi}\right)^3 &= 28\,660.367\,33(29) \times 10^{-11} \\ &= 24\,581.821\,55(24) \times 10^{-8} a_\mu \\ A_2^{(6)}(m_\mu/m_\tau) \left(\frac{\alpha}{\pi}\right)^3 &= 0.451\,85(26) \times 10^{-11} \\ &= 0.387\,55(22) \times 10^{-8} a_\mu. \end{aligned} \quad (\text{C10})$$

The contribution of $A_2^{(6)}(m_\mu/m_\tau)$ to $a_\mu(\text{th})$ is sufficiently small that the contribution from the next coefficient in that series, which is $A_2^{(8)}(m_\mu/m_\tau)$, and from higher-order coeffi-

cients may be assumed to be negligible. This is not the case for the contribution of the next coefficient in the series $A_2^{(2n)}(m_\mu/m_e)$, which is $A_2^{(8)}(m_\mu/m_e)$. The calculation of this coefficient is based mainly on numerical evaluations by Kinoshita and co-workers of the corresponding 469 Feynman diagrams. The current best estimate is

$$A_2^{(8)}(m_\mu/m_e) = 127.50(41), \quad (\text{C11})$$

where the quoted uncertainty is due to the uncertainty of the numerical integrations. Recent work leading to Eq. (C11) has been carried out by Kinoshita *et al.* (1990); Kinoshita (1993); Laporta (1993a); and Baikov and Broadhurst (1995). The contribution of this coefficient to $a_\mu(\text{th})$ is

$$\begin{aligned} A_2^{(8)}(m_\mu/m_e) \left(\frac{\alpha}{\pi} \right)^4 &= 371.2(1.2) \times 10^{-11} \\ &= 318.3(1.0) \times 10^{-8} a_\mu. \end{aligned} \quad (\text{C12})$$

The contribution itself is significant, but its uncertainty is of little consequence.

An estimate of the next coefficient in the series, which is $A_2^{(10)}(m_\mu/m_e)$, is

$$A_2^{(10)}(m_\mu/m_e) = 930(170), \quad (\text{C13})$$

based on the work of Kinoshita *et al.* (1990) and Karshenboim (1993b). Its contribution to $a_\mu(\text{th})$ is

$$\begin{aligned} A_2^{(10)}(m_\mu/m_e) \left(\frac{\alpha}{\pi} \right)^5 &= 6.3(1.1) \times 10^{-11} \\ &= 5.4(1.0) \times 10^{-8} a_\mu. \end{aligned} \quad (\text{C14})$$

The contribution itself is of marginal significance, and its uncertainty is of little consequence. In view of the smallness of this contribution, it is assumed that higher-order coefficients in the series may be neglected.

In analogy with the electron, the lowest-order nonvanishing coefficient in the term $A_3(m_\mu/m_e, m_\mu/m_\tau)$ is $A_3^{(6)}(m_\mu/m_e, m_\mu/m_\tau)$. Evaluating the series expansion of Czarnecki and Skrzypek (1999) for this coefficient using the 1998 recommended values of the mass ratios, we obtain

$$A_3^{(6)}(m_\mu/m_e, m_\mu/m_\tau) = 0.000\,527\,63(17), \quad (\text{C15})$$

where the uncertainty is due mainly to the uncertainty of m_τ . This result is consistent with the evaluation of the analytic expression for $A_3^{(6)}(m_\mu/m_e, m_\mu/m_\tau)$ (Lautrup, 1977; Samuel and Li, 1991) by numerical integration. The contribution of this coefficient to $a_\mu(\text{th})$ is

$$\begin{aligned} A_3^{(6)}(m_\mu/m_e, m_\mu/m_\tau) \left(\frac{\alpha}{\pi} \right)^3 &= 0.661\,26(21) \times 10^{-11} \\ &= 0.567\,16(18) \times 10^{-8} a_\mu, \end{aligned} \quad (\text{C16})$$

which is of no practical consequence. Nevertheless, the next coefficient in the series has been estimated numerically. The result is (Kinoshita *et al.*, 1990)

$$A_3^{(8)}(m_\mu/m_e, m_\mu/m_\tau) = 0.079(3), \quad (\text{C17})$$

and its contribution to $a_\mu(\text{th})$ is

$$\begin{aligned} A_3^{(8)}(m_\mu/m_e, m_\mu/m_\tau) \left(\frac{\alpha}{\pi} \right)^4 &= 0.2300(87) \times 10^{-11} \\ &= 0.1973(75) \times 10^{-8} a_\mu, \end{aligned} \quad (\text{C18})$$

which again is of no practical consequence. In view of the smallness of this contribution, higher-order coefficients are assumed to be negligible.

The electroweak contribution to $a_\mu(\text{th})$ can be characterized by the number of closed loops in the relevant Feynman diagrams:

$$a_\mu(\text{weak}) = a_\mu^{(1\ell)}(\text{weak}) + a_\mu^{(2\ell)}(\text{weak}) + \cdots, \quad (\text{C19})$$

where 1ℓ indicates one loop, 2ℓ indicates two loops, etc. The dominant contribution to $a_\mu(\text{weak})$ arises from one-loop diagrams involving W and Z bosons; the contribution from the Higgs boson is negligible for any reasonable estimated value of its mass. The two-loop contribution is further divided into fermionic and bosonic contributions:

$$a_\mu^{(2\ell)}(\text{weak}) = a_\mu^{(2\ell)}(\text{ferm}) + a_\mu^{(2\ell)}(\text{bos}), \quad (\text{C20})$$

where $a_\mu^{(2\ell)}(\text{ferm})$ denotes the two-loop contribution arising from closed fermion loops, and $a_\mu^{(2\ell)}(\text{bos})$ denotes the remaining two-loop contribution.

The electroweak contribution may be written as (Czarnecki, Krause, and Marciano, 1995)

$$\begin{aligned} a_\mu(\text{weak}) &= \frac{G_F m_\mu^2}{8\pi^2 \sqrt{2}} \frac{5}{3} \\ &\times \left[1 + \frac{1}{5} (1 - 4 \sin^2 \theta_W)^2 + C \frac{\alpha}{\pi} + \cdots \right], \end{aligned} \quad (\text{C21})$$

where G_F is the Fermi coupling constant; θ_W is the weak mixing angle with $\sin^2 \theta_W = 1 - (m_W/m_Z)^2$, where m_W/m_Z is the ratio of the mass of the W^\pm to the mass of the Z^0 ; and the value $C = -97$ has been calculated by Czarnecki *et al.* (1996) and accounts for fermion and boson two-loop contributions to $a_\mu(\text{weak})$. Equation (C21) yields $a_\mu(\text{weak}) = 151(4) \times 10^{-11}$, where the standard uncertainty is that quoted by Czarnecki *et al.* (1996) and is due to uncertainties in the Higgs mass, quark two-loop effects, and possible three- or higher-loop contributions. In recent work, Degrandi and Giudice (1998) have calculated the dependence of the coefficients of the leading logarithmic terms of $a_\mu^{(2\ell)}(\text{ferm})$ on $\sin^2 \theta_W$ and the leading logarithmic terms of the three-loop contribution $a_\mu^{(3\ell)}(\text{ferm})$. These additional terms provide small corrections to the value of Czarnecki *et al.* (1996); the combined result is (Degrandi and Giudice, 1998)

$$\begin{aligned} a_\mu(\text{weak}) &= 153(3) \times 10^{-11} \\ &= 131(3) \times 10^{-8} a_\mu. \end{aligned} \quad (\text{C22})$$

[Other work related to $a_\mu(\text{weak})$ has been carried out by Kuraev, Kukhto, and Schiller (1990); Kukhto *et al.* (1992);

and Peris, Perrottet, and de Rafael (1995).] The electroweak contribution to $a_\mu(\text{th})$ is significant, but its uncertainty is of little consequence.

The hadronic contribution to $a_\mu(\text{th})$ may be written as

$$a_\mu(\text{had}) = a_\mu^{(4)}(\text{had}) + a_\mu^{(6a)}(\text{had}) + a_\mu^{(\gamma\gamma)}(\text{had}) + \cdots, \quad (\text{C23})$$

where $a_\mu^{(4)}(\text{had})$ and $a_\mu^{(6a)}(\text{had})$ arise from hadronic vacuum polarization and are of order $(\alpha/\pi)^2 \text{ had}$ and $(\alpha/\pi)^3$, respectively; and $a_\mu^{(\gamma\gamma)}(\text{had})$ arises from hadronic light-by-light vacuum polarization. [The a in the superscript of $a_\mu^{(6a)}(\text{had})$ indicates that not all of the sixth-order terms are included. Further, $a_\mu^{(\gamma\gamma)}(\text{had})$ is also of sixth order.]

The most accurate calculation of the contribution $a_\mu^{(4)}(\text{had})$ is that of Davier and Höcker (1998b) and is based on improved theory together with experimental data from both the production of hadrons in e^+e^- collisions and the decay of the τ into hadrons. Their result is

$$a_\mu^{(4)}(\text{had}) = 6924(62) \times 10^{-11}, \quad (\text{C24})$$

where the quoted standard uncertainty is due to uncertainties in both the theory and experimental data. This value, which is the one that we shall employ, is in agreement with but has a smaller uncertainty than earlier results, some of which were based on e^+e^- scattering data alone (Davier and Höcker, 1998a; Alemany, Davier, and Höcker, 1998; Alemany, 1997; Brown and Worstell, 1996; Jegerlehner, 1996; Eidelman and Jegerlehner, 1995).

For $a_\mu^{(6a)}(\text{had})$ we take the value calculated by Krause (1997),

$$a_\mu^{(6a)}(\text{had}) = -101(6) \times 10^{-11}. \quad (\text{C25})$$

This result is a refinement of the earlier estimate of Kinoshita, Nižić, and Okamoto (1985) and incorporates an improved theoretical method. Further, it is based on the analysis by Eidelman and Jegerlehner (1995) of the experimental data for the process $e^+e^- \rightarrow \text{hadrons}$, and that analysis includes more recent data than the earlier estimate.

For $a_\mu^{(\gamma\gamma)}(\text{had})$ we take the value

$$a_\mu^{(\gamma\gamma)}(\text{had}) = -79.2(15.4) \times 10^{-11}, \quad (\text{C26})$$

quoted by Hayakawa and Kinoshita (1998), which is consistent with but has a smaller uncertainty than the result $a_\mu^{(\gamma\gamma)}(\text{had}) = -92(32) \times 10^{-11}$ of Bijmans, Pallante, and Prades (1996). Both of these estimates include the effect of the η' meson in addition to the effects of the π^0 and η mesons in the diagram that makes the largest contribution to $a_\mu^{(\gamma\gamma)}(\text{had})$. These results may be compared to the estimate $a_\mu^{(\gamma\gamma)}(\text{had}) = -52(18) \times 10^{-11}$, which does not include the effect of the η' (Hayakawa, Kinoshita, and Sanda, 1996).

Adding Eqs. (C24), (C25), and (C26), one obtains

$$\begin{aligned} a_\mu(\text{had}) &= 6744(64) \times 10^{-11} \\ &= 5784(55) \times 10^{-8} a_\mu. \end{aligned} \quad (\text{C27})$$

Clearly, the uncertainty of $a_\mu(\text{had})$ is the dominant contribution to the uncertainty of $a_\mu(\text{th})$.

Following the same procedure as with $a_e(\text{th})$ in Appendix B, by adding terms in $a_\mu(\text{QED})$ that have like powers of α/π , including the results for A_1 given in that Appendix, we summarize the theory of a_μ as follows:

$$a_\mu(\text{th}) = a_\mu(\text{QED}) + a_\mu(\text{weak}) + a_\mu(\text{had}), \quad (\text{C28})$$

where

$$\begin{aligned} a_\mu(\text{QED}) &= C_\mu^{(2)} \left(\frac{\alpha}{\pi} \right) + C_\mu^{(4)} \left(\frac{\alpha}{\pi} \right)^2 + C_\mu^{(6)} \left(\frac{\alpha}{\pi} \right)^3 \\ &\quad + C_\mu^{(8)} \left(\frac{\alpha}{\pi} \right)^4 + C_\mu^{(10)} \left(\frac{\alpha}{\pi} \right)^5 + \cdots, \end{aligned} \quad (\text{C29})$$

with

$$\begin{aligned} C_\mu^{(2)} &= 0.5 \\ C_\mu^{(4)} &= 0.765\,857\,376(27) \\ C_\mu^{(6)} &= 24.050\,508\,98(44) \\ C_\mu^{(8)} &= 126.07(41) \\ C_\mu^{(10)} &= 930(170), \end{aligned} \quad (\text{C30})$$

and where

$$a_\mu(\text{weak}) = 153(3) \times 10^{-11} \quad (\text{C31})$$

and

$$a_\mu(\text{had}) = 6744(64) \times 10^{-11}. \quad (\text{C32})$$

The standard uncertainty of $a_\mu(\text{th})$ from the uncertainties of the terms listed above, other than that due to α , is

$$u[a_\mu(\text{th})] = 6.4 \times 10^{-10} = 55 \times 10^{-8} a_\mu \quad (\text{C33})$$

and is primarily due to the uncertainty of $a_\mu(\text{had})$. In fact, if $a_\mu(\text{had})$ were exactly known, the standard uncertainty of $a_\mu(\text{th})$ would be only $3.4 \times 10^{-11} = 2.9 \times 10^{-8} a_\mu$ and would be due mainly to the uncertainty of $a_\mu(\text{weak})$. If both $a_\mu(\text{had})$ and $a_\mu(\text{weak})$ were exactly known, the uncertainty of $a_\mu(\text{th})$ would be only $1.7 \times 10^{-11} = 1.4 \times 10^{-8} a_\mu$, which is just the uncertainty of $a_\mu(\text{QED})$. [Note that the uncertainties of $C_\mu^{(4)}$ and $C_\mu^{(6)}$ are negligible.]

In a manner similar to that for $a_e(\text{th})$, for the purpose of the least-squares calculations carried out in Sec. 4, we define an additive correction δ_μ to $a_\mu(\text{th})$ to account for the lack of exact knowledge of $a_\mu(\text{th})$, and hence the complete theoretical expression for the muon anomaly is

$$a_\mu(\alpha, \delta_\mu) = a_\mu(\text{th}) + \delta_\mu. \quad (\text{C34})$$

Our theoretical estimate of δ_μ is zero and its standard uncertainty is $u[a_\mu(\text{th})]$:

$$\delta_\mu = 0.0(6.4) \times 10^{-10}. \quad (\text{C35})$$

Although $a_\mu(\text{th})$ and $a_e(\text{th})$ have common components of uncertainty, due mainly to the uncertainty of $A_1^{(8)}$, $u[a_\mu(\text{th})]$ is so large due to the uncertainty of $a_\mu(\text{had})$ that the covariance of δ_μ and δ_e is negligible.

Appendix D. Theory of Muonium Ground-State Hyperfine Splitting

This Appendix gives a brief summary of the present theory of $\Delta\nu_{\text{Mu}}$, the ground-state hyperfine splitting of muonium (μ^+e^- atom). The dominant part of the splitting is given by the Fermi formula (Fermi, 1930)

$$\Delta\nu_{\text{F}} = \frac{16}{3} c R_{\infty} Z^3 \alpha^2 \frac{m_e}{m_{\mu}} \left[1 + \frac{m_e}{m_{\mu}} \right]^{-3}, \quad (\text{D1})$$

where the last factor is the reduced mass correction. (Note that although the charge of the muon is e , some of the expressions in this Appendix correspond to a muon with charge Ze in order to indicate the nature of various terms.) The full theoretical expression may be written as

$$\Delta\nu_{\text{Mu}}(\text{th}) = \Delta\nu_{\text{D}} + \Delta\nu_{\text{rad}} + \Delta\nu_{\text{rec}} + \Delta\nu_{\text{r-r}} + \Delta\nu_{\text{weak}} + \Delta\nu_{\text{had}}, \quad (\text{D2})$$

where the terms labeled D, rad, rec, r-r, weak, and had account for the Dirac (relativistic), radiative, recoil, radiative-recoil, electroweak, and hadronic (i.e., strong interaction) contributions to the hyperfine splitting, respectively. [See Sapirstein and Yennie (1990) and Bodwin, Yennie, and Gregorio (1985) for reviews of the early work.]

The contribution $\Delta\nu_{\text{D}}$ is given by the Dirac equation and was calculated exactly to all orders in $Z\alpha$ by Breit (1930). The first few terms in the power-series expansion in $Z\alpha$ are

$$\Delta\nu_{\text{D}} = \Delta\nu_{\text{F}}(1 + a_{\mu}) \left[1 + \frac{3}{2}(Z\alpha)^2 + \frac{17}{8}(Z\alpha)^4 + \dots \right], \quad (\text{D3})$$

where a_{μ} is the muon magnetic moment anomaly (see Appendix C).

The radiative corrections are of the form

$$\Delta\nu_{\text{rad}} = \Delta\nu_{\text{F}}(1 + a_{\mu}) \left[D^{(2)}(Z\alpha) \left(\frac{\alpha}{\pi} \right) + D^{(4)}(Z\alpha) \left(\frac{\alpha}{\pi} \right)^2 + \dots \right], \quad (\text{D4})$$

where the functions $D^{(2n)}(Z\alpha)$ are contributions associated with n virtual photons. In the limit $Z\alpha \rightarrow 0$, each of these functions is equal to the corresponding coefficient $A_1^{(2n)}$ in the theoretical expression for a_e as discussed in Appendix B. [The mass-dependent QED, electroweak, and hadronic contributions to a_e are negligible in the context of $\Delta\nu_{\text{Mu}}(\text{th})$ and need not be considered.] The functions $D^{(2n)}(Z\alpha)$ are as follows:

$$\begin{aligned} D^{(2)}(Z\alpha) &= A_1^{(2)} + (\ln 2 - \frac{5}{2})\pi Z\alpha \\ &+ \left[-\frac{2}{3}\ln^2(Z\alpha)^{-2} + \left(\frac{281}{360} - \frac{8}{3}\ln 2 \right) \ln(Z\alpha)^{-2} \right. \\ &+ 16.9037\dots \left. \right] (Z\alpha)^2 \\ &+ \left[\left(\frac{5}{2}\ln 2 - \frac{547}{96} \right) \ln(Z\alpha)^{-2} \right] \pi (Z\alpha)^3 \\ &+ G(Z\alpha)(Z\alpha)^3, \end{aligned} \quad (\text{D5})$$

where $A_1^{(2)} = \frac{1}{2}$, as given in Appendix B. The number 16.9037... includes a numerical integration that is readily carried out to high accuracy. The function $G(Z\alpha)$ accounts for all higher-order contributions in powers of $Z\alpha$ and can be divided into parts that correspond to a self-energy Feynman diagram and a vacuum polarization diagram, $G(Z\alpha) = G_{\text{SE}}(Z\alpha) + G_{\text{VP}}(Z\alpha)$. The self-energy part is estimated to be $G_{\text{SE}}(Z\alpha) = -12.0(2.0)$. The vacuum polarization part G_{VP} is expected to be negligible compared to the uncertainty of the self-energy part. Work relevant to Eq. (D5) has been carried out by Schneider, Greiner, and Soff (1994); Nio (1995); Karshenboim (1996a); Pachucki (1996); Nio and Kinoshita (1997); Blundell, Cheng, and Sapirstein (1997a); and Sunnergren *et al.* (1998).

For $D^{(4)}(Z\alpha)$ we have

$$\begin{aligned} D^{(4)}(Z\alpha) &= A_1^{(4)} + 0.7717(4)\pi Z\alpha + \left[-\frac{1}{3}\ln^2(Z\alpha)^{-2} \right. \\ &\quad \left. - 86(18) \right] (Z\alpha)^2 + \dots, \end{aligned} \quad (\text{D6})$$

where $A_1^{(4)}$ is as given in Appendix B. The number 0.7717(4) is the sum of various contributions, some of which are evaluated numerically (Eides, Karshenboim, and Shelyuto, (1989b); Eides, Karshenboim, and Shelyuto, 1990; Eides, Karshenboim and Shelyuto, 1991; Karshenboim, Shelyuto, and Eides, 1992; Kinoshita and Nio, 1994; Eides and Shelyuto, 1995; Kinoshita and Nio, 1996). The $\ln^2(Z\alpha)^{-2}$ contribution is from Karshenboim, (1993a). The number $-86(18)$ [corresponding to $-0.110(23)$ kHz] is an estimate of the contribution of a $\ln(Z\alpha)^{-2}$ term and a constant term (Nio, 1995; Kinoshita, 1996).

Finally,

$$D^{(6)}(Z\alpha) = A_1^{(6)} + \dots, \quad (\text{D7})$$

where only the leading contribution is given for the sixth-order term, because no binding correction has yet been calculated. Higher-order functions $D^{(2n)}(Z\alpha)$ with $n > 3$ are expected to be negligible.

The recoil contribution is given by

$$\begin{aligned} \Delta\nu_{\text{rec}} &= \Delta\nu_{\text{F}} \frac{m_e}{m_{\mu}} \left\{ -\frac{3}{1 - (m_e/m_{\mu})^2} \ln \left(\frac{m_{\mu}}{m_e} \right) \frac{Z\alpha}{\pi} \right. \\ &+ \frac{1}{(1 + m_e/m_{\mu})^2} \left[\ln(Z\alpha)^{-2} - 8\ln 2 + \frac{65}{18} \right] (Z\alpha)^2 \\ &+ \left[-\frac{3}{2} \ln \left(\frac{m_{\mu}}{m_e} \right) \ln(Z\alpha)^{-2} - \frac{1}{6} \ln^2(Z\alpha)^{-2} \right. \\ &\quad \left. \left. - 57(22) \right] \frac{(Z\alpha)^3}{\pi} \right\} + \dots, \end{aligned} \quad (\text{D8})$$

where the number $-57(22)$ [corresponding to $-0.151(60)$ kHz] is an estimate of the contribution of a $\ln(Z\alpha)^{-2}$ term and a constant term (Nio, 1995; Kinoshita, 1996). The term of order $\ln(m_{\mu}/m_e) \ln(Z\alpha)^{-2} (Z\alpha)^3/\pi$ is discussed by Karshenboim (1994), by Nio (1995), and by Kinoshita and Nio (1994). The term of order $\ln^2(Z\alpha)^{-2} (Z\alpha)^3/\pi$ is from Karshenboim (1993a).

The radiative-recoil contribution is

$$\begin{aligned} \Delta\nu_{r-r} = & \nu_F \left(\frac{\alpha}{\pi} \right)^2 \frac{m_e}{m_\mu} \left\{ \left[-2 \ln^2 \left(\frac{m_\mu}{m_e} \right) + \frac{13}{12} \ln \left(\frac{m_\mu}{m_e} \right) \right. \right. \\ & + \frac{21}{2} \zeta(3) + \frac{\pi^2}{6} + \frac{35}{9} \left. \right] + \frac{4}{3} \pi \alpha \ln^2 \alpha^{-2} \\ & + \left[-\frac{4}{3} \ln^3 \left(\frac{m_\mu}{m_e} \right) + \frac{4}{3} \ln^2 \left(\frac{m_\mu}{m_e} \right) + 43.1 \right] \frac{\alpha}{\pi} \left. \right\} \\ & - \nu_F \alpha^2 \left(\frac{m_e}{m_\mu} \right)^2 \left(6 \ln 2 + \frac{13}{6} \right) + \dots, \quad (D9) \end{aligned}$$

where for simplicity the explicit dependence on Z is not shown. The number 43.1 (corresponding to 0.012 kHz) is an estimate of the $\ln(m_\mu/m_e)$ and constant terms. The more recent work on which this equation is based was carried out by Eides and Shelyuto (1984); Eides, Karshenboim, and Shelyuto (1989a); Li, Samuel, and Eides (1993); Karshenboim (1993a); and Eides, Grotch, and Shelyuto (1998).

The electroweak contribution due to the exchange of a Z^0 boson (Bég and Feinberg, 1974; Eides, 1996) and the hadronic contribution due to vacuum polarization involving hadrons (Sapirstein, Terray, and Yennie, 1984; Karimkhodzhaev and Faustov, 1991; Faustov, Karimkhodzhaev, and Martynenko, 1999) are given by

$$\Delta\nu_{\text{weak}} = -0.065 \text{ kHz} \quad (D10)$$

$$\Delta\nu_{\text{had}} = 0.240(7) \text{ kHz}. \quad (D11)$$

The standard uncertainty of $\Delta\nu_{\text{Mu}}(\text{th})$, not including the uncertainties of the quantities R_∞ , α , m_e/m_μ , and a_μ , consists of the following components: 0.009 kHz [0.2×10^{-8}] due to the uncertainty 2.0 of $G_{\text{SE}}(Z\alpha)$ in the function $D^{(2)}(Z\alpha)$; 0.023 kHz [0.5×10^{-8}] from the uncertainty 18 of the number 86 in the function $D^{(4)}(Z\alpha)$ [the uncertainty 0.0004 of the number 0.7717 in $D^{(4)}(Z\alpha)$ is negligible]; 0.060 kHz [1.3×10^{-8}] due to the uncertainty 22 of the number 57 in $\Delta\nu_{\text{rec}}$; 0.008 kHz [0.2×10^{-8}] to reflect a possible uncalculated recoil contribution with absolute value of order $\Delta\nu_F(m_e/m_\mu)(Z\alpha)^4 \ln^2(Z\alpha)^{-2}$; 0.104 kHz [2.3×10^{-8}] to reflect possible uncalculated radiative-recoil contributions with absolute values of order $\Delta\nu_F(\alpha/\pi)^2(m_e/m_\mu)\pi\alpha \ln \alpha^{-2}$ and $\Delta\nu_F(\alpha/\pi)^2(m_e/m_\mu)\pi\alpha$; and 0.007 kHz [0.2×10^{-8}] due to the uncertainty of $\Delta\nu_{\text{had}}$. Note that the uncertainties arising from the uncalculated terms are standard uncertainties based on hypothetical numerical coefficients suggested by analogous calculated terms in $\Delta\nu_{\text{Mu}}(\text{th})$. Any contribution to $\Delta\nu_{\text{Mu}}(\text{th})$ not explicitly included in Eqs. (D3)–(D11) or reflected in the uncertainty evaluation is assumed to be less than about 0.005 kHz [0.1×10^{-8}], and therefore negligible at the level of uncertainty of current interest.

Combining the above components, we obtain for the standard uncertainty of $\Delta\nu_{\text{Mu}}(\text{th})$

$$u[\Delta\nu_{\text{Mu}}(\text{th})] = 0.12 \text{ kHz} \quad [2.7 \times 10^{-8}]. \quad (D12)$$

In analogy with our treatment of inexactly known theoretical expressions in the previous three appendices, we represent the theoretical uncertainty of $\Delta\nu_{\text{Mu}}(\text{th})$ by adding to it the term

$$\delta_{\text{Mu}} = 0.00(12) \text{ kHz}. \quad (D13)$$

The theory summarized above predicts

$$\Delta\nu_{\text{Mu}} = 4\,463\,302.67(27) \text{ kHz} \quad [6.1 \times 10^{-8}], \quad (D14)$$

based on values of the constants obtained from a variation of the 1998 least-squares adjustment that omits the two LAMPF measured values of $\Delta\nu_{\text{Mu}}$. The main source of uncertainty is that of the mass ratio m_e/m_μ that appears in the theoretical expression as an overall factor. However, the relative standard uncertainty is about one-half that of the LAMPF-99 value of m_e/m_μ given in Eq. (156), Sec. 3.3.9.c, because in the least-squares adjustment the theoretical expression for $\Delta\nu_{\text{Mu}}(\text{th})$ is used in the observational equation for the LAMPF values of $\nu(f_p)$ [see Eq. (142), Sec. 3.3.9.b]. The explicit dependence of $\Delta\nu_{\text{Mu}}(\text{th})$ on the mass ratio modifies the relation between m_e/m_μ and $\nu(f_p)$ in such a way that the uncertainty of the resulting value of the mass ratio is about half as large as the value in Eq. (156). An alternative approach to the calculation of the theoretical value of $\Delta\nu_{\text{Mu}}$ would be to use an experimental value of $\Delta\nu_{\text{Mu}}$ in the observational equation, but such an approach would yield a result that is dependent on the experimental value.

The predicted and experimental values of $\Delta\nu_{\text{Mu}}$ [see Eqs. (144) and (152) of Secs. 3.3.9.b and 3.3.9.c] are in good agreement, as expected from the inferred values of α discussed in Sec. 3.3.9.d.

Appendix E. Method of Least Squares

This Appendix gives a concise summary of the least-squares method as it is used to obtain a unique set of values of the fundamental constants from the available data. The resulting set of constants may be regarded as conventional values or best estimates, depending on one's point of view. The method of least squares has its origins in the work of Legendre (1805); Gauss (1809); Laplace (1812); and Gauss (1823). More recently, Aitken (1934) [see also Sheppard (1912)] has considered the case in which the data are not independent, and we follow his approach. Cohen (1951) has emphasized the fact that correlations among the data should be taken into account in an evaluation of the fundamental constants.

We suppose that there are N measured (or in some cases calculated) values q_i of various quantities with standard uncertainties $u_i = u(q_i)$, variances $u_{ii} = u_i^2$, and covariances $u_{ij} = u(q_i, q_j)$, where $u_{ji} = u_{ij}$. For example, q_1 could be a measured value of the anomalous magnetic moment of the electron a_e , q_2 a measured value of the Josephson constant K_J , etc. These values are called *input data* or *observational data*.

A set of M quantities z_j with $M \leq N$, called *adjusted constants*, is then chosen such that each input datum q_i can be

expressed as a function f_i of one or more of the adjusted constants z_j through the set of N *observational equations*

$$q_i \doteq f_i(z) \equiv f_i(z_1, z_2, \dots, z_M); \quad i = 1, 2, \dots, N. \quad (\text{E1})$$

For example, z_1 could be the fine-structure constant α and z_2 the Planck constant h . There is no unique choice for the adjusted constants; however, they must be chosen such that none can be expressed as a function of the others and the value of each is determined by some subset of the expressions in Eq. (E1). The dotted equal sign \doteq in Eq. (E1) denotes the fact that in general the left and right sides are not equal, since the set of equations may be, and usually is, overdetermined ($N \geq M$). For the example of the Josephson constant given above, the observational equation is

$$q_2 \doteq \left(\frac{8z_1}{\mu_0 c z_2} \right)^{1/2}, \quad (\text{E2})$$

where $z_1 = \alpha$ and $z_2 = h$.

Most of the observational equations in the 1998 adjustment are nonlinear, so in order to apply linear matrix methods, we linearize Eq. (E1) using a first-order Taylor series around starting (sometimes called fiducial) values s_j that are nearly equal to the expected values of the adjusted constants:

$$q_i \doteq f_i(s) + \sum_{j=1}^M \frac{\partial f_i(s)}{\partial s_j} (z_j - s_j) + \dots \quad (\text{E3})$$

We then define new variables

$$\begin{aligned} y_i &= q_i - f_i(s) \\ x_j &= z_j - s_j \end{aligned} \quad (\text{E4})$$

to obtain to first order

$$y_i \doteq \sum_{j=1}^M a_{ij} x_j, \quad (\text{E5})$$

where

$$a_{ij} = \frac{\partial f_i(s)}{\partial s_j}. \quad (\text{E6})$$

In matrix notation, Eq. (E5) may be written simply as

$$\mathbf{Y} \doteq \mathbf{A}\mathbf{X}, \quad (\text{E7})$$

where \mathbf{Y} is a column matrix with N elements y_1, y_2, \dots, y_N , \mathbf{A} is a rectangular matrix with N rows and M columns with elements $a_{11}, a_{12}, \dots, a_{1M}, \dots, a_{N1}, a_{N2}, \dots, a_{NM}$, and \mathbf{X} is a column matrix with M elements x_1, x_2, \dots, x_M . Similarly $q_i, f_i(s), z_j$, and s_j are elements of matrices $\mathbf{Q}, \mathbf{F}, \mathbf{Z}$, and \mathbf{S} .

To obtain the best value of \mathbf{X} , and hence of \mathbf{Z} , we minimize the product

$$\mathbf{S} = (\mathbf{Y} - \mathbf{A}\mathbf{X})^\top \mathbf{V}^{-1} (\mathbf{Y} - \mathbf{A}\mathbf{X}) \quad (\text{E8})$$

with respect to \mathbf{X} , where the symbol $^\top$ indicates transpose, and \mathbf{V} is the $N \times N$ *covariance matrix* of the input data, also

denoted $\text{cov}(\mathbf{Y})$, with elements u_{ij} ($\mathbf{W} = \mathbf{V}^{-1}$ is often called the *weight matrix*). The solution $\hat{\mathbf{X}}$, with elements \hat{x}_j , that minimizes \mathbf{S} is

$$\hat{\mathbf{X}} = \mathbf{G}\mathbf{A}^\top \mathbf{V}^{-1} \mathbf{Y}, \quad (\text{E9})$$

where

$$\mathbf{G} = (\mathbf{A}^\top \mathbf{V}^{-1} \mathbf{A})^{-1}. \quad (\text{E10})$$

The covariance matrix of the solution $\hat{\mathbf{X}}$, which follows from the propagation of uncertainty relation (see Appendix F), is \mathbf{G} :

$$\text{cov}(\hat{\mathbf{X}}) = (\mathbf{G}\mathbf{A}^\top \mathbf{V}^{-1}) \mathbf{V} (\mathbf{G}\mathbf{A}^\top \mathbf{V}^{-1})^\top = \mathbf{G}. \quad (\text{E11})$$

We take $\hat{\mathbf{Y}}$ as the best estimate of \mathbf{Y} , where

$$\hat{\mathbf{Y}} = \mathbf{A}\hat{\mathbf{X}}, \quad (\text{E12})$$

with

$$\text{cov}(\hat{\mathbf{Y}}) = \mathbf{A}\mathbf{G}\mathbf{A}^\top. \quad (\text{E13})$$

We thus have

$$\hat{\mathbf{Y}} = \mathbf{C}\mathbf{Y}, \quad (\text{E14})$$

where

$$\mathbf{C} = \mathbf{A}(\mathbf{A}^\top \mathbf{V}^{-1} \mathbf{A})^{-1} \mathbf{A}^\top \mathbf{V}^{-1}. \quad (\text{E15})$$

The elements of $\hat{\mathbf{Y}}$ so obtained are the best estimates for the quantities represented by \mathbf{Y} in the following sense: If we consider an estimate of the quantities represented by \mathbf{Y} of the form $\mathbf{Y}' = \mathbf{D}\mathbf{Y}$ such that the sum of the squares of the uncertainties of \mathbf{Y}' as given by the trace of the covariance matrix $\text{cov}(\mathbf{Y}') = \mathbf{D}\mathbf{V}\mathbf{D}^\top$ is a minimum, subject to the condition that the matrix \mathbf{D} reproduces any set of data of the form $\mathbf{A}\mathbf{X}$ (that is, $\mathbf{D}\mathbf{A}\mathbf{X} = \mathbf{A}\mathbf{X}$ for any \mathbf{X}), then $\mathbf{D} = \mathbf{C}$, where \mathbf{C} is just the matrix in Eq. (E15) obtained by the least-squares method, and hence $\mathbf{Y}' = \hat{\mathbf{Y}}$ (Aitken, 1934).

Of course, we are not interested in $\hat{\mathbf{X}}$ and $\hat{\mathbf{Y}}$ per se, but rather the best estimate $\hat{\mathbf{Z}}$ of the adjusted constants and the best estimate $\hat{\mathbf{Q}}$, corresponding to the measured quantities \mathbf{Q} , given by

$$\begin{aligned} \hat{\mathbf{Z}} &= \mathbf{S} + \hat{\mathbf{X}} \\ \hat{\mathbf{Q}} &= \mathbf{F} + \hat{\mathbf{Y}}. \end{aligned} \quad (\text{E16})$$

Since \mathbf{S} and \mathbf{F} have no uncertainty associated with them, we have

$$\begin{aligned} \text{cov}(\hat{\mathbf{Z}}) &= \text{cov}(\hat{\mathbf{X}}) = \mathbf{G} \\ \text{cov}(\hat{\mathbf{Q}}) &= \text{cov}(\hat{\mathbf{Y}}) = \mathbf{A}\mathbf{G}\mathbf{A}^\top. \end{aligned} \quad (\text{E17})$$

In general, the values of the adjusted constants $\hat{\mathbf{Z}}$ are correlated; their variances and covariances are the elements of the covariance matrix \mathbf{G} . Thus this matrix is necessary for the evaluation of the uncertainty of a quantity calculated from two or more adjusted constants, as discussed in Appendix F.

Since the observational equations are nonlinear, the solution of the linear approximation described above does not provide an exact solution of the nonlinear problem, even though it provides values of the adjusted constants that are an improvement over the starting (fiducial) values. To obtain more precise values, we use the improved values of the adjusted constants as starting values for a new linear approximation. This procedure is iterated until the new values and the starting values differ by a very small fraction of the uncertainties of the adjusted constants $u(\hat{z}_j) = u(\hat{x}_j)$. Our convergence condition is

$$\sum_{j=1}^M \frac{\hat{x}_j^2}{u^2(\hat{x}_j)} < 10^{-20}. \quad (\text{E18})$$

In most cases, two iterations are sufficient to reach convergence, although in some cases more may be necessary. The number of iterations needed depends on how close the original starting values of the s_j are to the values of the \hat{z}_j in the final iteration.

Once the iterative process is complete, F , A , and C can be evaluated at the final values of the adjusted constants \hat{z}_j (denoted by \hat{F} , \hat{A} , and \hat{C}) and we have

$$\hat{Q} = \hat{F} + \hat{C}(Q - \hat{F}), \quad (\text{E19})$$

which implicitly describes the relation between small changes in the input data Q and the best estimates of the corresponding quantities \hat{Q} . If the elements of Q are exactly the input data values, then the second term on the right-hand side of Eq. (E19) vanishes. However, it is of interest to ask to what extent a change in a particular input datum q_i causes a change in its best estimated value \hat{q}_i . The relationship between these changes is given by

$$\frac{\partial \hat{q}_i}{\partial q_i} = \hat{c}_{ii}, \quad (\text{E20})$$

where \hat{c}_{ii} is the i, i element of \hat{C} . For convenience, we call \hat{c}_{ii} the self-sensitivity coefficient S_c of a particular input datum because it measures the influence of that datum on the best estimated value of the corresponding quantity. For the final 1998 least-squares adjustment, all of the coefficients lie in the range $0 < S_c \leq 1$, even though this limit is not a necessary condition when there are correlations among the input data. If S_c for a particular input datum is of the order of 0.01 or less, the datum does not play a significant role in determining the best estimated value of the corresponding quantity and could be discarded with little effect. The reason for such a small value for S_c could be the existence of another input datum of the same type with a significantly smaller uncertainty, or the generation by other input data of an *indirect* value of the corresponding quantity with a very small uncertainty.

A measure of the consistency of the input data is obtained by computing the Birge ratio

$$R_B = \sqrt{\chi^2/\nu}, \quad (\text{E21})$$

where $\nu = N - M$ is the degrees of freedom of the least-squares calculation, and χ^2 is given by

$$\chi^2 = (Q - \hat{Q})^T V^{-1} (Q - \hat{Q}), \quad (\text{E22})$$

which is the minimum value of S as given by Eq. (E8) evaluated in the final iteration. To the extent that correlations among the data may be neglected, the contribution to χ^2 of each item of data is r_i^2 , where r_i is the *normalized residual* of q_i :

$$r_i = \frac{q_i - \hat{q}_i}{u_i}, \quad (\text{E23})$$

and in the limit of a large number of degrees of freedom, the Birge ratio is the square root of the average of the squares of the normalized residuals. A Birge ratio substantially larger than one suggests that the data are inconsistent. Similarly, a normalized residual r_i significantly larger than one for an input datum suggests that the datum is inconsistent with the other data.

Inconsistencies among input data in a least-squares adjustment of the constants are not likely to be purely statistical, because the uncertainties of the data are in general dominated by Type B components associated with systematic effects and there is an insufficient number of experiments and calculations to treat the collection of results statistically. Further, hindsight shows that disagreements between measured (or calculated) results are usually due to unrecognized effects for which no allowance has been made in the uncertainty evaluation. Nevertheless, for comparison purposes (i.e., as general indicators), we can still consider the values of χ^2 and R_B that are expected in a purely statistical analysis.

If the probability distribution associated with each input datum is assumed to be normal with mean q_i and variance u_i^2 , then the expected value of χ^2 is $\nu = N - M$ with standard deviation $\sqrt{2\nu}$. Thus a value of the Birge ratio greater than $1 + \sqrt{2/\nu}$ would suggest a possible inconsistency in the data. In addition, for a given value of ν , the probability that an observed value of chi square would exceed χ^2 is (Abromowitz and Stegun, 1965)

$$Q(\chi^2|\nu) = \frac{1}{\Gamma\left(\frac{\nu}{2}\right)} \int_{\chi^2}^{\infty} dx \left(\frac{x}{2}\right)^{\nu/2} \frac{e^{-x/2}}{x}. \quad (\text{E24})$$

Hence the function $Q(\chi^2|\nu)$ evaluated with χ^2 equal to the observed value is the likelihood of obtaining an observed value that large or larger. A value of $Q(\chi^2|\nu)$ much less than one would therefore indicate that χ^2 is significantly larger than expected, suggesting a possible inconsistency in the data.

If an input datum that is independent of all other input data, together with a corresponding new adjusted constant, is added to an adjustment, then the Birge ratio remains unchanged, because the contribution of the new datum to χ^2 is zero and the degrees of freedom $\nu = N - M$ remains unchanged. More generally, any number of data for a quantity that is independent of the rest of the adjustment, as would be

the case for the Newtonian constant of gravitation G , may be treated separately by an application of the least-squares method. Such a one-variable least-squares computation is identical to calculating the weighted mean of these values. In the one-dimensional case, the observational equation is $q_i = z$, so the matrix \mathbf{A} is a single-column matrix with all elements equal to 1, and the matrix \mathbf{C} in Eq. (E15) has elements given by

$$c_{ij} = \sum_{k=1}^N w_{kj} / \sum_{n,m=1}^N w_{nm}, \quad (\text{E25})$$

where the w_{ij} are elements of the weight matrix $\mathbf{W} = \mathbf{V}^{-1}$. Since the observational equation is linear, we may take $\mathbf{F} = 0$ and only one iteration is needed. In this case, Eq. (E14) yields

$$\hat{q}_i = \sum_{j=1}^N c_{ij} q_j, \quad (\text{E26})$$

with standard uncertainty

$$u(\hat{q}_i) = \left(\sum_{n,m=1}^N w_{nm} \right)^{-1/2}. \quad (\text{E27})$$

In the case where there are only two observations, the equations for their weighted mean take a simple form:

$$\begin{aligned} \hat{q}_i &= \frac{(u_2^2 - u_{12})q_1 + (u_1^2 - u_{12})q_2}{u_1^2 + u_2^2 - 2u_{12}} \\ u(\hat{q}_i) &= \left(\frac{u_1^2 u_2^2 - u_{12}^2}{u_1^2 + u_2^2 - 2u_{12}} \right)^{1/2}. \end{aligned} \quad (\text{E28})$$

Appendix F. Use of the Covariance Matrix

As pointed out in Appendix E, the values of the adjusted constants resulting from a least-squares fit are correlated. Consequently, proper evaluation of the uncertainty of the value of a quantity based on two or more adjusted constants must take these correlations into account. This appendix reviews the law of propagation of uncertainty and indicates how the uncertainties of many of the 1998 recommended values can be calculated from the condensed covariance matrix given in Table 25. As noted in Sec. 5.1, the covariances of all the 1998 recommended values are given in the form of correlation coefficients at the Web site of the NIST Fundamental Constants Data Center: physics.nist.gov/constants.

The 1998 recommended values of the constants are calculated as functions of the 57 adjusted constants, as described in Sec. 5.2. Most of these functions are simple products of powers of a few of the adjusted constants. With the adjusted constants denoted by \hat{z}_j and the recommended constants by \hat{p}_i , these relations are indicated by

$$\hat{p}_i(\hat{z}_1, \hat{z}_2, \dots, \hat{z}_M); \quad i = 1, 2, \dots, K, \quad (\text{F1})$$

where M is the number of adjusted constants and K is the total number of recommended constants. Functions of the form $\hat{p}_3 = \hat{z}_2$ are, of course, included. The standard formula

for the propagation of uncertainty gives the covariances of the recommended constants $u(\hat{p}_k, \hat{p}_l)$ [as well as variances $u(\hat{p}_k)^2 = u(\hat{p}_k, \hat{p}_k)$] in terms of the covariances of the adjusted constants $u(\hat{z}_i, \hat{z}_j)$ (ISO, 1993a):

$$u(\hat{p}_k, \hat{p}_l) = \sum_{i,j=1}^M \frac{\partial \hat{p}_k}{\partial \hat{z}_i} \frac{\partial \hat{p}_l}{\partial \hat{z}_j} u(\hat{z}_i, \hat{z}_j). \quad (\text{F2})$$

The covariances $u(\hat{z}_i, \hat{z}_j)$ are the elements of the covariance matrix $\hat{\mathbf{G}}$ given by

$$\hat{\mathbf{G}} = (\hat{\mathbf{A}}^\top \mathbf{V}^{-1} \hat{\mathbf{A}})^{-1}, \quad (\text{F3})$$

where $\hat{\mathbf{A}}$ and \mathbf{V} are as defined in Appendix E; that is, $\hat{\mathbf{A}}$ is the matrix defined by Eq. (E6) evaluated in the final iteration of the least-squares calculation, and \mathbf{V} is the covariance matrix of the observational data. In our evaluation of the recommended constants, the partial derivatives in Eq. (F2) (most of which are zero) are both calculated analytically and translated into FORTRAN by computer.

In Eq. (F2) the set of variables \hat{z}_j can be extended to include any number of the derived constants \hat{p}_i in addition to the original adjusted constants on the right-hand side. Of course, the range of the covariance calculation, the \hat{p}_i on the left-hand side of Eq. (F2), can also be extended to combinations of constants not included in the 1998 set of recommended values. As an example of an application of Eq. (F2) in a case where the z_j have been extended, we consider the uncertainty of the 1998 recommended value of the Bohr magneton μ_B based on the expression

$$\mu_B = \frac{e\hbar}{2m_e} = \frac{eh}{4\pi m_e}. \quad (\text{F4})$$

The relevant derivatives are just

$$\begin{aligned} \frac{\partial \mu_B}{\partial e} &= \frac{\mu_B}{e} \\ \frac{\partial \mu_B}{\partial h} &= \frac{\mu_B}{h} \\ \frac{\partial \mu_B}{\partial m_e} &= -\frac{\mu_B}{m_e}, \end{aligned} \quad (\text{F5})$$

and the resulting relation takes a particularly simple form if expressed in terms of relative variances $u_r^2(x_i) = u^2(x_i)/x_i^2 = u(x_i, x_i)/x_i^2$ and relative covariances $u_r(x_i, x_j) = u(x_i, x_j)/(x_i x_j)$:

$$\begin{aligned} u_r^2(\mu_B) &= u_r^2(e) + u_r^2(h) + u_r^2(m_e) \\ &\quad + 2u_r(e, h) - 2u_r(e, m_e) \\ &\quad - 2u_r(h, m_e). \end{aligned} \quad (\text{F6})$$

Substitution of the appropriate numbers from Table 25 yields $u_r(\mu_B) = 4.0 \times 10^{-8}$, in agreement with the value listed in Table 24. It is of interest to note that the result would be 1.2×10^{-7} if covariances were neglected.

The matrix form of uncertainty propagation is applied in a number of instances in Appendix E. If we have a set of quantities $\hat{y}_k(\hat{x}_1, \hat{x}_2, \dots, \hat{x}_M)$ that depend on M quantities \hat{x}_i , then the covariance $u(\hat{y}_k, \hat{y}_l)$ of \hat{y}_k and \hat{y}_l is related to the covariance $u(\hat{x}_i, \hat{x}_j)$ of \hat{x}_i and \hat{x}_j by

$$u(\hat{y}_k, \hat{y}_l) = \sum_{i,j=1}^M \frac{\partial \hat{y}_k}{\partial \hat{x}_i} \frac{\partial \hat{y}_l}{\partial \hat{x}_j} u(\hat{x}_i, \hat{x}_j). \quad (\text{F7})$$

If the relationship between \hat{x}_i and \hat{y}_k is linear as in Eq. (E12) of Appendix E, then it is useful to write Eq. (F7) in matrix form following the definitions of that Appendix. In particular, from Eq. (E12) we have

$$\frac{\partial \hat{y}_k}{\partial \hat{x}_i} = a_{ki}, \quad (\text{F8})$$

where a_{ki} is an element of the matrix \mathbf{A} . Further, if $\text{cov}(\hat{\mathbf{X}})$ and $\text{cov}(\hat{\mathbf{Y}})$ are the covariance matrices of $\hat{\mathbf{X}}$ and $\hat{\mathbf{Y}}$ with matrix elements $u(\hat{x}_i, \hat{x}_j)$ and $u(\hat{y}_k, \hat{y}_l)$, respectively, then we have

$$\text{cov}(\hat{\mathbf{Y}})_{kl} = \sum_{i,j=1}^M a_{ki} a_{lj} \text{cov}(\hat{\mathbf{X}})_{ij}, \quad (\text{F9})$$

or

$$\text{cov}(\hat{\mathbf{Y}}) = \mathbf{A} \text{cov}(\hat{\mathbf{X}}) \mathbf{A}^T, \quad (\text{F10})$$

which corresponds to Eq. (E13).

Finally, we note that the general law of propagation of uncertainty in Eq. (F7) [see also Eq. (F2)] as applied to the uncertainty of a quantity is often written in the form

$$u^2(y_k) = \sum_{i=1}^N \left(\frac{\partial y_k}{\partial x_i} \right)^2 u^2(x_i) + 2 \sum_{i=1}^{N-1} \sum_{j=i+1}^N \frac{\partial y_k}{\partial x_i} \frac{\partial y_k}{\partial x_j} u(x_i, x_j). \quad (\text{F11})$$

The covariance in this equation can also be written in terms of the correlation coefficient of x_i and x_j defined by

$$r(x_i, x_j) = \frac{u(x_i, x_j)}{u(x_i)u(x_j)}, \quad (\text{F12})$$

where $-1 \leq r(x_i, x_j) \leq 1$.

9. References

- Abramowitz, M., and I. A. Stegun, *Handbook of Mathematical Functions* (Dover Publications, Inc., New York, NY, 1965).
- Adam, J., V. Hnatowicz, and A. Kugler, Czech. J. Phys. **B33**(4), 465–468 (1983).
- Aitken, A. C., Proc. R. Soc. Edinburgh **55**, 42–48 (1934).
- Aleman, R., Nucl. Phys. B (Proc. Suppl.) **55C**, 341–357 (1997).
- Aleman, R., M. Davier, and A. Höcker, Eur. Phys. J. C **2**(1), 123–135 (1998).
- Amin, S. R., C. D. Caldwell, and W. Lichten, Phys. Rev. Lett. **47**(18), 1234–1238 (1981).
- Andreae, T., W. König, R. Wynands, D. Leibfried, F. Schmidt-Kaler, C. Zimmermann, D. Meschede, and T. W. Hänsch, Phys. Rev. Lett. **69**(13), 1923–1926 (1992).
- Arnautov, G. P., Y. D. Boulanger, G. D. Karner, and S. N. Shcheglov, BMR J. Austral. Geol. Geophys. **4**, 383–393 (1979).
- Artemyev, A. N., V. M. Shabaev, and V. A. Yerokin, J. Phys. B **28**(24), 5201–5206 (1995).
- Audi, G., and A. H. Wapstra, Nucl. Phys. **A565**(1), 1–65 (1993).
- Audi, G., and A. H. Wapstra, Nucl. Phys. **A595**(4), 409–480 (1995).
- Audi, G., and A. H. Wapstra (private communication, 1998).
- Audi, G., and A. H. Wapstra (private communication, 1999).
- Auer, H., Ann. Phys. (Leipzig) **5**(18), 593–612 (1933).
- Bachmair, H., (private communication, 1997).
- Bachmair, H., (private communication, 1999).
- Bachmair, H., T. Funck, R. Hanke, and H. Lang, IEEE Trans. Instrum. Meas. **44**(2), 440–442 (1995).
- Bagley, C. H., and G. G. Luther, Phys. Rev. Lett. **78**(16), 3047–3050 (1997).
- Baikov, P. A., and D. J. Broadhurst, in *New Computing Techniques in Physics Research IV. International Workshop on Software Engineering and Artificial Intelligence for High Energy and Nuclear Physics*, edited by B. Denby and D. Perret-Gallix (World Scientific, Singapore, 1995), pp. 167–172.
- Bailey, J., et al., Nucl. Phys. **B150**(1), 1–75 (1979).
- Bailey, J., W. Bartl, G. von Bochmann, R. C. A. Brown, F. J. M. Farley, M. Giesch, H. Jöstlein, S. van Der Meer, E. Picasso, and R. W. Williams, Nuovo Cimento **A9**(4), 369–432 (1972).
- Barker, W. A., and F. N. Glover, Phys. Rev. **99**(1), 317–324 (1955).
- Barr, J. R. M., J. M. Girkin, J. M. Tolchard, and A. I. Ferguson, Phys. Rev. Lett. **56**(6), 580–583 (1986).
- Basile, G., A. Bergamin, G. Cavagnero, G. Mana, and G. Zosi, IEEE Trans. Instrum. Meas. **38**(2), 210–216 (1989).
- Basile, G., A. Bergamin, G. Cavagnero, G. Mana, E. Vittone, and G. Zosi, Phys. Rev. Lett. **72**(20), 3133–3136 (1994).
- Basile, G., A. Bergamin, G. Cavagnero, G. Mana, E. Vittone, and G. Zosi, IEEE Trans. Instrum. Meas. **44**(2), 526–529 (1995a).
- Basile, G., A. Bergamin, M. Oberto, and G. Zosi, Lett. Nuovo Cimento **23**(9), 324–326 (1978).
- Basile, G., et al., IEEE Trans. Instrum. Meas. **44**(2), 538–541 (1995b).
- Bearden, J. A., and J. S. Thomsen, Nuovo Cimento Suppl. **5**(2), 267–360 (1957).
- Beausoleil, R. G., Ph.D. Thesis, Stanford University, 1986.
- Beausoleil, R. G., D. H. McIntyre, C. J. Foot, E. A. Hildum, B. Couillaud, and T. W. Hänsch, Phys. Rev. A **35**(11), 4878–4881 (1987).
- Becker, P. (private communication, 1997).
- Becker, P. (private communication, 1998).
- Becker, P., and G. Mana, Metrologia **31**(3), 203–209 (1994).
- Becker, P., and H. Siegert, in *Precision Measurement and Fundamental Constants II*, edited by B. N. Taylor and W. D. Phillips (NBS Spec. Pub. 617, US Government Printing Office, Washington, DC, 1984), pp. 317–320.
- Becker, P., H. Bettin, L. Koenders, J. Martin, A. Nicolaus, and S. Röttger, PTB Mitt. **106**(5), 321–329 (1996).
- Becker, P., et al., Phys. Rev. Lett. **46**(23), 1540–1543 (1981).
- Becker, P., P. Seyfried, and H. Siegert, Z. Phys. B **48**, 17–21 (1982).
- Beer, W., B. Jeanneret, B. Jeckelmann, P. Richard, A. Courteville, Y. Salvadé, and R. Dändliker, IEEE Trans. Instrum. Meas. **48**(2), 192–195 (1999).
- Bég, M. A. B., and G. Feinberg, Phys. Rev. Lett. **33**(10), 606–610 (1974). Erratum: **35**(2), 130–130 (1975).
- Bego, V., J. Butorac, and D. Ilić, IEEE Trans. Instrum. Meas. **48**(2), 212–215 (1999).
- Bego, V., K. Poljančić, J. Butorac, and G. Gašljević, IEEE Trans. Instrum. Meas. **42**(2), 335–337 (1993).
- Beltrami, I., et al., Nucl. Phys. **A451**(4), 679–700 (1986).
- Belyi, V. A., E. A. Il'ina, and V. Y. Shifrin, Izmer. Tekh. **29**(7), 18–19 (1986). [Meas. Tech. **29**(7), 613–616 (1986)].
- Bender, P. L., and R. L. Driscoll, IRE Trans. Instrum. **I-7**(3 & 4), 176–180 (1958).
- Bennett, L. H., C. H. Page, and L. J. Swartzendruber, J. Res. Natl. Bur. Stand. **83**(1), 9–12 (1978).

- Bergamin, A., G. Cavagnero, G. Mana, and G. Zosi, *J. Appl. Phys.* **82**(11), 5396–5400 (1997a).
- Bergamin, A., G. Cavagnero, G. Mana, and G. Zosi, *Eur. Phys. J. B* **9**(2), 225–232 (1999).
- Bergamin, A., G. Cavagnero, L. Cordiali, and G. Mana, *IEEE Trans. Instrum. Meas.* **46**(2), 196–200 (1997b).
- Bergamin, A., G. Cavagnero, L. Cordiali, G. Mana, and G. Zosi, *IEEE Trans. Instrum. Meas.* **46**(2), 576–579 (1997c).
- Berkeland, D. J., E. A. Hinds, and M. G. Boshier, *Phys. Rev. Lett.* **75**(13), 2470–2473 (1995).
- Bettin, H., M. Gläser, F. Spieweck, H. Toth, A. Sacconi, A. Peuto, K. Fujii, M. Tanaka, and Y. Nezu, *IEEE Trans. Instrum. Meas.* **46**(2), 556–559 (1997).
- Bhatia, A. K., and R. J. Drachman, *J. Phys. B* **27**(7), 1299–1305 (1994).
- Bhatt, G., and H. Grotch, *Phys. Rev. Lett.* **58**(5), 471–474 (1987).
- Bijnens, J., E. Pallante, and J. Prades, *Nucl. Phys. B* **474**(2), 379–417 (1996).
- BIPM, *Le Système International d'Unités (SI)*, 7th ed. (Bureau International des Poids et Mesures, Sèvres, France, 1998).
- Biraben, F., and F. Nez (private communication, 1998).
- Biraben, F., J. C. Garreau, and L. Julien, *Europhys. Lett.* **2**(12), 925–932 (1986).
- Biraben, F., J. C. Garreau, L. Julien, and M. Allegrini, *Phys. Rev. Lett.* **62**(6), 621–624 (1989).
- Birge, R. T., *Rev. Mod. Phys.* **1**(1), 1–73 (1929).
- Birge, R. T., *Nuovo Cimento Suppl.* **6**(1), 39–67 (1957).
- Bloch, F., *Phys. Rev. Lett.* **21**(17), 1241–1243 (1968).
- Bloch, F., *Phys. Rev. B* **2**(1), 109–121 (1970).
- Blundell, S. A., K. T. Cheng, and J. Sapirstein, *Phys. Rev. Lett.* **78**(26), 4914–4917 (1997a).
- Blundell, S. A., K. T. Cheng, and J. Sapirstein, *Phys. Rev. A* **55**(3), 1857–1865 (1997b).
- Bodwin, G. T., and D. R. Yennie, *Phys. Rev. D* **37**(2), 498–523 (1988).
- Bodwin, G. T., D. R. Yennie, and M. A. Gregorio, *Rev. Mod. Phys.* **57**(3), 723–782 (1985).
- Boikova, N. A., Y. N. Tyukhtyaev, and R. N. Faustov, *Yad. Fiz.* **61**(5), 866–870 (1998). [*Phys. At. Nucl.* **61**(5), 781–784 (1998)].
- Bonse, U., and M. Hart, *Appl. Phys. Lett.* **6**(8), 155–156 (1965).
- Bonse, U., and W. Graeff, in *Topics in Applied Physics: X-ray Optics*, edited by H. J. Quessier, Vol. 33 (Springer-Verlag, Berlin, 1977), pp. 93–143.
- Borer, K., and F. Lange, *Nucl. Instrum. Methods* **143**(2), 219–225 (1977).
- Boshier, M. G. (private communication, 1998).
- Boshier, M. G., *et al.*, *Nature (London)* **330**(6147), 463–465 (1987).
- Boshier, M. G., *et al.*, *Phys. Rev. A* **40**(11), 6169–6183 (1989).
- Boshier, M. G., *et al.*, *Phys. Rev. A* **52**(3), 1948–1953 (1995).
- Boulanger, J. D., G. P. Arnautov, and S. N. Scheglov, *Bull. Inf. Bur. Grav. Int.* **52**, 99–124 (1983).
- Bourzeix, S., B. de Beauvoir, F. Nez, M. D. Plimmer, F. de Tomasi, L. Julien, and F. Biraben, in *Symposium on Frequency Standards and Metrology*, edited by J. C. Bergquist (World Scientific, Singapore, 1996a), pp. 145–150.
- Bourzeix, S., B. de Beauvoir, F. Nez, M. D. Plimmer, F. de Tomasi, L. Julien, F. Biraben, and D. N. Stacey, *Phys. Rev. Lett.* **76**(3), 384–387 (1996b).
- Bower, V. E., and R. S. Davis, *J. Res. Natl. Bur. Stand.* **85**(3), 175–191 (1980).
- Bradley, M. P., J. V. Porto, S. Rainville, J. K. Thompson, and D. E. Pritchard, *Phys. Rev. Lett.* **83**(22), 4510–4513 (1999).
- Breit, G., *Nature (London)* **122**(3078), 649–649 (1928).
- Breit, G., *Phys. Rev.* **35**(12), 1447–1451 (1930).
- Breit, G., and I. I. Rabi, *Phys. Rev.* **38**(11), 2082–2083 (1931).
- Breskman, D., and A. Kanofsky, *Phys. Lett. B* **33**(4), 309–311 (1970).
- Broersma, S., *J. Chem. Phys.* **17**(10), 873–882 (1949).
- Brown, D. H., and W. A. Worstell, *Phys. Rev. D* **54**(5), 3237–3249 (1996).
- Brown, L., G. Gabrielse, K. Helmerson, and J. Tan, *Phys. Rev. Lett.* **55**(1), 44–47 (1985a).
- Brown, L. S., G. Gabrielse, K. Helmerson, and J. Tan, *Phys. Rev. A* **32**(6), 3204–3218 (1985b).
- Cabiati, F., *IEEE Trans. Instrum. Meas.* **40**(2), 110–114 (1991).
- Cage, M. E. (private communication, 1989).
- Cage, M. E. (private communication, 1997).
- Cage, M. E., R. F. Dziuba, C. T. Van Degriift, and D. Yu, *IEEE Trans. Instrum. Meas.* **38**(2), 263–269 (1989a).
- Cage, M. E., *et al.*, *IEEE Trans. Instrum. Meas.* **38**(2), 284–289 (1989b).
- Camani, M., F. N. Gyax, E. Klempt, W. Rüegg, A. Schenck, H. Schilling, R. Schulze, and H. Wolf, *Phys. Lett. B* **77**(3), 326–330 (1978).
- Carey, R. M., *et al.*, *Phys. Rev. Lett.* **82**(8), 1632–1635 (1999).
- Caso, C., *et al.*, *Eur. Phys. J. C* **3**(1–4), 1–794 (1998).
- Casperson, D. E., *et al.*, *Phys. Rev. Lett.* **38**(17), 956–959 (1977). Erratum: **38**(25), 1504–1504 (1977).
- Castro, M., J. Keller, and A. Schenck, *Hyp. Int.* **6**, 439–442 (1979).
- Chen, W. Y., J. R. Purcell, P. T. Olsen, W. D. Phillips, and E. R. Williams, in *Advances in Cryogenic Engineering*, edited by R. W. Fast, Vol. 27 (Plenum, New York, 1982), pp. 97–104.
- Chiao, W., R. Liu, and P. Shen, *IEEE Trans. Instrum. Meas.* **IM-29**(4), 238–242 (1980).
- Chu, S., J. M. Hensley, and B. C. Young (private communication, 1998).
- Clarke, J., *Am. J. Phys.* **38**(9), 1071–1095 (1970).
- Close, F. E., and H. Osborn, *Phys. Lett. B* **34**(5), 400–404 (1971).
- Clothier, W. K., *Metrologia* **1**(2), 36–55 (1965a).
- Clothier, W. K., *Metrologia* **1**(4), 181–184 (1965b).
- Clothier, W. K., G. J. Sloggett, and H. Bairnsfather, *Opt. Eng.* **19**(6), 834–842 (1980).
- Clothier, W. K., G. J. Sloggett, H. Bairnsfather, M. F. Curry, and D. J. Benjamin, *Metrologia* **26**(1), 9–46 (1989).
- CODATA, CODATA Bull. No. 11, pp. 1–7 (1973).
- Cohen, E. R., *Phys. Rev.* **81**(1), 162–162 (1951).
- Cohen, E. R., and B. N. Taylor, *J. Phys. Chem. Ref. Data* **2**(4), 663–734 (1973).
- Cohen, E. R., and B. N. Taylor, CODATA Bull. No. 63, pp. 1–32 (1986).
- Cohen, E. R., and B. N. Taylor, *Rev. Mod. Phys.* **59**(4), 1121–1148 (1987).
- Cohen, E. R., and J. W. M. DuMond, *Rev. Mod. Phys.* **37**(4), 537–594 (1965).
- Cohen, E. R., and P. Giacomo, *Physica (Utrecht)* **146A**(1–2), 1–68 (1987).
- Cohen, E. R., J. W. M. DuMond, T. W. Layton, and J. S. Rollett, *Rev. Mod. Phys.* **27**(4), 363–380 (1955).
- Colclough, A. R., *Metrologia* **9**(2), 75–98 (1973).
- Colclough, A. R., *Proc. R. Soc. London, Ser. A* **365**(1722), 349–370 (1979a).
- Colclough, A. R., *Acustica* **42**(1), 28–36 (1979b).
- Colclough, A. R. (private communication, 1984a).
- Colclough, A. R., in *Precision Measurement and Fundamental Constants II*, edited by B. N. Taylor and W. D. Phillips (NBS Spec. Pub. 617, US Government Printing Office, Washington, DC, 1984b), pp. 263–275.
- Colclough, A. R., T. J. Quinn, and T. R. D. Chandler, *Proc. R. Soc. London, Ser. A* **368**(1732), 125–139 (1979).
- Combley, F., F. J. M. Farley, and E. Picasso, *Phys. Rep.* **68**(2), 93–119 (1981).
- Combley, F. H., *Rep. Prog. Phys.* **42**(11), 1889–1935 (1979).
- Cook, A. H., *Philos. Trans. R. Soc. London, Ser. A* **254**(1038), 125–154 (1961).
- Cook, A. H., and N. W. B. Stone, *Philos. Trans. R. Soc. London, Ser. A* **250**(978), 279–323 (1957).
- Coplen, T. B., *Pure Appl. Chem.* **68**(12), 2339–2359 (1996).
- Cotton, A., and G. Dupouy, in *Comptes Rendus Des Travaux De La Deuxième Section of Du Congrès International D'Électricité*, edited by R. De Valbreuze, Vol. 12 (Gauthier Villars, Paris, 1932), pp. 208–229, 740.
- Craig, D. N., J. I. Hoffman, C. A. Law, and W. J. Hamer, *J. Res. Natl. Bur. Stand. Sect. A* **64A**(5), 381–402 (1960).
- Crowe, K. M., J. F. Hague, J. E. Rothberg, A. Schenck, D. L. Williams, R. W. Williams, and K. K. Young, *Phys. Rev. D* **5**(9), 2145–2161 (1972).
- Cutkosky, R. D., *J. Res. Natl. Bur. Stand. Sect. A* **65A**(3), 147–158 (1961).
- Cutkosky, R. D., *IEEE Trans. Instrum. Meas.* **IM-23**(4), 305–309 (1974).
- Czarnecki, A., and B. Krause, *Nucl. Phys. B (Proc. Suppl.)* **51C**, 148–153 (1996).
- Czarnecki, A., and M. Skrzypek, *Phys. Lett. B* **449**(3–4), 354–360 (1999).
- Czarnecki, A., B. Krause, and W. J. Marciano, *Phys. Rev. D* **52**(5), R2619–R2623 (1995).
- Czarnecki, A., B. Krause, and W. J. Marciano, *Phys. Rev. Lett.* **76**(18), 3267–3270 (1996).
- Czarnecki, A., K. Melnikov, and A. Yelkhovsky, *Phys. Rev. Lett.* **82**(2), 311–314 (1999).

- Davies, M., and A. Höcker, Phys. Lett. B **419**(1-4), 419–431 (1998a).
- Davies, M., and A. Höcker, Phys. Lett. B **435**(3-4), 427–440 (1998b).
- Davis, R. S. (private communication, 1997).
- Davis, R. S., Metrologia **35**(1), 49–55 (1998).
- Davis, R. S., and V. E. Bower, J. Res. Natl. Bur. Stand. **84**(2), 157–160 (1979).
- de Beauvoir, B., F. Nez, L. Julien, B. Cagnac, F. Biraben, D. Touahri, L. Hilico, O. Acef, A. Clairon, and J. J. Zondy, Phys. Rev. Lett. **78**(3), 440–443 (1997).
- De Bièvre, P., *et al.*, IEEE Trans. Instrum. Meas. **46**(2), 592–595 (1997).
- Degrassi, G., and G. F. Giudice, Phys. Rev. D **58**, 053007, 5 pp. (1998).
- Dehmelt, H., in *Atomic Physics 7*, edited by D. Kleppner and F. M. Pipkin (Plenum, New York, 1981), pp. 337–372.
- Dehmelt, H., Proc. Natl. Acad. Sci. USA **91**(14), 6308–6309 (1994a).
- Dehmelt, H., Proc. Natl. Acad. Sci. USA **91**(11), 5043–5045 (1994b).
- Dehmelt, H. G., and R. S. Van Dyck, Jr. (private communication, 1996).
- Dehmelt, H., R. Van Dyck, Jr., and F. Palmer, Proc. Natl. Acad. Sci. USA **89**(5), 1681–1684 (1992).
- Delahaye, F., Metrologia **26**(1), 63–68 (1989).
- Delahaye, F., A. Fau, D. Dominguez, and M. Bellon, IEEE Trans. Instrum. Meas. **IM-36**(2), 205–207 (1987).
- Delahaye, F., A. Satrapinsky, and T. J. Witt, IEEE Trans. Instrum. Meas. **38**(2), 256–259 (1989).
- Delahaye, F., and D. Bournaud, IEEE Trans. Instrum. Meas. **40**(2), 237–240 (1991).
- Delahaye, F., T. J. Witt, B. Jeckelmann, and B. Jeanneret, Metrologia **32**(5), 385–388 (1996).
- Delahaye, F., T. J. Witt, E. Pesel, B. Schumacher, and P. Warnecke, Metrologia **34**(3), 211–214 (1997).
- Delahaye, F., T. J. Witt, F. Piquemal, and G. Genevès, IEEE Trans. Instrum. Meas. **44**(2), 258–261 (1995).
- Deslattes, R. D., in *Proceedings of Course LXVIII "Metrology and Fundamental Constants"*, edited by A. F. Milone and P. Giacomo (North-Holland, Amsterdam, 1980), pp. 38–113.
- Deslattes, R. D., in *The Art of Measurement*, edited by B. Kramer (VCH, Weinheim, 1988), pp. 193–201.
- Deslattes, R. D., A. Henins, H. A. Bowman, R. M. Schoonover, C. L. Carroll, I. L. Barnes, L. A. Machlan, L. J. Moore, and W. R. Shields, Phys. Rev. Lett. **33**(8), 463–466 (1974).
- Deslattes, R. D., A. Henins, R. M. Schoonover, C. L. Carroll, and H. A. Bowman, Phys. Rev. Lett. **36**(15), 898–900 (1976).
- Deslattes, R. D., and A. Henins, Phys. Rev. Lett. **31**(16), 972–975 (1973).
- Deslattes, R. D., and E. G. Kessler, Jr., IEEE Trans. Instrum. Meas. **40**(2), 92–97 (1991).
- Deslattes, R. D., and E. G. Kessler, Jr., IEEE Trans. Instrum. Meas. **48**(2), 238–241 (1999).
- Deslattes, R. D., M. Tanaka, G. L. Greene, A. Henins, and E. G. Kessler, Jr., IEEE Trans. Instrum. Meas. **IM-36**(2), 166–169 (1987).
- Dickinson, W. C., Phys. Rev. **81**(5), 717–731 (1951).
- DiFilippo, F., V. Natarajan, K. R. Boyce, and D. E. Pritchard, Phys. Rev. Lett. **73**(11), 1481–1484 (1994).
- DiFilippo, F., V. Natarajan, M. Bradley, F. Palmer, and D. E. Pritchard, Phys. Scr. **T59**, 144–154 (1995a).
- DiFilippo, F., V. Natarajan, M. Bradley, F. Palmer, and D. E. Pritchard, in *Atomic Physics 14*, edited by D. J. Wineland, C. E. Wieman, and S. J. Smith, AIP Conf. Proc. 323, 149–175 (1995b).
- Drake, G. W. F., and R. A. Swainson, Phys. Rev. A **41**(3), 1243–1246 (1990).
- Drake, G. W. F., and W. C. Martin, Can. J. Phys. **76**(9), 679–698 (1998).
- Drumm, H., C. Eck, G. Petrucci, and O. Runólfsson, Nucl. Instrum. Methods **158**(2-3), 347–362 (1979).
- Dupouy, G., and R. Jouaust, J. Phys. Radium **6**(3), 123–134 (1935).
- Eberhardt, K. R. (private communication, 1981).
- Eidelman, S., and F. Jegerlehner, Z. Phys. C **67**(4), 585–601 (1995).
- Eides, M. I., Phys. Rev. A **53**(5), 2953–2957 (1996).
- Eides, M. I., and H. Grotch, Phys. Rev. A **52**(4), 3360–3361 (1995a).
- Eides, M. I., and H. Grotch, Phys. Rev. A **52**(2), 1757–1760 (1995b).
- Eides, M. I., and H. Grotch, Ann. Phys. (N.Y.) **260**(1), 191–200 (1997a).
- Eides, M. I., and H. Grotch, Phys. Rev. A **56**(4), R2507–R2509 (1997b).
- Eides, M. I., and H. Grotch, Phys. Rev. A **55**(5), 3351–3360 (1997c).
- Eides, M. I., and V. A. Shelyuto, Phys. Lett. B **146**(3-4), 241–243 (1984).
- Eides, M. I., and V. A. Shelyuto, Phys. Rev. A **52**(2), 954–961 (1995).
- Eides, M. I., H. Grotch, and V. A. Shelyuto, Phys. Rev. A **55**(3), 2447–2449 (1997).
- Eides, M. I., H. Grotch, and V. A. Shelyuto, Phys. Rev. D **58**, 013008, 12 pp. (1998).
- Eides, M. I., S. G. Karshenboim, and V. A. Shelyuto, Phys. Lett. B **216**(3-4), 405–408 (1989a).
- Eides, M. I., S. G. Karshenboim, and V. A. Shelyuto, Phys. Lett. B **229**(3), 285–288 (1989b).
- Eides, M. I., S. G. Karshenboim, and V. A. Shelyuto, Phys. Lett. B **249**(3-4), 519–522 (1990).
- Eides, M. I., S. G. Karshenboim, and V. A. Shelyuto, Phys. Lett. B **268**(3-4), 433–436 (1991). Errata: **316**(4), 631–631 (1993), **319**(4), 545–545 (1993).
- Elkhovskii, A. S., Zh. Éksp. Teor. Fiz. **110**(2), 431–442 (1996) [Sov. Phys. JETP **83**(2), 230–235 (1996)].
- Elmqvist, R. E. (private communication, 1997).
- Elmqvist, R. E., and R. F. Dziuba, IEEE Trans. Instrum. Meas. **46**(2), 322–324 (1997).
- Erickson, G. W., J. Phys. Chem. Ref. Data **6**(3), 831–869 (1977).
- Erickson, G. W., and D. R. Yennie, Ann. Phys. (N.Y.) **35**(1), 271–313 (1965).
- Farley, F. J. M., and E. Picasso, Ann. Rev. Nucl. Part. Sci. **29**, 243–282 (1979).
- Farley, F. J. M., and E. Picasso, in *Quantum Electrodynamics*, edited by T. Kinoshita (World Scientific, Singapore, 1990), Chap. 11, pp. 479–559.
- Farnham, D. L., R. S. Van Dyck, Jr., and P. B. Schwinberg, Phys. Rev. Lett. **75**(20), 3598–3601 (1995).
- Faustov, R., Phys. Lett. B **33**(6), 422–424 (1970).
- Faustov, R. N., A. Karimkhodzhaev, and A. P. Martyneko, Phys. Rev. A **59**(3), 2498–2499 (1999).
- Fee, M. S., S. Chu, A. P. Mills, Jr., R. J. Chichester, D. M. Zuckerman, E. D. Shaw, and K. Danzmann, Phys. Rev. A **48**(1), 192–219 (1993).
- Fei, X., IEEE Trans. Instrum. Meas. **44**(2), 501–504 (1995).
- Fei, X., Bull. Am. Phys. Soc. **41**, 1271 (1996).
- Fei, X., V. W. Hughes, and R. Prigl, Nucl. Instrum. Methods **A394**(3), 349–356 (1997).
- Fellmuth, B. (private communication, 1999).
- Fermi, E., Z. Phys. **60**(5-6), 320–333 (1930).
- Feynman, R. P., R. B. Leighton, and M. L. Sands, *The Feynman Lectures on Physics*, Vol. 1 (Addison Wesley, Reading, MA, 1963).
- Fitzgerald, M. P., and T. R. Armstrong, Meas. Sci. Technol. **10**(6), 439–444 (1999).
- Flowers, J. L., B. W. Petley, and M. G. Richards, J. Phys. B **23**(8), 1359–1362 (1990).
- Flowers, J. L., B. W. Petley, and M. G. Richards, Metrologia **30**(2), 75–87 (1993).
- Flowers, J. L., C. J. Bickley, P. W. Josephs-Franks, and B. W. Petley, IEEE Trans. Instrum. Meas. **46**(2), 104–107 (1997).
- Flowers, J. L., N. J. Cleaton, P. W. Josephs-Franks, and B. W. Petley, IEEE Trans. Instrum. Meas. **48**(2), 209–211 (1999).
- Flowers, J. L., P. W. Franks, and B. W. Petley, IEEE Trans. Instrum. Meas. **44**(2), 488–490 (1995a).
- Flowers, J. L., P. W. Franks, and B. W. Petley, IEEE Trans. Instrum. Meas. **44**(2), 572–574 (1995b).
- Forkert, J., and W. Schlesok, Metro. Abh. des ASMW **6**(3-4), 165–175 (1986).
- Friar, J. L., Z. Phys. A **292**(1), 1–6 (1979a); Erratum: **303**(1), 84–84 (1981).
- Friar, J. L., Ann. Phys. (N.Y.) **122**(1), 151–196 (1979b).
- Friar, J. L. (private communication, 1998).
- Friar, J. L., and G. L. Payne, Phys. Rev. C **56**(2), 619–630 (1997a).
- Friar, J. L., and G. L. Payne, Phys. Rev. A **56**(6), 5173–5175 (1997b).
- Friar, J. L., and G. L. Payne, Phys. Rev. C **55**(6), 2764–2767 (1997c).
- Friar, J. L., J. Martorell, and D. W. L. Sprung, Phys. Rev. A **56**(6), 4579–4586 (1997).
- Friar, J. L., J. Martorell, and D. W. L. Sprung, Phys. Rev. A **59**(5), 4061–4063 (1999).
- Fujii, K., E. R. Williams, R. L. Steiner, and D. B. Newell, IEEE Trans. Instrum. Meas. **46**(2), 191–195 (1997).
- Fujii, K., M. Tanaka, Y. Nezu, A. Sakuma, A. Leistner, and W. Giardini, IEEE Trans. Instrum. Meas. **44**(2), 542–545 (1995).
- Fujii, Y., F. Shiota, Y. Miki, K. Nakayama, and T. Morokuma, IEEE Trans. Instrum. Meas. **48**(2), 200–204 (1999).

- Fujimoto, H., K. Nakayama, M. Tanaka, and G. Misawa, *Jpn. J. Appl. Phys.* **34**(9A), 5065–5069 (1995a). Erratum: **34**(12A), 6546–6546 (1995a).
- Fujimoto, H., M. Tanaka, and K. Nakayama, *IEEE Trans. Instrum. Meas.* **44**(2), 471–474 (1995b).
- Fulton, T. A., *Phys. Rev. B* **7**(3), 981–982 (1973).
- Funck, T., and V. Sienknecht, *IEEE Trans. Instrum. Meas.* **40**(2), 158–161 (1991).
- Gabrielse, G., and J. Tan, in *Cavity Quantum Electrodynamics. Advances in Atomic, Molecular, and Optical Physics. Supplement 2*, edited by P. R. Berman (Academic Press, San Diego, 1994), pp. 267–299.
- Gabrielse, G., J. Tan, and L. S. Brown, in *Quantum Electrodynamics*, edited by T. Kinoshita (World Scientific, Singapore, 1990a), Chap. 9, pp. 389–418.
- Gabrielse, G., X. Fei, L. A. Orozco, R. L. Tjoelker, J. Haas, H. Kalinowsky, T. A. Trainor, and W. Kells, *Phys. Rev. Lett.* **65**(11), 1317–1320 (1990b).
- Gardner, C. J., *et al.*, *Phys. Rev. Lett.* **48**(17), 1168–1171 (1982).
- Garreau, J. C., M. Allegrini, L. Julien, and F. Biraben, *J. Phys. (Paris)* **51**(20), 2263–2273 (1990a).
- Garreau, J. C., M. Allegrini, L. Julien, and F. Biraben, *J. Phys. (Paris)* **51**(20), 2275–2292 (1990b).
- Garreau, J. C., M. Allegrini, L. Julien, and F. Biraben, *J. Phys. (Paris)* **51**(20), 2293–2306 (1990c).
- Gauss, C. F., *Theoria Motus Corporum Coelestium in Sectionibus Conicis Solem Ambientium* (Perthes and Besser, Hamburg, 1809).
- Gauss, C. F., in *Theoria Combinationis Observationum Erroribus Minimis Obnoxiae* (Royal Society of Göttingen, Göttingen, 1823), pp. 33–62.
- Genevès, G., J.-P. Lo-Hive, D. Reymann, and T. J. Witt, *Metrologia* **30**(5), 511–512 (1993).
- Gillespie, A. D., K. Fujii, D. B. Newell, P. T. Olsen, A. Picard, R. L. Steiner, G. N. Stenbakken, and E. R. Williams, *IEEE Trans. Instrum. Meas.* **46**(2), 605–608 (1997).
- Gillies, G. T., *Rep. Prog. Phys.* **60**(2), 151–225 (1997).
- Gläser, M., *Rev. Sci. Instrum.* **62**(10), 2493–2494 (1991).
- Goidenko, I., L. Labzowsky, A. Nefiodov, G. Plunien, and G. Soff, *Phys. Rev. Lett.* **83**(12), 2312–2315 (1999).
- Golosov, E. A., A. S. Elkhovskii, A. I. Mil'shtein, and I. B. Khriplovich, *Zh. Eksp. Teor. Fiz.* **107**(2), 393–400 (1995). [*JETP* **80**(2), 208–211 (1995)].
- Gonfiantini, R., P. De Bièvre, S. Valkiers, and P. D. P. Taylor, *IEEE Trans. Instrum. Meas.* **46**(2), 566–571 (1997).
- Gorshkov, M. V., Y. I. Neronov, E. N. Nikolaev, Y. V. Tarbeev, and V. L. Tal'roze, *Dokl. Akad. Nauk SSSR* **305**, 1362–1364 (1989) [*Sov. Phys. Dokl.* **34**(4), 362–363 (1989)].
- Greene, G. L., E. G. Kessler, Jr., R. D. Deslattes, and H. Börner, *Phys. Rev. Lett.* **56**(8), 819–822 (1986).
- Greene, G. L., N. F. Ramsey, W. Mampe, J. M. Pendlebury, K. Smith, W. B. Dress, P. D. Miller, and P. Perrin, *Phys. Rev. D* **20**(9), 2139–2153 (1979).
- Greene, G. L., N. F. Ramsey, W. Mampe, J. M. Pendlebury, K. Smith, W. D. Dress, P. D. Miller, and P. Perrin, *Phys. Lett. B* **71**(2), 297–300 (1977).
- Grohmann, K., and H. Luther, in *Temperature: Its Measurement and Control in Science and Industry*, edited by J. F. Schooley, Vol. 6, part 1 (American Institute of Physics, New York, 1992), pp. 21–26.
- Grotch, H., *Phys. Rev. Lett.* **24**(2), 39–42 (1970a).
- Grotch, H., *Phys. Rev. A* **2**(4), 1605–1607 (1970b).
- Grotch, H., in *Precision Measurement and Fundamental Constants*, edited by D. N. Langenberg and B. N. Taylor (NBS Spec. Pub. 343, US Government Printing Office, Washington, DC, 1971), pp. 421–425.
- Grotch, H. (private communication, 1997).
- Grotch, H., and R. A. Hegstrom, *Phys. Rev. A* **4**(1), 59–69 (1971).
- Gundlach, J. H., *Meas. Sci. Technol.* **10**(6), 454–459 (1999).
- Hagley, E. W., and F. M. Pipkin, *Phys. Rev. Lett.* **72**(8), 1172–1175 (1994).
- Hall, J. L., C. J. Bordé, and K. Uehara, *Phys. Rev. Lett.* **37**(20), 1339–1342 (1976).
- Halperin, B. I., *Sci. Am.* **254**(4), 52–60 (1986).
- Hamer, W. J., *Standard Cells: Their Construction, Maintenance, and Characteristics* (NBS Monograph 84, US Government Printing Office, Washington, DC, 1965).
- Hamilton, C. A., C. J. Burroughs, and S. P. Benz, *IEEE Trans. Appl. Supercon.* **7**(2), 3756–3761 (1997).
- Hanada, H., T. Tsubokawa, B. Murphy, J. Williams, K. Shibuya, and K. Kaminuma, *Bull. Inf. Bur. Grav. Int.* **74**, 25–29 (1994).
- Hand, L. N., D. G. Miller, and R. Wilson, *Rev. Mod. Phys.* **35**(2), 335–349 (1963).
- Harris, W. S., *Trans. R. Soc. Edinburgh* **12**, 206–221 (1834).
- Hart, M., *Proc. R. Soc. London, Ser. A* **346**(1644), 1–22 (1975).
- Hartland, A., G. J. Davies, and D. R. Wood, *IEEE Trans. Instrum. Meas.* **IM-34**(2), 309–314 (1985).
- Hartland, A., K. Jones, J. M. Williams, B. L. Gallagher, and T. Galloway, *Phys. Rev. Lett.* **66**(8), 969–973 (1991).
- Hartland, A., R. G. Jones, and D. J. Legg, Document CCE/88-9 submitted to the 18th meeting of the Comité Consultatif d'Électricité of the CIPM (1988).
- Hartland, A., R. G. Jones, B. P. Kibble, and D. J. Legg, *IEEE Trans. Instrum. Meas.* **IM-36**(2), 208–213 (1987).
- Hartle, J. B., D. J. Scalapino, and R. L. Sugar, *Phys. Rev. B* **3**(5), 1778–1781 (1971).
- Härtwig, J., S. Grosswig, P. Becker, and D. Windisch, *Phys. Status Solidi A* **125**(1), 79–89 (1991).
- Hayakawa, M., and T. Kinoshita, *Phys. Rev. D* **57**(1), 465–477 (1998).
- Hayakawa, M., T. Kinoshita, and A. I. Sanda, *Phys. Rev. D* **54**(5), 3137–3153 (1996).
- Hegstrom, R. A., *Phys. Rev.* **184**(1), 17–22 (1969). Erratum: *Phys. Rev. A* **1**(2), 536–537 (1970).
- Hegstrom, R. A., in *Precision Measurement and Fundamental Constants*, edited by D. N. Langenberg and B. N. Taylor (NBS Spec. Pub. 343, US Government Printing Office, Washington, DC, 1971), pp. 417–420.
- Hensley, J. M. (private communication, 1999).
- Heyl, P. R., *J. Res. Natl. Bur. Stand.* **5**(256), 1243–1290 (1930).
- Heyl, P. R., and P. Chrzanowski, *J. Res. Natl. Bur. Stand.* **29**(1480), 1–31 (1942).
- Hildum, E. A., U. Boesl, D. H. McIntyre, R. G. Beausoleil, and T. W. Hänsch, *Phys. Rev. Lett.* **56**(6), 576–579 (1986).
- Hinds, E. A., in *The Spectrum of Atomic Hydrogen: Advances*, edited by G. W. Series (World Scientific, Singapore, 1988), Chap. 4, pp. 243–292.
- Huber, A., T. Udem, B. Gross, J. Reichert, M. Kourogi, K. Pachucki, M. Weitz, and T. W. Hänsch, *Phys. Rev. Lett.* **80**(3), 468–471 (1998).
- Hubler, B., A. Cornaz, and W. Kündig, *Phys. Rev. D* **51**(8), 4005–4016 (1995).
- Hudson, R. P., *Metrologia* **19**(4), 163–177 (1984).
- Hughes, V. W., in *A Gift of Prophecy*, edited by E. C. G. Sudarshan (World Scientific, Singapore, 1994), pp. 222–250.
- Hughes, V. W., in *Atomic Physics Methods in Modern Research*, edited by K. Jungmann, J. Kowalski, I. Reinhard, and F. Träger (Springer-Verlag, Berlin, 1997), pp. 21–41.
- Hughes, V. W., in *Frontier Tests of QED and Physics of the Vacuum*, edited by E. Zavattini, D. Bakalov, and C. Rizzo (Heron Press, Sofia, 1998), pp. 97–116.
- Hughes, V. W., and G. zu Putlitz, in *Quantum Electrodynamics*, edited by T. Kinoshita (World Scientific, Singapore, 1990), Chap. 16, pp. 822–904.
- Hughes, V. W., and J. Kuti, *Annu. Rev. Nucl. Part. Sci.* **33**, 611–644 (1983).
- Hughes, V. W., and T. Kinoshita, *Rev. Mod. Phys.* **71**(2), S133–S139 (1999).
- Hughes, W. M., and H. G. Robinson, *Phys. Rev. Lett.* **23**(21), 1209–1212 (1969).
- Hylton, D. J., *Phys. Rev. A* **32**(3), 1303–1309 (1985).
- IEC, *IEC 27: Letter symbols to be used in electrical technology*, 6th ed. (International Electrotechnical Commission, Geneva, Switzerland, 1992).
- ISO, *Guide to the Expression of Uncertainty in Measurement* (International Organization for Standardization, Geneva, Switzerland, 1993a; corrected and reprinted, 1995).
- ISO, *ISO Standards Handbook: Quantities and Units*, 3rd ed. (International Organization for Standardization, Geneva, Switzerland, 1993b).
- Janßen, M., O. Viehweger, U. Fastenrath, and J. Hajdu, *Introduction to the Theory of the Integer Quantum Hall Effect* (VCH, Weinheim, Germany, 1994).
- Jeanneret, B., B. Jeckelmann, H. Bühlmann, R. Houdré, and M. Ilegems, *IEEE Trans. Instrum. Meas.* **44**(2), 254–257 (1995).
- Jeckelmann, B., B. Jeanneret, and D. Inglis, *Phys. Rev. B* **55**(19), 13124–13134 (1997).

- Jeffery, A.-M., R. E. Elmquist, L. H. Lee, J. Q. Shields, and R. F. Dziuba, *IEEE Trans. Instrum. Meas.* **46**(2), 264–268 (1997).
- Jeffery, A., R. E. Elmquist, J. Q. Shields, L. H. Lee, M. E. Cage, S. H. Shields, and R. F. Dziuba, *Metrologia* **35**(2), 83–96 (1998).
- Jegerlehner, F., *Nucl. Phys. B (Proc. Suppl.)* **51C**, 131–141 (1996).
- Jentschura, U., and K. Pachucki, *Phys. Rev. A* **54**(3), 1853–1861 (1996).
- Jentschura, U. D., G. Soff, and P. J. Mohr, *Phys. Rev. A* **56**(3), 1739–1755 (1997).
- Jentschura, U. D., P. J. Mohr, and G. Soff, *Phys. Rev. Lett.* **82**(1), 53–56 (1999).
- Johnson, C. E., and H. G. Robinson, *Phys. Rev. Lett.* **45**(4), 250–252 (1980).
- Johnson, W. R., and G. Soff, *At. Data. Nucl. Data Tables* **33**(3), 405–446 (1985).
- Johnson, W. R., and K. T. Cheng, *Phys. Rev. A* **53**(3), 1375–1378 (1996).
- Jones, R. G., and B. P. Kibble, *IEEE Trans. Instrum. Meas.* **IM-34**(2), 181–184 (1985).
- Josephson, B. D., *Phys. Lett.* **1**(7), 251–253 (1962).
- Jungmann, K. (private communication, 1999).
- Karagioz, O. V., V. P. Izmaylov, and G. T. Gillies, *Grav. Cosmol.* **4**(3), 239–245 (1998).
- Karagyozy, O. V., A. H. Silin, and V. F. Izmaylov, *Izv. Akad. Nauk SSSR, Fiz. Zemli.* **17**(1), 92–97 (1981) [*Izv. Acad. Sci. USSR, Phys. Solid Earth.* **17**(1), 66–70 (1981)].
- Karimkhodzhaev, A., and R. N. Faustov, *Yad. Fiz.* **53**, 1012–1014 (1991) [*Sov. J. Nucl. Phys.* **53**(4), 626–627 (1991)].
- Karshenboim, S. G., in *1994 Conference on Precision Electromagnetic Measurements Digest*, edited by E. DeWeese and G. Bennett (IEEE, Piscataway, NJ, 1994), pp. 225–226. IEEE Catalog number 94CH3449-6.
- Karshenboim, S. G., *J. Phys. B* **28**(4), L77–L79 (1995).
- Karshenboim, S. G., *Z. Phys. D* **36**(1), 11–15 (1996a).
- Karshenboim, S. G., *J. Phys. B* **29**(2), L29–L31 (1996b).
- Karshenboim, S. G., *Z. Phys. D* **39**(2), 109–113 (1997a).
- Karshenboim, S. G., *Phys. Lett. A* **225**(1–3), 97–106 (1997b).
- Karshenboim, S. G., *Zh. Éksp. Teor. Fiz.* **103**(4), 1105–1117 (1993a) [*JETP* **76**(4), 541–546 (1993)].
- Karshenboim, S. G., *Yad. Fiz.* **56**, 252–254 (1993b) [*Phys. At. Nucl.* **56**(6), 857–858 (1993)].
- Karshenboim, S. G., *Zh. Éksp. Teor. Fiz.* **106**(2), 414–424 (1994) [*JETP* **79**(2), 230–235 (1994)].
- Karshenboim, S. G., *Zh. Éksp. Teor. Fiz.* **107**(4), 1061–1079 (1995) [*JETP* **80**(4), 593–602 (1995)].
- Karshenboim, S. G., *Zh. Éksp. Teor. Fiz.* **109**(3), 752–761 (1996) [*Sov. Phys. JETP* **82**(3), 403–408 (1996)].
- Karshenboim, S. G., V. A. Shelyuto, and M. I. Éides, *Yad. Fiz.* **55**, 466–474 (1992) [*Sov. J. Nucl. Phys.* **55**(2), 257–261 (1992)].
- Kawall, D., in *Frontier Tests of QED and Physics of the Vacuum*, edited by E. Zavattini, D. Vakalov, and C. Rizzo (Heron Press, Sofia, 1998), pp. 138–150.
- Kelly, R. L., *J. Phys. Chem. Ref. Data* **16**, Suppl. No. 1, 1–649 (1987).
- Kessler, E. G., A. Henins, R. D. Deslattes, L. Nielsen, and M. Arif, *J. Res. Natl. Inst. Stand. Technol.* **99**(1), 1–18 (1994). Erratum: **99**(3), 285–285 (1994).
- Kessler, E. G., M. S. Dewey, R. D. Deslattes, A. Henins, H. G. Börner, M. Jentschel, C. Doll, and H. Lehmann, *Phys. Lett. A* **255**(4–6), 221–229 (1999a).
- Kessler, Jr., E. G. (private communication, 1999).
- Kessler, Jr., E. G., J. E. Schweppe, and R. D. Deslattes, *IEEE Trans. Instrum. Meas.* **46**(2), 551–555 (1997).
- Kessler, Jr., E. G., R. D. Deslattes, and A. Henins, *Phys. Rev. A* **19**(1), 215–218 (1979).
- Kessler, Jr., E. G., S. M. Owens, A. Henins, and R. D. Deslattes, *IEEE Trans. Instrum. Meas.* **48**(2), 221–224 (1999b).
- Khriplovich, I. B. (private communication, 1998).
- Khriplovich, I. B., and R. A. Sen'kov, *Phys. Lett. A* **249**, (5–6), 474–476 (1998).
- Kibble, B. P., in *Atomic Masses and Fundamental Constants 5*, edited by J. H. Sanders and A. H. Wapstra (Plenum Press, New York, 1975), pp. 545–551.
- Kibble, B. P. (private communication, 1981).
- Kibble, B. P. (private communication, 1997).
- Kibble, B. P., and G. J. Hunt, *Metrologia* **15**(1), 5–30 (1979).
- Kibble, B. P., and I. A. Robinson (private communication, 1998).
- Kibble, B. P., and I. Robinson, *Feasibility Study for a Moving Coil Apparatus to Relate the Electrical and Mechanical SI Units* (National Physical Laboratory, Teddington, Middlesex, UK, 1977). NPL Report DES 40.
- Kibble, B. P., I. A. Robinson, and J. H. Belliss, *Metrologia* **27**(4), 173–192 (1990).
- Kibble, B. P., R. C. Smith, and I. A. Robinson, *IEEE Trans. Instrum. Meas.* **IM-32**(1), 141–143 (1983).
- Kim, C. G., B. C. Woo, P. G. Park, K. S. Ryu, and C. S. Kim, *IEEE Trans. Instrum. Meas.* **44**(2), 484–487 (1995).
- Kinoshita, T., in *Quantum Electrodynamics*, edited by T. Kinoshita (World Scientific, Singapore, 1990), Chap. 7, pp. 218–321.
- Kinoshita, T., *Phys. Rev. D* **47**(11), 5013–5017 (1993).
- Kinoshita, T., *Phys. Rev. Lett.* **75**(26), 4728–4731 (1995).
- Kinoshita, T., *Rep. Prog. Phys.* **59**(11), 1459–1492 (1996).
- Kinoshita, T., *IEEE Trans. Instrum. Meas.* **46**(2), 108–111 (1997).
- Kinoshita, T. (private communication, 1998).
- Kinoshita, T., and M. Nio, *Phys. Rev. Lett.* **72**(24), 3803–3806 (1994).
- Kinoshita, T., and M. Nio, *Phys. Rev. D* **53**(9), 4909–4930 (1996).
- Kinoshita, T., and W. J. Marciano, in *Quantum Electrodynamics*, edited by T. Kinoshita (World Scientific, Singapore, 1990), Chap. 10, pp. 419–478.
- Kinoshita, T., B. Nižić, and Y. Okamoto, *Phys. Rev. D* **31**(8), 2108–2119 (1985).
- Kinoshita, T., B. Nižić, and Y. Okamoto, *Phys. Rev. D* **41**(2), 593–610 (1990).
- Kirk-Othmer, *Kirk-Othmer Encyclopedia of Chemical Technology*, Vol. 4 (Wiley, New York, 1978).
- Kleinevoss, U., H. Meyer, A. Schumacher, and S. Hartmann, *Meas. Sci. Technol.* **10**(6), 492–492 (1999).
- Klempt, E., R. Schulze, H. Wolf, M. Camani, F. Gyax, W. Rüegg, A. Schenck, and H. Schilling, *Phys. Rev. D* **25**(3), 652–676 (1982).
- Kleppner, D. (private communication, 1997).
- Koch, W. F., in *Atomic Masses and Fundamental Constants 6*, edited by J. A. Nolen and W. Benenson (Plenum, New York, 1980), pp. 167–172.
- Koehler, C., D. Livingston, J. Castilleja, A. Sanders, and D. Shiner, in *Applications of Accelerators in Research and Industry*, edited by J. L. Duggan and I. L. Morgan, AIP Conf. Proc. 475, pp. 185–188 (1999).
- Kol'chenko, A. P., S. G. Rautian, and R. I. Sokolovskii, *Zh. Éksp. Teor. Fiz.* **55**, 1864–1873 (1968) [*Sov. Phys. JETP* **28**(5), 986–990 (1969)].
- Kotochigova, S., P. J. Mohr, and B. N. Taylor (private communication, 1999).
- Krause, B., *Phys. Lett. B* **390**(1–4), 392–400 (1997).
- Krüger, E., W. Nistler, and W. Weirauch, *J. Phys. (Paris) Colloq.* **C3**, 217–222 (1984a).
- Krüger, E., W. Nistler, and W. Weirauch, in *Precision Measurement and Fundamental Constants II*, edited by B. N. Taylor and W. D. Phillips (NBS Spec. Pub. 617, US Government Printing Office, Washington, DC, 1984b), pp. 369–373.
- Krüger, E., W. Nistler, and W. Weirauch, *Metrologia* **22**(3), 172–173 (1986).
- Krüger, E., W. Nistler, and W. Weirauch, *PTB Mitt.* **99**(5), 318–322 (1989a).
- Krüger, E., W. Nistler, and W. Weirauch, *Nucl. Instrum. Methods A* **284**(1), 143–146 (1989b).
- Krüger, E., W. Nistler, and W. Weirauch, *Metrologia* **32**(2), 117–128 (1995).
- Krüger, E., W. Nistler, and W. Weirauch, *Metrologia* **35**(3), 203–209 (1998).
- Krüger, E., W. Nistler, and W. Weirauch, *Metrologia* **36**(2), 147–148 (1999).
- Kukhto, T. V., E. A. Kuraev, A. Schiller, and Z. K. Silagadze, *Nucl. Phys.* **B371**(3), 567–596 (1992).
- Kuraev, E. A., T. V. Kukhto, and A. Schiller, *Yad. Fiz.* **51**, 1631–1637 (1990) [*Sov. J. Nucl. Phys.* **51**(6), 1031–1035 (1990)].
- Kuroda, K., *Phys. Rev. Lett.* **75**(15), 2796–2798 (1995).
- Kuroda, K., *Meas. Sci. Technol.* **10**(6), 435–438 (1999).
- Kuznetsov, V. A., V. Y. Kaminskii, S. N. Libedev, V. M. Pudalov, V. V. Sazhin, S. G. Semenchinsky, and A. K. Yanysh, Document CCE/88-3

- submitted to the 18th meeting of the Comité Consultatif d'Électricité of the CIPM (1988).
- Lamb, Jr., W. E., Phys. Rev. **60**(11), 817–819 (1941).
- Lambe, E. B. D., in *Polarisation Matière et Rayonnement* (Société Française de Physique, Paris, 1968), pp. 441–454.
- Lampard, D. G., Proc. IEEE **104C**, 271–280 (1957).
- Langenberg, D. N., and J. R. Schrieffer, Phys. Rev. B **3**(5), 1776–1778 (1971).
- Laplace, marquis de, P. S., *Théorie Analytique des Probabilités*, Vol. II (Ve. Courcier, Paris, 1812).
- Laporta, S., Phys. Lett. B **312**(4), 495–500 (1993a).
- Laporta, S., Nuovo Cimento **106**(5), 675–683 (1993b).
- Laporta, S., Phys. Rev. D **47**(10), 4793–4795 (1993c).
- Laporta, S., Phys. Lett. B **343**(1-4), 421–426 (1995).
- Laporta, S., and E. Remiddi, Phys. Lett. B **265**(1-2), 182–184 (1991).
- Laporta, S., and E. Remiddi, Phys. Lett. B **301**(4), 440–446 (1993).
- Laporta, S., and E. Remiddi, Phys. Lett. B **356**(2-3), 390–397 (1995).
- Laporta, S., and E. Remiddi, Phys. Lett. B **379**(1-4), 283–291 (1996).
- Larson, D. J., and N. F. Ramsey, Phys. Rev. A **9**(4), 1543–1548 (1974).
- Larson, D. J., P. A. Valberg, and N. F. Ramsey, Phys. Rev. Lett. **23**(24), 1369–1372 (1969).
- Lautrup, B., Phys. Lett. B **69**(1), 109–111 (1977).
- Legendre, A. M., *Nouvelles Méthodes pour la Détermination des Orbites des Comètes* (F. Didot, Paris, 1805).
- Li, G., M. A. Samuel, and M. I. Eides, Phys. Rev. A **47**(2), 876–878 (1993).
- Li, G., R. Mendel, and M. A. Samuel, Phys. Rev. D **47**(4), 1723–1725 (1993).
- Lieb, E. H., Philos. Mag. **46**(374), 311–316 (1955).
- Likharev, K. K., *Dynamics of Josephson Junctions and Circuits* (Gordon and Breach, Amsterdam, 1986).
- Liu, H., R. Liu, P. Shen, T. Jin, Z. Lu, X. Du, and B. Yu, Document CCE/88-11 submitted to the 18th meeting of the Comité Consultatif d'Électricité of the CIPM (1988).
- Liu, R. (private communication, 1997).
- Liu, R. (private communication, 1998).
- Liu, R. H. Liu, S. Xue, and Z. Zhang, Supplement to the Digest of the 1996 Conference on Precision Electromagnetic Measurements (1996).
- Liu, R., *et al.*, Acta Metrol. Sin. **16**(3), 161–168 (1995).
- Liu, W., and D. Kwall (private communication, 1998).
- Liu, W., *et al.*, Phys. Rev. Lett. **82**(4), 711–714 (1999).
- Lowes, F. J., Proc. R. Soc. London, Ser. A **337**(1611), 555–567 (1974).
- Lundeen, S. R., and F. M. Pipkin, Metrologia **22**(1), 9–54 (1986).
- Luo, J., Z. K. Hu, X. H. Fu, S. H. Fan, and M. X. Tang, Phys. Rev. D **59**, 042001, 6 pp. (1999).
- Luther, G. G., and W. R. Towler, Phys. Rev. Lett. **48**(3), 121–123 (1982).
- Luther, G. G., and W. R. Towler, in *Precision Measurement and Fundamental Constants II*, edited by B. N. Taylor and W. D. Phillips (NBS Spec. Pub. 617, US Government Printing Office, Washington, DC, 1984), pp. 573–576.
- Luther, H., K. Grohmann, and B. Fellmuth, Metrologia **33**(4), 341–352 (1996).
- Maas, F. E., *et al.*, Phys. Lett. A **187**(3), 247–254 (1994).
- Mallampalli, S., and J. Sapirstein, Phys. Rev. A **54**(4), 2714–2717 (1996).
- Mallampalli, S., and J. Sapirstein, Phys. Rev. Lett. **80**(24), 5297–5300 (1998).
- Mana, G., and E. Vittone, Z. Phys. B **102**(2), 189–196 (1997a).
- Mana, G., and E. Vittone, Z. Phys. B **102**(2), 197–206 (1997b).
- Mana, G., and G. Zosi, Rev. Nuovo Cimento **18**(3), 1–23 (1995).
- Mariam, F. G., Ph.D. thesis, Yale University, 1981.
- Mariam, F. G. (private communication, 1982).
- Mariam, F. G., *et al.*, Phys. Rev. Lett. **49**(14), 993–996 (1982).
- Marinenko, G., and J. K. Taylor, Anal. Chem. **40**(11), 1645–1651 (1968).
- Marson, I., *et al.*, Metrologia **32**(3), 137–144 (1995).
- Martin, J. E., and P. R. Haycocks, Metrologia **35**(4), 229–233 (1998).
- Martin, J. E., N. P. Fox, and P. J. Key, Metrologia **21**(3), 147–155 (1985).
- Martin, J., H. Bettin, U. Kuetsgens, D. Schiel, and P. Becker, IEEE Trans. Instrum. Meas. **48**(2), 216–220 (1999).
- Martin, J., U. Kuetsgens, J. Stümpel, and P. Becker, Metrologia **35**(6), 811–817 (1998).
- Martin, W. C. (private communication, 1998).
- Matsumura, S., N. Kanda, T. Tomaru, H. Ishizuka, and K. Kuroda, Phys. Lett. A **244**(1-3), 4–8 (1998).
- McIntyre, D. H., R. G. Beausoleil, C. J. Foot, E. A. Hildum, B. Couillaud, and T. W. Hänsch, Phys. Rev. A **39**(9), 4591–4598 (1989).
- McSkimin, H. J., J. Appl. Phys. **24**(8), 988–997 (1953).
- Mergell, P., U.-G. Meißner, and D. Dreschel, Nucl. Phys. A **596**(3-4), 367–396 (1996).
- Michaelis, W., H. Haars, and R. Augustin, Metrologia **32**(4), 267–276 (1996).
- Millman, S., I. I. Rabi, and J. R. Zacharias, Phys. Rev. **53**(5), 384–391 (1938).
- Mills, I., T. Cvitaš, K. Homann, N. Kallay, and K. Kuchitsu, *Quantities, Units and Symbols in Physical Chemistry*, 2nd ed. (Blackwell Scientific Publications, for the International Union of Pure and Applied Chemistry, Oxford, 1993).
- Minardi, F., G. Bianchini, P. C. Pastor, G. Giusfredi, F. S. Pavone, and M. Inguscio, Phys. Rev. Lett. **82**(6), 1112–1115 (1999).
- Mittlemann, R., H. Dehmelt, and S. Kim, Phys. Rev. Lett. **75**(15), 2839–2842 (1995).
- Mittlemann, R. K., I. I. Ioannou, and H. G. Dehmelt, in *Trapped Charged Particles and Fundamental Physics*, edited by D. H. E. Dubin and D. Schneider, AIP Conf. Proc. 457, 13–21 (1999).
- Mohr, P. J., in *Beam-Foil Spectroscopy*, edited by I. A. Sellin and D. J. Pegg, Vol. 1 (Plenum, New York, 1975), pp. 89–96.
- Mohr, P. J., Phys. Rev. A **26**(5), 2338–2354 (1982).
- Mohr, P. J., At. Data. Nucl. Data Tables **29**(3), 453–466 (1983).
- Mohr, P. J., Phys. Rev. A **46**(7), 4421–4424 (1992).
- Mohr, P. J., in *Atomic, Molecular, & Optical Physics Handbook*, edited by G. W. F. Drake (American Institute of Physics, Woodbury, 1996), Chap. 28, pp. 341–351.
- Mohr, P. J., and G. Soff, Phys. Rev. Lett. **70**(2), 158–161 (1993).
- Mohr, P. J., and Y.-K. Kim, Phys. Rev. A **45**(5), 2727–2735 (1992).
- Moldover, M. R. (private communication, 1990).
- Moldover, M. R., J. Res. Natl. Inst. Stand. Technol. **103**(2), 167–175 (1998).
- Moldover, M. R., and J. P. M. Trusler, Metrologia **25**(3), 165–187 (1988).
- Moldover, M. R., J. P. M. Trusler, T. J. Edwards, J. B. Mehl, and R. S. Davis, J. Res. Natl. Bur. Stand. **93**(2), 85–144 (1988a).
- Moldover, M. R., J. P. M. Trusler, T. J. Edwards, J. B. Mehl, and R. S. Davis, Phys. Rev. Lett. **60**(4), 249–252 (1988b).
- Moldover, M. R., S. J. Boyes, C. W. Meyer, and A. R. H. Goodwin, J. Res. Natl. Inst. Stand. Technol. **104**(1), 11–46 (1999).
- Nakamura, H., N. Kasai, and H. Sasaki, IEEE Trans. Instrum. Meas. **IM-36**(2), 196–200 (1987).
- Nakayama, K., and H. Fujimoto, IEEE Trans. Instrum. Meas. **46**(2), 580–583 (1997).
- Nakayama, K., H. Fujimoto, M. Tanaka, and K. Kuroda, IEEE Trans. Instrum. Meas. **42**(2), 401–404 (1993).
- Nakayama, K., M. Tanaka, and K. Kuroda, IEEE Trans. Instrum. Meas. **40**(2), 108–109 (1991a).
- Nakayama, K., M. Tanaka, F. Shiota, and K. Kuroda, Metrologia **28**(6), 483–502 (1991b).
- Neronov, Y. I., A. E. Barzakh, and K. Mukhamadiev, Zh. Éksp. Teor. Fiz. **69**, 1872–1882 (1975) [Sov. Phys. JETP **42**(6), 950–954 (1975)].
- Neronov, Y. I., and A. E. Barzakh, Zh. Éksp. Teor. Fiz. **72**(5), 1659–1669 (1977) [Sov. Phys. JETP **45**(5), 871–876 (1977)].
- Neronov, Y. I., and A. E. Barzakh, Zh. Éksp. Teor. Fiz. **75**, 1521–1540 (1978) [Sov. Phys. JETP **48**(5), 769–778 (1978)].
- Newman, R. D., and M. K. Bantel, Meas. Sci. Technol. **10**(6), 445–453 (1999).
- Newton, G., D. A. Andrews, and P. J. Unsworth, Philos. Trans. R. Soc. London, Ser. A **290**(1373), 373–404 (1979).
- Nez, F., *et al.*, Phys. Rev. Lett. **69**(16), 2326–2329 (1992).
- Nez, F., M. D. Plimmer, S. Bourzeix, L. Julien, F. Biraben, R. Felder, Y. Millerieux, and P. De Natale, Europhys. Lett. **24**(8), 635–640 (1993).
- Niebauer, T. M., G. S. Sasagawa, J. E. Faller, R. Hilt, and F. Klocking, Metrologia **32**(3), 159–180 (1995).
- Nier, A. O., Phys. Rev. **77**(6), 789–793 (1950).
- Nio, M., Ph.D. thesis, Cornell University, 1995.
- Nio, M., and T. Kinoshita, Phys. Rev. D **55**(11), 7267–7290 (1997).
- Nolting, F., J. Schurr, S. Schlamminger, and W. Kündig, Meas. Sci. Technol. **10**(6), 487–491 (1999).
- Olsen, P. T., and E. R. Williams, IEEE Trans. Instrum. Meas. **IM-23**(4), 302–305 (1974).

- Olsen, P. T., M. E. Cage, W. D. Phillips, and E. R. Williams, *IEEE Trans. Instrum. Meas.* **IM-29**(4), 234–237 (1980a).
- Olsen, P. T., R. E. Elmquist, W. D. Phillips, E. R. Williams, G. R. Jones, Jr., and V. E. Bower, *IEEE Trans. Instrum. Meas.* **38**(2), 238–244 (1989).
- Olsen, P. T., V. E. Bower, W. D. Phillips, E. R. Williams, and G. R. Jones, Jr., *IEEE Trans. Instrum. Meas.* **IM-34**(2), 175–181 (1985).
- Olsen, P. T., W. D. Phillips, and E. R. Williams, *J. Res. Natl. Bur. Stand.* **85**(4), 257–272 (1980b).
- Olsen, P. T., W. D. Phillips, and E. R. Williams, in *Precision Measurement and Fundamental Constants II*, edited by B. N. Taylor and W. D. Phillips (NBS Spec. Pub. 617, US Government Printing Office, Washington, DC, 1984), pp. 475–478.
- Olsen, P. T., W. L. Tew, Jr., E. R. Williams, R. E. Elmquist, and H. Sasaki, *IEEE Trans. Instrum. Meas.* **40**(2), 115–120 (1991).
- Pachucki, K., *Phys. Rev. A* **48**(4), 2609–2614 (1993a).
- Pachucki, K., *Ann. Phys. (N.Y.)* **226**(1), 1–87 (1993b).
- Pachucki, K., *Phys. Rev. A* **48**(1), 120–128 (1993c).
- Pachucki, K., *Phys. Rev. Lett.* **72**(20), 3154–3157 (1994).
- Pachucki, K., *Phys. Rev. A* **52**(2), 1079–1085 (1995).
- Pachucki, K., *Phys. Rev. A* **54**(3), 1994–1998 (1996).
- Pachucki, K. (private communication, 1998).
- Pachucki, K., and H. Grotch, *Phys. Rev. A* **51**(3), 1854–1862 (1995).
- Pal'chikov, V. G., Y. L. Sokolov, and V. P. Yakovlev, *Metrologia* **21**(3), 99–105 (1985).
- Pal'chikov, V. G., Y. L. Sokolov, and V. P. Yakovlev, *Phys. Scr.* **55**(1), 33–40 (1997).
- Patterson, J. B., and D. B. Prowse, *Metrologia* **21**(3), 107–113 (1985).
- Patterson, J. B., and D. B. Prowse, *Metrologia* **25**(2), 121–123 (1988).
- Patterson, J. B., and E. C. Morris, *Metrologia* **31**(4), 277–288 (1994).
- Peil, S., and G. Gabrielse, *Phys. Rev. Lett.* **83**(7), 1287–1290 (1999).
- Pendrill, L. R., *J. Phys. B* **29**(16), 3581–3586 (1996).
- Peris, S., M. Perrotet, and E. de Rafael, *Phys. Lett. B* **355**(3-5), 523–530 (1995).
- Persson, H., S. Salomonson, P. Sunnergren, and I. Lindgren, *Phys. Rev. A* **56**(4), R2499–R2502 (1997).
- Petermann, A., *Helv. Phys. Acta* **30**(5), 407–408 (1957).
- Petermann, A., *Nucl. Phys.* **5**(4), 677–683 (1958).
- Peters, A., K. Y. Chung, B. Young, J. Hensley, and S. Chu, *Philos. Trans. R. Soc. London, Ser. A* **355**(1733), 2223–2233 (1997).
- Petit, P., M. Desaintfuscien, and C. Audoin, *Metrologia* **16**(1), 7–14 (1980); Erratum: **16**(4), 184–184 (1980).
- Petley, B. W., and R. W. Donaldson, *Metrologia* **20**(3), 81–83 (1984).
- Phillips, W. D., D. Kleppner, and F. G. Walther (private communication, 1984).
- Phillips, W. D., W. E. Cooke, and D. Kleppner, *Metrologia* **13**(4), 179–195 (1977).
- Philo, J. S., and W. M. Fairbank, *J. Chem. Phys.* **72**(8), 4429–4433 (1980).
- Piccard, A., and A. Devaud, *Arch. Sci. Phys. Nat.* **2**, 455–485 (1920).
- Pichanick, F. M. J., and V. W. Hughes, in *Quantum Electrodynamics*, edited by T. Kinoshita (World Scientific, Singapore, 1990), Chap. 17, pp. 905–936.
- Pipkin, F. M., in *Quantum Electrodynamics*, edited by T. Kinoshita (World Scientific, Singapore, 1990), Chap. 14, pp. 696–773.
- Piquemal, F., B. Etienne, J.-P. Andre, and J.-N. Patillon, *IEEE Trans. Instrum. Meas.* **40**(2), 234–236 (1991).
- Pontikis, C., *C. R. Acad. Sci. Ser. B* **274**, 437–440 (1972).
- Pöpel, R., *Metrologia* **29**(2), 153–174 (1992).
- Powell, L. J., T. J. Murphy, and J. W. Gramlich, *J. Res. Natl. Bur. Stand.* **87**(1), 9–19 (1982).
- Prange, R. E., and S. M. Girvin, *The Quantum Hall Effect*, 2nd ed. (Springer-Verlag, Berlin, 1990).
- Preston-Thomas, H., *Metrologia* **5**(2), 35–44 (1969).
- Preston-Thomas, H., *Metrologia* **27**(1), 3–10 (1990).
- Prigl, R., U. Haeberlen, K. Jungmann, G. zu Putlitz, and P. von Walter, *Nucl. Instrum. Methods* **A374**(1), 118–126 (1996).
- Quinn, T. J., *Metrologia* **26**(1), 69–74 (1989).
- Quinn, T. J., *IEEE Trans. Instrum. Meas.* **40**(2), 81–85 (1991).
- Quinn, T. J., *Metrologia* **30**(5), 523–541 (1993).
- Quinn, T. J., *Metrologia* **31**(1), 63–68 (1994).
- Quinn, T. J., *Metrologia* **33**(3), 271–287 (1996).
- Quinn, T. J., A. R. Colclough, and T. R. D. Chandler, *Philos. Trans. R. Soc. London, Ser. A* **283**(1314), 367–420 (1976).
- Quinn, T. J., and J. E. Martin, *Philos. Trans. R. Soc. London, Ser. A* **316**(1536), 85–189 (1985).
- Ramsey, N. F., *Phys. Rev.* **85**(4), 688–688 (1952).
- Ramsey, N. F., *Phys. Rev. A* **1**(5), 1320–1322 (1970).
- Rao, S. R., and S. R. Govindarajan, *Proc. Indian Acad. Sci.* **15A**(1), 35–51 (1942).
- Rayner, G. H., *IEEE Trans. Instrum. Meas.* **IM-21**(4), 361–365 (1972).
- Raynes, W. T., and N. Panteli, *Mol. Phys.* **48**(3), 439–449 (1983).
- Reymann, D., and T. J. Witt, *IEEE Trans. Instrum. Meas.* **42**(2), 596–599 (1993).
- Reymann, D., T. J. Witt, D. Andreone, R. Cerri, and A. Godone, *Metrologia* **35**(1), 21–24 (1998).
- Richman, S. J., T. J. Quinn, C. C. Speake, and R. S. Davis, *Meas. Sci. Technol.* **10**(6), 460–466 (1999).
- Richtmyer, F. K., *Science* **75**(1931), 1–5 (1932).
- Ricketts, B. W., and M. E. Cage, *IEEE Trans. Instrum. Meas.* **IM-36**(2), 245–248 (1987).
- Ritter, M. W., P. O. Egan, V. W. Hughes, and K. A. Woodle, *Phys. Rev. A* **30**(3), 1331–1338 (1984).
- Roach, T. M., C. M. Levy, and G. Gabrielse, *Bull. Am. Phys. Soc.* **43**(3), 1316–1316 (1998).
- Robertsson, L. (private communication, 1999).
- Robinson, H. G., and W. M. Hughes, in *Precision Measurement and Fundamental Constants*, edited by D. N. Langenberg and B. N. Taylor (NBS Spec. Pub. 343, US Government Printing, Washington, DC, 1971), pp. 427–430.
- Robinson, I. A., and B. P. Kibble, *IEEE Trans. Instrum. Meas.* **46**(2), 596–600 (1997).
- Roskies, R. Z., E. Remiddi, and M. J. Levine, in *Quantum Electrodynamics*, edited by T. Kinoshita (World Scientific, Singapore, 1990), Chap. 6, pp. 162–217.
- Rosman, K. J. R., and P. D. P. Taylor, *J. Phys. Chem. Ref. Data* **27**(6), 1275–1287 (1998).
- Röttger, S., A. Paul, and U. Keyser, *IEEE Trans. Instrum. Meas.* **46**(2), 560–562 (1997).
- Rovera, G. D., and O. Acef, *IEEE Trans. Instrum. Meas.* **48**(2), 571–573 (1999).
- Rowlinson, J. S., and D. J. Tildesley, *Proc. R. Soc. London, Ser. A* **358**(1694), 281–286 (1977).
- Ruan, Y., X. Wang, T. Yin, and Z. Zhang, Document CCE/88-7 submitted to the 18th meeting of the Comité Consultatif d'Electricité of the CIPM (1988).
- Safinya, K. A., K. K. Chan, S. R. Lundeen, and F. M. Pipkin, *Phys. Rev. Lett.* **45**(24), 1934–1937 (1980).
- Sagitov, M. U., V. K. Milyukov, Y. A. Monakhov, V. S. Nazarenko, and K. G. Tadzhdinov, *Dokl. Akad. Nauk SSSR* **245**(3), 567–569 (1979) [*Sov. Phys. Dokl.* **245**(1-6), 20–22 (1981)].
- Samuel, M. A., and G. Li, *Phys. Rev. D* **44**(12), 3935–3942 (1991). Erratum: **48**(4), 1879–1881 (1993).
- Sapirstein, J. R., and D. R. Yennie, in *Quantum Electrodynamics*, edited by T. Kinoshita (World Scientific, Singapore, 1990), Chap. 12, pp. 560–672.
- Sapirstein, J. R., E. A. Terray, and D. R. Yennie, *Phys. Rev. D* **29**(10), 2290–2314 (1984).
- Sasagawa, G. S., F. Klopping, T. M. Niebauer, J. E. Faller, and R. L. Hilt, *Geophys. Res. Lett.* **22**(4), 461–464 (1995).
- Savithri, K., *Proc. Indian Acad. Sci.* **16A**(3), 196–206 (1943).
- Schmidt-Kaler, F., D. Leibfried, S. Seel, C. Zimmermann, W. König, M. Weitz, and T. W. Hänsch, *Phys. Rev. A* **51**(4), 2789–2800 (1995).
- Schneider, S. M., W. Greiner, and G. Soff, *Phys. Rev. A* **50**(1), 118–122 (1994).
- Schwarz, J. P., D. S. Robertson, T. M. Niebauer, and J. E. Faller, *Science* **282**(5397), 2230–2234 (1998).
- Schwarz, J. P., D. S. Robertson, T. M. Niebauer, and J. E. Faller, *Meas. Sci. Technol.* **10**(6), 478–486 (1999).
- Schwarz, W., *et al.*, *IEEE Trans. Instrum. Meas.* **44**(2), 505–509 (1995).
- Schwinberg, P. B., R. S. Van Dyck, Jr., and H. G. Dehmelt, *Phys. Rev. Lett.* **47**(24), 1679–1682 (1981).
- Schwinberg, P. B., R. S. Van Dyck, Jr., and H. G. Dehmelt, in *Precision Measurement and Fundamental Constants II*, edited by B. N. Taylor and W. D. Phillips (NBS Spec. Pub. 617, US Government Printing Office, Washington, DC, 1984), pp. 215–218.

- Schwinger, J., Phys. Rev. **73**(4), 416–417 (1948).
- Schwinger, J., Phys. Rev. **76**(6), 790–817 (1949).
- Schwob, C., L. Jozefowski, B. de Beauvoir, L. Hilico, F. Nez, L. Julien, and F. Biraben, Phys. Rev. Lett. **82**(25), 4960–4963 (1999).
- Seyfried, P., in *Precision Measurement and Fundamental Constants II*, edited by B. N. Taylor and W. D. Phillips (NBS Spec. Pub. 617, US Government Printing Office, Washington, DC, 1984), pp. 313–316.
- Shabaev, V. M., A. N. Artemyev, T. Beier, and G. Soff, J. Phys. B **31**(8), L337–L339 (1998).
- Sheppard, W. F., in *Proceedings of the Fifth International Congress of Mathematicians*, edited by E. W. Hobson and A. E. H. Love, Vol. ii (Cambridge University Press, Cambridge, 1912), pp. 348–384.
- Shida, K., T. Wada, H. Nishinaka, K. Segawa, and T. Igarashi, IEEE Trans. Instrum. Meas. **38**(2), 252–255 (1989).
- Shields, J. Q., R. F. Dziuba, and H. P. Layer, IEEE Trans. Instrum. Meas. **38**(2), 249–251 (1989).
- Shifrin, V. Y. (private communication, 1997).
- Shifrin, V. Y., P. G. Park, C. G. Kim, V. N. Khorev, and C. H. Choi, IEEE Trans. Instrum. Meas. **46**(2), 97–100 (1997).
- Shifrin, V. Y., P. G. Park, V. N. Khorev, C. H. Choi, and C. S. Kim, IEEE Trans. Instrum. Meas. **47**(3), 638–643 (1998a).
- Shifrin, V. Y., P. G. Park, V. N. Khorev, C. H. Choi, and S. Lee, IEEE Trans. Instrum. Meas. **48**(2), 196–199 (1999).
- Shifrin, V. Y., V. N. Khorev, P. G. Park, C. H. Choi, and C. S. Kim, Izmer. Tekh. **1998**(4), 68–72 (1998b).
- Shiner, D., R. Dixon, and P. Zhao, Phys. Rev. Lett. **72**(12), 1802–1805 (1994).
- Sick, I., and D. Trautmann, Nucl. Phys. **A637**(4), 559–575 (1998).
- Siebert, H., and P. Becker, in *Precision Measurement and Fundamental Constants II*, edited by B. N. Taylor and W. D. Phillips (NBS Spec. Pub. 617, US Government Printing Office, Washington, DC, 1984), pp. 321–324.
- Siebert, H., P. Becker, and P. Seyfried, Z. Phys. B **56**(4), 273–278 (1984).
- Sienknecht, V., and T. Funck, IEEE Trans. Instrum. Meas. **IM-34**(2), 195–198 (1985).
- Sienknecht, V., and T. Funck, Metrologia **22**(3), 209–212 (1986).
- Simon, G. G., C. Schmitt, F. Borkowski, and V. H. Walther, Nucl. Phys. **A333**, 381–391 (1980).
- Sloggett, G. (private communication, 1994).
- Small, G. W., IEEE Trans. Instrum. Meas. **IM-36**(2), 190–195 (1987).
- Small, G. W., B. W. Ricketts, and P. C. Coogan, IEEE Trans. Instrum. Meas. **38**(2), 245–248 (1989).
- Small, G. W., B. W. Ricketts, P. C. Coogan, B. J. Pritchard, and M. M. R. Sovierzoski, Metrologia **34**(3), 241–243 (1997).
- Sommerfield, C. M., Phys. Rev. **107**(1), 328–329 (1957).
- Sommerfield, C. M., Ann. Phys. (N.Y.) **5**(1), 26–57 (1958).
- Spagnolo, S., Eur. Phys. J. C **6**(4), 637–645 (1999).
- Stedman, R., J. Sci. Instrum. **1**(2), 1168–1170 (1968).
- Steiner, R. L., A. D. Gillespie, K. Fujii, E. R. Williams, D. B. Newell, A. Picard, G. N. Stenbakken, and P. T. Olsen, IEEE Trans. Instrum. Meas. **46**(2), 601–604 (1997).
- Steiner, R. L., D. B. Newell, and E. R. Williams, IEEE Trans. Instrum. Meas. **48**(2), 205–208 (1999).
- Stenbakken, G., R. Steiner, P. Olsen, and E. Williams, IEEE Trans. Instrum. Meas. **45**(2), 372–377 (1996).
- Stone, J. M., *Radiation and Optics* (McGraw-Hill, New York, 1963), p. 468.
- Stone, M., *Quantum Hall Effect* (World Scientific, Singapore, 1992).
- Storm, L., Metrologia **22**(3), 229–234 (1986).
- Storry, C. H., and E. A. Hessels, Phys. Rev. A **58**(1), R8–R11 (1998).
- Stratton, J. A., *Electromagnetic Theory* (McGraw-Hill, New York, 1941).
- Studentsov, N. V., V. N. Khorev, and V. Y. Shifrin, Izmer. Tekh. **24**(6), 56–57 (1981) [Meas. Tech. **24**(6), 501–502 (1981)].
- Sunnergren, P., H. Persson, S. Salomonson, S. M. Schneider, I. Lindgren, and G. Soff, Phys. Rev. A **58**(2), 1055–1069 (1998).
- Tan, J., and G. Gabrielse, Phys. Rev. Lett. **67**(22), 3090–3093 (1991).
- Tan, J., and G. Gabrielse, Phys. Rev. A **48**(4), 3105–3122 (1993).
- Tanaka, M., K. Nakayama, and K. Kuroda, IEEE Trans. Instrum. Meas. **38**(2), 206–209 (1989).
- Taqqu, D. et al. Hyp. Int. **119**(1–4), 311–315 (1999).
- Tarbeeve, Y. V. (private communication, 1981).
- Tarbeeve, Y. V., V. Y. Shifrin, V. N. Khorev, and N. V. Studentsov, Izmer. Tekh. **32**(4), 3–4 (1989) [Meas. Tech. **32**(4), 279–394 (1989)].
- Tarbeeve, Y. V., E. D. Koltik, V. I. Krzhimovsky, A. S. Katkov, O. P. Galakhova, S. V. Kozyrev, and S. E. Khabarov, Metrologia **28**(4), 305–307 (1991).
- Taylor, B. N., in *Precision Measurement and Fundamental Constants*, edited by D. N. Langenberg and B. N. Taylor (NBS Spec. Pub. 343, US Government Printing Office, Washington, DC, 1971), pp. 495–498.
- Taylor, B. N., J. Res. Natl. Bur. Stand. **90**(2), 91–94 (1985).
- Taylor, B. N., IEEE Trans. Instrum. Meas. **40**(2), 86–91 (1991).
- Taylor, B. N., *Guide for the Use of the International System of Units (SI)* (NIST Spec. Pub. 811, 1995 ed., US Government Printing Office, Washington, DC, 1995).
- Taylor, B. N., and C. E. Kuyatt, *Guidelines for Evaluating and Expressing the Uncertainty of NIST Measurement Results* (NIST Tech. Note 1297, 1994 ed., US Government Printing Office, Washington, DC, 1994).
- Taylor, B. N., and E. R. Cohen, J. Res. Natl. Inst. Stand. Technol. **95**(5), 497–523 (1990).
- Taylor, B. N., and P. J. Mohr, Metrologia **36**(1), 63–64 (1999).
- Taylor, B. N., and T. J. Witt, BIPM Com. Cons. Électricité **17**, E122–E136 (1986).
- Taylor, B. N., and T. J. Witt, Metrologia **26**(1), 47–62 (1989).
- Taylor, B. N., W. H. Parker, and D. N. Langenberg, Rev. Mod. Phys. **41**(3), 375–496 (1969).
- Taylor, B. N., W. H. Parker, D. N. Langenberg, and A. Denenstein, Metrologia **3**(4), 89–98 (1967).
- Thompson, A. M., Proc. IEEE **106B**, 307–310 (1959).
- Thompson, A. M., Metrologia **4**(1), 1–7 (1968).
- Thompson, A. M., and D. G. Lampard, Nature (London) **177**, 888–890 (1956).
- Tiedeman, J. S., and H. G. Robinson, Phys. Rev. Lett. **39**(10), 602–604 (1977).
- Tsai, J. S., A. K. Jain, and J. E. Lukens, Phys. Rev. Lett. **51**(4), 316–319 (1983); Erratum: **51**(12), 1109–1109 (1983).
- Udem, T., A. Huber, B. Gross, J. Reichert, M. Prevedelli, M. Weitz, and T. W. Hänsch, Phys. Rev. Lett. **79**(14), 2646–2649 (1997).
- Udem, T., J. Reichert, R. Holzwarth, and T. W. Hänsch, Phys. Rev. Lett. **82**(18), 3568–3571 (1999).
- Van Degrift, C. T., M. E. Cage, and S. M. Girvin, *The Integral and Fractional Quantum Hall Effects* (American Association of Physics Teachers, College Park, MD, 1991).
- Van Der Leun, C., and C. Alderliesten, Nucl. Phys. **A380**(2), 261–269 (1982).
- Van Dyck, Jr., R. S., in *Quantum Electrodynamics*, edited by T. Kinoshita (World Scientific, Singapore, 1990), Chap. 8, pp. 322–388.
- Van Dyck, Jr., R. S., in *Atomic, Molecular, and Optical Physics: Charged Particles*, edited by F. B. Dunning and R. G. Hulet (Academic, San Diego, 1995), Chap. 13, pp. 363–388. Experimental Methods in the Physical Sciences Series, Vol. 29A.
- Van Dyck, Jr., R. S. (private communication, 1999).
- Van Dyck, Jr., R. S., D. L. Farnham, and P. B. Schwinberg, Bull. Am. Phys. Soc. **38**, 946 (1993a).
- Van Dyck, Jr., R. S., D. L. Farnham, and P. B. Schwinberg, Bull. Am. Phys. Soc. **38**, 947 (1993b).
- Van Dyck, Jr., R. S., D. L. Farnham, and P. B. Schwinberg, Phys. Scr. **T59**, 134–143 (1995).
- Van Dyck, Jr., R. S., D. L. Farnham, S. L. Zafonte, and P. B. Schwinberg, in *Trapped Charged Particles and Fundamental Physics*, edited by D. H. E. Dubin and D. Schneider, AIP Conf. Proc. 457, 101–110 (1999a).
- Van Dyck, Jr., R. S., D. L. Farnham, S. L. Zafonte, and P. B. Schwinberg, Rev. Sci. Instrum. **70**(3), 1665–1671 (1999b).
- Van Dyck, Jr., R. S., F. L. Moore, D. L. Farnham, and P. B. Schwinberg, Bull. Am. Phys. Soc. **31**(3), 244–244 (1986a).
- Van Dyck, Jr., R. S., F. L. Moore, D. L. Farnham, P. B. Schwinberg, and H. G. Dehmelt, Phys. Rev. A **36**(7), 3455–3456 (1987a).
- Van Dyck, Jr., R. S., P. B. Schwinberg, and H. G. Dehmelt, in *Atomic Physics 9*, edited by R. S. Van Dyck, Jr. and E. N. Fortson (World Scientific, Singapore, 1984), pp. 53–74.
- Van Dyck, Jr., R. S., P. B. Schwinberg, and H. G. Dehmelt, Phys. Rev. D **34**(3), 722–736 (1986b).
- Van Dyck, Jr., R. S., P. B. Schwinberg, and H. G. Dehmelt, Phys. Rev. Lett. **59**(1), 26–29 (1987b).
- Van Dyck, Jr., R. S., P. B. Schwinberg, and H. G. Dehmelt, in *The Electron*,

- edited by D. Hestenes and A. Weingartshofer (Kluwer Academic, Netherlands, 1991), pp. 239–293.
- van Wijngaarden, A., F. Holuj, and G. W. F. Drake, *Can. J. Phys.* **76**(2), 95–103 (1998). Erratum: **76**(12), 993–993 (1998).
- van Wijngaarden, A., J. Kwela, and G. W. F. Drake, *Phys. Rev. A* **43**(7), 3325–3342 (1991).
- Vigoureux, P., and N. Dupuy, *Realization of the Ampere, and Measurement of the Gyromagnetic Ratio of the Proton* (National Physical Laboratory, Teddington, Middlesex, UK, 1980). NPL Report DES 59.
- von Klitzing, K., G. Dorda, and M. Pepper, *Phys. Rev. Lett.* **45**(6), 494–497 (1980).
- Vylov, T., V. M. Gorozhankin, K. Y. Gromov, A. I. Ivanov, I. F. Uchevatkin, and V. G. Chumin, *Yad. Fiz.* **36**, 812–814 (1982) [*Sov. J. Nucl. Phys.* **36**(3), 474–475 (1982)].
- Walther, F. G., W. D. Phillips, and D. Kleppner, *Phys. Rev. Lett.* **28**(18), 1159–1161 (1972).
- Wapstra, A. H., *Nucl. Instrum. Methods* **A292**(3), 671–676 (1990).
- Wapstra, A. H., and G. Audi, *Nucl. Phys.* **A432**(1), 1–54 (1985).
- Watson, G., *Contemp. Phys.* **37**(2), 127–143 (1996).
- Weirauch, W., *Nucl. Instrum. Methods* **131**(1), 111–117 (1975).
- Weirauch, W., in *Fundamental Physics with Reactor Neutrons and Neutrin*os, edited by T. von Egidy (IOP Conf. Ser. No. 42, Institute of Physics, London, 1978), Chap. 1, pp. 47–52.
- Weirauch, W., E. Krüger, and W. Nistler, in *Lecture Notes in Physics 128: Neutron Spin Echo*, edited by F. Mezei (Springer-Verlag, Berlin, 1980), pp. 94–103.
- Weiss, D. S., B. C. Young, and S. Chu, *Phys. Rev. Lett.* **70**(18), 2706–2709 (1993).
- Weiss, D. S., B. C. Young, and S. Chu, *Appl. Phys. B* **59**(3), 217–256 (1994).
- Weitz, M. (private communication, 1998).
- Weitz, M., A. Huber, F. Schmidt-Kaler, D. Leibfried, and T. W. Hänsch, *Phys. Rev. Lett.* **72**(3), 328–331 (1994).
- Weitz, M., *et al.*, *Phys. Rev. A* **52**(4), 2664–2681 (1995).
- Weyand, K., *IEEE Trans. Instrum. Meas.* **IM-34**(2), 167–173 (1985).
- White, D. R., *et al.*, *Metrologia* **33**(4), 325–335 (1996).
- Wichmann, E. H., and N. M. Kroll, *Phys. Rev.* **101**(2), 843–859 (1956).
- Williams, E. R. (private communication, 1997).
- Williams, E. R., and P. T. Olsen, *IEEE Trans. Instrum. Meas.* **IM-21**(4), 376–379 (1972).
- Williams, E. R., and P. T. Olsen, *Phys. Rev. Lett.* **42**(24), 1575–1579 (1979).
- Williams, E. R., G. R. Jones, J.-S. Song, W. D. Phillips, and P. T. Olsen, *IEEE Trans. Instrum. Meas.* **IM-34**(2), 163–167 (1985).
- Williams, E. R., G. R. Jones, Jr., S. Ye, R. Liu, H. Sasaki, P. T. Olsen, W. D. Phillips, and H. P. Layer, *IEEE Trans. Instrum. Meas.* **38**(2), 233–237 (1989).
- Williams, E. R., P. T. Olsen, and W. D. Phillips, in *Precision Measurement and Fundamental Constants II*, edited by B. N. Taylor and W. D. Phillips (NBS Spec. Pub. 617, US Government Printing Office, Washington, DC, 1984), pp. 497–503.
- Williams, E. R., R. L. Steiner, D. B. Newell, and P. T. Olsen, *Phys. Rev. Lett.* **81**(12), 2404–2407 (1998).
- Williams, R. W., *Phys. Lett. B* **34**(1), 63–64 (1971).
- Williams, W. L., and V. W. Hughes, *Phys. Rev.* **185**(4), 1251–1255 (1969).
- Wimett, T. F., *Phys. Rev.* **91**(2), 499–500 (1953).
- Windisch, D., and P. Becker, *Philos. Mag.* **58**(2), 435–443 (1988).
- Windisch, D., and P. Becker, *Phys. Status Solidi A* **118**(2), 379–388 (1990).
- Winkler, P. F., D. Kleppner, T. Myint, and F. G. Walther, *Phys. Rev. A* **5**(1), 83–114 (1972).
- Witt, T. J., *IEEE Trans. Instrum. Meas.* **44**(2), 208–210 (1995).
- Yelkhovsky, A. S., *Zh. Éksp. Teor. Fiz.* **113**, 865–879 (1998) [*JETP* **86**(3), 472–479 (1998)].
- Yennie, D. R., *Rev. Mod. Phys.* **59**(3), 781–824 (1987).
- Young, B. C., Ph.D. thesis, Stanford University, 1997.
- Young, B., M. Kasevich, and S. Chu, in *Atom Interferometry*, edited by P. R. Berman (Academic, New York, 1997), pp. 363–406.
- Zhang, T., and G. W. F. Drake, *Phys. Rev. A* **54**(6), 4882–4922 (1996).
- Zhang, Z., *Acta Metrol. Sin.* **6**(1), 33–38 (1985).
- Zhang, Z., D. Wang, T. Yin, Z. Hu, J. Zheng, F. Liu, J. Zhou, and L. Cai, Document CCE/88-8 submitted to the 18th meeting of the Comité Consultatif d'Électricité of the CIPM (1988).
- Zhang, Z., *et al.*, *IEEE Trans. Instrum. Meas.* **40**(6), 889–892 (1991).
- Zhang, Z., D. Wang, Z. Hu, J. Zheng, and Q. He, *Acta Metrol. Sin.* **14**(2), 81–86 (1993).
- Zhang, Z., D. Wang, Z. Hu, J. Zheng, Q. He, and R. Liu, Document CCE/92-66 submitted to the 19th meeting of the Comité Consultatif d'Électricité of the CIPM (1992).
- Zhang, Z., X. Wang, D. Wang, X. Li, Q. He, and Y. Ruan, *Acta Metrol. Sin.* **16**(1), 1–5 (1995).
- Zhao, P., W. Lichten, H. Layer, and J. Bergquist, *Phys. Rev. Lett.* **58**(13), 1293–1295 (1987); Erratum: **58**(23), 2506–2506 (1987).
- Zhao, P., W. Lichten, Z.-X. Zhou, H. P. Layer, and J. C. Bergquist, *Phys. Rev. A* **39**(6), 2888–2898 (1989).
- Zhao, P., W. Lichten, H. P. Layer, and J. C. Bergquist, *Phys. Rev. A* **34**(6), 5138–5141 (1986); Erratum: **36**(3), 1511–1511 (1987).